

Modulation of the Mitogen Activated Protein Kinase
Pathway Spatiotemporal Signalling Components:
Influence on Pathway Activation Behaviour Using an
Agent Based Model



Aban Shuaib

A thesis submitted for the degree of Doctor of Philosophy

Department of Cardiovascular Science and Computer
Science

School of Medicine and Biomedical Sciences

University of Sheffield

March 2016

Supervisors: Dr Endre Kiss-Toth and Professor Mike
Holcombe

Abstract

Cells use biochemical pathways to interpret their environment and respond accordingly. The mitogen activated protein kinase (MAPK) cascade forms a pathway central to translating external environmental signals into multiple and diverse responses. The mechanisms for decoding the environment by MAPKs and ensuring specificity and fidelity of responses are of great interest. Understanding these mechanisms will open the door to comprehending the molecular basis of dysregulated cellular behaviour, which leads to diseases such as cancer and atherosclerosis. Mathematical and computer models of the pathway provide useful tools to test and examine how these mechanisms give rise to specificity and fidelity where experimental tools cannot. We used an agent-based computational model (ABM) to examine MAPK activation behaviour when pathway components are present in confined compartments and assessed the impact of altered balance between activating and de-activating mechanisms on pathway dynamics, *i.e.* spatiotemporal regulation of the MAPK pathway. We show that multi-compartments contribute to the emergence of oscillatory behaviour and play a role in ensuring a robust response despite variation in the temporal activating mechanism. The emergent behaviour in the model replicated MAPK activation behaviour observed in *in vitro* experimental systems in regard to the levels of pMAPK and the time taken to achieve E_{\max} . Thus, ABM shows promise to model, examine and provide novel insights into the control of MAPK pathway dynamics.

Acknowledgements

I would like to thank the following people without whom this work could have not been achieved. I would like to thank my supervisors Dr Endre Kiss-Toth and professor Mike Holcombe for their guidance and support. I am deeply appreciative to Dave Rhodes and Simon Coakley for their continuous assistance and support in the development of the computational model.

I extend my appreciation and thanks to Manuel Guzmáno and Dr Guillermo Velasco for giving me the opportunity to carry out my experimental work in the Cannabinoid signalling group at Complutense University Madrid. I would like to acknowledge Dr David Dávila for his assistance with data analysis and presentation and his supervision during that period. I also extend my thanks to all the lab members for their support, comments and continuous help.

Last but not least, to my family. I am deeply grateful for everything they have done.

Declaration

This I declare that this thesis was composed by myself and the work contained herein is my own except where explicitly stated otherwise in the text. This work has not been submitted for any other degree or professional qualification except as specified.

Aban Shuaib

“If one assumes that the total volume of water on Earth is humanity’s knowledge about this topic, then this body of work is equivalent to five barrels of water... a giant leap for a man; a small step for mankind... However; remember, ‘The journey of a thousand miles begins with one step’... Anonymous

Contents

I. Overview of the mitogen activated protein kinase (MAPK) pathway and its signalling behaviour	XXVI
II. Research objectives	XXIX
III. Contribution to knowledge	XXX
IV. Abstracts, presentations & posters	XXXI
V. Publications:	XXXIII
Chapter 1 Cell signalling, and signal propagation through the mitogen activated protein kinase (MAPK)	1
1.1 A general introduction to cell signalling	1
1.2 The MAPK signalling pathway	3
1.2.1 Extracellular signal-regulated kinase ERK1/2	8
1.2.2 p38 pathway	10
1.2.3 Jun N-terminal kinases JNK.....	12
1.3 The complexity and mystery of the MAPK pathway	13
1.3.1 Regulation of the MAPK pathway	16
1.3.1.1.1 <i>Negative feedback</i>	19
1.4 Conclusion	33
Chapter 2 Computational modelling of biological systems	35
2.1 The complexity of the physiological system	35

2.2	The rise of Systems Biology (SB) and increased importance of <i>in silico</i> modelling	36
2.2.1	SB and use of <i>in silico</i> models: aims and benefits	37
2.2.2	Modelling intracellular signalling events	43
2.3	Conclusion	68
Chapter 3	Characterising the MAPK signalling pathway agent-based model (ABM)	71
3.1	The Modelling process: universal practice	71
3.2	Model specification	74
3.2.1	Defining the system boundaries.....	74
3.2.2	Physical environment.....	83
3.2.3	Important behaviour	85
3.3	Model formulation: Defining the agent based model (ABM) of the MAPK pathway	93
3.3.1	Creating the system boundaries:	95
3.3.2	Agent behaviour:.....	103
3.3.3	Model inputs and outputs.....	110
3.4	Initial conditions and parameters for the agent-based models (ABMs)	111
3.5	ABMs calibration, rule validation and analysis	115
3.5.1	Model rule validation and optimisation	115

3.6	Conclusion	126
Chapter 4	Results.....	127
4.1	ABMs time calibration	127
4.1.1	Sensitivity analysis of the agent based models.....	128
4.2	Examination of the spatial regulatory element on MAPK activation dynamics.	129
4.2.1	Results.....	134
4.2.2	Discussion and conclusion.....	148
4.3	The combination of spatiotemporal regulations play a role in shaping pathway activation behaviour	154
4.3.1	Results.....	158
4.3.2	Discussion and conclusion.....	167
4.4	Variation of the spatiotemporal regulatory elements and their effect on the MAPK global activation.....	174
4.4.1	Results.....	175
4.4.2	Discussion and conclusion:.....	183
Chapter 5	Conclusions and Future work	192
5.1	Conclusions	192
5.2	Limitations and future work	195
5.2.1	<i>In silico</i> modelling, future work.....	195

References.....	205
Appendix A.....	242
a. Agents' descriptions:.....	242
i. The multi-state models.....	242
1. Agent memory parameters.....	242
b. The multi-agent ABM	248
i. Agent memory parameters.....	248
ii. Agent messages	253
Appendix B.....	257
Appendix C. References used to calibrate pMAPK activation time in the ABM.	271
Appendix D. Tribbles mediate a differential response to THC-dependent cell death through alteration in protein-protein interaction with different binding partners	275
a. Introduction	275
b. Materials and methods.	280
<i>i. Cell culture and transfection.....</i>	280
<i>ii. Tribbles siRNA Knock Down (K.D).....</i>	282
<i>1. RNA isolation and Real-time quantitative PCR (RT-qPCR)</i>	282
iii. Tetrahydrocannabinol (THC) survival assay.....	284
<i>iv. Co-Immunoprecipitation (CO-IP).....</i>	285
1. Covalent coupling Trib3 antibody to protein G-sepharose.....	285

2. Covalent coupling Trib3 antibody to protein G-sepharose	286
v. <i>Luciferase assay preparation</i>	290
1. Plasmids (Bacterial transformation and plasmid isolation):	290
2. Restriction enzyme digests and gel electrophoresis.....	290
3. Fluorescence microscopy	291
4. Luciferase assay: Fluorescence microscopy:.....	291
c. <i>Results</i>	292
i. <i>Altering TRIB proteins levels cause a differential response to apoptosis</i> 292	
ii. <i>Altering TRIB proteins levels cause a differential response to apoptosis</i>	293
iii. <i>Knock down (KD) of tribbles family members' expression levels influence protein-protein interaction between TRIB3 and its interaction partners.</i>	295
iv. Over expression of TRIB1 and TRIB2 are capable of considerable reduction of p38 and ERK mediated gene expression events but with no notable difference between homo and heterodimer species.....	298
d. <i>Discussion</i>	299
e. <i>References</i>	307
Appendix E. Publications	313

List of Figures

Figure 1. 1 A schematic representation of the MAPK pathway architecture and its activation during response to an external stimulus.	4
Figure 1. 2 The different MAPK pathways and their correspondent MAP3K, MAP2K and MAPK.....	6
Figure 1. 3 A schematic representation of the ERK MAPK pathway and its correspondent MAP3K, MAP2K and phosphorylation target.....	8
Figure 1. 4 A schematic representation of the ERK MAPK pathway and its correspondent MAP3K, MAP2K and phosphorylation target.....	9
Figure 1. 5 A schematic representation of the ERK MAPK pathway and its correspondent MAP3K, MAP2K and phosphorylation target.....	12
Figure 1. 6 MAPK pathway mediates two distinct cellular outcomes.....	14
Figure 1. 7 The modulation of the MAPK pathway using feedback mechanisms.	19
Figure 1. 8 Compartmentalisation and scaffold proteins influence on the MAPK pathway.....	30
Figure 3. 1 A flowchart summarising modelling process <i>in silico</i>	73
Figure 3. 2 The MAPK activation dynamics observed <i>in vitro</i> and <i>in silico</i>	88
Figure 3. 3 shows activity diagrams for each agent and the processes leading to its state change.....	96

Figure 3. 4 Stategraph for the agents in the Agent Based Model (ABM) illustrating the processes of state change, communication and message input/out by the three primary agents in the ABM.	98
Figure 3. 5 Representation of the re-activation delay period (RADP) stochastic (I) and deterministic (periodic, (II)) modelling schemes.	107
Figure 3. 6 A sensitivity analysis of ExR [recdel] value on MAPK activation dynamics.....	109
Figure 3. 7 Agent based-model (ABM) simulations to validate agents' interaction, behaviour and state change.....	117
Figure 3. 8 Successful interactions between agents results in their state change and consequently alteration of their number in the ABM.	119
Figure 3. 9 Nuclear events, interaction of activated MAPK (pMAPK) with its nuclear binding partners.	121
Figure 3. 10 Validation of interaction of pMAPKK and the inhibitor protein TRIB.....	123
Figure 3. 11 Comparison between the multi-state and the multi-agent agent based models (ABMs) run times.....	124
Figure 4. 1: Data distribution and analysis of MAPK activation and the time-scale to achieve maximal pMAPK levels.....	128
Figure 4. 2 Different spatial ABMs used to investigate the significance of MAPKK and MAPK spatial arrangement on the MAPK.....	130

Figure 4. 3: Spatial modulation of the MAPK pathway using the ABM combined with models sensitivity analysis.....	133
Figure 4. 4 Multi-compartment ABM sensitivity analyses assessing the effect of agent levels alteration on MAPK and MAPKK activation.....	136
Figure 4. 5 Validation of the ABM models via comparison with published literature.....	138
Figure 4. 6 Significant difference in MAPK activation behaviour between two and multi-compartment models.....	139
Figure 4. 7 The effect of reducing the cytoplasmic volume on the MAPK activation dynamics in a two-compartment model.	140
Figure 4. 8 The effect of reducing the cytoplasmic volume on the MAPK activation dynamics in a multi-compartment ABM.	142
Figure 4. 9 The effect of reducing individual compartments volume on the MAPK activation dynamics in a multi-compartment ABM.....	143
Figure 4. 10 A two-compartment ABM simulating of pMAPK-dependent nuclear events and the effect of modulating MAPK activation by tribbles protein agents (TRIB).	145
Figure 4. 11 <i>in vitro</i> data demonstrating the ability of TRIB to significantly modulate the MAPK pathway.....	146
Figure 4. 12 Assessment of the disruption of MAPK activation dynamics at the level of MAPKK in the two-compartment model.....	147
Figure 4. 13 MAPK pathway regulation through feedback loops.....	154

Figure 4. 14 Analysis of the re-activation delay period (RADP) to confirm its stochasticity.	159
Figure 4. 15 The effect of altering spatiotemporal regulatory elements on the MAPK activation dynamics.	160
Figure 4. 16 The effect of spatiotemporal modulation on the MAPK activation dynamics.	162
Figure 4. 17 The effect of minimal stochasticity of RADP on the MAPK activation.	164
Figure 4. 18: (Fig 4.16) The effect of spatiotemporal modulation on the MAPK activation dynamics using deterministic re-activation delay periods.	165
Figure 4. 19 Modulation of the re-activation delay period (RADP) in a two compartment model of MAPK pathway.	167
Figure 4. 20 Validation of the emergent pMAPK oscillatory behaviour in the multi-compartment ABM against the oscillatory behaviour in the MAPK pathway first demonstrated by Shankaran et al.	169
Figure 4. 21 Modulation of the spatial regulatory element of the MAPK pathway results into emergence of two phase MAPK.	174
Figure 4. 22. The activation dynamics of MAPK in a MAPKK-MAPK signosome cluster ABM.	177
Figure 4. 23 The activation dynamics of MAPKK in a MAPKK-MAPK signosome cluster ABM.	179

Figure 4. 24 Modulation of the temporal regulatory element continuously and its impact on the dynamics of MAPK activation.....	186
Figure 4. 25 MAPK activation dynamics in endosomal compartments and in an agent-based model (ABM) containing cytosolic signalsome cluster.....	187
Figure 5. 1 A summary of future improvements and modifications process required for the ABM.....	196
Appendix A, Figure 1 Introduction of the tribbles protein agent into the two compartment agent based model (ABM).....	256
Appendix B, Figure 1 An agent based-model (ABM) simulation to validate agent interaction, behaviour and state change.....	257
Appendix B, Figure 2 A 3D visualisation of the ABMs. The red sphere in the middle represents the nucleus and marks the nuclear membrane.....	257
Appendix B, Figure 3 Multiple runs of the two compartment agent based mode (ABM) illustrating low variance for each time point. (.....	258
Appendix B, Figure 4 Low variability between multiple and different two compartment ABM runs demonstrating no statistical significant difference between ABM models run for 3, 5, 10 or 30 times.....	259

Appendix B, Figure 5 Multiple runs of the multi-compartment ABM showing low variance for each time point and the visual similarities between the different simulations.	260
Appendix B, Figure 6 low variability between multiple and different multi-compartment ABM runs demonstrating no statistical difference between ABM models run for 3, 5, 10 or 30 times.	261
Appendix B, Figure 7 Sensitivity analysis to examine the effect MAPKK and MAPK level variation on the activation behaviour in multi-compartment models.	264
Appendix B, Figure 8	265
Appendix B, Figure 9 Significant difference in the rate of pMAPK formation between the two and multi-compartment ABMs.	266
Appendix B, Figure 10 Introduction of the tribbles (TRIB) protein agent has no marked effect on the MAPK activation behaviour in the two compartment agent based model (ABM).	266
Appendix B, Figure 11 Comparison of temporal modulation effect between a multi-compartment and a two-compartment ABMs.	267
Appendix B, Figure 12 no extensive variation in pMAPK magnitude generated in a two compartment model where stochastic and deterministic configurations of re-activation delay period (RADP) were investigated.	268
Appendix B, Figure 13 Short and long ($0 < \text{RADP} < 90 \text{ s}$ and $0 < \text{RADP} < 22.64 \text{ min}$, respectively) MAPKK re-activation delay periods (RADP) configurations modulate MAPK activation behaviour.	269

Appendix B, Figure 14 Simultaneous modulation of the spatiotemporal regulatory elements in the MAPK pathway impact MAPK activation behaviour.	270
Appendix D, Figure 1 A schematic representation of the PathDetect system in the presence of constitutively active MEK3 mutant	281
Appendix D, Figure 2 Modulating TRIB levels impact survival in U87 cell line	293
Appendix D, Figure 3 Altering TRIB 1 and TRIB2 levels have differential impact on activation of the MAPK pathways and TRIB3 interaction with MEK4 and MEK7.	294
Appendix D, Figure 4 Analysis of CO-IP shown in Appendix D, Figure 2.(A).	296
Appendix D, Figure 5 Analysis of protein levels observed in Western blots in Appendix D, Figure 2 (B).	297
Appendix D, Figure 6	299
Appendix D, Figure 7	300

List of Tables

Table 3. 1 Summarises the mapping between the domain model and the model specification step presented in section 3.2 and their implementation in the ABMs presents in section 3.3. The literature column provides the evidence for both the modelled natural behaviour and previous models which simulated said behaviour	75
Table 3. 2 number of agents used in the agent based models (ABMs) and their derivation.....	113
Appendix A, Table 1 Summary descriptions of the memory parameters used for the protein-agent.....	243
Appendix A, Table 2 Table outlining memory parameters for the receptor agent with descriptions of each parameter and its classification.....	244
Appendix A, Table 3 Outline and description of the transition functions used by the protein-agents needed for executing movement and specifying the three dimensional coordinates of the agent.....	245
Appendix A, Table 4 Table displaying the transition function of receptor-agent with description of their flow and messages inputted and outputted to them.	246
Appendix A, Table 5 Illustration of the message outputted by agents to finalise the binding interaction and bond formation.....	247

Appendix A, Table 6 The parameters which constitute the memory of MAPKK (MAPKK) agents which are updated every time-step.....	248
Appendix A, Table 7 Shows the parameters which constitute the memory of MAPK (MK) agents which are updated every time-step.....	249
Appendix A, Table 8 Parameters constituting the memory of exporting receptor (ExR) agents which are updated every time-step.....	249
Appendix A, Table 9 Summary of the transition functions used to control MAPKK generic protein behaviour or specialised MAPKK behaviour.	250
Appendix A, Table 10 Summary of the transition functions used to control MAPK behaviour.	251
Appendix A, Table 11 Summary of the transition functions used to control the exporting receptor behaviour.	252
Appendix A, Table 12 Messages outputted by MAPKK into libmboard.	253
Appendix A, Table 13 Messages outputted by MAPK agents into the libmboard to allow for communication between the agent and its interacting partners.	254
Appendix A, Table 14 Messages outputted by exporting receptor agents (ExR).	255
Appendix B, Table 1 pMAPK levels in multi-compartment ABMs showing the values demonstrated in figure B6 and B7 in tabular form.....	262
Appendix B, Table 2 pMAPKK levels in multi-compartment ABM showing the values demonstrated in figure B6 and B7 in tabular form.....	262

Appendix B, Table 3 pMAPK levels in two compartment ABM with multiple model runs..... 263

Appendix B, Table 4 pMAPKK levels in two compartment ABM with multiple model runs..... 263

Appendix D, Table 1 TRIB trnasfection conditions using the PathDetect System 280

Appendix D, Table 2 Effects of knocking down (KD) tribbles family members on the activation of AKT and MAPKs. 295

Abbreviations

GRB2	Growth Factor Receptor-Bound Protein 2
5'	The 5 prime end of nucleic acid sequence
ABM	Agent Based Modelling
ADP	Adenosine Diphosphate
AKAP	A-Kinase Anchor Proteins
ASK	Apoptosis Signal-Regulating Kinase
ATF	Activating Transcription Factor
ATP	Adenosine Triphosphate
cAMP	Cyclic Adenosine Monophosphate
CHO	Chinese Hamster Ovary Cells
CHOP	C/EBP Homologous Protein
c-Myc	Cellular Myelocytomatosis Oncogene
CREB	Camp Response Element-Binding Protein
DMEM	Dulbecco's Modified Eagle's Medium
DUSP	Dual-Specificity Phosphatase(S)
DMSO	Dimethyl Sulfoxide
EDTA	Ethylenediaminetetraacetic Acid
EGF	Epidermal Growth Factor
EGFP	Enhanced Green Fluorescent Protein
eIF4E	The Eukaryotic Initiation Factor-4E
ELISA	Enzyme-Linked Immunosorbent Assay
eNOS	Endothelial Nitric Oxide Synthase
EPAC	Exchange Proteins Activated By Camp

ER	Endoplasmic Reticulum
ERK	The Extracellular Signal-Regulated Kinase
FBS	Fetal Bovine Serum
FCS	Fetal Calf Serum
FLAME	Flexible Large-Scale Agent Modelling Environment
GRAB2	Growth Factor Receptor-Bound Protein 2
GEF	Guanine-Exchange Factor
GPCR	G-Protein Coupled Receptors
GTPase	Guanine-Trisphosphatase
h	Hour
H3	Chromatin Structural Protein Histone Residue H3 Present In Eukaryotic Cells
HEPES	4-(2-Hydroxyethyl)-1-Piperazineethanesulfonic Acid
HRP	Horseradish Peroxidase
HSP25/27	Heat Shock Protein 25/27
IEGs	Immediate Early Genes
IL1	Interleukin 1 Protein
JIP	JNK-Interacting Protein
JNK	Jun N-Terminal Kinases
KD	Knock Down
kDa	Kilodalton And/Or Kilodaltons
KO	Knock Out
KSR	Kinase Suppressor Of Ras
MAP2	Microtubule Associated Protein 2

MAPK/MK	Mitogen Activated Protein Kinase
MAPKAPK	MAPK Activated Protein Kinase
MAPKK/MKK	MAPK Kinase
MAPKKK/MKKK/MAP3K/M3K	MAPKK Kinase
Max/Myc	Myc-Associated Factor X
MEF	Mouse Embryonic Fibroblast
MEK	MAPK/ERK Kinase
MEKK	MAPK/ERK Kinase Kinase
min	Minute Or Minutes
MKP	MAP Kinase Phosphatase(S)
MLK	Mixed-Lineage Kinases
MNK	MAPK Interacting Protein
MNK	MAPK Interacting Protein1
MP-1	MEK Partner 1
MSK	Mitogen- And Stress-Activated Kinase
mTOR	Mammalian Target Of Rapamycin
NF- κ B	Nuclear Factor Kappa-Light-Chain-Enhancer Of Activated B Cells
NGF	Nerve Growth Factor
ODE	Ordinary Differential Equations
OXTR	Oxytocin Receptor
PAGE	Polyacrylamide Gel Electrophoresis
PBS	Phosphate Buffered Saline
PC12	A Rat Adrenal Pheochromocytoma Cell Line
PCR	Polymerase Chain Reaction

PDGF	Platelet-Derived Growth Factor
PI3K	Phosphoinositide 3-Kinase
PIP3	Phosphatidylinositol 3,4,5-Trisphosphate
PKA	Protein Kinase A
PKB/AKT	Protein Kinase B
PKC	Protein Kinase C
PLA2	Phospholipase A2
PMSF	Phenylmethylsulfonyl Fluoride
PP-2B	Phosphatase Protein-2B
PTP	Protein Tyrosin Phosphatase(S)
PSP	Protein Serine/Threonine Phosphatase
Ras	Rat Sarcoma
RNA	Ribonucleic Acid
RTK	Receptor Tyrosine Kinase
s	Second(s)
SD	Standard Deviations
SDS	Sodium Dodecyl Sulfate
SOS	Son Of Sevenless
SWI/SNF	Switch/Sucrose Non-fermentable
TAK	TGF B-Activated Kinase
TAO	Thousand And One Amino Acid
TBS	Tris-Buffered Saline
TCR	T-Cell Receptor
TF	Transcription Factor
TLRs	Toll-Like Receptors

TNF

Tumor Necrosis Factors

TRB

Tribbles

U87

human glioblastoma primary cell line also known
as u-87 MG

Preface

I. Overview of the mitogen activated protein kinase (MAPK) pathway and its signalling behaviour

The mitogen activated protein kinase (MAPK) signalling pathway is a biochemical pathway used by all cells in the body to interpret their environment and respond appropriately (Raff et al., 2002). The MAPK pathway mediates multiple and varied cellular responses such as proliferation, differentiation and programmed cell death (apoptosis) (Chambard et al., 2007, Smith et al., 2004, Sun et al., 2006).

The MAPK pathway is a three tiered biochemical pathway, which relies on phosphorylation events to propagate the signal from activated receptors at the cell surface into the cell cytoplasm and nucleus, ultimately, leading to a cellular response (Rubinfeld and Seger, 2005). The three tiers of the pathway are formed by the MAPK kinase kinases (MAPKKK), MAPK kinase (MAPKK) and MAPK proteins in that respective order. The activated MAPK protein is primarily responsible for mediating the cellular response (Lewis et al., 1998a). The pathway molecular architecture and basic biochemical steps which lead to the activation of MAPK proteins are evolutionarily conserved between species and between different cell types. Nonetheless, the pathway is capable of inducing diverse cellular outcomes (Tian and Harding, 2014). These cellular responses vary both within the cell and between different cell-types. In addition, there is a high degree of signal fidelity, where a ligand induces the same responses downstream of its receptor (Hu et al., 2009).

Therefore, given the identical architectural and biochemical similarities, understanding the manner in which this biochemical pathway mediates the diverse and sometimes opposing, cellular responses within a cell and between different cells is of great interest (Kholodenko and Birtwistle, 2009).

Initially, this was attributed to the different MAPK protein families. MAPK is divided into four protein families (ERK, JNK, p38 and ERK5). These families were discovered in different cellular contexts and were previously shown to be able to mediate specific responses. For instance, ERK was discovered to mediate cellular response to growth factors, JNK was first shown to be recruited in cellular response to stress (such as ultraviolet light and cycloheximide) and p38 was shown to be induced in response to inflammatory stimuli. However, further investigation showed that a specific cellular response was not linked to a specific MAPK protein family. These pieces of evidence include the ability of the different MAPK protein families to induce the same response as the other families. For instance, JNK and p38 are both capable of mediating responses to stress. Furthermore, in PC12 cells ERK was shown to induce two distinct responses when recruited by either NGF or EGF. In addition, ERK (and the other MAPK family members) were shown to be able to induce cell-specific responses. For instance, ERK activation mediates pro-apoptotic effects in tumour cells while in other cell (such as Chinese hamster lung fibroblast cell line CC139) it mediates anti-apoptotic effects. These observations were explained by crosstalk whereby the different MAPKs share protein targets downstream of their cascades (Fey et al., 2012).

However, MAPK signalling and signal transduction is additionally complicated by crosstalk between the different MAPK family members operating at the three different tiers of the pathway (Fey et al., 2012, Ganiatsas et al., 1998, Junttila et al., 2008). This, as a result, showed that the MAPK signalling family members form a signalling network. This was contradictory to the original belief that each MAPK family had an independent linear pathway; thereby, further complicating the search for how specificity and fidelity to external stimuli, as well as cell-type specific responses arise, though evidence points to regulatory mechanisms imposed on the MAPK signalling network.

These regulatory mechanisms, which were shown to affect the MAPK signalling network, are spatiotemporal in nature. Spatial regulation of the pathway includes the compartmentalisation of the proteins involved in the cascades within cellular compartments (or domains) (Chiu et al., 2002, Ebisuya et al., 2005), and the involvement of regulatory proteins (such as scaffolds and adaptor proteins) and binding/interaction partners (Wunderlich et al., 2001, Teis et al., 2002). Temporal regulation involves mechanisms that control the duration of MAPK activation and the level of active MAPK generated during the response. Temporal regulatory processes were shown to be linked to feedback mechanisms, both positive and negative.

Although both spatial and temporal mechanisms were shown to modulate the activation behaviour and dynamics of the MAPK pathway both *in vitro* and *in silico*, their combination and how those influence the MAPK activation dynamics and emergence of specificity and fidelity are not investigated widely.

II. Research objectives

The aim of this thesis is to investigate the complex interaction between spatial and temporal regulatory components and how they influence MAPK activation dynamics. Furthermore, a key motivation was to capture the manner by which the different spatiotemporal combinations result into the emergence of specificity and fidelity of MAPK-dependent cellular response. Examining these different combinations and their influence on the MAPK is very challenging experimentally due to issues of protein redundancy, the unavailability of potent inhibitors and network adaptation; therefore, an agent based computational model (ABM) was constructed. This model will allow the following questions to be addressed:

- I. Does the combination of spatiotemporal regulatory components on MAPK activation have a substantial effect on the activation dynamics? How does this happen?
- II. What are the important spatiotemporal combinations which result into marked change in MAPK activation dynamics?
- III. Does altering and varying spatial components (interactions) give rise to different activation dynamics?
- IV. Do localised/compartmentalised MAPK activation responses alter global MAPK activation?
- V. What are the mechanisms and processes involved which allow specificity and fidelity to develop in the MAPK pathway?
- VI.

In order to address these questions the following steps were taken:

1. Reviewing previously published models of the MAPK pathway to aid building a basic ABM
2. Developing an ABM of the MAPK pathway
3. Dissecting the important components needed for the model
4. Comparing the simulation generated from the ABM with both *in silico* and *in vitro* data, an output for the signalling dynamics has to be determined
5. Model validation and sensitivity analyses to establish model accuracy
6. Further optimisation.

III. Contribution to knowledge

This body of work has resulted into a novel ABM which addresses the effect of multi-compartments on the activation dynamics of the MAPK pathway (See publications section and appendix E for further information) (Shuaib et al., 2016).

This work demonstrated that a multi-compartment model provides a better alternative to the classical two-compartment model. This is because the emergent MAPK activation behaviour from our multi-compartment ABM was captured with more accuracy than the activation dynamics observed in previously published *in vitro* and *in silico* data which compared with the two-compartment ABM.

The ABM presented here demonstrates the potential effect of combining spatiotemporal regulation on diversification of the MAPK activation behaviour and the emergence of oscillatory behaviour in the MAPK pathway.

The ABM investigated the contribution of signalling clusters and their dissipation in the deactivation of MAPK response and signal turn-off.

This body of work also provides experimental data as a base for building a more detailed ABM, which would integrate the inhibitory proteins tribbles. Part of this data is now published (see publication section below and appendix E) (Guan et al., 2016).

IV. Abstracts, presentations & posters

1. A. Shuaib, M. Holcombe, E. Kiss-Toth. "SpatioTemporal Regulation of Mitogen Activated Protein Kinase (MAPK) By The Tribbles (Trbs) Protein Family". Presented at The Joint EMBL-EBI and Wellcome Trust In Silico Systems Biology: Network Based Modelling and Analysis; April 2012; Wellcome Trust Genome Campus, Hinxton, Cambridgeshire, UK. **[Abstract, Poster & Presentation]**
2. A. Shuaib, M. Holcombe, E. Kiss-Toth. Regulation of The Mitogen Activated Protein Kinase (MAPK) Pathway By The Tribbles Protein Family: An Agent

Based Modelling Approach. **Seminar**; June 2013; Universidad Complutense de Madrid, Spain

3. A. Shuaib, M. Holcombe, E. Kiss-Toth. An Agent Based Computer Model To Study The Dynamics Of The Mitogen Activated Protein Kinase (MAPK). Presented at Mathematical and Statistical Aspects of Molecular Biology 2014 meeting at Sheffield Institute for Translational Neuroscience (SITraN); April 2014; Sheffield, UK. **[Abstract and Poster]**

4. A. Shuaib, M. Holcombe, E. Kiss-Toth. MAPK pathway dynamics and behaviour are significantly influenced by the compartmentalisation of the pathway components into multi-compartments; and the mode of stimulation at the level of MAPKK. Presented at University of Sheffield's Interdisciplinary Postgraduate Research Showcase (IPRS); July 2014; Sheffield, UK. **[Abstract and Poster]**

5. A. Shuaib, M. Holcombe, E. Kiss-Toth. Investigating the of The Mitogen Activated Protein Kinase (MAPK) Pathway activation through the modulation of the SpatioTemporal. **Seminar**; June 2013; A* STaR (Agency of Science, Technology and Research), Singapore Universidad Complutense de Madrid, Spain

6. A. Shuaib, M. Holcombe, E. Kiss-Toth. SpatioTemporal Regulation of The MAPK Pathway Relies On Multi-Compartmentalisation For The Emergence of Ultrasensitivity And Oscillatory Behaviour Thereby Impacting On Fidelity And Specificity of Cellular Response. To be presented at the ICSB 2014 - 15th International Conference on Systems Biology; September 2014; Melbourne, Australia. **[Abstract and Poster]**

V. Publications:

1. SHUAIB, A., HARTWELL, A., KISS-TOTH, E. & HOLCOMBE, M. 2016. Multi-Compartmentalisation in the MAPK Signalling Pathway Contributes to the Emergence of Oscillatory Behaviour and to Ultrasensitivity. PLoS One, 11, e0156139. (Refer to appendix E)

2. GUAN, H., SHUAIB, A., LEON, D. D., ANGYAL, A., SALAZAR, M., VELASCO, G., HOLCOMBE, M., DOWER, S. K. & KISS-TOTH, E. 2016. Competition between members of the tribbles pseudokinase protein family shapes their interactions with mitogen activated protein kinase pathways. Sci Rep, 6, 32667. (Refer to appendix E)

Chapter 1 Cell signalling, and signal propagation through the mitogen activated protein kinase (MAPK)

This chapter provides the biological background to cell signalling *via* the MAPK pathway. The pathway's components and its basic architecture are presented. The ability of the pathway to mediate diverse cellular responses is described. Additionally, the complex mechanisms which give rise to signal specificity and fidelity are presented and discussed.

1.1 A general introduction to cell signalling

In order for the body to function properly, it must respond to the environment proportionally and accurately. As a result the body uses a plethora of mechanisms with which it generates a physiological response (Uings and Farrow, 2000). These responses occur at different levels of an organism; ranging from the organ systems to the molecular level. Many diseases occur due to perturbation of these mechanisms. Diseases such as cancer, inflammatory diseases and atherosclerosis occur due to disturbance of the mechanisms used to interpret the environment at cellular and molecular levels. Cells are regarded as the building units of the body. Cells' collective response to their micro-environment produces an organ response, and different organs' responses are integrated to generate the bodily response. Thus, looking at how cells interpret the environment around them and how they respond to it and its changes, provides an insight into how diseases arise when

those mechanisms are perturbed. Developing the aforementioned knowledge provides the basis for drug discovery and drug development (Lawrence et al., 2008, Kumar et al., 2004). To interpret the environment around them, cells employ different mechanisms. All of these mechanisms are termed as signal transduction mechanisms and/or cell signalling mechanisms.

The general theme for signal transduction begins with the reception of an external signal, *via* receptors. Receptors undergo a three dimensional (3D) conformational change when activated by the external stimuli. This is transduced intracellularly into a cellular response *via* biochemical events which recruit intracellular signalling pathways. As a result, this allows for the interpretation of the original stimulus to a cellular response.

There are several biochemical pathways which are utilised for signal transduction. Some signal transduction pathways are heavily used in particular scenarios. For instance, during embryonic development and cell differentiation, these include Notch, Wnt and retinoic acid pathways (Andersson et al., 2011, Louvi and Artavanis-Tsakonas, 2006, Rhinn and Dollé, 2012, Sokol, 2011, van Amerongen and Nusse, 2009) On the other hand, other cell signalling pathways are widely used to mediate diverse cellular responses such as cell motility, cell survival and cell proliferation in different cell types. Examples of these include: cAMP, calcium and the MAPK signalling pathways. Signalling through calcium and cAMP is extensively studied and is reviewed comprehensively in the literature. Therefore, for more thorough description and details regarding these pathways these reviews are recommended

(Arora et al., 2013, Billington and Hall, 2012, Clapham, 2007, Fimia and Sassone-Corsi, 2001, Stewart et al., 2015, Uhlén and Fritz, 2010)

1.2 The MAPK signalling pathway

The MAPK signalling pathway is an evolutionarily conserved biochemical signalling pathway, it is used by most, if not all cells in the body in order to respond to the environment around them. Cellular responses include differentiation, proliferation and cell survival (Chambard et al., 2007, Smith et al., 2004, Sun et al., 2006, Traverse et al., 1992, Xia et al., 1995). Perturbation in the pathway by mutations or abnormal activation leads to diseases such as myocardial hypertrophy, cancer (McCubrey et al., 2007, Weber et al., 2010, del Barco Barrantes and Nebreda, 2012, Shin et al., 2013) and inflammatory diseases (Kyriakis and Avruch, 2001). The pathway is composed of three tiers and relies primarily on phosphorylation events for signal transduction (Brunet et al., 1999, Khokhlatchev et al., 1998, Seger et al., 1994). Phosphorylation events are used to propagate the signal downstream of the pathway and they are carried out by protein kinases placed at each tier of the pathway (Lewis et al., 1998a). These kinases are the mitogen activated protein kinase kinase kinase (MAPKKK also known as MAP3K), the mitogen activated protein kinase kinase (MAPKK also known as MAP2K) and the mitogen activated protein kinase (MAPK). The MAPK pathway was originally discovered and characterised as part of the cellular response to mitogenic factors such as nerve growth factor (NGF) , epidermal growth (EGF) (Boulton et al., 1991, Gómez et al., 1990, Gomez and Cohen, 1991, Gotoh et al., 1990, Landreth et al., 1990, Rowland et al., 1987) and platelet derived growth factors (PDGF) (L'Allemain et al., 1992).

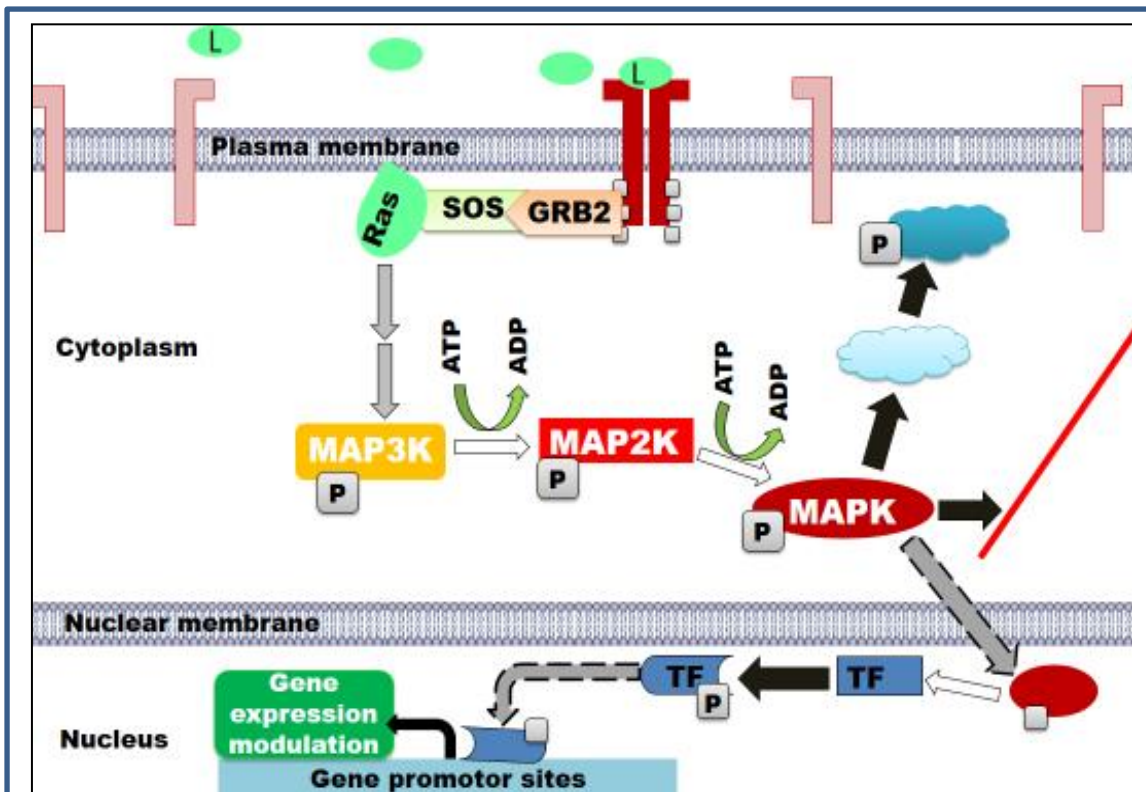
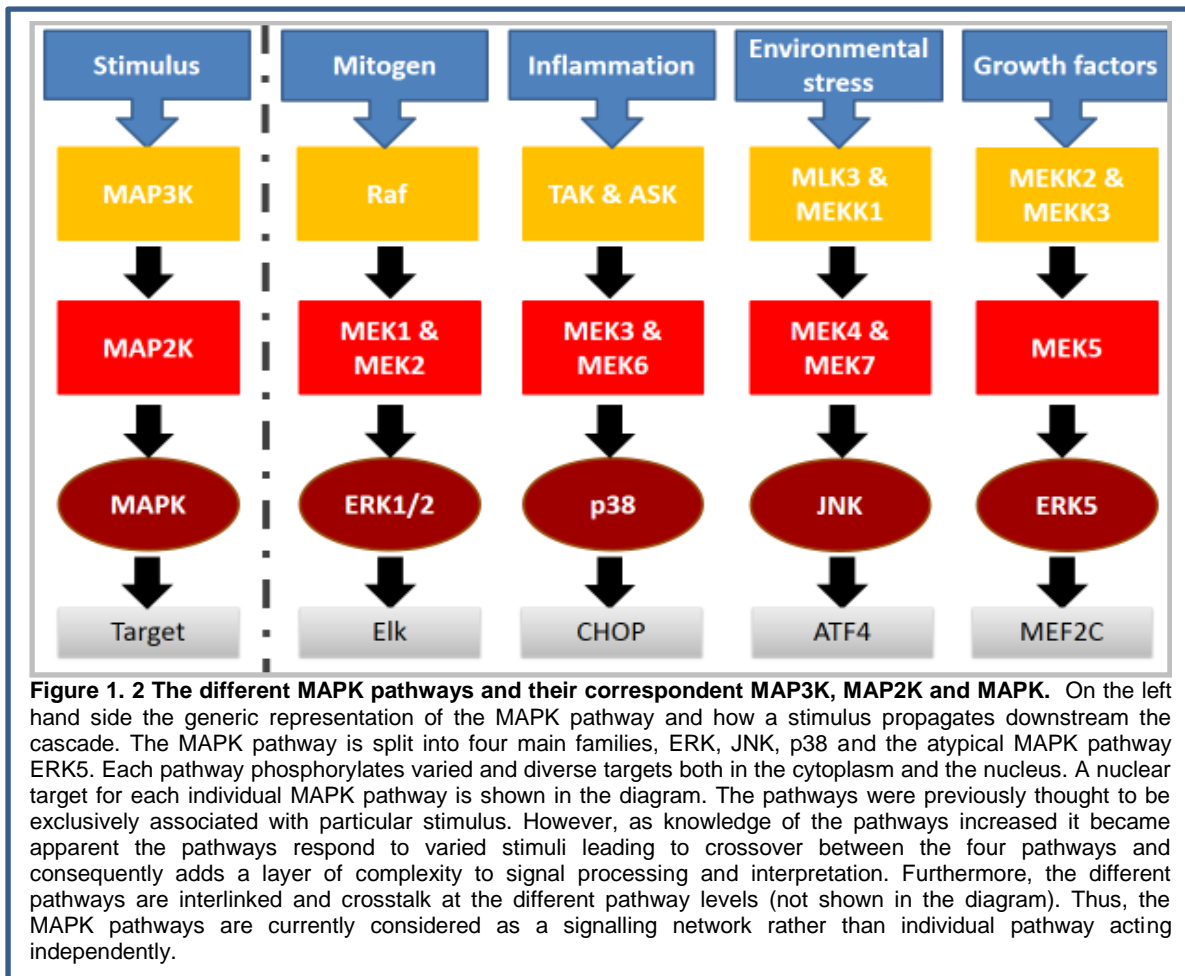


Figure 1. 1 A schematic representation of the MAPK pathway architecture and its activation during response to an external stimulus. This is a general outline of the cascade encompassing its three tiered architecture, sequence of events and the role of phosphorylation in propagating the signal downstream of the pathway. Cells receive signals from the external environment where extracellular ligands (L) bind to their consecutive receptors found at the plasma membrane. The ligand-receptor interaction causes receptor activation and commences signal transduction intracellularly. In the case of the MAPK pathway, RTK are the main receptors which transduce external stimuli into cellular mechanisms. These receptors found in the plasma membrane as monomers (light brown receptors) dimerise and autophosphorylate (dark brown receptors) allowing them to become docking sites for adaptor proteins GRB2 and SOS, which in return activate the Ras family proteins. Ras proteins result into the activation and phosphorylation of MAP3K which bind to and activate MAP2K, MAP2K in turn activate MAPK. MAPK activation is pivotal for mediating the MAPK cascade action. MAPK phosphorylate both cytoplasmic and nuclear targets. For the former, MAPK has direct access while for the latter nuclear translocation is necessary. These nuclear targets are usually transcription factors (TF) which bind to DNA at promoter sites, hence controlling gene expression events. Cytoplasmic targets such as the actin filament (red line) and phosphatases (light blue shape) are easily accessible to activated MAPK and mediate rapid actions. Phosphorylation events are marked by white arrows, curly arrows denote hydrolysis of ATP to ADP and a phosphate group (P) and round grey spheres, stands for the phosphate groups attached to proteins as a result of phosphorylation events. Dotted grey arrows denote movement of protein. Thick black arrows show activation events. ATP denotes adenosine triphosphate and ADP represents denosine diphosphate

These mitogenic growth factors share in common the use of receptor tyrosine kinases (RTK), which bind the mitogenic factors at the extracellular interface of the plasma membrane (Figure 1. 1) (Lemmon and Schlessinger, 2010, Lenormand et al., 1993).

The mitogenic ligands bind to two RTKs simultaneously causing their dimerisation and, ultimately, their autophosphorylation and activation (Lemmon and Schlessinger, 2010, Margolis and Skolnik, 1994). The phosphorylated sites allow for the recruitment of adaptor proteins, such as the growth factor receptor-bound protein 2 (GRB2) (Lowenstein et al., 1992, Rozakis-Adcock et al., 1992). GRB2 recruit the Guanine-exchange factor (GEF) protein son of sevenless (SOS) to the plasma membrane, hence forming a complex with the RTK. SOS in turn recruits the membrane bound guanine-trisphosphatase (GTPase) Ras to the receptor complex (Cicchetti et al., 1992, Medema and Bos, 1993). SOS allows for the exchange of guanine-diphosphate (GDP) molecule bound to Ras with a guanine-trisphosphate molecule (GTP). This exchange activates the Ras protein and thus allows for its conformational change. The conformational change of Ras allows for the recruitment of MAPKKK (MAP3K) (Dent et al., 1992, Van Aelst et al., 1993, Vojtek et al., 1993, Howe et al., 1992, Kyriakis et al., 1992). In addition to the Ras family of proteins, MAP3K was also shown to be activated by scaffold proteins such as kinase suppressor of Ras (KSR) (Nguyen et al., 2002, Xing et al., 1997) and g-protein coupled receptors (GPCRs) (Lange-Carter et al., 1993). MAPKKK is serine/threonine kinase which binds to MAPKK proteins and phosphorylates them at two sites and thus insures their activation (Huang et al., 1993, Johnson et al., 2005, Kyriakis et al., 1992, Moodie et al., 1993, Van Aelst et al., 1993).

The mitogen protein kinase kinase protein (referred to as MAP2K and/or MAPKK), is also a diverse kinases family (Uhlik et al., 2004). The family has the unique ability to phosphorylate both threonine and serine residues (Gotoh et al., 1994, Yan and Templeton, 1994, Zheng and Guan, 1994). Certain members of the MAPKK family

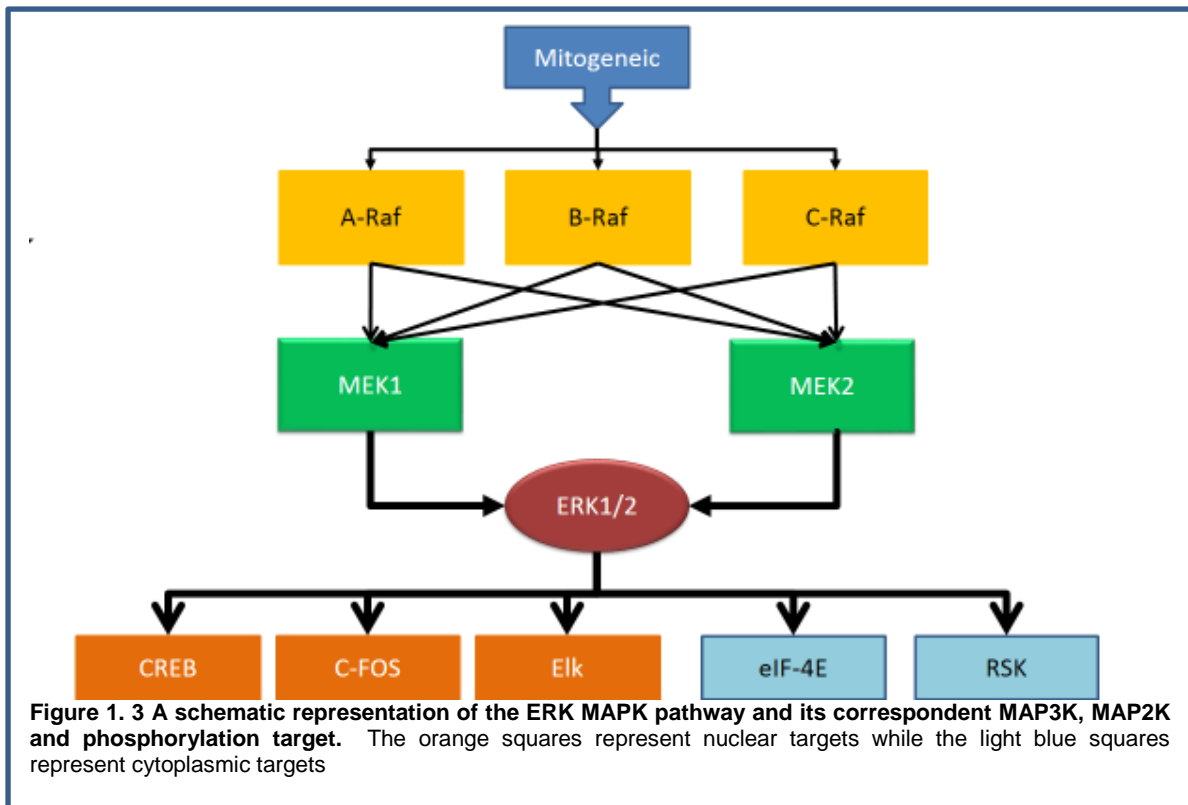


were shown to interact with scaffold proteins which increase their activation and the time period during which they remain active (Uhlik et al., 2003, Whitmarsh et al., 1998). The family specifically phosphorylates the MAPK proteins as they recognise a specific amino acid sequence (Matsuda et al., 1992). This allows them to phosphorylate the MAPK at two phosphorylation sites (Alvarez et al., 1991, Anderson et al., 1990, Boulton et al., 1991). Furthermore, it was demonstrated that each MAPKK exhibits a high level of specificity to its MAPK target which allows for limited overlap between the different MAPK pathways. This was one of the rationales for establishing the linear representation of the pathways (see Figure 1. 2).

Phosphorylation and activation of the MAPK proteins are the focal events in the cascade (Alessi et al., 1995, Anderson et al., 1990, Burack, 1997).

Once activated, MAPK either translocates to the nucleus or resides in the cytoplasm (Lenormand et al., 1993, Sanghera et al., 1992, Seth et al., 1992). In both intracellular compartments (the cytoplasm and the nucleus) MAPKs phosphorylate a diverse array of proteins. Phosphorylating proteins at the two compartments gives the MAPK pathway a temporal dimension to execute its effects. Phosphorylation of cytoplasmic targets allows for rapid tuning of the signal, therefore mediating short term and immediate effects of the signal. Phosphorylating nuclear targets, such as transcription factors influence gene-expression events; thus, allowing for a long term and delayed signal outcomes. Cytoplasmic targets of the MAPK proteins include the MAPK activated protein kinases (MAPKAPK and abbreviated as MK), the Eukaryotic Initiation Factor-4E [eIF4E] and the actin cytoskeleton (Stokoe et al., 1992). MAPKAPK control gene expression during transcription and post-transcription; eIF4E factors play a role in protein synthesis and the translational phase of gene expression (Gavin and Schorderet-Slatkine, 1997). Control of the actin cytoskeleton affects cellular morphology. Once translocation to the nucleus takes place, MAPK phosphorylates nuclear targets. These include the transcription factors c-FOSs, FOXO and CHOP (Efimova et al., 2002, Xu et al., 2004). These transcription factors play a role in cellular responses such as proliferation, survival and adaptation to cellular stress respectively.

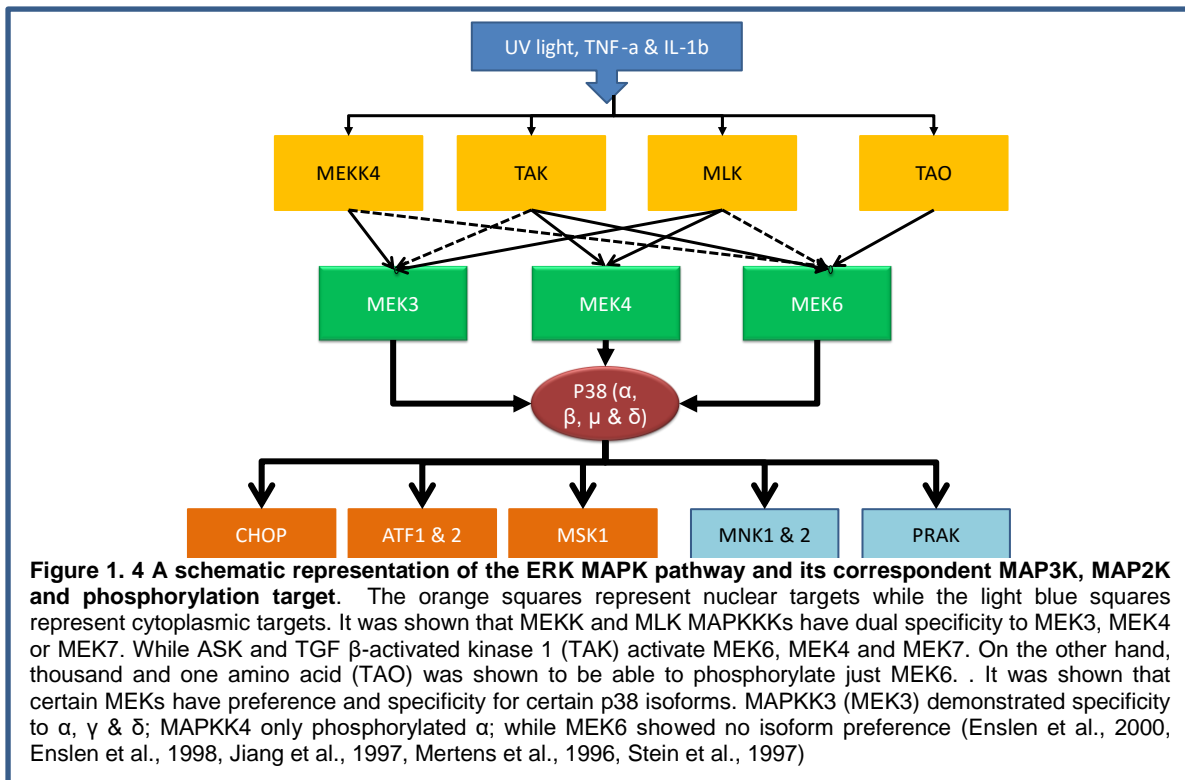
The MAPK proteins are grouped into four families, with each family including several members. These families are the extracellular signal-regulated kinase (ERK), p38, Jun N-terminal kinases (JNK) and the relatively newly discovered ERK5. The ERK



family is composed of two proteins: ERK1 and ERK2. The p38 includes p38 α , β , γ , δ . The JNK family is composed of JNK1, JNK2 and JNK3. ERK5 shares a 50% sequence homology with the ERK1/2, however ERK5 has diverse and different types of substrates compared to ERK1/2. The different MAPKs were discovered separately and in different cellular contexts, thus each MAPK had given its name to the cascade which leads to its activation. **Below is a summary of each of the families, their activation dynamics and the cellular functions they mediate.** The aim is to demonstrate the complexity of the individual pathways.

1.2.1 Extracellular signal-regulated kinase ERK1/2

The protein is a 44/42 kDa and is abundantly expressed in all cells. It is found as two isoforms ERK1/2 which are simultaneously expressed in cells. However, ERK2 knock out (KO) mice were embryonically lethal, while ERK1 were viable and only



demonstrated a disruption of thymocyte activation. This suggested that ERK2 is capable of functionally substituting and replacing ERK1. ERK was the first MAPK to be discovered. The discovery was during application of mitogenic stimuli (insulin and the nerve growth factor (NGF)) which lead to the phosphorylation and activation of the microtubule associated protein 2 (MAP2). ERK is widely established to respond and mediate the action of mitogenic signals such as proliferation, growth and survival (Boulton et al., 1991). ERK activation is achieved *via* the MAPKKK RAF family, which were then shown to activate the MAPKK, MEK1 leading to ERK activation (see Figure 1. 3). This linear sequence is regarded as the ERK MAPK pathway. This pathway is the most studied of the MAPK pathways and was shown to be primarily responsible for growth induction and regulation of the cell cycle. ERK has cytoplasmic and nuclear targets. Cytoplasmic targets include p90 ribosomal protein S6 (RSK) (Frödin and Gammeltoft, 1999, Jones et al., 1988) and MAPK interacting protein1 (MNK1). These two targets were demonstrated to play a role in the regulation gene expression events (De Cesare et al., 1998, Xing et al., 1996),

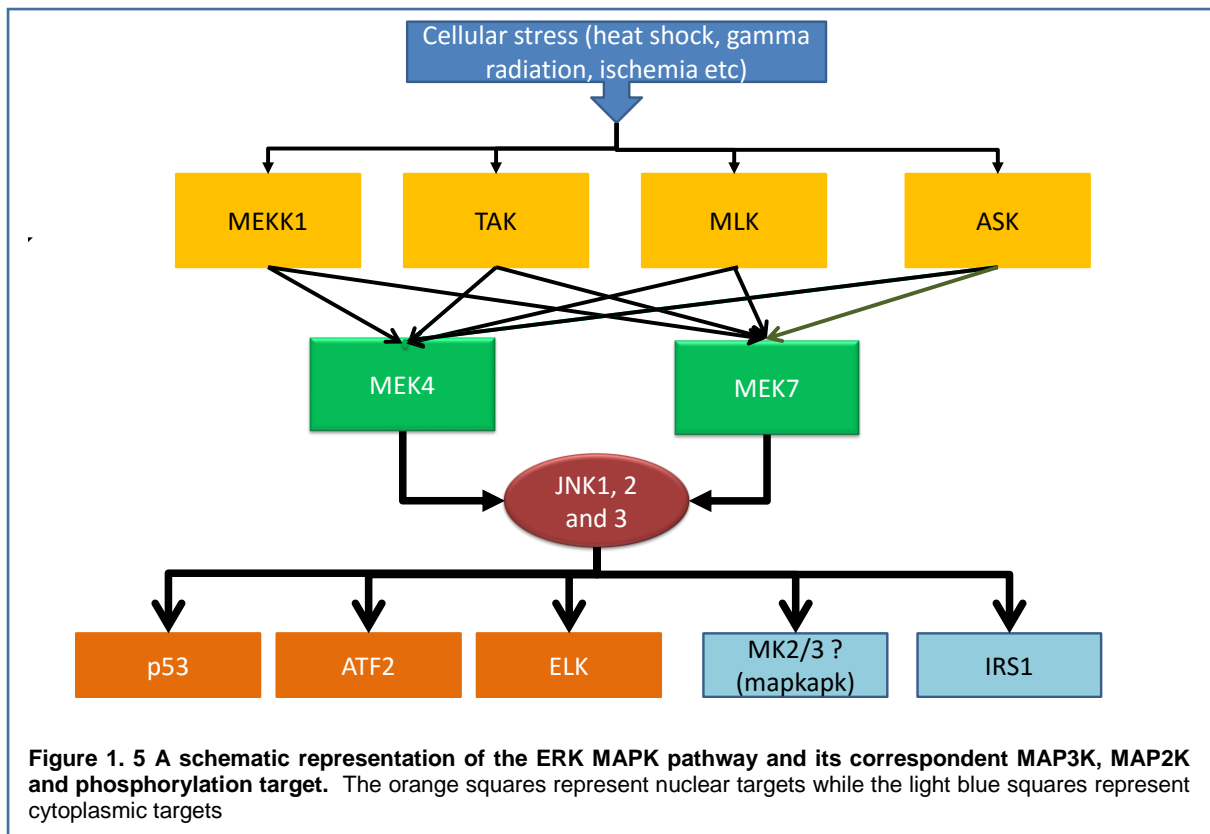
therefore, ERK imposes an indirect control of the process (Fukunaga and Hunter, 1997, Pyronnet et al., 1999, Sonenberg and Gingras, 1998, Waskiewicz et al., 1997). Nuclear targets for ERK are primarily transcription factors which are involved in the regulation of the cell cycle and growth, these include Elk, c-Myc and the mitogen and stress activated protein kinase (MSK) (Gille et al., 1992, Seth et al., 1992).

1.2.2 p38 pathway

p38 is a 38 kDa protein found in four isoforms: p38 α , β , γ and δ . p38 members are widely expressed, however their expression levels vary (Cuenda and Rousseau, 2007). p38 involvement in cellular responses to stress, DNA damage and apoptosis was revealed by Cuenda A *et al* . In addition to the p38 activation *via* RTKs, it is also activated by Toll-like receptors (TLRs) and T-cell receptor (TCR). The pathway activation was shown to be elevated in inflammatory diseases such as rheumatoid arthritis. The p38 pathway is activated by inflammatory stimuli and stress such as exposure to UV light, oxidative stress and osmotic stress (Brewster et al., 1993, Hazzalin et al., 1996, Runchel et al., 2010). The pathway regulates the production of inflammatory mediators such as interleukin 1 (IL1), DNA repair and apoptosis (Choi et al., 2011, Ghatan et al., 2000, Herrera et al., 2005, Hazzalin et al., 1996). Therefore, the p38 isoforms were regarded as a valuable drug target. Many MAPKKs are involved in the activation of p38 (Figure 1.4). These include apoptosis signal-regulating kinase-1 (ASK), MAPK/ERK kinase kinase (MEKK) and mixed-lineage kinases (MLK). p38 proteins are activated by either of one of a three MAPKK proteins MEK3, MEK6 and MEK4 (Derijard et al., 1995). The linear sequence of the

abovementioned MAPKKs, MAPKKs and p38 constitute the p38 MAPK pathway (see Figure 1. 4).

p38 is capable of phosphorylating many proteins in both the cytoplasm and the nucleus. Cytoplasmic targets include Phospholipase A2 (PLA2), MNK1/2 and MAPKAPK2 (Ghatan et al., 2000, Kim et al., 2006, Kramer et al., 1996, Scheper et al., 2001, Waskiewicz et al., 1997). p38 also translocates to the nucleus and phosphorylates nuclear targets. These include transcription factors such as C/EBP homologous protein (CHOP), Elk, ATF1 and 2. ATF2 has been shown to be activated by p38 γ and δ (Efimova et al., 2002, Perdiguero and Muñoz-Cánoves, 2008). p38 was shown to regulate other transcription factors indirectly by the phosphorylation and activation of the MSK family; these transcription factors include Max/Myc complex and CREB (Lee et al., 2002, Pierrat et al., 1998). p38 was also shown to modulate gene expression by chromatin remodelling by phosphorylation of the histone complex thus the accessibility of transcription factors to genes and their promoter sites (Drobic et al., 2010). Another nuclear target for p38 is MAPK activating protein kinase 2 (MAPKAPK2) which phosphorylates and activates the heat shock protein 25/27 (HSP25/27) (Freshney et al., 1994, McLaughlin et al., 1996). HSP25/27 plays a role in cell migration. (Denouel-Galy et al., 1998, Joneson et al., 1998, Rousseau et al., 1997, Sugimoto et al., 1998) It is also involved in mediating responses during oxidative stress (Huot et al., 1997, Macario and Conway de Macario, 2000) and a role in mouse embryo implantation and progression beyond the 16 cell stage (Natale et al., 2004).



1.2.3 Jun N-terminal kinases JNK

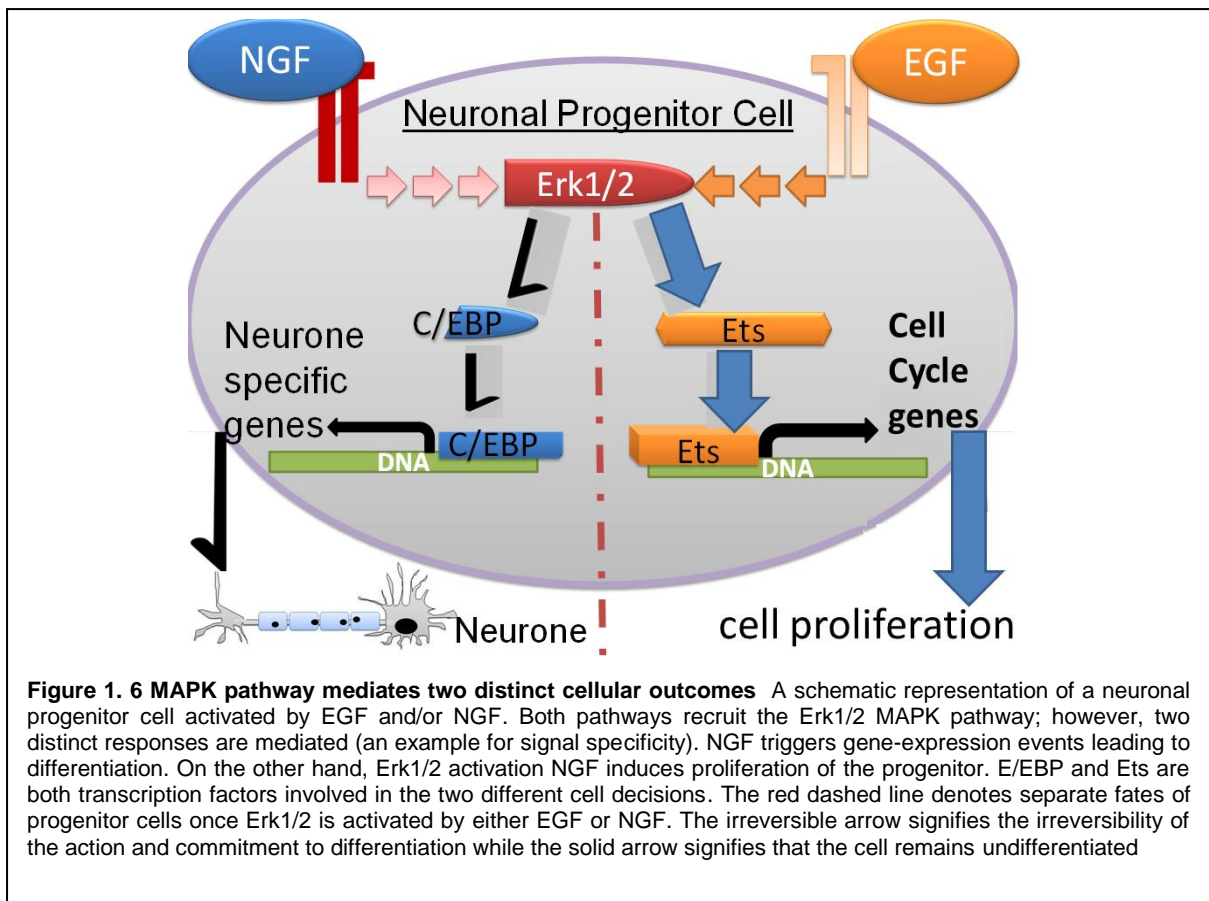
JNK (also known as stress-activated protein kinase (SAPK)) is a 46-54 kDa protein which exists in three isoforms, JNK1, 2 and 3 (Dérillard et al., 1994, Gupta et al., 1996, Sluss et al., 1994). These isoforms share >80% sequence homology. JNK1 and 2 are ubiquitously expressed while JNK3 are expressed in the brain, heart and the testis (Gupta et al., 1996, Yang et al., 1997a). JNK was discovered and linked to ERK during cycloheximide treatment in liver cells, where it phosphorylates MAP2 (Mukhopadhyay et al., 1992, Kyriakis and Avruch, 1990). This was further confirmed when JNK was shown to phosphorylate the transcription factor c-Jun during UV exposure (Dérillard et al., 1994, Pulverer et al., 1991). JNK is activated by MEK4 and MEK7 which are activated by MEKK, MLK, TAK and ASK (Davis, 2000, Derijard et al., 1995, Tournier et al., 1999, Sanchez et al., 1994, Yao et al., 1997). This linear sequence constitutes the JNK pathway (see Figure 1. 5). The JNK pathway is the

second most studied MAPK pathway because it is highly associated with stress-induced responses, for instance: ischemia, heat shock and ER stress (Pombo et al., 1994, Sluss et al., 1994, Tournier et al., 1997). The main effect is that JNK mediates apoptosis induced by extracellular stimuli or through the mitochondria (Schroeter et al., 2003). The expression of a dominant negative JNK resulted in rescuing cells from apoptosis when they were exposed to NGF withdrawal, heat shock or irradiation. Cells derived from JNK1 or JNK2 KO mice demonstrate resistance to apoptosis *via* stress stimuli. Knocking down both isoforms in MEF cells resulted into an increased resistance to stress induced stimuli compared to wild type cells (Tournier et al., 2000). JNK1 and JNK2 KO mice were viable and survived to adulthood, however double KO mice were embryonically lethal due to defects of the formation of the neural tube and brain regions (Yang et al., 1997b).

JNK phosphorylates targets both in the cytoplasm and the nucleus. Its nuclear targets include ATF2, AP-1, p53 and Elk1 (Devary et al., 1992, Gupta et al., 1995, Hibi et al., 1993, Whitmarsh et al., 1995). Some of the cytoplasmic targets include the pro-apoptotic Bcl family of proteins Bcl-2 and Bcl-xL.

1.3 The complexity and mystery of the MAPK pathway

Historically the MAPK pathways were identified in different biological contexts; as a result, a cellular response was thought to be mediated by a particular MAPK pathway. However, continuous research showed that the three pathway crosstalk at



different levels of the cascades. The MAPKs share several targets in the cytoplasm and the nucleus as demonstrated in Figure 1. 3, Figure 1. 4 and Figure 1. 5 (Gaestel, 2006). They are also capable of modulating each other's activation behaviour (Kockel et al., 1997). For instance, it was shown that p38 negatively feeds back onto ERK pathway and active ERK imposes negative feedback onto the JNK pathway (Junttila et al., 2008, Monick et al., 2006, Paumelle et al., 2000, Westermarck et al., 2001). Therefore, the view of the three main MAPK cascades had moved from three independent modules to an interlinking MAPK signalling network. Consequently, in order to define and understand the cellular responses generated by the activation of the MAPK pathways, they should not be considered in isolation.

Although signalling through the MAPK pathway is a complex process due to the different pathways and the high degree of overlap between them; nonetheless, there is a high degree of specificity and fidelity maintained when the signal is transduced to a cellular response. For instance, in pheochromocytoma (PC12) cells, stimulation with EGF and NGF activate the ERK pathway; however, the former triggers proliferation while the latter induces differentiation. This is an example of signal specificity. An example of signal fidelity is the perpetual yet unequivocal ability of ERK to recruit the same downstream proteins in response to EGF-dependent activation from a wide array of targets. Furthermore, the outcome of MAPK stimulation is thought to be cell specific. For instance, although ERK pathway activation triggers proliferation in PC12 cells, it mediates pro-apoptotic effects in tumour cells while in CC139 cell (lung fibroblast cell line) it mediates anti-apoptotic effects (Hübner et al., 2008, Javvadi et al., 2008, Ley et al., 2003, Obitsu et al., 2013, Weston et al., 2003). Additionally, although the three classical MAPK pathways are capable of mediating the same effects in cells, one pathway is more dominant than others. For example JNK and p38 are both capable of mediating responses to stress; however cells use JNK to undergo apoptosis.

How the MAPK pathways maintain specificity and fidelity to the original signal and what mechanisms are employed to insure that, are fundamental questions which the field of MAPK signalling is tackling. There are many theories of how those behaviours emerge, all of them centre on the tight regulation the MAPK signalling network is exposed to. Regulatory mechanisms involve the attenuation of spatial and temporal elements of signalling. This is thought to involve regulation of the duration

of MAPK activation, the levels of active MAPK produced, and the location of their intracellular targets.

1.3.1 Regulation of the MAPK pathway

There are multiple mechanisms utilised for the regulation of MAPK signalling. The majority of these rely on other proteins to regulate the activation behaviour/dynamics in the cell; and direct protein-protein interactions. This section underlines the main mechanisms involved in the regulation of the MAPK pathway.

1.3.1.1 Regulating the magnitude and duration of phosphorylated MAPK levels

The first work to determine how specificity and fidelity appeared in the MAPK pathway came from work with the PC12 cell line (Marshall, 1995, Tombes et al., 1998, Traverse et al., 1992). PC12 cells responded to both NGF and EGF *via* the recruitment of the MAPK ERK pathway. However, the activation dynamics and cellular response generated were different. EGF mediates a transient activation of ERK which resulted into proliferation. Conversely, NGF triggered a sustained activation of ERK and resulted into the differentiation of PC12 cells into neuronal cells. Similarly, Khan *et al* reported that activation of the fibroblasts by non-mitogenic signal had resulted into activation of the ERK pathway lasting for less than 60 minutes and no proliferation, while the use of growth factors had resulted into a sustained ERK activation lasting for 6 hours and causing the cells to enter into the cell cycle (Sasagawa et al., 2005a). The same was reported with JNK activation.

Mouse embryonic fibroblasts (MEF) cells activated by UV light sustain JNK activation and undergo apoptosis. This effect is rescued by the inhibition of JNK sustained activation. Conversely, transient JNK activation with TNF-alpha in these cells is associated with survival. Inhibition of TNF-alpha dependent JNK activation resulted into DNA defragmentation and apoptosis. These further affirmed the hypothesis that duration of the MAPK activation was the source of specificity and fidelity (Marshall, 1995). Further evidence of that was obtained both experimentally and using *in silico* models of the cascade (Albeck et al., 2013).

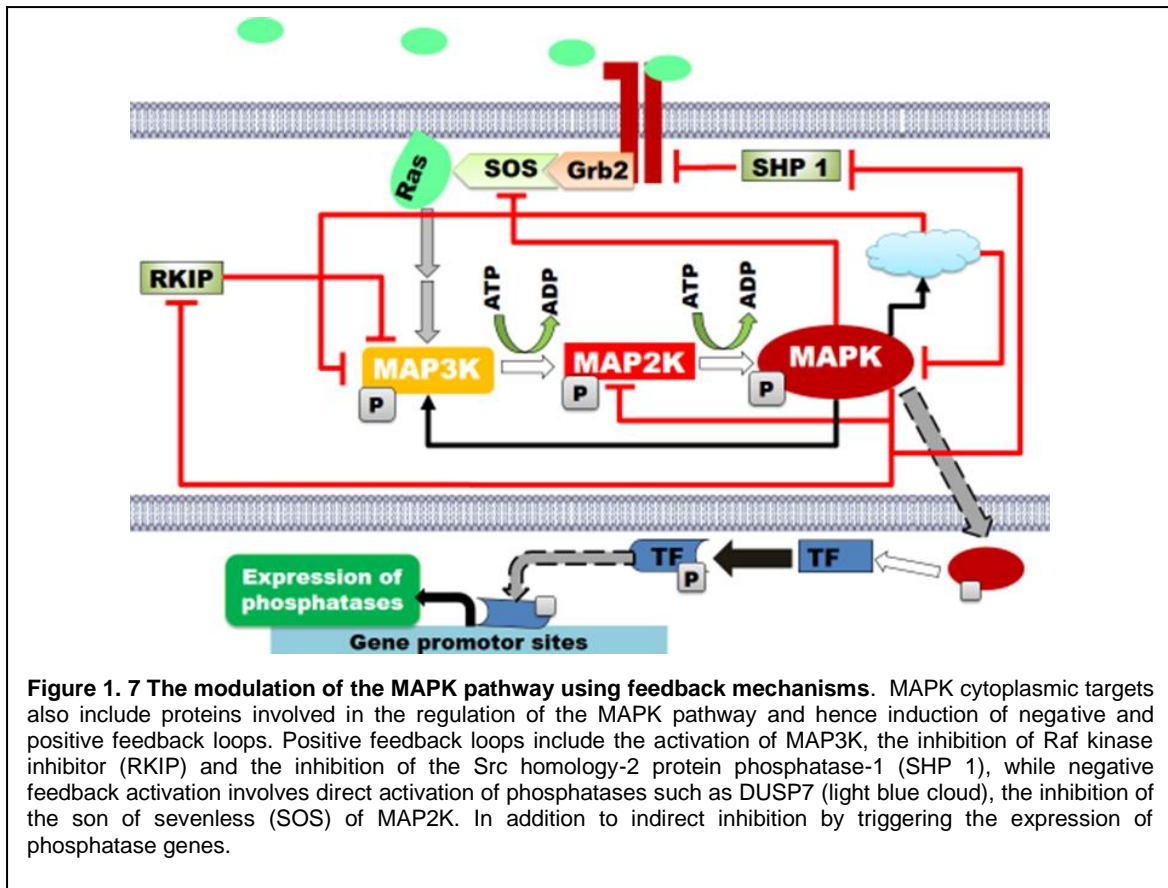
The magnitude was also shown to be important for specifying cellular response. The magnitude is measured as the maximal level of phosphorylated (active) MAPK generated during signal initiation (E_{max}). Sewing and Woods *et al* had previously shown that high intensity of Raf activation mediated cell cycle arrest while low Raf activation intensity triggered proliferation (Sewing et al., 1997, Woods et al., 1997). In addition, with high levels of active ERK, cells became resistant to apoptosis induced by serum starvation, while low levels of phosphorylated ERK did not (Le Gall et al., 2000a). In corneal epithelial cells the magnitude of the MAPK response was shown to mediate different cellular outcomes. This was also shown in intestinal cancers where high levels of ERK1/2 activity correlate with increased proliferation while low and sustained activation was linked with differentiation (Aliaga et al., 1999, Le Gall et al., 2000b). Furthermore, the control of duration and magnitude was shown to influence immediate early genes (IEG) and thus the protein constitution of cells, and ultimately, their proteome and how they respond to stimuli in the future (Cook et al., 1999, Sabbagh et al., 2001, Murphy et al., 2004).

Some *in silico* models explained that kinases are responsible for controlling the magnitude of the response while phosphatases were the main regulators of activation duration (Shin et al., 2013). This was further confirmed by Horinberg *et al*'s experimentally by monitoring the sensitivity of the initial activation peak to MEK antagonism and phosphatase inhibition. They also studied the sustained response and showed it was more sensitive to inhibition of phosphatases in comparison to MEK inhibitors. In addition they also confirmed Heinrich *et al* findings *in silico* (Hornberg et al., 2005b). It is interesting, however, that in cancer cells where sustained MAPK activation is ongoing, differentiation of the cancer cells is not induced, but continue to proliferate uncontrollably.

Duration and magnitude determine the cellular response, and play a role in specificity and fidelity; nonetheless, both the magnitude and duration are simply products of the balance between activating and inhibiting inputs. This balance is linked to feedback loops (Santos et al., 2007b).

1.3.1.1.1 Feedback loops

Some MAPK targets are proteins involved in pathway regulatory mechanisms, which either form negative or positive feedback loops. These result into either prolonged activation, response reduction or termination. Feedback mechanisms are regarded as a temporal regulatory mechanism for the MAPK network.



1.3.1.1.1 Negative feedback

Negative feedback is a process or a mechanism triggered by the activation of the MAPKs, leading to the cessation or reduction of phosphorylated MAPK (pMAPK) levels intracellularly. This is achieved by phosphorylation of proteins either upstream or downstream of MAPK, which ultimately reduce activating inputs into MAPKs. As shown in Figure 1. 7, some of the targets are RTKs, SOS and MAPKK (Matsuda et al., 1993). In EGF signalling it was shown that activation of ERK resulted in phosphorylation of the EGFRs and their internalisation, thus reducing the response to EGF ligand. Phosphorylation of SOS by ERK was shown to reduce its recruitment of Ras and reduce its GEF activity. It was shown that several MAPKs are capable of phosphorylating MAPKKs once they are activated, which is in line with the cooperative/competitive inhibition theory (Chickarmane et al., 2007).

Other modulators of the negative feedback mechanism are phosphatase enzymes. Phosphatase enzymes are regarded as the primary inducers of negative feedback inhibition. Phosphatases are activated by phosphorylation in the cytoplasm and mediate their action by the hydrolysis of phosphate groups on MAPKs and MAPKKs. This results in an immediate inhibitory response to the signal. Gene expression of phosphatases genes are also initiated by transcription factors activated by the MAPK proteins. This mediates a long-term regulation of MAPK activation and is considered to be the main force to fully curtail the activation of MAPK to base levels.

1.3.1.1.1.1 Phosphatases

Phosphatases play a role in mediating specific MAPK responses *via* different mechanisms. These include differential interaction with the MAPK proteins, compartmentalising MAPK proteins into different intracellular locations, and determining the MAPK interaction partners.

Phosphatases hydrolyse phosphate groups which were added to proteins exposed to kinase activity. Phosphatase proteins are abundant both intracellularly and in all tissues as many cellular activities rely on phosphorylation events (60% of total cellular proteins are phosphorylated at any given time) (Kondoh and Nishida, 2007, Newman et al., 2014). Therefore, regulation of phosphorylation events is important. Phosphatases are capable of dephosphorylating many proteins involved in different pathways and intracellular mechanisms to modulate cell functionality.

As described previously in section 1.3.1.1, the main regulators of the duration of MAPK activation are the phosphatase enzymes (Hanada et al., 1998, Takekawa et al., 1998). MAPKs are phosphorylated on two sites, both containing tyrosine and threonine. Since it is considered that only dually phosphorylated MAPK species are fully active, dephosphorylation of either of the phosphorylation sites is thought to be sufficient for reducing the MAPK activity. The MAPK pathways are modulated by the three phosphatase families, however the Dual-Specificity Phosphatase family (DUSP) contains members which have the most affinity to the MAPKs and many of these members are implicated in MAPKs' dephosphorylation. These family members are the MAP Kinase Phosphatases (MKPs). Therefore, there is a research focus on MKPs and their regulation of the MAPK cascades and consequently this section will be focused on this family; nevertheless, other phosphatases families there will be cited within the appropriate context.

The MAPK cascades were shown to be modulated by 10 MKPs. Some of MKPs were shown to display a differential preference to the different MAPK proteins. VHR/DUSP3 and hVH3/DUSP5 are exclusive for ERK, MKP8/DUSP26 exclusively dephosphorylates p38 and DUSP18 was shown to only mediate JNK deactivation. Nonetheless, there are MKPs with broad, yet varied preference. MKP1/DUSP1 was shown to deactivate ERK, JNK and p38, however, it exerted more inhibition on p38 and JNK. MEFs from MKP1 KO mice showed no altered levels of ERK activation in presence of serum, and had hyper-activated p38 and JNK. However, the cells exhibited high level of apoptosis. These KO mice also revealed that MKP1 plays an important role in immune response modulation. This was also reported in MKP4 and

PAC-1 KO mice (Jeffrey et al., 2006, Zhao et al., 2006). MKP-X/DUSP7 was shown to dephosphorylate both JNK and ERK but was found to have preference for ERK.

Further to their substrate preference and structural homology, MKP proteins have differential cellular localisation. They were observed to be expressed either in the nucleus, the cytoplasm or both compartments (Karlsson et al., 2004, Mandl et al., 2005, Masuda et al., 2001). An interesting observation was that MKP proteins which localise to both compartments targeted p38 and JNK but not ERK. Furthermore, nuclear MKPs genes were shown to be inducible by mitogenic and stress stimuli and were identified as members of the inducible immediate early genes (IEG). This had rendered them important in negatively regulating the MAPK pathways.

MAPKs and phosphatases influence each other's expression. MAPKs are capable of inducing their phosphatases; this is observed with the induction of MKP1 by ERK in response to growth factor stimulation as an IEG of ERK (Kucharska et al., 2009). MKP1 gene was also shown to be induced in response to oxidative stress *via* p38 signalling. MKP3 gene was also induced after FGF stimulation in mammalian and yeast cells. The protein serine-threonine phosphatases (PSPs) protein phosphatase 1 (PP1) and PP2 were also shown to be induced by the activation of the MAPK cascades, where PP2A gene was shown to be induced by p38 activation. This is linked to the long-term modulation and negative feedback of the MAPK signalling. MAPK were shown to phosphorylate MKPs and enhance their activity (Camps et al., 1998, Castelli et al., 2004, Katagiri et al., 2005). This was established to be due to inhibition of phosphatase degradation *via* the ubiquitin pathway and enhanced phosphatase activity due to the addition of the phosphate group (Brondello et al.,

1999, Marchetti et al., 2005). This protein-protein induced regulation is believed to be part of the short-term modulation and regulation of the MAPK signalling. The short-term regulation is believed to play a part in modulating the magnitude in the initial phase of MAPK activation. Phosphatases regulation of MAPKs activity in addition to dephosphorylation is by competing with MAPK substrates for the kinase site, thus acting as competitive antagonists.

In addition, it was shown that MKP-X functions as a scaffold for ERK, as a result providing a new mechanism with which MKPs modulate the MAPK activity. This is in line with work showing that phosphatase enzymes are capable of anchoring MAPKs into specific compartments. Mandl *et al* have shown previously that nuclear MKPs anchor ERK protein in the nucleus although ERK had been dephosphorylated (Karlsson et al., 2004, Mandl et al., 2005). PP2A was also shown to anchor the MAPK in the cytosol and in specific cytosolic locations. Roy *et al* had shown that the interaction of the MEK-ERK scaffold protein IQGAP1 with E-cadherines at cell-cell junctions is dependent on its interaction with PP2A (Roy et al., 2005, Takahashi et al., 2006). This suggests that phosphatases may play a role in regulating specific MAPK responses by fine-tuning MAPK activity inside specific compartments (these can be specialised compartments or within the cytoplasm). Additionally, PSP phosphatases are capable of forming heterotrimeric complexes with MAPKs. These complexes are found to be with different and diverse proteins, including PSP regulatory subunits. This might be connected to mediating different MAPK responses by dictating the protein targets immediately available for the MAPK. This was shown with the ability of PP2A to contain regulatory subunits B56 to inhibit ERK phosphorylation in *Drosophila* S2 cells; however the overexpression of PP2A in PC6–3 cell line with the regulatory subunit B55 γ resulted into a sustained activity of

ERK. Conversely, the overexpression of the regulatory subunits B55 α and δ dephosphorylated ERK and reduced its activation. PP2A interaction with hepatocyte growth factor (HGF) RTK Met1 results into an increased receptor sensitivity, further suggesting that the signal outcome which relies on PP2A is dependent on PP2A binding partners.

As shown with Mel, phosphatases are capable of modulating the MAPK signalling through the interaction with proteins upstream of MAPK in the cascade (Figure 1. 7). Protein tyrosine phosphatases (PTPs) in particular were shown to dephosphorylate RTKs and as a result reduce the activating input to MAPK proteins (Haj et al., 2003, Mattila et al., 2005). PP2A was shown to dephosphorylate MAPKK3 within the p38 pathway (creating a negative feedback loop). The use of transgenic mice expressing dominant negative PP2A resulted into enhanced phosphorylation of MEK1, thus further demonstrated phosphatase action at the level of MAPKK. Additionally, PP2A was shown to complex with Shc protein inhibiting its phosphorylation and thus signal propagation. PP2A was also shown to modulate Raf, however it was reported that PP2A was activating Raf. This is regarded as one of the positive regulatory mechanisms implemented in the cascade.

As demonstrated, the phosphatases play a role in deactivating the MAPK pathway and return the cell back to basal conditions. The phosphatases form part of the feedback mechanisms which are thought to be important for the regulation of the MAPK signalling dynamics. These feedback mechanisms are discussed below.

1.3.1.1.1.2 Positive feedback

Contrary to negative feedback, positive feedback regulation is capable of augmenting MAPK activation and thus further enhances MAPK-dependent response. This regulation depends on autocatalysis where MAPKs phosphorylate targets which ensure the continuation and/or the increase of signalling through the pathway. This results in either sustaining a high pMAPK level or its further increase. The first report of positive feedback in the pathway came from Gotoh *et al*, Ferrell *et al* and Bagowski *et al* (Bagowski and Ferrell Jr, 2001, Gotoh *et al.*, 1995, Ferrell and Machleder, 1998). Their work showed that *Xenopus* oocytes maturation during the initial phases of embryogenesis require the activation of both p42/p44 (ERK) and JNK pathways. Positive feedback is achieved by different patterns, termed collectively as loops (Figure 1. 7). One involves direct activation of upstream activators of the pathway. In *Xenopus* oocyte maturation, ERK was shown to phosphorylate the *Xenopus* MAPKKK protein Mos, which in turn causes further phosphorylation and activation of p42/p44. JNK mediation of positive feedback was shown to involve the modulation of Ras and Raf interaction, leading to enhanced activation of p42/p44 and thus oocyte maturation (Adler *et al.*, 2005). This activation of MAPKKK by MAPK was also demonstrated with ERK positive feedback to Raf. Balan *et al* (2006) showed *in vitro and in vivo* that ERK phosphorylates Raf-1 at three phosphorylation sites allowing for augmented ERK activation. Other observed direct activation events *via* MAPK were by inducing RTKs activation (Balan *et al.*, 2006, Baljuls *et al.*, 2008). This was observed at the gene expression level by either inducing the production of growth factors such as ErbB or receptors such as EGFR (Santos *et al.*, 2007b, Schulze *et al.*, 2004, Shilo, 2005).

Another configuration for positive feedback loops involves the blockade of inhibitory mechanism (*i.e.* a double negative feedback). This is observed in the ability of ERK to phosphorylate DUSP1/MKP1 at Ser296 and Ser323 which leads to its ubiquitination and therefore degradation (Lin et al., 2003, Lin and Yang, 2006). Another example of this type of positive feedback is through the phosphorylation of Raf kinase inhibitory protein (RKIP), thus suppressing MEK deactivation (Shin et al., 2009a). Also the inhibition of the RasGAP was demonstrated to contribute to positive feedback regulation in the pathway (von Kriegsheim et al., 2009).

1.3.1.2 *Direct protein-protein interactions: binding partners*

Specificity and fidelity of the MAPK pathways were shown to be influenced by direct interaction of the MAPK with other proteins. These direct interactions are achieved using scaffold proteins, regulatory proteins and the use of compartments to facilitate specific interactions.

1.3.1.2.1 Scaffold proteins

Scaffold proteins are regulatory proteins which interact and bind with multiple proteins tethering them into complexes, and thus mediate more efficient interaction and improve pathway organisation. Scaffolds influence MAPK signalling by increasing the efficiency of interaction between the three tiers of the cascade (predominantly the interaction between the three kinases). This is achieved by the ability of these proteins to bind to two or more of the kinases, provide an interface for phosphorylation events to occur and thus increase the probability of interaction (Behar et al., 2007, Ferrell, 2000). There is also evidence for scaffolds being capable

of linking different MAPK pathways together, thus controlling the dynamics of the entire signalling network. In addition, it was shown that these scaffold proteins are capable of localising into specific compartments (Teis et al., 2006, Teis et al., 2002) within the cell, thus allowing for a local response to MAPK cascade excitation.

There are many scaffold proteins which were shown to play a role in the MAPK signalling pathway; however the most studied members of this family are kinase suppressor of Ras (KSR) (Kornfeld et al., 1995, Sundaram and Han, 1995), MEK1-partner (MP-1) and JNK-interacting protein-1 (JIP). JIP-1 was initially reported as an inhibitory scaffold for several components of the JNK pathway (Whitmarsh et al., 1998), while KSR and MP1 are largely thought of as enhancers of MAPK signal (Ito et al., 1999, Kornfeld et al., 1995, Schaeffer et al., 1998). These scaffold proteins were shown to influence the specificity of the MAPK in a concentration dependent manner (Ferrell, 2000, Levchenko et al., 2000, Locasale et al., 2007b). Their influence on the MAPK pathway was demonstrated to be of a bell-shaped curve; where optimum influence on the MAPK pathway relies on an intermediate critical concentration, while low and high expression cause the opposite effect on the cascade. Over-expression of KSR in mammalian cells had caused an inhibition of ERK1/2 activation and a reduction in ERK1/2 signal propagation (Denouel-Galy et al., 1998, Joneson et al., 1998, Sugimoto et al., 1998). Yet, over-expression in PC12 cells caused an amplification of EGF and NGF signal (Müller et al., 2001, Nguyen et al., 2002). In addition work on PC12 cells has shown that KSR is capable of switching the outcome of EGF mediated signal from proliferation to differentiation. Further analysis for this discrepancy showed that the concentration of KSR, which was inhibitory, was much higher compared to the concentrations generated in the

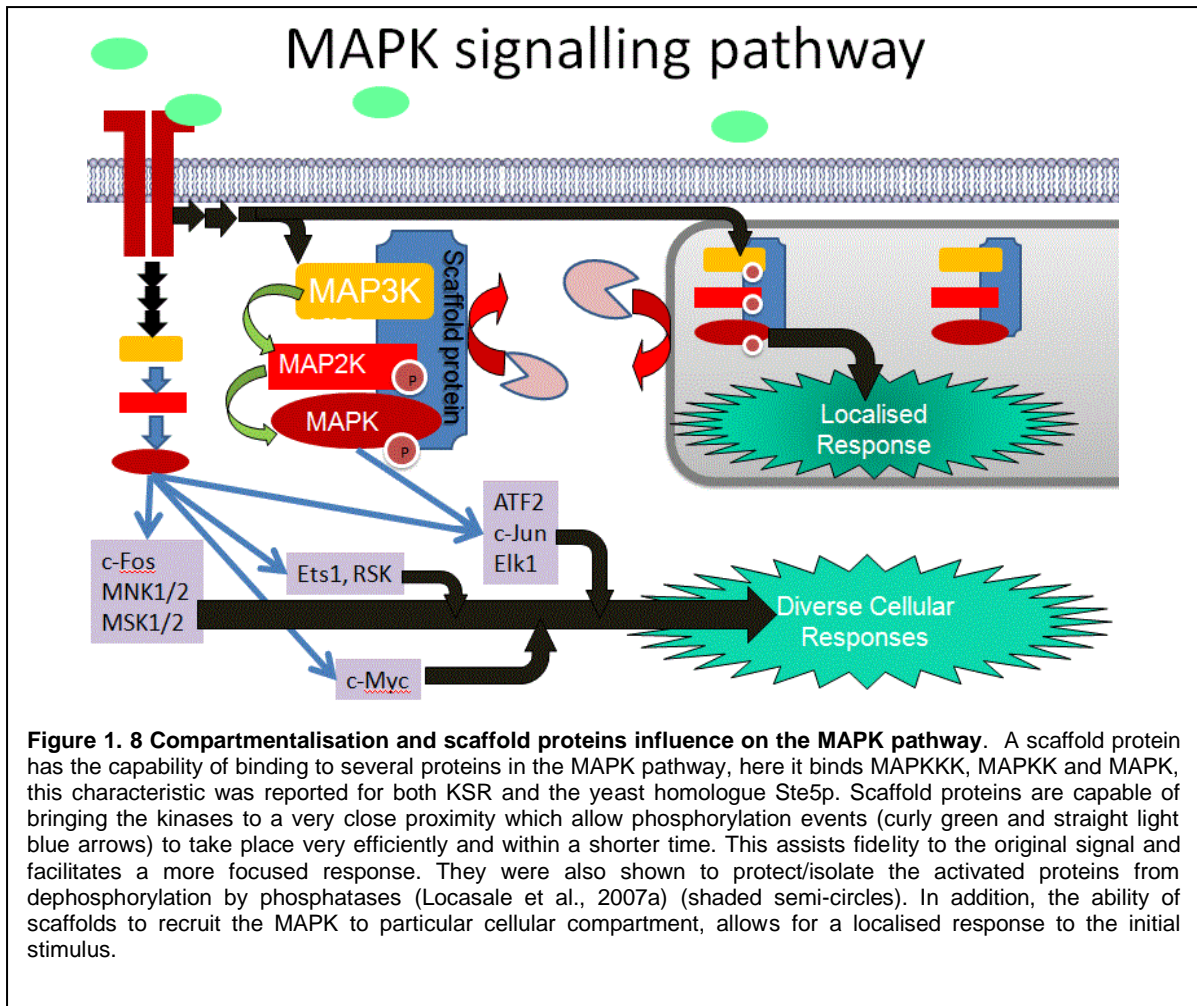
PC12 experiments. Thus, KSR critical concentration was achieved, while in the initial experiments KSR was operating outside of the optimum concentration. Related observation was reported with JIP-1; when JIP was first discovered, its interaction with JNK was shown to antagonise JNK mediated cellular responses, however in neurons and during excitotoxicity, JNK-JIP1 complexes were increased which resulted into an increase in neuronal apoptosis (Figuroa et al., 2003, Kim et al., 2002).

Reports of the ability of these scaffolds to fine-tune MAPK signalling *via* regulation of protein-protein interactions have been published. KSR binds Raf, MEK and ERK (Cacace et al., 1999, Therrien et al., 1996, Yu et al., 1998), once ERK1/2 is activated and translocates to the nucleus, it switches on negative feedback mechanisms which reduce the sustainability of the ERK1/2 pathway. In addition, ERK1/2 is capable of phosphorylating KSR, causing a conformational change which in turn results in Raf release and the diminishing of the signal. Reported mutations in this phosphorylation site in KSR caused a sustained activation of the ERK1/2 pathway. In addition, it was demonstrated that Raf activation was directly proportional to KSR concentrations (Douziech M, 2006) and that was independent from the KSR critical concentration theory. JIP-1 interacts with dual leucine zipper-bearing kinase (DLK) and JNK. DLK and JNK were shown to compete with each other to bind JIP-1. At cell resting state, the dominant complex is JIP-1-DLK, due to JIP-1 high affinity to DLK (Nihalani et al., 2001, Nihalani et al., 2003). However, once the JNK pathway is recruited, JIP-1's affinity to JNK increased, thus more JIP-1-JNK complexes formed and DLK was released from the complexes. This resulted into the DLK dimerisation and the mediation of DLK-dependent signals.

Another mechanism reported to influence the MAPK signalling by these scaffolds is *via* compartmentalising the MAPK components to cell-specific domains. One of the best examples which demonstrated this came from work with the MP-1 scaffold. MP-1 was shown to interact with ERK1/2 and MEK1. MP-1 interaction with p14 protein localises it to the late endosome and lysosomal compartments (Teis et al., 2006, Teis et al., 2002, Wunderlich et al., 2001), hence, localising ERK1/2 pathway to these compartments once activated. RNAi knockdown experiments for MP-1 had caused reduction of the overall EGF dependent response. While work with MP-1 KO mice had shown similar effects, with the cytoplasmic response of EGF not affected, the endosomal response was demolished. This was shown to be due to lowered activation of endosomal ERK1/2 but an intact cytoplasmic ERK1/2 activation.

1.3.1.2.2 Compartmentalisation

Localising proteins involved in the MAPK pathway in intracellular compartments is recognised as a regulatory mechanism of the MAPK pathways (**Figure 1. 8**). Compartments provide spatial regulation for the MAPK signalling and are thought to be a source for signal specificity and fidelity. These compartments are usually membrane bound and include the Golgi, endosome, caveolae and the mitochondria. The Raf-MEK-ERK pathway in particular is reported to reside in many of these compartments (Fan et al., 2008, Lee et al., 2011). The ability of the MAPK signalling components to reside in these compartments insulates them from exposure to the cytoplasmic environment and regulatory processes, such as dephosphorylation by phosphatases and/or degradation *via* ubiquitination. The compartments also provide



a localised environment where subsets of the MAPKs target proteins are available for phosphorylation. This includes other localised signalling pathways which are capable of crosstalking with the MAPK pathways (Arora et al., 2013, Canal et al., 2011, Kholodenko, 2002, Wunderlich et al., 2001). These additional signalling pathways are also subsets/branches of the complete networks found in the cell, thus specific and miniature crosstalk networks within the compartment will be established.

Compartmentalisation of the MAPK pathways was shown to provide an element of specificity and diversification of the response to the original signal. In cavioline-rich compartments, β arrestins were shown to recruit both ERK and JNK and mediate their signalling. However, β -arrestin1 was demonstrated to be specialised in

mediating ERK- dependent signalling while β -arrestin2 and 3 bind JNK2 and 3 and transmit their signal (Ahn et al., 2004, Luttrell et al., 2001, Shenoy et al., 2006). Furthermore, it was shown that altering the localisation of ERK from the plasma membrane to caveolae compartments modulates the cellular response. For instance, the oxytocin receptor (OXTR) localised to caveolea microdomains was observed to mediate ERK-dependent cell growth. However, OXTR localised out of caveolae triggered cell proliferation (Guzzi et al., 2002). Contribution of compartmentalised MAPK to specific subcellular domains was demonstrated at the endosome. Disrupting MAPK compartmentalisation at the endosome revealed the importance of this local MAPK population in endosomal function. It was shown that the adaptor proteins p18, p14 and the scaffold protein MEK partner 1 (MP-1) are important components in localising the MAPK in the endosomal compartment (Brahma and Dalby, 2007, Teis et al., 2006, Teis et al., 2002, Wunderlich et al., 2001). Disturbing this complex and its formation, both *in vitro* and *in vivo* caused malfunction and aberrant distribution of both late endosome and lysosomal compartments. The cellular phenotypes reported for the p14 knockdown were identical to those reported for MEK1 knock down, which showed that the MAPK has a role in the formation and function of the endosomal compartment. These defects are also observed in mutations of p14 protein in the human population

In addition to adaptor proteins (such as p14 and beta-arrestins), some scaffold proteins play a role in localising the MAPK pathway components to specific compartments. This tethering of the MAPK signalling apparatus to different cellular organelles or locations *via* scaffolds prompt diversity in the MAPK activation and hence its outcome. Connector enhancer of KSR 2 (CNK) was shown to allow

neuronal precursors to distinguish between the proliferative and neurotropic signals. Difference in response elicited by EGF in neuronal cells at the cell body and distal membranes (either axons or the synapse) (Canal et al., 2011) is thought to be due to the involvement of KSR and how it isolates both pools of ERK locally. This diversity in response due to scaffold tethering was also shown in neuronal cells with the scaffold Sur-8. There are reported observations of altered response specificity once the scaffold-MAPK-signalling complex was disrupted

The ability of tethering by scaffolds to induce two separate MAPK responses were also shown with the scaffold Sef (similar expression to fgf genes) (Torii et al., 2004). Sef was shown to localise in the Golgi where it binds to ERK. However, it was shown to have preferential affinity to phosphorylated ERK bound to MEK1. Therefore, Sef restricted the active ERK to the cytoplasmic compartments by blocking ERK translocation to the nucleus, thus confining ERK-mediated phosphorylation to cytoplasmic targets. In addition, Sef behaviour demonstrated that scaffolds attenuate the activated signal, in addition to anchoring MAPKs at a specific location and their substrates.

Furthermore, other mediators of the MAPK pathway were shown to also localise into different cellular compartments. Phosphatase protein PP-2B and PKC were shown to bind to the A-kinase anchoring proteins AKAP79/150. The AKAP79 were shown to localise to the postsynaptic densities on the internal surfaces of excitatory synapses and thus influence MAPK activation behaviour there. Furthermore, variation in AKAPs amino acid sequence target them to different compartments and potentially

therefore localising MAPK proteins to these compartments. For instance, AKAP1/AKAP149 were shown to be anchored at ER, the prenuclear membrane and the mitochondria. AKAP1/AKAP149 was shown to complex with Protein Phosphatase 1 (PP1) and targets it to these compartments. Furthermore, it has been shown that AKAP79 is capable of forming diverse complexes with other proteins, therefore, adding diversity to how the MAPK activation dynamics are transduced and regulated.

1.4 Conclusion

This chapter has outlined the components and processes in the MAPK pathway involved in its activation behaviour and ultimately generation of cellular responses. The chapter also highlighted how the MAPK activation is regulated in space and time *via* compartmentalisation and modulation of activating inputs. The chapter also introduced how combinations of these components and regulatory mechanisms play a role in the emergence of specificity and fidelity.

Furthermore, the chapter introduced the perplexing notion that, although the pathway is ubiquitously expressed, has a universal architecture and consistent activating mechanisms in all cells, signal fidelity and specificity still emerges. Decoding how spatiotemporal regulation determines the MAPK activation behaviour and, consequently, cellular response, will play a role in drug discovery and combating disease. The aim of the thesis was to investigate the influence of spatiotemporal modulation of the pathway on activation behaviour.

Chapter 2 focus on *in silico* modelling of biological systems and previous models of the MAPK pathway. There the methodology for modelling the MAPK pathway in this thesis is outlined. Chapter 3 presents the modelling methodology implemented in the thesis using an agent-based model (ABM). Chapter 4 presents the results obtained from the MAPK pathway ABM and discusses their implication.

Chapter 2 Computational modelling of biological systems

This chapter addresses the use of the *in silico* approach to model biological systems. An argument is provided for the need to model biological systems *in silico* and the advantages offered by this approach. An overview of the different modelling approaches is presented. A review of previous models of mitogen activated protein kinase (MAPK) cascade along with their contribution to the field are provided. The section also introduces our approach for modelling the cascade *via* the agent based modelling (ABM) paradigm, its fundamental characteristics and its contribution to understanding biological systems.

2.1 The complexity of the physiological system

Physiology focuses on studying a living system both in health and disease. This may begin at the molecular level with the interaction of small molecules (*e.g.* nucleic acids forming DNA), to the interaction of organisms between themselves and their environment. Since the second half of the 20th century, the investigative approach has focused on various hierarchical levels in isolation: referred to as the *reductionist* approach (Hess, 1970, Stent, 1968). Consequently, this (at the molecular level) has given birth to areas which focus on the genome, transcriptome and proteome, which is collectively referred to as omic data.

Though the study of living systems is complex both at the macro and micro scales, nevertheless, it is increasingly difficult to study them in isolation *via* the reductionist approach; because it does not account for the interplay between the different system scales in addition to environmental factors. Since the beginning of the 21st century, and in particular in the past ten years there has been an increase in data which link the different system scales (Kitano, 2002b, Kitano, 2002c). These emphasised the interplay and connectivity across the scales. Consequently, a better understanding and appreciation now exists of physiological phenomena as product of the overall interaction across system scales. Thus, a system approach is becoming more popular. This systematic and integrative approach is termed Systems Biology (SB).

2.2 The rise of Systems Biology (SB) and increased importance of *in silico* modelling

The principle that a systemic understanding allows for the betterment of our knowledge of the world around us in general and of physiology specifically, was first emphasised by Claude Bernard in his *Introduction à l'Étude de la Médecine Expérimentale*. This was further emphasised by Polyani, von Bertalanffy and Weiss (Bernard, 1865, Von Bertalanffy, 1950, Von Bertalanffy and Rapoport, 1963, Mostert, 1974). However, in that period, this approach was restricted due to the inadequacy of the available technology and the limited data existing across the system scales. In addition, breakthroughs at the molecular scale emphasised the use of the reductionist approach (Hogeweg, 2011). Thus, the system-based approach entered dormancy (Noble, 2008, Saks et al., 2009). Meanwhile, the reductionist approach gained momentum and generated extensive and expansive data (the omic data).

Although this data shed light on how genes, proteins and molecules interact leading to the construction of genomic and signalling networks; it provided a static knowledge as it did not give an account of how the genetic and protein networks collectively adapted to extrinsic and intrinsic disruption and modulation (Saks et al., 2009, Scott, 2004).

The 'omic data, in combination with major breakthroughs in experimental techniques and computational technology, resurrected the systemic approach. Kitano's publication in Nature and Science has highlighted the need for systemic approach in biology and the role SB can play to advance our understanding of physiological systems and in combating disease (Kitano, 2002b, Kitano, 2002c). After Kitano's publications, SB generated interest and currently the systemic approach is being encouraged; evident from the many publications and journals which address biological questions using a SB approach as well as the establishment of world class SB research institutes worldwide (Institute of Molecular Systems Biology, 2016, Institute, 2005-2016).

2.2.1 SB and use of *in silico* models: aims and benefits

The use of a systemic approach is not straightforward from a practical aspect. In the post-genome research environment the data generated is vast, complex and often difficult to interpret (Joyce and Palsson, 2006). Consequently, it is becoming gruelling and extremely challenging to audit and integrate this data into the systemic understanding using only human comprehension. Computation and the construction of *in silico* models are the main tools used to assist assembly and integration of omic

data. These models examine the different mechanisms and configurations which connect the system at the macro and micro scales. Thus, the models investigate the interplay within and between the different scales. This approach is complementary to experimentation, both *in vitro* and *in vivo*.

In silico modelling and simulation of natural systems are approaches which have been used extensively (Crick, 1970, McDougall et al., 2006, Wolpert, 1969) (Turing, 1952). A model is an abstract representation of a real system, while simulation refers to operating a model under a configuration of interest to reproduce the natural system's behaviour. The objective behind modelling natural systems is to further understand the underpinning mechanisms by undertaking hypothesis testing through a validated model and to predict system behaviour in response to modulation, which assists in exploiting the knowledge (available following the hypothesis testing step). The use of *in silico* models and simulations are beneficial especially when the subject under investigation is difficult to solve analytically: in short complex (Kaul and Ventikos, 2015). These are due to information (regarding the system or its behaviour) that is either not accessible, incomplete, or not precisely determined. Furthermore, a model can be used to assess the system's fundamental components which are needed for its functionality and to exhibit its behaviour, either in integration with other components or, if desired, in isolation. One example of modelling which encompass the abovementioned notions is seen during World War II with the development of the nuclear bomb at the Manhattan Project, where knowledge regarding subatomic particles and their interactions was relatively unknown.

In silico models are either mathematical models or computational models. Mathematical models in general describe relationships between quantities by describing a process *via* a set of equations (Murray, 2002). In biology this process may be differentiation, proliferation, biochemical reactions, etc. Depending on the system, its mathematical representation can be statistical or dynamic. In the former, a description of the relationship between observed variables are quantified whereby dependencies and correlations are established; however, it does not describe how the change occurs (Draghici et al., 2007, Jeong et al., 2000). The dynamic representation expresses the mechanisms of change and specifies how dependencies and correlations arise with respect to specific variables, such as time. In the dynamical representation, the mathematical description of the system is derived, then solved or approximated analytically (Anderson et al., 2000, McDougall et al., 2006). Mathematical models are simulated *via* computers to elucidate solutions of equations. Furthermore, analytic methods for mathematical models are numerous. Conversely, computational models describe interactions between identified components in the real world represented using algorithms written in a programming language and executed by an abstract machine to simulate real world behaviour. A computational model, simplistically, is a set of instructions which describe mechanisms and parameters that integrate the identified components of the system together. These instructions are executed in a particular sequence by a computer. Computational models are used to examine complex problems where analytical solutions are difficult to obtain (Fisher and Henzinger, 2007, Hunt et al., 2008, Kaul and Ventikos, 2015).

2.2.1.1 Modelling approaches

Computational SB employs algorithms and data structures to assemble and incorporate the omic data to construct a faithful *in silico* representation of the biological system and its behaviour. This is generally achieved using one of the two main paradigms: a top-down or bottom up approach.

2.2.1.1.1 Top-down approach:

The top-down approach examines biological behaviour at systemic scale and correlates observations with interactions occurring at lower scales. Effectively, the approach focuses on understanding the systemic behaviour and then disassembles it into its quiddity. Once the components and their interactions are identified, these are interrogated further, if required, by disassembling and dissecting them into smaller interactions and constituents (Bruggeman and Westerhoff, 2007, Katagiri, 2003). This approach includes traditional statistical models, pattern recognition and machine learning. In SB, this approach is utilised to infer mechanistic details from omic data, both at the genome and protein level, where cell behaviour is correlated to interactions between genes and/or proteins and the networks they form (Tenazinha and Vinga, 2011). As such, cell behaviour (such as differentiation or proliferation) can be explained. For example, clustering analyses were initially used to derive correlation between genes and their activity as seen in microarray data (Chu et al., 1998). Independent Component Analysis (ICA) and Reconstruction of Accurate Cellular Networks (ARACNE) are used to build both metabolic and transcription control networks by recognising data obtained from high throughput technologies (Liao et al., 2003, Margolin et al., 2006).

However, there are disadvantages associated with the top-down approach. Relying on observations inferred from systemic behaviour to elucidate the interacting components often masks important or even fundamental interactions at the lower levels (Castiglione et al., 2014). This is sometimes referred to as “unknown unknowns” (Logan, 2009, Sadeh et al., 2013). “Unknown-unknowns” are information, mechanisms and/or components within the system that are not yet discovered or even contemplated. Thus these “unknown unknowns”, once identified, lead to two scenarios, either an increase in our understanding of the system, or a fundamental change in our perception of the system. In both cases, identification of the “unknown unknown” components changes established opinions of the system. “Unknown unknowns” are appreciated in retrospect; for instance, the concept of crosstalk within the MAPK signalling pathways is currently common knowledge within the field, however, this was not true during the early 1990s where the majority of these signalling were characterised as separate pathways. Consequently therefore, during the 90s, crosstalk between signalling pathways is regarded as an “unknown unknown” (Burack and Shaw, 2000, Suderman and Deeds, 2013, Xia et al., 1995).

2.2.1.1.2 Bottom-up approach

In contrast to the top-down approach, the bottom-up approach investigates how components of the system and the interactions between them yield systemic behaviour. The approach relies on detailed knowledge and/or understanding of the system components and their interactions (Nurse, 2008). In SB, this translates to identifying the genes or proteins which compose the system, mapping their interactions and examining how the mechanistic properties of the system (such as

differentiation or triggering of gene expression events) emerge *via* computer simulations (Scott, 2004). The approach takes advantage of the bountiful high-throughput data. This methodology includes system dynamic models, kinetic models and stochastic methods (Edwards et al., 2011). The approach is also advantageous in designing and planning wet-lab experiments as the computational models explore modification of specific system components or parameters which can also be disrupted *in vitro* and/or *in vivo* (Kholodenko, 2002).

The bottom-up approach is not without disadvantages. A detailed knowledge of the system's components and their interactions is required, and such information is not always available. Moreover, modelling some components of the system and their interactions might not yield the observed system behaviour; though this is insightful in its own right as it highlights gaps in our knowledge, thereby leading to expansion of the model. Subsequently, however, the models become large and more computationally expensive. Furthermore, the recursive process of model development and modification can take years (Bianca and Pennisi, 2012, Cakir and Khatibipour, 2014, Castiglione et al., 2014, Kaul and Ventikos, 2015).

Regardless of the approach, a better perception is developed of what contributes to system behaviour across system scales. This improved understanding of connections and interplay within the system results into a better representation of the system (Castiglione et al., 2014). This is important to in understanding the transition from health to disease and vice versa, and is evident from the use of computer models to elucidate new drug targets, pharmacokinetic and pharmacodynamics

computer models, and the use of models to simulate clinical trials (Draghici et al., 2007, Edwards and Thiele, 2013). These will, ultimately, influence drug discovery and development (Kitano, 2002a), thus improving patient treatment and bettering health care. It is of no surprise that SB integrative approach is seen to be increasingly employed in studies of diseases such as cancer, inflammation and infectious diseases (Draghici et al., 2007, Orton et al., 2009).

2.2.2 Modelling intracellular signalling events

The upsurge in omic data was in part due to the interest in disease development at the molecular and cellular levels. Most diseases under investigation (such as cancer, immunological diseases and age-related diseases) have molecular and cellular roots, with cell signalling processes receiving considerable attention. As mentioned in Chapter 1, cell signalling mechanisms are used by cells to interpret their environment and their break-down causes many diseases (Krauss, 2004). With the prominence of SB and the extensive data available, *in silico* modelling of cell signalling mechanisms and events is increasing. These include models of important signalling networks such as the NF- κ B, the mitogen activated protein kinase (MAPK), PI3K and in some cases signalling networks which encompass crosstalk between two signalling pathways (Grieco et al., 2013, Haack et al., 2015, Orton et al., 2009). Said computational models have shed light on the signal transduction mechanisms and provided insights into the regulation of several signalling pathways in time and space; the influence of feedback mechanisms on signal modulation; and the effect of crosstalk between different pathways. One pathway that has been pervasively modelled is the MAPK pathway, due to its ubiquitous use by cells to mediate a

multitude of cellular responses (Kolch et al., 2005, Orton et al., 2005) . The reader is referred to Chapter 1 for a detailed description of the pathway, the cellular responses it mediates and its (complex) regulation. The following section will address the *in silico* models of the MAPK pathway, how it is modelled and the advances made in understanding the MAPK signalling behaviour.

2.2.2.1 *In silico models of the MAPK pathway.*

The increase in MAPK related omic data, which demonstrated a high level of cross talk between the three MAPK pathways at the three tiers of the pathway, has meant that it is no longer viewed as a linear pathway (Oda et al., 2005, Taniguchi et al., 2006). Furthermore, the MAPK pathways are known to interact with other signalling cascades to modulate cellular responses (Aksamitiene et al., 2010, Aksamitiene et al., 2012) (Nakakuki et al., 2010). Additionally, feedback mechanisms have an impact on MAPK activation (Santos et al., 2007a) (Kholodenko, 2000, Ingolia and Murray, 2007, Brandman and Meyer, 2008, Shin et al., 2009b, Avraham and Yarden, 2011). Given this complexity, nonetheless, the MAPK signalling network still exhibits specificity and fidelity to the original signal. *In silico* models of the MAPK pathway were constructed in order to explain and discern the underlying mechanisms which mediate the emergence of the MAPK global activation behaviour at the molecular and cellular levels. The MAPK pathway was modelled using several formalisms; these are divided into two mainstream formalisms: continuous (quantitative) and discrete (qualitative).

2.2.2.1.1 Continuous modelling approach

The continuum approach is a frequently used approach for modelling biological events and the MAPK pathway in particular (EMBL-EBI, 1991-2016, Chylek et al., 2014). It relies on the continuity of the parameters used in the model such as concentrations, reaction rates, and volumes. The approach describes numerical changes in parameters that define the system. These parameters are usually dependent on specific variables such as time, concentration or space, and therefore, this paradigm captures dynamic change in the system with respect to these predetermined variables (Hu et al., 2009). Mathematical equations (predominantly differential equations) describe the initial conditions, system behaviour and the boundary conditions, and therefore define the relation between the system parameters and the rate of change. The equations are then discretised and solved either numerically or estimated analytically. The mathematical expressions are also used to generate numerical algorithms for computational execution. These differential equations are either ordinary differential equations (ODEs) or partial differential equations (PDEs) (Eungdamrong and Iyengar, 2004). In the former, the changes are all in relation to one variable - typically time. While the latter look at the dynamic changes in the system with respect to multiple parameters: usually time and space. ODEs are more frequently utilised in modelling biological systems. The continuum approach assigns time-dependency to both measurable and non-measurable variables. Changes are then postulated *via* the sum of rate changes due to increases and/or decreases in the variables quantities.

For the MAPK pathway, the first models of the MAPK pathway investigated how the ultrasensitive response emerged using (ODEs) of enzyme reaction kinetics and

studied change in protein kinases concentration with respect to time (Ferrell, 2000, Blüthgen et al., 2009, Levchenko et al., 2000, Huang and Ferrell, 1996, Ferrell, 1997). The work of Huang and Ferrell, 1996 and Kholodenko *et al.*, 1998 had demonstrated that the kinetic mechanism and the three tiered design contribute to ultrasensitivity (Kholodenko et al., 1999, Huang and Ferrell, 1996). Ballhalla *et al* 1999 identified the essential components of the signalling network (such as feedback loops) and how these contribute to emergent behaviour in the network (for instance, bistability) (Bhalla and Iyengar, 1999, Markevich et al., 2006, Bhalla et al., 2002, Xiong and Ferrell, 2003). Kholodenko *et al* 2000 had further investigated the role of feedback loops on MAPK activation dynamics. They found that inclusion of negative feedback resulted into sustained oscillatory behaviour (Hilioti et al., 2008, Kholodenko, 2000). Considering that oscillatory activation behaviour was only demonstrated *in vitro* in 2009, predictions by Kholodenko and co-workers are momentous and reveal the capabilities of computational simulations in providing fundamental insights into system behaviour (Aoki et al., 2013a, Shankaran et al., 2009).

The complexity around the MAPK pathway is that it is capable of triggering cellular responses which are both cell-type specific and ligand specific. This occurs despite the architecture of the cascade in all cells being indistinguishable and the proteins constituting the cascade being ubiquitously expressed in each cell. Therefore, the demonstration of the role feedback loops play in MAPK activation dynamics resulted into further investigation into the wiring of these loops. Brightman & Fell (2000) had investigated differential feedback loops in the ERK pathway stimulated by either EGF or NGF (refer to section 1.3.1.1 in Chapter 1 for a detailed description of MAPK

signalling in both cascades, (Brightman and Fell, 2000)). They showed that the variance in activation behaviour of ERK was due to differential negative feedback from ERK to SOS and Grb2. EGF employs a negative feedback loop which causes transient ERK activation, while the lack of this feedback loop in NGF-mediated ERK activation was suggested to be the cause of the sustained ERK activation. Schoeberl *et al* (2002) had built a model to address the link between the original stimulus and signal specificity in addition to assaying the efficiency of signal propagation through the pathway (Schoeberl, 2002). They built a comprehensive model which elaborated on events between EGF receptor (EGFR) and MAPKKK. Their model showed that activation dynamics of MAPK and pathway sensitivity was not dramatically influenced by the concentration of EGF. However, the model presented did not integrate the negative feedback loop from ERK to SOS. Heinrich *et al* assessed the role of phosphatases and kinases in shaping the MAPK response (Heinrich *et al.*, 2002). They postulated that phosphatases have more influence on the duration of MAPK activation, while kinases affect the amplitude of MAPK activation. Hatakeyama *et al* had also looked at the interplay between kinases and phosphatases on MAPK activation amplitude (HATAKEYAMA *et al.*, 2003); however, their model integrated crosstalk between the MAPK and PI3K pathways. Their work showed that kinases demonstrated a higher activation rate in the initial phases of MAPK activation while phosphatases reaction rates increased gradually and they maintained a high reaction rate at later stages of pathway activation. Altan-Bonnet *et al* 2003 and Honberg *et al* 2005 examined the interplay between negative and positive feedback loops and how those influence the activation behaviour of the MAPK (Altan-Bonnet and Germain, 2005, Hornberg *et al.*, 2005a). Altan-Bonnet had demonstrated that the balance between the two loops contribute to how T-cell

receptors distinguish between activating signals (*i.e.* a suggestion of how fidelity emerges). Honberg *et al* were interested in the signal flow through the pathway and which reactions and protein interactions were critical in determining information flow. They examined 148 reactions in the EGF-dependent MAPK pathway and their influence on MAPK activation amplitude and duration. They found that only eight reactions were crucial for signal flow in the pathway and that these reactions were connected to Raf, MEK and ERK. Their work also demonstrated that there were two pools of active ERK in the cell, distributed between the cytoplasm and the plasma membrane. This suggested that spatial distribution of MAPK affect the activation behaviour. In 2004 Bhalla *et al* had suggested that spatial arrangement of MAPK proteins into small volumes play a role in the emergence of bistability in the pathway (Bhalla, 2004a). Bistability is a characteristic in the pathway where the proteins in the pathway are thought to exist in active and inactive states. Bhalla had suggested that this characteristic is responsible for the emergence of the ultrasensitive response. Mechanistically, this is thought to be linked to the phosphorylation state of the kinases and the mechanisms involved. Markevich *et al* and Ortega showed that distributive phosphorylation of MAPK play a role in the emergence of both bistability and the ultrasensitive responses (Bagowski and Ferrell, 2001, Ferrell and Machleder, 1998, Markevich et al., 2004, Ortega et al., 2006). Nonetheless, Santos *et al* 2007 had suggested that bistability should emerge in the existence of active positive feedback loops (Santos et al., 2007b, Qiao et al., 2007). Ortega argued that distributive phosphorylation without any feedback is sufficient for bistability activation behaviour to appear. Santos *et al* 2007 confirmed that EGF-dependent MAPK activation behaviour was associated with negative feedback while NGF-dependent MAPK activation was connected with positive feedback. They also showed that

bistability emerged in NGF-mediated activation which supported the link between bistability and positive feedback. The latter was linked to molecular memory, which Ortega *et al* 2006 also alluded to. Santos *et al* (2007) also demonstrated that ERK impose an inhibitory effect on MEK and, thus, created an additional negative feedback loop *via* competitive bidding (Ortega *et al.*, 2006, Santos *et al.*, 2007b). They confirmed their findings *in vitro* by re-wiring the NGF and EGF pathways in pheochromocytoma (PC12) where EGF was exposed to positive feedback while NGF was connected to negative feedback loops. The outcome was that EGF induced PC12 differentiation and NGF mediated cell proliferation. Sturm *et al* 2010 demonstrated that negative feedback loops acted as negative feedback amplifiers in an attempt to explain how robustness and signal stabilisation emerge at the system level (Sturm *et al.*, 2010b, Romano *et al.*, 2014). Their model attempted to explain the modest change in MAPK activation amplitude with variation in the ligand concentration. Fritsche-Guenther *et al* 2011 in addition to confirming the role of negative feedback loops had further investigated robustness in the pathway and the molecular mechanisms which lead to its appearance (Fritsche-Guenther *et al.*, 2011). They showed that robustness does not rely on dual specificity phosphatases (DUSP), or saturation of MEK; but on post-translational modification at the level of Raf proteins. Furthermore, their model revealed that concentration of ERK had no effect on the emergence of robustness. Sarma *et al* 2012 showed that robustness in the pathway was the product of the interaction between kinases and phosphatases, which leads to phosphatase sequestration (Sarma and Ghosh, 2012). Their model demonstrated that phosphatase sequestration modulate the duration of MAPK activation behaviour. Sarma *et al* 2012 also investigated the design of coupled positive and negative feedback loops. They showed that the characteristics of the

oscillatory behaviour (such as amplitude and frequency) were linked to the design of the coupled feedback loops.

The aforementioned models had used ODEs with the assumption that the proteins were homogeneously expressed and well mixed intracellularly. However, this is not the case physiologically as heterogeneity in protein distribution is well documented for proteins involved in the MAPK pathway (Perlson et al., 2005). In addition, Bhalla had shown that small volumes might play a role in the emergence of bistability in the pathway (Bhalla, 2004b, Bhalla, 2004a). Therefore, PDEs were used to address the effect of the spatial element on the activation behaviour of the pathway. The initial models had addressed different localisation of kinases and phosphatases and their effect on signalling) (Brown and Kholodenko, 1999, van Albada and ten Wolde, 2007). Models which investigated the MAPK in particular demonstrated the formation of a phospho-protein gradient due to spatial segregation between kinases and phosphatases. The gradient was dependent on diffusion when cell diameter was more than $1\mu\text{m}$ (Kholodenko et al., 2000, Naka et al., 2006). Nevertheless, this is problematic as the concentration of activated MAPK considerably diminishes intracellularly (Kholodenko et al., 1999). Kholodenko *et al* 2006 demonstrated that bistability through dualphosphorylation of MAPK and positive feedback to MAPKK (Markevich et al., 2006, Markevich et al., 2004) allow for the signal to be propagated deeper into the cell and with high frequency, while others argued that propagation of the signal were protected by scaffold proteins and/or residing within the endosomal compartment (Ferrell, 2000, Lee et al., 2002). Neves *et al* 2008 illustrated with their model that diffusion did not play a significant role in shaping the activation behaviour of MAPK, yet protein heterogeneous distribution did (Neves and Iyengar, 2009).

They also determined that cell shape, negative regulatory loops and key reaction kinetics contribute to the MAPK activation behaviour. Munoz-Garcia *et al* 2009 had demonstrated that unlike Heinrich's ODE model, the amplitude of the propagating signal was dependent on ratio between activation and deactivation (*via* kinases and phosphatases respectively) (Munoz-Garcia *et al.*, 2009). This also ensured a more robust signal compared to those observed in ODE models. Kazmierczak *et al* 2010 demonstrated that for a signal to propagate from the receptor at the cell membrane intracellularly, the kinase diffusion coefficient must be small (Kazmierczak and Lipniacki, 2009, Kazmierczak and Lipniacki, 2010). This also has an effect over positive feedback and its potency. Though there is a growing realisation of the importance of the spatial element in mediating cell signalling in general and the MAPK activation behaviour in particular, however, PDEs addressing the whole cascade are not abundant.

In addition to investigating MAPK activation dynamics with respect to time and space, the continuum formalism was used to shed light on the role of scaffold proteins in modulating pathway activation behaviour and their role in specificity and fidelity. The initial models of Levchenko *et al* 2000 and Heinrich *et al* 2002 had demonstrated that scaffold concentration is important in determining the augmentation or antagonism of MAPK activation (Heinrich *et al.*, 2002, Levchenko *et al.*, 2000). Levchenko had demonstrated that scaffold works biphasically, promoting MAPK activation when they were present within an optimal concentration (OC), while concentrations above or below OC reduced MAPK activation. For scaffold concentrations above the OC, the inhibitory effect is suggested to be due to the distribution of the kinases into incomplete scaffold-kinase complex, thus preventing

efficient activation propagation in the pathway. Conversely, concentrations below OC result into a smaller number of the complete scaffold-kinase complexes. Chan and Tian T *et al* argue that scaffolds contribute to bistability (Chan et al., 2012) (Tian et al., 2007, Tian et al., 2009). Chan Y *et al* (2012) showed that scaffolds mediate a processive phosphorylation of the kinases and that is linked to the emergence of bistability within the MAPK pathway. However, Tian *et al* and Thalhauser T *et al* showed the contrary and that scaffolds are responsible for emergence of graded MAPK activation behaviour as opposed to ultrasensitive activation (Thalhauser and Komarova, 2010, Tian and Harding, 2014). The latter was demonstrated physiologically. Nonetheless, others had shown that this only occurs when certain parameters are fulfilled which include the presence of negative feedback and low scaffold-kinase binding affinity.

The continuous approach has several advantages. Practically, the quantitative data it generates is related to what is measured biologically. For instance, the concentrations of protein species in the cell, rate of activation and enzyme kinetics. Other advantages of the continuum approach are: (1) the availability of analytical and validation methodology to analyse and substantiate the data generated; (2) model execution is not computationally expensive and often do not require a long time to run; and (3) translation of the theoretical concepts into mathematical equations is not highly complex (Murray, 2002, Eungdamrong and Iyengar, 2004).

Nevertheless, the continuous approach has some disadvantages. One of these is the incapability of ODE models to account for the heterogeneity within the system

(Costa et al., 2009), which is not accurate physiologically because an inherent characteristic of biological systems is their variability and heterogeneity (Li and Xie, 2011, Eberwine and Kim, 2015). The models usually represent the average behaviour of the system as they assume its homogeneity; therefore, contribute to understanding the global dynamics and behaviour of the pathway rather than localised behaviour where there is variation in concentration, pH, diffusivity and porosity (such as activation within a compartment) (Mayer et al., 2009). These elements affect protein behaviour and kinetics. The collection of these local behaviours give rise to the global behaviour (or ultimately the global activation behaviour). Thus the continuum approach is appropriate for a top-down representation of the system (Jeon et al., 2010). Furthermore, in order to build models with differential equations, quantitative knowledge of the system's parameters is essential. These include dissociation constants, reaction rates and concentrations of the different proteins involved in the cascade. However, the majority of this quantitative data are either extremely difficult to obtain (both *in vitro* and/or *in vivo*) or currently impossible due to unavailability of the technology to allow for accurate measurements. Subsequently, many of the parameters required to build complete and comprehensive ODE/PDE models of the MAPK signalling network are unknown, such as the local concentrations within compartments, and hence modellers resort to estimating these values to populate the model. Consequently, this limits the formalism to modelling small signalling network and limits the expansion of models to include the MAPK signalling network in its entirety (Aldridge et al., 2006).

2.2.2.1.2 Discrete models using logical models

To overcome the aforementioned caveats of the continuous formalism, other non-continuous (discrete) approaches were used to model the MAPK pathway (Calder et al., 2006a, Singh et al., 2012, Samaga et al., 2009). There has been a growth in the application of these models within the last decade. The marked advantage of these formalisms is their ability to model the signalling network without the need for complete kinetic information and data. These include many paradigms, such models utilising graph theory (petri-nets), logical models (Boolean logic) and rule-based models (RBM).

The first non-continuous model of the MAPK pathway was a statistical model developed by Brown *et al.*(1999). In this model of ERK activation by EGF and NGF, they demonstrated that specific signalling modules are responsible for the differential cellular outcome mediated by the two ligands (Brown and Kholodenko, 1999). In addition, Brown and colleagues had illustrated for the first time the concept of sloppiness in cell signalling and how it is an inherent characteristic for cellular function. Their model had shown that discrete modelling of MAPK signalling has the potential of improving the understanding of signal transduction, signal dynamics and how that is related to signal specificity and fidelity. This resulted into an increase of discrete (qualitative) models of the MAPK pathway. Earlier methods took advantage of structural models and information flow theory, where the structure and architecture of the pathway was taken into consideration, because signalling pathways are usually presented (by cell and molecular biologists) as graphical notations. In principle; signal transduction is considered a process where information is rallied from the external environment intracellularly. This is advantageous, since

mathematical models usually do not consider the flow of information. Furthermore, in this post-genomic era, there is a prodigious qualitative data from high throughput methods, in addition to the representation of signalling networks and the signal flow in graphical notations. Petri-nets is a method which takes advantage of this representation of signalling networks and it was used to investigate the MAPK signalling network (Chaouiya, 2007). Therefore, petri-nets are useful as a top-down approach for modelling the MAPK pathway. This formalism has shed light on crosstalk between different signalling pathways and its role in modulating MAPK activity and vice versa. Ruth *et al* had studied the MAPK and AKT signalling pathways downstream of the EGFR with a petri-net model and confirmed experimental findings where inhibition of protein Raptor caused the reduction of p70S6K levels in MDA231 breast cancer cell line (Ruths et al., 2008). Although their model showed the same effect in the BT549 cell line, this was contradictory to previous published data. However, they speculated the observation to arise due to the mutation of retinoblastoma protein (p16INK4a/RB) in aforesaid cell line. Sackmann *et al*'s petri-net model of the mating pheromone pathway in the yeast *S.cerevisiae* demonstrated that phosphorylation of MAPK is dependent on MAPKK activation, thus, demonstrating, *in silico*, the role of MAPKK as a bottleneck for cascade activation (Sackmann et al., 2006).

Another formalism which does not require prior knowledge of network kinetics is Boolean logic. Boolean logic is a branch of algebra where an event (a variable) is modelled as true or false with the events assigned numerical values of 1 and 0 respectively. The logic defines two events (A and B) and mapped to three possibilities which are as follows: (1) either both events occur simultaneously

(denoted with the operator AND); (2) when either event (A or B) occur designated by the operator OR, and (3) when one of the events does not occur (referred to with operator NOT). Huang S *et al* in 2000 had highlighted the potential for use of Boolean logic to infer how cells commit to cellular decision making, such as proliferation and/or differentiation, using the MAPK pathway as an example (Huang and Ingber, 2000). Helikar, T *et al* used Boolean logic to examine how cellular decision making emerges in a signalling network which included the AKT, MAPKs (including p38, JNK and ERK), Rac and CDC42 (Helikar et al., 2008). Their work showed that for ERK activation *via* the extracellular matrix receptors (integrins) and G-protein coupled receptors is highly dependent on EGFR transactivation. However, for integrin and EGFR-dependent ERK activation, ligands levels for both receptors have to be high. Saez-Rodriguez *et al* using their Boolean model discovered a new locus of crosstalk and interplay between the MAPK and the AKT pathway in inflammatory signalling at the level of insulin receptor substrate (IRS) (Klamt et al., 2006, Samaga et al., 2009). Recently, Mori *et al* had demonstrated with their Boolean model that in the *S.cervasea* MAPK pathway, the appearance of oscillatory behaviour depends on the attributes of the negative feedback loop. They demonstrated that in a deterministic model of MAPK pathway the oscillatory behaviour is sustained, while the introduction of negative feedback results into desynchronisation of the oscillatory behaviour (Mori et al., 2015).

Handorf T *et al* had examined the role of crosstalk between the MAPK pathway and Wnt pathway to commit cells to differentiation or proliferation (Handorf and Klipp, 2012, Haack et al., 2015). Their results showed that both beta-catinin and ERK activation exhibited oscillatory activation behaviour in the presence of basal level of

Wnt. However, the activation of both proteins become sustained when Wnt levels were increased and were maintained at high levels. These outcomes agreed with (Kim et al., 2007) model which utilised the continuous paradigm. Samaga *et al* had built a logical model of the EGFR signalling network which included the MAPK signalling pathway. Their work showed that the MAPK signalling network contains redundant substructures, similar to the postulation by Honberg *et al* (Hornberg et al., 2005a, Samaga et al., 2009). Their work also displayed that in hepatocytes p38 and JNK activation is independent of PI3K/AKT pathway activation. Grieco L *et al* built a logical model of the EGFR-FGFR signalling network (which included MAPK pathway in addition to AKT pathway), which demonstrated that ERK activation is essential for the cell to make a decision between proliferative and non-proliferative responses (Grieco et al., 2013). However, this switch positively correlated with the presence of AKT. In addition, their model had illustrated that crosstalk between the two cascades is vital for cell fate decisions. Recently, petri-nets formalism is being integrated with other methods such as Boolean logic or constraint-based analysis in order to take advantage of analytical methods and to allow for the exchange between different modelling formalisms; thus, maximising our understanding of the MAPK pathway (Grieb et al., 2015, Honglin and Shitong, 2009)

The disadvantage of using Boolean logic lies in the inability to model intermediate events which determine if an event will occur or not. Therefore, this limits the integration of molecular mechanisms such as protein-protein interactions: dynamic events where the strength of feedback mechanisms change or events where concentrations of proteins change. In addition, conceptually, cells and proteins are not logical machines and the emergent behaviours observed (including the wiring of

the signalling networks) did not evolve due to logical decisions, but due to biochemical rules. However, lately, modelling formalisms incorporating uncertainty into Boolean logic models or utilising fuzzy logic have become available to tackle this challenge (Grieb et al., 2015, Honglin and Shitong, 2009).

Another disadvantage which applies to both continuous and described qualitative paradigms is combinatorial complexity (Mayer et al., 2009, Hlavacek et al., 2003, Deeds et al., 2012). Cells are dynamic and heterogeneous; they sense and respond to changes in conditions surrounding them (Grinev et al., 2013). Cell signalling is characterised by self-organisation and the emergence of behaviour due to the interaction between the lower-scale entities which constitute the cell. Protein-protein interactions are central to signal propagation, particularly for the MAPK pathway, where these interactions include the ability of proteins within the cascade to bind to multiple partners (such as the scaffold KSR and the adaptor protein Grb2) and also the presence of multiple sites for post-translational modifications. Thus, a given protein can assume multiple states depending on its interaction partners (Suderman and Deeds, 2013). To represent all these possibilities (*i.e.* protein states) using differential equations requires specifying a reaction per state change per protein species. This will also require determining the concentrations of these protein species and the kinetic rates for their forward and backward reactions. It is worth iterating that if a protein contains eight modifiable domains, it can occupy 256 states (Hlavacek et al., 2003). If we consider that two proteins (with the same number of modifiable domains) form heterodimers, the heterodimeric complexes can assume 65,000 possible states (Blinov et al., 2006, Danos et al., 2007, Deeds et al., 2012). Consequently, modelling all of these states and the reaction associated with them

leads to models which are highly arduous but less informative. Therefore, other modelling paradigms had been adapted to model the MAPK pathway where protein-protein interactions are integrated into the models: this is the rule-based modelling paradigm (RBM) (Chylek et al., 2015, Hlavacek et al., 2006).

In this approach a protein is treated as an object (or agent) with defined structure and the reactions which govern their behaviour as rules. This is different from kinetic models because it is not required to explicitly define and specify all the molecules and reactions involved. The rules can also include interactions with partners, post-translational modification, and the ability to form homo and/or heterodimers etc. The proteins are capable of adapting numerous states once the rules that dictate state transition are satisfied. Blinov *et al* 2005 used RBM to investigate early activation events of the EGFR with Kholodenko's as a guideline; nonetheless, their model integrated phosphorylation events of specific sites on the EGFR contrary to Kholodenko's model which only modelled this as one step (Blinov et al., 2006, Kholodenko et al., 1999). Blinov's RBM showed that the outcome for mutating tyrosine residues in both EGFR and Shc is identical, which is contradictory to Kholodenko's predictions. However, both Blinov's and Kholodenko's models showed that eliminating Shc-dependent SOS recruitment to the receptor was primarily responsible in mediating an increase of overall SOS recruitment. Furthermore, due to their expanded model, Blinov and colleagues predicted SOS interaction with more partners, thus predicting more diversity in the cellular outcome. Creamer *et al* 2012 had reconstructed using a RBM the EGFR receptor signalling model which Chen *et al* and Birtwistle *et al* had previously built using ODE models (Birtwistle et al., 2007, Chen et al., 2009, Creamer et al., 2012). This RBM included ERK and AKT proteins

and the crosstalk between them. Their extended model had demonstrated the ability of RBM to handle model expansions which will be impossible for ODEs given the combinatorial complexity. Suderman *et al* had used rule-based modelling to build the yeast pheromone signalling network in the presence of the scaffold Ste5 (Suderman and Deeds, 2013). Their model, although it replicated the responses associated with pheromone activation, did not inhibit the activation at high concentration of Ste5, contradicting Levchenko's OC hypothesis (Levchenko et al., 2000). Kocieniewski *et al* 2012, using the RBM, also investigated the role of scaffolds in modulating the MAPK activation behaviour and proposed that scaffolds are required to transmit activation through the pathway in the presence of low signals (Kocieniewski et al., 2012). The model illustrated that dual phosphorylation in the presence of scaffolds is necessary for signal specificity to emerge in the system.

A disadvantage of RBM currently is the inability to account for the spatial element and compartmentalisation of signalling modules, though recent publications have attempted to address this issue (Regev et al., 2004, Pedersen et al., 2015). On the other hand, the agent-based modelling (ABM) formalism provides a better approach to integrating temporal regulation, spatial elements and rules into the model.

2.2.2.2 *Our approach, the use of agent-based modelling (ABM) to simulate the MAPK pathway*

Behaviour at the cellular scale evolves from interaction between the different molecules at the molecular scale, such as nucleic acids, proteins and lipids. For instance, the process of gene transcription and translation is a cycle of interaction between proteins and nucleic acids. This is parallel to the bottom-up paradigm.

Proteins are regarded as the key functional units (or machines) in the cell due to their abundance and involvement in the majority of cellular activity, especially cell signalling (Kiel and Serrano, 2012, Bray, 1995, Roux, 2011). Each protein has biochemical and biophysical properties which allow it to interact with its environment and other molecules which reside in the environment (Sikosek and Chan, 2014). This intractability gives proteins a social dimension (Wooldridge and Jennings, 1995, Bankes, 2002). More importantly, proteins interact with each other and conduct their action without a set-goal or consciousness of the objective of the interaction (Bandini et al., 2009). Furthermore, each protein in the cell is an autonomous entity in its interactions and functionality and, therefore, independently responds to modulation and separately follows biochemical and biophysical roles to achieve its function. A protein, due to its ability to form multiple interactions, can adopt multiple states, such as bound or free, phosphorylated or unphosphorylated, active or inactive, mobile or immobile etc. Satisfaction of biochemical and biophysical rules allow the protein to circulate between these various and diverse states. All of the above descriptions qualify proteins to be molecular machines and/or molecular agents; therefore, an ABM paradigm is an appropriate choice to model the MAPK pathway.

ABM is a bottom up, object-oriented, ruled based *in silico* approach, where the essential components of the system are modelled as heterogeneous interacting autonomous agents, in order to examine and understand the emergent behaviour(s) at the system level from the intractability between the agents (DeAngelis, 1994, Robinson et al., 2005, Robinson et al., 2008). The ABM formalism models the essential components in the system and their core interactions. This is achieved by specifying simplified rules, which are capable of generating complex behaviour(s)

and patterns at the global level. Pertinent demonstrations of how simple interaction roles are capable of generating complex system patterns and behaviour are the Mandelbrot set and The Game of Life invented by John Conway (Gardner, 1970). In The Game of Life, a grid is composed of several cells (squares); each cell is governed by four basic rules. A cell is “viable” (or on) if it is surrounded by two or three “viable” cells. A cell “dies” (turned off) if it is surrounded by fewer than two or more than three “viable” cells. A dead cell becomes viable if surrounded by three viable cells. Running simulations of these rules results into complex behaviour and patterning in the grid.

In order for an agent to adapt a protein-state, it requires several attributes. These include memory, intractability and in some cases adaptability or learning capabilities. The memory allows a protein-agent to memorise important characteristics such as its state, the rules it is governed with and its location within the intracellular environment. Intractability is based on the rules governing the execution of these rules by the agent. Learning capabilities are related to both memory and rule execution. Recollection of current and previous state(s), environmental conditions and rules executed allow agents to adapt and improve its response to future inputs.

ABM is effective in capturing the rise of complex behaviour in the systems *via* modelling the interaction of the system’s components with each other and their environment. This is demonstrated at both the macro and micro system levels in different research fields such as economics, ecology and cell biology. In biology, at the macro system level, ABM had shed light on ants foraging behaviour (Jackson et

al., 2004, Robinson et al., 2005). At the cellular level, ABM was used to model T-cells activation in lymph nodes (Bogle and Dunbar, 2009, Bogle and Dunbar, 2010, Bogle and Dunbar, 2012) and epidermis wound-healing and self-organisation. The Epithelome project had illustrated the role (TGF-beta) in wound healing and illustrated that self-organisation of keratinocytes depended on cell-cell interaction and cell-substrate interaction (Adra et al., 2010, Sun et al., 2008). At the molecular scale, the work of Chapa J *et al* had demonstrated for the first time the role of RUNX3 in the FLAME is capable of running on various computing systems including parallel high performance computers (HPC). The latter feature allows for the inclusion the of actin filaments in the regulation of the NF-κB signalling pathway (Pogson et al., 2008, Holcombe et al., 2012, Pogson et al., 2006). In addition to the aforementioned benefits of the ABM paradigm in comparison to other approaches, ABM data demonstrate a robustness in imitating natural systems, which is important when correlating findings to biological data (Jeong et al., 2000, Kriete, 2013, Grinev et al., 2013, Stelling et al., 2004).

2.2.2.3 Flexible Large Scale Agent Modelling .Environment (FLAME)

FLAME is an off-lattice discrete modelling framework used to simulate agent based models (ABMs). The framework is a generic ABM modelling system and therefore it is used in numerous research domains such as economics, crowd movement and molecular biology. Another distinctive feature is its ability to create models in 3D, an important characteristic for the investigation presented in this thesis. Furthermore, FLAME is capable of running on various computing systems including parallel high

performance computers (HPC) . The latter feature allows for the inclusion of a large number of agents (in the magnitude of millions) and thus utilises models which incorporate multitudes of interactions and communications between the agents. The ability to include millions of agents is a feature unique to FLAME in comparison to other ABM platforms such as NetLogo and Biocellion (Kang et al., 2014, Kaul and Ventikos, 2015). FLAME provides a robust solution for running large models (Hao Bai et al., 2014)

FLAME uses logical communicating extended finite state machines principles in particular X-machines. A finite state machine is an abstract state machine which can adapt finite number of states. However, these states are achieved asynchronously, whereby the state machine must transit between the different states it can potentially occupy. In order to achieve this transition, state machines exploit transition functions. The transition functions stipulate restrictive conditions and/or events that, when met, specify the appropriate state the machine will adapt next. An X-machine is analogous to finite state machines, however, the main difference is that X-machines include machine memory. Thus, transition between states incorporate memory transition and its modification. A communicating X-machine is a machine which communicates with other machines by exchanging messages. These communication messages are outputted to a common library (in FLAME this is libmboard), which the X-machines can access and read the particular messages as shown in **Figure 2. 1**. The concept of X-machines can be described quantitatively as following (see also **Figure 2. 1**):

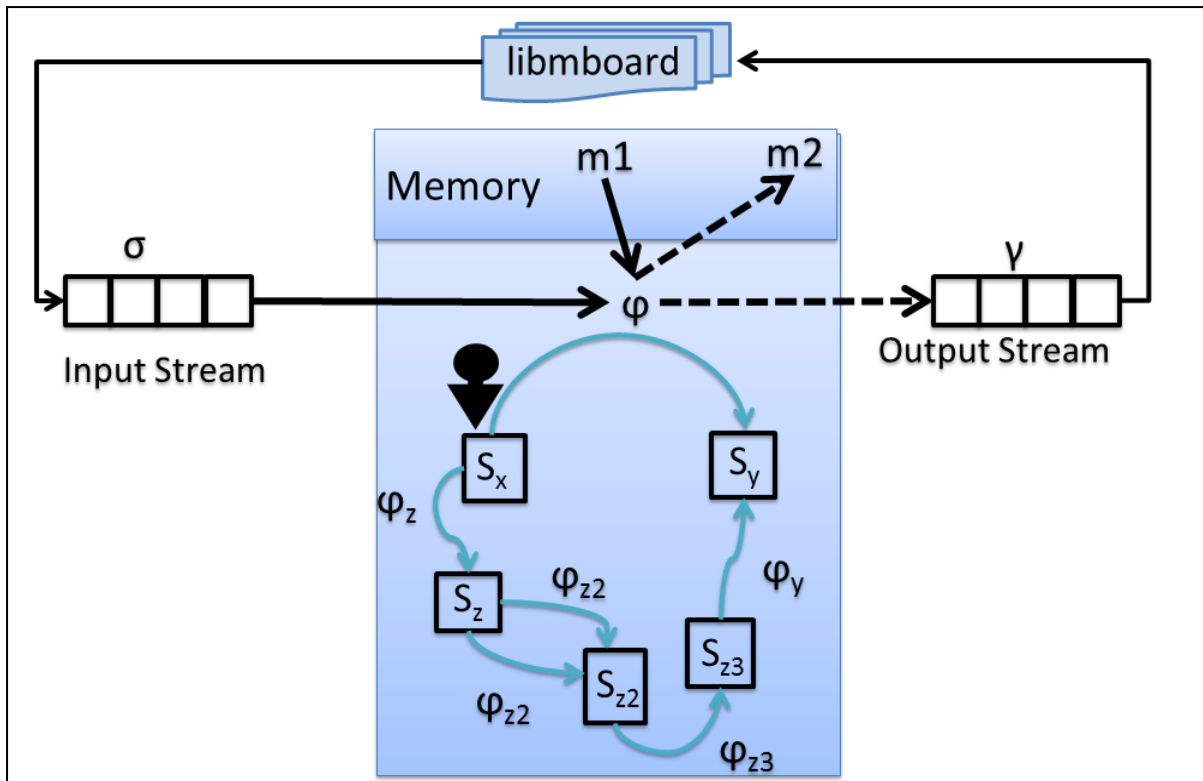
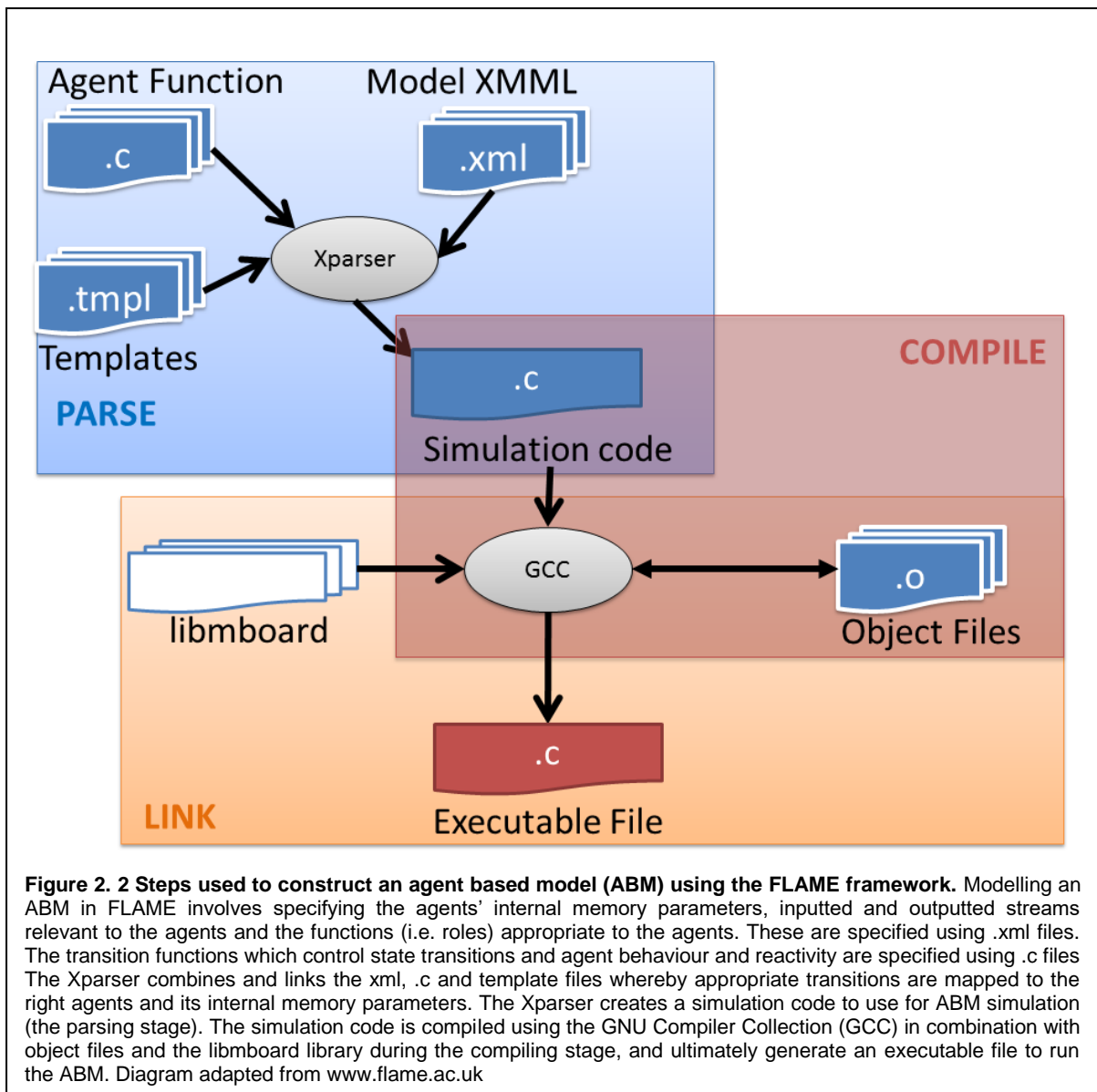


Figure 2. 1 A schematic representation of a finite X-machine. An X-machine or agent is capable of assuming many states (S_n) to adopt any of these an agent is required to transit from state (S_x) to state (S_y). Transition between these different states is achieved using transition functions ϕ_n . For S_x to transfer to another state (S_z) another transition function ϕ_z is utilised. To execute a transition function the X-machine receives input streams from either other agents or its environment. Once the transition is executed, the X-machine memory is updated from $m1$ to $m2$. After transition, the state-machine creates output stream, in FLAME this is the outputted messages. The diagram was adapted from the FLAME user manual available at www.flame.ac.uk

$$X=(\sigma,\gamma,S,M, \Phi,F,s_0,m_0)$$

where σ are input set, γ are output set, S denotes the infinite set of states a machine can adapt, M denotes possible finite memory variables, Φ denotes the set of partial functions (ϕ) that map an input and memory variable to an output and a change in the memory variable, which can be represented as follows: $\phi: \sigma \times M \rightarrow \gamma \times M$, F is the next state transition function: whereby $F: S \times \phi \rightarrow S$, s_0 is the initial state and m_0 is the initial memory . ϕ is a state transition function which integrate inputs from the environment σ , the current state and memory of the X-machine (s_0 and m_0) (FLAME.co.uk, 2016). In order for the agent to transit from s_0 to the next state s_1 , particular conditions needed to be met, which the X-machine read as inputs in libmboard. Once the conditions are met, the transition function ϕ is executed,



consequently, a new state, s_1 , is achieved and the memory is updated to m_1 .

Forthwith communicating X-machines are referred to as agents

FLAME is a template based parallel simulation code generator. The user describes the agents' memory parameters, the model and the environmental conditions using the extensible markup language (XML) and utilises C coding language to detail transition function algorithms. The XML files which describe the agents are termed X-machine markup language XMML. FLAME is composed of two components, the

Xparser and the libmboard (message board library). The former is the tool that parses the XMML files into a simulation source code which can be run in parallel or serially; it also generates state diagrams and Make files to allow model execution using main.exe. While libmboard supports a library that manage agent messages (inputs and outputs), thus it allows the agents to interact efficiently. Furthermore, libmboard models can act as Message Passing Interface to run models in parallel on multi-node systems. The simulation code, in combination with libmboard and the initial conditions file (0.xml) are used to execute the model simulation (see **Figure 2. 2**).

There are other numerous ABM platforms available which utilise different programming languages (Nikolai and Madey, 2009), use diverse operating systems and have the option of coupling the framework to other programmes. The most popular ABM framework used are NetLogo, MASON, Repastm and Swarm (Railsback et al., 2006). Burkitt M had rigorously evaluated the aforementioned frameworks in addition to FLAME and he found that model implementation was simplest using FLAME in comparison to the other frameworks mentioned above. This allows the modeller to concentrate on writing the algorithms for the transition functions and agents specification. This is ideal for investigators who have limited expertise in computer science and computational biology, thus making the modelling process uncomplicated and accessible. In addition, FLAME automates the management of agents' lists and their operations, in contrast to the other frameworks. He also found that FLAME performance was faster when run on the Grid using a large number of cores (Burkitt, 2011). However, the caveat of FLAME in comparison to the other platforms is the lack of a complete built in analysis library or

tools while MASON and Repast contain such tools. Furthermore, FLAME allows the incorporation of user defined data sets and the simulating models in 3D.

The aim of this thesis is to investigate the combined effect of spatiotemporal modulation of the MAPK pathway on MAPK activation behaviour and its implication in fidelity and specificity. Modelling the pathway using ABM formalism provides a suitable tool to achieve this objective due to its capability of modulating the spatiotemporal elements simultaneously and independently for each agent. In addition, the ABM formalism allow for expanding the model to include more protein-agents, new mechanisms (*i.e.* rules) and to modify a coarse-grained process to a fine-grained process (zooming in) and vice versa.

2.3 Conclusion

This chapter provided an overview of the systemic approach to understand system behaviour, and outlined the objectives of Systems Biology (SB). The purpose, aims and benefits of *in silico* modelling of natural systems, in general, and cell biology, in particular, were emphasised. The different approaches for modelling in SB were introduced. Modelling of the MAPK signalling pathway was outlined and the different paradigms utilised for modelling were presented. The agent-based modelling (ABM) paradigm was introduced and its suitability to model the MAPK pathway was underlined.

There is extensive biological evidence for the importance of spatiotemporal regulatory mechanisms in modulating the MAPK pathway activation behaviour and the emergence of fidelity and specificity. However, there are not many models which address spontaneous spatiotemporal regulation of the pathway and none to our knowledge which examine the rule of compartmentalisation in modulating MAPK activation behaviour and the emergence of specificity and fidelity within the pathway. Therefore, the ABM paradigm was used to address these issues.

Chapter three highlights the modelling process and describes the conceptual model of the MAPK pathway. Chapter four presents the computational implementation and the results obtained from the ABM model of the MAPK pathway.

Hypotheses

Based on the information presented in the introduction, indicates that temporal and spatial elements within the MAPK signalling pathway influence activation magnitude, duration and ultimately specificity and fidelity of the cellular response, hence, it can be hypothesised that concurrent modulations of the pathway temporal and spatial elements impact the activation dynamics of the MAPK pathway. Additionally, it can also be speculated that different combinations of the spatial and temporal modulations lead to the emergence of distinct activation behaviour and thus contribute to the emergence of fidelity and specificity of the MAPK-dependent cellular responses. Said hypotheses can be dissected and presented as following:

1. Spatially restricting the proteins involved in the MAPK pathway into multi-compartments impacts MAPK activation behaviours differently compared to a homogeneously distributed scheme.
2. Simultaneous modifications of the spatiotemporal elements can substantially affect MAPK activation behaviour.
3. Using different combinations of spatial and temporal elements cause differential activation behaviour in the MAPK pathway.

Chapter 3 Characterising the MAPK signalling pathway agent-based model (ABM)

This chapter aims to provide a link between the biological descriptions of the MAPK system described in the introduction (peruse Chapter 1) and computational implementation into the MAPK ABMs presented in Chapter 4. The universal modelling process was conveyed in section 3. 1, a description of the MAPK pathway conceptual model and its components which were utilised to create the MAPK ABMs were emphasised in section 3. 2. The processes of transforming the conceptual model into the ABM are underlined in the subsequent section 3. 3.

3.1 The Modelling process: universal practice

To build a reliable model of a particular system or behaviour, a definition process takes place. This begins with (i) a conceptual model of the system or the behaviour under focus. The conceptual model is a scrutinised aggregation of the literature, thus represents current and common knowledge of the system and its behaviour. It is an abstract, static and simplified representation of the system, its behaviour and the interaction between its components. (ii) The second step involves formulating questions for interrogating the identified conceptual model. (iii) Characterising components within the conceptual model that are associated with the questions imposed in point (ii). (iv) Identifying the modelling paradigm suitable to address and

integrate points (ii) and (iii). This definition process identifies fundamental elements of the system and its behaviour allowing the elimination of nonessential or trivial components, therefore reducing combinatorial complexity. Following said definition process, a functional model is constructed to simulate the selected components and elements within the identified conceptual model. This functional model translates the selected components and elements into a quantitative and dynamic representation using mathematical description and computer programme/algorithms (Defranoux et al., 2005, Saks et al., 2009).

Computational modelling is generally an iterative process as shown in Figure 3. 1. It relies on cycles of model building, experimentation and modification. The model construction process starts with the literature which contributes the conceptual model (as described in the previous paragraph). Experimentation, both *in silico* and in the lab, provides results which can be used to validate the computational model; thereby aid model modification and improvement, and ultimately, lead to a computational model that reliably depicts the natural system and its behaviour. Once validated, further experimentations using the computational model are conducted to uncover mechanistic explanations for the system and its behaviour. It is highly desirable that *in silico* experimentation are coupled with *in vitro* or *in vivo* experiments to allow for one-to-one validation, amending the developed model and improving its accuracy. However, this sometimes is not realistic due to technical/methodological difficulties in performing the laboratory experiments. These Issues arise due to limited resources, ethical boundaries and/or due to practical/technical considerations.

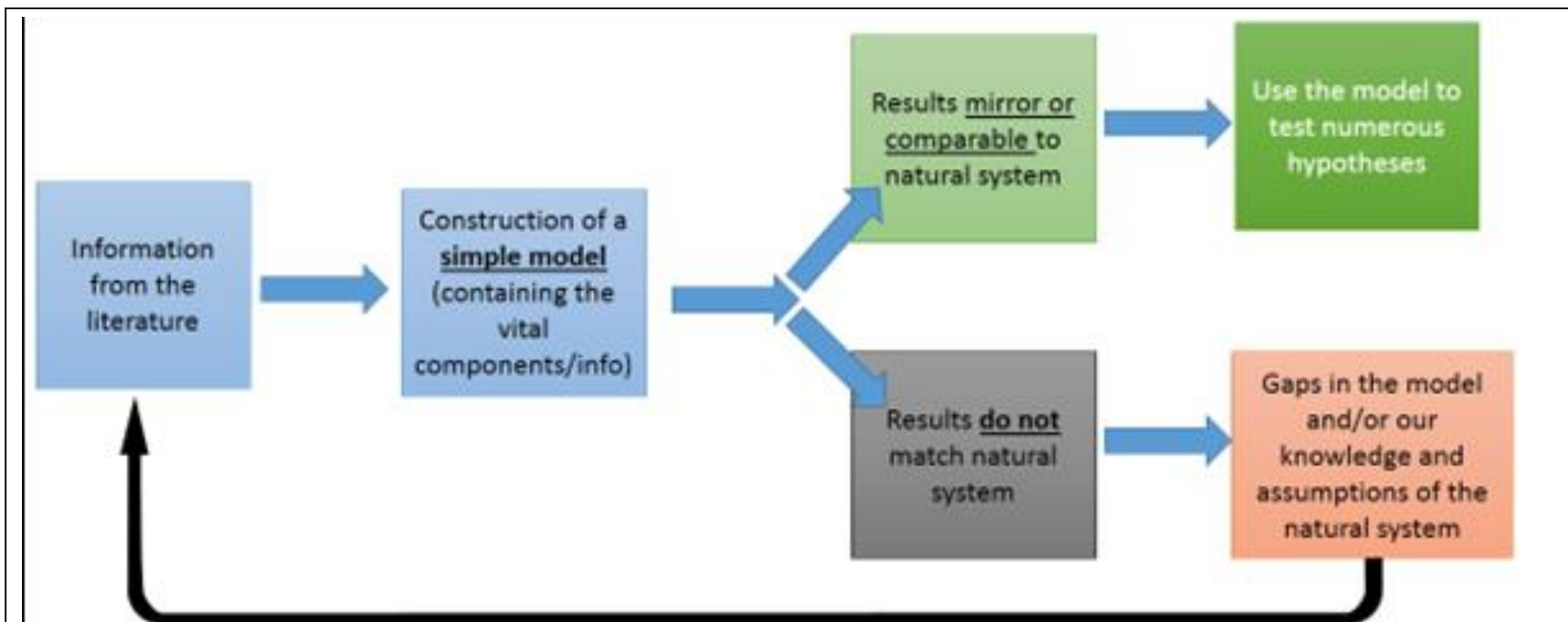


Figure 3. 1 A flowchart summarising modelling process *in silico*. Prior to the construction of a model to represent and examine natural systems a process of abstraction takes place. In this process information about the natural system to be modelled is gathered, the objective and questions the model is trying to address are defined and outlined. Consequently, the essential information and data required to build a model to address these particular objectives are extracted from the literature. The models usually are simple and only contain information and mechanisms which the field consider as the main processes which drive the system. The model is simulated, and the data generated is analysed. The analysed data is compared to experimental outcomes, whether obtained in house or published previously in the literature. This step is part of model validation process. The data generated from the model either does not match the behaviour of the natural system, which demonstrates a gap in knowledge, perception and/or assumptions about the natural system. This requires cycles of model modification and improvement to allow for the model to faithfully mimic the natural system. Once the model reaches that phase, it is utilised to formulate, examine and explore hypotheses regarding the natural system and its behaviour, which are impossible or impractical to perform experimentally.

Let us put the universal modelling process in context in relation to the work presented in this thesis; in regard to point (i) the state-of-the-art conceptual model of the MAPK signalling system was presented in chapter 1 and 2. Considering point (ii) questions about the MAPK signalling system were formulated and imposed as hypotheses in the hypothesis section on page 71. Characterisation of the components and translation into a modelling paradigm (points (iii) and (iv)) are presented in this chapter and summarised in table 3. 1

3.2 Model specification

This section summarises the specifications used to formulate a functional MAPK model. It also describes how this functional model was transformed to the MAPK pathway ABM. Furthermore, what is being emphasised in this section are the common features of the presented ABMs. Within the appropriate result sections the adjustments applied to the generic ABM are described in more detail.

3.2.1 Defining the system boundaries

Firstly, system boundaries were defined to construct the functional model. These are the components which define the behaviour or the system to be modelled and ultimately distinguishing elements which links the model with actual behaviour. For instance, the physical environment, the individuals involved in the behaviour/system and identifying the time scales associated with model and actual behaviour.

Table 3. 1 Summarises the mapping between the domain model and the model specification step presented in section 3.2 and their implementation in the ABMs presents in section 3.3. The literature column provides the evidence for both the modelled natural behaviour and previous models which simulated said behaviour

<u>Domain model</u>	<u>Literature</u>	<u>ABM implementation</u>
<u>Physical environment</u>		
The cell as site for signal transduction	<u>(Alberts et al. 2002)</u> <u>(Karr et al. 2012)</u> <u>(Pogson et al. 2006;</u> <u>Rhodes et al. 2014)</u>	Modelled as a 3D spherical cell with a radius of 20µm
The cytoplasm is where cell signalling occurs. It is a semifluid environment with 80% water content where micro and macromolecules reside and move.	<u>(Alberts et al. 2002)</u> <u>(L'Allemain et al. 1992)</u> <u>(Luby-Phelps 2000)</u> <u>(Shepherd 2006)</u>	Modelled as a 3D fluid space with no macromolecule obstacles and where proteins move freely by Brownian motion.
Compartments and organelles: The cytoplasm contains cellular organelles which are thought to play role in signal specificity and fidelity	<u>(Hudder et al. 2003)</u> <u>(Takamori et al. 2006)</u> <u>(Settembre et al. 2013)</u>	In the multi-compartment ABM, these were modelled as 10 cubic compartments with a length of 1µm, equivalent to the length of a mitochondrion. The number of compartments was arbitrary as compartments such as the ER, endosomes and Golgi apparatus are continuous compartments.
Spatial separation: The cell contains highly specialised domains. These are created via lipids by layers and/or diffusion gradients	<u>(Arora et al. 2013)</u> <u>(Canal et al. 2011)</u> <u>(Chiu et al. 2002)</u> <u>(Kholodenko 2002)</u> <u>(Donovan et al. 2016)</u>	These were modelled as cytoplasm, nucleus and cytoplasmic compartments in the ABMs. The two-compartment model was designed to emulate classical methodology of simulating the pathway by assuming a homogenous well-mixed cell. The multicompartment ABM is emulating a physiologically accurate representation of the cell where extensive evidence illustrate distinct heterogeneity of biomolecules in the cytoplasm
Physical boundaries by membranes	<u>(Resat et al. 2011)</u> <u>(Klann et al. 2011)</u> <u>(Sjöstrand 1959)</u>	The separation was specified as roles within the agents transitional functions where the movement is restricted to

		within particular compartments
The nucleus as a domain for cell signalling and gene expression	(Seth et al. 1992) (Volmat et al. 2001)	The speculation that the nucleus is the sight for the termination of pMAPK signalling was utilised in the ABM by the transition of pMAPK state to MAPK state once it is exported out of the nucleus
Individuals within the environment	(Ferrell and Bhatt 1997) (Ferrell 1997) (Kholodenko 2000)	The MAPK cascade is a three tiered cascade where activation commences by triggering MAPKKK. This was applied in the ABM by simulating the cascade downstream of MAPKKK where MAPKKK were assumed to be fully active at t_0
The MAPK cascade: The cascade relies on phosphorylation events to propagate the signal downstream. Phosphorylation occurs when kinases activation sites are at close proximity to phosphorylation sites on their target proteins	(Ferrell 1997) (Widmann et al. 1999)	In the ABM interacting agents, when in close proximity, bind together and if they are available to form bonds, activation ensues. This simulates the final outcome of the phosphorylation process.
MAPKKK \Leftrightarrow pMAPKKK process	(Craig et al. 2008)	Was assumed to be fully active at t_0 .
MAPKK \Leftrightarrow pMAPKK process	(Matsuda et al. 1993) (Takekawa et al. 2005)	Modelled as two states of a communicating x-machine, active state (pMAPKK) and inactive state (MAPKK). State transition occurs when the appropriate conditions in the transition functions are satisfied.
MAPK \Leftrightarrow pMAPK	(Seger and Krebs 1995) (Zhang et al. 2002) (Kocieniewski et al. 2012)	Modelled as two states of a communicating x-machine, active state (pMAPK) and inactive state (MAPK). As conditions within the algorithm are met, the agent change state using its transition function.

Temporal environment	<u>(Tomida and Taichiro 2014)</u>	
Continuous stimulus	<u>(Tomida et al. 2012)</u> <u>(Macia et al. 2009)</u> <u>(Tombes et al. 1998)</u>	The ABMs simulated activation via an acute signal. However a continuous signal was also applied to examine pMAPK response to dynamic signalling. Refer to section 4.4.1.2
Acute stimulation	<u>(Tombes et al. 1998)</u>	Received at t_0
Sustained pMAPK activation	<u>(Sasagawa et al. 2005)</u> <u>(Tomida et al. 2012)</u> <u>(Traverse et al. 1992)</u>	These behaviours were not specifically modelled because they are emergent behaviours, and consequently were outputs for detection.
Transient pMAPK activation	<u>(Sasagawa et al. 2005)</u> <u>(Tomida et al. 2012)</u>	
re-establishment of basal pMAPK levels	<u>(Lefkowitz 2005)</u> <u>(Traverse et al. 1992)</u>	
Full activation at 5-10 min	<u>(Tomida et al. 2015)</u> <u>(Chang and Karin 2001)</u>	
<u>Important behaviour</u>		
MAPK activation dynamics	<u>(Anderson et al. 1990)</u> <u>(Kocieniewski et al. 2012)</u>	
Processive phosphorylation: The process where a protein is phosphorylated on multiple sites by the same kinase. Recent publication emphasis processive phosphorylation dominance, especially in the presence of scaffold proteins	<u>(Kocieniewski et al. 2012)</u> <u>(Ouldrige and Rein ten Wolde 2014)</u> <u>(Heinrich et al. 2002)</u> <u>(Levchenko et al. 2000)</u> <u>(Burack and Shaw 2000)</u> <u>(Aoki et al. 2011)</u>	pMAPKK interaction and phosphorylation of MAPK to was simulated as a processive process whereby pMAPKK was assumed to dual phosphorylate MAPK.
Distributive phosphorylation: The process where a protein is phosphorylated on two sites by two different kinases and involves the dissociation of the proteins from the original complex	<u>(Markevich et al. 2004)</u> <u>(Burack and Sturgill 1997)</u> <u>(Ferrell and Bhatt 1997)</u> <u>(Huang and Ferrell 1996)</u>	This was not considered in the ABMs as evidence suggest that phosphorylation within the MAPK pathway is a processive process

to complete phosphorylation of the second site		
Oscillatory pMAPK response	<u>(Kholodenko 2000)</u> <u>(Shankaran et al. 2009)</u> <u>(Weber et al. 2010)</u> <u>(Tomida et al. 2015)</u>	As these behaviours are products of the formation and therefore levels of pMAPK , they were not specifically modelled in the ABM, but were emergent behaviour of the models, and therefore were assessed as the ABM outputs
Graded pMAPK response	<u>(Ferrell and Machleder 1998)</u> <u>(MacKeigan et al. 2005)</u>	
Ultrasensitive pMAPK response	<u>(Ferrell and Bhatt 1997)</u> <u>(Ferrell 1997)</u>	
Nuclear translocation: The precise mechanism for import is debated to be either passive, active or a combination of both,	<u>(Horgan and Stork 2003)</u> <u>(Karlsson et al. 2004)</u> <u>(Furuno et al. 2001)</u> <u>(Khokhlatchev et al. 1998)</u> <u>(Masuda et al. 2001)</u> Importin: <u>(Lorenzen et al. 2001)</u> <u>(Plotnikov et al. 2011)</u>	pMAPK import was simulated as instantaneous translocation of pMAPK into the nucleus from the cytoplasm.
Nuclear translocation: The time taken to translocate pMAPK into the nucleus	<u>(Ahmed et al. 2014)</u> <u>(Costa et al. 2006)</u> <u>(Volmat et al. 2001)</u> <u>(Lenormand 1993)</u> <u>(Lenormand et al. 1998)</u>	The time to achieve full pMAPK translocation into the nucleus is within 5 minutes and is shown to be instantaneous. Hence, pMAPK agents translocated into the nucleus once they changed state. The time to achieve full translocation into the nucleus was an emergent behaviour monitored in the ABM
Gene expression events: Activated pMAPK triggers gene expression events in the nucleus. Gene expression and transcription involves multimeric protein complexes	<u>(Winkles 1997)</u> <u>(Murphy et al. 2002)</u> <u>(Matsushita et al. 2009)</u> <u>(Funnell and Merlin 2012)</u> <u>(Scott and Pawson 2009)</u> <u>(Soufi et al. 2008)</u>	The ABM modelled the interaction with transcription factors (TF) to mediate gene expression initiation events. pMAPK interacted with different TF states: monomeric-DNA bound, monomeric-unbound, multimeric-DNA bound and multimeric-unbound. Only DNA-bound multimericTF state mediated gene

		transcription initiation events.
Nuclear export of pMAPK to the cytoplasm was shown to involve protein-protein interactions with various proteins	<u>(Karlsson et al. 2004)</u> <u>(Adachi et al. 2000)</u> <u>(Plotnikov et al. 2011)</u> <u>(Adachi et al. 1999)</u> <u>(Gaumont-Leclerc et al. 2004)</u>	Nuclear export was modelled as an active process which involved the interaction of pMAPK with an exporting nuclear receptor (ExR). Binding interaction between the two agents resulted into the export of pMAPK into the cytoplasm and/or cytoplasmic compartment and change state to MAPK
MAPKK activation dynamics		
The MAPKK is a bottleneck where activating and deactivating inputs coverage. Balance between activating and deactivating signals determine pMAPK magnitudes and duration	<u>(Cuenda 1995)</u> <u>(Favata et al. 1998)</u> <u>(Haeusgen et al. 2011)</u>	This property was utilised in the ABM by the use of pMAPKK agent activation behaviour to temporally adjust pathway activation
Cooperative inhibition is the process where pMAPK phosphorylates pMAPKK, thus inhibits the latter and modifies MAPK activation dynamics	<u>(Kim and Ferrell 2007)</u> <u>(Legewie et al. 2007)</u> <u>(Eblen et al. 2004)</u> <u>(Chickarmane et al. 2007)</u> <u>(Ortega et al. 2006)</u>	Binding interaction of pMAPKK with MAPK resulted into the phosphorylation of pMAPK. This in turn phosphorylates pMAPKK leading to its inactivation and formation of a dormant MAPKK. The dormancy period was modelled as re-activation delay period (RADP)
Phosphatases: Inhibition of the kinases in the MAPK pathway was shown to be mediated by phosphatase protein families which determine the time the kinases remain in the phosphorylated/active state	<u>(Kins et al. 2003)</u> <u>(Silverstein et al. 2002)</u> <u>(Sontag et al. 1993)</u> <u>(Westermarck et al. 2001)</u>	The inhibitory action of phosphatases on MAPK signalling was integrated in the ABM as a black-box parameter within the RADP.
Ubiquitination: MAPKK was shown to be regulated by ubiquitination which impact the MAPK activation behaviour and	<u>(Hurst and Dohlman 2013)</u> <u>(Wang 2002)</u>	Irreversible inhibition and breakdown of pMAPKK was simulated in one experiment in the two compartment ABM by including algorithm for

MAPKK levels in the cytoplasm		MAPKK-agent removal from the model
Deactivation by other proteins: MAPKKs activity is reported to be influenced by several binding partners such as tribbles, scaffold proteins and adaptor proteins.	<u>(Sung et al. 2007)</u> <u>(Kiss-Toth et al. 2004)</u>	Reversible inhibition of the MAPKK by binding partners such as the tribbles family (TRIB) was modelled in one ABM experiment in the two-compartment ABM by the introduction of a TRIB-agent. TRIB bound to pMAPKK changing its state to a MAPKK.
Protein intracellular movement		
Homogenous distribution of molecules in the cell is a prevalent representation of proteins in <i>in silico</i> models. However this assumption is becoming superannuated as more evidence indicate spatial separation and compartmentalisation of molecules within the cell	<u>(Klann et al. 2009)</u> <u>(Arora et al. 2013)</u> <u>(Canal et al. 2011)</u> <u>(Chiu et al. 2002)</u> <u>(Kholodenko 2002)</u> <u>(Donovan et al. 2016)</u>	A two compartment model was used where the appropriate proteins and kinases were homogeneously distributed in the cell. While in the multi-compartment ABM the proteins and kinases are distributed into cytosolic compartments
Brownian motion: Small and moderate sized molecules such as proteins move by Brownian motion in crowded environment and within the cytoplasm	<u>(Klann et al. 2011)</u> <u>(Klann et al. 2009)</u> <u>(Neves and Iyengar 2009)</u>	Each agent was assigned a transition function determining movement with a Brownian motion via an algorithm. The algorithm had an element of stochasticity where at each time step the rotation angles were chosen randomly by each agent
Molecular transport: Large objects such as organelles, chromosomes and endosomal vesicles are transported across the cytoplasm by intracellular transport system which involves large proteins such as kinesin and dynein	<u>(Voelzmann et al. 2016)</u>	The ABM did not address the movement of organelles or their transportation across the cytoplasm. Therefore, it was not included in the ABMs
Protein-protein interactions: Molecular behaviour involves chemical	<u>(Hlavacek et al. 2003)</u> <u>(Legewie et al. 2007)</u> <u>(Scott and Pawson 2009)</u> <u>(Suderman et al. 2013)</u>	The ABMs are driven by binding interactions between agents, whereby they determine their activation and inhibition status in addition to

<p>modifications preceded by collision, docking and molecular binding of molecules. Protein-protein interactions, by determining the identity of proteins in the complex and their spatial localisation, are driving molecular forces which were illustrated to influence cellular response.</p>		<p>their future interactions. This is analogous to the the natural system. Binding interaction is executed via transition functions and by message input-output exchange between agents via libmboard</p>
<p>Interactome determines response: The identity of the interacting proteins influence the outcome of the signal</p>	<p><u>(Santos et al. 2007)</u> <u>(Ahmed et al. 2014)</u> <u>(Romano et al. 2014)</u> <u>(Romano et al. 2014;</u> <u>Brahma et al. 2007)</u></p>	<p>This was utilised in the ABM by utilising the binding interaction between agents in the ABMs and allowing it to be the driving force of the ABMs. The concept was also utilised to facilitate the change of protein-agents (such as MAPK) to change to different states depending on its interaction partner.</p>
<p>Binding/docking and phosphorylation</p>	<p><u>(Hlavacek et al. 2003)</u> <u>(Legewie et al. 2007)</u> <u>(Scott and Pawson 2009)</u> <u>(Suderman et al. 2013)</u></p>	<p>Binding and docking was executed by transition functions whereby an agent scans the surrounding environment for its binding partners. When identified, the binding partners are notified, they confirm their interaction availability and consequently a bond is formed between the two agents</p>
<p>MAPKK-MAPK: A hallmark of the MAPK pathway is the interaction between the kinases especially the third tier MAPKK and MAPK whereby the main molecule MAPK is phosphorylated and activated. This involves their binding and the transfer of a phosphate group from ATP to MAPK</p>	<p><u>(Legewie et al. 2007)</u> <u>(Seger and Krebs 1995)</u> <u>(Zhang et al. 2002)</u></p>	<p>Interaction between MAPKK-MAPK was modelled when the two proteins came into close proximity. The intricate details of the phosphorylation step were not included in the ABM due to its rapid occurrence in relation to the calibrated run time in the ABMs. At every iteration, MAPK scanned the surrounding environment for the closest free pMAPKK. Once identified, the pMAPKK confirms the availability for binding and a bond forms</p>

		between the two agents.
<p>pMAPK-TF: pMAPK mediated gene expression events in the nucleus by phosphorylation of TFs that control the expression of particular genes. The event involves binding and phosphorylation of TF by pMAPK</p>	<p><u>(Efimova 2002)</u> <u>(Xu et al. 2004)</u> <u>(Volmat et al. 2001)</u> <u>(Mebratu et al. 2009)</u></p>	<p>pMAPK interaction mechanism with TF was identical to its interaction with MAPKK. The phosphorylation process was not included in detail due to the short time-scale of its occurrence; however, the outcome of phosphorylation (i.e. TF activation) is part of the model. Unlike the natural system, pMAPK involved in TF activation changed its state to allow to monitor the level of pMAPK involved in gene-expression initiation events</p>
<p>MAPK-ExR: Numerous MAPK nuclear export mechanisms are demonstrated in the literature, all involve interaction and binding with an exporting protein such as Importin 7</p>	<p><u>(Adachi et al. 2000)</u> <u>(Adachi et al. 1999)</u></p>	<p>The exporting mechanisms relied on binding interaction with a general exporting protein which was localised at the nuclear membrane. The mechanism of interaction are identical to those outlined for MAPKK-MAPK</p>
<p>MAPKKK-MAPKK: A hallmark of the MAPK cascade activation is signal propagation from first tier to second tier via MAPKKK phosphorylation and activation of MAPKK. This occurs by the co-binding of both proteins and the transfer of a phosphate group from ATP to MAPKK via a catalytic reaction conducted by MAPKKK</p>	<p><u>(Matsuda et al. 1993)</u> <u>(Takekawa et al. 2005)</u></p>	<p>Successful signal propagation from MAPKKK to MAPKK was initiated at t_0. MAPKK agents were in the dormant state and at t_0 MAPKKK were assumed to be fully active, and thus phosphorylated MAPKK leading to pMAPKK formation. MAPKK re-activation was integrated as part of RADD.</p>
<p>Regulation : feedback loops The MAPK pathway is tightly controlled via feedback loops which result into the modulation of the activation magnitude and duration. Regulatory loops are regarded as temporal regulatory mechanism.</p>	<p><u>(Brightman and Fell 2000)</u> <u>(Marshall 1995)</u></p>	

MAPKK was demonstrated to be a bottleneck for activating and inhibiting inputs		
Negative regulatory loops final outcome is to reduce levels of pMAPK to basal levels. The loops modulate the pathway at the three tiers. The involve the activation of phosphatases, inhibition of upstream cascade proteins such as MAPKK and SOS.	<u>(Lake et al. 2016)</u> <u>(Westermarck et al. 2001)</u> Inducible dusp expression: <u>(Kucharska et al. 2009)</u> <u>(Lin et al. 2003)</u>	Positive and negative regulation are both at play at any particular time, therefore the observed effect on the system is the outcome between a “tug of war” between both actions. Strong activation causes a prolonged activation of the cascade, while substantial inhibition result into brief activation and return to basal pMAPK levels in a short time. In the ABMs the net effect of inhibition and activation was translated via RADP. As MAPKK was regarded as the bottleneck for the pathway, RADP was implemented as a transition function rule governing MAPKK.
Positive regulatory loops involve enhancing the propagation of the signal downstream of the MAPK pathway. It was shown to be mediated through kinases and double negative loops. The final outcome is to increase pMAPK levels and increase the magnitude of the signal	<u>(Shin et al. 2009)</u>	
Receptor constitutive activity: whereby receptors are activated without the presence of their activating ligand and therefore automatically shift from active to inactive state	<u>(Rang 2006)</u> <u>(Bond and IJzerman 2006)</u> (Kleiman et al., 2011)	This property was used in the model to simulate the activation of the export receptor (ExR) via the memory parameter recdelay, where ExR automatically shift between active and dormant states. The former interacts with pMAPK to allow its nuclear export, while the latter does not interact with pMAPK

3.2.2 Physical environment

The process of cell signalling occurs within the internal cell environment (Alberts et al., 2002). Therefore, the cell was chosen to be the environment where model events

occur. Signalling through the MAPK pathway predominantly occurs within the cytoplasm and the nucleus, and ultimately drives cellular responses (Alberts et al., 2002, L'Allemain et al., 1992, Seth et al., 1992). Therefore, the cytoplasmic and nuclear compartments were chosen to be the site of interactions.

3.2.2.1 *Individuals within the environment:*

As highlighted in Chapter 1 and demonstrated in Figure 1. 1; the MAPK pathway is a three tiered cascade with the main proteins involved being MAPKKK, MAPKK and MAPK (Brunet et al., 1999). One of the main phenotypes of MAPK activation is its interaction and activation of nuclear proteins, predominantly transcription factors (TF) (Efimova et al., 2002, Xu et al., 2004). Therefore, TFs were considered in this model. Mechanisms to export activated MAPK (pMAPK) out of the nucleus to the cytoplasm are complex, however, it is reported that they rely on protein receptors which allow for pMAPK species to translocate out of the nucleus (Furuno et al., 2001, Horgan and Stork, 2003, Karlsson et al., 2004, Masuda et al., 2001).

3.2.2.2 *Temporal environment:*

The model aims to investigate the dynamics of MAPK activation, the influence of spatiotemporal changes on activation; and consequently their role in diversifying MAPK-dependent cellular responses. If the initial activation was through a temporary and abrupt signal, full activation of the pathway and deactivation events at the molecular level occurs and persists for minutes (Sasagawa et al., 2005b, Tomida et al., 2012). Given a continuous stimulus, the activation of MAPK can last for few hours (Macia et al., 2009).

3.2.3 Important behaviour

Chapter 1 described the complexity of the MAPK signalling network (see section 1.3). These include the multiple MAPK pathways, crosstalk and other mechanisms which influence MAPK activation dynamics, and ultimately determine cellular response. Subsequent sections identify and describe the important behaviours observed within the MAPK signalling pathway both at the cellular (system) and the protein (individual) levels.

3.2.3.1 Cellular environment and architecture

A typical cell is simply defined as “solution medium” (the cytoplasm) surrounded by a lipid membrane (plasma membrane) (Klann et al., 2011, Neves and Iyengar, 2009, Resat et al., 2011). The plasma membrane serves as the boundary which separates intracellular and extracellular environments. However, the cytoplasm is a complex fluid environment, composed of the fluid phase which dissolves both large and small molecules (such as proteins and monosaccharides respectively) and a network of cytoskeletal filaments (Luby-Phelps, 2000). The cytoplasm of eukaryotes encompasses several specialised membrane-bound compartments, such as the endoplasmic reticulum (ER) (Hudder et al., 2003, Takamori et al., 2006). In addition, the cytoplasm contains organelles such as the mitochondria and the ribosomes. Another important characteristic of eukaryotic cells is the presence of the nucleus where genetic material is stored and separated from the cytoplasmic environment by the nuclear membrane. In the nucleus, expression of genes is primarily controlled (Youngson, 2006). Separation between the compartments results in different compartments obtaining distinct characteristics and specialised functions, such as

the low pH of the lysosomes making it ideal as a site for protein degradation (Settembre et al., 2013). The classical assumption that the cytoplasm of eukaryotic cells is composed of homogeneously distributed proteins is outdated. Accumulating evidence demonstrates localised pools of proteins within specific cellular domains and within intracellular compartments (Arora et al., 2013, Canal et al., 2011, Chiu et al., 2002, Kholodenko, 2002). The separation provided by compartments insulates compartmentalised proteins from further enzymatic processing such as dephosphorylation and ubiquitination. Compartmentalisation also dictates protein-protein interaction as specific proteins are targeted into specific compartments. It was demonstrated that some compartments contain a 1-100 protein copy number in contrast to 1000s in the cytoplasm (Takamori et al., 2006).. Furthermore Takamori et al, also illustrated that the proteins stoichiometry within these compartments is regulated.

On page 103 the implementation of the cellular environment into the agent based model is outlined.

3.2.3.2 *MAPK pathway dynamics: ultrasensitivity and oscillatory behaviour*

Biologically, activation of the MAPK pathway is primarily characterised by two events (Figure 1. 1). The first is the increased phosphorylation of the MAPK proteins by MAPKK and hence phosphorylated MAPK (pMAPK) levels. (Seger and Krebs, 1995). The second event is the translocation of pMAPK proteins and the rapid increase of its levels in the nucleus. pMAPK interaction with transcription factors

(TFs) in the nucleus mediate gene expression events. MAPK phosphorylation and translocation occur almost simultaneously and in under 10 minutes (Ahmed et al., 2014, Costa et al., 2006, Kholodenko and Birtwistle, 2009).

Activation of MAPK and formation of pMAPK species, with respect to time, is characterised as either a digital/binary process (all or nothing), graded (analogue) or as an oscillatory process (Figure 3. 2) (Ferrell, 1997, Ferrell and Xiong, 2001, Tomida et al., 2012). The former activation behaviour appears as a nearly vertical sigmoidal curve, while the second appear as a sigmoidal curve where levels of pMAPK increase gradually (Ferrell and Machleder, 1998). In both the graded and the digital process the sigmoidal curve is composed of three phases. The initial phase is short and characterised by low and unchanged pMAPK levels. The second (middle phase) is characterised by a relatively short yet rapid increase in pMAPK formation. The third phase is characterised by the pMAPK levels reaching their peak and a deceleration in pMAPK formation leading to a plateau phase which lasts for few minutes. The digital/binary behaviour is termed the ultrasensitive response. Conversely, oscillatory activation behaviour exhibits an alternating increase and decrease in pMAPK levels (Figure 3. 2,) (Kholodenko, 2000, Wang et al., 2006). This behaviour was only recently demonstrated *in vitro*, although it was predicted by Kholodenko *et al in silico* when they investigated the effect of negative feedback loops on MAPK activation dynamics (Kholodenko, 2000, Shankaran et al., 2009).

The final outcome of modulation of gene expression by pMAPK is not immediate (Winkles, 1998). This is due to the lengthy period between modulation of

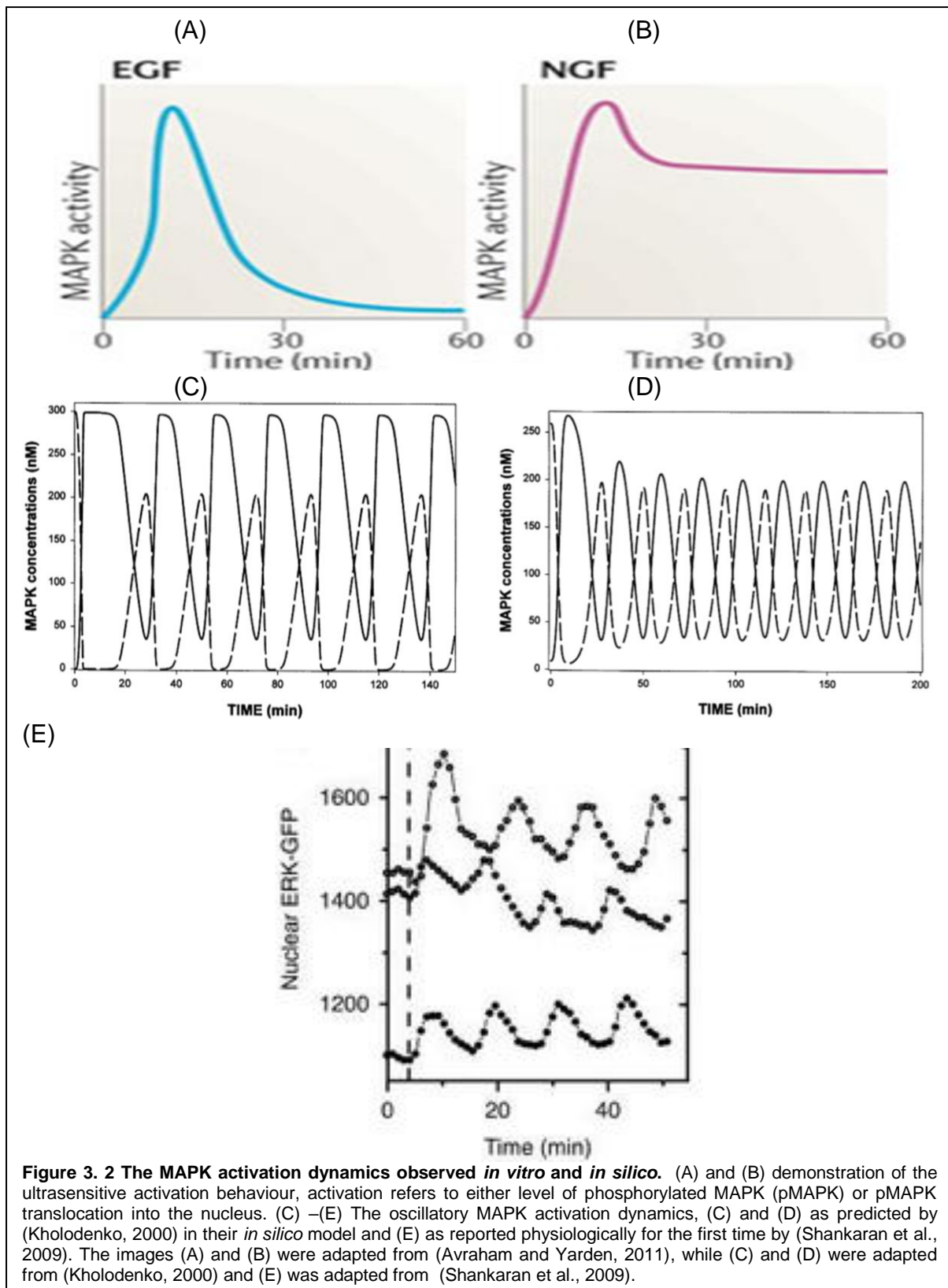


Figure 3.2 The MAPK activation dynamics observed *in vitro* and *in silico*. (A) and (B) demonstration of the ultrasensitive activation behaviour, activation refers to either level of phosphorylated MAPK (pMAPK) or pMAPK translocation into the nucleus. (C) –(E) The oscillatory MAPK activation dynamics, (C) and (D) as predicted by (Kholodenko, 2000) in their *in silico* model and (E) as reported physiologically for the first time by (Shankaran et al., 2009). The images (A) and (B) were adapted from (Avraham and Yarden, 2011), while (C) and (D) were adapted from (Kholodenko, 2000) and (E) was adapted from (Shankaran et al., 2009).

transcription and considerable alteration in the cellular protein levels (Matsushita et al., 2009). However, the immediate influence of pMAPK on gene expression events

can be monitored *in vitro* by several methods, for instance qPCR or microarrays measure mRNA levels of the gene(s) of interest (Murphy et al., 2002).

3.2.3.3 *MAPK pathway regulation*

Regulation of the MAPK pathway is either a prolonged response or a rapid deactivation (Brightman and Fell, 2000, Marshall, 1995). These are mainly mediated through feedback mechanisms and predominantly rely on protein-protein interactions (Nakakuki et al., 2010, Santos et al., 2007a), which were described in detail in Section 1.3.1.

3.2.3.4 *MAPKK activation dynamics:*

The MAPK pathway relies on propagation of phosphorylation events through the cascade (Alessi et al., 1995, Anderson et al., 1990, Burack and Shaw, 2000). Activation of MAPKK is believed to be the bottleneck for such a process (Alessi et al., 1995, Favata et al., 1998, Haeusgen et al., 2011). Activated MAPKK (pMAPKK) levels are elevated with persistent pathway activation due to constant activation of upstream cascade components such as the RTKs, or by positive feedback mechanisms, including the inhibition of the Raf kinase inhibitor protein (RKIP, Figure 1. 7) (Shin et al., 2009b). However, pMAPKK levels are reduced *via* several mechanisms including direct inhibition (Kim and Ferrell, 2007, Legewie et al., 2007) and dephosphorylation by phosphatase enzymes (Kins et al., 2003, Silverstein et al., 2002, Sontag et al., 1993). Phosphatase actions are outlined in Chapter 1 section 1.3.1.1.1.1.1. Phosphatase proteins are activated either immediately (phosphorylation *via* pMAPK) (Westermarck et al., 2001) or by the increased phosphatase gene expression (Kucharska et al., 2009, Lin et al., 2003). Other

mechanisms which result in the inhibition of MAPKK activity include protein degradation *via* ubiquitination, or inhibition. Inhibition is accomplished *via* the pMAPK (competitive inhibition, (Eblen et al., 2004)) and/or adaptor proteins such as the tribbles family of proteins (Kiss-Toth et al., 2004, Sung et al., 2006).

3.2.3.5 *Intracellular movement of the proteins.*

Intracellular protein movements occur within the cytoplasm and the nucleus. Physically, the cytoplasm is regarded as a semi-fluid compartment composed of a fluid and solid phase (Fels et al., 2009). The solid phase contains macromolecules such as polysaccharides, lipids and the cytoskeleton. The cytoplasm is composed of large compartments such as the Golgi apparatus and the endoplasmic reticulum (ER) (Raff et al., 2002). Smaller molecules such as amino acids, fatty acids and carbohydrates exist in the semi fluid phase. They and the macromolecules are thought to move through the cytoplasm by simple diffusion over short distances and *via* molecular transport over large distances (for instance from the cell body of neurones to the synapses) (Voelzmann et al., 2016). Computer models of cell signalling events, for simplicity, usually assume a homogeneously distributed and a well-mixed cytoplasm where molecules move through the cytoplasm by Brownian motion (Burrage, 2003, Burrage et al., 2006, Burrage et al., 2004).

3.2.3.6 *Translocation of pMAPK species*

After pMAPK formation, it translocates into the nucleus within few seconds. The precise mechanism of import into the nucleus is complex and many mechanistic features are proposed to be important (Costa et al., 2006, Liu and Geisbrecht, 2011,

Lorenzen et al., 2001). These include a passive translocation process, an importin protein-dependent process, or a pMAPK dimerization-dependent process. MAPK nuclear export is a rapid process and the precise molecular mechanism has not been resolved. However, the mechanisms proposed include the involvement of importin7, phosphatases and calcium immobilisation from nuclear stores (Liu and Geisbrecht, 2011, Lorenzen et al., 2001). There is also extensive evidence for the involvement of exporting proteins which shuttle MAPK out of the nucleus (Plotnikov et al., 2011).

3.2.3.7 *Protein-protein interactions*

The majority of cellular processes depend on proteins being in very close proximity and either binding *via* weak chemical forces or stronger covalent bonds (Hlavacek et al., 2003, Legewie et al., 2007, Scott and Pawson, 2009). These processes include transport across membranes, protein synthesis and cell signalling (Kholodenko et al., 2002, Nicolau et al., 2006, Suderman and Deeds, 2013)

3.2.3.7.1 Interaction of MAPKK and MAPK

Phosphorylation and activation of MAPK proteins involves MAPKKs binding to MAPK (Seger and Krebs, 1995). The kinase active site in MAPKK (with the presence of ATP molecule) catalyses the transfer of a phosphate group from ATP to either a threonine or tyrosine amino acids at MAPK activation loop, and consequently the formation of ADP molecules (Chang and Karin, 2001, Coulthard et al., 2009, Davies and Tournier, 2012). The addition of the phosphate group changes the MAPK tertiary conformation, thus stabilising and activating its kinase domain. It is widely believed

that the MAPK proteins require dual phosphorylation of the threonine and tyrosine residues for full MAPK activation (Ferrell and Bhatt, 1997, Kocieniewski et al., 2012, Ortega et al., 2006). However, there is speculation if this is a processive or distributive process (Burack and Shaw, 2000, Markevich et al., 2004, Ouldrige and Rein ten Wolde, 2014). Interaction of MAPK with MAPKK results in inhibition of MAPKK termed as competitive/cooperative inhibition (Chickarmane et al., 2007, Legewie et al., 2007, Ortega et al., 2006).

3.2.3.7.2 Interaction of MAPK with TF

Once pMAPK is imported into the nucleus, it interacts with several nuclear proteins to influence nuclear events (Efimova et al., 2002, Perdiguero and Muñoz-Cánoves, 2008, Xu et al., 2004). These include binding with TFs (such as Elk as c-Myc) to regulate gene expression. Gene expression events rely on binding of activated TFs to promoter sites in the DNA. Facilitating gene expression requires recruitment of RNA polymerases into promoters (Raff et al., 2002). This depends on the presence of specific combinations of TFs forming multimeric complexes (Funnell and Crossley, 2012, Scott and Pawson, 2009, Soufi and Jayaraman, 2008). The formation and activation of the right complex allows for mediation of gene expression events. pMAPK is capable of binding to monomer TF, or a multimeric complex where MAPK phosphorylation activates the complex and thus, ultimately, stimulates gene expression (Volmat et al., 2001).

3.2.3.7.3 Interaction with exporting receptors (ExR)

MAPK interaction with exporting proteins is required to allow for its export from the nucleus (Adachi et al., 1999, Adachi et al., 2000, Volmat et al., 2001). The process plays a role in inhibiting gene expression, because of reduced pMAPK availability to interact and activate TF complexes (Mebratu and Tesfaigzi, 2009, Volmat et al., 2001). The process is thought to involve the binding of the MAPK species with the exporting receptors at the internal interface of the nuclear membrane. The binding of pMAPK triggers a conformational change in ExR structure, leading to exporting pMAPK from the nucleus to the cytoplasmic interface of the nuclear membrane

3.3 Model formulation: Defining the agent based model (ABM) of the MAPK pathway

This section underlines how system specifications outlined in section 3.2 were implemented computationally.

A cellular response is dependent on molecular interactions. Molecular interactions rely on interaction of individual molecules (Deeds et al., 2012). The main interacting molecules in the MAPK pathway are the kinase proteins (Chang and Karin, 2001, Johnson and Lapadat, 2002). Every protein in the cascade varies in its activation state, interactivity and cellular location (Andreadi et al., 2012, Deeds et al., 2012, Harding et al., 2005b, Suderman and Deeds, 2013). These properties are important in shaping the activation dynamics of the pathway and the cellular response (refer to Chapter 1, section 1.3). Therefore, a molecular level ABM was used to model the

cascade downstream of MAPKKK, where MAPKKK being represented by the activation trigger occurring at t_0 , because MAPKKK activation signifies the initiation of MAPK pathway stimulation, which is immediately followed by MAPKK activation, consequently, the individuals included in the model were MAPKK and MAPK (Ferrell, 1997, Kholodenko, 2000). The individual behaviour of MAPKK, MAPK, TFs and ExR were defined by roles, which were executed by the agents. These roles (at the level of individual proteins) were used to examine spatiotemporal properties of the cascade and how they contribute to cellular MAPK activation dynamics.

Implementing the roles which closely depict the interaction and activation behaviour of the proteins involved in the cascade allows for investigating the effects of different interaction combinations and activation behaviours in space and time. As a result, assessment of the significance of these combinations, and their contribution to the complexity of the pathway activation dynamics can be conducted. The model, therefore, will allow us to look into molecular interactions, in space and time, which lead to emergence of ultrasensitivity and oscillatory activation behaviour. Furthermore, the model will allow for characterising the molecular mechanisms which return the system back to basal conditions, and exploring the potency of these mechanisms to down-regulate activation.

Most cells adhere to somewhat generic behaviour as they implement fundamentally identical mechanisms to achieve it. The presented ABMs were designed to emulate this and, thus were built as generic models. Furthermore, part of the mystery of the MAPK signalling pathway is that it is utilised by different cell types with similar activation dynamics, yet, the cellular outcomes differ. This is generally believed to be

due to alterations in molecular signalling parameters such as signal intensity and feedback mechanisms in space and time. The ultimate and long-term aims from using the ABM approach are: (1) examine how cell-specific behaviour develops, despite different cell types employing the same elements and generic behaviour; (2) identify which molecular parameters (both spatially and temporally) are altered to achieve this and (3) how these lead to cell-specific responses. Hence, obtaining the generic behaviour of *The Cell* is key to moving forward with future work and/or contributions to the field of MAPK signalling.

3.3.1 Creating the system boundaries:

This section describes computational translation and implementation of the boundaries (identified and described in section 3.2.1). Table 3.1 summarises the process.

3.3.1.1 *Physical environments*

Signalling through the MAPK pathway takes place intracellularly, predominantly in the cytoplasm and the nucleus. Therefore, a three-dimensional (3D) model of the cell was used as the global environment. Biologically, the main entities which create physical boundaries between these cellular compartments are lipid membranes. Therefore, nuclear and plasma membranes were specified as environments and their radii were specified as an environmental boundary in the model. The diameter of a cell is 10-100 μm and the nucleus diameter is 3-10 μm with an average of 6 μm . In FLAME, distance is divided into arbitrary points, thus every distance point was

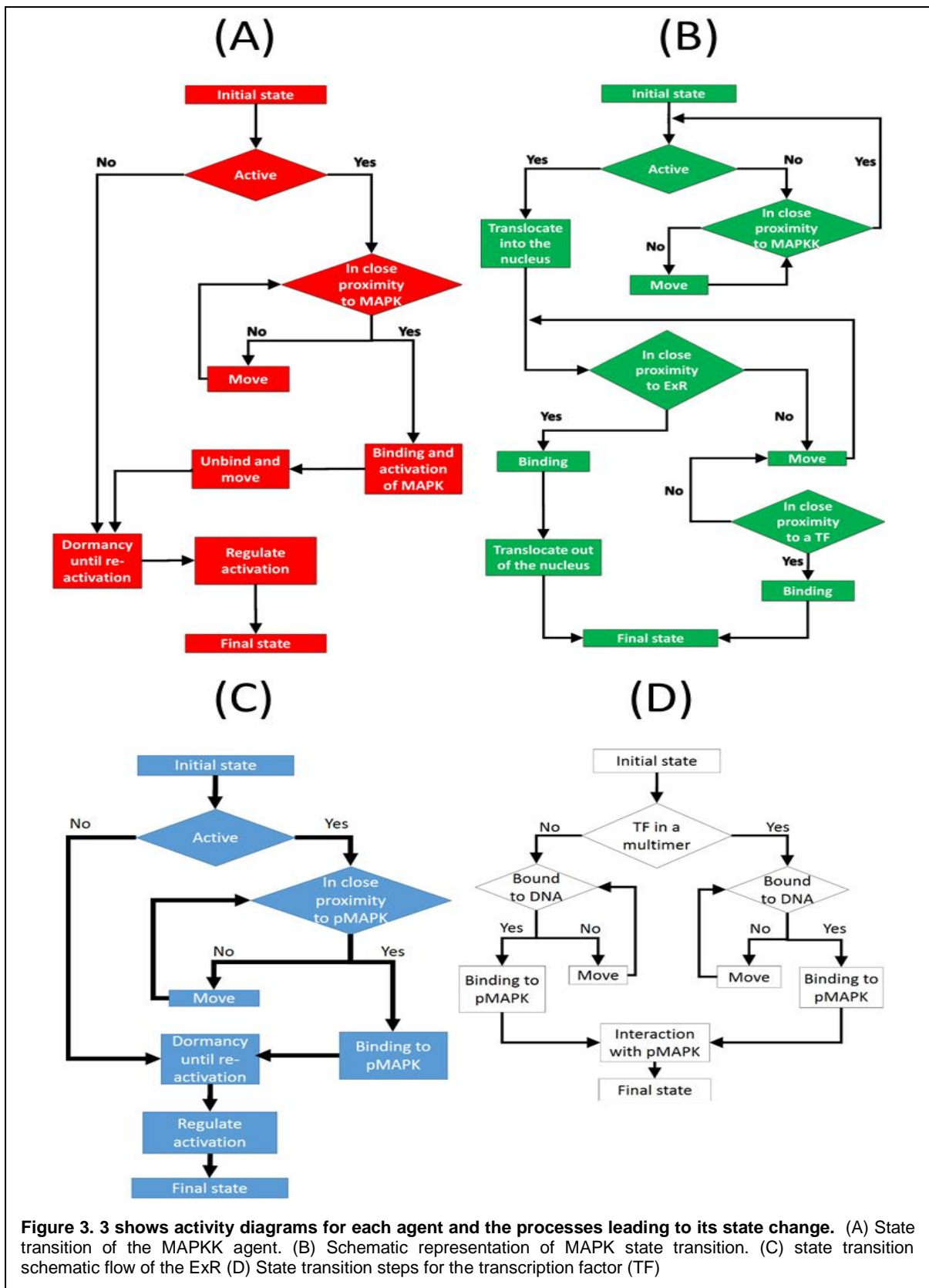


Figure 3.3 shows activity diagrams for each agent and the processes leading to its state change. (A) State transition of the MAPKK agent. (B) Schematic representation of MAPK state transition. (C) state transition schematic flow of the ExR (D) State transition steps for the transcription factor (TF)

assigned a value of 1nm. The cell size chosen for the ABM was double the size of the smallest cell (i.e. 20 μ m). While the size picked for the nucleus was a middle value between the average and the largest size of a nucleus (8 μ m in diameter).

Therefore, a moderate cytoplasmic volume is created to accommodate for the protein number. The membrane-bound intercellular compartments boundaries were also specified. The size selected for an individual compartment was 1µm which is equivalent to the size of a small mitochondrion (Raff et al., 2002). The protein agents were made to deflect away from the membrane once their 3D coordinates reached the membrane boundaries. For simplicity, viscosity and porosity of the cytoplasm and the nuclear environment were not considered in the model.

3.3.1.2 *Individual agents within the ABMs*

The MAPK pathway incorporate numerous proteins which are involved in pathway activation and regulation, Including all mechanisms and the proteins involved in the MAPK signalling network (at this stage) adds unnecessary complexity to the model, which renders it difficult for implementation, analysis and validation (Deeds et al., 2012, Suderman and Deeds, 2013). Therefore, using the evidence from the literature, only the primary proteins involved in the pathway and the mechanisms considered necessary for the MAPK pathway functionality were adapted and implemented in the presented ABMs. To overcome this a black-box approach was utilised to implement behaviour and components in the pathway such as feedback loops. Using the ABM formalism, said components can be improved and expanded in consequent models in the future. The individuals which were chosen to represent the pathway were predominantly the MAPKK, MAPK and ExR. Any additional agents or alteration of agents' behaviour(s) are highlighted and described in the appropriate result chapter. These autonomous agents can attain different states. Interaction

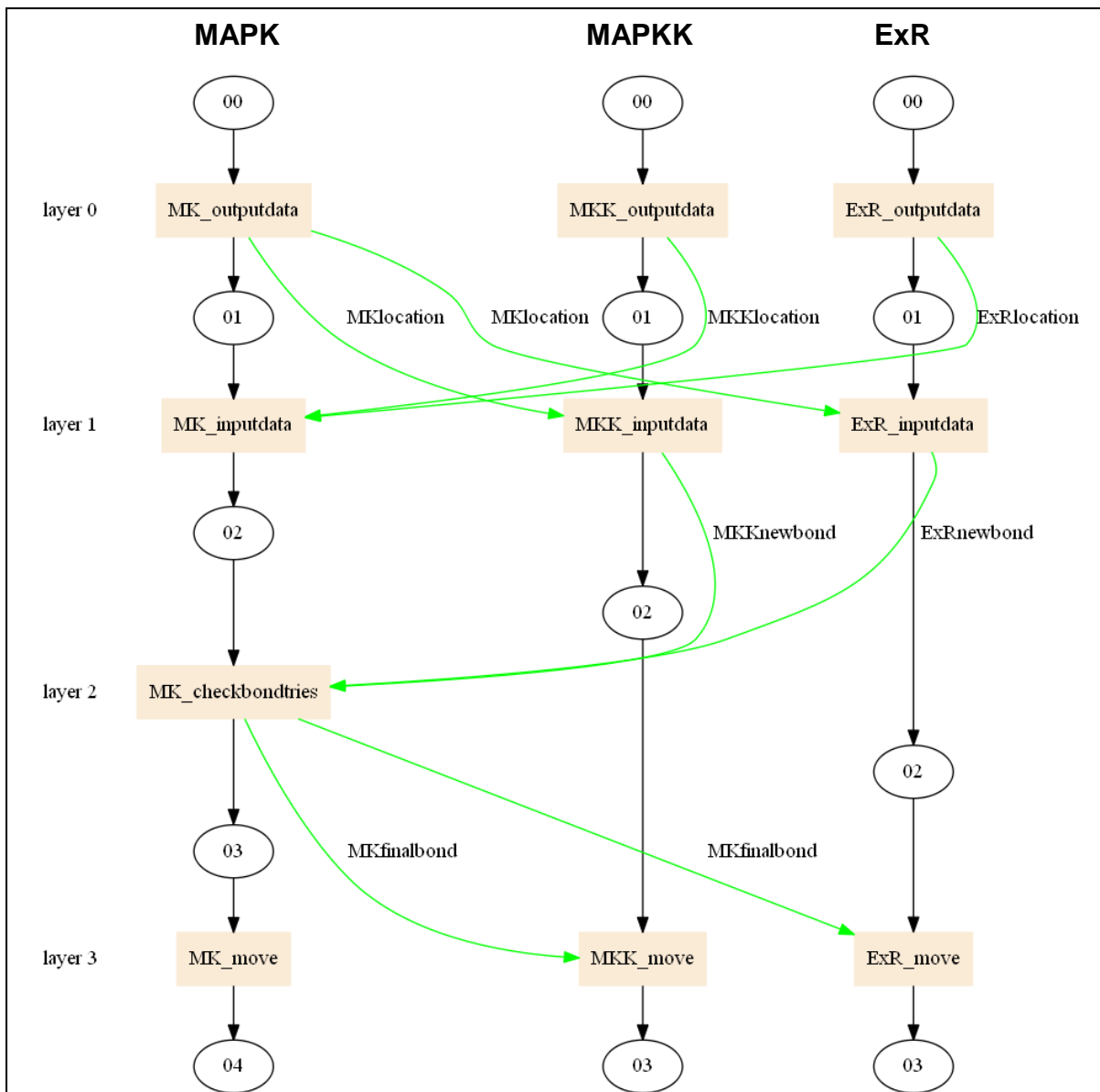


Figure 3. 4 Stategraph for the agents in the Agent Based Model (ABM) illustrating the processes of state change, communication and message input/out by the three primary agents in the ABM. The initial state 00 is the native state at the start of the simulation; agents execute the first transition function (indicated by the brown box). The execution of the transition function output messages (denoted by the green arrows). Transition function full execution allows the agent to occupy a new state (01). The new state executes a new transition function which may require a message input. The agent accesses messages from the libmboard. The process of state change, transition function execution and message input-output continue until the last transition function is completed. This marks the end of a simulation

between the agents relied on binding events and bond formation between them. A summary of the pivotal agents in the ABMs are described below.

3.3.1.2.1 MAPKK (total MAPKK (tMAPKK))

Intracellularly, MAPKK exists in either a phosphorylated or unphosphorylated states. The former is the active state while the latter is the inactive state (Raff et al., 2002). Therefore, MAPKK in the ABM was modelled to exist in either an active state (pMAPKK) or inactive/dormant state (henceforth referred to as MAPKK). Consequently, it is worth noting that tMAPKK (MAPKK in both active and inactive state) is referred to henceforward as tMAPKK. pMAPKK only interacts with the MAPK agents. tMAPKK was modelled to move by Brownian motion, which is further described in section 3.3.2.1.1 below (Klann et al., 2011, Pogson et al., 2006). In the two compartments ABM, this movement is restricted to the cytoplasm, where it is deflected off the plasma membrane and the nuclear membrane. Movement in the multi-compartment ABM is restricted to within the individual compartment boundaries. tMAPKK agents contain memory parameters which specify the 3D position in Cartesian and polar coordinates (see Appendix A, Table 1 and Appendix A, Table 6). The protein activation/phosphorylation state was monitored using the memory parameters [state] and [RADP]. To simplify agents' movement and diffusion, each was modelled as a single point. Interaction with MAPK was monitored using the memory parameter [boundindex]. pMAPKK interaction with MAPK occurred as the former agent reads locations messages of the different MAPK agents; determining the closest MAPK available for binding. pMAPKK sends location messages and binding status messages to neighbouring MAPK agents. Once binding availability confirmation is established between MAPK and pMAPKK, binding occurs. This leads to the change in pMAPKK status to MAPKK. MAPKK reverts back into pMAPKK after a lag phase (regulated by the parameter re-activation delay period, [RADP]).

tMAPKK activity is summarised in Figure 3. 3 (A), while its state transition is shown in Figure 3.4

3.3.1.2.2 MAPK

MAPK move by Brownian motion. Similar to tMAPKK, this is traced *via* memory parameters which record its 3D position in Cartesian and polar coordinates (peruse Appendix A, Table 3 and Appendix A, Table 7). However, the movements of the different states are distinct. Inactive MAPK is restricted to moving in the cytoplasm or within the boundary of its specific compartment, whereas pMAPK is restricted to the nucleus. To simplify MAPK agents' movement, they were considered as points. MAPK exists in two states: active (phosphorylated (pMAPK)) or inactive (MAPK). These were monitored by the memory parameter [state]. MAPK interaction with its binding partners relied on the memory parameter [radius]. MAPK interacts with a several agents in the model. This utilises the memory parameters [radius] and [state]. MAPK sends messages of its location and binding availability to be read by its interacting partners. Once binding availability is confirmed, the interaction between MAPK and its interaction partner occurs. MAPK interacts with pMAPKK in the cytoplasm and with ExR at the internal surface of the nuclear membrane. Interaction with pMAPKK leads to MAPK activation, change of status to pMAPK and nuclear translocation. In the nucleus, pMAPK interacts with ExR, leading to pMAPKs export to the cytoplasm or its specific compartment in the multi-compartment system, and subsequently, the re-formation of MAPK. Figure 3. 3 (B) summarises MAPK activity, while **Figure 3.4** illustrates its state transition.

3.3.1.2.3 Exporting receptor (ExR)

The movement of ExR was restricted to the circumference of the nuclear membrane. The movement was modelled as a Brownian motion within the circumference of the nuclear membrane (Nicolson, 2014). This was monitored using the memory parameters which recorded its 3D position in Cartesian and polar coordinates (found in Appendix A, Table 4 and Appendix A, Table 8). Receptors are shifting between active and inactive states and vice versa (Bond and IJzerman, 2006, Rang, 2006), thus ExR were modelled in two states, active (ExR) and inactive (iExR). These were specified by the memory parameter [state]. These two states are interchangeable. iExRs shift back to ExR after a lag phase (dormancy period) which is specified by the memory parameter [redelay]. ExR interacts with pMAPK, which utilises the memory parameters [state], [radius] and [boundindex]. An activity diagram of ExR is shown in Figure 3.3 (C), and ExR state transition is illustrated in Figure 3.4.

3.3.1.2.4 The MAPKK protein inhibitor tribbles (TRIB)

Tribbles is a family of pseudokinases which were shown to bind to MAPKK protein and induce an inhibitory action on MAPKK proteins in the MAPK pathway (Kiss-Toth et al., 2004). In the two compartments ABM TRIB proteins were modelled as a generic cytoplasmic protein which moves by Brownian motion. This was monitored using the memory parameters which recorded its 3D position in Cartesian and polar coordinates (see Appendix A, Table 1). TRIBs interact with pMAPKK agents when both proteins are within close proximity to each other (Hegedus et al., 2007, Sung et al., 2007). Successful binding of TRIB to pMAPK induce both protein agents to change state from active to inactive states (MAPKK and dTRIB respectively, see

Figure A. 1). Both protein agents revert back to their active state after few milliseconds. This interaction behaviour utilises the memory parameters [state], [radius] and [boundindex].

3.3.1.3 *Temporal environment*

The time to illicit full activation of MAPK *i.e.* by forming the maximum level of pMAPK species (E_{max}) was determined from the literature and was used in the ABMs. This is demonstrated and discussed further in section 3.3.2.2.1 on page 106. Briefly, 80 graphs from the literature demonstrating the time to achieve pMAPK E_{max} were manually analysed. The analysis illustrated that the representative time to reach pMAPK E_{max} was 7.63 min.

3.3.1.4 *Binding interactions time*

Binding of MAPKK and activating MAPK by the addition of phosphate groups is an important attribute of the MAPK pathway activation (Anderson et al., 1990, Chang and Karin, 2001). Individual chemical interactions and reactions occur within micro time-scales. The addition of a single phosphate group as a result of ATP hydrolysis occurs within femto-seconds (Perkins et al., 2010). Modelling these reactions accurately and within the natural time-frame is possible; nonetheless inclusion of these steps requires complex calculations as well as being computationally expensive due to model processing of individual binding events and the large data produced (Shaw et al., 2014, Stefan et al., 2014). Additionally, inclusion of these processes will not assist the ABM in investigating the spatiotemporal elements which affect MAPK signalling, as the purpose of the model is to investigate protein interactions after the formation of these bonds. Therefore, the precise mechanisms

were not included in the model and a simplified bond formation was modelled. Consequently, the time assigned for the full binding interaction in the model was estimated to be, and set to, 0.91 second per iteration (Daub et al., 2008, Olsen et al., 2006, Perkins et al., 2010).

3.3.2 Agent behaviour:

This section describes the behaviour of the agents within the model and the computational algorithms (transition functions) used to execute these behaviours. A sample of the transition functions that was used for each of the agents is in Appendix A, Table 3-Appendix A, Table 4 and Appendix A, Table 9-Appendix A, Table 11. In section 3.2.2, the fundamental properties and behaviour in the system were highlighted. The computational process by which these behaviours were converted into simulation is outlined below. The behaviours were divided into 1) individual behaviours, which are specific to an agent species (e.g. MAPKK agents) or 2) system level behaviour, where the behaviour applies to all the agent species. System level behaviours include agent movement, communication and binding interactions. Agent level behaviour includes the activation of MAPKK and MAPK, agents' protein-protein interactions, and MAPK nuclear import and export. Any additional or altered agent or system behaviours were mentioned and described in the appropriate result section.

3.3.2.1 System level behaviour

3.3.2.1.1 Movement of the agents

To be in line with the majority of previously published models of the MAPK pathway, the initial MAPK ABM was constructed for a cell with a homogenous distribution of proteins moving by Brownian motion. Conversely, the subsequent multi-compartment ABM had adapted a more biological representation of protein distribution by placing the proteins within multiple cytoplasmic compartments, where movement of the proteins within the compartment were assumed to occur through Brownian motion, as they are located within a very small volume.

All the agents were modelled to move by Brownian motion within the 3D space of the cell. This is to mimic simple diffusion of molecules within the cytoplasm. The function `[[Move]]` was designed to execute stochastic Brownian 3D movement using polar coordinates. This relied on specifying the polar angles phi and theta (`[movephi]` and `[movetheta]` respectively) and the radial coordinate `[mover]`. With each time-step, the value of phi and theta are updated and random angle values were chosen. These changes transferred into random motion. Once an agent reaches the environmental boundaries of either the plasma, nuclear or the intracellular-compartment membranes, the agents deflect from the membrane by reversing the value of phi and theta and the value of `[mover]`.

3.3.2.1.2 Communication between agents

This was achieved by the use of messages (see Appendix A, Table 5 and Appendix A, Table 12-Appendix A, Table 14). The messages are inputted and outputted using the agents functions (refer to Appendix A, Table 4 and Appendix A, Table 9-Appendix A, Table 11 for the messages inputted by individual functions). The messages are stored in FLAME's message library (libmboard) and individual agents accessed particular messages required for interaction with their binding partners. Agents went through state transitions and the memory parameters were updated once the messages were read and the functions were performed (based on the specified algorithm code and the conditions set within it).

3.3.2.1.3 Binding interaction

Binding interaction was executed by the transition functions [[outputdata]], [[inputdata]] and [[checkboxodtries]]. In summary, an agent surveys the environment for its closest binding partner, once this was located, the agent assesses if the binding partner is free for interaction. When the binding availability was confirmed the two agents bind, a confirmation for bond-formation is established and consequently both agents change state.

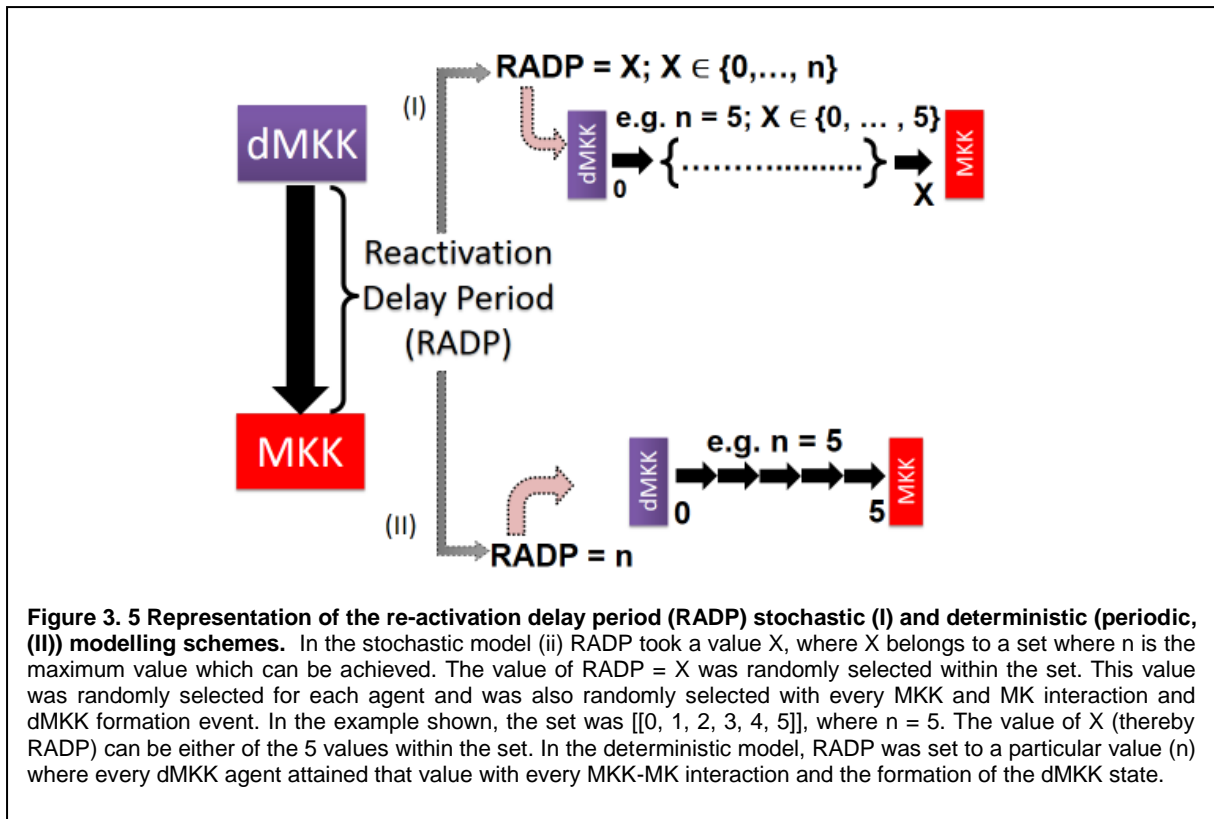
3.3.2.2 *Agent specific behaviour*

3.3.2.2.1 MAPK phosphorylation process and its activation dynamics

The model addresses the initial short-term MAPK activation phase (within the first 45 min of activation) and monitors the activation behaviour during that period.

Therefore, long-term activation responses, which involve modulation of gene expression events, are out of the scope of the model.

Activation/phosphorylation of MAPK agents was modelled as a change in state due to binding interactions with pMAPKK agents. The transition functions `[[MAPK_outputdata]]`, `[[MAPK_inputdata]]` and `[[MAPK_checkbodtries]]` with the memory parameter `[state]` executed such behaviour (Heinrich et al., 2002, Kocieniewski et al., 2012, Ouldrige and Rein ten Wolde, 2014). The phosphorylation process was modelled as a processive mechanism, whereby a pMAPKK undergoes the dual phosphorylation of MAPK in one binding interaction. pMAPK levels were measured to monitor the activation dynamics of the pathway. Since the ultrasensitive response is a characteristic based on the formation of pMAPK species, it was expected to emerge as a result of pMAPKK and MAPK agents interaction and pMAPK formation. This was used as the key output measurement for ABMs validation by measuring the time required to achieve pMAPK E_{max} and the time required to reach its EC_{50} . Furthermore, pMAPK species were modelled to translocate to the nucleus once state change takes place. Nuclear events and interaction with TF to initiate gene expression events were attempted in one of the ABMs to mimic the secondary pathway activation characteristic and, therefore, act as secondary measurable output for the model. This is to mimic biological experiments where levels of gene expression are measured using techniques such as microarrays where the levels of mRNA of a target gene are monitored with and without the activation of the MAPK pathway (Murphy et al., 2004).



3.3.2.2.2 MAPKK activation dynamics

MAPKK activation cues start at the beginning of model simulation; mimicking the phosphorylation event by the upstream kinase MAPKKK (Balan et al., 2006, Calipel et al., 2006, Craig et al., 2008). Transition functions $[[MAPKK_inputdata]]$ and $[[MAPKK_outputdata]]$ alongside the memory parameter $[state]$ control the process. Biologically, MAPKK proteins are under regulation by positive and negative feedback mechanisms and the balance between the two processes determine active MAPKK levels (and thus the intensity of signalling through the pathway) (Sturm et al., 2010a, Fritsche-Guenther et al., 2011, Tian and Harding, 2014). This was modelled by the memory parameter Re-Activation Delay Period $[RADP]$ which controlled the period of time MAPKK remained in the dormant phase, thus mimicking the net balance between exciting and inhibiting inputs at the level of MAPKK. Thus, $[RADP]$ represents the temporal regulatory mechanism for the cascade. pMAPKK interaction

with MAPK lead to MAPK activation and formation of MAPKK species represented biological inhibitory processes such as cooperative/competitive inhibition or due to negative feedback (Brunet et al., 1994, Eblen et al., 2004, Ortega et al., 2006). An RADP value is assigned to every tMAPKK agent and was updated when MAPKK was restored to pMAPKK state. The RADP value was updated either deterministically or stochastically (Figure 3. 4). For deterministic update, the value for every tMAPKK was identical and predetermined before commencing model simulations. For stochastic update, RADP was set (for individual tMAPKK agents) randomly between 0 and a pre-determined value.

3.3.2.2.3 MAPK nuclear export and interaction with ExR

Export of the pMAPK agent species was modelled as dependent on the interaction of pMAPK with ExR at nuclear membrane internal surface. Active ExR received location messages from pMAPK; the closest pMAPK confirmed availability to bind, once bound to ExR, pMAPK translocated out of the nucleus and both agents changed state: pMAPK to MAPK and ExR to iExR. MAPK nuclear export is mediated by the transition functions `[[ExR_inputdata]]`, `[[ExR_outputdata]]`, `[[ExR_move]]`, `[[MK_inputdata]]`, `[[MK_outputdata]]`, `[[MK_checkboundtries]]` and `[[MK_move]]`.

3.3.2.2.4 ExR automatic activation

The convention that receptors are in dynamic equilibrium between active and inactive states is well established pharmacological concept (Khilnani and Khilnani, 2011). Furthermore, automatic receptor activation is a well-documented phenomena among receptors (Bond and IJzerman, 2006, Vezzi et al., 2013) However, there is no

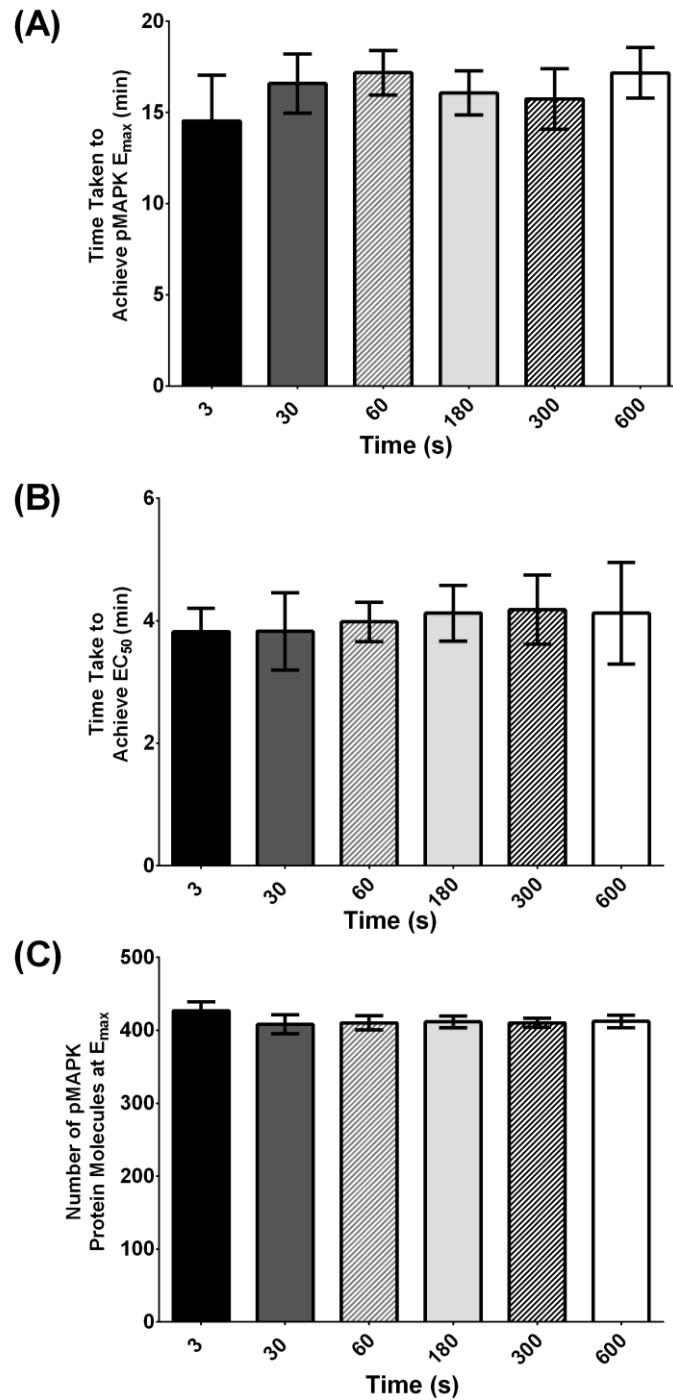


Figure 3.6 A sensitivity analysis of ExR [recdel] value on MAPK activation dynamics. The magnitude (A) and time to achieve E_{max} (B) and EC_{50} (C) were not significantly altered with increase in [recdel] value until the [recdel] value reached 6 min. Bar values represent mean \pm SD. * signifies a statistical significance where $p \leq 0.05$. $n = 10$ simulation per model.

evidence in the literature indicating the exact time frame for this shift between active and inactive states for receptors, and specifically for the exporting receptors involved in the MAPK translocation. Therefore, this behaviour was approximated in the ABM based on Kleiman et al study (Kleiman et al., 2011). First, the ExR was modelled to

exist in two states, active and inactive, and the agent cycles between the two states frequently, mimicking the natural state of constitutive activity of receptors demonstrated pharmacologically in vitro (Bond and IJzerman, 2006, Rang, 2006). This behaviour was mediated using the transition function $[[\text{ExR_inputdata}]]$ where $[\text{recdelay}]$ was controlled. The $[\text{redelay}]$ selected was stochastically modelled; however, it was within 3 s as reported by Kleiman et al (Kleiman et al., 2011). A sensitivity analysis was conducted for the values of $[\text{recdelay}]$ and the effect was of no statistical significance on the pMAPK E_{max} , and the time to achieve E_{max} and EC_{50} within the initial 10 min as shown in Figure 3. 6.

3.3.3 Model inputs and outputs.

The initial inputs of the model were the initial conditions at t_0 . These included starting position and direction of the agents, the compartment they reside in, their initial activation state, the predetermined $[\text{RADP}]$ value and their identity and availability for binding interactions. The output from the model (measured as emergent behaviour) included the updated activation state, the number of tMAPKK agents (both in the active and dormant state); the number of MAPK agents (both active and inactive), the number of pMAPK which interacted with TF; and the number of gene expression initiation events.

From the above outputted data, the following measurements were calculated:

- I. The maximum number of pMAPK, MAPK, MAPKK and dMAPK formed (E_{max}).

- II. Relative activation (number of pMAPK/total MAPK)

- III. The time to achieve E_{max} .

- IV. The half maximum number of pMAPK, MAPK, MAPKK and dMAPK (EC_{50}).

- V. The time required to achieve EC_{50} .

- VI. Rate of conversion of MAPK to pMAPK during the linear phase (second phase) of the ultrasensitive response.

- VII. Rate of conversion of pMAPKK to MAPKK.

3.4 Initial conditions and parameters for the agent-based models (ABMs)

Below are the conditions which were used to set-up the model at t_0 . These conditions were largely adapted/derived from the literature. When a quantitative value was not obtainable from published data, an informed estimation was conducted to derive a quantitative value.

3.4.1.1 *Activation trigger*

The model was designed from the point where the activation signal is transduced to MAPKK *via* phosphorylation of MAPKKK. At t_0 it is assumed that MAPKKK bound and interacted with MAPKK agents. In addition, to simulate physiological conditions of resting cells in this model, at t_0 the 99% of MAPKK agents were in an inactive state (MAPKK), and 0-50% of MAPK agents were not phosphorylated/activated (pMAPK).

3.4.1.2 *Total activation time*

Biologically, the highly characteristic ultrasensitive response of the MAPK pathway occurs within the first 5-10 minutes following stimulus reception. The peak and plateau phase are fully accomplished within 10 minutes. However, the deregulation and deactivation phases can be slow and require between 10-40 minutes (or more) depending on the balance between activating and deactivating inputs into the pathway. Thus, as the focus of this work was to investigate the activation dynamics of MAPK, simulations were run to cover 45 minutes from the initial activating cue.

3.4.1.3 *Numbers of agents*

The number of kinase agents in the cascade (MAPKK, pMAPKK, MAPK and pMAPK) used in the model at t_0 , was inferred from the concentration values calculated using an ODE model based on Huang *et al* (Huang and Ferrell, 1996). These concentrations were converted to moles by adapting the average number of mean corpuscular volume of red blood cells (≈ 90 femtoliter) as the volume these

	inactive MAPKK (dMAPKK)	active MAPKK (pMAPKK)	inactive MAPK (MAPK)	active MAPK (pMAPK)	TRB
Concentration (μM)	1.2	0.0003	1.2	0.6	2
Number of Moles	1.50E-16	3.75E-20	1.50E-16	7.50E-17	2.50E-16
Number of protein molecules	9.03E+07	2.26E+04	9.03E+07	4.52E+07	1.51E+08
Ratio between number of protein molecules	4.00E+03	1.00E+00	4.00E+03	2.00E+03	6.67E+03
Number of protein molecules used in the model	5.00E+02	≈ 0	5.00E+02	2.50E+02	8.33E+02

Table 3. 2 number of agents used in the agent based models (ABMs) and their derivation. The numbers of agents were stipulated from the concentration of their corresponding proteins as published by (Ferrell and Bhatt, 1997, Ferrell and Machleder, 1998). The table also demonstrate the number of agents used in the ABMs after simplification as referred to in section 3.4.1.3

proteins were present in. Moles were then converted into the number of protein molecules using Avogadro's number. Table 3. 2 summarises the process and shows the numerical values adapted in the model.

Converting the concentration of protein molecules into proteins numbers had resulted in protein numbers in the magnitude of millions. Consequently, a full scale model will require the total number of agents to be in the magnitude of hundreds of millions. This ultimately leads to a substantial time delay in executing the model per time step rendering the model computationally expensive, without obvious advantages. This is highly undesirable, especially at the model development phase. Therefore, to simplify this and to allow for more proficient model runs and development, the model was downscaled and the number of proteins were reduced to the magnitude of hundreds (Table 3. 2). The intention was to eventually upscale the model in future when it was completely validated and has demonstrated accuracy in replicating the behaviour of the real biological system.

Although the number of individual proteins was downsized, nonetheless, the ratio between the different protein species was kept constant. This is to closely emulate the cellular environment (as shown in Table 3. 2).

3.4.1.4 *Location and agent distribution*

Previous *in silico* models of the MAPK pathway assume a homogenous distribution of MAPKKK, MAPKK and MAPK in the cytoplasm in a well-mixed cell. To adhere to this assumption, MAPKK and MAPK agents were distributed randomly within the 3D environment of the cytoplasm and similarly for nuclear agents. However, ExR distribution was restricted to the nuclear membrane.

3.4.1.5 *The 3D environment*

Two main ABM models were used for simulating the MAPK pathway. Both were different in the architecture of the cytoplasmic 3D environment. The first ABM followed the conventional *in silico* models where the kinase proteins were distributed over two compartments (the cytoplasm and the nucleus). However, the second ABM adapted a more biologically accurate architecture of the cytoplasm and incorporated multiple cytoplasmic compartments where the kinase proteins reside. The size of a typical animal eukaryotic cell is 10-100 μ m in diameter and the average size of the nucleus is typically 6 μ m in diameter (with a range of 3-10 μ m in diameter). In FLAME, every arbitrary unit of distance was assigned to 1nm. The diameter of the cell was chosen to be 20 μ m in diameter to match the downscaling of protein content in the cell (see Table on page 103) while the chosen nucleus size was 8 μ m in diameter. In regard to the size of the individual compartments, these were modelled as 10 cubic compartments with a length of 1 μ m, equivalent to the length of a mitochondrion. The

number of compartments was arbitrary as compartments such as the ER, endosomes and Golgi apparatus are continuous compartments.

3.5 ABMs calibration, rule validation and analysis

This subsection is dedicated to the ABMs construction, validation and sensitivity analysis. Calibration of simulation time and its derivation from the literature is presented. Implementation of the models is then reviewed. These include (1) validating the application of the roles assigned to the agents; (2) sensitivity analysis conducted on the ABMs and (3) a comparison between the different spatial ABMs for the MAPK pathway.

3.5.1 Model rule validation and optimisation

Agent Based computational Modelling (ABM) is a bottom up modelling approach. It relies on modelling the essential components of the system and how these components interact with each other. The interaction of these components together defines the behaviour of the whole system. This modelling approach highlights the low level roles, which are critical contributors to system behaviour. The ABM approach has been successfully used in different fields such as ecology, economics and cell biology to explain and show how low level interactions play an important role in the emergence of behaviour at the system level. To our knowledge, a molecular ABM of the MAPK pathway was never attempted before, thus it was necessary during the model building process to validate and insure accuracy and efficiency of agent interactions, state transition and role execution. This section is devoted to

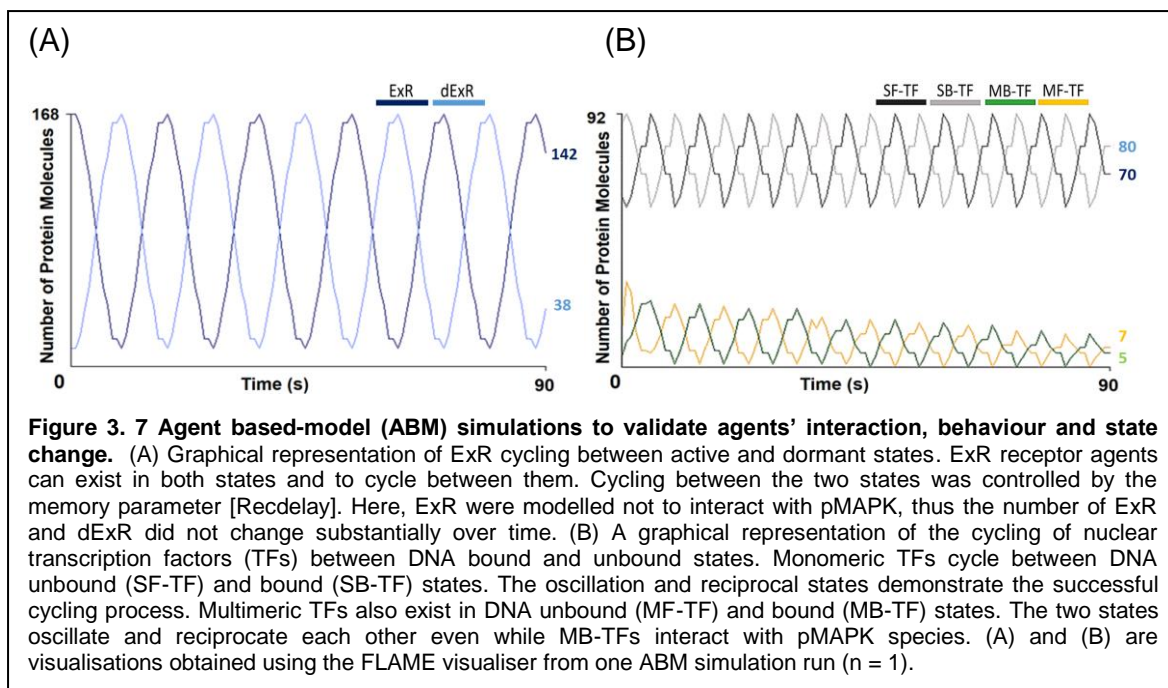
examining essential agent properties such as interaction with partners, state transitions and changes in internal memory parameters. The following sub-sections (4.1.2.1-4.1.2.5) demonstrate model assessment and validation methods at the initial stage of ABM construction. The properties examined and validated therein (such as agents' movements) were chosen as they are essential characteristics for the performance of the ABMs. The process of assessment, validation and improvement were performed at every stage of ABM development.

3.5.1.1 Validation of agents auto-state transition

Although the ABMs incorporated regulatory mechanisms to modulate the MAPK pathway, it was not possible to include all the regulatory mechanisms in these models. Therefore, in order for some agents to return to their initial state, they were modelled to cycle between active and inactive/dormant states. The agents concerned and the validation of the process is described below.

3.5.1.1.1 MAPKK cycling between active (pMAPKK) and inactive (MAPKK) states

Availability of pMAPKK to interact with MAPK agents is important to sustain MAPK pathway activation and signal propagation. Thus, it was necessary to allow for MAPKK to cycle between the two states. This was achieved *via* the re-activation delay period [RADP] parameter. Cycling between the two states was validated, and the successful cycling between the two states is demonstrated in video 4.1.



3.5.1.1.2 Exporting nuclear receptors (ExR) cycling between active (aExR) and dormant/inactive (iExR) states

Receptors are reported to cycle between active and inactive states (Kenakin and Miller, 2010, Rang, 2006, Yarden and Schlessinger, 1987). This characteristic was modelled by allowing ExR to cycle between the two states. [Recdelay] parameter was responsible for the execution of the cycling process. The oscillation and reciprocal levels between the two states demonstrated in **Figure 3. 7 (A)** illustrate a successful cycling process.

3.5.1.1.3 Transcription factors (TFs) cycle between different states

As shown in Figure 3. 3 (D), the TF agents were modelled to cycle between DNA-bound and unbound states. Validation of this process was conducted and shown in **Figure 3. 7 (B)** and Appendix B, Figure 1). The Figure illustrates continuous cycling

of monomeric TF states between bound and unbound states (SF-TF and SB-TF respectively) without a change in their total levels. Conversely, the multimeric TF states (MF-TF and MB-TF), although continuing to cycle between DNA bound and unbound states, decreased their levels in total. This is due to the incorporation of pMAPK binding to MB-TF and changing its state to an active MB-TF.

3.5.1.2 Validation of agents movement

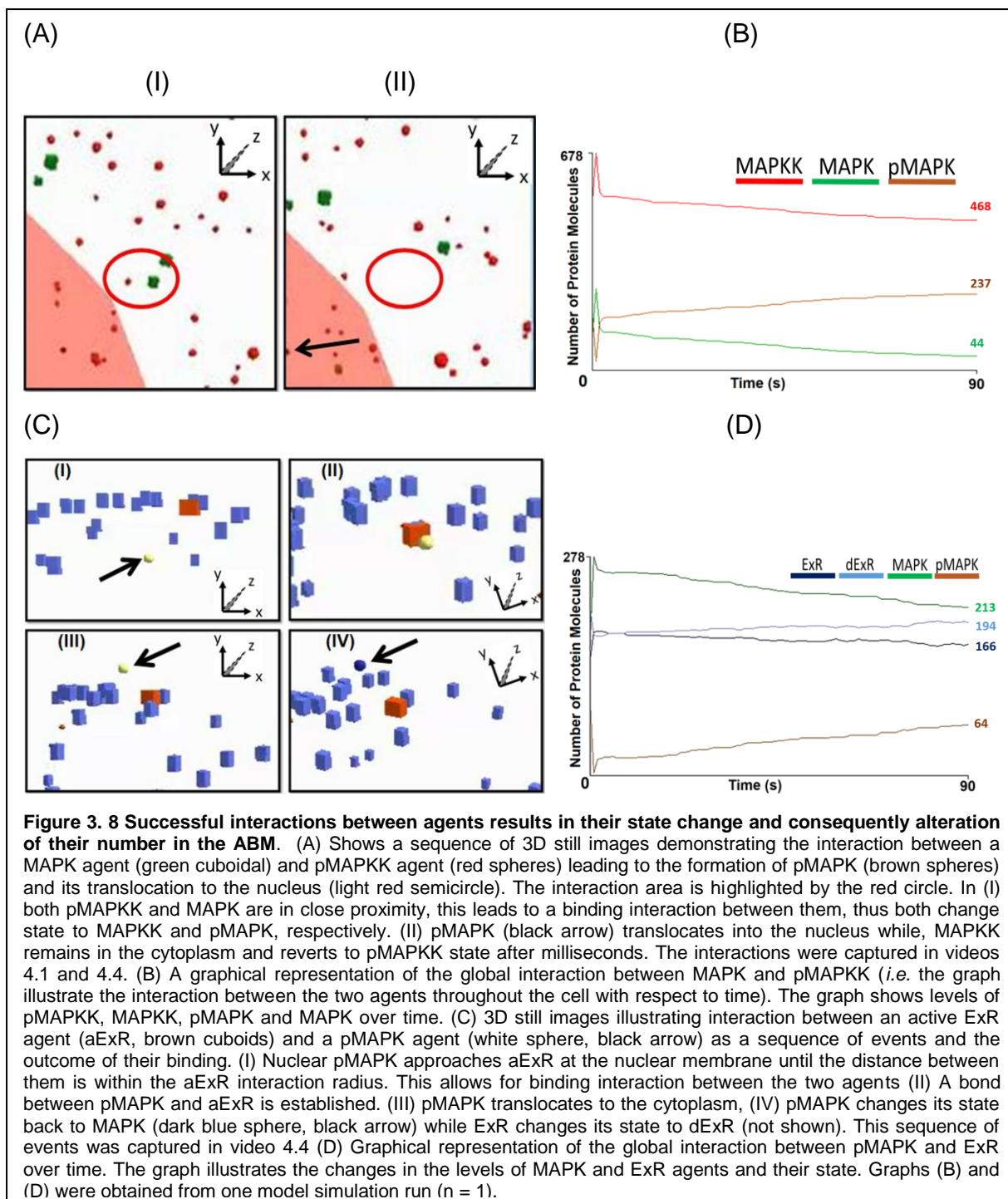
Agent movement was monitored during simulation to ensure all agents adhered to the movement roles specified.

3.5.1.2.1 MAPKK and MAPK movement restriction

Both agents were restricted to moving within the cytoplasm. In the two-compartment model, their movement algorithm restricted them to the cytoplasmic boundaries (the plasma and nuclear membranes). This is demonstrated in video 4.2. While in the multi-compartment model, the algorithm restricted their movement to the compartments the agents resided in. This is illustrated in video 4.3.

3.5.1.2.2 Active MAPK (pMAPK) import and export

pMAPK movement into, within and out of the nucleus was confirmed. Interaction of pMAPKK and MAPK results in an activation of MAPK and its translocation to the nucleus. **Figure 3. 8** (A) and (B) demonstrate the translocation of the pMAPK species into the nucleus. This interaction is also displayed in video 3.4. Once pMAPK resides in the nucleus, it moves by a Brownian motion in order to interact



with other nuclear agents (TFs and ExRs). This is demonstrated in video 3.6. Export of the pMAPK back to the cytoplasm is a result of its interaction with the active ExR. This is shown in Figure 3.7 (C) and (D). The process is also shown in videos 3.4 and 3.6.

3.5.1.2.3 Nuclear Exporting receptor (ExR) movement restriction within the nuclear membrane

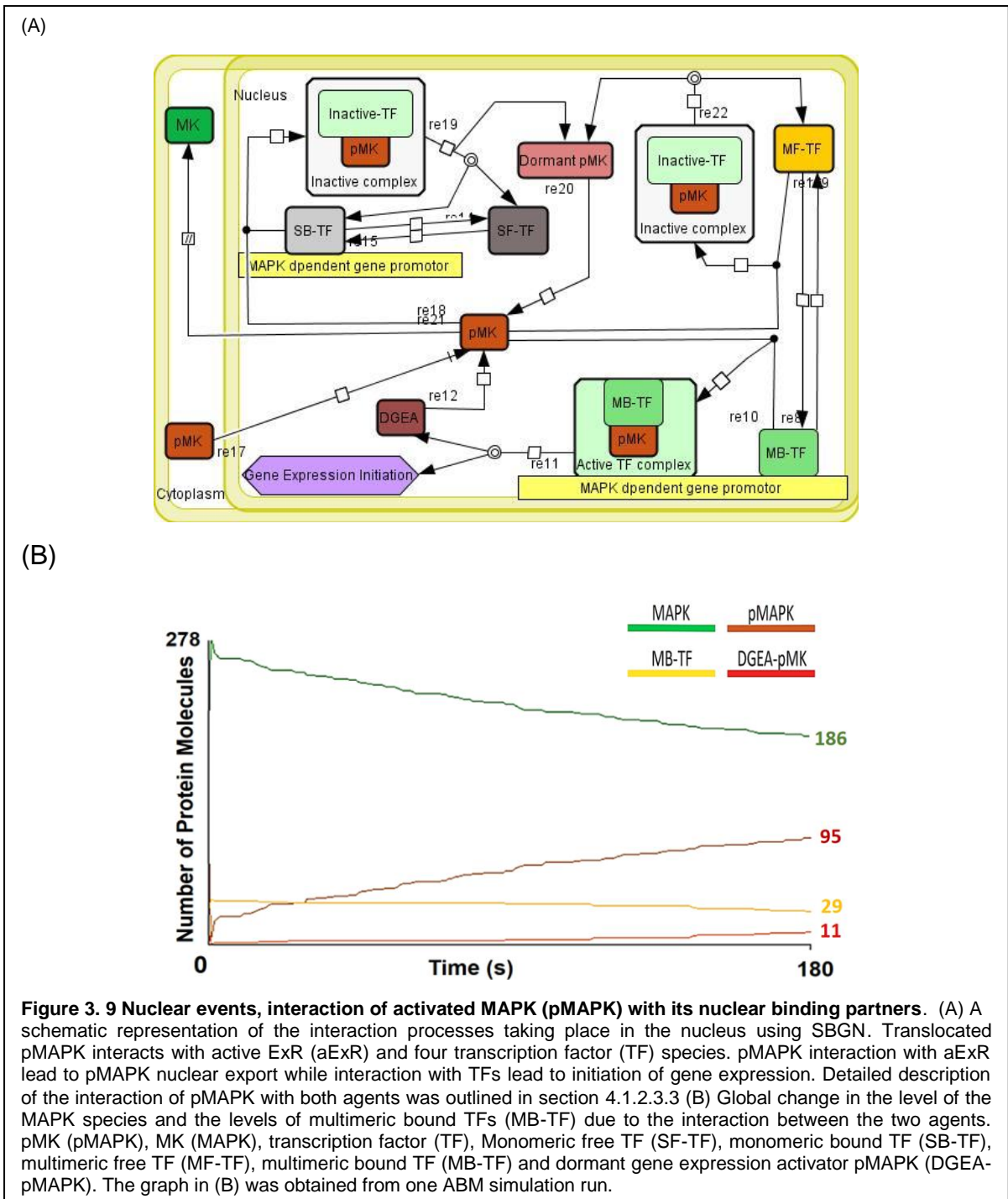
ExRs movement was modelled to be within the circumference of the nuclear membrane. Appendix B, Figure 1 demonstrates the distribution of the ExR agents within the nuclear membrane. Video 3.7 illustrates that movement clearly.

3.5.1.3 Validation of agent interactions and state transition

Agents binding interaction and the ensuing state change are an integral part of the model presented here. They are also fundamental for the MAPK pathway ABM simulation and its signalling behaviour; therefore, it was essential to validate these interactions. These are described below.

3.5.1.3.1 Active MAPKK (pMAPKK)-MAPK interaction

The interaction between the two agents is essential for the activation of the pathway, both biologically and *in silico*. The binding interaction was described comprehensively in Chapter 1 (section 3.2.3.7.1). The binding of pMAPKK with MAPK induced MAPK activation, its state change to pMAPK and its translocation to the nucleus (Figure 3. 7 (A) and (B)). The interaction also leads to pMAPKK state change to MAPKK. Figure 3. 7 (B) displays agent levels during a model simulation and the change in their number with respect to time. As expected the levels of pMAPKK and MAPK decreased while levels of pMAPK increased with respect to time. This is further demonstrated in video 3.8. Interaction of MAPKK and MAPK and



their state changes occur rapidly, therefore, for confirmation and validation the global change in their levels were monitored for the first 90 s of simulation.

3.5.1.3.2 pMAPK-exporting receptor (ExR) interaction

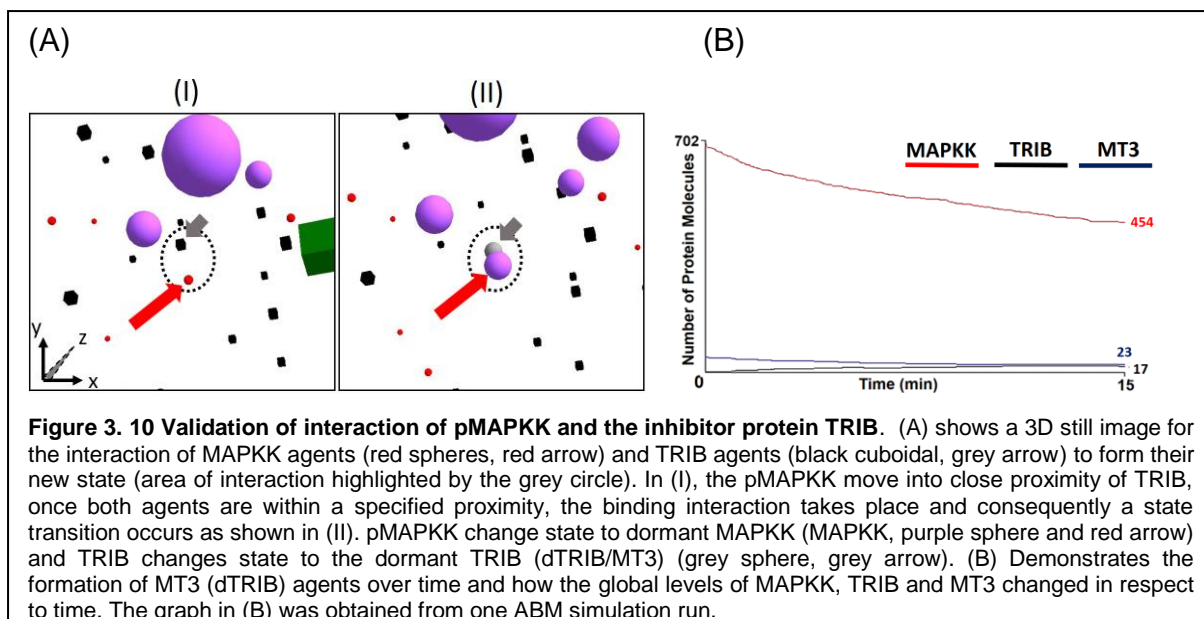
pMAPK nuclear export is an important process to sustain pMAPK-MAPK interaction and thus MAPK activation. Therefore, the interaction between the active ExR (aExR)

and pMAPK and their state change was monitored and validated. Figure 3. 7 (C) demonstrates the interaction between the two agents interacting at the inner nuclear membrane. This interaction causes pMAPK translocation to the cytoplasm and its state change. Figure 3. 7 (D) illustrates the global change in the level of pMAPK and aExR due to their interaction and state change. The levels of aExR and pMAPK decrease with time while levels of MAPK and dExR increase. Video 3.6 displays the full interaction process between the two agents during simulation.

3.5.1.3.3 pMAPK- transcription factors (TF) interaction

When in the nucleus, pMAPK interacts with TFs. Biologically, pMAPK interaction with TFs facilitates modulation and control of gene expression. This interaction was modelled as outlined in the Figure 3. 2 (B) and in **Figure 3. 9 (A)**. pMAPK interacts with four TF species, free monomeric TF (FS-TF) DNA-bound monomeric TF (BS-TF), free multimeric TF (FM-TF) and DNA-bound multimeric TF (BM-TF). As shown in Figure 3. 8 (A), only the interaction with BM-TF corresponds to the initiation of gene expression, mimicking the biological process where gene expression is triggered by specific multimeric TF complexes bound to DNA promoter sequences. The binding of pMAPK to BM-TF results into pMAPK changing state briefly to a dormant state (DGEA-pMAPK). In the two-compartment model the levels of DGEA-pMAPK and active MB-TF were used as a secondary output to measure MAPK activation behaviour.

As pMAPK agents accumulate in the nucleus its interaction with the TF species ensues. Figure 3. 8 (B) demonstrates that as the pMAPK levels increase, DGEA-



pMAPKK levels increase while MB-TF levels are reduced. Figure 3. 8 (B) illustrates the global change in the levels of TF species due to cycling between free and DNA-bound states. Reduction of the number of MB-TF coincides with an increase in the number of DEGA-pMAPK (DEGA-pMK).

3.5.1.3.4 MAPKK-TRIB interaction

The interaction between pMAPKK and one of its intracellular inhibitory proteins tribbles (TRIB) was modelled and validated (see Appendix A, Figure 1). The biological interaction between MAPKK and TRIB was comprehensively outlined in section appendix D. **Figure 3. 10** shows the successful interaction between the two agents. When both agents are in close proximity, binding interaction ensues and subsequently they change state; pMAPKK to MAPKK and TRIB to the dormant TRIB state MT3.

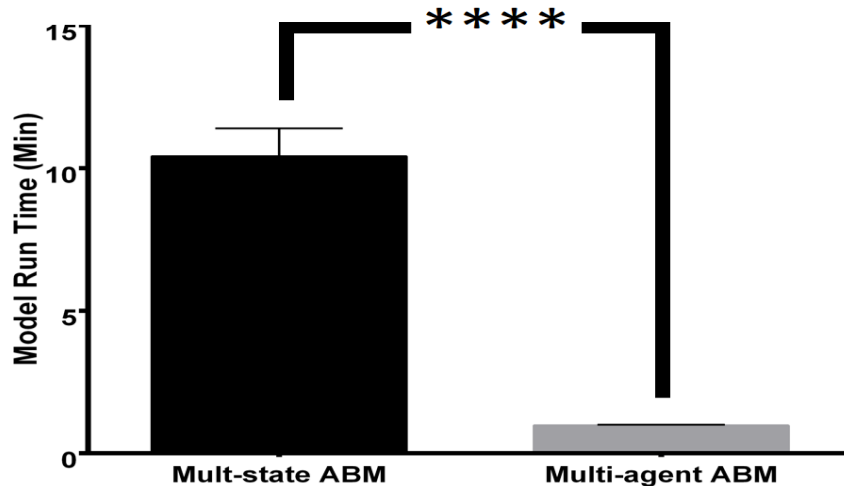


Figure 3. 11 Comparison between the multi-state and the multi-agent agent based models (ABMs) run times. A multi-agent ABM run time was significantly shorter, with run time 58.9 ± 1.5 (s), while multi-state ABMs run time was 10.42 ± 0.97 (min). The data shown represent mean \pm standard error of the mean (SEM), $n = 10$, each ABM was run for 250 iterations and the run time taken to complete the simulation was taken as run-time for the model. A student t-test was used for statistical analysis which showed a significant difference between the multi-state and multi-agent ABM schemes whereby $p < 0.0001$, indicated by **** in the figure.

3.5.1.4 Optimisation, multi-state ABM Vs multi-agent ABM

In order to optimise simulation run times and so obtain an efficient ABM, the ABMs were constructed using two schemes. The first composition/scheme was a multi-state ABM and the second was a multi-agent ABM. The former included two agent types in the system; these were the protein-agents and receptor-agents. In the latter scheme every protein was modelled as an independent agent.

In the multi-state ABM, protein-agents encompassed all the proteins in the cell (the MAPKK, MAPK and TRIB). However, the different proteins were specified as different states of the protein agent. This was specified by the memory parameter [state] (see Appendix A, Table 1). For instance, a protein-agent could be MAPKK, MAPK or TRIB proteins; however, the protein-agent memory parameter [state] determines which protein it is and thus dictated its behaviour. Activation and deactivation of these different protein states resulted in them obtaining a new state.

Receptor-agents were exclusive for the exporting receptors (ExR) and they cycled between active and inactive states. This was specified by the memory parameter [state] (see Appendix A, Table 2). All protein-agents in the model were able to access all the messages from FLAME libmboard with no discrimination between the different protein states. Agent states were annotated using numerical values, and state change was monitored by the alteration of these values.

In the multi-agent ABM, every protein was designated as an independent agent. The change from active to inactive state was assigned to the memory parameter [state] (see Appendix A, Table 6-Appendix A, Table 8). For instance, MAPKK is an agent with two states, an active (pMAPKK) and inactive (MAPKK). The MAPKK states were specified by the memory parameter [state]. Every agent accessed messages that are produced by its binding partners and executed their transition functions separately.

The run time of the different ABM schemes was measured and **Figure 3. 11** demonstrates that a multi-agent model is noticeably quicker to run and thus better and more appropriate to use for the MAPK pathway ABM construction and development from the conceptual model. Therefore, this approach was adopted for subsequent ABMs.

This section aimed to demonstrate that the fundamental roles deduced from the conceptual model (see section 3.2), such as state transition and binding behaviour, were modelled and executed accurately, and that the execution was computationally efficient.

It was indispensable to have confidence in the ABMs developed, how they are executed and their accurate simulation of the real-world behaviour. Therefore, model validation was an essential component for ABM construction and their further development. In this section it was demonstrated that the ABM roles (identified in section 3.3) were satisfactorily implemented and executed during model simulations, and consequently provided a level of confidence in the constructed ABMs.

3.6 Conclusion

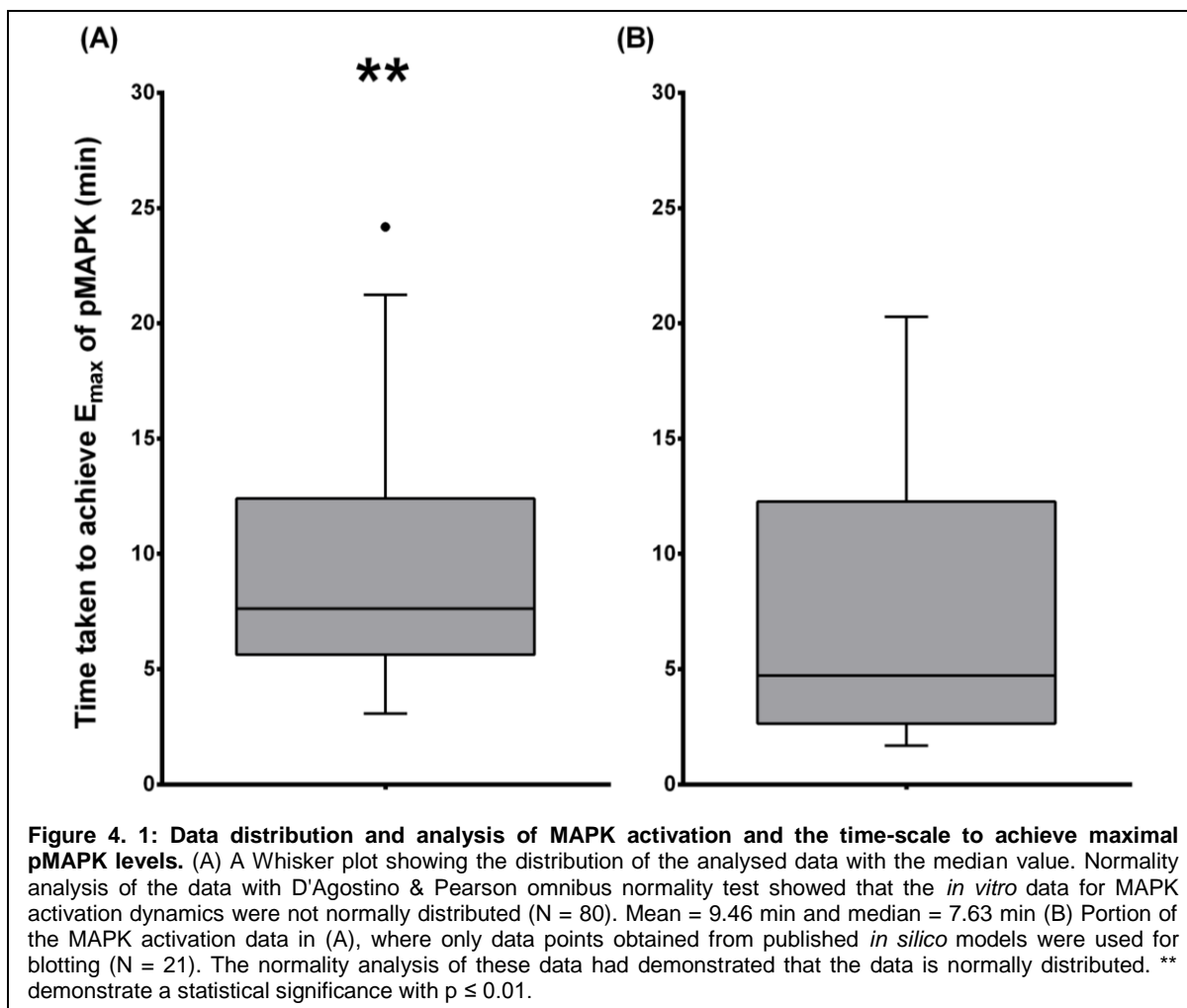
The aim of this chapter was to provide a detailed description of a conceptual model for the MAPK pathway the main components of the system and its behaviour. The chapter also provided an outline of how the conceptual model was transformed into roles used in the ABMs. Chapter 4 is dedicated to the computational implementation of the MAPK pathway ABMs and the data which has been generated from these models

Chapter 4 Results

This chapter is dedicated to the construction of agent-based models (ABMs) and the results generated from them. The chapter is divided into four sections. Section 4.1 describes the time calibration of simulation times in the ABM. Sections 4.2 to 4.4 are dedicated to *in silico* experimentation to investigate *spatiotemporal* regulatory mechanisms in the MAPK pathway and the modulatory role they play in shaping MAPK activation behaviour.

4.1 ABMs time calibration

This subsection discusses the calibration of simulation time and its derivation from the literature. The activation of the MAPK pathway is measured over time. The time to elicit the maximal level (E_{\max}) of pMAPK species is the commonly used measurement *in silico*, *in vitro* and *in vivo* experiments. Accumulation of the pMAPK species in the nucleus over time is also used. Therefore, in order to compare the output from the ABMs with the literature, the simulation time was calibrated. Subsequently, 80 graphs displaying MAPK activation were obtained from the literature and analysed (Figure 4.1 and appendix C). The time to achieve E_{\max} was manually determined from these graphs and plotted as shown in Figure 4.1 (A). These graphs had demonstrated that the average activation time to reach E_{\max} was (9.46 min). Nevertheless, normality analysis of all data points showed that the experimental data is not normally distributed (Figure 4. 1 (A) and (B)); therefore, the use of the mean activation time to reach E_{\max} is not an appropriate value to use for



model calibration. Hence the median time to achieve E_{\max} value (7.63 min) was used to calibrate simulation time.

4.1.1 Sensitivity analysis of the agent based models

Sensitivity analysis was conducted on the models when necessary. These were to confirm the robustness of the models to large variations in agent numbers. These analyses are presented in detail below, in section 4.2

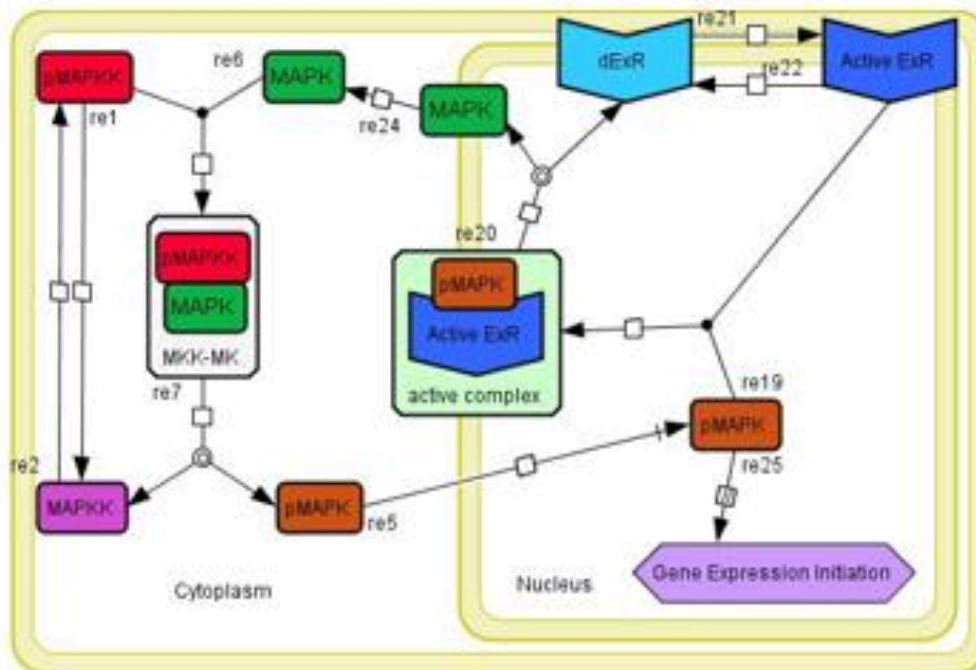
4.2 Examination of the spatial regulatory element on MAPK activation dynamics.

After validation and optimisation of the core ABMs, two models were constructed to investigate the effect of spatial modulation on the activation behaviour of the MAPK pathway. These were: a two-compartment ABM and multi-compartment ABM. This section is devoted to the experimentation conducted with the two models which include sensitivity analysis and validation.

In regard to the validation of the ABMs, as described in sections 3.3.2.2.1 (page 105) and section 4.1 (page 127), the magnitude of pMAPK generated (E_{\max}), the time to achieve E_{\max} and EC_{50} are commonly used to describe the MAPK activation behaviour of the pathway both *in vitro* and *in silico* (Aoki et al., 2013a, Aoki et al., 2013b, Tomida et al., 2015). Thus said behaviours were used to compare the results obtained from the ABMs with previous published *in vitro* data (presented in Figure 4.1).

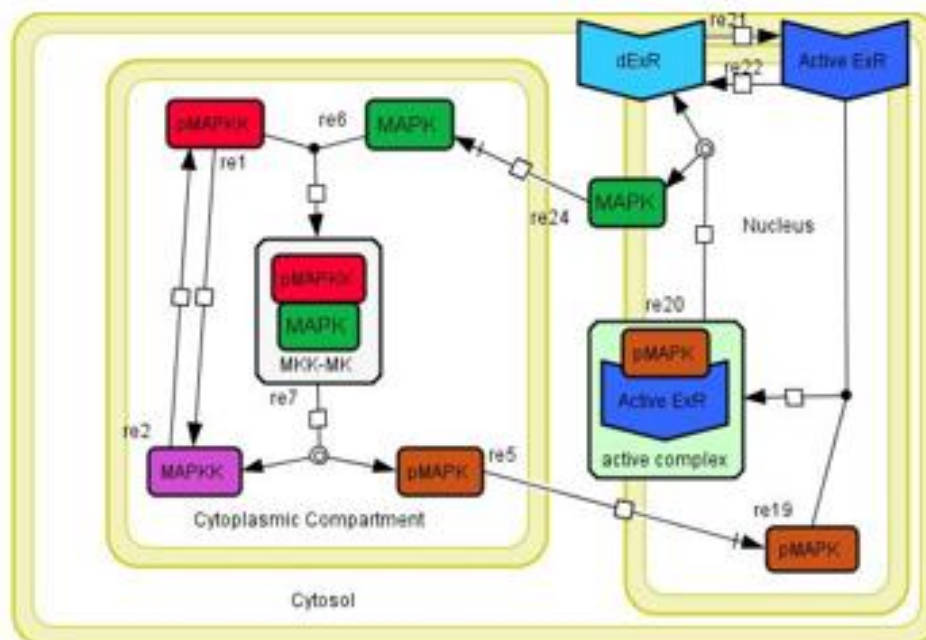
As described in section 3.4.1.5, the two-compartment model was constructed to emulate previously published *in silico* models of the MAPK pathway, while the multi-compartment model aimed to also incorporate the physiological three dimensional (3D) structure of the cell, where the proteins involved in the MAPK cascade reside in different cellular compartments. The null hypothesis for this section is the following: localising the proteins involved in the MAPK pathway into multi-compartments has

(A)



Two compartment model

(B)



Multi compartment model

Figure 4. 2 Different spatial ABMs used to investigate the significance of MAPKK and MAPK spatial arrangement on the MAPK activation behaviour. (A) A SBN graphical representation of the two compartments ABM. The main feature of the model is the homogenous distribution of MAPKK and MAPK within the cytoplasm. (B) A SBN graphical representation of the multi-compartment ABM. The main feature of this model is the spatial restriction of MAPKK and MAPK within the cytosolic compartments. Lipid membranes are represented by the yellow quadrilaterals. SBN simplifies the model and represent every protein and entity once For further description of the two models peruse section 3.3

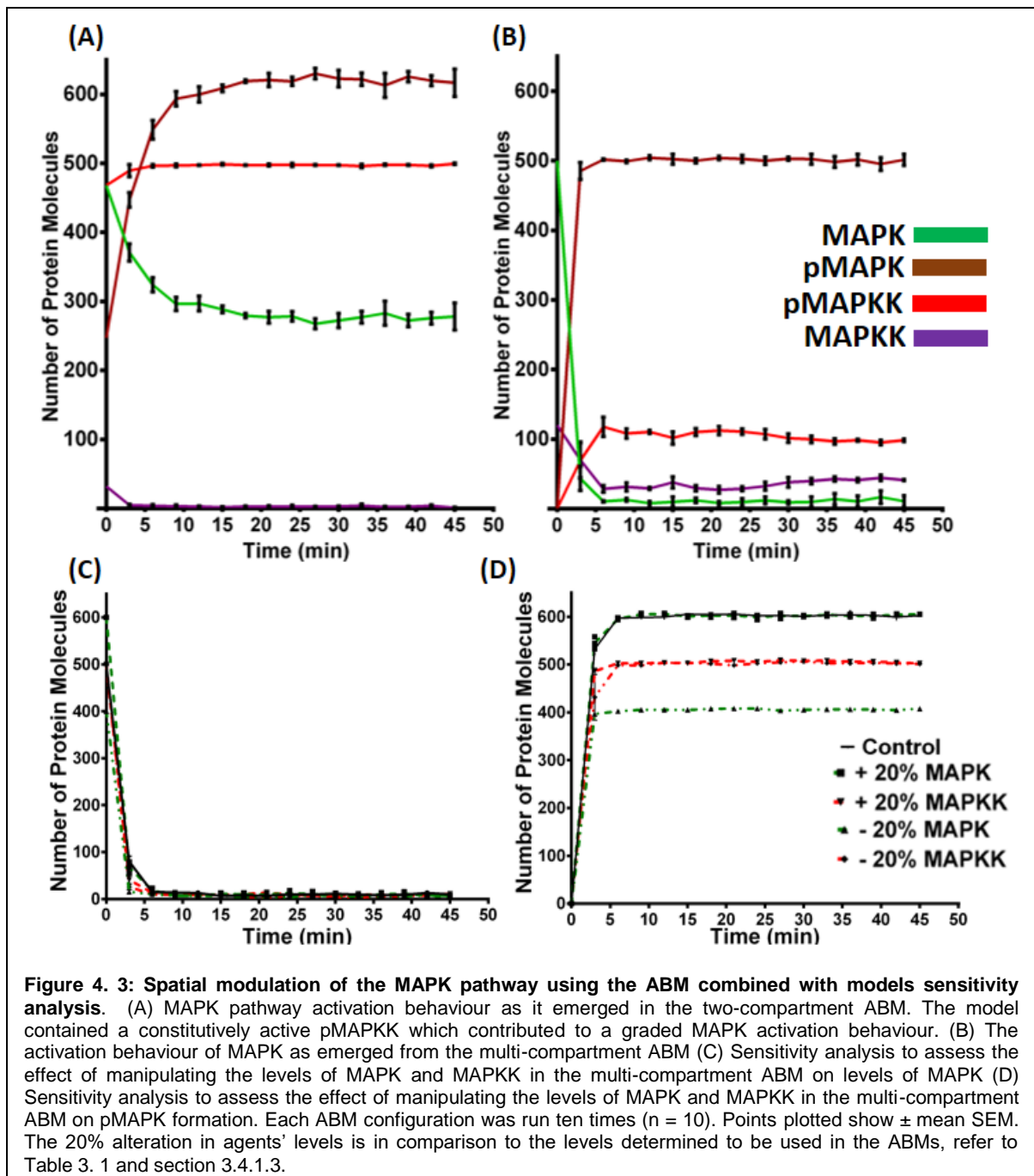
no significant effect on MAPK activation behaviour compared to a homogeneously distributed two compartment ABM.

MAPK pathway mediates responses with a high level of fidelity and specificity, and there is a growing realisation that these outcomes rely on the spatial distribution of the MAPK cascade components within the cell. The first observation of variant cellular outcomes from different MAPK spatial pools came from studies with fibroblast and embryonic carcinomas (Gaumont-Leclerc *et al.*, 2004, Smith *et al.*, 2004). In these cells, when ERK had translocated into the nucleus the cells had proliferated. However, prevention of ERK translocation to the nucleus resulted into the differentiation of the carcinoma cells and their senescence. It was also shown that MAPK responses are composed of two phases; the first phase relies on the presence of the MAPK components in the cytoplasm. This was initially shown with beta-adrenergic GPCRs, where they mediated a rapid and short ERK activation. However, when the caveolin-dependent pathway was knocked out (KO), ERK activation dynamics had switched to sustained and slow activation dynamics. This was also confirmed in other GPCR systems where the beta-arrestin components were knocked out using siRNA (Shenoy *et al.*, 2006). In these experiments the ERK response only included the rapid activation phase. On the other hand, inhibition of protein kinase C (PKC)-dependent activation of ERK demolished the rapid activation phase while the slow and sustained ERK activation was maintained (Wei *et al.*, 2003, Lefkowitz and Shenoy, 2005). Furthermore, it was also demonstrated in Chinese Hamster Ovary cells (CHO) that anchoring MEK2 (ERK kinase) into the endosomal compartment led to a sustained activation of ERK, while normally MEK2 causes a transient ERK activation. Moreover, the work of Ties *et al* had illustrated

that ERK was distributed into two cellular pools, one of which was endosomal (Brahma and Dalby, 2007, Teis *et al.*, 2006, Teis *et al.*, 2002, Wunderlich *et al.*, 2001). These two pools had mediated two separate actions of the MAPK response. Depletion of the endosomal pools had resulted in the loss of the endosomal dependent response and only returned by the re-introduction of these endosomal pools. In addition, scaffolds and adaptor proteins were shown to anchor the proteins involved in the MAPK cascade in different cellular localisations and limit their action in these compartments (Roy *et al.*, 2005, Takahashi *et al.*, 2006).

All of the above literature shows that compartmentalisation is playing an important role in determining and influencing MAPK activation behaviour and thus controlling of cellular responses. Therefore, the ABM addressed the issue of compartmentalisation and investigated the difference compartmentalisation of the MAPK components made on MAPK activation behaviour and pMAPK levels in comparison to those observed in the classical, two-compartment system model.

The structures of the two ABMs are demonstrated in Figure 4. 2 and Appendix B, Figure 2. Briefly, the two-compartment model had assumed a homogenous distribution of total MAPKK (both pMAPKK and MAPKK, henceforth referred to as tMAPKK) and MAPK proteins in the cytoplasm, while the multi-compartment model was composed of randomly localised cytoplasmic compartments where tMAPKK and MAPK proteins resided. Takamori *et al* demonstrated that a small cytoplasmic compartment such as an endoplasmic vesicle contains a small number of proteins (50- 100 proteins) (Takamori *et al.*, 2006). Furthermore, Ortega *et al* illustrated that



the ratio between MAPKK: MAPK to which produces an ultrasensitive response is 1:10 (Eblen et al., 2004, Ortega et al., 2006). Thus, the total number of proteins in a compartment in the multi-compartment ABM was approximated to 60, whereby the 1:10 MAPKK: MAPK ratio was maintained. Both models were simulated from the point where the MAPK pathway-activating signal had been transduced from MAPKKK to MAPKK. In both models, the activating cue was assumed to be intense, with negligible negative feedback mechanisms. Therefore, pMAPKK was assumed to

remain in the active state for an extended period. This was analogous to irreversible pathway activation in oocytes, investigated by Ferrell *et al* in the first *in silico* model of the MAPK pathway. The Flexible Large-scale Agent Modelling Environment (FLAME) was used for simulation and the results were visualised via the FLAME visualiser.

4.2.1 Results

4.2.1.1 *Sensitivity analysis*

Both ABMs were run multiple times (up to $n = 30$) to test their robustness and reproducibility. The levels of the agent species were plotted at every three minutes for each individual model run. The levels of pMAPKK, MAPKK, MAPK and pMAPK in both ABMs were plotted to assess the activation behaviour and the effect of compartmentalisation on the global MAPK activation (Figure 4. 3 (A) and (B)). The models were simulated in for 3, 5, 10 and 30 runs and demonstrated low standard error of the mean (SEM) for all protein levels at every time point. SEM between runs did not exceeded 3.3% at any of the time points in either of the models, even under conditions where SEM for pMAPKK was significantly greater. In addition, that increasing number of runs only reduced the value of SEM. Appendix B Figure 4 illustrates that the increase in the number of runs had no considerable effect on the activation behaviour. Therefore, simulating the model for 10 or 30 runs was sufficient, as there will be neither additional information nor knowledge gained if the run numbers were increased.

Subsequently, the number of MAPKK and MAPK agents were altered by 20% in the multi-compartment model and the effect of this alteration on pMAPK formation and MAPKK levels were examined in multiple model runs (Figure 4. 3 (C) and (D)). The levels of both pMAPK and MAPKK were plotted at set time points (every three minutes). Analysis showed that the variance value at each time point was between \pm 0.58- 22.07. Thus it was concluded that the models are robust (Appendix B, Figure 3-Appendix B, Figure 6 and Appendix B, Table 1-Appendix B, Table 4). The impact of the agents' numbers variation on MAPK activation behaviour and dynamics in the multi-compartment model was further analysed. This was via the analysis of the time pMAPK and MAPKK reached E_{max} and EC_{50} under the different model conditions (Figure 4. 4 (A)-(D)). One way ANOVA had verified that the 20% alteration in agent species number had no marked effect on MAPK activation dynamics and the time to achieve E_{max} and EC_{50} were not considerably different. Furthermore, analysing the effect of said alterations on pMAPK and MAPKK levels during the simulation also demonstrated no noticeable difference, apart from when MAPKK was increased by 20% (Figure 4. 4 (E) and (F) and Appendix B, Figure 7). Nonetheless, increasing MAPKK levels by 20% caused a marked change in the level of pMAPK during the simulation (Figure 4. 4 (F) and Appendix B, Figure 7).

4.2.1.2 Compartmentalisation contributes to the rapid responsiveness of the MAPK pathway and ultrasensitivity.

Figure 4. 4 (A) vs. (B), highlights the effect of compartmentalising the kinases on formation of pMAPK species (a component of the MAPK activation dynamics). In the two compartment ABM (Figure 4. 4 (A)) the ratio between the kinases used was 1:1,

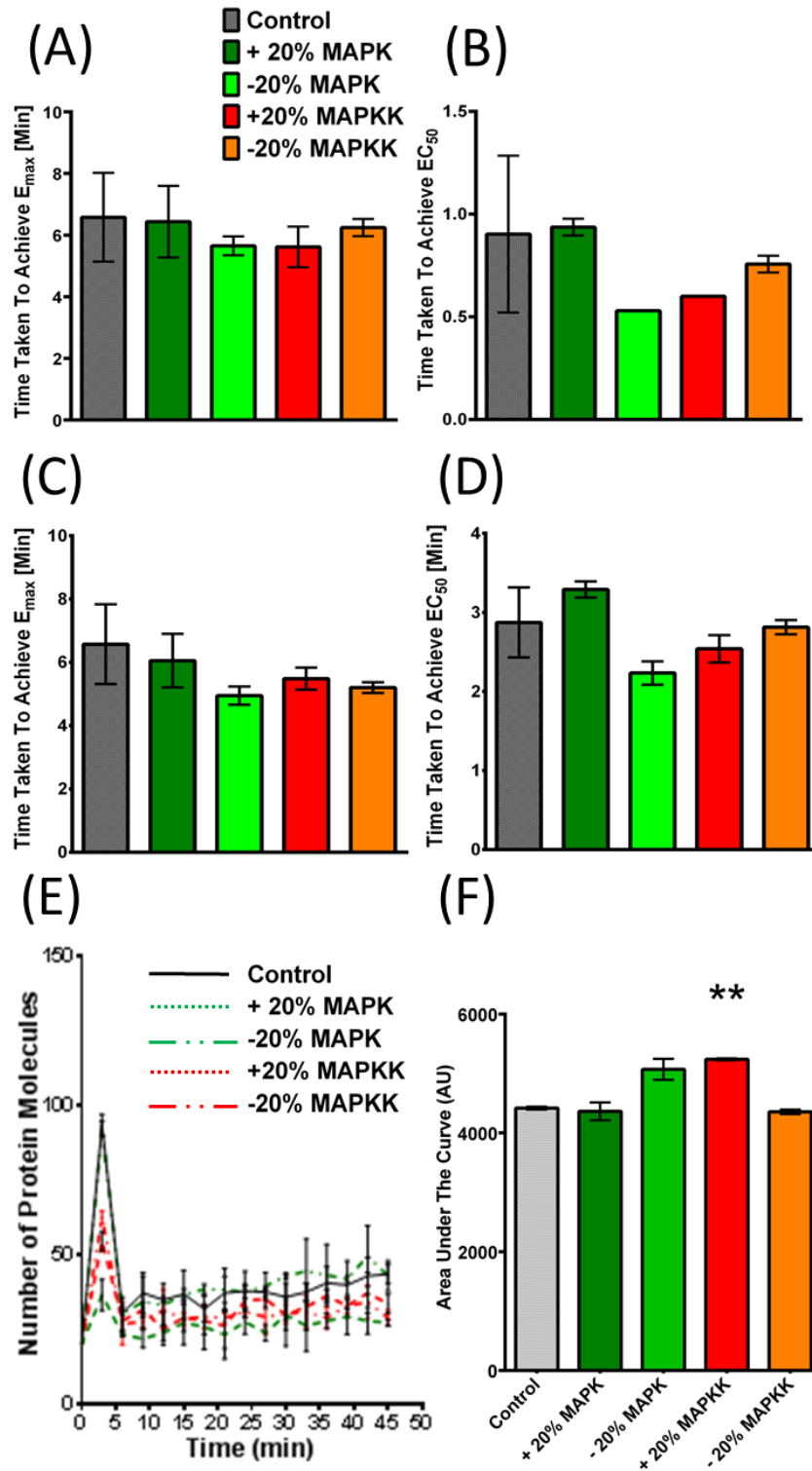


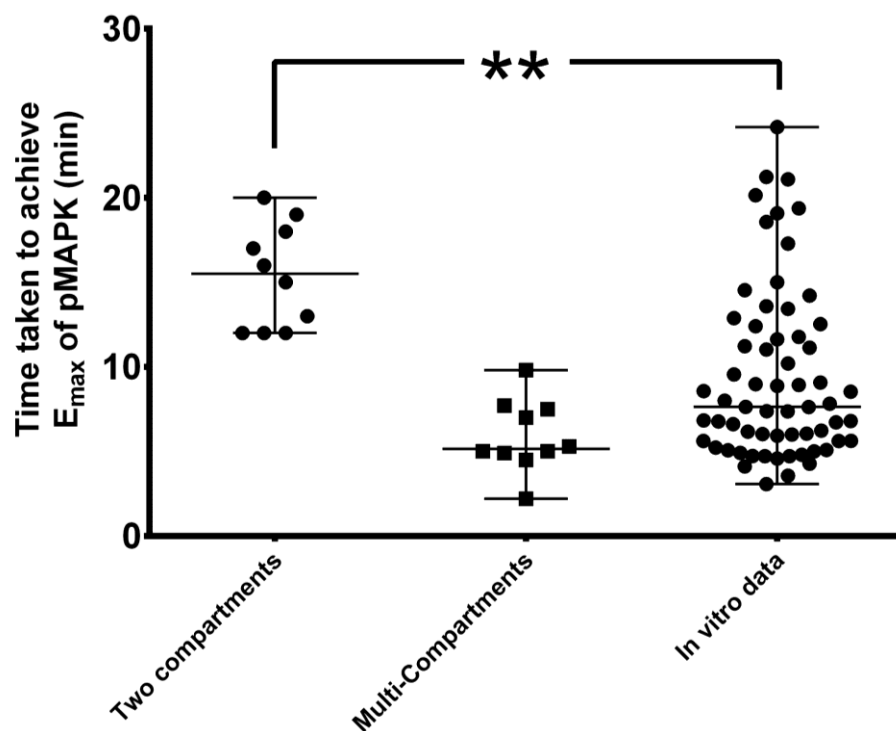
Figure 4.4 Multi-compartment ABM sensitivity analyses assessing the effect of agent levels alteration on MAPK and MAPKK activation. (A) The time taken pMAPK to reach E_{max} under varied starting levels of MAPKK and MAPK agents were measured and plotted. (B) Time taken for EC_{50} of to be established for the pMAPK species. (C) Comparison of the time taken for pMAPKK to reach E_{max} when levels of MAPKK and MAPK were varied. (D) A comparison between the time taken to establish pMAPKK EC_{50} when levels of agents were altered in the ABM. (E) Sensitivity analysis to examine the effect of altering MAPKK and MAPK levels on MAPKK formation during ABM simulation (F) Area under the curve of the MAPKK levels to determine if varying MAPKK and MAPK levels effect the pMAPKK formation during simulation. Simulations were repeated ten times ($n = 10$). Statistical analysis using one way ANOVA showed altering the numbers of MAPKK and MAPK had no significant effect on the time to establish E_{max} and EC_{50} for both pMAPK and pMAPKK. Bar values represent mean \pm SD. ** signifies a statistical significance where $p \leq 0.01$

in line with previously published *in silico* models (Table 3. 2). In this set-up, MAPKK activation was constitutively active and where 99% of tMAPKK species were assumed to be activated by MAPKKK at t_0 , consequent levels of MAPKK did not change over time. This resulted in a sharp formation of pMAPK and equilibrium was reached rapidly. However, a short lag-phase was observed prior to the global increase in pMAPK (~94 sec, Appendix B, Figure 8), this was an emergent behaviour from the model because the ABMs contained no algorithms specifying this activation behaviour.

The data obtained from both ABMs was validated against *in vitro* data from the literature as shown in Figure 4.5. The time to achieve E_{max} (A) and EC_{50} (B) were compared. Statistical analysis with nonparametric one-way ANOVA had shown that there is a significant difference between the *in vitro* data and the two compartment model, while the data obtained from the multi-compartment ABM showed no statistical difference with the *in vitro* data.

The multi-compartment model (Figure 4. 6 (B)), was highly sensitive to activation with a rapid rate of pMAPK formation ($\approx 176.86 \pm 0.18\%$ MAPK were converted to pMAPK/min (see Appendix B, Figure 9), allowing for almost instantaneous full activation of MAPK and establishment of equilibrium ($E_{max} = 5.89 \pm 2.13$ min, Figure 4. 6). Nonetheless, a short lag-phase was observed (~ 1.5 s, see Appendix B, Figure 8 (B)). Furthermore, in this model design, when E_{max} was achieved, $98 \pm 0.1\%$ of MAPK were converted to pMAPK species and were translocated to the nucleus. In contrast, in the two compartment model configuration, only $85.5 \pm 0.6\%$ MAPK were

(A)



(B)

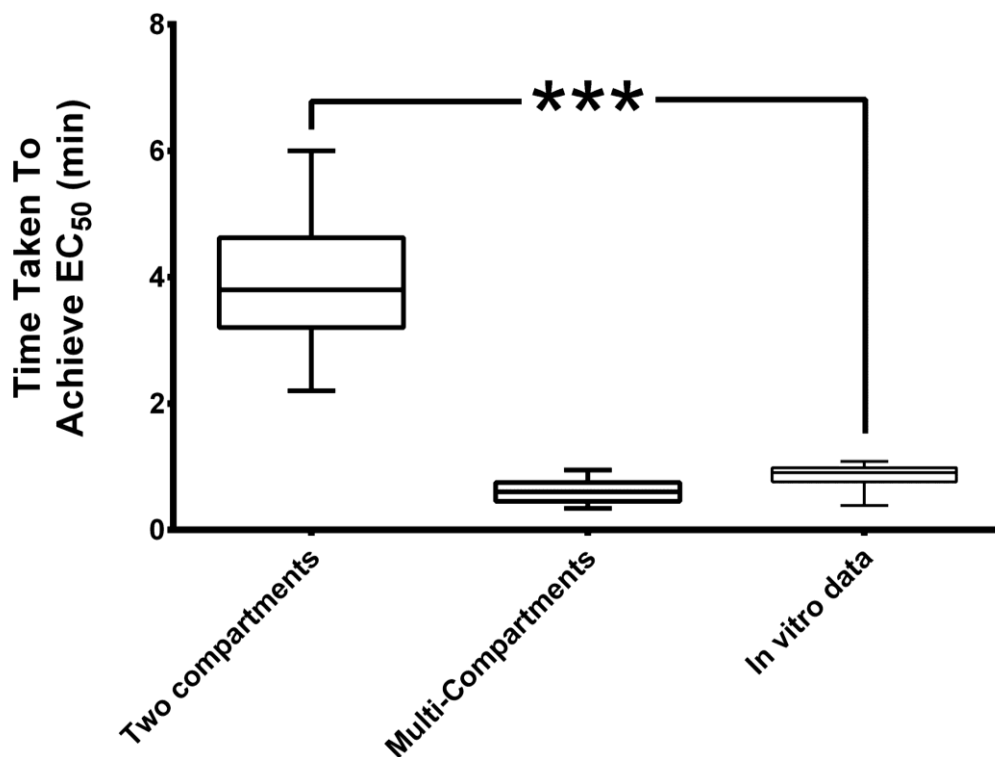
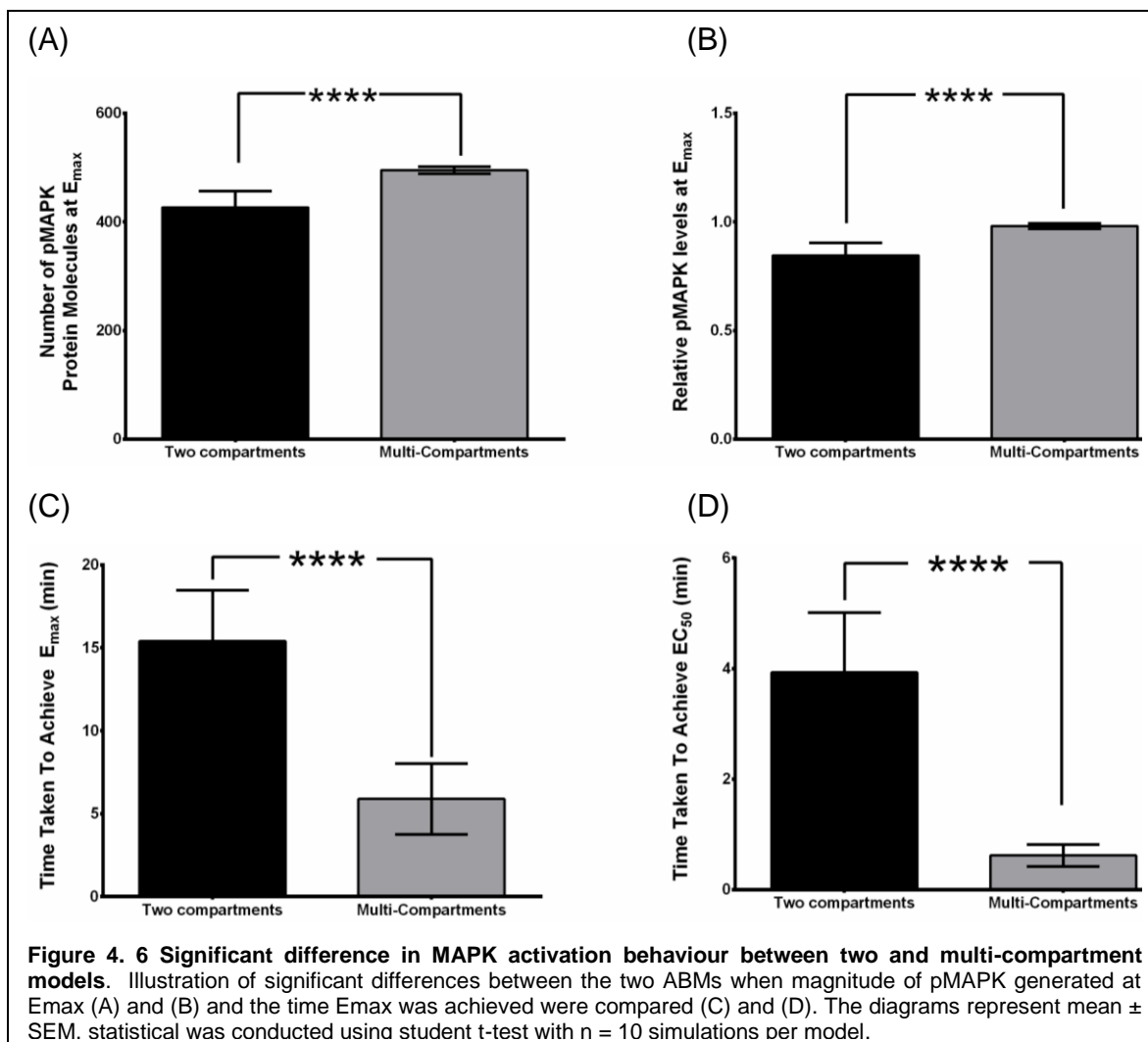


Figure 4. 5 Validation of the ABM models via comparison with published literature. (A) The time taken to achieve E_{max} obtained from both the two and multi-compartment ABMs were compared to those analysed from the literature (see figure 4.1). The data are presented using Box whisker blots with the median presented as the horizontal line. (B) The time taken to achieve EC_{50} was analysed from in vitro data and plotted against the time for EC_{50} in both ABMs. The blot illustrates that there is a significant difference between the two-compartment ABM values, while said values obtained from the multi-compartment ABM showed no significant difference between in vitro data and the ABM. The data is presented as a box and whisker blots with the median value presented as the horizontal line. For the ABMs $n = 10$, and $n = 64$ for in vitro data and n



converted to pMAPK when E_{max} was achieved, reflecting a system with lower activation potency. Furthermore, in the two compartment model, only $70.3 \pm 2.2\%$ of cytoplasmic MAPK were converted to pMAPK within the first 5 minutes, while in the multi-compartment ABM, 98% of MAPK were converted to pMAPK species.

4.2.1.3 *Downscaling the cytoplasmic volume did not alter the MAPK activation dynamics in either ABMs*

The impact of downscaling the cytoplasmic volume was investigated, as increasing molecular crowding is shown to influence biochemical behaviour in addition to

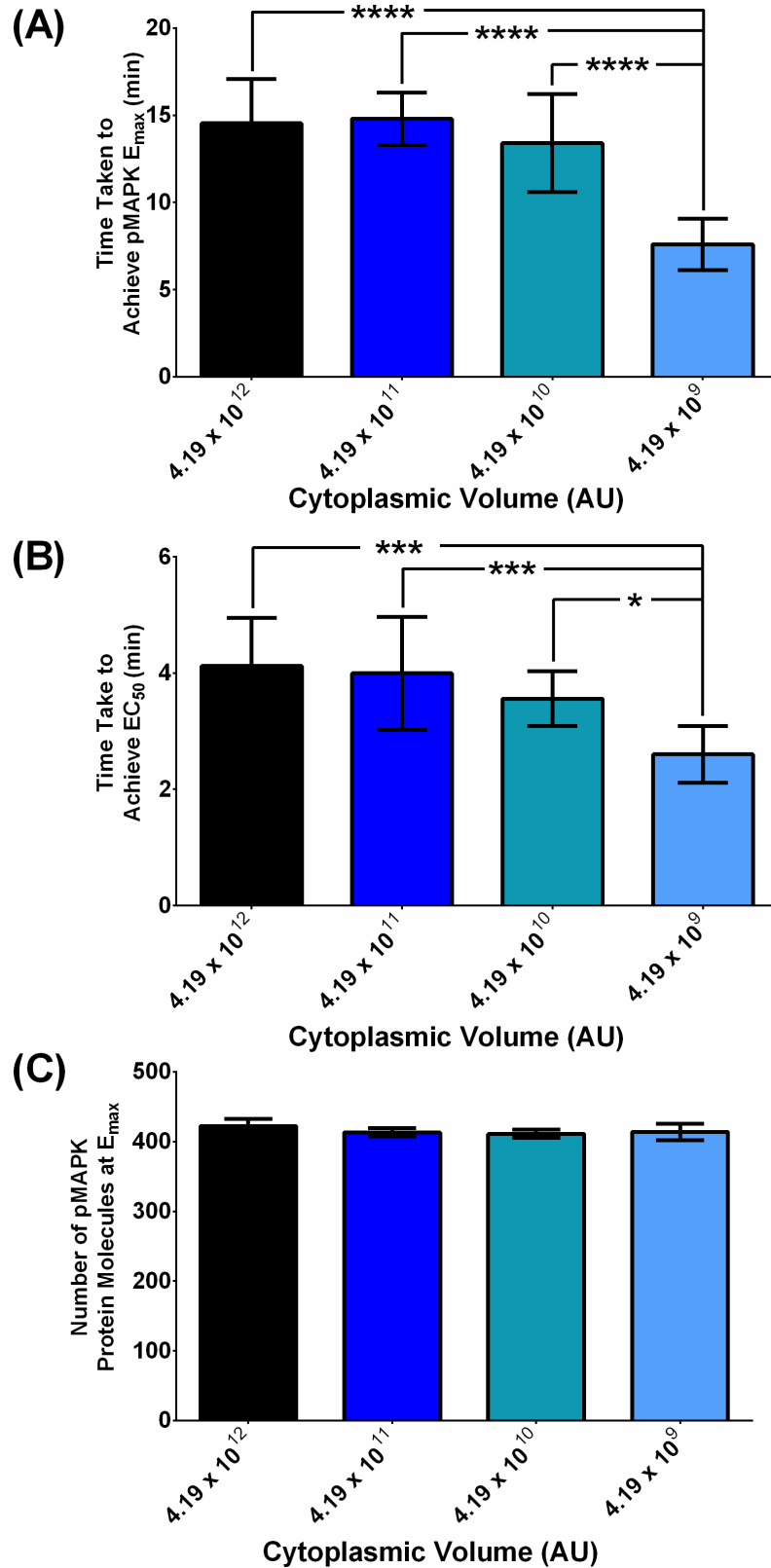


Figure 4.7 The effect of reducing the cytoplasmic volume on the MAPK activation dynamics in a two-compartment model. (A) The time to achieve E_{max} was measured after the modification of the total cellular volume. Reducing the cellular volume by 10 and 100 did not demonstrate any significant effect on time to reach E_{max} , however a significant effect emerged when the volume was reduced by 1000 fold. (B) The same effect was observed with the time to achieve EC_{50} . (C) Conversely, total volume reduction did not have an impact on the magnitude of pMAPK. The diagrams represent mean \pm SD, statistical was conducted using one way ANOVA with $n = 10$ simulations per model. **** indicate a p value where $p < 0.0001$, *** indicate a p value where $p < 0.001$. * indicate a p value where $p < 0.05$.

assessing if the downscaling of the number of proteins from magnitudes of millions to thousands influences the MAPK activation dynamics.

The chosen radius of the cell in both ABM was 10000 arbitrary units of distance, with a total cytoplasmic volume of 4.19×10^{12} arbitrary units of volume. The cytoplasmic volume was altered by two methods. The first was to downscale the total volume from 4.19×10^{12} to 4.19×10^{11} arbitrary units of volume (i.e. reduction of total volume by 10 fold) to adjust to the 8 fold downscaling factor which was applied to the number of agents (see table 3.2 page 112). The second method was downscaling the radius of the cytoplasm by 10 fold, thus the final volume of the cytoplasm became 4.19×10^9 arbitrary units of volume. Only at this cytoplasmic volume, a statistically significant increase in the time to achieve EC_{50} and E_{max} were achieved (see Figure 4.7). An indistinguishable approach was applied to downscale the cytoplasmic volume in the multicompartment ABM. There was no statistically significant impact on the magnitude of pMAPK generated, the time to achieve both E_{max} and EC_{50} (see Figure 4.8). Furthermore, reducing the volume of each individual compartment to 1×10^6 arbitrary units of volume, did not significantly shorten the time to achieve E_{max} and EC_{50} nor the magnitude of pMAPK at E_{max} (see Figure 4.8).

In relation to the multi-compartment model, the scaling process applied in the ABM could not have affected the activation dynamics of MAPK because each compartment occupied a volume of 1×10^9 arbitrary units of volume, while the cytoplasm occupied a 4.19×10^{12} arbitrary units of volume and downscaling the volume of the cytoplasm will unlikely change the dynamics of activation, as the

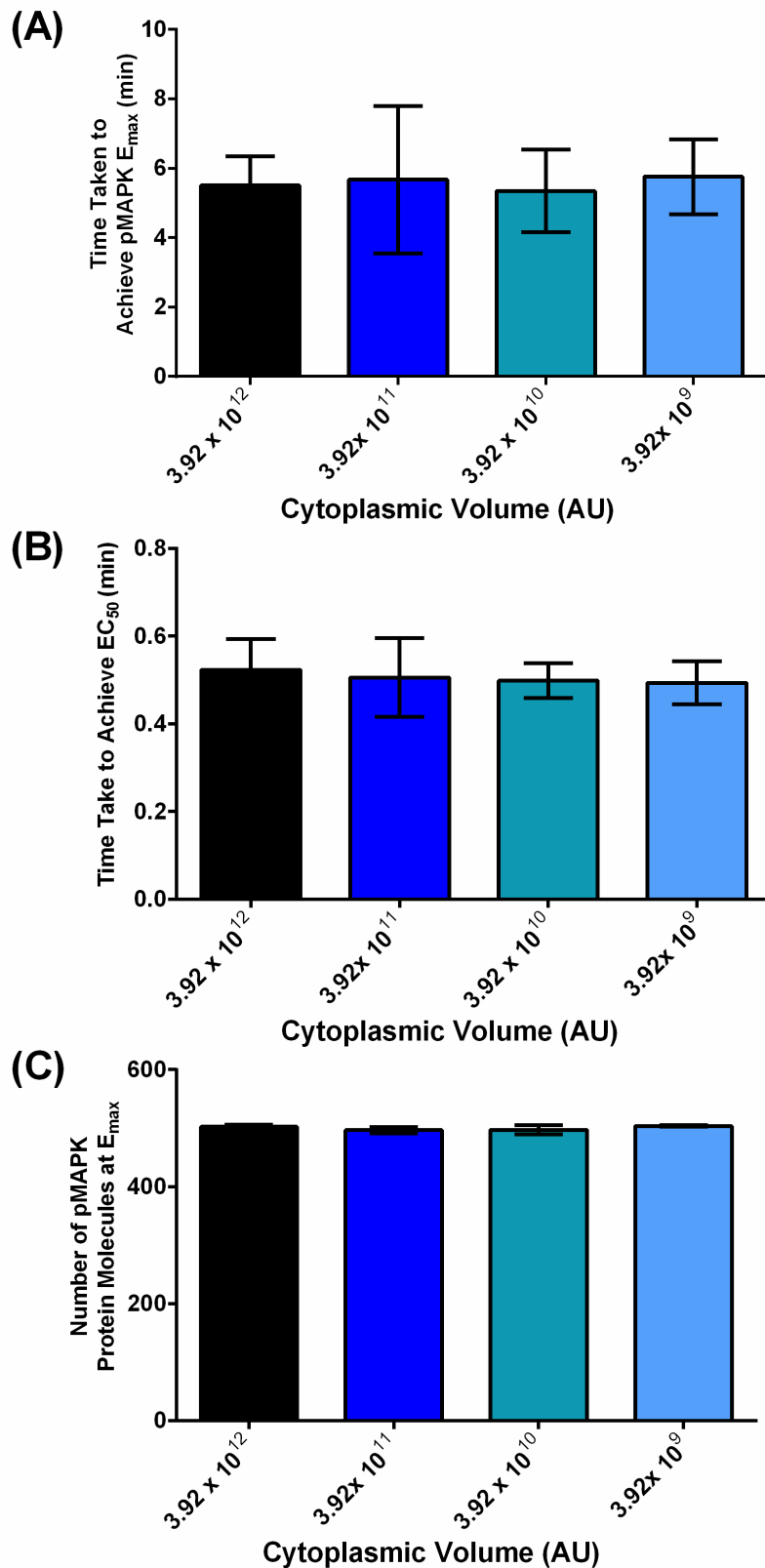


Figure 4. 8 The effect of reducing the cytoplasmic volume on the MAPK activation dynamics in a multi-compartment ABM. (A) The time to achieve E_{max} was measured after the modification of the total cellular volume. Reducing the cellular volume by 10, 100 and 1000 fold did not demonstrate any significant effect on time to reach E_{max} . (B) Identical effect was established with the time to achieve EC_{50} . (C) The pMAPK magnitude was not altered with changes in total volume. The diagrams represent mean \pm SD, statistical was conducted using one way ANOVA with $n = 10$ simulations per model.

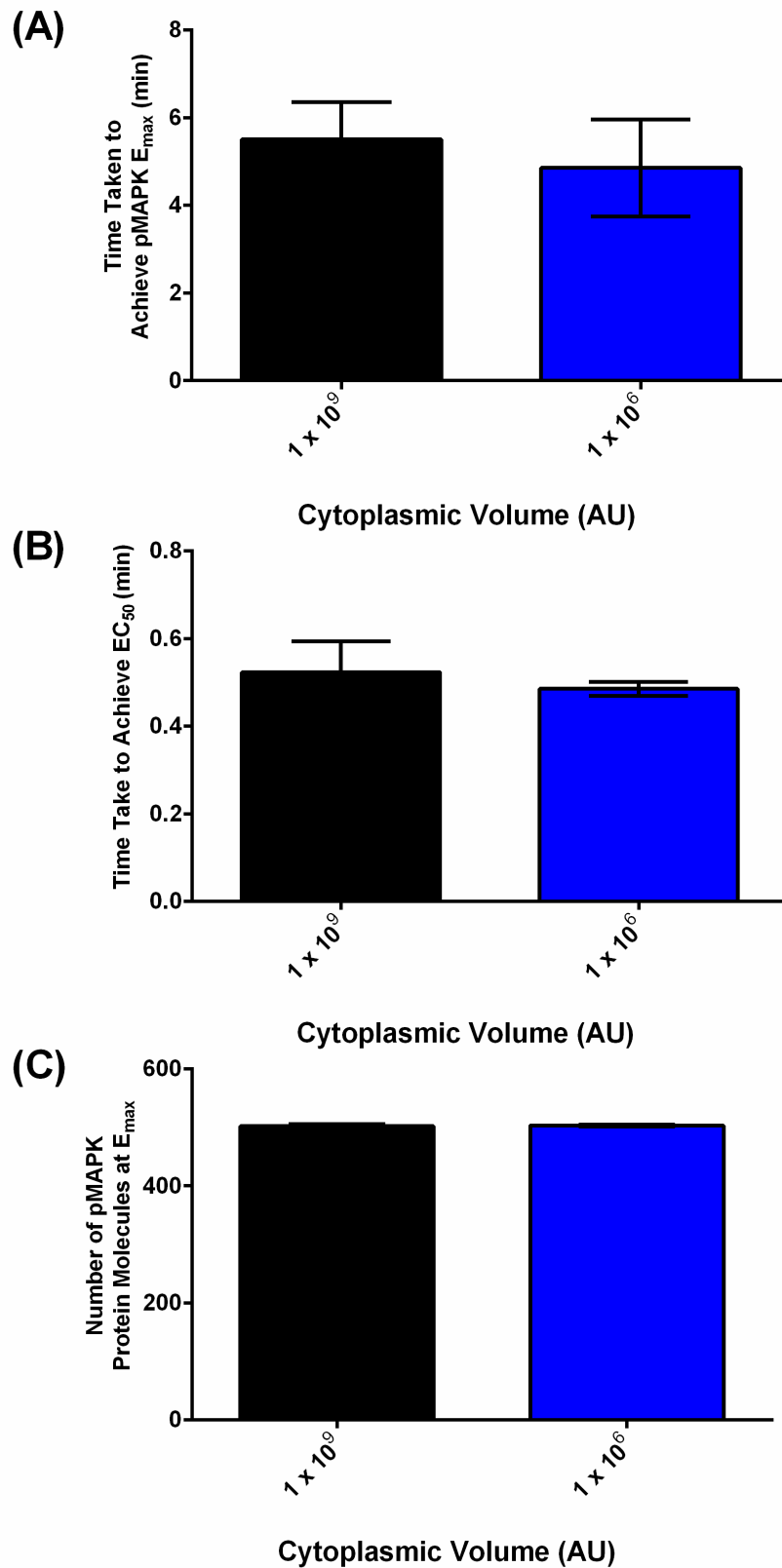


Figure 4. 9 The effect of reducing individual compartments volume on the MAPK activation dynamics in a multi-compartment ABM. (A) The time to achieve E_{max} was measured in two multi-compartment ABMs where the volume of each compartment was reduced by 1000 fold; however there was no significant effect noted. (B) No significant effect was observed with said alteration when the time to achieve EC_{50} was considered. (C) The pMAPK magnitude was not altered significantly with the changes in compartmental volume. The diagrams represent mean \pm SD, statistical was conducted using student t-test with $n = 10$ simulations per model.

agents are already present and compacted in small volume. This is further emphasised with the reduction of the volume of each compartment to 1×10^6 arbitrary units of volume, which did not statistically improve the MAPK activation dynamics (Figure 4. 9). With respect to the two compartments model, only the reduction of the total cytoplasmic volume to 4.19×10^9 illustrated a reduction in the time to achieve E_{\max} and EC_{50} . Considering that this volume is equivalent to the volume of 4 cytoplasmic compartments in the multi-compartment model, this improvement in pMAPK activation dynamics is not surprising. Furthermore, the abovementioned points are supported by the work of Rhodes et al. They have recently published an investigation to examine the effect of modulating the spatial parameter and cell volume in an ABM comprised of two agents, A and B, interacting to form a molecule C utilising FLAME (Rhodes et al., 2016). They conclude that the overall system behaviour remained largely unchanged, and that only when they changed the cell volume 2000 fold, that they have observed a significant change in the behaviour.

4.2.1.4 Further investigation of MAPK activation dynamics in the two compartment agent based model (ABM)

The majority of *in silico* literature investigating the MAPK dynamics (especially with ODEs) assume a two compartmental distribution of the kinases involved in the pathway. The two compartment ABM was further scrutinised to ensure that it captured the fundamental activation behaviour (outlined in section 3.2) prior to its expansion and refinement.

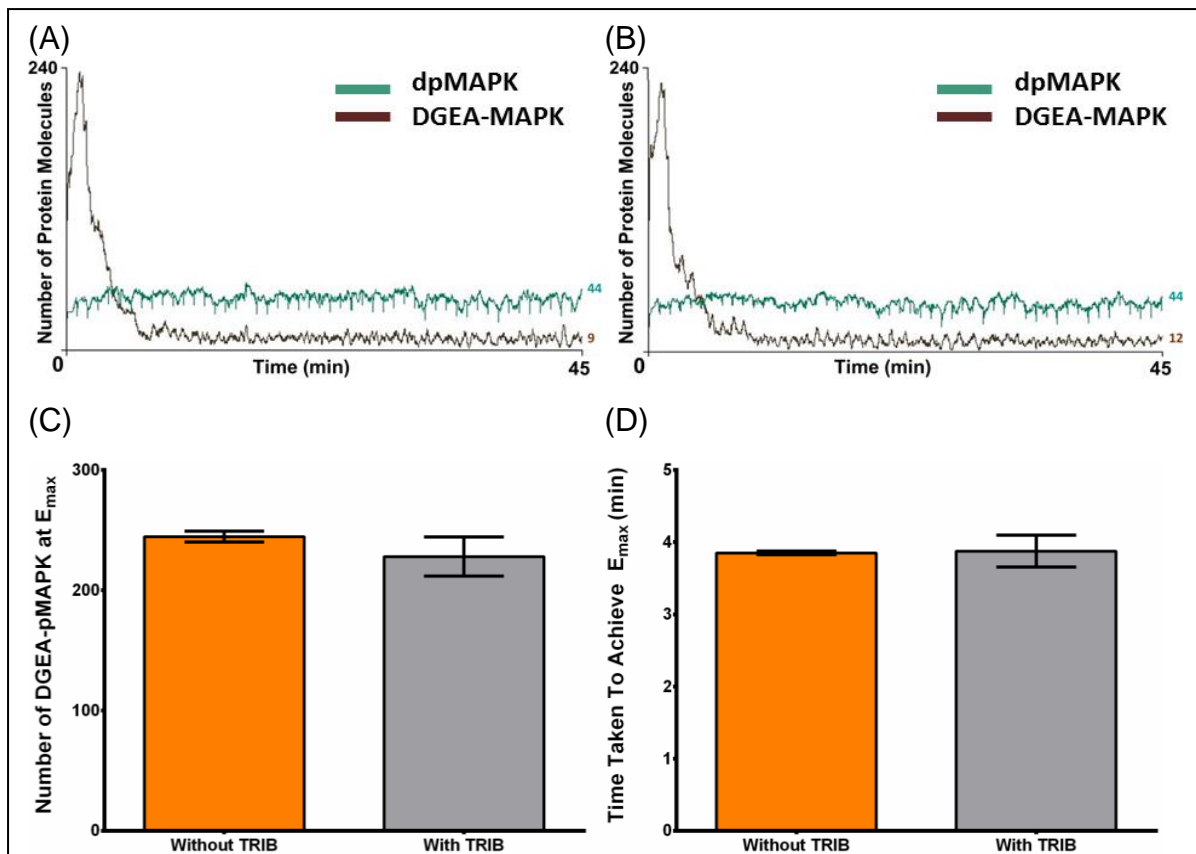
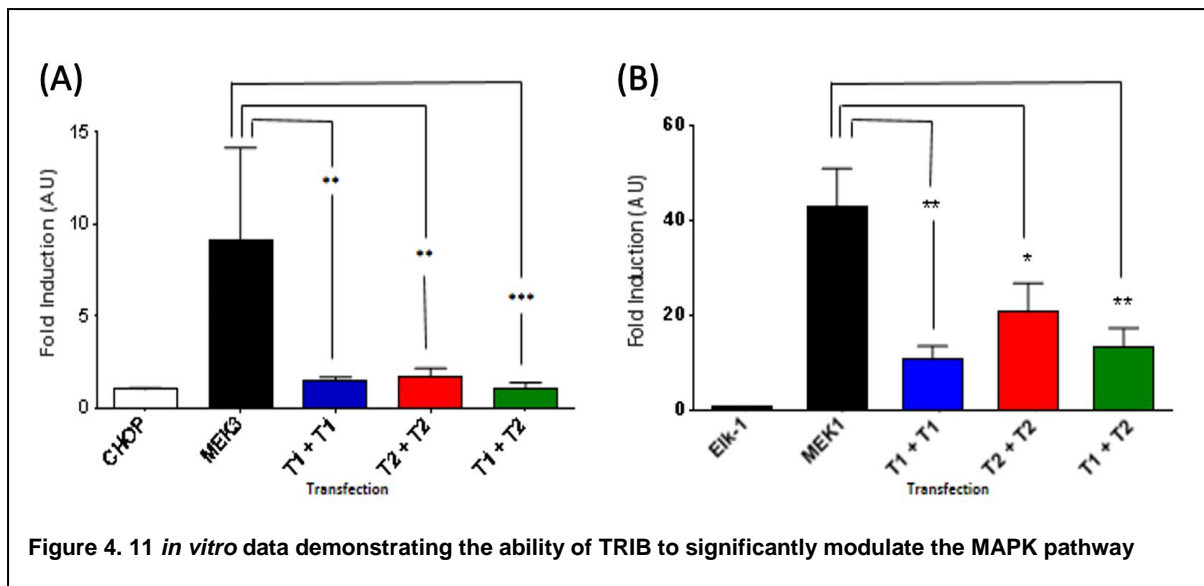


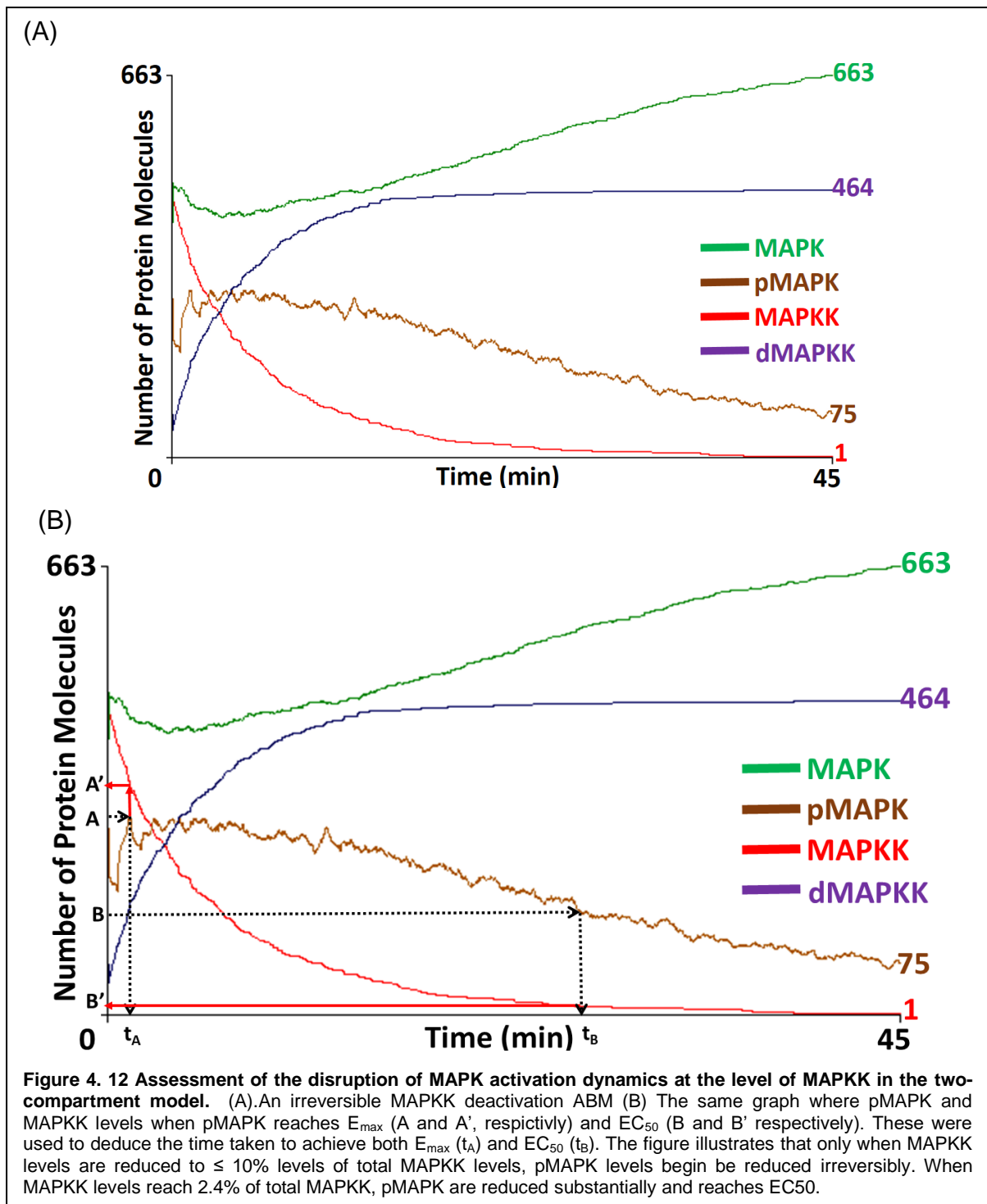
Figure 4.10 A two-compartment ABM simulating of pMAPK-dependent nuclear events and the effect of modulating MAPK activation by tribbles protein agents (TRIB). In reference to figure 3.9, pMAPK interacts with two transcription factor (TF) species, namely SB-TF and MB-TF. Interaction with the latter signals the initiation of the of pMAPK-dependent gene expression. (A) The interaction dynamics between pMAPK and MB-TFs in a two compartment model in the presence of constitutively active pMAPK. The initial phase sees a rapid increase in the number of DGEA-pMAPK and a moderate increase in active MB-TF, thus an increase in the initiation of gene expression events. However, the rapid increase in DGEA-pMAPK levels declines and reaches low levels within “8 minutes]. However, the levels of MB-TF do not diminish overtime (B) The effect of the TRIBprotein-agent introduction on the dynamics of gene-expression initiation within the constitutively active MAPK pathway ABM. The introduction of TRIB does not significantly (using a student t-test) alter the gene-expression initiation dynamics and levels of either DGEA-pMAPK or MB-TF. These conflicts with *in vitro* observations with the strong inhibitory effects tribbles have on MAPK-dependent gene-expression events. The presence of the MAPK inhibitor proteins TRIB has no significant effect on nuclear MAPK activation events in a two-compartment ABM. (C) levels of Dormant Gene Expression Activation pMAPK (DGEA-pMAPK) in the nucleus with and without the presence of TRIB protein-agent. The presence of TRIB does not significantly reduce the levels of DGEA-pMAPK formed. (D) Examination of the time DGEA-pMAPK reach their maximal level (E_{max})in the presence and absence of TRIB agents demonstrate no significant change in the time taken to achieve E_{max} . The model was simulated ten times ($n = 10$) The bars represent mean \pm SD. Student t-test was performed for statistical analysis to assess significance where $p > 0.05$ was considered insignificant effect.

This was done through examining the activation behaviour inside the nucleus and the effect blockade of signal propagation has on cytoplasmic and nuclear events. Thus, the formation of the pMAPK species and gene expression events were evaluated. As shown in Figure 3.9 (A), pMAPK species interact with transcription factors (TFs) in the nucleus. This interaction reflects MAPK-dependent initiation of gene expression events (Figure 4.10 (A) and (B)). Furthermore, the signal



propagation was blocked *via* the introduction of the MAPKK inhibitory proteins tribbles (TRIB). TRIB inhibitory protein agents were homogeneously distributed within the cytoplasm and their levels were as shown in Table 3. 2. The introduction of the tribbles protein, contrary to results obtained *in vitro* (Kiss-Toth et al., 2004, Sung et al., 2006, Sung et al., 2007), did not alter the initiation of gene expression events, and the levels of both DEGA-pMAPK and active MB-TF did not extensively change. This was also observed in the cytoplasmic events where pMAPK levels were not notably altered with the introduction of TRIB, although (as shown in Table 3. 2) the quantity of TRIB agents was more when compared to both tMAPKK and MAPK (Appendix B, Figure 10 (A), (B) and (C)).

To further investigate the level of MAPKK inhibition required to show a considerable alteration in MAPK activation dynamics, TRIB levels in the model were increased by 90%. This resulted in a substantial reduction in pMAPK levels and levels of DEGA-pMAPK and activated MB-TF (*i.e.* gene expression initiation events) were also altered. However, although the MAPK activation was inhibited both at the cytoplasmic and nuclear level, these alterations are not biologically sound. *In vitro*



experiments demonstrated that in order to inhibit gene-expression events *via* the introduction of TRIB proteins, TRIB concentration was only increased by $\sim 2\%$ in order to see a marked reduction in the MAPK-dependent gene expression event (Figure 4. 11 (A) and (B)). The effect of signal propagation blockade was further investigated in the ABM *via* a different approach. MAPKK species were modelled to

undergo irreversible deactivation once they activated MAPK proteins; this is akin to MAPKK degradation events intracellularly (Hurst and Dohlman, 2013). Therefore, the MAPKK activation was not sustained and MAPK levels returned to the levels at t_0 (Figure 4. 12). However, it was observed that when $85 \pm 2\%$ pMAPKK was degraded, pMAPK levels began to reduce irreversibly and continued to decrease until beyond those at basal levels at t_0 . This was also contradictory to previous findings, where a small reduction of MAPKK levels was demonstrated to have statistically significant effects on MAPK activation behaviour in yeast cells (Hurst and Dohlman, 2013).

4.2.2 Discussion and conclusion

The MAPK pathway was investigated thoroughly using *in silico* models, which contributed to the understanding of pathway behaviour (Brightman and Fell, 2000, Ferrell and Machleder, 1998, Ferrell and Xiong, 2001, Huang and Ferrell, 1996, Kholodenko, 2000, Kholodenko et al., 1999, Levchenko et al., 2000, Schoeberl, 2002). These models vary from statistical approaches, probabilistic models to deterministic models using differential equations. The majority of models of the MAPK pathway are deterministic and written using ordinary differential equations (ODEs). Some of the notable breakthroughs from ODE models came from the work of Ferrell *et al.*, (Ferrell and Machleder, 1998, Huang and Ferrell, 1996), Kholodenko *et al.*, (Kholodenko, 2000, Kholodenko, 2002) and Levchenko *et al.* (Levchenko et al., 2000). Levchenko had explained the contradictions observed experimentally regarding the concentrations of KSR1 scaffold protein. He showed that scaffolds have to be within an optimal concentration in order to enhance MAPK activation

behaviour Ferrell's model was one of the first for the MAPK pathway and it shed light on the pathway architecture and how that influences pathway dynamics. Models of the pathway which followed Ferrell's study had expanded to include feedback mechanisms. In these models positive and negative feedback loops were shown to be important, where their presence lead to the appearance of bistable and ultrasensitive activation behaviour in the pathway (Shin et al., 2009b, Tian et al., 2009, Tsai et al., 2008). Additionally, models that investigated the architecture of the feedback loops showed that two circuit designs of coupled positive and negative feedback-networks result in oscillatory behaviour (Sarma and Ghosh, 2012). The oscillatory behaviour of the MAPK pathway was only experimentally demonstrated recently (Shankaran et al., 2011, Shankaran et al., 2009, Weber et al., 2010).

However, investigating the spatial and temporal regulatory elements and their effect on pathway activations simultaneously, using ODEs is difficult, because ODEs do not have the capability to include spatial parameters (Angermann et al., 2012, Calder et al., 2006b, Klann et al., 2011, Mallavarapu et al., 2009). Furthermore, model amendments and improvements require the writing *de novo* equations. As a result, the most common representation of the MAPK pathway in the literature using ODEs is using the assumption of two compartments. This is understandable due to the continuum concept, which relies on representing the proteins as a population; and considering that, biologically, the majority of the kinases in the cell are distributed between the two compartments. However, there is strong evidence that the functional location of these kinases resides in subcellular compartments such as the endosome, Golgi or other cellular locations (Fan et al., 2008, Lee et al., 2011, Teis et al., 2002, Torii et al., 2004, Wunderlich et al., 2001). Since ABMs are able to

incorporate spatial parameters into the simulation, they are an excellent tool to use to meet the need for refined modelling. Furthermore, the ability of ABMs to model the interaction between proteins and with their environment, and its capability of giving autonomy to each component, provides a further advantage.

In this section, the effect of compartmentalisation on the MAPK pathway was investigated via the construction of two ABMs with two different 3D intracellular environments. The first contained only the cytoplasmic and nuclear compartments while the second model also included 10 cytosolic compartments. The ABMs reveal that homogeneous distribution of the MAPK kinases in a two compartment model did not lead to the emergence of MAPK activation dynamics, which are usually observed *in vitro* and *in silico*. Although the two compartment-ABM had demonstrated an activation pattern and pMAPK accumulation while MAPKK interacted with MAPK, the dynamics observed demonstrated an incremental increase in pMAPK levels (i.e. a graded/analogue activation behaviour) compared to the normally reported ultrasensitive response (Figure 4. 3 (A)). This occurred although the construction of the ABM was based on previous ODE models. These models implemented a one- or two-compartment architecture with well mixed MAPK components that are “assumed” to be moving randomly within the cytoplasm. Homogeneous expression of proteins coupled to their random movement caused the increase in their diffusion parameters and reduction in their probability to encounter and interact with other proteins (Bhalla, 2004a, Kholodenko et al., 2000, Kholodenko et al., 1999, Klann et al., 2011, Zhao et al., 2011). Therefore, this graded response in the ABM is due to the homogeneity and the Brownian motion of the kinases implemented in the model. An increase in diffusion parameters was shown to cause a reduction in reaction

order, and followed Michaelis–Menten kinetics. Reduction of the diffusion parameters showed an increase in the reaction order and the emergence of reaction behaviour with a sigmoidal activation curve. This is well documented in reactions involving scaffold proteins, such as KSR and MP-1, where the pathway kinases are brought together into closer proximity, thus reducing their diffusion coefficient, and therefore the probability of their interaction. Furthermore, this causes an increase in the level of phosphorylated MAPK species (Bray and Lay, 1997, Calder et al., 2006b, Ferrell, 2000, Klann et al., 2011, Levchenko et al., 2000).

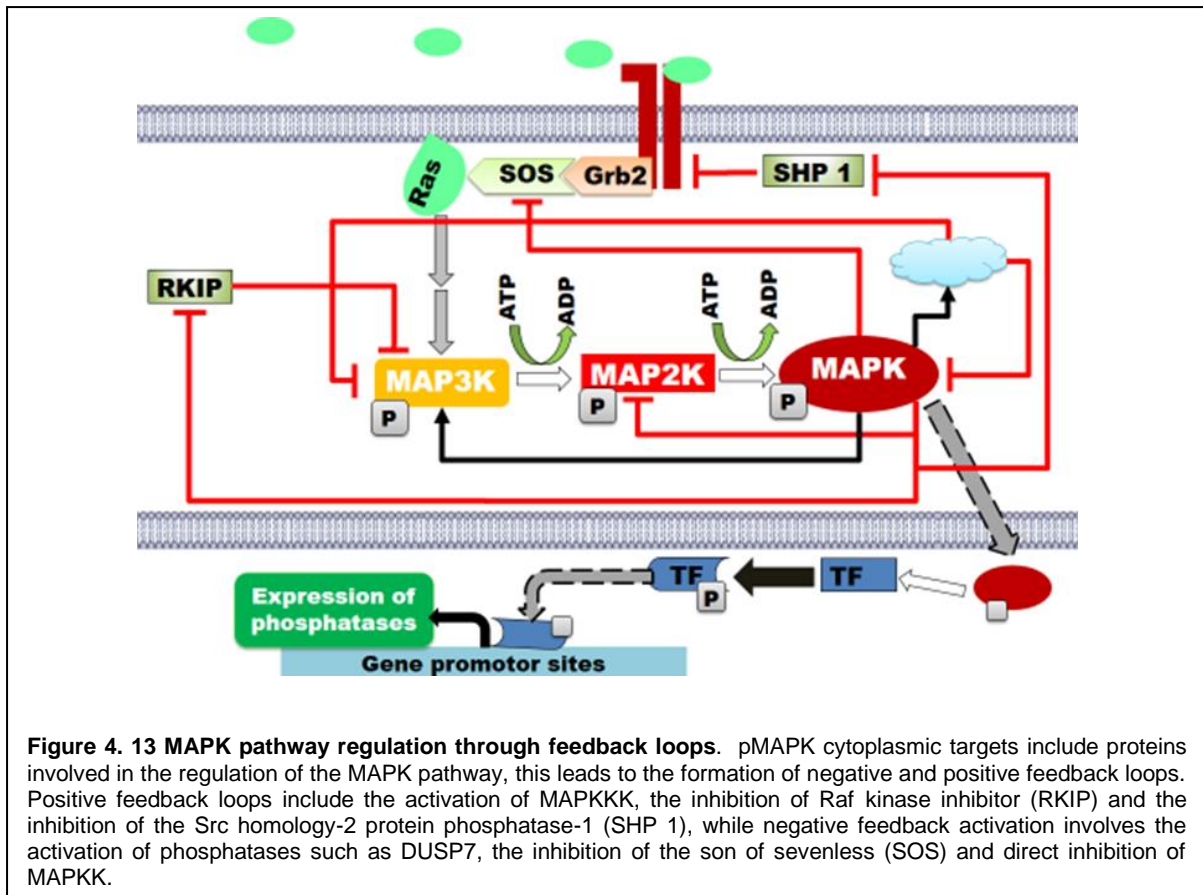
In the real world, homogeneous distribution of the kinases intracellularly renders them accessible to regulatory proteins such as phosphatases (Bhalla, 2004a, Kholodenko, 2003, Kholodenko, 2009, Kholodenko et al., 2000, Klann et al., 2011). This counterbalances the activation of the kinases, and thus further reduces the level of accumulated kinases, particularly the pMAPK species, thus slowing down or stopping signal propagation (Bhalla et al., 2002, Takekawa et al., 1998). Nonetheless, once a MAPK pathway is activated at the plasma membrane, the signal is propagated through the cytoplasm into the nucleus, despite presence of phosphatases in the cytoplasm, and also their activation by MAPK phosphorylation (Brondello et al., 1999, Katagiri et al., 2005, Kucharska et al., 2009, Lewis et al., 1998b, Marchetti et al., 2005). *In silico* models had demonstrated that to allow for signal spread, phosphatases and kinases are arranged in intracellular protein complexes leading to formation of active phospho-kinase species pools (Kholodenko, 2009, Mugler et al., 2012, Munoz-Garcia et al., 2009, Shvartsman et al., 2009, van Albada and ten Wolde, 2007). As a result, the signal either becomes localised to the regions that harbour these complexes or propagated into more

interior parts of the cell via waves of phosphorylation. These mechanisms for spreading the signal are thought to be active in neurons where excitation at the post-synaptic junctions has to be propagated through the axon to the nucleus, or to pre-synaptic junctions (Canal et al., 2011). This suggests that compartmentalising the MAPK components in intracellular domains is a crucial factor in shaping pathway activation behaviour, and consequently determining cell response.

All of the above arguments and ideas suggest that the integration of multi-compartments into the ABM will be a better model to investigate the MAPK activation dynamics. Biologically, intracellular compartmentalisation of the MAPK components is emerging as a fundamental mechanism in pathway regulation and mediating specificity and fidelity. Scaffold proteins such as KSR1, paxillin and p14, were also shown to be localised in special cellular compartments (for instance, Golgi, the endosome and the plasma membrane) (Canal et al., 2011, Ishibe et al., 2003, Schaeffer et al., 1998, Wunderlich et al., 2001). Thus, anchoring the kinases in these compartments and allowing them to be in close proximity while reducing diffusion parameters (van Albada and ten Wolde, 2007). The multi-compartment ABM presented here further supports the major role of intracellular compartments in influencing the pathway activation behaviour. In this ABM, the multi-compartments strengthened the ultrasensitive response and caused a more rapid activation of MAPK (Figure 4.3 (B) and Figure 4.6). This is reflected quantitatively by the shorter time to achieve both E_{max} and the EC_{50} ; the higher rate of activation (*i.e.* MAPK conversion to pMAPK) and higher levels of pMAPK achieved at E_{max} (Figure 4.6 (A) and Appendix B, Figure 9). Qualitatively, this is reflected by the emergence of the ultrasensitive activation behaviour in the model. It is worth highlighting that in the

multi-compartment ABM the total number of MAPKK in the model was only 10% of the two-compartment ABM. This was achieved through restricting MAPK and MAPKK to the compartments, which reduced their ability to diffuse into the cytoplasm. In addition, multi-compartments provided an interaction volume which brought the kinases into a closer proximity and increased the probability for interaction. This is analogous to the mechanisms proposed for the action of scaffold proteins to increase the efficiency of MAPK activation (Bhalla, 2004a, Klann et al., 2011, Neves and Iyengar, 2009).

In summary, the investigation presented here revealed that the use of a two-compartment model of the MAPK pathway with homogeneously distributed kinases, in addition to its physiological inaccuracy, leads to a graded and irreversible pathway activation behaviour, and does not produce the commonly biologically observed pathway activation behaviour that is the ultrasensitive response. Thus, this is a misrepresentation of the pathway. This is strengthened by the emergence of the expected pathway activation dynamics (rapid activation and an ultrasensitive response) when multi-compartmentalisation had been implemented in the model. This reinforces the notion that the ABM approach is capable of producing robust models that faithfully re-create pathway behaviours observed experimentally. Consequently, the multi-compartment model was taken forward to inspect temporal regulation, and how the combination of spatial and temporal elements impact on the activation dynamics of the pathway.



4.3 The combination of spatiotemporal regulations play a role in shaping pathway activation behaviour

In this subsection, both the temporal and spatial regulatory elements were combined in the ABM to assess how their combination and modification impact the activation behaviour of the pathway. This was achieved by implementing a temporal component in the multi-compartment ABM, which controlled the activation of MAPKK. This temporal component was the memory parameter re-activation delay period $[[RADP]]$. The null hypothesis is as follows: modification of the temporal element in a multi-compartment ABM has no substantial effect on the activation behaviour of MAPK.

The MAPK pathway is highly regulated (Figure 4. 13). These regulatory mechanisms either enhance or abate the original response, and are highly specific to the cellular and signalling state. As a result, the outcome from the pathway (output) is reliant on the balance between activating inputs and deactivating inputs (Bhalla et al., 2002, Cirit et al., 2010, Haj et al., 2003, James E, 1996, Jeffrey et al., 2006, Sewing et al., 1997, Shalom-Feuerstein et al., 2008). These include phosphorylation and dephosphorylation events mediated by kinases and phosphatase enzymes, respectively, as well as chemical and/or biological inhibitors.

Furthermore, MAPKK was shown previously to act as a bottleneck for the JNK pathway and by the use of chemical inhibitors such as U0126 and PD-098059 (Duesbery et al., 1998) (Alessi et al., 1995, Favata et al., 1998, Haeusgen et al., 2011). Thus, MAPKK was considered in the ABM as the point of convergence for these activating and deactivating inputs, which influence the pathway output. Given that the level of active MAPK generated (hence the strength of the output) relies on the balance between the activating inputs against the deactivating inputs at the level of MAPKK, the signalling output is proportional to the number of active MAPKK molecules present in the system.

As described in section 3.3.2.2.2, and shown in Figure 3. 5 (page 107), RADP exerted a control over the temporal element by dictating the time MAPKK remained in a dormant state. Thus, RADP regulates the number of active MAPKKs available in the cell. RADP was designed to represent the balance between activating and inhibiting inputs at the level of MAPKK. A strong activating signal, coupled with weak

inhibition results in a sustained propagation of the signal and high level of activated MAPKK. Conversely, a weak activating signal coupled with a strong inhibition results in a reduced number of active MAPKK species in the system, and ultimately inhibition of MAPK activation and signal propagation. This was implemented by varying RADP, whereby short RADPs result in high levels of active MAPKK, while long time periods cause the population of dormant MAPKK to increase. The time periods of 90 s, 4.5 min, 7.55 min and 22.6 min were chosen, as they associate with relevant time points in MAPK activation. This was based on the deduction made in section 4.1 that the median time for pMAPK to reach their E_{\max} was 7.63 (see Figure 4. 1). Therefore, the model opted to assess the significance of modulating the temporal activation behaviour on global MAPK activation at the chosen time-points. An activation cue is strongest at the initial phase, where activation is instantaneous and inhibitory inputs are minimal; at this time point the majority of MAPKKK has been activated and, therefore, pMAPKK proteins are also activated (Hornberg et al., 2005b, Santos et al., 2007c, Shin et al., 2013, Shin et al., 2009b) (Hanada et al., 1998, Takekawa et al., 1998). Hence, the initial 90 s of activation was chosen to investigate modulation of the temporal activation behaviour at that stage. The 4.5 min time point was chosen as it was within the linear and intermediate phase of the ultrasensitive response. This signifies the rapid activation of MAPK and its accumulation into the nucleus. Therefore, this provides a good assessment of the significance of altering the temporal activation dynamics at that stage. The 7.56 min time point was chosen as it is immediately before the median time to reach E_{\max} . This allowed for examining the significance of modifying the temporal activation dynamics at that stage. Biologically, the activation response elicited by a transient activating signal receded after 20 minutes, where levels of activated MAPKK and

MAPK reached basal levels. Therefore, the 22.6 min time point was chosen to assess the effect of modifying the temporal activation dynamics at this stage.

Biologically, a cell is exposed to two forms of stimulation environment; a sustained/periodic activation environment or a dynamic activating environment (Alberts et al., 2002). In a periodic activating environment, the cell is initially exposed to a high intensity yet transient stimulus, which is followed by strong inhibitory feedback. These include the exposure to growth factors (for instance FGF and growth hormone) or to neurotransmitters (acetylcholine and serotonin) (Atherton et al., 2015, Spiegel et al., 2000). For a dynamic activating environment, a tug-of-war is occurring between activating and inhibitory inputs. This is where positive and negative feedback loops are both activated, corresponding to a cell exposed simultaneously to pro-survival and pro-apoptotic signals; for instance, glioblastomas treated with the cannabinoid Δ 9-Tetrahydrocannabinol (THC) (Aguado et al., 2007, Aksamitiene et al., 2010, Wong et al., 2007). To accommodate for this, the RADP was modelled either deterministically or stochastically (Figure 3. 4). A deterministic RADP mimics the periodic and sustained activation environment. RADP was defined as a particular time point where every MAPKK species become re-activated. The time points are what were specified above. The stochastic RADP was to imitate the dynamic activation environment. Comparable to the real-world scenario, the activation state of a MAPKK molecule depends on the proteins which are in close proximity to it (for instance a MAPKKK, a phosphatase or MAPK), and hence the feedback apparatus in its environment. Therefore, a single MAPKK protein becomes activated and deactivated depending on which protein is in close proximity to it. Thus, molecularly, in such an environment, is the time a MAPKK molecule stays in

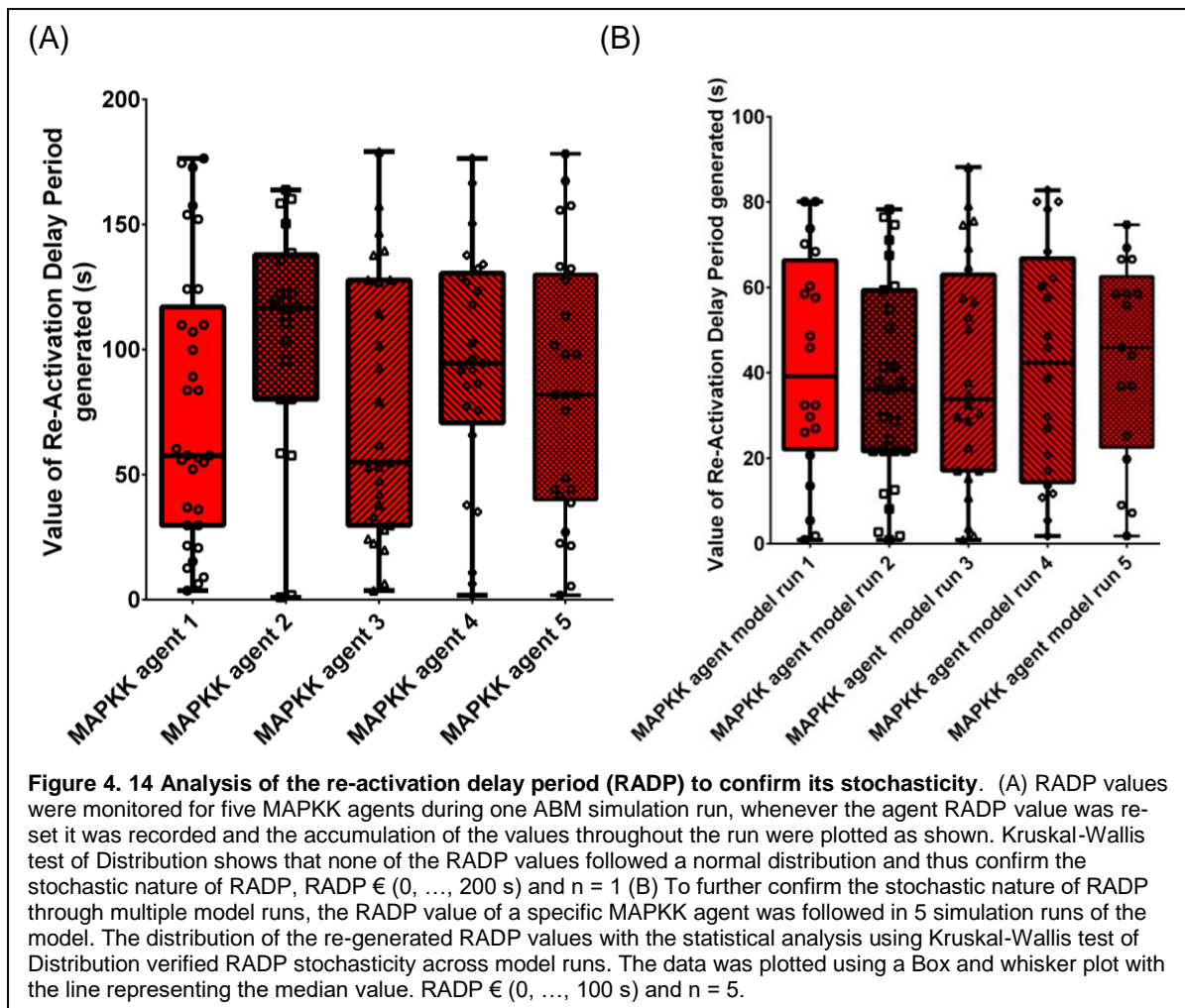
an active or inactive/dormant state, and will vary within the course of the stimulation. Furthermore, this time will also differ between the individual proteins in the population. RADP was modelled where the time point chosen (see above) represented a set of time which a MAPKK agent can adopt one of them with equal probability.

The simulations were run using the FLAME environment; visualisation and graph plotting were done using the FLAME visualiser. The following subsections outline the results obtained from the combination of the spatiotemporal regulatory elements and modification of the temporal activating behaviour in a multi-compartment environment.

4.3.1 Results

4.3.1.1 *Validating MAPKK Reactivation delay period (RADP) stochasticity*

RADP was modelled stochastically as described on page 138. Briefly, RADP was modelled to assume particular time intervals which maintain MAPKK in an inactive state. These time intervals were 90s, 4.5 min, 7.55 min and 22.6 min. A stochastic RADP with a time interval of 3 min, for instance, could adapt any time value from 0 to 3 min. The probability of each time point to be generated was equal i.e. modelled using a uniform distribution. Figure 4. 14 demonstrates this point. Within one model run the RADP value of 5 agents were monitored (Figure 4. 14 (A)), statistical analysis illustrates that there is no significant difference between the distributions, and when a normality test was conducted using a nonparametric test, and using



Kruskal-Wallis test of Distribution, the distribution was not Gaussian. RADP was also tested by monitoring the RADP value generated by one MAPKK agent in 5 ABM simulations. The distributions of RADP values were plotted as shown in Figure 4.14 (B). The Kruskal-Wallis test of Distribution confirmed that RADP values were stochastically generated.

4.3.1.2 *MAPKK re-activation delay influences the dynamics of pMAPK formation in a multi-compartment model*

The significance of modifying MAPKK re-activation delay period (RADP) on MAPK activation dynamics was investigated. This was done by comparing system

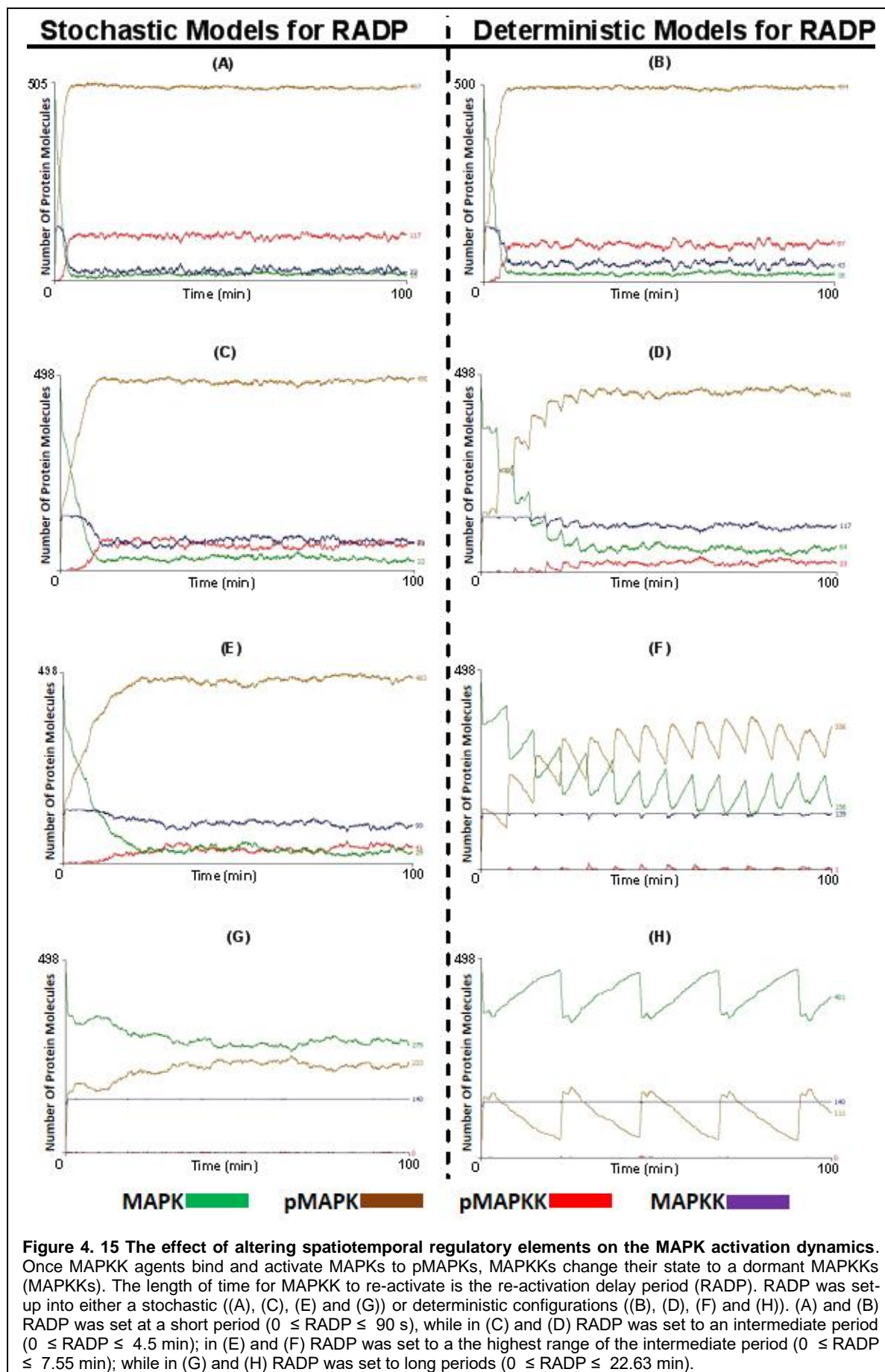
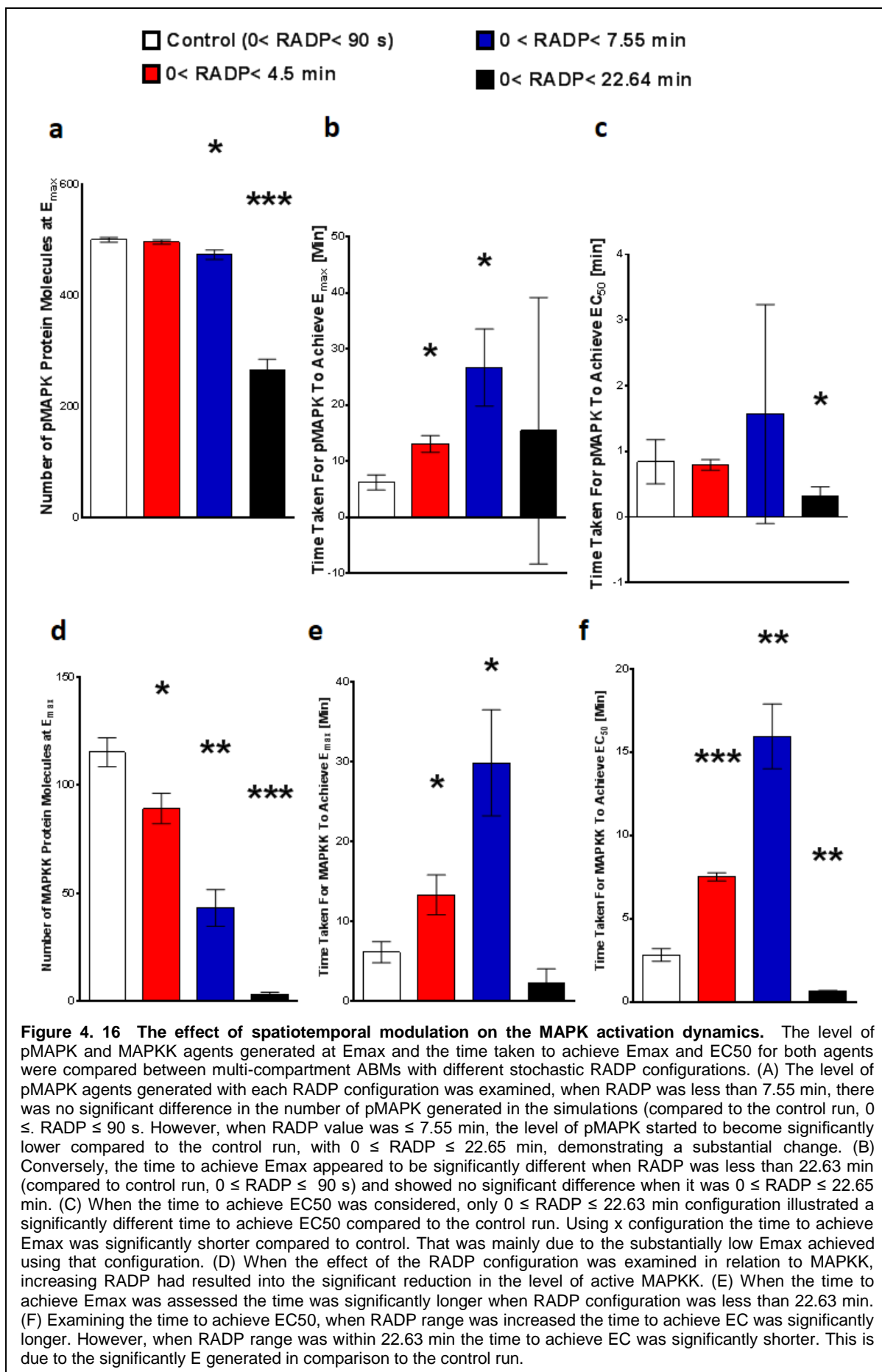


Figure 4.15 The effect of altering spatiotemporal regulatory elements on the MAPK activation dynamics. Once MAPKK agents bind and activate MAPKs to pMAPKs, MAPKKs change their state to a dormant MAPKKs (MAPKKs). The length of time for MAPKK to re-activate is the re-activation delay period (RADP). RADP was set-up into either a stochastic ((A), (C), (E) and (G)) or deterministic configurations ((B), (D), (F) and (H)). (A) and (B) RADP was set at a short period ($0 \leq \text{RADP} \leq 90$ s), while in (C) and (D) RADP was set to an intermediate period ($0 \leq \text{RADP} \leq 4.5$ min); in (E) and (F) RADP was set to a the highest range of the intermediate period ($0 \leq \text{RADP} \leq 7.55$ min); while in (G) and (H) RADP was set to long periods ($0 \leq \text{RADP} \leq 22.63$ min).

behaviour in stochastic vs. deterministic RADP configuration (Figure 4. 15). When short RADPs were investigated, the system maintained robust and rapid MAPK activation in both the stochastic ($0 \leq \text{RADP} < 90 \text{ s}$) and deterministic models of RADP (RADP=90 s) (Figure 4. 15 (A) and (B)). When the RADP value was switched to 4.55 min, although the stochastic model ($0 \leq \text{RADP} < 4.55 \text{ min}$) had maintained the robust and rapid MAPK activation behaviour signified by the pMAPK magnitude, and the time to reach E_{max} and EC_{50} (Figure 4. 15 (C) and Figure 4. 16 (a)-(c)), in the deterministic models (RADP = 4.55 min) an oscillatory behaviour started to emerge (Figure 4. 15 (D)). This behaviour was also visible in the stochastic model, when stochasticity was minimal (for instance, $4.38 \leq \text{RADP} < 4.53 \text{ min}$, Figure 4. 17). The data obtained from these experimentations were validated as following. Where the sustained oscillatory behaviour first emerged in the ABM, the wavelength between the pMAPK peaks and the deactivation phase of the oscillatory behaviour were validated against the data observed by Shankaran et al, (Shankaran et al., 2009). For the stochastic RADP model, due to the lack of technology which allows modulation of feedback loops at precise and exact time-points, the data were only validated against the specifications mentioned above (i.e. the time to achieve E_{max} and EC_{50} in addition to the magnitude of the pMAPK produced).

Next, longer RADP values were investigated ($0 \leq \text{RADP} < 7.56 \text{ min}$). Stochastic RADP models had maintained their ability to generate high levels of pMAPK species (MAPK levels were reduced to $93.9 \pm 1.7\%$ at E_{max} ; Figure 4. 16 (a)). Nonetheless, the rate of activation had been reduced and the time to achieve E_{max} increased by 4.3 fold (Figure 4. 16 (b)). However, when the stochasticity of the RADP configuration was at its minimal ($7.53 \leq \text{RADP} < 7.55 \text{ min}$), or the RADP value was



fixed to create a deterministic mode ($RADP = 7.55$ min), the minor oscillatory behaviour observed in earlier models (Figure 4. 15 (D)) evolved into complete oscillatory behaviour (shown in Figure 4. 15 (F)).

$RADP$ was set at 22.64 min and this was modelled stochastically and deterministically (Figure 4. 15 (G) and (H)). The stochastic model of $RADP$ had resulted in reduced MAPK activation. This was signified by a reduction of MAPK to $47.4 \pm 3.9\%$ from 100% levels at t_0 (Figure 4. 16 (a)). This is in contrast to a 95% reduction observed when $0 < RADP \leq 90s$ (Figure 4. 15 (A) and Figure 4. 16 (a)). This reduction in MAPK level magnitude at E_{max} is statistically different from the control (when $0 < RADP \leq 90s$); however, the MAPK levels were five times higher than EC_{50} values in the control. This was unexpected, as inhibiting MAPKK activation within 20-30 minutes was anticipated to cause insignificant change in MAPK values and the return of pMAPK levels to baseline at t_0 . Yet, when $RADP$ was set to $RADP = 22.64$ min, MAPK and pMAPK levels approached their basal levels, and levels lower than their EC_{50} as seen in Figure 4. 15 (G).

Nevertheless, using this configuration, the model retained a degree of responsiveness to the initial stimulus. This appears to have emerged due to the ability of low levels of activated MAPKK to maintain a high level of pMAPK in the model. Conversely, in the deterministic configuration (*i.e.* $RADP = 22.6$ min), the MAPK activation dynamic evolved into a sustained oscillatory behaviour (Figure 4. 15 (H)).

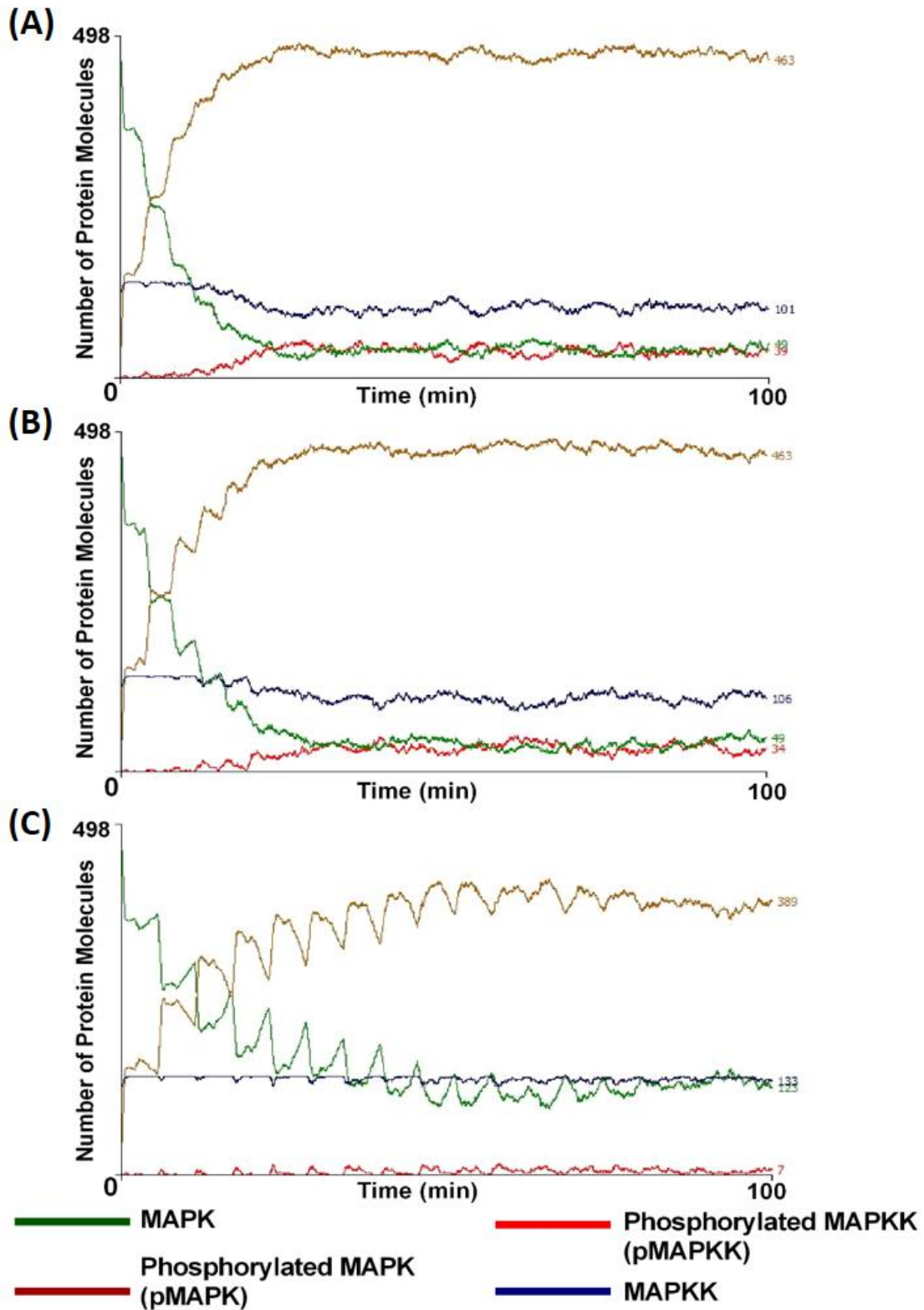


Figure 4. 17 The effect of minimal stochasticity of RADP on the MAPK activation. Stochastic models of RADP were tested with several ranges, as the ranges were lowered, the stochasticity of RADP reduced, this was evident as these models with minimal stochasticity demonstrated MAPK activation dynamics identical to those of the deterministic RADP models in regard to the magnitude of pMAPK and time to achieve EC50 and Emax. (A) RADP was set into this range $3.77 \leq \text{RADP} < 4.53$ min, the figure illustrates the beginning of the emergence of the minor oscillatory responses at the initial activation phase. (B) shows the model with $4.15 \leq \text{RADP} < 4.53$ min, the initial phase of MAPK activation demonstrate sharper miniature oscillatory activity at the initial activation stage. (C) demonstrates a model with $4.38 \leq \text{RADP} < 4.53$ min.

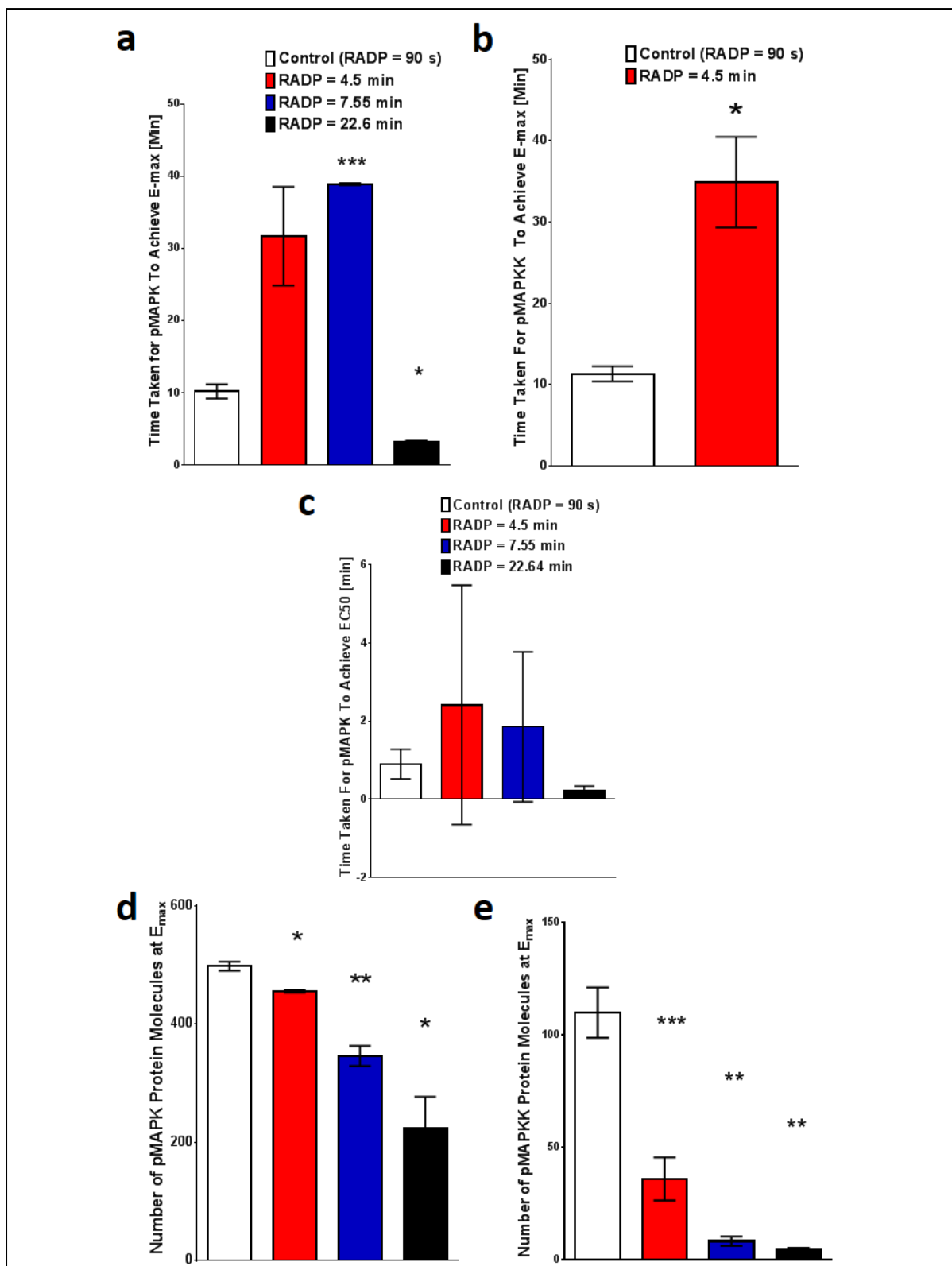


Figure 4. 18: (Fig 4.16) The effect of spatiotemporal modulation on the MAPK activation dynamics using deterministic re-activation delay periods. The multi-compartment ABM utilising deterministic RADP configurations were analysed. (A) Time to achieve pMAPK E_{max}. (B) Time to achieve E_{max} for active MAPKK (pMAPKK). Only the times for RADP =90 s and RADP = 4.5 min are shown due to the low levels of pMAPKK generated when RADP was set at 7.55 min and 22.6 min. Thus, it was difficult to deduce the true E_{max} values. (C) There was no significant difference in the time to achieve EC₅₀ for pMAPK with the different RADP configurations. Due to difficulty to achieve a true EC₅₀ for pMAPKK, the time to achieve EC₅₀ for was not postulated for pMAPKK (D) The levels of pMAPK at E_{max} for are significantly lower as RADP is increased. (E) The levels of pMAPKK at E_{max} with the different RADP configurations. Increasing RADP value significantly lowers the levels of pMAPKK at E_{max}.

4.3.1.3 Global MAPK activation dynamics depend on simultaneous spatiotemporal regulation and the mode of MAPKK activation

To confirm that the emergent behaviours observed in the spatiotemporal models outlined above were due to the simultaneous modulation of spatiotemporal regulatory elements of the MAPK pathway at the level of MAPKK, the RADP models outlined previously were implemented in a two compartment model (Figure 4. 19). The time points chosen for this assessment were 90s and 22.6 min, as these two time points represent two extremes. The former is the time point where the model demonstrated the least difference in MAPK activation behaviour, when RADP assumed both stochastic and deterministic configurations, while the contrary was observed when 22.6 min were used (see Figure 4.16). The stochastic and deterministic models for these time points were used in the two compartment model. In these configurations neither an ultrasensitive response nor oscillatory behaviour emerged with either stochastic (Figure 4. 19 (A) and (C)) or deterministic configurations (Figure 4. 19 (B) and (D)) of RADP. Statistical analysis shows that there was no significant difference between these models in regard to pMAPK formation, MAPKK activation or re-establishment of MAPK levels (Appendix B, Figure 11). Nevertheless, in these RADP models, the characteristic graded MAPK activation response emerged, albeit, the level of pMAPK generated in these models were lower in comparison to those in the multi-compartment models with a statistical significance of $p < 0.01\%$ (see Appendix B, Figure 11 (A)). Additionally, the graded MAPK response observed in these two-compartment models was at least 1.5 fold

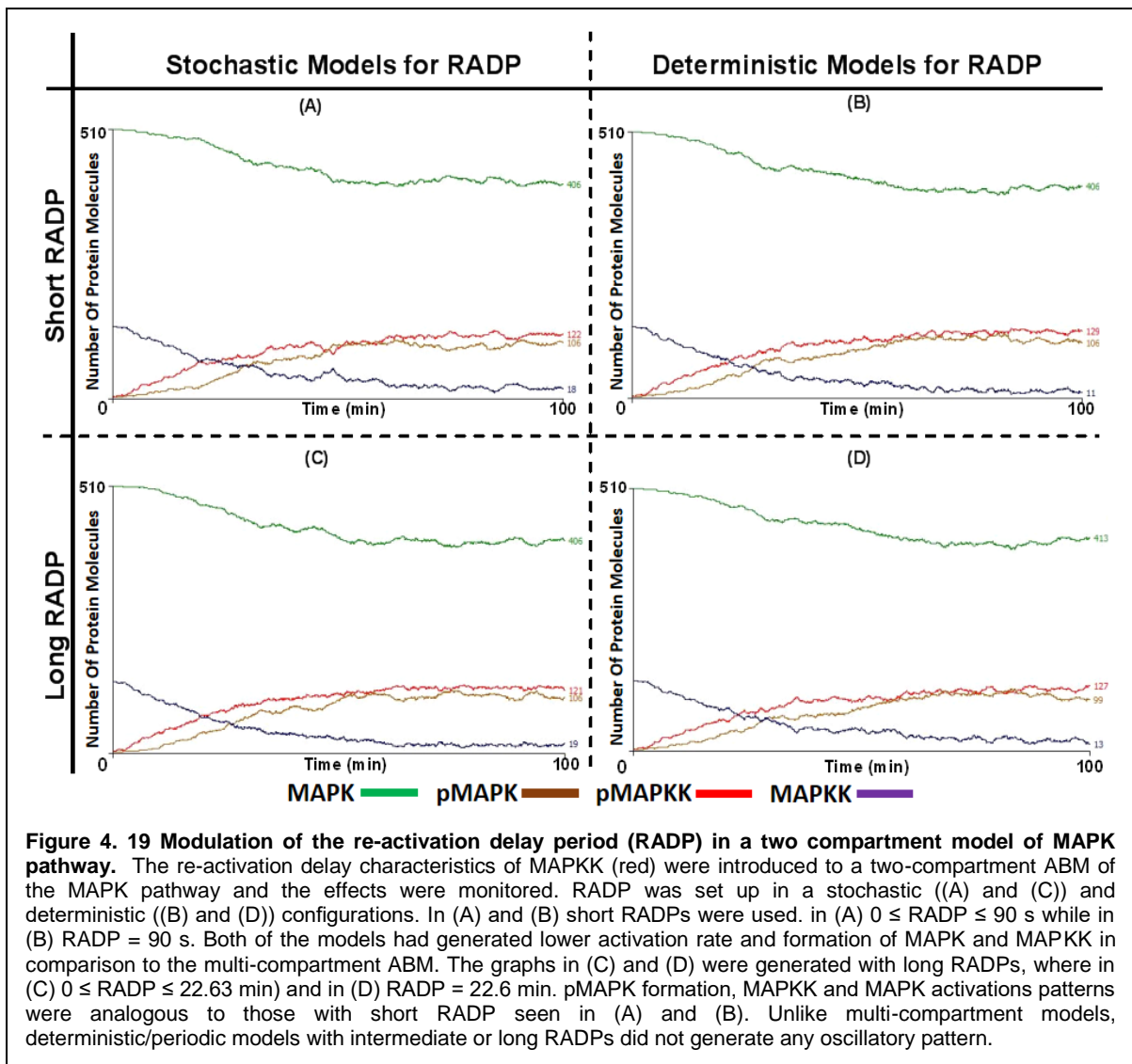


Figure 4. 19 Modulation of the re-activation delay period (RADP) in a two compartment model of MAPK pathway. The re-activation delay characteristics of MAPKK (red) were introduced to a two-compartment ABM of the MAPK pathway and the effects were monitored. RADP was set up in a stochastic ((A) and (C)) and deterministic ((B) and (D)) configurations. In (A) and (B) short RADPs were used. in (A) $0 \leq \text{RADP} \leq 90$ s while in (B) $\text{RADP} = 90$ s. Both of the models had generated lower activation rate and formation of MAPK and MAPKK in comparison to the multi-compartment ABM. The graphs in (C) and (D) were generated with long RADPs, where in (C) $0 \leq \text{RADP} \leq 22.63$ min and in (D) $\text{RADP} = 22.6$ min. pMAPK formation, MAPKK and MAPK activations patterns were analogous to those with short RADP seen in (A) and (B). Unlike multi-compartment models, deterministic/periodic models with intermediate or long RADPs did not generate any oscillatory pattern.

slower in comparison to those observed in the multi-compartment ABMs (see Appendix B, Figure 11 (B)).

4.3.2 Discussion and conclusion

Negative and positive feedback loops play a role in the dynamics of the MAPK pathway. These mechanisms modulate the intensity and the duration of MAPK activation. As shown in Figure 4. 13, the pathway is heavily regulated by feedback loops. The inclusion of RADP in the ABM was to introduce a temporal regulatory element into the MAPK pathway, and to integrate feedback mechanisms into the

multi-compartment ABM. This introduction revealed several characteristics of the activation behaviour. The first is that activating and inhibiting inputs at the level of MAPKK plays an important part in the activation dynamics. The second is that distinctive activation dynamic behaviour emerges from variation in the nature of input at this level of the cascade. Finally, compartmentalisation and periodic RADP together were necessary for the emergence of oscillatory MAPK activation behaviour. These results are in line with the theories that negative and positive feedback loops are important in controlling the activation dynamics of the pathway, especially ultrasensitivity and bistability (Butcher et al., 2003, Cai et al., 2008, Ferrell Jr, 2002, Hayashi et al., 2001, Neves and Iyengar, 2009). The emergent oscillatory behaviour in the ABM was validated against Shanakran et al, where the oscillatory behaviour in the MAPK pathway was demonstrated for the first time (Figure 4. 20).

At short RADPs no distinct differences in the activation dynamics were observed between deterministic and stochastic configurations of RADP in the ABMs (Figure 4. 15 (A) and (B)). This suggests that once the pathway is activated, and the balance of inputs is shifted towards activating inputs, the manner of feedback is irrelevant, as the priority is to respond to the signal. Consider that at basal level, activating and inactivating inputs are balanced (*i.e.* at equilibrium). When an intense signal initiates MAPK pathway activation, the balance is tipped towards the activating inputs. As the median E_{\max} value is achieved within 7.73 min, any shift in the balance between activating and deactivating inputs prior to that time is overcome by the strength of the activating signal. In addition any periodicity in deactivating inputs which is shorter than that median time is incapable of overcoming the initial activating input.

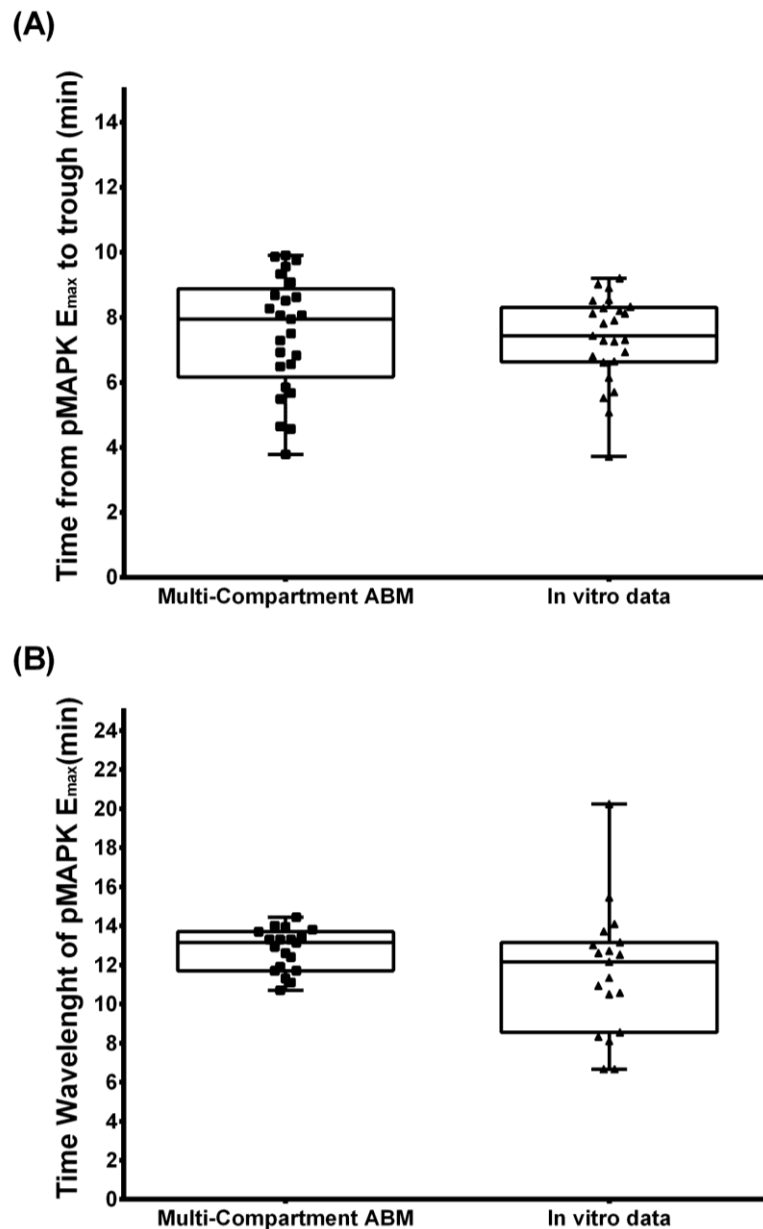


Figure 4. 20 Validation of the emergent pMAPK oscillatory behaviour in the multi-compartment ABM against the oscillatory behaviour in the MAPK pathway first demonstrated by Shankaran et al. (A) The time between peak and trough pMAPK levels were manually analysed from the publication of Shankaran et al and compared to the oscillatory behaviour first observed in the ABM multi-compartment ($0 \leq \text{RADP} \leq 7.55$ min) model. The data show no statistical significance between the two data sets (B) The time between every pMAPK peak was analysed in both Shankaran's data and the ABM and conducting statistical analysis with nonparametric analysis illustrate no significant difference between them.

ABM with intermediate and stochastic RADP ($4 \leq \text{RADP} \leq 10$ min) were still capable of generating an ultrasensitive response (Figure 4. 15 (C), (E) & (G)). However, this became graded as the time to achieve E_{max} increased to 30 min and thus the sigmoidal curve shifted to the right. A stochastic model of the RADP was designed to model a continuous and dynamic activating signal (Macia et al., 2009, Tomida,

2015). The degree of balance (*i.e.* equilibrium) between activating and deactivating inputs and the shift between them were taken into consideration with the length of RADP. With long RADP ($\text{RADP} \leq 15 \text{ min}$), the deactivating inputs are more dominant than activating inputs, leading to substantial reduction in MAPK activating behaviour. Though the deactivating inputs are more dominant, the aptitude to generate the response was not completely lost in the presence of multi-compartments. The activation behaviour was lost when strong deactivating inputs are present ($\text{RADP} \geq 15 \text{ min}$, Figure 4. 15 (G)).

Therefore, considering that the MAPK pathway is under dynamic stimulation, and the emergent activation behaviour is robust and exhibits a degree of resistance to modulation of temporal the regulatory element, it can be postulated that compartmentalisation is linked to signal memory and so signal fidelity. The emergent behaviour of this dynamic system suggests that the system is set up to remember the original activating signal and the initial conditions. This ensures that once the balance shifts back to the activating inputs, re-establishment of the activation dynamics can be facilitated with ease. This is in line with the mechanisms proposed of how MAPK play a role in long term potentiation and development of neuronal plasticity. (Gao et al., 2011, Mayford et al., 2012, Miyamoto, 2006, Schrick et al., 2007)

Previous *in silico* models argue that oscillation in the MAPK pathway emerge randomly and it does not rely on regulatory mechanisms (Legewie et al., 2007, Ortega et al., 2006, Qiao et al., 2007). Oscillation also emerged in the ABM.

However, contradictorily, the ABM suggests that in order for oscillatory behaviour to appear, three conditions are needed. These conditions are: compartmentalisation; MAPKK as the bottleneck for activating-deactivating inputs; and a shift in activation-deactivation balance with periodicity ≥ 4.5 min. The time restriction appears to be essential for determining if the oscillatory behaviour is sustained or transient. Oscillatory activation dynamics in the MAPK system have been reported both *in silico* (Kholodenko, 2000, Sarma and Ghosh, 2012, Shin et al., 2009b, Tian et al., 2009, Wang et al., 2006) and recently *in vitro* (Hilioti et al., 2008, Nakayama et al., 2008, Shankaran et al., 2009, Weber et al., 2010). In *in silico* models, oscillation was initially thought to be solely reliant on negative feedback. Models with strong feedback loops generate oscillatory behaviour (Cirit et al., 2010, Kholodenko, 2000, Lim et al., 2009, Novak and Tyson, 2008). This supports the outcome of the model presented here with long deterministic RADPs (simulating a system where deactivating inputs are dominant). However, this idea is changing, as the interaction between positive and negative feedback loops are considered to play a part in the emergence of oscillation in the cascade. This was shown by several investigators *in silico* (Ferrell et al., 2009, Ingolia and Murray, 2007, Sarma and Ghosh, 2012, Tsai et al., 2008). Our model strengthens this idea, as RADP integrates negative and positive feedbacks at the level of MAPKK. Furthermore, although the ABM designed only included the fundamental behaviour and individuals of the MAPK pathway, oscillation still emerged. All of the above strongly suggests that in order for oscillation to occur in the real-world system a few conditions have to be met. The ABM revealed that these conditions are purely intracellular settings, and thus suggest an explanation as to why oscillatory behaviour is visible at *in vitro* single-cell

experiments, while being difficult to detect in *in vitro* experiments which assess populations of cells.

We looked at formation of pMAPK in the ABM model and compared it to published data. We compared the ABM data to the recently published results by Shankaran et al. where they demonstrated the oscillation of pMAPK levels experimentally (Shankaran et al., 2009). Our ABM models statistically show parallelism with their *in vitro* data in terms of MAPK activation dynamics (Figure 4. 20). Their stimulation of cells with EGF showed a temporal dynamics of pMAPK formation similar to that of the periodic RADP ABM model (RADP = 7.55 min). Furthermore, when comparing the oscillatory behaviour shown by Shankaran and colleagues, the ABM model matches several features in the pMAPK response. Both Shankaran's data and the ABM model show similar "turn off" dynamics for all the oscillatory waves and the maintenance of the oscillatory behaviour past the first response trigger. This is evident in Figure 4.20 (A) where the time between pMAPK peak levels and troughs was not statistically different between Shankran's data and those observed in the ABM. The time between pMAPK peaks was also not statistically different (Figure 4. 20 (B)). The ABM (with $4.5 \leq \text{RADP} \leq 7.5$ min) and some of the oscillatory behaviour in Shankaran's paper demonstrated graded responses, while continuing oscillate until the levels of pMAPK were close to E_{max} . We also noted similarities at the phase between the turn-on and turn-off phase in the oscillatory waves. Both the ABM (when $6 \leq \text{RADP} \leq 23$ min) and some of the *in vitro* data at the initial response show some fluctuations in pMAPK levels before the "turn off" phase. In our model, we observed that this was due to a second wave of MAPKK activation which were either dormant or not in a close enough proximity to bind to MAPK during the initial wave of

activation. However, the small number of available active MAPKK agents, and their lengthy RADP, hindered further activation of the recently available MAPKs.

The amplitude and frequency of MAPK activation dynamics are thought to play a role in signal specificity and fidelity (Hancock and Parton, 2005, Murphy et al., 2004, Sewing et al., 1997). This is shown with how amplitude of phosphorylated ERK influences the expressions of genes such as c-Fos (Cai et al., 2008, Lim et al., 2009, Murphy et al., 2004, Murphy et al., 2002). This is intriguing as the multi-compartment ABM presented demonstrated that shifting the balance between activating and deactivating inputs has a major effect on levels of pMAPK. Alteration of the balance through RADP in a two-compartment system did not generate such differences in amplitude (Appendix B, Figure 12) This further supports the idea that a multi-compartment model of the MAPK pathway is a more appropriate model compared to a two-compartment model (Figure 4. 3, Figure 4. 6 and Figure 4. 15). Oscillation in the MAPK pathway has been proposed as a mechanism to regulate MAPK-mediated events in the cytoplasm (Murphy et al., 2004), where oscillation frequency and amplitude encodes the appropriate response; similar to what has been demonstrated in calcium signalling with calcium oscillation (Ullah et al., 2007). The model represented here further supports this concept because the presence of cytoplasmic multi-compartments was necessary for the emergence of oscillation. We propose that within these cytoplasmic compartments periodic shifts in the activation and deactivation inputs at the level of MAPKK can act as filters and signal modulators for local responses. MAPKs are present in the compartment and have direct access to their targets in these compartments. If there are multiple targets available, the frequency and the amplitude of the oscillatory behaviour can be differentially decoded by the different targets. This also suggests an interaction hierarchy where

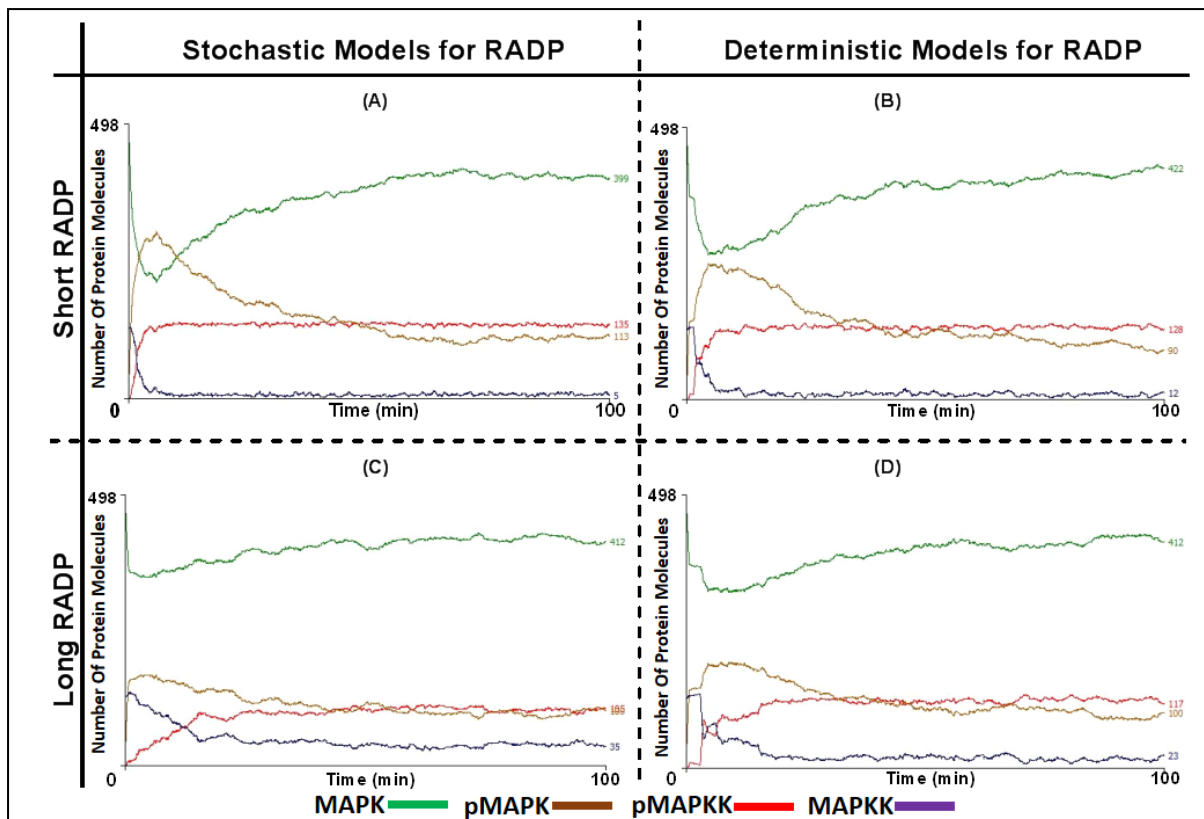


Figure 4. 21 Modulation of the spatial regulatory element of the MAPK pathway results into emergence of two phase MAPK activation behaviour, irrespective of the temporal regulatory element. (A) The MAPKK-MAPK signalosome-cluster ABM assessed the effect of disassembly of the MAPKK-MAPK complex in tandem with modulation of the re-activation delay period (RADP). The ABM utilised stochastic ((A) and (C)) and deterministic ((B) and (D)) configurations. These were using short RADP values (where in (A) $0 \leq \text{RADP} \leq 90$ s for the stochastic configuration and in (B) $\text{RADP} = 90$ s for the deterministic configuration) and long RADP values (where in (C) $0 \leq \text{RADP} \leq 22.6$ min for the stochastic configuration and in (D) $\text{RADP} = 22.6$ min for the deterministic configuration).

some MAPK phosphorylation targets are more sensitive to MAPK activation compared to others.

4.4 Variation of the spatiotemporal regulatory elements and their effect on the MAPK global activation.

In the previous sections, the attempt was made to modulate either the spatial or temporal regulatory elements separately, while maintaining the second element unchanged. In this section the attempt was made to modulate both the

spatiotemporal elements simultaneously. The null hypothesis for this section is that concurrent modulation of the spatiotemporal parameters results in no significant effect on the MAPK activation behaviour. This was done using a signalosome cluster ABM and a multi-compartment ABM which interchanged between dynamic and periodic stimulation.

4.4.1 Results

4.4.1.1 *Spatiotemporal elements modification using a MAPKK-MAPK signalosome cluster model.*

Signalosome clusters have been reported previously to modulate cell signalling. These include plasma membrane clusters, such as lipid rafts, and the nanoclusters of rapidly accelerated fibrosarcoma1 [RAF1] and rat sarcoma (Ras) (Lingwood and Simons, 2010). In these signalling apparatus RAF-1 and Ras are brought together into close proximity and randomly assemble and disassemble (Harding et al., 2005a, Shalom-Feuerstein et al., 2008). This concept was applied to the ABM by altering the multi-compartment model to a model with assembled MAPKK-MAPK signalosome clusters at the arrival of the activating signal; these clusters then disassemble and the signalosome components diffused into the cytoplasm by Brownian motion. The temporal element was altered by using either a stochastic or deterministic RADP models. The RADP values that were chosen to be applied were 90 s and 22.6 min. The null hypothesis is altering the spatial element by modification of cluster assembly and disassembly, in conjunction with modulating the temporal element by using stochastic and deterministic time points, has no substantial effect on the MAPK activation behaviour. These models had resulted in the emergence of a biphasic

MAPK activation response composed of an activation (“turn on”) phase and a deactivation (“turn off”) phase (Figure 4. 21). The model results were validated against the *in vitro* data obtained from Lefkowitz et al, investigating the MAPK activation dynamics within the endosomal compartment, as their system examines MAPK-GPCR- β -arrestin signalosome clusters within the endosomal compartment.

Considering that the pMAPK formation is a proxy for MAPK activation, there was a statistically significant difference between the stochastic (Figure 4. 21 (A) and (C)) and deterministic RADP (Figure 4. 21 (B) and (D)) signalosome cluster models. A statistically significant difference in MAPK activation behaviour was also observed when RADP value was increased. These observations were at the level of pMAPK generated at E_{max} , the time to achieve both E_{max} and EC_{50} . All models exhibited a rapid MAPK activation and pMAPK accumulation in the initial phase, followed by a slow deactivation phase. The use of different RADP configurations (*i.e.* stochastic and deterministic) had primarily impacted pMAPK levels generated at E_{max} (Figure 4. 22 and Appendix B, Figure 13). When RADP was at 90 s, the stochastic configuration resulted in statistically significant lower pMAPK levels. Alternatively, when RADP was 22.64 min, deterministic configuration generated considerably higher pMAPK levels (Figure 4. 22 (A) and (B)). Furthermore, although there was no considerable difference statistically in the time to reach EC_{50} between stochastic and deterministic configurations of RADP, when RADP was set up at 90 s (Figure 4. 22 (C)), when RADP was set-up at 22.64 min, the time to reach E_{max} markedly increased in the deterministic RADP configuration, in comparison to the stochastic (Figure 4. 22 (D)). Nonetheless, the time to reach EC_{50} had been extensively reduced in ABMs adopting deterministic RADP, in comparison to the stochastic

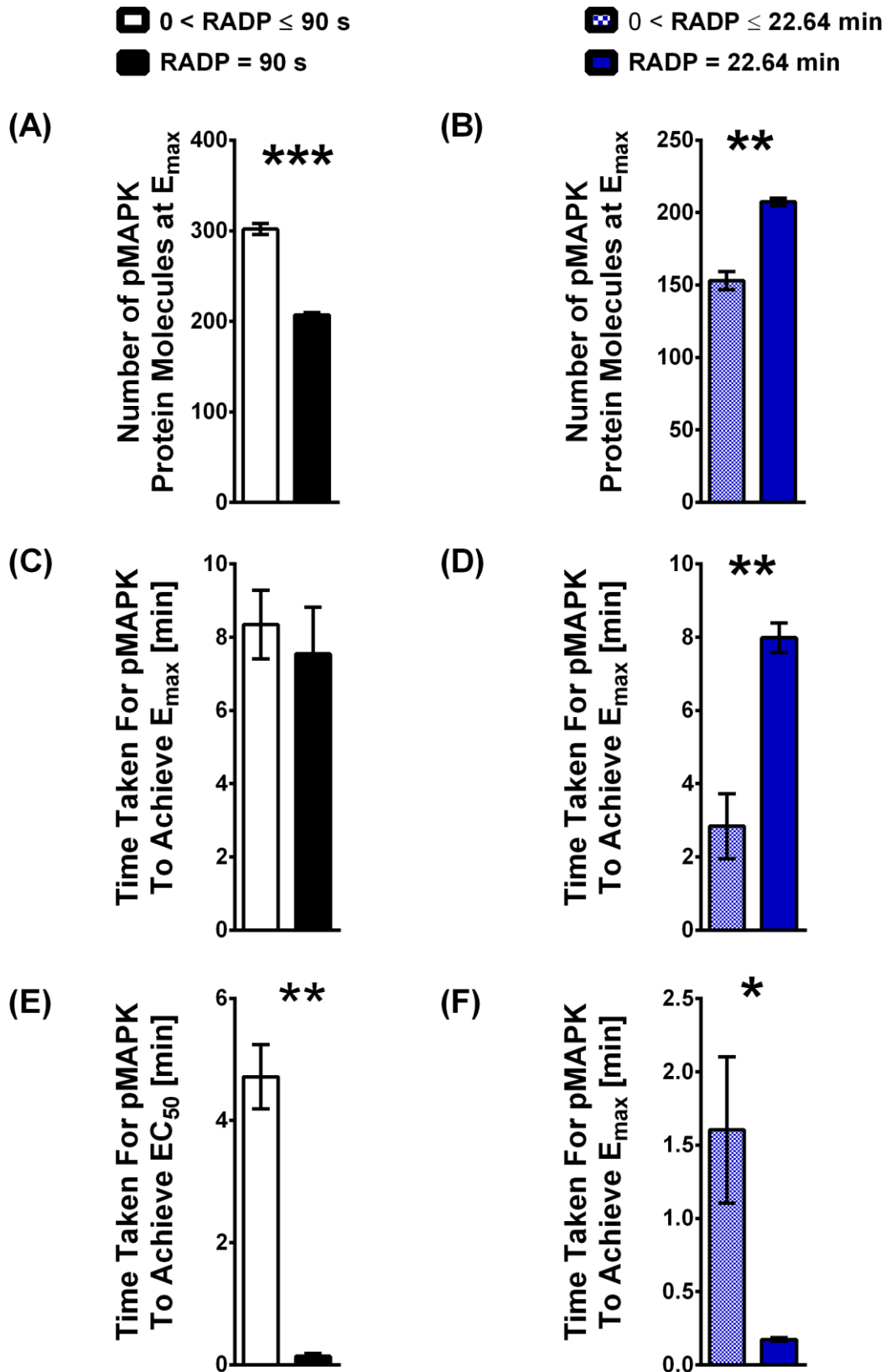


Figure 4. 22. The activation dynamics of MAPK in a MAPKK-MAPK signlosome cluster ABM. An assessment of the effect of using RADP stochastic and deterministic configurations on the level of MAPK at E_{\max} (A) and (B), the time to achieve E_{\max} (C) and (D) and the time to achieve EC_{50} (E) and (F). Values represent mean \pm standard error of the mean (SEM) and student t-test statistical analysis was performed to find statistically significant difference. *, ** and *** illustrate $p < 0.05$, $p < 0.01$ and $p < 0.001$ respectively.

configuration using both 90 s and 22.64 min (Figure 4. 22 (E) and (F)). Furthermore, when the effect of increasing RADP values on MAPK activation behaviour was assessed, it was observed that pMAPK levels were greatly reduced, regardless of the RADP configuration used (Appendix B, Figure 13 (A) and (B)). Nonetheless, RADP stochastic configurations illustrated more substantial reductions at E_{\max} (Appendix B, Figure 13 (A) and (B)). Notably, however, when RADP was set at the stochastic configuration, increasing its value resulted in a statistically significant reduction in the time to achieve both E_{\max} and EC_{50} (Appendix B, Figure 13 (C) and (E)). Conversely, when RADP was set up into a deterministic configuration, there was no noticeable change in the time to achieve E_{\max} and EC_{50} (Appendix B, Figure 13 (D) and (F)).

Considering the activation of MAPKK, in this MAPKK-MAPK signalling cluster ABM, the RADP configuration did not influence the level of MAPKK at E_{\max} (Figure 4. 23 (A) and (B)). However, when the RADP value assumed 90s, the time to achieve E_{\max} increased substantially in deterministic configuration, coupled with no observed change in the time to achieve EC_{50} (Figure 4. 23 (C) and (E)). Yet, when RADP was set-up to 22.64 min the observed change in the time to achieve E_{\max} was statistically insignificant when stochastic and deterministic configurations were compared (Figure 4. 23 (D)), even though there was a statistical difference in the time to achieve EC_{50} (Figure 4. 23 (F)). Increasing RADP value resulted in a statistically significant reduction in the level of MAPKK at E_{\max} using the stochastic configuration (Appendix B, Figure 14 (A)). However, in the deterministic configuration, increasing RADP from 90 s to 22.64 min did not change MAPKK levels at E_{\max} (Appendix B, Figure 14 (B)). Additionally, in a stochastic configuration, increasing RADP from 90 s to 22.64

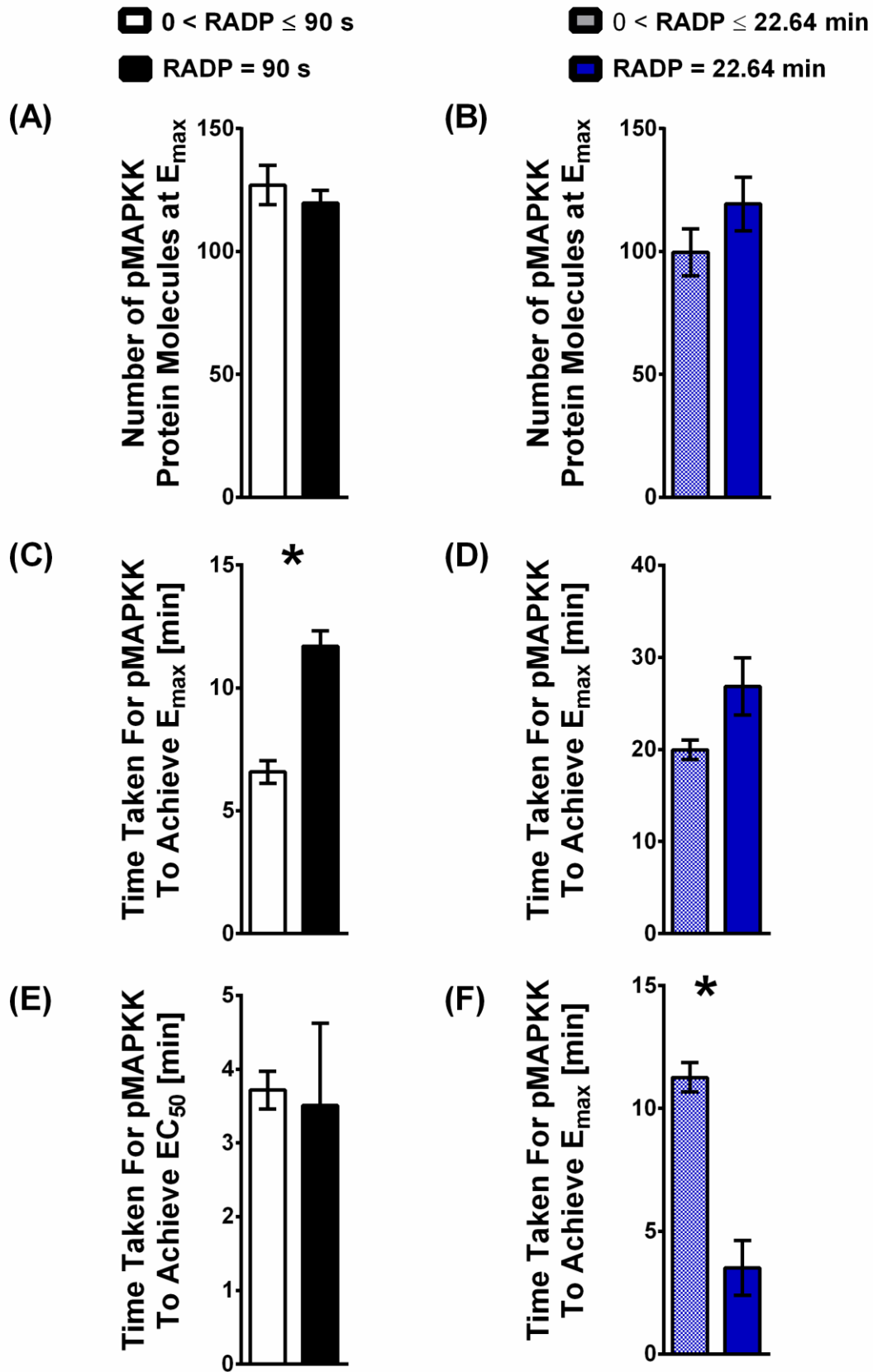


Figure 4. 23 The activation dynamics of MAPKK in a MAPKK-MAPK signlosome cluster ABM. An assessment of the effect of using RADP stochastic and deterministic configurations on the level of MAPK at E_{\max} (A) and (B), the time to achieve E_{\max} (C) and (D) and the time to achieve EC_{50} (E) and (F). Values represent mean \pm standard error of the mean (SEM) and student t-test statistical analysis was performed to find differences of statistical significance. *, ** and *** illustrate $p < 0.05$, $p < 0.01$ and $p < 0.001$ respectively.

caused an increase in the time to achieve both E_{\max} and EC_{50} (Appendix B, Figure 14 (C) and (E)). This increase was also observed in the RADP deterministic configuration (Appendix B, Figure 14 (D) and (F)). It is of interest that in this model, in contrast to what was reported in the prior multi-compartment ABMs, the levels of pMAPKK, MAPKK, MAPK and pMAPK returned to levels close to baseline at t_0 .

4.4.1.2 *Investigating alteration of the spatiotemporal regulatory elements via diversification of feedback mechanisms.*

In this ABM, a few RADP configurations were used during one model simulation. The null hypothesis here is that change in feedback behaviour, via the use of different RADP configurations, results in the same MAPK activation dynamics.

Cells are exposed to ever-changing signalling conditions. These take the form of different extracellular ligands, different stimulation modes (dynamic Vs periodic), and/or the initiation of different feedback mechanisms. The collective of these conditions ultimately influences cellular responses and behaviour. Dynamic signalling conditions are present during embryonic development and cell differentiation. An extensively studied example of these signalling conditions is during somatogenesis in vertebrate animals. Somitogenesis involves the sequential transition of paraxial mesoderm into somites, as the primitive streak regresses along the embryo anterior-posterior axis (Christ and Ordahl, 1995, Palmeirim et al., 1997). The process is periodic and occurs at regular intervals. The behaviour is believed to emerge due to molecular oscillatory clock, where cells are exposed to vigorous activating signals and potent feedback control mechanisms, which are also periodic

and oscillatory in nature. Where certain developmental genes are exposed to cycles of activation and inhibition (Kageyama et al., 2012, Kicheva et al., 2012, Le Dreau and Marti, 2012). This oscillatory behaviour is observed at the gene expression level (Palmeirim et al., 1997). The genes which exhibit this oscillatory behaviour express components of signalling pathways, such as fibroblast growth factor (FGF) (Dubrulle et al., 2001, Dubrulle and Pourquie, 2004), Wnt (Aulehla et al., 2003), Notch (Jiang et al., 1997) and MAPK phosphatases (Dequéant et al., 2006, Niwa et al., 2007, Niwa et al., 2011). It is believed that negative feedback mechanisms are the prime contributors to the appearance of oscillatory behaviour. The MAPK pathway is thought to be triggered during somatogenesis by fibroblast growth factor (FGF) with ERK and dual specificity phosphatase gene Dusp4 both playing a role in this process (Niwa et al., 2011, Niwa et al., 2007). However, it is still not understood in great detail how this oscillatory signalling behaviour influences the signalling pathways involved in somatogenesis either individually or globally (*i.e.* as a signalling network).

Considering that in somatogenesis the oscillatory behaviour is believed to develop due to signal modulation *via* negative feedback loops (*i.e.* the modulation of the temporal regulatory element), the multi-compartment ABM was used to test the effect of ongoing modulation of the temporal regulatory element on MAPK activation dynamics. This was undertaken by emulating the dynamic changes in external signals that have previously been reported experimentally in the literature (Kageyama et al., 2012, Niwa et al., 2011). However, due to the lack of experimental techniques permitting varying stimulating inputs within the same experiment, in addition to monitoring their effects on MAPK activation in real-time, this ABM

experiment was not validated against *in vitro* data due to the lack of biological data, and a methodology which can be mapped to the ABM.

To model a cellular environment where diverse and flexible signalling dynamics are at action, this model implemented three different RADP models in one simulation. During somatogenesis, the balance between activating and inhibitory inputs is thought to be mediating the observed oscillatory behaviour. When the initial stimulus arrives, activating inputs are more dominant in comparison to inhibitory inputs. Therefore, a model which implemented a short-stochastic RADP ($0 \leq \text{RADP} < 90$ s, Figure 4. 24, solid green line) was used. Once the system stabilised and reached equilibrium, RADP was re-set to an intermediate-deterministic RADP model (RADP = 7.55 min, Figure 4. 24, solid blue line). Biologically, after the arrival of the initial stimulus, negative feedback mechanisms are triggered and they become increasingly more dominant, yet the activating inputs are still present and continue to impose activation. Therefore, in this ABM the intermediate-deterministic RADP configuration (RADP = 7.55 min) mimicked that biological scenario. Once equilibrium was achieved, RADP was re-set to an intermediate-stochastic RADP configuration ($0 \leq \text{RADP} < 7.55$ min, Figure 4. 24, with the solid dark lines). A cell is exposed to strong and sustained activating inputs in addition to strong inhibitory inputs where the latter is capable of substantial inhibition of activating inputs. This was also run until equilibrium was achieved. The only difference between the models applied here were within the transition function `[[MKK_outputdata]]` which controlled the mode of RADP.

Initiating the response by using a short-stochastic RADP ($0 \leq \text{RADP} < 90$ s, Figure 4. 24, solid green line) resulted in an ultrasensitive response for both MAPKK and MAPK and establishment of E_{max} at 4.92 min and 4.55 respectively. When the RADP was re-set to the intermediate-deterministic configuration (RADP = 7.55 min, bold blue line) levels of pMAPK and MAPK had rapidly been reduced, with the lowest level of pMAPK reached at 121.73 min from t_0 (and within 56.88 min from the switch to deterministic RADP configuration). However, the levels of pMAPK were only reduced by 46.81% compared to those when RADP was set at $0 \leq \text{RADP} < 90$ s. These levels were 53.13% higher compared to basal levels. Alternatively, MAPKK levels were reduced by (98.7%) within 12.86 min of re-setting RADP to the intermediate-deterministic configuration. Once the RADP was switched to an intermediate-stochastic RADP configuration, ($0 \leq \text{RADP} < 7.55$ min, bold black line), pMAPK activation increased by 90.08%, compared to levels at t_0 (57.88% increase compared to when the configuration was RADP = 7.55 min) and the pMAPK ultrasensitive response re-emerged within the system. Simultaneously, a graded ultrasensitive response of active MAPK was produced with the levels only reaching 11.85% of total active MAPKK, which can be generated in the system.

4.4.2 Discussion and conclusion:

This section was dedicated to investigating the effects of manipulating the spatiotemporal elements on MAPK activation dynamics. Firstly, the spatial element was modified using the signalosome-cluster ABM. In this ABM, the spatial element modification was in tandem with manipulation of the temporal element (Figure 4. 21). The second attempt was to look at continuous alterations in temporal components,

with the spatial element intact, to emulate a dynamic signalling environment. In both configurations, the ABMs generated insightful data which shed light on the interplay between the spatiotemporal regulatory element and the effect their modulation have on the MAPK activation behaviour. The key finding with these ABMs is the emergence of the inactivation dynamics of the pMAPK, and the re-establishment of agents levels close to basal levels.

The deactivation of the MAPK signal is thought to involve a spatial regulatory element. This was argued for by Kholodenko et al, and shown for the first time experimentally by Lekowitz et al. When the spatial element was modified using the signalosome-cluster ABM, the emergent behaviour observed was biphasic, whereby it comprised an activation and deactivation phase. The pMAPK dynamics seen in these models incorporating MAPKK-MAPK signalosome cluster assembly and disassembly were similar to the results obtained with compartmentalised MAPK signalling at the endosome (Figure 4. 21 and Figure 4. 24). Lefkowitz (and others after him) had shown *in vitro* that a typical response of MAPK, involving the endosome and G protein-coupled receptors (GPCRs), was divided into two phases; a GPCR phase and a β -arrestin-dependent phase (Figure 4. 25 (A)). The GPCR-dependent phase was characterised by an initial ultrasensitive MAPK activation, followed by a rapid secondary “turn-off” phase (Ahn et al., 2004, Luttrell et al., 2001, Shenoy et al., 2006, Wei et al., 2003). Conversely, the secondary phase is endosomal and β -arrestin-dependent, and is characterised by slow deactivation phases and a continuous reduction of the pMAPK magnitude. The activation dynamics of the MAPK ERK (a target of the GPCR induced signalling) incorporated both the GPCR- and β -arrestin-dependent responses. In Figure 4. 21 and Figure 4.

24 the ABM produced a biphasic MAPK activation response: a rapid activation at the initial phase followed by a slow deactivation phase. The deactivation phase was capable of lowering the levels of pMAPK to levels closer to basal conditions. These qualitative characteristics produced by the ABM are similar to the endosomal MAPK activation dynamics demonstrated *in vitro* by Lefkowitz (Lefkowitz and Shenoy, 2005). This suggests that the formation of signalosome clusters at subcellular compartments generate signals comparable to those triggered at membrane clusters.

MAPKK-MAPK-signalosome ABM also proposed a role for clustered signalosome and their disassembly play a role in shaping the activation dynamics of the MAPK pathway (Figure 4. 22 and Figure 4. 23). The ABM showed that the integrity of signalosome clusters plays a role in the generation of the initial MAPK activation phase, and that when MAPKK-MAPK clusters defragment/disassemble dominate, MAPK deactivation preponderates. Signalosome clusters are widely reported to have a role in mediating MAPK activation and signal initiation. These mainly include lipid rafts and Ras nanoclusters, which are commonly present at cell membranes (Harding and Hancock, 2008, Lingwood and Simons, 2010, Murakoshi et al., 2004, Plowman et al., 2008). As aforementioned, endosomal MAPK activation is composed of two phases. The slow deactivating phase was shown to be mediated through the endocytic population of MAPK, as pharmacological inhibition, or the knocking down of β -arrestin shows a complete repression of the second phase (Figure 4.25 (A)). The abatement is thought to be due to the internalisation of the MAPKK-MAPK signalosome, and their diffusion into the cytoplasm, thus halting MAPK signalling propagation *via* restricting activation of cytoplasmic targets. The

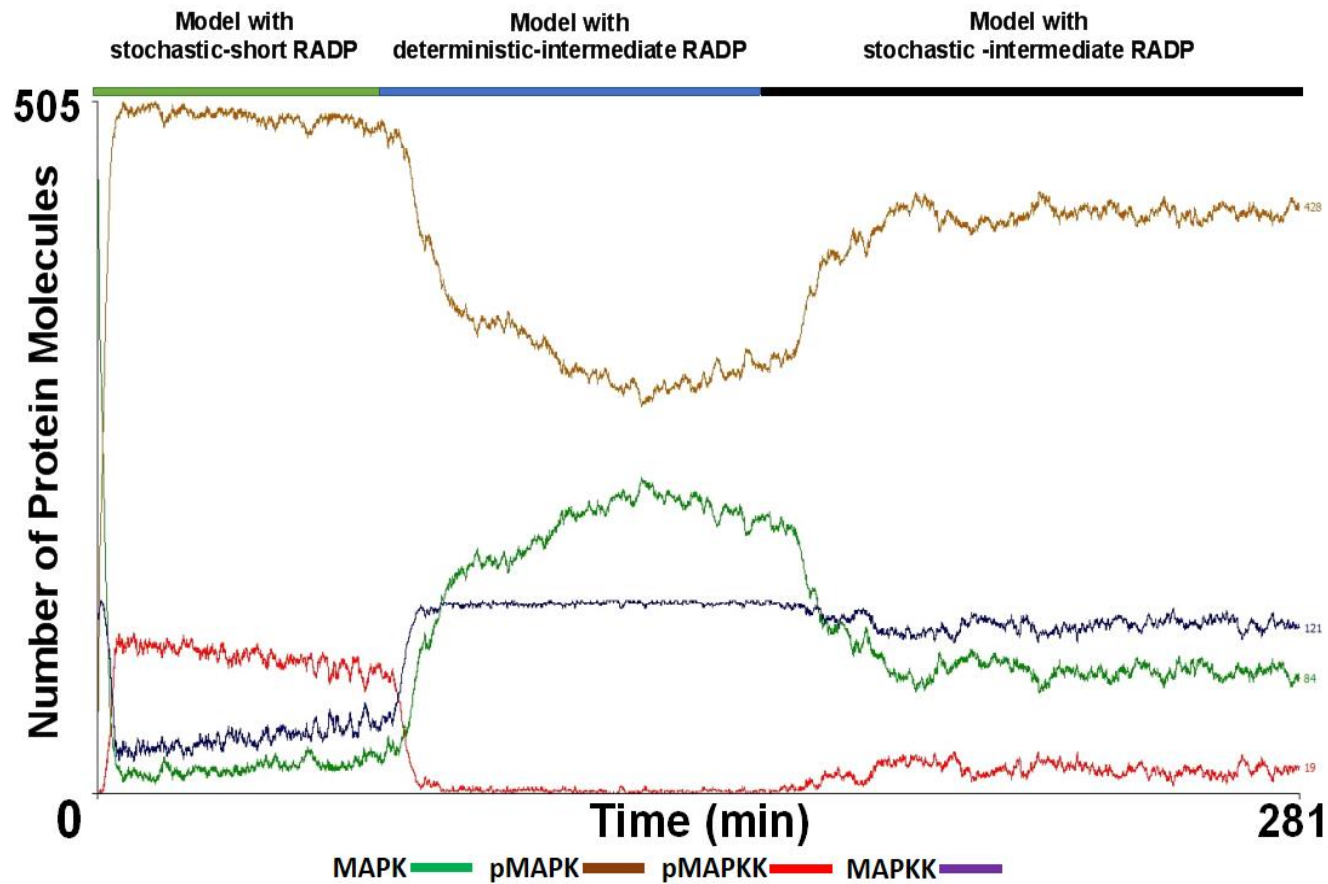


Figure 4. 24 Modulation of the temporal regulatory element continuously and its impact on the dynamics of MAPK activation. The A multi-compartment ABM was used with different re-activation delay period (RADP) configurations. In a single simulation of the ABM, the RADP configurations were modulated in order to emulate dynamic signalling environment such as those observed during development and differentiation. These where a cell is initially faced with a strong, yet short activating signal, followed by the take-over of the inhibitory mechanisms and then followed by a moderate and persistent signal. Biologically, the temporal element is control *via* feedback loops. The ABM implemented this by the use of a highly stochastic model of MAPKK re-activation delay with a short delay period ($0 \leq \text{RADP} \leq 90$ s, [green solid line]), once pMAPK level reached its maximum and was at equilibrium, the simulation was switched to deterministic-intermediate RADP model ($\text{RADP} = 7.54$ min [solid blue lines]). Once the level of pMAPK reached its lowest and was at equilibrium, the re-activation delay was switched to a model with stochastic-intermediate RADP ($0 \leq \text{RADP} \leq 7.54$ min; [solid black line]). This combination of the different modes of the MAPKK re-activation suggests that when strong activation inputs of MAPKK are substantially reduced, prolonged deactivating inputs at MAPKK are capable of rapidly reducing the levels of pMAPK. However, they are still not capable of re-establishing the initial levels of MAPK seen at t_0 (only 58.7% of t_0 MAPK level was re-established). The final stage of the simulation (solid blue lines), reflects that in a multi-compartment system, even with a high stochasticity for MAPKK activation, a low number of active MAPKK is sufficient to fundamentally increase and maintain high pMAPK levels.

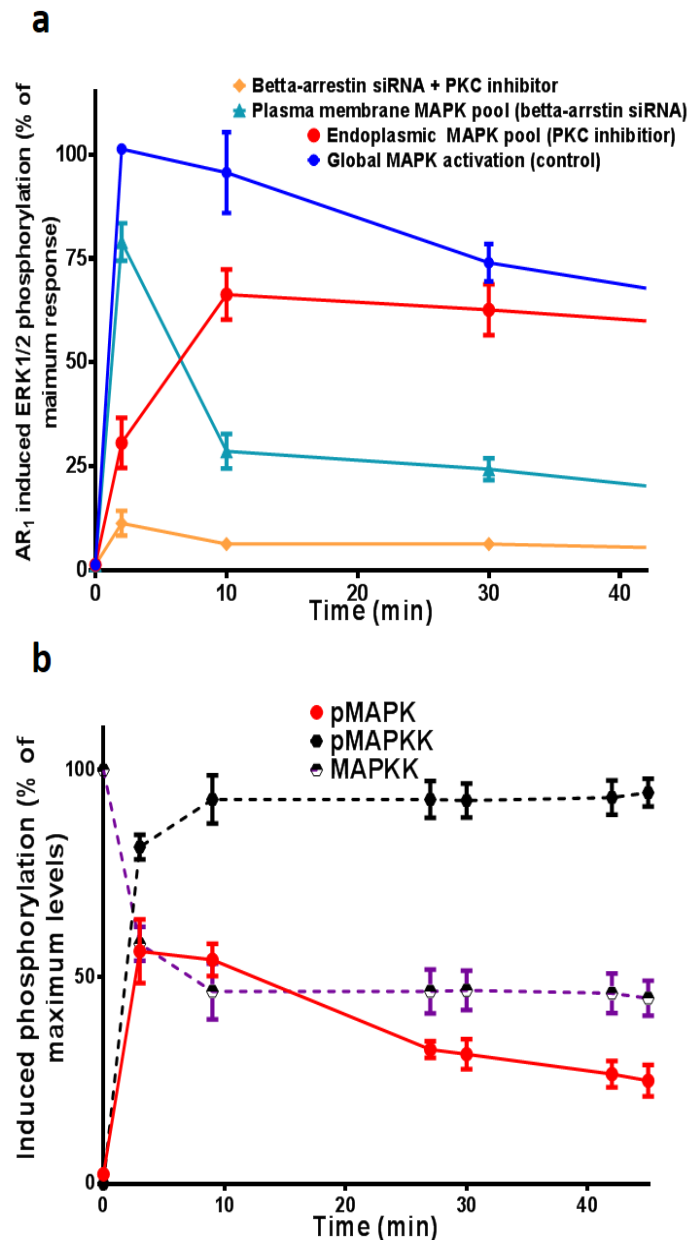


Figure 4. 25 MAPK activation dynamics in endosomal compartments and in an agent-based model (ABM) containing cytosolic signalsome cluster. (A) In vitro data demonstrating the two phase activation dynamics of ERK. This had demonstrated that intracellular pools of MAPK are responsible for mediating slow ERK1/2 deactivation and maintaining pERK at high level over time. The data was adapted from Lefkowitz RJ, Shenoy SK (2005) Transduction of Receptor Signals by β -Arrestins. *Science* 308: 512-517. (B) Data from the ABM which integrated intracellular clusters, where the MAPK activation dynamics replicates the *in vitro* data in (A).

ABM model which incorporated MAPKK-MAPK signalsome cluster formation and dissociation had resulted in the appearance of the second slow deactivation phase (Figure 4. 21). However, the model shows that this behaviour appeared due to the increased dissociation and disassembly of the MAPK's signalsome clusters inside the multi-compartments, and not just due to the alleviation of the global MAPK

activation, and maintenance of local activation. On the contrary, the ABMs in section 4.3 demonstrated that a localised (*i.e.* compartmentalised) signal was able to generate a large E_{\max} magnitude (Figure 4. 15, Figure 4. 16 and Figure 4. 18). Consequently, this outcome further supports the notion that compartmentalisation of the MAPK components can be important in mediating specific cellular responses. In these compartments there is a need for rapid mechanisms to curb and/or inhibit the expeditious activation, and reduce the magnitude of pMAPK generated; dissociation of the signalosome components in the compartments provides a rapid and efficient mechanism to perform this.

Previously, Tian *et al*, and others had shown that plasma membrane Ras nanoclusters are the central components for the generation of the initial MAPK activation phase (Harding et al., 2005a, Shalom-Feuerstein et al., 2008, Tian et al., 2007). This was in line with work which showed that the initial activation dynamics were β -arrestin independent. The signalosome-cluster ABM shows that the initial activation phase is also dependent on MAPKK-MAPK interaction inside the multi-compartments. However, others (such as (Chiu et al., 2002, Markevich et al., 2004)) have shown that Ras nanoclusters are not exclusively located at the plasma membrane, and they do exist in other membrane bound organelles, such as Golgi and the endosomal compartment (Chiu et al., 2002, Murakoshi et al., 2004, Plowman et al., 2008, Shalom-Feuerstein et al., 2008). Considering that the maximum pMAPK amplitude (E_{\max}) generated using the signalosome cluster ABM was only ~55% of the E_{\max} observed in the initial multi-compartment ABM, this implies that the initial phase of activation recruits compartmentalised Ras nanoclusters, in addition to the plasma membrane Ras nanoclusters. This is plausible, considering that ERK and other

MAPK compartmentalisation in the endosome can occur without requiring β -arrestin (Inder et al., 2008, Schaeffer et al., 1998, Teis et al., 2006, Wunderlich et al., 2001). Furthermore, the assumption is also valid given that cytoplasmic Ras nanoclusters were shown to be activated by the plasma membrane compartmentalised MAPKKK Raf1 (Fan et al., 2008, Inder et al., 2008, Lee et al., 2011).

Considering that in order to trigger the downstream components of the MAPK cascade plasma membrane Ras nanoclusters will still rely on diffusion into the cytoplasm, or the recruitment of the downstream proteins into the plasma membrane (Brown and Kholodenko, 1999, Eblen et al., 2004, Kholodenko et al., 2000, Mugler et al., 2012, Murakoshi et al., 2004), the shift between the coming activating inputs and these robust deactivating mechanisms provides an additional obstacle to signal propagation, it can be postulated that cytoplasmic nanoclusters are needed to overcome the obstacle diffusion present for the propagation of the signal. *Videlicet*, compartmentalised Ras nanoclusters can be regarded as amplifiers of an activation signal which was depleted due to diffusion from the plasma membrane to the cell interior.

Biologically, assuming these conditions are all in force, the MAPK pathway is fully activated, both plasma membrane and compartmentalised Ras nanoclusters were triggered simultaneously and with equal potency; and that negative feedback is minimal, it is expected that pMAPK generation is to be very potent. Hence, the initial activation phase (levels of pMAPK) should be propagated for an extended time period before the deactivation phase commences. Additionally, or alternatively, the

secondary phase should demonstrate a slower decay behaviour. Nonetheless, this is not what is observed *in vitro*.

Another interpretation for the *in vitro* observed endosomal MAPK activation behaviour is the deployment of efficient negative feedback mechanisms. These can be through insulation and/or disassembly of the signalosome clusters. This perception is supported with the concurrent modulation of the spatiotemporal regulatory elements shown with the signalosome-cluster ABM, namely with long RADPs (*i.e.* where deactivating inputs are dominant, (Figure 4. 21 (C) & (D))). With these configurations of RADP, pMAPK were characterised with a lower E_{max} compared to those of the same signalosome cluster model with shorter RADPs (Appendix B, Figure 13 (A) & (B)). To allow for rapid and efficient modulation of MAPK activation within the compartment, negative feedback mechanisms must be employed at amplification points (such as the MAPKK protein) within the cascade. The ABMs tested thus far reveal that imposing short bursts of negative feedback at the level of MAPKK is sufficient to reduce pMAPK levels considerably. Consequently, this provides an element of periodicity in the shift between the coming activating inputs and these robust deactivating mechanisms, subsequently, providing a mechanism for the generation of oscillatory behaviour in MAPK activation dynamics.

Therefore, the following ABM addressed the effect of dynamic modulation of negative feedback regulations by modulating the temporal regulatory element (RADP) in the multi-compartment ABM (Figure 4. 15). From that ABM, a dynamic

MAPK activation response was generated, implying that the ABM is capable of modelling dynamic signalling conditions. These conditions included the variation of the temporal element and the constant alterations in the number of protein-agent species in the simulation. The model had revealed that periodic RADP is capable of reducing the levels of pMAPK in the system in a relatively short period, thus providing a strong de-activating mechanism. Biologically, this will mean that employing periodic and efficacious phases of inhibitory mechanisms results in more potent deactivating behaviour. Nonetheless, this is not adequate by itself to get the system back to t_0 . Stochastic models with RADP, though with similar periods as the deterministic model, produced an activating response, although rationally it would lead one to believe that a model which is more stochastic and with long RADPs will generate an inhibitory system which reduces the pMAPK number to basal levels (*i.e.* at t_0). The model demonstrated further that MAPK deactivating is more optimal when utilised deterministically. Still, the model suggested that activating mechanisms exhibit a level of periodicity to ensure no complete superiority of the deactivating mechanisms while the activating stimuli/input is present to allow the system not to fully deactivate.

Chapter 5 Conclusions and Future work

This chapter is dedicated to summarising the findings from the MAPK agent based model (ABM), and how these findings contribute to the field of cell signalling and MAPK activation dynamics. The objective of this thesis was to investigate how spatiotemporal regulatory elements affect the MAPK pathway activation, and how these elements promote specificity and fidelity of cellular response. This chapter commences by reviewing the research objectives outlined in the preface section and how they were achieved. That review is followed up by an outline of future work needed to further refine and develop the ABM. These improvements provide the progression of the model to allow for more thorough and detailed investigations of MAPK activation dynamics, and how the modulation of spatiotemporal regulatory mechanisms determine the final cellular outcome.

5.1 Conclusions

The objectives of the study were summarised in the preface as follows:

1. To build an agent-based model (ABM) of the MAPK pathway
2. A survey of previously published models of the MAPK pathway to aid building of a basic ABM model and integrating the essential components
3. Dissect the important components needed for the model
4. To be able to compare the simulation generated from the ABM with both *in silico* and *in vitro* data, an output for the signalling dynamics has to be determined

5. Model validation and sensitivity analysis to be conducted to certify the model accuracy
6. Once a complete model is established, whereby it is fully validated both in regard to the algorithms accuracy and functionality, in addition to the model's reproducibility of biological behaviour, experimental "wet" data are used to further improve and allow the modelling to address more specific questions related to spatiotemporal regulation of the MAPK pathway.

These objectives were achieved, as summarised below.

Objective (1): In this thesis and in chapter 4, a basic ABM model for MAPK pathway was constructed. Section 4.1 assessed the "construction" process and demonstrated that the agents adhered to the behaviour assigned to them within the algorithms. Building on that, an ABM was constructed to investigate modulating the pathway's spatial element (peruse, section 4.2) by using two models, a two-compartment and a multi-compartment ABM. Once it was concluded that the multi-compartment model provided a better ABM to investigate the MAPK activation dynamics, the model was used to examine the effect of altering both spatial and temporal regulatory elements simultaneously (review section 4.3 and 4.4).

Objective (2): The literature was surveyed comprehensively to assess previously modelled MAPK pathways, and the essential components required to build a basic molecular model of the pathway were identified. This was included in chapter one, where the computational and biological background to the thesis were reviewed and

described. A practical application of this process is shown in the ABM collaboration of activation time, which is shown in section 4.4.1.

Objective (3): This objective was addressed in Chapter 3 where the important components required for the model construction were described and analysed. This included the definition of the conceptual model of the MAPK pathway, and specifying the essential behaviour and individual properties, which are thought to play an important role in the emergence of real-world system behaviour, or dynamics. The following section was devoted to the transition of the conceptual model into an ABM.

Objective (4): This objective was achieved in section 3.3.3 where the measurable outputs from the ABM were specified. These outputs were used for comparison between the data generated using the ABM approach and previously published data. This objective is also addressed in section 4.1.1 where time calibration of the ABM was implemented. The data generated using the multi-compartment model was compared to previously published data from *in vitro* and *in silico* experimentation (refer to section 4.3).

Objective (5): This was achieved by the multiple model runs, statistical analysis and comparison with previously published data, as reviewed and discussed in section 4.2.1 and 4.4.

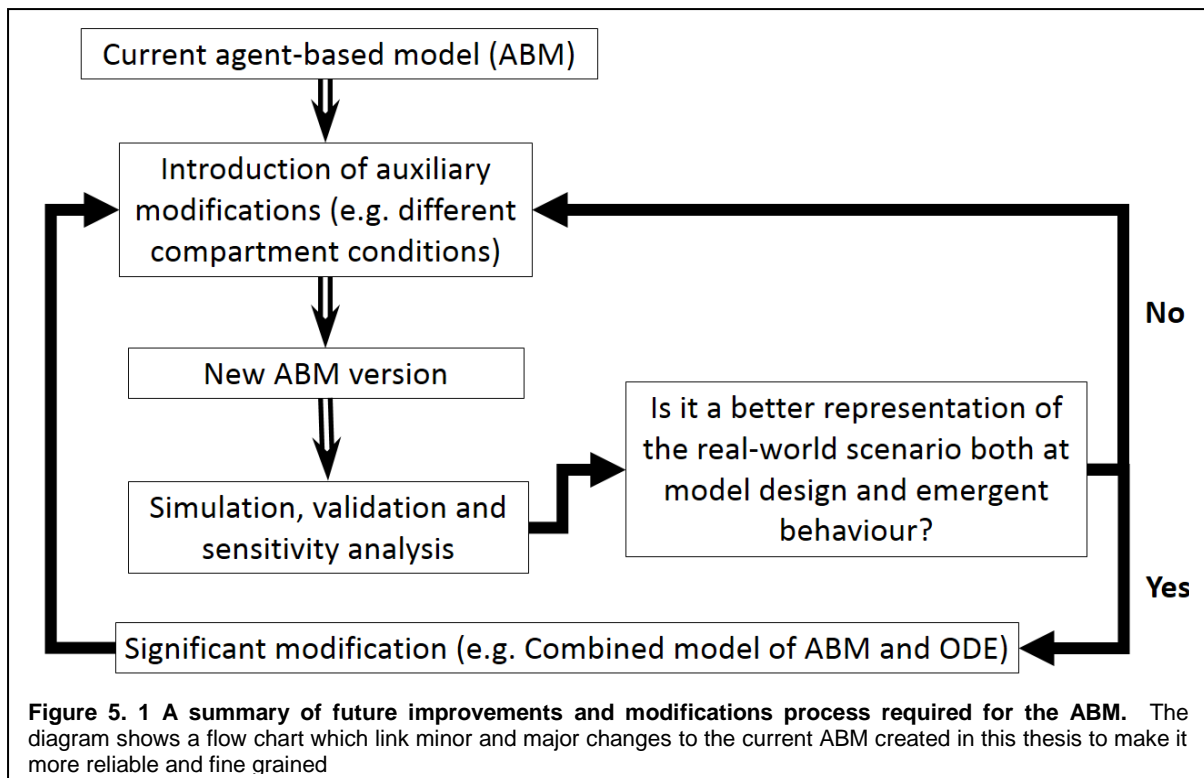
Objective (6): This was demonstrated in the Appendix, where *in vitro* experiments were performed to investigate how cellular responses to stressful stimuli were altered by the modulation of the MAPKK inhibitory proteins tribbles (TRIBs). These experiments will provide the basis for further examination of the regulation of the spatiotemporal modulation of the MAPK pathway using the multi-compartment ABM. The *in vitro* data presented illustrate that the TRIBs are capable of mediating cell death in response to external stimuli differentially, with TRIB3 being important in driving cells towards a cell death pathway. The data also suggested that this differential mediation of stress-induced cell death may be due to the change in the MAPK signalosome cluster, in addition to change in the balance of the signalling within the ERK-JNK-p38-AKT signalling network.

5.2 Limitations and future work

5.2.1 *In silico* modelling, future work

Though the models presented in this thesis have provided novel insights which will be of interest to the field, nonetheless, I do recognise limitations in the model and the requirement for its further development and improvements. These improvements are divided into limited/minor modifications and extensive modifications.

The auxiliary modifications require minimal improvements of the multi-compartment ABM components and/or the addition of few agents to it. These modifications/improvements represent a continuation of the recursive process of



model development. Thus, in these circumstances the use of the current ABM will continue, because these improvements are complementary and do not result in a complete renovation of the current model and its configuration. These include the following:

- The effect of distributive or processive phosphorylation on the activation dynamics of the MAPK pathway
- Different compartmental conditions
- Investigating the effects of the reported emergent MAPK activation behaviour observed on gene expression events.
- Introduction of inhibitory components such as TRIBs
- An agent based model (ABM) combining compartmentalised and homogeneously distributed MAPKK and MAPK agents in the cytoplasm

Extensive modifications require the introduction of a new computational algorithm, multiple new agents and introduction of mathematical equations within the model. Introducing the later changes mean the development of new ABMs built on the insights generated from the auxiliary ABMs (Figure 5. 1). This is similar to the movement from a two compartment model to the multi-compartment model. These extensive changes are not immediately necessary as the current multi-compartment ABM is sufficient to provide a level of understanding of the MAPK activation dynamics. Therefore, these changes will be conducted once the smaller changes were introduced into the available ABM, and the effects of the changes were assessed (Figure 5. 1).

5.2.1.1 Auxiliary modifications and adjustments to the current multi-compartment ABM.

5.2.1.1.1 The effect of distributive or processive phosphorylation on the activation dynamics of the MAPK pathway.

For MAPK proteins to become fully active, they are dually phosphorylated at two phosphorylation sites by pMAPKKs. There are two mechanisms by which MAPKK achieve this. The first is the processive process whereby a pMAPKK phosphorylates MAPK at one site and releases it into the cytoplasm where it interacts with a second pMAPKK which phosphorylates the other site, while the distributive process is when pMAPKK interacts with a MAPK and phosphorylates both phosphorylation sites, and a fully active MAPK is released into the cytoplasm. The current model relies on processive phosphorylation mechanisms for full activation of the MAPK proteins. We

would like to modify the multi compartment ABM slightly by allowing the MAPK to become fully activated *via* distributive process, and monitor how it affects the activation dynamics observed. This will be achieved by the introduction of a basic double phosphorylation model, where in order for MAPK agent to become fully activated, it goes through two state transitions (from inactive MAPK to a mono-phosphorylated MAPK (pMAPK), to a double phosphorylated MAPK (ppMAPK). This modified model will also be used in combination with the stochastic and periodic RADP models to monitor if distributive MAPK phosphorylation influences the emergence of oscillatory behaviour observed in the multi-compartment model.

5.2.1.1.2 Different compartmental conditions

Given that in the natural system compartmentalisation influences the MAPK pathway activation dynamics, and that the current ABM presented proposes some of the mechanisms by which this is achieved, a model which models variability in the conditions inside these compartments will be insightful. Given the assumption that compartments are sources for the emergence of specificity and fidelity in the natural system (Ferrell et al., 2009, Burack, 1997), it will be interesting to monitor if variation of the conditions inside these compartments influences the global dynamics of MAPK activation. In addition, it will be interesting to monitor the local activation dynamics within each compartment. The conditions which can be changed are the variation in the numbers of MAPKK and MAPK agents per compartment, and changes in the ratio between MAPKK and MAPK per compartment as well as variation in the number of mono and non-phosphorylated MAPK species, and how that influences activation dynamics.

5.2.1.1.3 Investigating the effects of the emergent MAPK activation behaviour observed on gene expression events.

Using the established multi-compartment ABM with the various RADP models, it will be interesting to reintroduce the TF agents into the nucleus and monitor the nuclear events during activation of the MAPK pathway within the multi-compartment model. Will there be different MAPK-dependent gene expression initiation dynamics observed in comparison to those observed with the two compartmental model? Additionally, it will be interesting to see how the nuclear events change with the change of the mode of activation at the MAPKK level. What impact an oscillatory *versus* a robust system have on the outcome of the gene expression events?

5.2.1.1.4 Introduction of inhibitory components such as TRIBs

The tribbles proteins were shown to have an inhibitory action on MAPK signalling at the level of MAPKK, which the ABM showed to be important in facilitating the emergence of oscillatory behaviour in the model. Therefore, investigating how inhibitory components such as tribbles (TRIB) affect the dynamics of MAPK activation, by modulating MAPKK interaction with MAPK, will be insightful. This modification is interesting in the context of global activation dynamics, and the MAPK-dependent gene expression events, once the TF agents were introduced into the model. This modified model will make use of the *in vitro* experimental data where TRIBs were shown to modulate the MAPK pathway and its activation dynamics (see appendix A). Furthermore, this introduction of the TRIB agents is complementary to the signalosome cluster ABM (peruse section 4.4.1.1), because the results

demonstrated in appendix A illustrate that the identity of proteins which compose the MAPK signalosome cluster influence the final cellular outcome.

5.2.1.1.5 An agent based model (ABM) combining compartmentalised and homogeneously distributed MAPKK and MAPK agents in the cytoplasm

Biologically, only a fraction of the overall MAPK signalling components reside inside the intracellular compartments. The multi-compartment ABM demonstrated that a fraction of active MAPKK species (~20% of proposed levels see Table 3. 1) are capable of eliciting full MAPK activation, and also sustaining a high level of pMAPK species. This is in line with observations *in vitro/in silico* that show levels of active MAPKK are lower than the total number of inactive MAPKK species (see Table 3. 1). therefore, suggesting that there is a residual number of MAPKKs within the cell which does not contribute to the activation process. Consequently, we would like to test a hybrid model of the multi compartment and the homogeneously distributed MAPKK and MAPK (two compartment) ABM and monitor the activation dynamics and how such a model influences activation dynamics and responds to temporal activation.

5.2.1.2 Extensive changes and additions to the ABM

The extensive changes to the model will include the following:

5.2.1.2.1 Introduction of new agents upstream and downstream of the current model.

The current ABM included components of the MAPK pathway downstream of MAPKKK with the integration of activating and inactivating inputs at the level of the MAPKK. That was sufficient to generate the MAPK activation dynamics observed in the literature and yielded insightful data. However, in order to further increase confidence in the model and its ability to better simulate the natural system, maintaining a degree of faithfulness to the MAPK pathway natural is desirable. These include the addition of upstream components/proteins such as MAPKKK, Ras and the RTKs as independent agents to the model and hence substitute their abstract representation in the model.

Furthermore, RADP presented an output of the final outcome between a "tug of war" between activating and inactivating inputs (positive and negative feedback loops), which ultimately feeds into MAPKK. The next step will be to integrate negative and positive feedback mechanisms by including protein agents responsible for mediating these processes such as phosphatase agents and RKIP agents (refer to Figure 4.14). Furthermore, it was previously shown *in vitro* that phosphatases are found in the nucleus and they dephosphorylate translocated pERK within few minutes from their arrival. Nevertheless, the accumulation of ERK continued with the ERK levels higher in the nucleus compared to the cytoplasm. Inhibition of phosphatase activity allowed for the reappearance of pERK staining in the nucleus (Volmat et al., 2001, Brondello et al., 1999, Keyse, 2000). This shows that the phosphatase activity in the nucleus is important. Therefore, phosphatase agents will be introduced to the cytoplasm and

the nucleus to investigate their effect on MAPK dynamics both at the cytoplasm and nucleus.

Additionally, in the nucleus, the multimeric transcription factor complex (BM-TF) will be substituted with individual proteins which form the BM-TF complex. These proteins will be the transcription factors which are influenced by the MAPK proteins in the nucleus (such as elk, chop and creb). Furthermore, the mechanisms involved for the formation of the MB-TF complex (from a single TF to the complex) will be simulated in the ABM by incorporating binding kinetics, probability roles and Boolean logic.

5.2.1.2.2 MAPK translocation and export to the nucleus

To simulate the rapid translocation of MAPK proteins to the nucleus, translocation was automatic and immediate in the current implementations of the ABM. To improve this, the modified model will include better nuclear translocation and export mechanisms. The design will allow pMAPK to move towards the nucleus as a linear vector with high trajectory/displacement. In a similar fashion, the movement of the exported MAPK will be in a straight line into its compartment of origin.

5.2.1.2.3 Move from a generic MAPK agent-based model (ABM) to a multiple MAPK pathways.

The ultimate desire is to move from the generic MAPK pathway into an ABM which include ERK, p38 and JNK as different MAPK states or, preferably, as independent agents. Consequently, these independent agents interact with the different nuclear

and cytoplasmic targets. Using the same approach, the different MAPKK proteins can be introduced as independent entities into the ABM. Subsequently, introduction of different binding partners and signalosome clusters will follow. These examine the effects of altering the cluster composition on MAPK activation dynamics. This will be monitored for both the MAPK species (p38, JNK and ERK) globally in the cell and within the specific compartments. The last will allow validation of the data we obtained experimentally (peruse appendix D)

5.2.1.2.4 Improvements of binding kinetics and linking the ABM to ODE and probabilistic models

Integrating the binding kinetics between MAPK, MAPKK and MAPKKK by including the calculation of binding coefficients and affinity of one agent to another will be of benefit. That is because it will allow for an additional level of realism into the model and consequently, a further increase in confidence of the model and its ability to adhere to and simulate cell physiology.

The addition of binding kinetics will allow for modulating protein-protein binding. This is important as it is believed that affinity of tribbles proteins (TRIBs) to their binding partners (the MAPKK proteins) play an important role in the differential regulation of MAPKKs by TRIBs. For The incorporation of binding kinetics equations will also be applied when modelling the interaction of transcription factors (TFs) with activated MAPKs and with DNA to facilitate gene expression events. This is will be of benefit to the model because TFs in different phosphorylation states demonstrate differential affinity and binding behaviour to both the pMAPK and DNA, thus this might affect the emergent gene expression behaviour.

5.2.1.2.5 Modification of the nuclear events

The two compartment model contained TFs to model MAPK-dependent gene expression events and in that configuration, the model relied on MAPK activation of multimeric TF species bound to the DNA (MB-TF). The activation of the multimeric TF (MB-TF) initiates gene expression. This is a limitation in the model because activation and binding of the active multimeric TFs to DNA marks initiation of gene expression event but not its final outcome. Considering that the binding of one MB-TF to DNA is a single event, nonetheless this binding event mediate an "n" number of gene transcription events as MB-TF continue to bind to DNA and recruit the gene transcription machinery. Thus, it is complicated to correlate a gene expression initiation event with biological data which rely on transcribed mRNA levels as reading outputs for gene expression. This may explain the observations in the two compartmental ABM with the inhibitory protein agent TRIB showing no notable effect on the gene expression events in comparison with an ABM without (review section 4.2.1.4 and Figure 4. 14) Thus, future models should incorporate DNA, DNA polymerase agents and mRNA agents to monitor the dynamics of gene expression appropriately.

References

- ADACHI, M., FUKUDA, M. & NISHIDA, E. 1999. Two co-existing mechanisms for nuclear import of MAP kinase: passive diffusion of a monomer and active transport of a dimer. *EMBO J*, 18, 5347-58.
- ADACHI, M., FUKUDA, M. & NISHIDA, E. 2000. Nuclear Export of Map Kinase (ERK) Involves a Map Kinase Kinase (Mek-Dependent) Active Transport Mechanism. *The Journal of Cell Biology*, 148, 849-856.
- ADLER, V., QU, Y., SMITH, S. J., IZOTOVA, L., PESTKA, S., KUNG, H.-F., LIN, M., FRIEDMAN, F. K., CHIE, L., CHUNG, D., BOUTJDIR, M. & PINCUS, M. R. 2005. Functional Interactions of Raf and MEK with Jun-N-Terminal Kinase (JNK) Result in a Positive Feedback Loop on the Oncogenic Ras Signaling Pathway†. *Biochemistry*, 44, 10784-10795.
- ADRA, S., SUN, T., MACNEIL, S., HOLCOMBE, M. & SMALLWOOD, R. 2010. Development of a Three Dimensional Multiscale Computational Model of the Human Epidermis. *PLoS ONE*, 5, e8511.
- AGUADO, T., CARRACEDO, A., JULIEN, B., VELASCO, G., MILMAN, G., MECHOULAM, R., ALVAREZ, L., GUZMAN, M. & GALVE-ROPERH, I. 2007. Cannabinoids induce glioma stem-like cell differentiation and inhibit gliomagenesis. *J Biol Chem*, 282, 6854-62.
- AHMED, S., GRANT, K. G., EDWARDS, L. E., RAHMAN, A., CIRIT, M., GOSHE, M. B. & HAUGH, J. M. 2014. Data-driven modeling reconciles kinetics of ERK phosphorylation, localization, and activity states. *Molecular Systems Biology*, 10, 718.
- AHN, S., SHENOY, S. K., WEI, H. & LEFKOWITZ, R. J. 2004. Differential Kinetic and Spatial Patterns of β -Arrestin and G Protein-mediated ERK Activation by the Angiotensin II Receptor. *Journal of Biological Chemistry*, 279, 35518-35525.
- AKSAMITIENE, E., KHOLODENKO, B. N., KOLCH, W., HOEK, J. B. & KIYATKIN, A. 2010. PI3K/Akt-sensitive MEK-independent compensatory circuit of ERK activation in ER-positive PI3K-mutant T47D breast cancer cells. *Cellular signalling*, 22, 1369-1378.
- AKSAMITIENE, E., KIYATKIN, A. & KHOLODENKO, B. N. 2012. Cross-talk between mitogenic Ras/MAPK and survival PI3K/Akt pathways: a fine balance. *Biochem Soc Trans*, 40, 139-46.
- ALBECK, J. G., MILLS, G. B. & BRUGGE, J. S. 2013. Frequency-modulated pulses of ERK activity transmit quantitative proliferation signals. *Mol Cell*, 49, 249-61.
- ALBERTS, B., JOHNSON, A., LEWIS, J., RAFF, M., ROBERTS, K. & WALTER, P. 2002. General principles of cell communication.
- ALDRIDGE, B. B., BURKE, J. M., LAUFFENBURGER, D. A. & SORGER, P. K. 2006. Physicochemical modelling of cell signalling pathways. *Nat Cell Biol*, 8, 1195-203.
- ALESSI, D. R., CUENDA, A., COHEN, P., DUDLEY, D. T. & SALTIEL, A. R. 1995. PD 098059 Is a Specific Inhibitor of the Activation of Mitogen-activated Protein Kinase Kinase in Vitro and in Vivo. *Journal of Biological Chemistry*, 270, 27489-27494.

- ALIAGA, J. C., DESCHENES, C., BEAULIEU, J. F., CALVO, E. L. & RIVARD, N. 1999. Requirement of the MAP kinase cascade for cell cycle progression and differentiation of human intestinal cells. *Am J Physiol*, 277, G631-41.
- ALTAN-BONNET, G. & GERMAIN, R. N. 2005. Modeling T Cell Antigen Discrimination Based on Feedback Control of Digital ERK Responses. *PLoS Biology*, 3, e356.
- ALVAREZ, E., NORTHWOOD, I. C., GONZALEZ, F. A., LATOUR, D. A., SETH, A., ABATE, C., CURRAN, T. & DAVIS, R. J. 1991. Pro-Leu-Ser/Thr-Pro is a consensus primary sequence for substrate protein phosphorylation. Characterization of the phosphorylation of c-myc and c-jun proteins by an epidermal growth factor receptor threonine 669 protein kinase. *Journal of Biological Chemistry*, 266, 15277-15285.
- ANDERSON, A. R. A., CHAPLAIN, M. A. J., NEWMAN, E. L., STEELE, R. J. C. & THOMPSON, A. M. 2000. Mathematical Modelling of Tumour Invasion and Metastasis. *Journal of Theoretical Medicine*, 2.
- ANDERSON, N. G., MALLER, J. L., TONKS, N. K. & STURGILL, T. W. 1990. Requirement for integration of signals from two distinct phosphorylation pathways for activation of MAP kinase. *Nature*, 343, 651-653.
- ANDERSSON, E. R., SANDBERG, R. & LENDAHL, U. 2011. Notch signaling: simplicity in design, versatility in function. *Development*, 138, 3593-3612.
- ANDREADI, C., NOBLE, C., PATEL, B., JIN, H., AGUILAR HERNANDEZ, M. M., BALMANN, K., COOK, S. J. & PRITCHARD, C. 2012. Regulation of MEK/ERK pathway output by subcellular localization of B-Raf. *Biochem Soc Trans*, 40, 67-72.
- ANGERMANN, B. R., KLAUSCHEN, F., GARCIA, A. D., PRUSTEL, T., ZHANG, F., GERMAIN, R. N. & MEIER-SCHELLERSHEIM, M. 2012. Computational modeling of cellular signaling processes embedded into dynamic spatial contexts. *Nat Methods*, 9, 283-9.
- AOKI, K., KUMAGAI, Y., SAKURAI, A., KOMATSU, N., FUJITA, Y., SHIONYU, C. & MATSUDA, M. 2013a. Stochastic ERK Activation Induced by Noise and Cell-to-Cell Propagation Regulates Cell Density-Dependent Proliferation. *Molecular Cell*, 52, 529-540.
- AOKI, K., TAKAHASHI, K., KAIZU, K. & MATSUDA, M. 2013b. A quantitative model of ERK MAP kinase phosphorylation in crowded media. *Sci Rep*, 3, 1541.
- ARORA, K., SINHA, C., ZHANG, W., REN, A., MOON, C., YARLAGADDA, S. & NAREN, A. 2013. Compartmentalization of cyclic nucleotide signaling: a question of when, where, and why? *Pflügers Archiv - European Journal of Physiology*, 465, 1397-1407.
- ATHERTON, L. A., DUPRET, D. & MELLOR, J. R. 2015. Memory trace replay: the shaping of memory consolidation by neuromodulation. *Trends in Neurosciences*, 38, 560-570.
- AULEHLA, A., WEHRLE, C., BRAND-SABERI, B., KEMLER, R., GOSSLER, A., KANZLER, B. & HERRMANN, B. G. 2003. Wnt3a plays a major role in the segmentation clock controlling somitogenesis. *Dev Cell*, 4, 395-406.
- AVRAHAM, R. & YARDEN, Y. 2011. Feedback regulation of EGFR signalling: decision making by early and delayed loops. *Nat Rev Mol Cell Biol*, 12, 104-117.
- BAGOWSKI, C. P. & FERRELL, J. E., JR. 2001. Bistability in the JNK cascade. *Curr Biol*, 11, 1176-82.

- BAGOWSKI, C. P. & FERRELL JR, J. E. 2001. Bistability in the JNK cascade. *Current Biology*, 11, 1176-1182.
- BALAN, V., LEICHT, D. T., ZHU, J., BALAN, K., KAPLUN, A., SINGH-GUPTA, V., QIN, J., RUAN, H., COMB, M. J. & TZIVION, G. 2006. Identification of Novel In Vivo Raf-1 Phosphorylation Sites Mediating Positive Feedback Raf-1 Regulation by Extracellular Signal-regulated Kinase. *Molecular Biology of the Cell*, 17, 1141-1153.
- BALJULS, A., SCHMITZ, W., MUELLER, T., ZAHEDI, R. P., SICKMANN, A., HEKMAN, M. & RAPP, U. R. 2008. Positive Regulation of A-RAF by Phosphorylation of Isoform-specific Hinge Segment and Identification of Novel Phosphorylation Sites. *Journal of Biological Chemistry*, 283, 27239-27254.
- BANDINI, S., MANZONI, S. & VIZZARI, G. 2009. Agent Based Modeling and Simulation: An Informatics Perspective. *Journal of Artificial Societies and Social Simulation*, 12, 4.
- BANKES, S. C. 2002. Agent-based modeling: a revolution? *Proc Natl Acad Sci U S A*, 99 Suppl 3, 7199-200.
- BEHAR, M., DOHLMAN, H. G. & ELSTON, T. C. 2007. Kinetic insulation as an effective mechanism for achieving pathway specificity in intracellular signaling networks. *Proceedings of the National Academy of Sciences*, 104, 16146-16151.
- BERNARD, C. 1865. *Introduction à l'étude de la médecine expérimentale*, Baillière.
- BHALLA, U. S. 2004a. Signaling in small subcellular volumes. I. Stochastic and diffusion effects on individual pathways. *Biophys J*, 87, 733-44.
- BHALLA, U. S. 2004b. Signaling in Small Subcellular Volumes. II. Stochastic and Diffusion Effects on Synaptic Network Properties. *Biophysical Journal*, 87, 745-753.
- BHALLA, U. S. & IYENGAR, R. 1999. Emergent properties of networks of biological signaling pathways. *Science*, 283, 381-7.
- BHALLA, U. S., RAM, P. T. & IYENGAR, R. 2002. MAP kinase phosphatase as a locus of flexibility in a mitogen-activated protein kinase signaling network. *Science*, 297, 1018-23.
- BIANCA, C. & PENNISI, M. 2012. Immune system modeling by top-down and bottom-up approaches. *International Mathematical Forum*, 7.
- BILLINGTON, C. K. & HALL, I. P. 2012. Novel cAMP signalling paradigms: therapeutic implications for airway disease. *British Journal of Pharmacology*, 166, 401-410.
- BIRTWISTLE, M. R., HATAKEYAMA, M., YUMOTO, N., OGUNNAIKE, B. A., HOEK, J. B. & KHOLODENKO, B. N. 2007. Ligand-dependent responses of the ErbB signaling network: experimental and modeling analyses. *Molecular Systems Biology*, 3.
- BLAZQUEZ, C., CARRACEDO, A., SALAZAR, M., LORENTE, M., EGIA, A., GONZALEZ-FERIA, L., HARO, A., VELASCO, G. & GUZMAN, M. 2008a. Down-regulation of tissue inhibitor of metalloproteinases-1 in gliomas: a new marker of cannabinoid antitumoral activity? *Neuropharmacology*, 54, 235-43.
- BLAZQUEZ, C., CASANOVA, M. L., PLANAS, A., GOMEZ DEL PULGAR, T., VILLANUEVA, C., FERNANDEZ-ACENERO, M. J., ARAGONES, J., HUFFMAN, J. W., JORCANO, J. L. & GUZMAN, M. 2003. Inhibition of tumor angiogenesis by cannabinoids. *FASEB J*, 17, 529-31.

- BLAZQUEZ, C., GONZALEZ-FERIA, L., ALVAREZ, L., HARO, A., CASANOVA, M. L. & GUZMAN, M. 2004. Cannabinoids inhibit the vascular endothelial growth factor pathway in gliomas. *Cancer Res*, 64, 5617-23.
- BLAZQUEZ, C., SALAZAR, M., CARRACEDO, A., LORENTE, M., EGIA, A., GONZALEZ-FERIA, L., HARO, A., VELASCO, G. & GUZMAN, M. 2008b. Cannabinoids inhibit glioma cell invasion by down-regulating matrix metalloproteinase-2 expression. *Cancer Res*, 68, 1945-52.
- BLINOV, M. L., FAEDER, J. R., GOLDSTEIN, B. & HLAVACEK, W. S. 2006. A network model of early events in epidermal growth factor receptor signaling that accounts for combinatorial complexity. *Biosystems*, 83, 136-151.
- BLÜTHGEN, N., LEGEWIE, S., KIELBASA, S. M., SCHRAMME, A., TCHERNITSA, O., KEIL, J., SOLF, A., VINGRON, M., SCHÄFER, R., HERZEL, H. & SERS, C. 2009. A systems biological approach suggests that transcriptional feedback regulation by dual-specificity phosphatase 6 shapes extracellular signal-related kinase activity in RAS-transformed fibroblasts. *FEBS Journal*, 276, 1024-1035.
- BOGLE, G. & DUNBAR, P. R. 2009. Agent-based simulation of T-cell activation and proliferation within a lymph node. *Immunol Cell Biol*, 88, 172-179.
- BOGLE, G. & DUNBAR, P. R. 2010. T cell responses in lymph nodes. *Wiley Interdisciplinary Reviews: Systems Biology and Medicine*, 2, 107-116.
- BOGLE, G. & DUNBAR, P. R. 2012. On-Lattice Simulation of T Cell Motility, Chemotaxis, and Trafficking in the Lymph Node Paracortex. *PLoS ONE*, 7, e45258.
- BOND, R. A. & IJZERMAN, A. P. 2006. Recent developments in constitutive receptor activity and inverse agonism, and their potential for GPCR drug discovery. *Trends in pharmacological sciences*, 27, 92-96.
- BOULTON, T. G., NYE, S. H., ROBBINS, D. J., IP, N. Y., RADZLEJEWSKA, E., MORGENBESSER, S. D., DEPINHO, R. A., PANAYOTATOS, N., COBB, M. H. & YANCOPOULOS, G. D. 1991. ERKs: A family of protein-serine/threonine kinases that are activated and tyrosine phosphorylated in response to insulin and NGF. *Cell*, 65, 663-675.
- BRAHMA, A. & DALBY, K. N. 2007. Regulation of protein phosphorylation within the MKK1-ERK2 complex by MP1 and the MP1*P14 heterodimer. *Arch Biochem Biophys*, 460, 85-91.
- BRANDMAN, O. & MEYER, T. 2008. Feedback loops shape cellular signals in space and time. *Science*, 322, 390-5.
- BRAY, D. 1995. Protein molecules as computational elements in living cells. *Nature*, 376, 307-312.
- BRAY, D. & LAY, S. 1997. Computer-based analysis of the binding steps in protein complex formation. *Proc Natl Acad Sci U S A*, 94, 13493-8.
- BREWSTER, J., DE VALOIR, T., DWYER, N., WINTER, E. & GUSTIN, M. 1993. An osmosensing signal transduction pathway in yeast. *Science*, 259, 1760-1763.
- BRIGHTMAN, F. A. & FELL, D. A. 2000. Differential feedback regulation of the MAPK cascade underlies the quantitative differences in EGF and NGF signalling in PC12 cells. *FEBS Letters*, 482, 169-174.
- BRONDELLO, J. M., POUYSSEGUR, J. & MCKENZIE, F. R. 1999. Reduced MAP kinase phosphatase-1 degradation after p42/p44MAPK-dependent phosphorylation. *Science*, 286, 2514-7.
- BROWN, G. C. & KHOLODENKO, B. N. 1999. Spatial gradients of cellular phosphoproteins. *FEBS Lett*, 457, 452-4.

- BRUGGEMAN, F. J. & WESTERHOFF, H. V. 2007. The nature of systems biology. *Trends Microbiol*, 15, 45-50.
- BRUNET, A., PAGES, G. & POUYSSEGUR, J. 1994. Growth factor-stimulated MAP kinase induces rapid retrophosphorylation and inhibition of MAP kinase kinase (MEK1). *FEBS Lett*, 346, 299-303.
- BRUNET, A., ROUX, D., LENORMAND, P., DOWD, S., KEYSE, S. & POUYSSEGUR, J. 1999. Nuclear translocation of p42/p44 mitogen-activated protein kinase is required for growth factor-induced gene expression and cell cycle entry. *EMBO J*, 18, 664-674.
- BURACK, W. R. & SHAW, A. S. 2000. Signal transduction: hanging on a scaffold. *Curr Opin Cell Biol*, 12, 211-6.
- BURACK, W. R. A. S., T. W. 1997. The activating dual phosphorylation of MAPK by MEK is nonprocessive. *Biochemistry*, 36.
- BURRAGE, K., BURRAGE, P., JEFFREY, S., PICKETT, T., SIDJE, R., TIAN, T., . 2003. A grid implementation of chemical kinetic simulation methods in genetic regulation. Proceedings of the APAC03 Conference on Advanced Computing, Grid Applications and eResearch.
- BURRAGE, K., HEGLAND, M., MACNAMARA, S. & SIDJE, R. A Krylov-based finite state projection algorithm for solving the chemical master equation arising in the discrete modelling of biological systems. Proc. of The AA Markov 150th Anniversary Meeting, 2006. 21-37.
- BURRAGE, K., TIAN, T. & BURRAGE, P. 2004. A multi-scaled approach for simulating chemical reaction systems. *Progress in Biophysics and Molecular Biology*, 85, 217-234.
- BUTCHER, G. Q., LEE, B. & OBRIETAN, K. 2003. Temporal regulation of light-induced extracellular signal-regulated kinase activation in the suprachiasmatic nucleus. *J Neurophysiol*, 90, 3854-63.
- CACACE, A. M., MICHAUD, N. R., THERRIEN, M., MATHES, K., COPELAND, T., RUBIN, G. M. & MORRISON, D. K. 1999. Identification of Constitutive and Ras-Inducible Phosphorylation Sites of KSR: Implications for 14-3-3 Binding, Mitogen-Activated Protein Kinase Binding, and KSR Overexpression. *Molecular and Cellular Biology*, 19, 229-240.
- CAI, L., DALAL, C. K. & ELOWITZ, M. B. 2008. Frequency-modulated nuclear localization bursts coordinate gene regulation. *Nature*, 455, 485-90.
- CAKIR, T. & KHATIBIPOUR, M. J. 2014. Metabolic network discovery by top-down and bottom-up approaches and paths for reconciliation. *Frontiers in Bioengineering and Biotechnology*, 2.
- CALDER, M., DUGUID, A., GILMORE, S. & HILLSTON, J. 2006a. Stronger Computational Modelling of Signalling Pathways Using Both Continuous and Discrete-State Methods. In: PRIAMI, C. (ed.) *Computational Methods in Systems Biology*. Springer Berlin Heidelberg.
- CALDER, M., GILMORE, S. & HILLSTON, J. 2006b. Modelling the Influence of RKIP on the ERK Signalling Pathway Using the Stochastic Process Algebra PEPA. In: PRIAMI, C., INGÓLFSDÓTTIR, A., MISHRA, B. & RIIS NIELSON, H. (eds.) *Transactions on Computational Systems Biology VII*. Springer Berlin Heidelberg.
- CALIPEL, A., MOURIAUX, F., GLOTIN, A.-L., MALECAZE, F., FAUSSAT, A.-M. & MASCARELLI, F. 2006. Extracellular Signal-regulated Kinase-dependent Proliferation Is Mediated through the Protein Kinase A/B-Raf Pathway in

- Human Uveal Melanoma Cells. *Journal of Biological Chemistry*, 281, 9238-9250.
- CAMPS, M., NICHOLS, A., GILLIERON, C., ANTONSSON, B., MUDA, M., CHABERT, C., BOSCHERT, U. & ARKINSTALL, S. 1998. Catalytic activation of the phosphatase MKP-3 by ERK2 mitogen-activated protein kinase. *Science*, 280, 1262-5.
- CANAL, F., PALYGIN, O., PANKRATOV, Y., CORREA, S. A. & MULLER, J. 2011. Compartmentalization of the MAPK scaffold protein KSR1 modulates synaptic plasticity in hippocampal neurons. *FASEB J*, 25, 2362-72.
- CARRACEDO, A., GIRONELLA, M., LORENTE, M., GARCIA, S., GUZMAN, M., VELASCO, G. & IOVANNA, J. L. 2006a. Cannabinoids induce apoptosis of pancreatic tumor cells via endoplasmic reticulum stress-related genes. *Cancer Res*, 66, 6748-55.
- CARRACEDO, A., LORENTE, M., EGIA, A., BLAZQUEZ, C., GARCIA, S., GIROUX, V., MALICET, C., VILLUENDAS, R., GIRONELLA, M., GONZALEZ-FERIA, L., PIRIS, M. A., IOVANNA, J. L., GUZMAN, M. & VELASCO, G. 2006b. The stress-regulated protein p8 mediates cannabinoid-induced apoptosis of tumor cells. *Cancer Cell*, 9, 301-12.
- CASTELLI, M., CAMPS, M., GILLIERON, C., LEROY, D., ARKINSTALL, S., ROMMEL, C. & NICHOLS, A. 2004. MAP kinase phosphatase 3 (MKP3) interacts with and is phosphorylated by protein kinase CK2alpha. *J Biol Chem*, 279, 44731-9.
- CASTIGLIONE, F., PAPPALARDO, F., BIANCA, C., RUSSO, G. & MOTTA, S. 2014. Modeling Biology Spanning Different Scales: An Open Challenge. *BioMed Research International*, 2014, 902545.
- CHAMBARD, J.-C., LEFLOCH, R., POUYSSÉGUR, J. & LENORMAND, P. 2007. ERK implication in cell cycle regulation. *Biochimica et Biophysica Acta (BBA) - Molecular Cell Research*, 1773, 1299-1310.
- CHAN, C., LIU, X., WANG, L., BARDWELL, L., NIE, Q. & ENCISO, G. 2012. Protein Scaffolds Can Enhance the Bistability of Multisite Phosphorylation Systems. *PLoS Comput Biol*, 8, e1002551.
- CHANG, L. & KARIN, M. 2001. Mammalian MAP kinase signalling cascades. *Nature*, 410, 37-40.
- CHAOUIYA, C. 2007. Petri net modelling of biological networks. *Brief Bioinform*, 8, 210-9.
- CHEN, W. W., SCHOEBERL, B., JASPER, P. J., NIEPEL, M., NIELSEN, U. B., LAUFFENBURGER, D. A. & SORGER, P. K. 2009. Input-output behavior of ErbB signaling pathways as revealed by a mass action model trained against dynamic data. *Molecular Systems Biology*, 5.
- CHICKARMANE, V., KHOLODENKO, B. N. & SAURO, H. M. 2007. Oscillatory dynamics arising from competitive inhibition and multisite phosphorylation. *J Theor Biol*, 244, 68-76.
- CHIU, V. K., BIVONA, T., HACH, A., SAJOUS, J. B., SILLETTI, J., WIENER, H., JOHNSON, R. L., 2ND, COX, A. D. & PHILIPS, M. R. 2002. Ras signalling on the endoplasmic reticulum and the Golgi. *Nat Cell Biol*, 4, 343-50.
- CHOI, T. G., LEE, J., HA, J. & KIM, S. S. 2011. Apoptosis signal-regulating kinase 1 is an intracellular inducer of p38 MAPK-mediated myogenic signalling in cardiac myoblasts. *Biochimica et Biophysica Acta (BBA) - Molecular Cell Research*, 1813, 1412-1421.

- CHRIST, B. & ORDAHL, C. P. 1995. Early stages of chick somite development. *Anat Embryol (Berl)*, 191, 381-96.
- CHU, S., DERISI, J., EISEN, M., MULHOLLAND, J., BOTSTEIN, D., BROWN, P. O. & HERSKOWITZ, I. 1998. The transcriptional program of sporulation in budding yeast. *Science*, 282, 699-705.
- CHYLEK, L. A., HARRIS, L. A., FAEDER, J. R. & HLAVACEK, W. S. 2015. Modeling for (physical) biologists: an introduction to the rule-based approach. *Phys Biol*, 12, 045007.
- CHYLEK, L. A., HARRIS, L. A., TUNG, C.-S., FAEDER, J. R., LOPEZ, C. F. & HLAVACEK, W. S. 2014. Rule-based modeling: a computational approach for studying biomolecular site dynamics in cell signaling systems. *Wiley interdisciplinary reviews. Systems biology and medicine*, 6, 13-36.
- CICCHETTI, P., MAYER, B. J., THIEL, G. & BALTIMORE, D. 1992. Identification of a protein that binds to the SH3 region of Abl and is similar to Bcr and GAP-rho. *Science*, 257, 803-806.
- CIRIT, M., WANG, C. C. & HAUGH, J. M. 2010. Systematic quantification of negative feedback mechanisms in the extracellular signal-regulated kinase (ERK) signaling network. *J Biol Chem*, 285, 36736-44.
- CLAPHAM, D. E. 2007. Calcium Signaling. *Cell*, 131, 1047-1058.
- COOK, S. J., AZIZ, N. & MCMAHON, M. 1999. The repertoire of fos and jun proteins expressed during the G1 phase of the cell cycle is determined by the duration of mitogen-activated protein kinase activation. *Mol Cell Biol*, 19, 330-41.
- COSTA, M., MARCHI, M., CARDARELLI, F., ROY, A., BELTRAM, F., MAFFEI, L. & RATTO, G. M. 2006. Dynamic regulation of ERK2 nuclear translocation and mobility in living cells. *Journal of Cell Science*, 119, 4952-4963.
- COSTA, M. N., RADHAKRISHNAN, K., WILSON, B. S., VLACHOS, D. G. & EDWARDS, J. S. 2009. Coupled Stochastic Spatial and Non-Spatial Simulations of ErbB1 Signaling Pathways Demonstrate the Importance of Spatial Organization in Signal Transduction. *PLoS ONE*, 4, e6316.
- COULTHARD, L. R., WHITE, D. E., JONES, D. L., MCDERMOTT, M. F. & BURCHILL, S. A. 2009. p38MAPK: stress responses from molecular mechanisms to therapeutics. *Trends in Molecular Medicine*, 15, 369-379.
- CRAIG, E. A., STEVENS, M. V., VAILLANCOURT, R. R. & CAMENISCH, T. D. 2008. MAP3Ks as central regulators of cell fate during development. *Developmental Dynamics*, 237, 3102-3114.
- CREAMER, M. S., STITES, E. C., AZIZ, M., CAHILL, J. A., TAN, C. W., BERENS, M. E., HAN, H., BUSSEY, K. J., VON HOFF, D. D., HLAVACEK, W. S. & POSNER, R. G. 2012. Specification, annotation, visualization and simulation of a large rule-based model for ERBB receptor signaling. *BMC Systems Biology*, 6, 107-107.
- CRICK, F. 1970. Diffusion in embryogenesis. *Nature*, 225, 420-2.
- CUENDA, A. & ROUSSEAU, S. 2007. p38 MAP-Kinases pathway regulation, function and role in human diseases. *Biochimica et Biophysica Acta (BBA) - Molecular Cell Research*, 1773, 1358-1375.
- DANOS, V., FERET, J., FONTANA, W., HARMER, R. & KRIVINE, J. 2007. Rule-Based Modelling of Cellular Signalling. In: CAIRES, L. & VASCONCELOS, V. (eds.) *CONCUR 2007 – Concurrency Theory*. Springer Berlin Heidelberg.
- DAUB, H., OLSEN, J. V., BAIRLEIN, M., GNAD, F., OPPERMANN, F. S., KORNER, R., GREFF, Z., KERI, G., STEMMANN, O. & MANN, M. 2008. Kinase-

- selective enrichment enables quantitative phosphoproteomics of the kinome across the cell cycle. *Mol Cell*, 31, 438-48.
- DAVIES, C. & TOURNIER, C. 2012. Exploring the function of the JNK (c-Jun N-terminal kinase) signalling pathway in physiological and pathological processes to design novel therapeutic strategies. *Biochem Soc Trans*, 40, 85-9.
- DAVIS, R. J. 2000. Signal Transduction by the JNK Group of MAP Kinases. *Cell*, 103, 239-252.
- DE CESARE, D., JACQUOT, S., HANAUER, A. & SASSONE-CORSI, P. 1998. Rsk-2 activity is necessary for epidermal growth factor-induced phosphorylation of CREB protein and transcription of c-fos gene. *Proceedings of the National Academy of Sciences of the United States of America*, 95, 12202-12207.
- DEANGELIS, D. L., ROSE, K.A., HUSTON, M.A., 1994. *Individual oriented approaches to modelling ecological populations and communities*, Berlin, Springer.
- DEEDS, E. J., KRIVINE, J., FERET, J., DANOS, V. & FONTANA, W. 2012. Combinatorial complexity and compositional drift in protein interaction networks. *PLoS One*, 7, e32032.
- DEFRANOUX, N. A., STOKES, C. L., YOUNG, D. L. & KAHN, A. J. 2005. In silico modeling and simulation of bone biology: a proposal. *J Bone Miner Res*, 20, 1079-84.
- DEL BARCO BARRANTES, I. & NEBREDA, A. R. 2012. Roles of p38 MAPKs in invasion and metastasis. *Biochem Soc Trans*, 40, 79-84.
- DENOUEL-GALY, A., DOUVILLE, E. M., WARNE, P. H., PAPIN, C., LAUGIER, D., CALOTHY, G., DOWNWARD, J. & EYCHÈNE, A. 1998. Murine Ksr interacts with MEK and inhibits Ras-induced transformation. *Current biology : CB*, 8, 46-55.
- DENT, P., HASER, W., HAYSTEAD, T., VINCENT, L. A., ROBERTS, T. M. & STURGILL, T. W. 1992. Activation of mitogen-activated protein kinase kinase by v-Raf in NIH 3T3 cells and in vitro. *Science*, 257, 1404-1407.
- DEQUÉANT, M.-L., GLYNN, E., GAUDENZ, K., WAHL, M., CHEN, J., MUSHEGIAN, A. & POURQUIÉ, O. 2006. A Complex Oscillating Network of Signaling Genes Underlies the Mouse Segmentation Clock. *Science*, 314, 1595-1598.
- DÉRIJARD, B., HIBI, M., WU, I. H., BARRETT, T., SU, B., DENG, T., KARIN, M. & DAVIS, R. J. 1994. JNK1: A protein kinase stimulated by UV light and Ha-Ras that binds and phosphorylates the c-Jun activation domain. *Cell*, 76, 1025-1037.
- DERIJARD, B., RAINGEAUD, J., BARRETT, T., WU, I., HAN, J., ULEVITCH, R. & DAVIS, R. 1995. Independent human MAP-kinase signal transduction pathways defined by MEK and MKK isoforms. *Science*, 267, 682-685.
- DEVARY, Y., GOTTLIEB, R. A., SMEAL, T. & KARIN, M. 1992. The mammalian ultraviolet response is triggered by activation of src tyrosine kinases. *Cell*, 71, 1081-1091.
- DOUZIECH M, S. M., LABERGE G, THERRIEN M 2006. A KSR/CNK complex mediated by HYP, a novel SAM domain-containing protein, regulates RAS-dependent RAF activation in *Drosophila*. *Genes & Development*, 20, 807-819.
- DRAGHICI, S., KHATRI, P., TARCA, A. L., AMIN, K., DONE, A., VOICHITA, C., GEORGESCU, C. & ROMERO, R. 2007. A systems biology approach for pathway level analysis. *Genome Res*, 17, 1537-45.

- DROBIC, B., PÉREZ-CADAHÍA, B., YU, J., KUNG, S. K.-P. & DAVIE, J. R. 2010. Promoter chromatin remodeling of immediate-early genes is mediated through H3 phosphorylation at either serine 28 or 10 by the MSK1 multi-protein complex. *Nucleic Acids Research*, 38, 3196-3208.
- DUBRULLE, J., MCGREW, M. J. & POURQUIE, O. 2001. FGF signaling controls somite boundary position and regulates segmentation clock control of spatiotemporal Hox gene activation. *Cell*, 106, 219-32.
- DUBRULLE, J. & POURQUIE, O. 2004. fgf8 mRNA decay establishes a gradient that couples axial elongation to patterning in the vertebrate embryo. *Nature*, 427, 419-22.
- DUESBERY, N. S., WEBB, C. P., LEPPLA, S. H., GORDON, V. M., KLIMPEL, K. R., COPELAND, T. D., AHN, N. G., OSKARSSON, M. K., FUKASAWA, K., PAULL, K. D. & VANDE WOUDE, G. F. 1998. Proteolytic Inactivation of MAP-Kinase-Kinase by Anthrax Lethal Factor. *Science*, 280, 734-737.
- EBERWINE, J. & KIM, J. 2015. Cellular Deconstruction: Finding Meaning in Individual Cell Variation. *Trends Cell Biol*, 25, 569-78.
- EBISUYA, M., KONDOH, K. & NISHIDA, E. 2005. The duration, magnitude and compartmentalization of ERK MAP kinase activity: mechanisms for providing signaling specificity. *J Cell Sci*, 118, 2997-3002.
- EBLEN, S. T., SLACK-DAVIS, J. K., TARCSAFALVI, A., PARSONS, J. T., WEBER, M. J. & CATLING, A. D. 2004. Mitogen-activated protein kinase feedback phosphorylation regulates MEK1 complex formation and activation during cellular adhesion. *Mol Cell Biol*, 24, 2308-17.
- EDER, K., GUAN, H., SUNG, H. Y., WARD, J., ANGYAL, A., JANAS, M., SARMAY, G., DUDA, E., TURNER, M., DOWER, S. K., FRANCIS, S. E., CROSSMAN, D. C. & KISS-TOTH, E. 2008. Tribbles-2 is a novel regulator of inflammatory activation of monocytes. *International Immunology*, 20, 1543-1550.
- EDWARDS, L. M., ASHRAFIAN, H. & KORZENIEWSKI, B. 2011. In silico studies on the sensitivity of myocardial PCr/ATP to changes in mitochondrial enzyme activity and oxygen concentration. *Mol Biosyst*, 7, 3335-42.
- EDWARDS, L. M. & THIELE, I. 2013. Applying systems biology methods to the study of human physiology in extreme environments. *Extreme Physiology & Medicine*, 2, 8-8.
- EFIMOVA, T., DEUCHER, A., KUROKI, T., OHBA, M. & ECKERT, R. L. 2002. Novel Protein Kinase C Isoforms Regulate Human Keratinocyte Differentiation by Activating a p38 δ Mitogen-activated Protein Kinase Cascade That Targets CCAAT/Enhancer-binding Protein α . *Journal of Biological Chemistry*, 277, 31753-31760.
- EMBL-EBI. 1991-2016. *BioModels Database* [Online]. Wellcome Genome Campus, Hinxton, Cambridgeshire, CB10 1SD, UK The European Bioinformatics Institute. Available: <https://www.ebi.ac.uk/biomodels-main/search-models.do?cmd=TEXT:SEARCH> 2016].
- ENSLEN, H., BRANCHO, D. M. & DAVIS, R. J. 2000. Molecular determinants that mediate selective activation of p38 MAP kinase isoforms. *The EMBO Journal*, 19, 1301-1311.
- ENSLEN, H., RAINGEAUD, J. & DAVIS, R. J. 1998. Selective activation of p38 mitogen-activated protein (MAP) kinase isoforms by the MAP kinase kinases MKK3 and MKK6. *Journal of Biological Chemistry*, 273, 1741-1748.
- EUNG DAMRONG, N. J. & IYENGAR, R. 2004. Computational approaches for modeling regulatory cellular networks. *Trends in Cell Biology*, 14, 661-669.

- FAN, F., FENG, L., HE, J., WANG, X., JIANG, X., ZHANG, Y., WANG, Z. & CHEN, Y. 2008. RKTG sequesters B-Raf to the Golgi apparatus and inhibits the proliferation and tumorigenicity of human malignant melanoma cells. *Carcinogenesis*, 29, 1157-63.
- FAVATA, M. F., HORIUCHI, K. Y., MANOS, E. J., DAULERIO, A. J., STRADLEY, D. A., FEESER, W. S., VAN DYK, D. E., PITTS, W. J., EARL, R. A., HOBBS, F., COPELAND, R. A., MAGOLDA, R. L., SCHERLE, P. A. & TRZASKOS, J. M. 1998. Identification of a Novel Inhibitor of Mitogen-activated Protein Kinase Kinase. *Journal of Biological Chemistry*, 273, 18623-18632.
- FELS, J., ORLOV, S. N. & GRYGORCZYK, R. 2009. The Hydrogel Nature of Mammalian Cytoplasm Contributes to Osmosensing and Extracellular pH Sensing. *Biophysical Journal*, 96, 4276-4285.
- FERRELL, J. E. & BHATT, R. R. 1997. Mechanistic Studies of the Dual Phosphorylation of Mitogen-activated Protein Kinase. *Journal of Biological Chemistry*, 272, 19008-19016.
- FERRELL, J. E., JR. 1997. How responses get more switch-like as you move down a protein kinase cascade. *Trends Biochem Sci*, 22, 288-9.
- FERRELL, J. E., JR. 2000. What Do Scaffold Proteins Really Do? *Sci. STKE*, 2000, pe1-.
- FERRELL, J. E., JR., POMERENING, J. R., KIM, S. Y., TRUNNELL, N. B., XIONG, W., HUANG, C. Y. & MACHLEDER, E. M. 2009. Simple, realistic models of complex biological processes: positive feedback and bistability in a cell fate switch and a cell cycle oscillator. *FEBS Lett*, 583, 3999-4005.
- FERRELL, J. E. & MACHLEDER, E. M. 1998. The Biochemical Basis of an All-or-None Cell Fate Switch in *Xenopus* Oocytes. *Science*, 280, 895-898.
- FERRELL, J. E. & XIONG, W. 2001. Bistability in cell signaling: How to make continuous processes discontinuous, and reversible processes irreversible. *Chaos*, 11, 227-236.
- FERRELL JR, J. E. 2002. Self-perpetuating states in signal transduction: positive feedback, double-negative feedback and bistability. *Current Opinion in Cell Biology*, 14, 140-148.
- FEY, D., CROUCHER, D. R., KOLCH, W. & KHOLODENKO, B. N. 2012. Crosstalk and Signaling Switches in Mitogen-Activated Protein Kinase Cascades. *Frontiers in Physiology*, 3, 355.
- FIGUEROA, C., TARRAS, S., TAYLOR, J. & VOJTEK, A. B. 2003. Akt2 Negatively Regulates Assembly of the POSH-MLK-JNK Signaling Complex. *Journal of Biological Chemistry*, 278, 47922-47927.
- FIMIA, G. M. & SASSONE-CORSI, P. 2001. Cyclic AMP signalling. *Journal of Cell Science*, 114, 1971-1972.
- FISHER, J. & HENZINGER, T. A. 2007. Executable cell biology. *Nat Biotech*, 25, 1239-1249.
- FLAME.CO.UK. 2016. *Documentation* [Online]. Available: <http://www.flame.ac.uk/2014>].
- FRESHNEY, N. W., RAWLINSON, L., GUESDON, F., JONES, E., COWLEY, S., HSUAN, J. & SAKLATVALA, J. 1994. Interleukin-1 activates a novel protein kinase cascade that results in the phosphorylation of hsp27. *Cell*, 78, 1039-1049.
- FRITSCH-GUENTHER, R., WITZEL, F., SIEBER, A., HERR, R., SCHMIDT, N., BRAUN, S., BRUMMER, T., SERS, C. & BLÜTHGEN, N. 2011. Strong

- negative feedback from Erk to Raf confers robustness to MAPK signalling. *Molecular Systems Biology*, 7, 489-489.
- FRÖDIN, M. & GAMMELTOFT, S. 1999. Role and regulation of 90 kDa ribosomal S6 kinase (RSK) in signal transduction. *Molecular and Cellular Endocrinology*, 151, 65-77.
- FUKUNAGA, R. & HUNTER, T. 1997. MNK1, a new MAP kinase-activated protein kinase, isolated by a novel expression screening method for identifying protein kinase substrates. *EMBO Journal*, 16, 1921-1933.
- FUNNELL, A. P. & CROSSLEY, M. 2012. Homo- and heterodimerization in transcriptional regulation. *Protein Dimerization and Oligomerization in Biology*. Springer.
- FURUNO, T., HIRASHIMA, N., ONIZAWA, S., SAGIYA, N. & NAKANISHI, M. 2001. Nuclear shuttling of mitogen-activated protein (MAP) kinase (extracellular signal-regulated kinase (ERK) 2) was dynamically controlled by MAP/ERK kinase after antigen stimulation in RBL-2H3 cells. *J Immunol*, 166, 4416-21.
- GAESTEL, M. 2006. MAPKAP kinases — MKs — two's company, three's a crowd. *Nat Rev Mol Cell Biol*, 7, 120-130.
- GALVE-ROPERH, I., SANCHEZ, C., CORTES, M. L., GOMEZ DEL PULGAR, T., IZQUIERDO, M. & GUZMAN, M. 2000. Anti-tumoral action of cannabinoids: involvement of sustained ceramide accumulation and extracellular signal-regulated kinase activation. *Nat Med*, 6, 313-9.
- GANIATSAS, S., KWEE, L., FUJIWARA, Y., PERKINS, A., IKEDA, T., LABOW, M. A. & ZON, L. I. 1998. SEK1 deficiency reveals mitogen-activated protein kinase cascade crossregulation and leads to abnormal hepatogenesis. *Proceedings of the National Academy of Sciences*, 95, 6881-6886.
- GAO, C., FRAUSTO, S. F., GUEDEA, A. L., TRONSON, N. C., JOVASEVIC, V., LEADERBRAND, K., CORCORAN, K. A., GUZMÁN, Y. F., SWANSON, G. T. & RADULOVIC, J. 2011. IQGAP1 regulates NR2A signaling, spine density, and cognitive processes. *The Journal of neuroscience : the official journal of the Society for Neuroscience*, 31, 8533-8542.
- GAONI, Y. & MECHOULAM, R. 1964. Isolation, Structure, and Partial Synthesis of an Active Constituent of Hashish. *Journal of the American Chemical Society*, 86, 1646-1647.
- GARDNER, M. 1970. MATHEMATICAL GAMES: The fantastic combinations of John Conway's new solitaire game "life". *Scientific American USA*: Gerard Piel.
- GAVIN, A. C. & SCHORDERET-SLATKINE, S. 1997. Ribosomal S6 kinase p90(rsk) and mRNA cap-binding protein eIF4E phosphorylations correlate with MAP kinase activation during meiotic reinitiation of mouse oocytes. *Molecular Reproduction and Development*, 46, 383-391.
- GHATAN, S., LARNER, S., KINOSHITA, Y., HETMAN, M., PATEL, L., XIA, Z., YOULE, R. J. & MORRISON, R. S. 2000. p38 Map Kinase Mediates Bax Translocation in Nitric Oxide-Induced Apoptosis in Neurons. *The Journal of Cell Biology*, 150, 335-348.
- GILLE, H., SHARROCKS, A. D. & SHAW, P. E. 1992. Phosphorylation of transcription factor p62TCF by MAP kinase stimulates ternary complex formation at c-fos promoter. *Nature*, 358, 414-417.
- GOMEZ, N. & COHEN, P. 1991. Dissection of the protein kinase cascade by which nerve growth factor activates MAP kinases. *Nature*, 353, 170-173.

- GÓMEZ, N., TONKS, N. K., MORRISON, C., HARMAR, T. & COHEN, P. 1990. Evidence for communication between nerve growth factor and protein tyrosine phosphorylation. *FEBS Letters*, 271, 119-122.
- GOTOH, Y., MASUYAMA, N., DELL, K., SHIRAKABE, K. & NISHIDA, E. 1995. Initiation of Xenopus Oocyte Maturation by Activation of the Mitogen-activated Protein Kinase Cascade. *Journal of Biological Chemistry*, 270, 25898-25904.
- GOTOH, Y., MATSUDA, S., TAKENAKA, K., HATTORI, S., IWAMATSU, A., ISHIKAWA, M., KOSAKO, H. & NISHIDA, E. 1994. Characterization of recombinant Xenopus MAP kinase kinases mutated at potential phosphorylation sites. *Oncogene*, 9, 1891-1898.
- GOTOH, Y., NISHIDA, E., YAMASHITA, T., HOSHI, M., KAWAKAMI, M. & SAKAI, H. 1990. Microtubule-associated-protein (MAP) kinase activated by nerve growth factor and epidermal growth factor in PC12 cells. *European Journal of Biochemistry*, 193, 661-669.
- GREENHOUGH, A., PATSOS, H. A., WILLIAMS, A. C. & PARASKEVA, C. 2007. The cannabinoid delta(9)-tetrahydrocannabinol inhibits RAS-MAPK and PI3K-AKT survival signalling and induces BAD-mediated apoptosis in colorectal cancer cells. *Int J Cancer*, 121, 2172-80.
- GRIEB, M., BURKOVSKI, A., STRÄNG, J. E., KRAUS, J. M., GROß, A., PALM, G., KÜHL, M. & KESTLER, H. A. 2015. Predicting Variabilities in Cardiac Gene Expression with a Boolean Network Incorporating Uncertainty. *PLoS ONE*, 10, e0131832.
- GRIECO, L., CALZONE, L., BERNARD-PIERROT, I., RADVANYI, F., KAHN-PERLÈS, B. & THIEFFRY, D. 2013. Integrative Modelling of the Influence of MAPK Network on Cancer Cell Fate Decision. *PLoS Comput Biol*, 9, e1003286.
- GRINEV, V. V., RAMANOUSKAYA, T. V. & GLOUSHEN, S. V. 2013. Multidimensional control of cell structural robustness. *Cell Biol Int*, 37, 1023-37.
- GUAN, H., SHUAIB, A., LEON, D. D., ANGYAL, A., SALAZAR, M., VELASCO, G., HOLCOMBE, M., DOWER, S. K. & KISS-TOTH, E. 2016. Competition between members of the tribbles pseudokinase protein family shapes their interactions with mitogen activated protein kinase pathways. *Sci Rep*, 6, 32667.
- GUPTA, S., BARRETT, T., WHITMARSH, A. J., CAVANAGH, J., SLUSS, H. K., DERIJARD, B. & DAVIS, R. J. 1996. Selective interaction of JNK protein kinase isoforms with transcription factors. *The EMBO journal*, 15, 2760.
- GUPTA, S., CAMPBELL, D., DERIJARD, B. & DAVIS, R. 1995. Transcription factor ATF2 regulation by the JNK signal transduction pathway. *Science*, 267, 389-393.
- GUZMAN, M. 2003. Cannabinoids: potential anticancer agents. *Nat Rev Cancer*, 3, 745-55.
- GUZZI, F., ZANCHETTA, D., CASSONI, P., GUZZI, V., FRANCOLINI, M., PARENTI, M. & CHINI, B. 2002. Localization of the human oxytocin receptor in caveolin-1 enriched domains turns the receptor-mediated inhibition of cell growth into a proliferative response. *Oncogene*, 21, 1658-67.
- HAACK, F., LEMCKE, H., EWALD, R., RHARASS, T. & UHRMACHER, A. M. 2015. Spatio-temporal Model of Endogenous ROS and Raft-Dependent WNT/Beta-Catenin Signaling Driving Cell Fate Commitment in Human Neural Progenitor Cells. *PLoS Computational Biology*, 11, e1004106.

- HAEUSGEN, W., HERDEGEN, T. & WAETZIG, V. 2011. The bottleneck of JNK signaling: Molecular and functional characteristics of MKK4 and MKK7. *European Journal of Cell Biology*, 90, 536-544.
- HAI, F. G., MARKOVA, B., KLAMAN, L. D., BOHMER, F. D. & NEEL, B. G. 2003. Regulation of receptor tyrosine kinase signaling by protein tyrosine phosphatase-1B. *J Biol Chem*, 278, 739-44.
- HANADA, M., KOBAYASHI, T., OHNISHI, M., IKEDA, S., WANG, H., KATSURA, K., YANAGAWA, Y., HIRAGA, A., KANAMARU, R. & TAMURA, S. 1998. Selective suppression of stress-activated protein kinase pathway by protein phosphatase 2C in mammalian cells. *FEBS Lett*, 437, 172-6.
- HANCOCK, J. F. & PARTON, R. G. 2005. Ras plasma membrane signalling platforms. *Biochem J*, 389, 1-11.
- HANDORF, T. & KLIPP, E. 2012. Modeling mechanistic biological networks: An advanced Boolean approach. *Bioinformatics*, 28, 557-563.
- HAO BAI, MATTHEW D. ROLFE, WENJING JIA, SIMON COAKLEY, ROBERT K. POOLE, GREEN, J. & HOLCOMBE, A. M. 2014. Agent-Based Modeling of Oxygen-responsive Transcription Factors in Escherichia coli. *PLOS Comput Biol*, In press.
- HARDING, A., TIAN, T., WESTBURY, E., FRISCHE, E. & HANCOCK, J. F. 2005a. Subcellular localization determines MAP kinase signal output. *Curr Biol*, 15, 869-73.
- HARDING, A., TIAN, T., WESTBURY, E., FRISCHE, E. & HANCOCK, J. F. 2005b. Subcellular localization determines MAP kinase signal output. *Curr Biol*, 15.
- HARDING, A. S. & HANCOCK, J. F. 2008. Using plasma membrane nanoclusters to build better signaling circuits. *Trends Cell Biol*, 18, 364-71.
- HATAKEYAMA, M., KIMURA, S., NAKA, T., KAWASAKI, T., YUMOTO, N., ICHIKAWA, M., KIM, J.-H., SAITO, K., SAEKI, M., SHIROUZU, M., YOKOYAMA, S. & KONAGAYA, A. 2003. A computational model on the modulation of mitogen-activated protein kinase (MAPK) and Akt pathways in heregulin-induced ErbB signalling. *Biochemical Journal*, 373, 451-463.
- HAYASHI, Y., SANADA, K. & FUKADA, Y. 2001. Circadian and photic regulation of MAP kinase by Ras- and protein phosphatase-dependent pathways in the chick pineal gland. *FEBS Lett*, 491, 71-5.
- HAZZALIN, C. A., CANO, E., CUENDA, A., BARRATT, M. J., COHEN, P. & MAHADEVAN, L. C. 1996. p38/RK is essential for stress-induced nuclear responses: JNK/SAPKs and c-Jun/ATF-2 phosphorylation are insufficient. *Current Biology*, 6, 1028-1031.
- HEGEDUS, Z., CZIBULA, A. & KISS-TOTH, E. 2007. Tribbles: A family of kinase-like proteins with potent signalling regulatory function. *Cellular Signalling*, 19, 238-250.
- HEINRICH, R., NEEL, B. G. & RAPOPORT, T. A. 2002. Mathematical Models of Protein Kinase Signal Transduction. *Molecular Cell*, 9, 957-970.
- HELIKAR, T., KONVALINA, J., HEIDEL, J. & ROGERS, J. A. 2008. Emergent decision-making in biological signal transduction networks. *Proceedings of the National Academy of Sciences*, 105, 1913-1918.
- HERRERA, B., CARRACEDO, A., DIEZ-ZAERA, M., GUZMAN, M. & VELASCO, G. 2005. p38 MAPK is involved in CB2 receptor-induced apoptosis of human leukaemia cells. *FEBS Lett*, 579, 5084-8.
- HESS, E. L. 1970. Origins of molecular biology. *Science*, 168, 664-9.

- HIBI, M., LIN, A., SMEAL, T., MINDEN, A. & KARIN, M. 1993. Identification of an oncoprotein- and UV-responsive protein kinase that binds and potentiates the c-Jun activation domain. *Genes & Development*, 7, 2135-2148.
- HILIOTI, Z., SABBAGH, W., JR., PALIWAL, S., BERGMANN, A., GONCALVES, M. D., BARDWELL, L. & LEVCHENKO, A. 2008. Oscillatory phosphorylation of yeast Fus3 MAP kinase controls periodic gene expression and morphogenesis. *Curr Biol*, 18, 1700-6.
- HILL, M. M. & HEMMING, B. A. 2002. Inhibition of protein kinase B/Akt. implications for cancer therapy. *Pharmacol Ther*, 93, 243-51.
- HLAVACEK, W. S., FAEDER, J. R., BLINOV, M. L., PERELSON, A. S. & GOLDSTEIN, B. 2003. The complexity of complexes in signal transduction. *Biotechnol Bioeng*, 84, 783-94.
- HLAVACEK, W. S., FAEDER, J. R., BLINOV, M. L., POSNER, R. G., HUCKA, M. & FONTANA, W. 2006. Rules for Modeling Signal-Transduction Systems. *Science Signaling*, 2006, re6-re6.
- HOGEWEG, P. 2011. The Roots of Bioinformatics in Theoretical Biology. *PLoS Comput Biol*, 7, e1002021.
- HOLCOMBE, M., ADRA, S., BICAK, M., CHIN, S., COAKLEY, S., GRAHAM, A. I., GREEN, J., GREENOUGH, C., JACKSON, D., KIRAN, M., MACNEIL, S., MALEKI-DIZAJI, A., MCMINN, P., POGSON, M., POOLE, R., QWARNSTROM, E., RATNIEKS, F., ROLFE, M. D., SMALLWOOD, R., SUN, T. & WORTH, D. 2012. Modelling complex biological systems using an agent-based approach. *Integr Biol (Camb)*, 4, 53-64.
- HONGLIN, X. & SHITONG, W. Fuzzy Logical on Boolean Networks as Model of Gene Regulatory Networks. Artificial Intelligence, 2009. JCAI '09. International Joint Conference on, 25-26 April 2009 2009. 501-505.
- HORGAN, A. M. & STORK, P. J. 2003. Examining the mechanism of Erk nuclear translocation using green fluorescent protein. *Exp Cell Res*, 285, 208-20.
- HORNBERG, J. J., BINDER, B., BRUGGEMAN, F. J., SCHOEBERL, B., HEINRICH, R. & WESTERHOFF, H. V. 2005a. Control of MAPK signalling: from complexity to what really matters. *Oncogene*, 24, 5533-5542.
- HORNBERG, J. J., BRUGGEMAN, F. J., BINDER, B., GEEST, C. R., DE VAATE, A. J. M. B., LANKELMA, J., HEINRICH, R. & WESTERHOFF, H. V. 2005b. Principles behind the multifarious control of signal transduction. *FEBS Journal*, 272, 244-258.
- HOWE, L. R., LEEVERS, S. J., GÓMEZ, N., NAKIELNY, S., COHEN, P. & MARSHALL, C. J. 1992. Activation of the MAP kinase pathway by the protein kinase raf. *Cell*, 71, 335-342.
- HU, B., RAPPEL, W.-J. & LEVINE, H. 2009. Mechanisms and Constraints on Yeast MAPK Signaling Specificity. *Biophysical Journal*, 96, 4755-4763.
- HUANG, C. Y. & FERRELL, J. E. 1996. Ultrasensitivity in the mitogen-activated protein kinase cascade. *Proceedings of the National Academy of Sciences*, 93, 10078-10083.
- HUANG, H. & TINDALL, D. J. 2011. Regulation of FOXO protein stability via ubiquitination and proteasome degradation. *Biochim Biophys Acta*, 1813, 1961-4.
- HUANG, S. & INGBER, D. E. 2000. Shape-Dependent Control of Cell Growth, Differentiation, and Apoptosis: Switching between Attractors in Cell Regulatory Networks. *Experimental Cell Research*, 261, 91-103.

- HUANG, W., ALESSANDRINI, A., CREWS, C. M. & ERIKSON, R. L. 1993. Raf-1 forms a stable complex with Mek1 and activates Mek1 by serine phosphorylation. *Proceedings of the National Academy of Sciences*, 90, 10947-10951.
- HÜBNER, A., BARRETT, T., FLAVELL, R. A. & DAVIS, R. J. 2008. Multi-site Phosphorylation Regulates Bim Stability and Apoptotic Activity. *Molecular cell*, 30, 415-425.
- HUDDER, A., NATHANSON, L. & DEUTSCHER, M. P. 2003. Organization of mammalian cytoplasm. *Mol Cell Biol*, 23, 9318-26.
- HUNT, C. A., ROPELLA, G. E. P., PARK, S. & ENGELBERG, J. 2008. Dichotomies between computational and mathematical models. *Nat Biotech*, 26, 737-738.
- HUOT, J., HOULE, F., MARCEAU, F. & LANDRY, J. 1997. Oxidative stress-induced actin reorganization mediated by the p38 mitogen-activated protein kinase/heat shock protein 27 pathway in vascular endothelial cells. *Circulation research*, 80, 383-392.
- HURST, J. H. & DOHLMAN, H. G. 2013. Dynamic Ubiquitination of the Mitogen-activated Protein Kinase Kinase (MAPKK) Ste7 Determines Mitogen-activated Protein Kinase (MAPK) Specificity. *Journal of Biological Chemistry*, 288, 18660-18671.
- INDER, K., HARDING, A., PLOWMAN, S. J., PHILIPS, M. R., PARTON, R. G. & HANCOCK, J. F. 2008. Activation of the MAPK module from different spatial locations generates distinct system outputs. *Mol Biol Cell*, 19, 4776-84.
- INGOLIA, N. T. & MURRAY, A. W. 2007. Positive-feedback loops as a flexible biological module. *Curr Biol*, 17, 668-77.
- INSTITUTE OF MOLECULAR SYSTEMS BIOLOGY, Z. 2016. Zurich: <http://www.imsb.ethz.ch/>. Available: <http://www.imsb.ethz.ch/> [Accessed 15/02 2015].
- INSTITUTE, T. S. B. 2005-2016. Japan: The Systems Biology Institute - Japan. [Accessed February 2015 2015].
- ISHIBE, S., JOLY, D., ZHU, X. & CANTLEY, L. G. 2003. Phosphorylation-dependent paxillin-ERK association mediates hepatocyte growth factor-stimulated epithelial morphogenesis. *Mol Cell*, 12, 1275-85.
- ITO, M., YOSHIOKA, K., AKECHI, M., YAMASHITA, S., TAKAMATSU, N., SUGIYAMA, K., HIBI, M., NAKABEPPU, Y., SHIBA, T. & YAMAMOTO, K.-I. 1999. JSAP1, a Novel Jun N-Terminal Protein Kinase (JNK)-Binding Protein That Functions as a Scaffold Factor in the JNK Signaling Pathway. *Molecular and Cellular Biology*, 19, 7539-7548.
- JACKSON, D. E., HOLCOMBE, M. & RATNIEKS, F. L. W. 2004. Trail geometry gives polarity to ant foraging networks. *Nature*, 432, 907-909.
- JAMES E, F., JR. 1996. Tripping the switch fantastic: how a protein kinase cascade can convert graded inputs into switch-like outputs. *Trends in Biochemical Sciences*, 21, 460-466.
- JAVVADI, P., SEGAN, A. T., TUTTLE, S. W. & KOUMENIS, C. 2008. The chemopreventive agent curcumin is a potent radiosensitizer of human cervical tumor cells via increased reactive oxygen species production and overactivation of the mitogen-activated protein kinase pathway. *Molecular pharmacology*, 73, 1491-1501.
- JEFFREY, K. L., BRUMMER, T., ROLPH, M. S., LIU, S. M., CALLEJAS, N. A., GRUMONT, R. J., GILLIERON, C., MACKAY, F., GREY, S., CAMPS, M., ROMMEL, C., GERONDAKIS, S. D. & MACKAY, C. R. 2006. Positive

- regulation of immune cell function and inflammatory responses by phosphatase PAC-1. *Nat Immunol*, 7, 274-83.
- JEON, J., QUARANTA, V. & CUMMINGS, P. T. 2010. An Off-Lattice Hybrid Discrete-Continuum Model of Tumor Growth and Invasion. *Biophysical Journal*, 98, 37-47.
- JEONG, H., TOMBOR, B., ALBERT, R., OLTVAI, Z. N. & BARABASI, A. L. 2000. The large-scale organization of metabolic networks. *Nature*, 407, 651-4.
- JIANG, Y., GRAM, H., ZHAO, M., NEW, L., GU, J., FENG, L., DI PADOVA, F., ULEVITCH, R. J. & HAN, J. 1997. Characterization of the structure and function of the fourth member of p38 group mitogen-activated protein kinases, p38 δ . *Journal of Biological Chemistry*, 272, 30122-30128.
- JOHNSON, G. L., DOHLMAN, H. G. & GRAVES, L. M. 2005. MAPK kinase kinases (MKKKs) as a target class for small-molecule inhibition to modulate signaling networks and gene expression. *Current Opinion in Chemical Biology*, 9, 325-331.
- JOHNSON, G. L. & LAPADAT, R. 2002. Mitogen-activated protein kinase pathways mediated by ERK, JNK, and p38 protein kinases. *Science*, 298, 1911-2.
- JONES, S. W., ERIKSON, E., BLENIS, J., MALLER, J. L. & ERIKSON, R. 1988. A Xenopus ribosomal protein S6 kinase has two apparent kinase domains that are each similar to distinct protein kinases. *Proceedings of the National Academy of Sciences*, 85, 3377-3381.
- JONESON, T., FULTON, J. A., VOLLE, D. J., CHAIKA, O. V., BAR-SAGI, D. & LEWIS, R. E. 1998. Kinase Suppressor of Ras Inhibits the Activation of Extracellular Ligand-regulated (ERK) Mitogen-activated Protein (MAP) Kinase by Growth Factors, Activated Ras, and Ras Effectors. *Journal of Biological Chemistry*, 273, 7743-7748.
- JOYCE, A. R. & PALSSON, B. O. 2006. The model organism as a system: integrating 'omics' data sets. *Nat Rev Mol Cell Biol*, 7, 198-210.
- JUNTTILA, M. R., LI, S.-P. & WESTERMARCK, J. 2008. Phosphatase-mediated crosstalk between MAPK signaling pathways in the regulation of cell survival. *The FASEB Journal*, 22, 954-965.
- KAGEYAMA, R., NIWA, Y., ISOMURA, A., GONZALEZ, A. & HARIMA, Y. 2012. Oscillatory gene expression and somitogenesis. *Wiley Interdiscip Rev Dev Biol*, 1, 629-41.
- KANG, S., KAHAN, S., MCDERMOTT, J., FLANN, N. & SHMULEVICH, I. 2014. Biocellion: accelerating computer simulation of multicellular biological system models. *Bioinformatics*, 30, 3101-8.
- KARLSSON, M., MATHERS, J., DICKINSON, R. J., MANDL, M. & KEYSE, S. M. 2004. Both Nuclear-Cytoplasmic Shuttling of the Dual Specificity Phosphatase MKP-3 and Its Ability to Anchor MAP Kinase in the Cytoplasm Are Mediated by a Conserved Nuclear Export Signal. *Journal of Biological Chemistry*, 279, 41882-41891.
- KATAGIRI, C., MASUDA, K., URANO, T., YAMASHITA, K., ARAKI, Y., KIKUCHI, K. & SHIMA, H. 2005. Phosphorylation of Ser-446 determines stability of MKP-7. *J Biol Chem*, 280, 14716-22.
- KATAGIRI, F. 2003. Attacking Complex Problems with the Power of Systems Biology. *Plant Physiology*, 132, 417-419.
- KAUL, H. & VENTIKOS, Y. 2015. Investigating biocomplexity through the agent-based paradigm. *Brief Bioinform*, 16, 137-52.

- KAZMIERCZAK, B. & LIPNIACKI, T. 2009. Regulation of kinase activity by diffusion and feedback. *J Theor Biol*, 259, 291-6.
- KAZMIERCZAK, B. & LIPNIACKI, T. 2010. Spatial gradients in kinase cascade regulation. *IET Syst Biol*, 4, 348-55.
- KENAKIN, T. & MILLER, L. J. 2010. Seven transmembrane receptors as shapeshifting proteins: the impact of allosteric modulation and functional selectivity on new drug discovery. *Pharmacol Rev*, 62, 265-304.
- KEYSE, S. M. 2000. Protein phosphatases and the regulation of mitogen-activated protein kinase signalling. *Curr Opin Cell Biol*, 12, 186-92.
- KHILNANI, G. & KHILNANI, A. K. 2011. Inverse agonism and its therapeutic significance. *Indian Journal of Pharmacology*, 43, 492-501.
- KHOKHLATCHEV, A. V., CANAGARAJAH, B., WILSBACHER, J., ROBINSON, M., ATKINSON, M., GOLDSMITH, E. & COBB, M. H. 1998. Phosphorylation of the MAP Kinase ERK2 Promotes Its Homodimerization and Nuclear Translocation. *Cell*, 93, 605-615.
- KHOLODENKO, B. N. 2000. Negative feedback and ultrasensitivity can bring about oscillations in the mitogen-activated protein kinase cascades. *Eur J Biochem*, 267, 1583-8.
- KHOLODENKO, B. N. 2002. MAP kinase cascade signaling and endocytic trafficking: a marriage of convenience? *Trends Cell Biol*, 12, 173-7.
- KHOLODENKO, B. N. 2003. Four-dimensional organization of protein kinase signaling cascades: the roles of diffusion, endocytosis and molecular motors. *J Exp Biol*, 206, 2073-82.
- KHOLODENKO, B. N. 2009. Spatially distributed cell signalling. *FEBS Lett*, 583, 4006-12.
- KHOLODENKO, B. N. & BIRTWISTLE, M. R. 2009. Four-dimensional dynamics of MAPK information processing systems. *Wiley interdisciplinary reviews. Systems biology and medicine*, 1, 28-44.
- KHOLODENKO, B. N., BROWN, G. C. & HOEK, J. B. 2000. Diffusion control of protein phosphorylation in signal transduction pathways. *Biochem J*, 350 Pt 3, 901-7.
- KHOLODENKO, B. N., DEMIN, O. V., MOEHREN, G. & HOEK, J. B. 1999. Quantification of short term signaling by the epidermal growth factor receptor. *J Biol Chem*, 274, 30169-81.
- KHOLODENKO, B. N., KIYATKIN, A., BRUGGEMAN, F. J., SONTAG, E., WESTERHOFF, H. V. & HOEK, J. B. 2002. Untangling the wires: A strategy to trace functional interactions in signaling and gene networks. *Proceedings of the National Academy of Sciences of the United States of America*, 99, 12841-12846.
- KICHEVA, A., COHEN, M. & BRISCOE, J. 2012. Developmental pattern formation: insights from physics and biology. *Science*, 338, 210-2.
- KIEL, C. & SERRANO, L. 2012. Challenges ahead in signal transduction: MAPK as an example. *Curr Opin Biotechnol*, 23, 305-14.
- KIM, A. H., YANO, H., CHO, H., MEYER, D., MONKS, B., MARGOLIS, B., BIRNBAUM, M. J. & CHAO, M. V. 2002. Akt1 Regulates a JNK Scaffold during Excitotoxic Apoptosis. *Neuron*, 35, 697-709.
- KIM, B.-J., RYU, S.-W. & SONG, B.-J. 2006. JNK- and p38 Kinase-mediated Phosphorylation of Bax Leads to Its Activation and Mitochondrial Translocation and to Apoptosis of Human Hepatoma HepG2 Cells. *Journal of Biological Chemistry*, 281, 21256-21265.

- KIM, D., RATH, O., KOLCH, W. & CHO, K. H. 2007. A hidden oncogenic positive feedback loop caused by crosstalk between Wnt and ERK Pathways. *Oncogene*, 26, 4571-4579.
- KIM, S. Y. & FERRELL, J. E., JR. 2007. Substrate competition as a source of ultrasensitivity in the inactivation of Wee1. *Cell*, 128, 1133-45.
- KINS, S., KUROSIKI, P., NITSCH, R. M. & GOTZ, J. 2003. Activation of the ERK and JNK signaling pathways caused by neuron-specific inhibition of PP2A in transgenic mice. *Am J Pathol*, 163, 833-43.
- KISS-TOTH, E., BAGSTAFF, S. M., SUNG, H. Y., JOZSA, V., DEMPSEY, C., CAUNT, J. C., OXLEY, K. M., WYLLIE, D. H., POLGAR, T., HARTE, M., O'NEILL, L. A. J., QWARNSTROM, E. E. & DOWER, S. K. 2004. Human Tribbles, a Protein Family Controlling Mitogen-activated Protein Kinase Cascades. *Journal of Biological Chemistry*, 279, 42703-42708.
- KISS-TOTH, E., WYLLIE, D. H., HOLLAND, K., MARSDEN, L., JOZSA, V., OXLEY, K. M., POLGAR, T., QWARNSTROM, E. E. & DOWER, S. K. 2006. Functional mapping and identification of novel regulators for the Toll/Interleukin-1 signalling network by transcription expression cloning. *Cellular Signalling*, 18, 202-214.
- KITAMBI, SATISH S., TOLEDO, ENRIQUE M., USOSKIN, D., WEE, S., HARISANKAR, A., SVENSSON, R., SIGMUNDSSON, K., KALDERÉN, C., NIKLASSON, M., KUNDU, S., ARANDA, S., WESTERMARK, B., UHRBOM, L., ANDÄNG, M., DAMBERG, P., NELANDER, S., ARENAS, E., ARTURSSON, P., WALFRIDSSON, J., FORSBERG NILSSON, K., HAMMARSTRÖM, LARS G. J. & ERNFORS, P. 2014. Vulnerability of Glioblastoma Cells to Catastrophic Vacuolization and Death Induced by a Small Molecule. *Cell*, 157, 313-328.
- KITANO, H. 2002a. Computational systems biology. *Nature*, 420, 206-210.
- KITANO, H. 2002b. Looking beyond the details: a rise in system-oriented approaches in genetics and molecular biology. *Curr Genet*, 41, 1-10.
- KITANO, H. 2002c. Systems biology: a brief overview. *Science*, 295, 1662-4.
- KLAMT, S., SAEZ-RODRIGUEZ, J., LINDQUIST, J. A., SIMEONI, L. & GILLES, E. D. 2006. A methodology for the structural and functional analysis of signaling and regulatory networks. *BMC Bioinformatics*, 7, 56.
- KLANN, M. T., LAPIN, A. & REUSS, M. 2011. Agent-based simulation of reactions in the crowded and structured intracellular environment: Influence of mobility and location of the reactants. *BMC Syst Biol*, 5, 71.
- KLEIMAN, L. B., MAIWALD, T., CONZELMANN, H., LAUFFENBURGER, D. A. & SORGER, P. K. 2011. Rapid Phospho-Turnover by Receptor Tyrosine Kinases Impacts Downstream Signaling and Drug Binding. *Molecular cell*, 43, 723-737.
- KOCIENIEWSKI, P., FAEDER, J. R. & LIPNIACKI, T. 2012. The interplay of double phosphorylation and scaffolding in MAPK pathways. *Journal of Theoretical Biology*, 295, 116-124.
- KOCKEL, L., ZEITLINGER, J., STASZEWSKI, L. M., MLODZIK, M. & BOHMANN, D. 1997. Jun in Drosophila development: redundant and nonredundant functions and regulation by two MAPK signal transduction pathways. *Genes & Development*, 11, 1748-1758.
- KOLCH, W., CALDER, M. & GILBERT, D. 2005. When kinases meet mathematics: the systems biology of MAPK signalling. *FEBS Letters*, 579, 1891-1895.

- KONDOH, K. & NISHIDA, E. 2007. Regulation of MAP kinases by MAP kinase phosphatases. *Biochimica et Biophysica Acta (BBA) - Molecular Cell Research*, 1773, 1227-1237.
- KORNFELD, K., HOM, D. B. & HORVITZ, H. R. 1995. The ksr-1 gene encodes a novel protein kinase involved in Ras-mediated signaling in *C. elegans*. *Cell*, 83, 903-913.
- KRAMER, R. M., ROBERTS, E. F., UM, S. L., BÖRSCH-HAUBOLD, A. G., WATSON, S. P., FISHER, M. J. & JAKUBOWSKI, J. A. 1996. p38 mitogen-activated protein kinase phosphorylates cytosolic phospholipase A2 (cPLA2) in thrombin-stimulated platelets. Evidence that proline-directed phosphorylation is not required for mobilization of arachidonic acid by cPLA2. *Journal of Biological Chemistry*, 271, 27723-27729.
- KRAUSS, G. 2004. Front Matter. *Biochemistry of Signal Transduction and Regulation*. Wiley-VCH Verlag GmbH & Co. KGaA.
- KRIETE, A. 2013. Robustness and aging--a systems-level perspective. *Biosystems*, 112, 37-48.
- KUCAB, J. E., LEE, C., CHEN, C. S., ZHU, J., GILKS, C. B., CHEANG, M., HUNTSMAN, D., YORIDA, E., EMERMAN, J., POLLAK, M. & DUNN, S. E. 2005. Celecoxib analogues disrupt Akt signaling, which is commonly activated in primary breast tumours. *Breast Cancer Res*, 7, R796-807.
- KUCHARSKA, A., RUSHWORTH, L. K., STAPLES, C., MORRICE, N. A. & KEYSE, S. M. 2009. Regulation of the inducible nuclear dual-specificity phosphatase DUSP5 by ERK MAPK. *Cell Signal*, 21, 1794-805.
- KUMAR, A., TAKADA, Y., BORIEK, A. M. & AGGARWAL, B. B. 2004. Nuclear factor- κ B: Its role in health and disease. *Journal of Molecular Medicine*, 82, 434-448.
- KYRIAKIS, J. M., APP, H., ZHANG, X.-F., BANERJEE, P., BRAUTIGAN, D. L., RAPP, U. R. & AVRUCH, J. 1992. Raf-1 activates MAP kinase-kinase. *Nature*, 358, 417-421.
- KYRIAKIS, J. M. & AVRUCH, J. 1990. pp54 microtubule-associated protein 2 kinase. A novel serine/threonine protein kinase regulated by phosphorylation and stimulated by poly-L-lysine. *Journal of Biological Chemistry*, 265, 17355-17363.
- KYRIAKIS, J. M. & AVRUCH, J. 2001. Mammalian mitogen-activated protein kinase signal transduction pathways activated by stress and inflammation. *Physiol Rev*, 81, 807-69.
- L'ALLEMAIN, G., HER, J. H., WU, J., STURGILL, T. W. & WEBER, M. J. 1992. Growth factor-induced activation of a kinase activity which causes regulatory phosphorylation of p42/microtubule-associated protein kinase. *Molecular and Cellular Biology*, 12, 2222-2229.
- LANDRETH, G. E., SMITH, D. S., MCCABE, C. & GITTINGER, C. 1990. Characterization of a Nerve Growth Factor-Stimulated Protein Kinase in PC12 Cells Which Phosphorylates Microtubule-Associated Protein 2 and pp250. *Journal of neurochemistry*, 55, 514-523.
- LANGE-CARTER, C. A., PLEIMAN, C. M., GARDNER, A. M., BLUMER, K. J. & JOHNSON, G. L. 1993. A divergence in the MAP kinase regulatory network defined by MEK kinase and Raf. *Science*, 260, 315-319.
- LAWRENCE, M. C., JIVAN, A., SHAO, C., DUAN, L., GOAD, D., ZAGANJOR, E., OSBORNE, J., MCGLYNN, K., STIPPEC, S., EARNEST, S., CHEN, W. & COBB, M. H. 2008. The roles of MAPKs in disease. *Cell Res*, 18, 436-42.

- LE DREAU, G. & MARTI, E. 2012. Dorsal-ventral patterning of the neural tube: a tale of three signals. *Dev Neurobiol*, 72, 1471-81.
- LE GALL, M., CHAMBARD, J.-C., BREITTMAYER, J.-P., GRALL, D., POUYSSEGUR, J. & VAN OBERGHEN-SCHILLING, E. 2000a. The p42/p44 MAP Kinase Pathway Prevents Apoptosis Induced by Anchorage and Serum Removal. *Molecular Biology of the Cell*, 11, 1103-1112.
- LE GALL, M., CHAMBARD, J. C., BREITTMAYER, J. P., GRALL, D., POUYSSEGUR, J. & VAN OBERGHEN-SCHILLING, E. 2000b. The p42/p44 MAP kinase pathway prevents apoptosis induced by anchorage and serum removal. *Mol Biol Cell*, 11, 1103-12.
- LEE, C. M., ONÉSIME, D., REDDY, C. D., DHANASEKARAN, N. & REDDY, E. P. 2002. JLP: a scaffolding protein that tethers JNK/p38MAPK signaling modules and transcription factors. *Proceedings of the National Academy of Sciences*, 99, 14189-14194.
- LEE, M. H., LEE, S. E., KIM, D. W., RYU, M. J., KIM, S. J., KIM, S. J., KIM, Y. K., PARK, J. H., KWEON, G. R., KIM, J. M., LEE, J. U., DE FALCO, V., JO, Y. S. & SHONG, M. 2011. Mitochondrial localization and regulation of BRAFV600E in thyroid cancer: a clinically used RAF inhibitor is unable to block the mitochondrial activities of BRAFV600E. *J Clin Endocrinol Metab*, 96, E19-30.
- LEFKOWITZ, R. J. & SHENOY, S. K. 2005. Transduction of Receptor Signals by β -Arrestins. *Science*, 308, 512-517.
- LEGEWIE, S., SCHOEBERL, B., BLUTHGEN, N. & HERZEL, H. 2007. Competing docking interactions can bring about bistability in the MAPK cascade. *Biophys J*, 93, 2279-88.
- LEMMON, M. A. & SCHLESSINGER, J. 2010. Cell signaling by receptor tyrosine kinases. *Cell*, 141, 1117-1134.
- LENORMAND, P., SARDET, C., PAGES, G., L'ALLEMAIN, G., BRUNET, A. & POUYSSEGUR, J. 1993. Growth factors induce nuclear translocation of MAP kinases (p42mapk and p44mapk) but not of their activator MAP kinase kinase (p45mapkk) in fibroblasts. *J Cell Biol*, 122, 1079-88.
- LEVCHENKO, A., BRUCK, J. & STERNBERG, P. W. 2000. Scaffold proteins may biphasically affect the levels of mitogen-activated protein kinase signaling and reduce its threshold properties. *Proceedings of the National Academy of Sciences*, 97, 5818-5823.
- LEWIS, T. S., SHAPIRO, P. S. & AHN, N. G. 1998a. Signal transduction through MAP kinase cascades. *Adv Cancer Res*, 74, 49-139.
- LEWIS, T. S., SHAPIRO, P. S. & AHN, N. G. 1998b. Signal Transduction through MAP Kinase Cascades. In: GEORGE, F. V. W. & GEORGE, K. (eds.) *Advances in Cancer Research*. Academic Press.
- LEY, R., BALMANN, K., HADFIELD, K., WESTON, C. & COOK, S. J. 2003. Activation of the ERK1/2 signaling pathway promotes phosphorylation and proteasome-dependent degradation of the BH3-only protein, Bim. *Journal of Biological Chemistry*, 278, 18811-18816.
- LI, G. W. & XIE, X. S. 2011. Central dogma at the single-molecule level in living cells. *Nature*, 475, 308-15.
- LIAO, J. C., BOSCOLO, R., YANG, Y. L., TRAN, L. M., SABATTI, C. & ROYCHOWDHURY, V. P. 2003. Network component analysis: reconstruction of regulatory signals in biological systems. *Proc Natl Acad Sci U S A*, 100, 15522-7.

- LIM, H. J., CROWE, P. & YANG, J. L. 2015. Current clinical regulation of PI3K/PTEN/Akt/mTOR signalling in treatment of human cancer. *J Cancer Res Clin Oncol*, 141, 671-89.
- LIM, S., PNUELI, L., TAN, J. H., NAOR, Z., RAJAGOPAL, G. & MELAMED, P. 2009. Negative feedback governs gonadotrope frequency-decoding of gonadotropin releasing hormone pulse-frequency. *PLoS One*, 4, e7244.
- LIN, Y.-W., CHUANG, S.-M. & YANG, J.-L. 2003. ERK1/2 Achieves Sustained Activation by Stimulating MAPK Phosphatase-1 Degradation via the Ubiquitin-Proteasome Pathway. *Journal of Biological Chemistry*, 278, 21534-21541.
- LIN, Y.-W. & YANG, J.-L. 2006. Cooperation of ERK and SCFSkp2 for MKP-1 Destruction Provides a Positive Feedback Regulation of Proliferating Signaling. *Journal of Biological Chemistry*, 281, 915-926.
- LINGWOOD, D. & SIMONS, K. 2010. Lipid Rafts As a Membrane-Organizing Principle. *Science*, 327, 46-50.
- LIU, Z. & GEISBRECHT, E. R. 2011. Moleskin is essential for the formation of the myotendinous junction in *Drosophila*. *Developmental Biology*, 359, 176-189.
- LOCASALE, J. W., SHAW, A. S. & CHAKRABORTY, A. K. 2007a. Scaffold proteins confer diverse regulatory properties to protein kinase cascades. *Proceedings of the National Academy of Sciences*, 104, 13307-13312.
- LOCASALE, J. W., SHAW, A. S. & CHAKRABORTY, A. K. 2007b. Scaffold proteins confer diverse regulatory properties to protein kinase cascades. *Proc Natl Acad Sci U S A*, 104, 13307-12.
- LOGAN, D. C. 2009. Known knowns, known unknowns, unknown unknowns and the propagation of scientific enquiry. *Journal of Experimental Botany*, 60, 712-714.
- LORENTE, M., CARRACEDO, A., TORRES, S., NATALI, F., EGIA, A., HERNANDEZ-TIEDRA, S., SALAZAR, M., BLAZQUEZ, C., GUZMAN, M. & VELASCO, G. 2009. Amphiregulin is a factor for resistance of glioma cells to cannabinoid-induced apoptosis. *Glia*, 57, 1374-85.
- LORENZEN, J. A., BAKER, S. E., DENHEZ, F., MELNICK, M. B., BROWER, D. L. & PERKINS, L. A. 2001. Nuclear import of activated D-ERK by DIM-7, an importin family member encoded by the gene moleskin. *Development*, 128, 1403-1414.
- LOUVI, A. & ARTAVANIS-TSAKONAS, S. 2006. Notch signalling in vertebrate neural development. *Nat Rev Neurosci*, 7, 93-102.
- LOWENSTEIN, E., DALY, R., BATZER, A., LI, W., MARGOLIS, B., LAMMERS, R., ULLRICH, A., SKOLNIK, E., BAR-SAGI, D. & SCHLESSINGER, J. 1992. The SH2 and SH3 domain-containing protein GRB2 links receptor tyrosine kinases to ras signaling. *Cell*, 70, 431-442.
- LUBY-PHELPS, K. 2000. Cytoarchitecture and physical properties of cytoplasm: volume, viscosity, diffusion, intracellular surface area. *Int Rev Cytol*, 192, 189-221.
- LUTTRELL, L. M., ROUDABUSH, F. L., CHOY, E. W., MILLER, W. E., FIELD, M. E., PIERCE, K. L. & LEFKOWITZ, R. J. 2001. Activation and targeting of extracellular signal-regulated kinases by beta-arrestin scaffolds. *Proc Natl Acad Sci U S A*, 98, 2449-54.
- MACARIO, A. J. L. & CONWAY DE MACARIO, E. 2000. Stress and molecular chaperones in disease. *International Journal of Clinical and Laboratory Research*, 30, 49-66.

- MACIA, J., REGOT, S., PEETERS, T., CONDE, N., SOLÉ, R. & POSAS, F. 2009. Dynamic Signaling in the Hog1 MAPK Pathway Relies on High Basal Signal Transduction. *Science Signaling*, 2, ra13-ra13.
- MALLAVARAPU, A., THOMSON, M., ULLIAN, B. & GUNAWARDENA, J. 2009. Programming with models: modularity and abstraction provide powerful capabilities for systems biology. *J R Soc Interface*, 6, 257-70.
- MANDL, M., SLACK, D. N. & KEYSE, S. M. 2005. Specific Inactivation and Nuclear Anchoring of Extracellular Signal-Regulated Kinase 2 by the Inducible Dual-Specificity Protein Phosphatase DUSP5. *Molecular and Cellular Biology*, 25, 1830-1845.
- MARCHETTI, S., GIMOND, C., CHAMBARD, J. C., TOUBOUL, T., ROUX, D., POUYSSEUR, J. & PAGES, G. 2005. Extracellular signal-regulated kinases phosphorylate mitogen-activated protein kinase phosphatase 3/DUSP6 at serines 159 and 197, two sites critical for its proteasomal degradation. *Mol Cell Biol*, 25, 854-64.
- MARGOLIN, A. A., NEMENMAN, I., BASSO, K., WIGGINS, C., STOLOVITZKY, G., DALLA FAVERA, R. & CALIFANO, A. 2006. ARACNE: an algorithm for the reconstruction of gene regulatory networks in a mammalian cellular context. *BMC Bioinformatics*, 7 Suppl 1, S7.
- MARGOLIS, B. & SKOLNIK, E. Y. 1994. Activation of Ras by receptor tyrosine kinases. *Journal of the American Society of Nephrology*, 5, 1288-99.
- MARKEVICH, N. I., HOEK, J. B. & KHOLODENKO, B. N. 2004. Signaling switches and bistability arising from multisite phosphorylation in protein kinase cascades. *J Cell Biol*, 164, 353-9.
- MARKEVICH, N. I., TSYGANOV, M. A., HOEK, J. B. & KHOLODENKO, B. N. 2006. Long-range signaling by phosphoprotein waves arising from bistability in protein kinase cascades. *Molecular Systems Biology*, 2, 61-61.
- MARSHALL, C. J. 1995. Specificity of receptor tyrosine kinase signaling: Transient versus sustained extracellular signal-regulated kinase activation. *Cell*, 80, 179-185.
- MASUDA, K., SHIMA, H., WATANABE, M. & KIKUCHI, K. 2001. MKP-7, a novel mitogen-activated protein kinase phosphatase, functions as a shuttle protein. *J Biol Chem*, 276, 39002-11.
- MATSUDA, S., GOTOH, Y. & NISHIDA, E. 1993. Phosphorylation of Xenopus mitogen-activated protein (MAP) kinase kinase by MAP kinase kinase kinase and MAP kinase. *Journal of Biological Chemistry*, 268, 3277-3281.
- MATSUDA, S., KOSAKO, H., TAKENAKA, K., MORIYAMA, K., SAKAI, H., AKIYAMA, T., GOTOH, Y. & NISHIDA, E. 1992. Xenopus MAP kinase activator: identification and function as a key intermediate in the phosphorylation cascade. *The EMBO journal*, 11, 973.
- MATSUSHITA, T., CHAN, Y. Y., KAWANAMI, A., BALMES, G., LANDRETH, G. E. & MURAKAMI, S. 2009. Extracellular signal-regulated kinase 1 (ERK1) and ERK2 play essential roles in osteoblast differentiation and in supporting osteoclastogenesis. *Mol Cell Biol*, 29, 5843-57.
- MATTILA, E., PELLINEN, T., NEVO, J., VUORILUOTO, K., ARJONEN, A. & IVASKA, J. 2005. Negative regulation of EGFR signalling through integrin- α 1 β 1-mediated activation of protein tyrosine phosphatase TCPTP. *Nat Cell Biol*, 7, 78-85.
- MAYER, B. J., BLINOV, M. L. & LOEW, L. M. 2009. Molecular machines or pleiomorphic ensembles: signaling complexes revisited. *J Biol*, 8, 81.

- MAYFORD, M., SIEGELBAUM, S. A. & KANDEL, E. R. 2012. Synapses and memory storage. *Cold Spring Harb Perspect Biol*, 4.
- MCALLISTER, S. D., CHAN, C., TAFT, R. J., LUU, T., ABOOD, M. E., MOORE, D. H., ALDAPE, K. & YOUNT, G. 2005. Cannabinoids selectively inhibit proliferation and induce death of cultured human glioblastoma multiforme cells. *J Neurooncol*, 74, 31-40.
- MCCUBREY, J. A., STEELMAN, L. S., CHAPPELL, W. H., ABRAMS, S. L., WONG, E. W. T., CHANG, F., LEHMANN, B., TERRIAN, D. M., MILELLA, M., TAFURI, A., STIVALA, F., LIBRA, M., BASECKE, J., EVANGELISTI, C., MARTELLI, A. M. & FRANKLIN, R. A. 2007. Roles of the Raf/MEK/ERK pathway in cell growth, malignant transformation and drug resistance. *Biochimica et Biophysica Acta (BBA) - Molecular Cell Research*, 1773, 1263-1284.
- MCDOUGALL, S. R., ANDERSON, A. R. & CHAPLAIN, M. A. 2006. Mathematical modelling of dynamic adaptive tumour-induced angiogenesis: clinical implications and therapeutic targeting strategies. *J Theor Biol*, 241, 564-89.
- MCLAUGHLIN, M. M., KUMAR, S., MCDONNELL, P. C., VAN HORN, S., LEE, J. C., LIVI, G. P. & YOUNG, P. R. 1996. Identification of mitogen-activated protein (MAP) kinase-activated protein kinase-3, a novel substrate of CSBP p38 MAP kinase. *Journal of Biological Chemistry*, 271, 8488-8492.
- MEBRATU, Y. & TESFAIGZI, Y. 2009. How ERK1/2 Activation Controls Cell Proliferation and Cell Death Is Subcellular Localization the Answer? *Cell cycle (Georgetown, Tex.)*, 8, 1168-1175.
- MEDEMA, R. H. & BOS, J. L. 1993. The role of p21ras in receptor tyrosine kinase signaling. *Critical reviews in oncogenesis*, 4, 615-615.
- MERTENS, S., CRAXTON, M. & GOEDERT, M. 1996. SAP kinase-3, a new member of the family of mammalian stress-activated protein kinases. *FEBS Letters*, 383, 273-276.
- MITSIADES, C. S., MITSIADES, N. & KOUTSILIERIS, M. 2004. The Akt pathway: molecular targets for anti-cancer drug development. *Curr Cancer Drug Targets*, 4, 235-56.
- MIYAMOTO, E. 2006. Molecular mechanism of neuronal plasticity: induction and maintenance of long-term potentiation in the hippocampus. *J Pharmacol Sci*, 100, 433-42.
- MONICK, M. M., POWERS, L. S., GROSS, T. J., FLAHERTY, D. M., BARRETT, C. W. & HUNNINGHAKE, G. W. 2006. Active ERK Contributes to Protein Translation by Preventing JNK-Dependent Inhibition of Protein Phosphatase 1. *The Journal of Immunology*, 177, 1636-1645.
- MOODIE, S. A., WILLUMSEN, B. M., WEBER, M. J. & WOLFMAN, A. 1993. Complexes of Ras. GTP with Raf-1 and mitogen-activated protein kinase kinase. *Science*, 260, 1658-1661.
- MORI, T., FLÖTTMANN, M., KRANTZ, M., AKUTSU, T. & KLIPP, E. 2015. Stochastic simulation of Boolean rxncon models: towards quantitative analysis of large signaling networks. *BMC Systems Biology*, 9, 45.
- MOSTERT, J. W. 1974. The Science of Life: The Living System—a System for Living by Paul A. Weiss (review). *Perspectives in Biology and Medicine*, 17, 592-593.
- MUGLER, A., BAILEY, A. G., TAKAHASHI, K. & TEN WOLDE, P. R. 2012. Membrane clustering and the role of rebinding in biochemical signaling. *Biophys J*, 102, 1069-78.

- MUKHOPADHYAY, N. K., PRICE, D. J., KYRIAKIS, J. M., PELECH, S., SANGHERA, J. & AVRUCH, J. 1992. An array of insulin-activated, proline-directed serine/threonine protein kinases phosphorylate the p70 S6 kinase. *Journal of Biological Chemistry*, 267, 3325-3335.
- MÜLLER, J., ORY, S., COPELAND, T., PIWNICA-WORMS, H. & MORRISON, D. K. 2001. C-TAK1 Regulates Ras Signaling by Phosphorylating the MAPK Scaffold, KSR1. *Molecular cell*, 8, 983-993.
- MUNOZ-GARCIA, J., NEUFELD, Z. & KHOLODENKO, B. N. 2009. Positional information generated by spatially distributed signaling cascades. *PLoS Comput Biol*, 5, e1000330.
- MURAKOSHI, H., IINO, R., KOBAYASHI, T., FUJIWARA, T., OHSHIMA, C., YOSHIMURA, A. & KUSUMI, A. 2004. Single-molecule imaging analysis of Ras activation in living cells. *Proc Natl Acad Sci U S A*, 101, 7317-22.
- MURPHY, L. O., MACKEIGAN, J. P. & BLENIS, J. 2004. A network of immediate early gene products propagates subtle differences in mitogen-activated protein kinase signal amplitude and duration. *Mol Cell Biol*, 24, 144-53.
- MURPHY, L. O., SMITH, S., CHEN, R. H., FINGAR, D. C. & BLENIS, J. 2002. Molecular interpretation of ERK signal duration by immediate early gene products. *Nat Cell Biol*, 4, 556-64.
- MURRAY, J. D. 2002. *Mathematical Biology I: An Introduction*, vol. 17 of *Interdisciplinary Applied Mathematics*. Springer, New York, NY, USA.
- NAKA, T., HATAKEYAMA, M., SAKAMOTO, N. & KONAGAYA, A. 2006. Compensation effect of the MAPK cascade on formation of phospho-protein gradients. *Biosystems*, 83, 167-77.
- NAKAKUKI, T., BIRTWISTLE, M. R., SAEKI, Y., YUMOTO, N., IDE, K., NAGASHIMA, T., BRUSCH, L., OGUNNAIKE, B. A., OKADA-HATAKEYAMA, M. & KHOLODENKO, B. N. 2010. Ligand-specific c-Fos expression emerges from the spatiotemporal control of ErbB network dynamics. *Cell*, 141, 884-896.
- NAKAYAMA, K., SATOH, T., IGARI, A., KAGEYAMA, R. & NISHIDA, E. 2008. FGF induces oscillations of Hes1 expression and Ras/ERK activation. *Current Biology*, 18, R332-R334.
- NATALE, D. R., PALIGA, A. J. M., BEIER, F., D'SOUZA, S. J. A. & WATSON, A. J. 2004. p38 MAPK signaling during murine preimplantation development. *Developmental Biology*, 268, 76-88.
- NEVES, S. R. & IYENGAR, R. 2009. Models of spatially restricted biochemical reaction systems. *J Biol Chem*, 284, 5445-9.
- NEWMAN, R. H., ZHANG, J. & ZHU, H. 2014. Toward a systems-level view of dynamic phosphorylation networks. *Frontiers in Genetics*, 5, 263.
- NGUYEN, A., BURACK, W. R., STOCK, J. L., KORTUM, R., CHAIKA, O. V., AFKARIAN, M., MULLER, W. J., MURPHY, K. M., MORRISON, D. K., LEWIS, R. E., MCNEISH, J. & SHAW, A. S. 2002. Kinase Suppressor of Ras (KSR) Is a Scaffold Which Facilitates Mitogen-Activated Protein Kinase Activation In Vivo. *Molecular and Cellular Biology*, 22, 3035-3045.
- NICOLAU, D. V., JR., BURRAGE, K., PARTON, R. G. & HANCOCK, J. F. 2006. Identifying optimal lipid raft characteristics required to promote nanoscale protein-protein interactions on the plasma membrane. *Mol Cell Biol*, 26, 313-23.
- NICOLSON, G. L. 2014. The Fluid—Mosaic Model of Membrane Structure: Still relevant to understanding the structure, function and dynamics of biological

- membranes after more than 40 years. *Biochimica et Biophysica Acta (BBA) - Biomembranes*, 1838, 1451-1466.
- NIHALANI, D., MEYER, D., PAJNI, S. & HOLZMAN, L. B. 2001. Mixed lineage kinase-dependent JNK activation is governed by interactions of scaffold protein JIP with MAPK module components. *EMBO J*, 20, 3447-3458.
- NIHALANI, D., WONG, H. N. & HOLZMAN, L. B. 2003. Recruitment of JNK to JIP1 and JNK-dependent JIP1 Phosphorylation Regulates JNK Module Dynamics and Activation. *Journal of Biological Chemistry*, 278, 28694-28702.
- NIKOLAI, C. & MADEY, G. 2009. Tools of the trade: A survey of various agent based modeling platforms. *Journal of Artificial Societies and Social Simulation*, 12, 2.
- NIWA, Y., MASAMIZU, Y., LIU, T., NAKAYAMA, R., DENG, C. X. & KAGEYAMA, R. 2007. The initiation and propagation of Hes7 oscillation are cooperatively regulated by Fgf and notch signaling in the somite segmentation clock. *Dev Cell*, 13, 298-304.
- NIWA, Y., SHIMOJO, H., ISOMURA, A., GONZALEZ, A., MIYACHI, H. & KAGEYAMA, R. 2011. Different types of oscillations in Notch and Fgf signaling regulate the spatiotemporal periodicity of somitogenesis. *Genes Dev*, 25, 1115-20.
- NOBLE, D. 2008. Claude Bernard, the first systems biologist, and the future of physiology. *Experimental Physiology*, 93, 16-26.
- NOVAK, B. & TYSON, J. J. 2008. Design principles of biochemical oscillators. *Nat Rev Mol Cell Biol*, 9, 981-91.
- NURSE, P. 2008. Life, logic and information. *Nature*, 454, 424-6.
- OBITSU, S., SAKATA, K., TESHIMA, R. & KONDO, K. 2013. Eleostearic acid induces RIP1-mediated atypical apoptosis in a kinase-independent manner via ERK phosphorylation, ROS generation and mitochondrial dysfunction. *Cell Death & Disease*, 4, e674.
- ODA, K., MATSUOKA, Y., FUNAHASHI, A. & KITANO, H. 2005. A comprehensive pathway map of epidermal growth factor receptor signaling. *Molecular Systems Biology*, 1.
- OLSEN, J. V., BLAGOEV, B., GNAD, F., MACEK, B., KUMAR, C., MORTENSEN, P. & MANN, M. 2006. Global, in vivo, and site-specific phosphorylation dynamics in signaling networks. *Cell*, 127, 635-48.
- ÖRD, D. & ÖRD, T. 2005. Characterization of human NIPK (TRB3, SKIP3) gene activation in stressful conditions. *Biochemical and Biophysical Research Communications*, 330, 210-218.
- ORTEGA, F., GARCES, J. L., MAS, F., KHOLODENKO, B. N. & CASCANTE, M. 2006. Bistability from double phosphorylation in signal transduction. Kinetic and structural requirements. *FEBS J*, 273, 3915-26.
- ORTON, R. J., ADRIAENS, M. E., GORMAND, A., STURM, O. E., KOLCH, W. & GILBERT, D. R. 2009. Computational modelling of cancerous mutations in the EGFR/ERK signalling pathway. *BMC Systems Biology*, 3, 100-100.
- ORTON, R. J., STURM, O. E., VYSHEMIRSKY, V., CALDER, M., GILBERT, D. R. & KOLCH, W. 2005. Computational modelling of the receptor-tyrosine-kinase-activated MAPK pathway. *Biochem J*, 392, 249-61.
- OULDRIDGE, THOMAS E. & REIN TEN WOLDE, P. 2014. The Robustness of Proofreading to Crowding-Induced Pseudo-Processivity in the MAPK Pathway. *Biophysical Journal*, 107, 2425-2435.

- PALMEIRIM, I., HENRIQUE, D., ISH-HOROWICZ, D. & POURQUIE, O. 1997. Avian hairy gene expression identifies a molecular clock linked to vertebrate segmentation and somitogenesis. *Cell*, 91, 639-48.
- PAUMELLE, R., TULASNE, D., LEROY, C., COLL, J., VANDENBUNDER, B. & FAFEUR, V. 2000. Sequential Activation of ERK and Repression of JNK by Scatter Factor/Hepatocyte Growth Factor in Madin-Darby Canine Kidney Epithelial Cells. *Molecular Biology of the Cell*, 11, 3751-3763.
- PEDERSEN, M., PHILLIPS, A. & PLOTKIN, G. D. 2015. A high-level language for rule-based modelling. *PLoS One*, 10, e0114296.
- PERDIGUERO, E. & MUÑOZ-CÁNOVES, P. 2008. Transcriptional regulation by the p38 MAPK signaling pathway in mammalian cells. *In: POSAS, F. & NEBREDA, A. (eds.) Stress-Activated Protein Kinases*. Springer Berlin Heidelberg.
- PERKINS, J. R., DIBOUN, I., DESSAILLY, B. H., LEES, J. G. & ORENCO, C. 2010. Transient protein-protein interactions: structural, functional, and network properties. *Structure*, 18, 1233-43.
- PERLSON, E., HANZ, S., BEN-YAAKOV, K., SEGAL-RUDER, Y., SEGER, R. & FAINZILBER, M. 2005. Vimentin-dependent spatial translocation of an activated MAP kinase in injured nerve. *Neuron*, 45, 715-26.
- PERTWEE, R. G. 2008. The diverse CB1 and CB2 receptor pharmacology of three plant cannabinoids: delta9-tetrahydrocannabinol, cannabidiol and delta9-tetrahydrocannabivarin. *Br J Pharmacol*, 153, 199-215.
- PIERRAT, B., DA SILVA CORREIA, J., MARY, J. L., TOMÁS-ZUBER, M. & LESSLAUER, W. 1998. RSK-B, a novel ribosomal S6 kinase family member, is a CREB kinase under dominant control of p38 α mitogen-activated protein kinase (p38 α (MAPK)). *Journal of Biological Chemistry*, 273, 29661-29671.
- PLOTNIKOV, A., ZEHORAI, E., PROCACCIA, S. & SEGER, R. 2011. The MAPK cascades: Signaling components, nuclear roles and mechanisms of nuclear translocation. *Biochimica et Biophysica Acta (BBA) - Molecular Cell Research*, 1813, 1619-1633.
- PLOWMAN, S. J., ARIOTTI, N., GOODALL, A., PARTON, R. G. & HANCOCK, J. F. 2008. Electrostatic interactions positively regulate K-Ras nanocluster formation and function. *Mol Cell Biol*, 28, 4377-85.
- POGSON, M., HOLCOMBE, M., SMALLWOOD, R. & QWARNSTROM, E. 2008. Introducing Spatial Information into Predictive NF- κ B Modelling – An Agent-Based Approach. *PLoS ONE*, 3, e2367.
- POGSON, M., SMALLWOOD, R., QWARNSTROM, E. & HOLCOMBE, M. 2006. Formal agent-based modelling of intracellular chemical interactions. *Biosystems*, 85, 37-45.
- POMBO, C. M., BONVENTRE, J. V., AVRUCH, J., WOODGETT, J. R., KYRIAKIS, J. M. & FORCE, T. 1994. The stress-activated protein kinases are major c-Jun amino-terminal kinases activated by ischemia and reperfusion. *Journal of Biological Chemistry*, 269, 26546-26551.
- PREET, A., GANJU, R. K. & GROOPMAN, J. E. 2008. Delta9-Tetrahydrocannabinol inhibits epithelial growth factor-induced lung cancer cell migration in vitro as well as its growth and metastasis in vivo. *Oncogene*, 27, 339-46.
- PULVERER, B. J., KYRIAKIS, J. M., AVRUCH, J., NIKOLAKAKI, E. & WOODGETT, J. R. 1991. Phosphorylation of c-jun mediated by MAP kinases. *Nature*, 353, 670-674.

- PYRONNET, S., IMATAKA, H., GINGRAS, A. C., FUKUNAGA, R., HUNTER, T. & SONENBERG, N. 1999. Human eukaryotic translation initiation factor 4G (eIF4G) recruits mnk1 to phosphorylate eIF4E. *The EMBO journal*, 18, 270-279.
- QIAO, L., NACHBAR, R. B., KEVREKIDIS, I. G. & SHVARTSMAN, S. Y. 2007. Bistability and oscillations in the Huang-Ferrell model of MAPK signaling. *PLoS Comput Biol*, 3, 1819-26.
- RAFF, M., ALBERTS, B., LEWIS, J., JOHNSON, A. & ROBERTS, K. 2002. *Molecular Biology of the Cell* 4th edition.
- RAMER, R. & HINZ, B. 2008. Inhibition of Cancer Cell Invasion by Cannabinoids via Increased Expression of Tissue Inhibitor of Matrix Metalloproteinases-1. *Journal of the National Cancer Institute*, 100, 59-69.
- RANG, H. P. 2006. The receptor concept: pharmacology's big idea. *British Journal of Pharmacology*, 147, S9-S16.
- REGEV, A., PANINA, E. M., SILVERMAN, W., CARDELLI, L. & SHAPIRO, E. 2004. BioAmbients: an abstraction for biological compartments. *Theoretical Computer Science*, 325, 141-167.
- RESAT, H., COSTA, M. N. & SHANKARAN, H. 2011. Spatial aspects in biological system simulations. *Methods Enzymol*, 487, 485-511.
- RHINN, M. & DOLLÉ, P. 2012. Retinoic acid signalling during development. *Development*, 139, 843-858.
- RHODES, D. M., HOLCOMBE, M. & QWARNSTROM, E. E. 2016. Reducing complexity in an agent based reaction model-Benefits and limitations of simplifications in relation to run time and system level output. *Biosystems*, 147, 21-7.
- ROBINSON, E. J. H., JACKSON, D. E., HOLCOMBE, M. & RATNIEKS, F. L. W. 2005. Insect communication: 'No entry' signal in ant foraging. *Nature*, 438, 442-442.
- ROBINSON, E. J. H., RATNIEKS, F. L. W. & HOLCOMBE, M. 2008. An agent-based model to investigate the roles of attractive and repellent pheromones in ant decision making during foraging. *Journal of Theoretical Biology*, 255, 250-258.
- ROMANO, D., NGUYEN, L. K., MATAILLANAS, D., HALASZ, M., DOHERTY, C., KHOLODENKO, B. N. & KOLCH, W. 2014. Protein interaction switches coordinate Raf-1 and MST2/Hippo signalling. *Nat Cell Biol*, 16, 673-684.
- ROUSSEAU, S., HOULE, F., LANDRY, J. & HUOT, J. 1997. P38 MAP kinase activation by vascular endothelial growth factor mediates actin reorganization and cell migration in human endothelial cells. *Oncogene*, 15, 2169-2177.
- ROUX, B. 2011. *Molecular machines*, World Scientific.
- ROWLAND, E. A., MÜLLER, T. H., GOLDSTEIN, M. & GREENE, L. A. 1987. Cell-free detection and characterization of a novel nerve growth factor-activated protein kinase in PC12 cells. *Journal of Biological Chemistry*, 262, 7504-7513.
- ROY, M., LI, Z. & SACKS, D. B. 2005. IQGAP1 Is a Scaffold for Mitogen-Activated Protein Kinase Signaling. *Molecular and Cellular Biology*, 25, 7940-7952.
- ROZAKIS-ADCOCK, M., MCGLADE, J., MBAMALU, G., PELICCI, G., DALY, R., LI, W., BATZER, A., THOMAS, S., BRUGGE, J. & PELICCI, P. 1992. Association of the Shc and Grb2/Sem5 SH2-containing proteins is implicated in activation of the Ras pathway by tyrosine kinases. *Nature*, 360, 689-692.
- RUBINFELD, H. & SEGER, R. 2005. The ERK cascade. *Molecular biotechnology*, 31, 151-174.

- RUNCHEL, C., MATSUZAWA, A. & ICHIJO, H. 2010. Mitogen-Activated Protein Kinases in Mammalian Oxidative Stress Responses. *Antioxidants & Redox Signaling*, 15, 205-218.
- RUTHS, D., MULLER, M., TSENG, J.-T., NAKHLEH, L. & RAM, P. T. 2008. The Signaling Petri Net-Based Simulator: A Non-Parametric Strategy for Characterizing the Dynamics of Cell-Specific Signaling Networks. *PLoS Comput Biol*, 4, e1000005.
- SABBAGH, W., JR., FLATAUER, L. J., BARDWELL, A. J. & BARDWELL, L. 2001. Specificity of MAP kinase signaling in yeast differentiation involves transient versus sustained MAPK activation. *Mol Cell*, 8, 683-91.
- SACKMANN, A., HEINER, M. & KOCH, I. 2006. Application of Petri net based analysis techniques to signal transduction pathways. *BMC Bioinformatics*, 7, 482-482.
- SADEH, M. J., MOFFA, G. & SPANG, R. 2013. Considering Unknown Unknowns: Reconstruction of Nonconfoundable Causal Relations in Biological Networks. *Journal of Computational Biology*, 20, 920-932.
- SAKS, V., MONGE, C. & GUZUN, R. 2009. Philosophical basis and some historical aspects of systems biology: from Hegel to Noble - applications for bioenergetic research. *Int J Mol Sci*, 10, 1161-92.
- SALAZAR, M., CARRACEDO, A., SALANUEVA, I. J., HERNANDEZ-TIEDRA, S., LORENTE, M., EGIA, A., VAZQUEZ, P., BLAZQUEZ, C., TORRES, S., GARCIA, S., NOWAK, J., FIMIA, G. M., PIACENTINI, M., CECCONI, F., PANDOLFI, P. P., GONZALEZ-FERIA, L., IOVANNA, J. L., GUZMAN, M., BOYA, P. & VELASCO, G. 2009. Cannabinoid action induces autophagy-mediated cell death through stimulation of ER stress in human glioma cells. *J Clin Invest*, 119, 1359-72.
- SALAZAR, M., LORENTE, M., GARCIA-TABOADA, E., HERNANDEZ-TIEDRA, S., DAVILA, D., FRANCIS, S. E., GUZMAN, M., KISS-TOTH, E. & VELASCO, G. 2013. The pseudokinase tribbles homologue-3 plays a crucial role in cannabinoid anticancer action. *Biochim Biophys Acta*, 1831, 1573-8.
- SAMAGA, R., SAEZ-RODRIGUEZ, J., ALEXOPOULOS, L. G., SORGER, P. K. & KLAMT, S. 2009. The Logic of EGFR/ErbB Signaling: Theoretical Properties and Analysis of High-Throughput Data. *PLoS Comput Biol*, 5, e1000438.
- SANCHEZ, C., GALVE-ROPERH, I., CANOVA, C., BRACHET, P. & GUZMAN, M. 1998. Delta9-tetrahydrocannabinol induces apoptosis in C6 glioma cells. *FEBS Lett*, 436, 6-10.
- SANCHEZ, I., HUGHES, R. T., MAYER, B. J., YEE, K., WOODGETT, J. R., AVRUCH, J., KYRIAKLS, J. M. & ZON, L. I. 1994. Role of SAPK/ERK kinase-1 in the stress-activated pathway regulating transcription factor c-Jun. *Nature*, 372, 794-798.
- SANCHEZ, M. G., RUIZ-LLORENTE, L., SANCHEZ, A. M. & DIAZ-LAVIADA, I. 2003. Activation of phosphoinositide 3-kinase/PKB pathway by CB(1) and CB(2) cannabinoid receptors expressed in prostate PC-3 cells. Involvement in Raf-1 stimulation and NGF induction. *Cell Signal*, 15, 851-9.
- SANGHERA, J., PETER, M., NIGG, E. & PELECH, S. 1992. Immunological characterization of avian MAP kinases: evidence for nuclear localization. *Molecular biology of the cell*, 3, 775-787.
- SANTOS, S. D., VERVEER, P. J. & BASTIAENS, P. I. 2007a. Growth factor-induced MAPK network topology shapes Erk response determining PC-12 cell fate. *Nature cell biology*, 9, 324-330.

- SANTOS, S. D., VERVEER, P. J. & BASTIAENS, P. I. 2007b. Growth factor-induced MAPK network topology shapes Erk response determining PC-12 cell fate. *Nat Cell Biol*, 9, 324-30.
- SANTOS, S. D. M., VERVEER, P. J. & BASTIAENS, P. I. H. 2007c. Growth factor-induced MAPK network topology shapes Erk response determining PC-12 cell fate. *Nat Cell Biol*, 9, 324-330.
- SARMA, U. & GHOSH, I. 2012. Oscillations in MAPK cascade triggered by two distinct designs of coupled positive and negative feedback loops. *BMC Res Notes*, 5, 287.
- SASAGAWA, S., OZAKI, Y.-I., FUJITA, K. & KURODA, S. 2005a. Prediction and validation of the distinct dynamics of transient and sustained ERK activation. *Nat Cell Biol*, 7, 365-373.
- SASAGAWA, S., OZAKI, Y., FUJITA, K. & KURODA, S. 2005b. Prediction and validation of the distinct dynamics of transient and sustained ERK activation. *Nat Cell Biol*, 7, 365-73.
- SCHAEFFER, H. J., CATLING, A. D., EBLEN, S. T., COLLIER, L. S., KRAUSS, A. & WEBER, M. J. 1998. MP1: A MEK Binding Partner That Enhances Enzymatic Activation of the MAP Kinase Cascade. *Science*, 281, 1668-1671.
- SCHEPER, G. C., MORRICE, N. A., KLEIJN, M. & PROUD, C. G. 2001. The Mitogen-Activated Protein Kinase Signal-Integrating Kinase Mnk2 Is a Eukaryotic Initiation Factor 4E Kinase with High Levels of Basal Activity in Mammalian Cells. *Molecular and Cellular Biology*, 21, 743-754.
- SCHOEBERL, B., EICHLER-JONSSON, C., GILLES, E. D. AND MULLER, G. 2002. Computational modeling of the dynamics of the MAP kinase cascade activated by surface and internalized EGF receptors. *Nat. Biotechnol*, 20, 370-375.
- SCHRICK, C., FISCHER, A., SRIVASTAVA, D. P., TRONSON, N. C., PENZES, P. & RADULOVIC, J. 2007. N-Cadherin Regulates Cytoskeletally Associated IQGAP1/ERK Signaling and Memory Formation. *Neuron*, 55, 786-798.
- SCHROETER, H., BOYD, C. S., AHMED, R., SPENCER, J. P. E., DUNCAN, R. F., RICE-EVANS, C. & CADENAS, E. 2003. c-Jun N-terminal kinase (JNK)-mediated modulation of brain mitochondria function: new target proteins for JNK signalling in mitochondrion-dependent apoptosis. *Biochemical Journal*, 372, 359-369.
- SCHULZE, A., NICKE, B., WARNE, P. H., TOMLINSON, S. & DOWNWARD, J. 2004. The Transcriptional Response to Raf Activation Is Almost Completely Dependent on Mitogen-activated Protein Kinase Kinase Activity and Shows a Major Autocrine Component. *Molecular Biology of the Cell*, 15, 3450-3463.
- SCOTT, A. 2004. Reductionism revisited. *Journal of Consciousness Studies*, 11, 51-68.
- SCOTT, J. D. & PAWSON, T. 2009. Cell Signaling in Space and Time: Where Proteins Come Together and When They're Apart. *Science*, 326, 1220-1224.
- SEGER, R. & KREBS, E. G. 1995. The MAPK signaling cascade. *FASEB J*, 9, 726-35.
- SEGER, R., SEGER, D., RESZKA, A. A., MUNAR, E. S., ELDAR-FINKELMAN, H., DOBROWOLSKA, G., JENSEN, A. M., CAMPBELL, J. S., FISCHER, E. H. & KREBS, E. G. 1994. Overexpression of mitogen-activated protein kinase kinase (MAPKK) and its mutants in NIH 3T3 cells. Evidence that MAPKK involvement in cellular proliferation is regulated by phosphorylation of serine

- residues in its kinase subdomains VII and VIII. *Journal of Biological Chemistry*, 269, 25699-709.
- SETH, A., GONZALEZ, F. A., GUPTA, S., RADEN, D. L. & DAVIS, R. J. 1992. Signal transduction within the nucleus by mitogen-activated protein kinase. *Journal of Biological Chemistry*, 267, 24796-24804.
- SETTEMBRE, C., FRALDI, A., MEDINA, D. L. & BALLABIO, A. 2013. Signals from the lysosome: a control centre for cellular clearance and energy metabolism. *Nat Rev Mol Cell Biol*, 14, 283-296.
- SEWING, A., WISEMAN, B., LLOYD, A. C. & LAND, H. 1997. High-intensity Raf signal causes cell cycle arrest mediated by p21Cip1. *Mol Cell Biol*, 17, 5588-97.
- SHALOM-FEUERSTEIN, R., PLOWMAN, S. J., ROTBLAT, B., ARIOTTI, N., TIAN, T., HANCOCK, J. F. & KLOOG, Y. 2008. K-ras nanoclustering is subverted by overexpression of the scaffold protein galectin-3. *Cancer Res*, 68, 6608-16.
- SHANKARAN, H., CHRISLER, W. B., SONTAG, R. L. & WEBER, T. J. 2011. Inhibition of ERK oscillations by ionizing radiation and reactive oxygen species. *Mol Carcinog*, 50, 424-32.
- SHANKARAN, H., IPPOLITO, D. L., CHRISLER, W. B., RESAT, H., BOLLINGER, N., OPRESKO, L. K. & WILEY, H. S. 2009. Rapid and sustained nuclear-cytoplasmic ERK oscillations induced by epidermal growth factor. *Mol Syst Biol*, 5, 332.
- SHAW, D. E., GROSSMAN, J., BANK, J. A., BATSON, B., BUTTS, J. A., CHAO, J. C., DENEROFF, M. M., DROR, R. O., EVEN, A. & FENTON, C. H. Anton 2: raising the bar for performance and programmability in a special-purpose molecular dynamics supercomputer. Proceedings of the International Conference for High Performance Computing, Networking, Storage and Analysis, 2014. IEEE Press, 41-53.
- SHENOY, S. K., DRAKE, M. T., NELSON, C. D., HOUTZ, D. A., XIAO, K., MADABUSHI, S., REITER, E., PREMONT, R. T., LICHTARGE, O. & LEFKOWITZ, R. J. 2006. beta-arrestin-dependent, G protein-independent ERK1/2 activation by the beta2 adrenergic receptor. *J Biol Chem*, 281, 1261-73.
- SHILO, B.-Z. 2005. Regulating the dynamics of EGF receptor signaling in space and time. *Development*, 132, 4017-4027.
- SHIN, S.-Y., RATH, O., CHOO, S.-M., FEE, F., MCFERRAN, B., KOLCH, W. & CHO, K.-H. 2009a. Positive- and negative-feedback regulations coordinate the dynamic behavior of the Ras-Raf-MEK-ERK signal transduction pathway. *Journal of Cell Science*, 122, 425-435.
- SHIN, S. H., PARK, S. Y. & KANG, G. H. 2013. Down-regulation of dual-specificity phosphatase 5 in gastric cancer by promoter CpG island hypermethylation and its potential role in carcinogenesis. *Am J Pathol*, 182, 1275-85.
- SHIN, S. Y., RATH, O., CHOO, S. M., FEE, F., MCFERRAN, B., KOLCH, W. & CHO, K. H. 2009b. Positive- and negative-feedback regulations coordinate the dynamic behavior of the Ras-Raf-MEK-ERK signal transduction pathway. *J Cell Sci*, 122, 425-35.
- SHUAIB, A., HARTWELL, A., KISS-TOTH, E. & HOLCOMBE, M. 2016. Multi-Compartmentalisation in the MAPK Signalling Pathway Contributes to the Emergence of Oscillatory Behaviour and to Ultrasensitivity. *PLoS One*, 11, e0156139.

- SHVARTSMAN, S. Y., COPPEY, M. & BEREZHKOVSII, A. M. 2009. MAPK signaling in equations and embryos. *Fly (Austin)*, 3, 62-7.
- SIKOSEK, T. & CHAN, H. S. 2014. Biophysics of protein evolution and evolutionary protein biophysics. *J R Soc Interface*, 11, 20140419.
- SILVERSTEIN, A. M., BARROW, C. A., DAVIS, A. J. & MUMBY, M. C. 2002. Actions of PP2A on the MAP kinase pathway and apoptosis are mediated by distinct regulatory subunits. *Proc Natl Acad Sci U S A*, 99, 4221-6.
- SINGH, A., NASCIMENTO, J. M., KOWAR, S., BUSCH, H. & BOERRIES, M. 2012. Boolean approach to signalling pathway modelling in HGF-induced keratinocyte migration. *Bioinformatics*, 28, i495-i501.
- SLUSS, H. K., BARRETT, T., DÉRIJARD, B. & DAVIS, R. J. 1994. Signal transduction by tumor necrosis factor mediated by JNK protein kinases. *Molecular and Cellular Biology*, 14, 8376-8384.
- SMITH, E. R., SMEDBERG, J. L., RULA, M. E. & XU, X. X. 2004. Regulation of Ras-MAPK pathway mitogenic activity by restricting nuclear entry of activated MAPK in endoderm differentiation of embryonic carcinoma and stem cells. *J Cell Biol*, 164, 689-99.
- SOKOL, S. Y. 2011. Maintaining embryonic stem cell pluripotency with Wnt signaling. *Development*, 138, 4341-4350.
- SONENBERG, N. & GINGRAS, A.-C. 1998. The mRNA 5' cap-binding protein eIF4E and control of cell growth. *Current opinion in cell biology*, 10, 268-275.
- SONTAG, E., FEDOROV, S., KAMIBAYASHI, C., ROBBINS, D., COBB, M. & MUMBY, M. 1993. The interaction of SV40 small tumor antigen with protein phosphatase 2A stimulates the map kinase pathway and induces cell proliferation. *Cell*, 75, 887-97.
- SOUFI, A. & JAYARAMAN, P. S. 2008. PRH/Hex: an oligomeric transcription factor and multifunctional regulator of cell fate. *Biochem J*, 412, 399-413.
- SPIEGEL, K., LEPROULT, R., COLECCHIA, E. F., L'HERMITE-BALÉRIAUX, M., NIE, Z., COPINSCHI, G. & VAN CAUTER, E. 2000. Adaptation of the 24-h growth hormone profile to a state of sleep debt. *American Journal of Physiology - Regulatory, Integrative and Comparative Physiology*, 279, R874-R883.
- STEFAN, M. I., BARTOL, T. M., SEJNOWSKI, T. J. & KENNEDY, M. B. 2014. Multi-state modeling of biomolecules. *PLoS Comput Biol*, 10, e1003844.
- STEIN, B., YANG, M. X., YOUNG, D. B., JANKNECHT, R., HUNTER, T., MURRAY, B. W. & BARBOSA, M. S. 1997. p38-2, a novel mitogen-activated protein kinase with distinct properties. *Journal of Biological Chemistry*, 272, 19509-19517.
- STELLING, J., SAUER, U., SZALLASI, Z., DOYLE, F. J., 3RD & DOYLE, J. 2004. Robustness of cellular functions. *Cell*, 118, 675-85.
- STENT, G. S. 1968. That was the molecular biology that was. *Science*, 160, 390-5.
- STEWART, T. A., YAPA, K. T. & MONTEITH, G. R. 2015. Altered calcium signaling in cancer cells. *Biochim Biophys Acta*, 1848, 2502-11.
- STOKOE, D., CAMPBELL, D., NAKIELNY, S., HIDAKA, H., LEEVERS, S., MARSHALL, C. & COHEN, P. 1992. MAPKAP kinase-2; a novel protein kinase activated by mitogen-activated protein kinase. *The EMBO journal*, 11, 3985.
- STURM, O. E., ORTON, R., GRINDLAY, J., BIRTWISTLE, M., VYSHEMIRSKY, V., GILBERT, D., CALDER, M., PITT, A., KHOLODENKO, B. & KOLCH, W.

- 2010a. The Mammalian MAPK/ERK Pathway Exhibits Properties of a Negative Feedback Amplifier. *Science Signaling*, 3, ra90-ra90.
- STURM, O. E., ORTON, R., GRINDLAY, J., BIRTWISTLE, M., VYSHEMIRSKY, V., GILBERT, D., CALDER, M., PITT, A., KHOLODENKO, B. & KOLCH, W. 2010b. The mammalian MAPK/ERK pathway exhibits properties of a negative feedback amplifier. *Sci Signal*, 3, ra90.
- SUDERMAN, R. & DEEDS, E. J. 2013. Machines vs. Ensembles: Effective MAPK Signaling through Heterogeneous Sets of Protein Complexes. *PLoS Computational Biology*, 9, e1003278.
- SUGIMOTO, T., STEWART, S., HAN, M. & GUAN, K.-L. 1998. The kinase suppressor of Ras (KSR) modulates growth factor and Ras signaling by uncoupling Elk-1 phosphorylation from MAP kinase activation. *EMBO J*, 17, 1717-1727.
- SUN, P., WATANABE, H., TAKANO, K., YOKOYAMA, T., FUJISAWA, J.-I. & ENDO, T. 2006. Sustained activation of M-Ras induced by nerve growth factor is essential for neuronal differentiation of PC12 cells. *Genes to Cells*, 11, 1097-1113.
- SUN, T., MCMINN, P., HOLCOMBE, M., SMALLWOOD, R. & MACNEIL, S. 2008. Agent Based Modelling Helps in Understanding the Rules by Which Fibroblasts Support Keratinocyte Colony Formation. *PLoS ONE*, 3, e2129.
- SUNDARAM, M. & HAN, M. 1995. The *C. elegans* ksr-1 gene encodes a novel raf-related kinase involved in Ras-mediated signal transduction. *Cell*, 83, 889-901.
- SUNG, H. Y., FRANCIS, S. E., CROSSMAN, D. C. & KISS-TOTH, E. 2006. Regulation of expression and signalling modulator function of mammalian tribbles is cell-type specific. *Immunology Letters*, 104, 171-177.
- SUNG, H. Y., GUAN, H., CZIBULA, A., KING, A. R., EDER, K., HEATH, E., SUVARNA, S. K., DOWER, S. K., WILSON, A. G., FRANCIS, S. E., CROSSMAN, D. C. & KISS-TOTH, E. 2007. Human Tribbles-1 Controls Proliferation and Chemotaxis of Smooth Muscle Cells via MAPK Signaling Pathways. *Journal of Biological Chemistry*, 282, 18379-18387.
- TAKAHASHI, K., NAKAJIMA, E. & SUZUKI, K. 2006. Involvement of protein phosphatase 2A in the maintenance of E-cadherin-mediated cell-cell adhesion through recruitment of IQGAP1. *Journal of Cellular Physiology*, 206, 814-820.
- TAKAMORI, S., HOLT, M., STENIUS, K., LEMKE, E. A., GRONBORG, M., RIEDEL, D., URLAUB, H., SCHENCK, S., BRUGGER, B., RINGLER, P., MULLER, S. A., RAMMNER, B., GRATER, F., HUB, J. S., DE GROOT, B. L., MIESKES, G., MORIYAMA, Y., KLINGAUF, J., GRUBMULLER, H., HEUSER, J., WIELAND, F. & JAHN, R. 2006. Molecular anatomy of a trafficking organelle. *Cell*, 127, 831-46.
- TAKEKAWA, M., MAEDA, T. & SAITO, H. 1998. Protein phosphatase 2 α inhibits the human stress-responsive p38 and JNK MAPK pathways. *EMBO J*, 17, 4744-52.
- TANIGUCHI, C. M., EMANUELLI, B. & KAHN, C. R. 2006. Critical nodes in signalling pathways: insights into insulin action. *Nat Rev Mol Cell Biol*, 7, 85-96.
- TEIS, D., TAUB, N., KURZBAUER, R., HILBER, D., DE ARAUJO, M. E., ERLACHER, M., OFFTERDINGER, M., VILLUNGER, A., GELEY, S., BOHN, G., KLEIN, C., HESS, M. W. & HUBER, L. A. 2006. p14-MP1-MEK1 signaling

- regulates endosomal traffic and cellular proliferation during tissue homeostasis. *The Journal of Cell Biology*, 175, 861-868.
- TEIS, D., WUNDERLICH, W. & HUBER, L. A. 2002. Localization of the MP1-MAPK Scaffold Complex to Endosomes Is Mediated by p14 and Required for Signal Transduction. *Developmental cell*, 3, 803-814.
- TENAZINHA, N. & VINGA, S. 2011. A survey on methods for modeling and analyzing integrated biological networks. *IEEE/ACM Trans Comput Biol Bioinform*, 8, 943-58.
- THALHAUSER, C. J. & KOMAROVA, N. L. 2010. Signal Response Sensitivity in the Yeast Mitogen-Activated Protein Kinase Cascade. *PLoS ONE*, 5, e11568.
- THERRIEN, M., MICHAUD, N. R., RUBIN, G. M. & MORRISON, D. K. 1996. KSR modulates signal propagation within the MAPK cascade. *Genes & Development*, 10, 2684-2695.
- TIAN, T. & HARDING, A. 2014. How MAP kinase modules function as robust, yet adaptable, circuits. *Cell Cycle*, 13, 2379-2390.
- TIAN, T., HARDING, A., INDER, K., PLOWMAN, S., PARTON, R. G. & HANCOCK, J. F. 2007. Plasma membrane nanoswitches generate high-fidelity Ras signal transduction. *Nat Cell Biol*, 9, 905-14.
- TIAN, X. J., ZHANG, X. P., LIU, F. & WANG, W. 2009. Interlinking positive and negative feedback loops creates a tunable motif in gene regulatory networks. *Phys Rev E Stat Nonlin Soft Matter Phys*, 80, 011926.
- TOMBES, R. M., AUER, K. L., MIKKELSEN, R., VALERIE, K., WYMAN, M. P., MARSHALL, C. J., MCMAHON, M. & DENT, P. 1998. The mitogen-activated protein (MAP) kinase cascade can either stimulate or inhibit DNA synthesis in primary cultures of rat hepatocytes depending upon whether its activation is acute/phasic or chronic. *Biochem J*, 330 (Pt 3), 1451-60.
- TOMIDA, T. 2015. Visualization of the spatial and temporal dynamics of MAPK signaling using fluorescence imaging techniques. *The Journal of Physiological Sciences*, 65, 37-49.
- TOMIDA, T., ODA, S., TAKEKAWA, M., IINO, Y. & SAITO, H. 2012. The temporal pattern of stimulation determines the extent and duration of MAPK activation in a *Caenorhabditis elegans* sensory neuron. *Sci Signal*, 5, ra76.
- TOMIDA, T., TAKEKAWA, M. & SAITO, H. 2015. Oscillation of p38 activity controls efficient pro-inflammatory gene expression. *Nat Commun*, 6, 8350.
- TORII, S., KUSAKABE, M., YAMAMOTO, T., MAEKAWA, M. & NISHIDA, E. 2004. Sef Is a Spatial Regulator for Ras/MAP Kinase Signaling. *Developmental Cell*, 7, 33-44.
- TOURNIER, C., HESS, P., YANG, D. D., XU, J., TURNER, T. K., NIMNUAL, A., BAR-SAGI, D., JONES, S. N., FLAVELL, R. A. & DAVIS, R. J. 2000. Requirement of JNK for Stress- Induced Activation of the Cytochrome c-Mediated Death Pathway. *Science*, 288, 870-874.
- TOURNIER, C., THOMAS, G., PIERRE, J., JACQUEMIN, C., PIERRE, M. & SAUNIER, B. 1997. Mediation by arachidonic acid metabolites of the H₂O₂-induced stimulation of mitogen-activated protein kinases (extracellular-signal-regulated kinase and c-Jun NH₂-terminal kinase). *European Journal of Biochemistry*, 244, 587-595.
- TOURNIER, C., WHITMARSH, A. J., CAVANAGH, J., BARRETT, T. & DAVIS, R. J. 1999. The MKK7 Gene Encodes a Group of c-Jun NH₂-Terminal Kinase Kinases. *Molecular and Cellular Biology*, 19, 1569-1581.

- TRAVERSE, S., GOMEZ, N., PATERSON, H., MARSHALL, C. & COHEN, P. 1992. Sustained activation of the mitogen-activated protein (MAP) kinase cascade may be required for differentiation of PC12 cells. Comparison of the effects of nerve growth factor and epidermal growth factor. *Biochemical Journal*, 288, 351-355.
- TSAI, T. Y., CHOI, Y. S., MA, W., POMERENING, J. R., TANG, C. & FERRELL, J. E., JR. 2008. Robust, tunable biological oscillations from interlinked positive and negative feedback loops. *Science*, 321, 126-9.
- TURING, A. M. 1952. The chemical basis of morphogenesis. *Philosophical Transactions of the Royal Society of London B: Biological Sciences*, 237, 37-72.
- UHLÉN, P. & FRITZ, N. 2010. Biochemistry of calcium oscillations. *Biochemical and Biophysical Research Communications*, 396, 28-32.
- UHLIK, M. T., ABELL, A. N., CUEVAS, B. D., NAKAMURA, K. & JOHNSON, G. L. 2004. Wiring diagrams of MAPK regulation by MEKK1, 2, and 3. *Biochemistry and Cell Biology*, 82, 658-663.
- UHLIK, M. T., ABELL, A. N., JOHNSON, N. L., SUN, W., CUEVAS, B. D., LOBEL-RICE, K. E., HORNE, E. A., DELL'ACQUA, M. L. & JOHNSON, G. L. 2003. Rac-MEKK3-MKK3 scaffolding for p38 MAPK activation during hyperosmotic shock. *Nature cell biology*, 5, 1104-1110.
- UINGS, I. J. & FARROW, S. N. 2000. Cell receptors and cell signalling. *Mol Pathol*, 53, 295-9.
- ULLAH, G., JUNG, P. & MACHACA, K. 2007. Modeling Ca²⁺ signaling differentiation during oocyte maturation. *Cell calcium*, 42, 556-564.
- VAN AELST, L., BARR, M., MARCUS, S., POLVERINO, A. & WIGLER, M. 1993. Complex formation between RAS and RAF and other protein kinases. *Proceedings of the National Academy of Sciences*, 90, 6213-6217.
- VAN ALBADA, S. B. & TEN WOLDE, P. R. 2007. Enzyme localization can drastically affect signal amplification in signal transduction pathways. *PLoS Comput Biol*, 3, 1925-34.
- VAN AMERONGEN, R. & NUSSE, R. 2009. Towards an integrated view of Wnt signaling in development. *Development*, 136, 3205-3214.
- VARA, D., SALAZAR, M., OLEA-HERRERO, N., GUZMAN, M., VELASCO, G. & DIAZ-LAVIADA, I. 2011. Anti-tumoral action of cannabinoids on hepatocellular carcinoma: role of AMPK-dependent activation of autophagy. *Cell Death Differ*, 18, 1099-111.
- VEZZI, V., ONARAN, H. O., MOLINARI, P., GUERRINI, R., BALBONI, G., CALO, G. & COSTA, T. 2013. Ligands raise the constraint that limits constitutive activation in G protein-coupled opioid receptors. *J Biol Chem*, 288, 23964-78.
- VOELZMANN, A., OKENVE-RAMOS, P., QU, Y., CHOJNOWSKA-MONGA, M., DEL CAÑO-ESPINEL, M., PROKOP, A. & SANCHEZ-SORIANO, N. 2016. Tau and spectraplakins promote synapse formation and maintenance through Jun kinase and neuronal trafficking. *eLife*, 5, e14694.
- VOJTEK, A. B., HOLLENBERG, S. M. & COOPER, J. A. 1993. Mammalian Ras interacts directly with the serine/threonine kinase raf. *Cell*, 74, 205-214.
- VOLMAT, V., CAMPS, M., ARKINSTALL, S., POUYSSEGUR, J. & LENORMAND, P. 2001. The nucleus, a site for signal termination by sequestration and inactivation of p42/p44 MAP kinases. *J Cell Sci*, 114, 3433-43.
- VON BERTALANFFY, L. 1950. The theory of open systems in physics and biology. *Science*, 111, 23-29.

- VON BERTALANFFY, L. & RAPOPORT, A. 1963. *General systems*, JSTOR.
- VON KRIEGSHEIM, A., BAIOCCHI, D., BIRTWISTLE, M., SUMPTON, D., BIENVENUT, W., MORRICE, N., YAMADA, K., LAMOND, A., KALNA, G., ORTON, R., GILBERT, D. & KOLCH, W. 2009. Cell fate decisions are specified by the dynamic ERK interactome. *Nat Cell Biol*, 11, 1458-1464.
- WANG, X., HAO, N., DOHLMAN, H. G. & ELSTON, T. C. 2006. Bistability, stochasticity, and oscillations in the mitogen-activated protein kinase cascade. *Biophys J*, 90, 1961-78.
- WASKIEWICZ, A. J., FLYNN, A., PROUD, C. G. & COOPER, J. A. 1997. Mitogen-activated protein kinases activate the serine/threonine kinases Mnk1 and Mnk2. *EMBO Journal*, 16, 1909-1920.
- WEBER, T. J., SHANKARAN, H., WILEY, H. S., OPRESKO, L. K., CHRISLER, W. B. & QUESENBERRY, R. D. 2010. Basic fibroblast growth factor regulates persistent ERK oscillations in premalignant but not malignant JB6 cells. *J Invest Dermatol*, 130, 1444-56.
- WEI, H., AHN, S., SHENOY, S. K., KARNIK, S. S., HUNYADY, L., LUTTRELL, L. M. & LEFKOWITZ, R. J. 2003. Independent beta-arrestin 2 and G protein-mediated pathways for angiotensin II activation of extracellular signal-regulated kinases 1 and 2. *Proc Natl Acad Sci U S A*, 100, 10782-7.
- WEI, S. C., ROSENBERG, I. M., CAO, Z., HUETT, A. S., XAVIER, R. J. & PODOLSKY, D. K. 2012. Tribbles 2 (Trib2) is a novel regulator of toll-like receptor 5 signaling. *Inflamm Bowel Dis*, 18, 877-88.
- WESTERMARCK, J., LI, S.-P., KALLUNKI, T., HAN, J. & KÄHÄRI, V.-M. 2001. p38 Mitogen-Activated Protein Kinase-Dependent Activation of Protein Phosphatases 1 and 2A Inhibits MEK1 and MEK2 Activity and Collagenase 1 (MMP-1) Gene Expression. *Molecular and Cellular Biology*, 21, 2373-2383.
- WESTON, C. R., BALMANN, K., CHALMERS, C., HADFIELD, K., MOLTON, S. A., LEY, R., WAGNER, E. F. & COOK, S. J. 2003. Activation of ERK1//2 by [Delta]Raf-1[thinsp]:[thinsp]ER[ast] represses Bim expression independently of the JNK or PI3K pathways. *Oncogene*, 22, 1281-1293.
- WHITMARSH, A. J., CAVANAGH, J., TOURNIER, C., YASUDA, J. & DAVIS, R. J. 1998. A Mammalian Scaffold Complex That Selectively Mediates MAP Kinase Activation. *Science*, 281, 1671-1674.
- WHITMARSH, A. J., SHORE, P., SHARROCKS, A. D. & DAVIS, R. J. 1995. Integration of MAP kinase signal transduction pathways at the serum response element. *Science*, 269, 403-407.
- WINKLES, J. A. 1998. Serum- and polypeptide growth factor-inducible gene expression in mouse fibroblasts. *Prog Nucleic Acid Res Mol Biol*, 58, 41-78.
- WOLPERT, L. 1969. Positional information and the spatial pattern of cellular differentiation. *J Theor Biol*, 25, 1-47.
- WONG, M. L., KAYE, A. H. & HOVENS, C. M. 2007. Targeting malignant glioma survival signalling to improve clinical outcomes. *J Clin Neurosci*, 14, 301-8.
- WOODS, D., PARRY, D., CHERWINSKI, H., BOSCH, E., LEES, E. & MCMAHON, M. 1997. Raf-induced proliferation or cell cycle arrest is determined by the level of Raf activity with arrest mediated by p21Cip1. *Mol Cell Biol*, 17, 5598-611.
- WOOLDRIDGE, M. & JENNINGS, N. R. 1995. Intelligent agents: Theory and practice. *Knowledge engineering review*, 10, 115-152.
- WUNDERLICH, W., FIALKA, I., TEIS, D., ALPI, A., PFEIFER, A., PARTON, R. G., LOTTSPREICH, F. & HUBER, L. A. 2001. A Novel 14-Kilodalton Protein

- Interacts with the Mitogen-Activated Protein Kinase Scaffold Mp1 on a Late Endosomal/Lysosomal Compartment. *The Journal of Cell Biology*, 152, 765-776.
- XIA, Z., DICKENS, M., RAINGEAUD, J., DAVIS, R. J. & GREENBERG, M. E. 1995. Opposing Effects of ERK and JNK-p38 MAP Kinases on Apoptosis. *Science*, 270, 1326-1331.
- XING, H., KORNFELD, K. & MUSLIN, A. J. 1997. The protein kinase KSR interacts with 14-3-3 protein and Raf. *Current Biology*, 7, 294-300.
- XING, J., GINTY, D. D. & GREENBERG, M. E. 1996. Coupling of the RAS-MAPK pathway to gene activation by RSK2, a growth factor-regulated CREB kinase. *Science*, 273, 959-963.
- XIONG, W. & FERRELL, J. E., JR. 2003. A positive-feedback-based bistable 'memory module' that governs a cell fate decision. *Nature*, 426, 460-5.
- XU, L.-G., LI, L.-Y. & SHU, H.-B. 2004. TRAF7 Potentiates MEKK3-induced AP1 and CHOP Activation and Induces Apoptosis. *Journal of Biological Chemistry*, 279, 17278-17282.
- YAN, M. & TEMPLETON, D. J. 1994. Identification of 2 serine residues of MEK-1 that are differentially phosphorylated during activation by raf and MEK kinase. *Journal of Biological Chemistry*, 269, 19067-19073.
- YANG, D. D., KUAN, C.-Y., WHITMARSH, A. J., RINOCN, M., ZHENG, T. S., DAVIS, R. J., RAKIC, P. & FLAVELL, R. A. 1997a. Absence of excitotoxicity-induced apoptosis in the hippocampus of mice lacking the Jnk3 gene. *Nature*, 389, 865-870.
- YANG, D. D., KUAN, C.-Y., WHITMARSH, A. J., RINÓCN, M., ZHENG, T. S., DAVIS, R. J., RAKIC, P. & FLAVELL, R. A. 1997b. Absence of excitotoxicity-induced apoptosis in the hippocampus of mice lacking the Jnk3 gene. *Nature*, 389, 865-870.
- YAO, Z., DIENER, K., WANG, X. S., ZUKOWSKI, M., MATSUMOTO, G., ZHOU, G., MO, R., SASAKI, T., NISHINA, H., HUI, C. C., TAN, T.-H., WOODGETT, J. P. & PENNINGER, J. M. 1997. Activation of Stress-activated Protein Kinases/c-Jun N-terminal Protein Kinases (SAPKs/JNKs) by a Novel Mitogen-activated Protein Kinase Kinase (MKK7). *Journal of Biological Chemistry*, 272, 32378-32383.
- YARDEN, Y. & SCHLESSINGER, J. 1987. Self-phosphorylation of epidermal growth factor receptor: evidence for a model of intermolecular allosteric activation. *Biochemistry*, 26, 1434-1442.
- YOUNGSON, R. M. 2006. *Collins dictionary of human biology*, Collins.
- YU, W., FANTL, W. J., HARROWE, G. & WILLIAMS, L. T. 1998. Regulation of the MAP kinase pathway by mammalian Ksr through direct interaction with MEK and ERK. *Current Biology*, 8, 56-64.
- ZHAO, Q., WANG, X., NELIN, L. D., YAO, Y., MATTA, R., MANSON, M. E., BALIGA, R. S., MENG, X., SMITH, C. V., BAUER, J. A., CHANG, C. H. & LIU, Y. 2006. MAP kinase phosphatase 1 controls innate immune responses and suppresses endotoxic shock. *J Exp Med*, 203, 131-40.
- ZHAO, Q., YI, M. & LIU, Y. 2011. Spatial distribution and dose-response relationship for different operation modes in a reaction-diffusion model of the MAPK cascade. *Phys Biol*, 8, 055004.
- ZHENG, C. F. & GUAN, K. L. 1994. Activation of MEK family kinases requires phosphorylation of two conserved Ser/Thr residues. *EMBO Journal*, 13, 1123-1131.

Appendices

Appendix A.

a. Agents' descriptions:

Below are tables which summarise the description of agent' memory parameters, agent functions and agents' messages which are exported to the libmboard.

i. The multi-state models.

As aforementioned in section 3.5.1.4 (page 124), during the construction of the ABMs, an assessment between multi-agent and multi-state ABMs was conducted. The information related to the multi-state ABM is summarised below in table form.

1. Agent memory parameters

Here the parameters which constituted agent memory in the ABM and their attributes are illustrated and described in tabular form.

PROTEIN agent Memory		
Name	type	Description
<u>ID</u>	int	Identity tag for the agent
Postheta	double	Agent position in the spherical coordinate system (θ is the angle rotating about the y-axis, where y coordinates is expressed as the function $\text{Sin}\theta\text{Sin}\varphi$)
Posphi	double	Agent position in the spherical coordinate system (φ is the angle rotating about the Z-axis, where Z coordinate is expressed as the function $\text{Cos}\varphi$)
Posr	double	The position of the agent expressed in radians
Posx	double	The position of the agent on the X-axis
Posy	double	The position of the agent on the Y-axis
Posz	double	The position of the agent on the Z-axis
Movetheta	double	Movement angle in the spherical coordinate system (θ is the angle between z-axis and r)
Movephi	double	Movement angle in the spherical coordinate system (φ is the angle between x-axis and $r.\text{cos}\theta$)
Mover	double	The displacement of the agent in the spherical coordinate system ($\sim r$ or p)
State	int	Agent state (e.g. MKK, MK, pMK, etc)
RADP	int	The Re-Activation Delay Period defines the number of iterations and or time period a protein state lasts before it changes to or reverts back to another state
<u>Iradius</u>	double	Distance between two agents which allow them to interact
Disval	int	The rate at which molecules such as MKK breakdown to their essential components

Appendix A, Table 1 Summary descriptions of the memory parameters used for the protein-agent. Parameters written in bold font are updated after the end of each time-step and model run. Underlined parameters written in red font are not updated or modified throughout model runs.

RECEPTOR agent Memory		
Name	type	description
<u>Id</u>	int	ID for the agent
Posteta	double	Agent position in the spherical coordinate system (θ is the angle rotating about the y-axis, where y coordinate is expressed as the function $\text{Sin}\theta\text{Sin}\varphi$)
Posphi	double	Agent position in the spherical coordinate system (φ is the angle rotating about the Z-axis, where Z coordinates are expressed as the function $\text{Cos}\varphi$)
Posr	double	the position of the agent expressed in radians
Posx	double	the position of the agent on the X-axis
Posy	double	the position of the agent on the Y-axis
Posz	double	the position of the agent on the Z-axis
Movetheta	double	Movement angle in the spherical coordinate system (θ is the angle between z-axis and r)
Movephi	double	Movement angle in the spherical coordinate system (φ is the angle between x-axis and $r.\text{cos}\theta$)
Mover	double	The displacement of the agent in the spherical coordinate system ($\sim r$ or p)
State	int	Agent state (e.g. active and inactive ExR)
Recdelay	int	The delay with which the receptor can hold the bound pMK to it before it releases it to the cytoplasm
boundindex	int	The id of the agent that the receptor is bound to
<u>radius</u>	double	Distance between two agents which allow them to interact
Disval	int	The rate at which molecules such as MKK breakdown to their essential components

Appendix A, Table 2 Table outlining memory parameters for the receptor agent with descriptions of each parameter and its classification. Parameters written in bold font are updated after the end of each time-step and model run. Underlined parameters written in red font are not updated or modified throughout model runs. Agents' functions:

PROTEIN agent FUNCTIONS)		
Name	Protein_outputdata	
Description	Outputs location message	
Current state	0	
Next state	1	
<u>Inputs</u>		
Message name	Filter/Operation	From agent
n/a	n/a	n/a
<u>Outputs</u>		
Message name	To agent	
Location	All agents	
Name	Protein_move	
Description	Controls protein movement	
Current state	3	
Next state	4	
<u>Inputs</u>		
Message name	Filter/Operation	From agent
finalbond	n/a	All agents
<u>Outputs</u>		
Message name	To agent	
n/a	n/a	
FUNCTIONS (for PROTEIN agent)		
Name	Protein_inputdata	
Description	Read all messages from other agents	
Current state	1	
Next state	2	
<u>Inputs</u>		
Message name	Filter/Operation	From agent
startbond	n/a	Receptor agents
location	n/a	All agents
<u>Outputs</u>		
Message name	To agent	
newbond	All protein agents	
Name	Protein_checkbondtries	
Description	Check bond tries	
Current state	2	
Next state	3	
<u>Inputs</u>		
Message name	Filter/Operation	From agent
newbond	n/a	All agents
<u>Outputs</u>		
Message name	To agent	
finalbond	All agents	

Appendix A, Table 3 Outline and description of the transition functions used by the protein-agents needed for executing movement and specifying the three dimensional coordinates of the agent.

RECEPTOR agent FUNCTIONS		
Name	Receptor_outputdata	
Description	Output location message and check nuclear receptor timers	
Current state	0	
Next state	1	
Inputs		
Message name	Filter/Operation	From agent
n/a	n/a	n/a
Outputs		
Message name	To agent	
location	All agents	
startbond	All protein agents	
Name	Receptor_inputdata	
Description	Read all messages from other agents	
Current state	1	
Next state	2	
Inputs		
Message name	Filter/Operation	From agent
location	n/a	All agents
Outputs		
Message name	To agent	
newbond	All protein agents	
Name	Receptor_move	
Description	movement and check bond messages	
Current state	2	
Next state	3	
Inputs		
Message name	Filter/Operation	From agent
finalbond	n/a	All protein agents
Outputs		
Message name	To agent	
n/a	n/a	

Appendix A, Table 4 Table displaying the transition function of receptor-agent with description of their flow and messages inputted and outputted to them.

Agent messages:

MESSAGES		
Name	<u>Location</u>	
Description	Check location of agent	
Elements		
Name	Type	Description
Id	int	id of the agent
X	double	x coordinates
Y	double	y coordinates
Z	double	z coordinates
State	int	agent state
Range	double	the agent's message range
Name	<u>Startbond</u>	
Description	To make bonds	
Elements		
Name	Type	Description
idfrom	int	From agent id
statefrom	int	From agent state
idto	int	To agent id
bindunbind	int	Whether to bind or not
distance	double	Distance between agents
range	double	The agent's message range
x	double	x coordinates
y	double	y coordinates
z	double	z coordinates
Name	<u>Newbond</u>	
Description	To make bonds (after assessing which is the best bond to form)	
Elements		
Name	Type	Description
idfrom	int	From agent id
statefrom	int	From agent state
idto	int	To agent id
bindunbind	int	Whether to bind or not
distance	double	Distance between agents
range	double	The agent's message range
X	double	x coordinates
Y	double	y coordinates
Z	double	z coordinates
Name	<u>Finalbond</u>	
Description	To make bonds (the final bond formed)	
Elements		
Name	Type	Description
idfrom	int	From agent id
statefrom	int	From agent state
idto	int	To agent id
bindunbind	int	Whether to bind or not
distance	double	Distance between agents
range	double	The agent's message range
X	double	x coordinates
Y	double	y coordinates
Z	double	z coordinates

Appendix A, Table 5 Illustration of the message outputted by agents to finalise the binding interaction and bond formation.

b. The multi-agent ABM

i. Agent memory parameters

MAPKK		
Name	Type	Description
Id	int	ID for agent
Comptag	double	Tag to identify which compartment MAPKK resides in
Postheta	double	Agent position in the spherical coordinate system (θ is the angle rotating about the y-axis, where y coordinates is expressed as the function $\text{Sin}\theta\text{Sin}\varphi$)
Posphi	double	Agent position in the spherical coordinate system (φ is the angle rotating about the Z-axis, where Z coordinate is expressed as the function $\text{Cos}\varphi$)
Posr	double	the position of the agent expressed in radians
Posx	double	the position of the agent on the X-axis
Posy	double	the position of the agent on the Y-axis
Posz	double	the position of the agent on the Z-axis
movetheta	double	Movement angle in the spherical coordinate system (θ is the angle between z-axis and r)
movephi	double	Movement angle in the spherical coordinate system (φ is the angle between x-axis and $r.\text{cos}\theta$)
mover	double	The displacement of the agent in the spherical coordinate system ($-r$ or p)
State	int	MAPKK state (e.g. MAPKK or dMAPKK)
RADP	int	The re-activation delay periods which defines the time period which dMAPKK stays dormant before it reverts back to MAPKK
boundindex	int	Determines the bound state of MAPKK to MK
lradius	Double	which defines the number of iterations a protein state lasts before it changes to or reverts back to another state

Appendix A, Table 6 The parameters which constitute the memory of MAPKK (MAPKK) agents which are updated every time-step

MAPK		
Name	Type	Description
Id	int	ID for agent
comptag	double	Tag to identify which compartment MAPK resides in
postheta	double	Agent position in the spherical coordinate system (θ is the angle rotating about the y-axis, where y coordinates is expressed as the function $\text{Sin}\theta\text{Sin}\phi$)
posphi	double	Agent position in the spherical coordinate system (ϕ is the angle rotating about the Z-axis, where Z coordinate is expressed as the function $\text{Cos}\phi$)
Posr	double	the position of the agent expressed in radians
Posx	double	the position of the agent on the X-axis
Posy	double	the position of the agent on the Y-axis
Posz	double	the position of the agent on the Z-axis
movetheta	double	Movement angle in the spherical coordinate system (θ is the angle between z-axis and r)
movephi	double	Movement angle in the spherical coordinate system (ϕ is the angle between x-axis and $r.\text{cos}\theta$)
mover	double	The displacement of the agent in the spherical coordinate system ($\sim r$ or p)
State	int	MAPK state (e.g. MAPK or phosphor-MK)
iradius	double	which defines the number of iterations a protein state lasts before it changes to or reverts back to another state

Appendix A, Table 7 Shows the parameters which constitute the memory of MAPK (MK) agents which are updated every time-step

ExR		
Name	Type	Description
Id	int	ID for agent
postheta	double	Agent position in the spherical coordinate system (θ is the angle rotating about the y-axis, where y coordinates is expressed as the function $\text{Sin}\theta\text{Sin}\phi$)
posphi	double	Agent position in the spherical coordinate system (ϕ is the angle rotating about the Z-axis, where Z coordinate is expressed as the function $\text{Cos}\phi$)
Posr	double	the position of the agent expressed in radians
Posx	double	the position of the agent on the X-axis
Posy	double	the position of the agent on the Y-axis
Posz	double	the position of the agent on the Z-axis
movetheta	double	Movement angle in the spherical coordinate system (θ is the angle between z-axis and r)
movephi	double	Movement angle in the spherical coordinate system (ϕ is the angle between x-axis and $r.\text{cos}\theta$)
Mover	double	The displacement of the agent in the spherical coordinate system ($\sim r$ or p)
State	int	ExR state (e.g. ExR or dExR)
recdelay	int	The re-activation delay periods which defines the time period which ExR stays active before it changes to dExR and the time period dExR state exist before it it reverts back to ExR
boundindex	int	Determines the bound state of ExR to phospho-MK
Iradius	double	which defines the number of iterations a protein state lasts before it changes to or reverts back to another state

Appendix A, Table 8 Parameters constituting the memory of exporting receptor (ExR) agents which are updated every time-step

Agent functions

MAPKK FUNCTIONS		
Function Name		
MAPKK_outputdata		
Description		
Outputs location message		
Current state		
0		
Next state		
1		
<u>Inputs</u>		
n/a		
<u>Outputs</u>		
Message name		
To agent		
MAPKK Location		
MAPK agents		
Function Name		
MAPKK_inputdata		
Description		
Read all messages from other agents		
Current state		
1		
Next state		
2		
<u>Inputs</u>		
Message name		
Filter/Operation		
From agent		
MAPK location	n/a	MAPK agents
<u>Outputs</u>		
Message name		
To agent		
MAPKK newbond		
MAPK agents		
Function Name		
MAPKK_move		
Description		
Controls protein movement and checks binding status of MAPKK		
Current state		
2		
Next state		
3		
<u>Inputs</u>		
Message name		
Filter/Operation		
From agent		
MKfinalbond	n/a	MAPK agents
<u>Outputs</u>		
n/a		

Appendix A, Table 9 Summary of the transition functions used to control MAPKK generic protein behaviour or specialised MAPKK behaviour. MAPKK behaviours are controlled by three transition functions, namely MAPKK_outputdata, MAPKK_inputdata and MAPKK_move. MAPKK_outputdata and MAPKK_inputdata are agent specific functions while MAPKK_move is a system level transition function. Each of these agents is associated with either the reading/importing or exporting of messages to limboard. MAPKK_outputdata controls the calculation of re-activation delay period (RADP) timer, thus the transition from dormant state to active state. This function also outputs the location of the MAPKK agents as MAPKK_location. MAPKK_inputdata controls the reading of messages from MAPK agents to the closest binding partner and the possibility of interaction. This function outputs MAPKK_newbond message to signal to the MAPK agent in close proximity to its binding availability and is an "invitation" for interaction.

MAPK FUNCTIONS		
Function Name	MK_outputdata	
Description	Outputs location message	
Current state	0	
Next state	1	
<u>Inputs</u>		
n/a		
<u>Outputs</u>		
Message name	To agent	
MKLocation	MAPKK agents	
Function Name	MK_inputdata	
Description	Read all messages from other agents	
Current state	1	
Next state	2	
<u>Inputs</u>		
Message name	Filter/Operation	From agent
MAPKK location	n/a	MAPKK agents
ExRlocation	n/a	ExR agents
<u>Outputs</u>		
n/a		
Function Name	MK_checkbondtries	
Description	Check if there were any binding attempts between MAPK and MAPKK or ExR	
Current state	2	
Next state	3	
<u>Inputs</u>		
Message name	Filter/Operation	From agent
MAPKK newbond	n/a	MAPKK agents
ExRnewbond	n/a	ExR agents
<u>Outputs</u>		
Message name	To agent	
MAPK finalbond	All agents	
Function Name	MK_move	
Description	Controls protein movement and checks binding status of MAPKK	
Current state	3	
Next state	4	
<u>Inputs</u>		
n/a		
<u>Outputs</u>		
n/a		

Appendix A, Table 10 Summary of the transition functions used to control MAPK behaviour. . MAPK behaviours are controlled by three transition functions, namely MAPK_outputdata, MAPK_inputdata and MAPK_move. MAPK_outputdata and MAPK_inputdata are agent specific functions while MAPK_move is a system level transition function. Each of these agents is associated with either the reading/importing or exporting of messages to limboard. MAPK_outputdata outputs the location of MAPK as MAPK_location. MAPK_inputdata controls the reading of messages from MAPKK and ExR agents to the closest binding partner and the possibility of their interaction with MAPK. MK_checkbondtries assesses the interaction between MAPKK and its interaction partners and outputs its binding status and binding availability to other agents. MK_move controls MK movement and assesses the bond status with MAPKK

ExR FUNCTIONS		
Function Name	ExR_outputdata	
Description	Output location message and check nuclear receptor timers	
Current state	0	
Next state	1	
Inputs		
n/a		
Outputs		
Message name	To agent	
ExRlocation	MAPK agents	
Function Name	ExR_inputdata	
Description	Read all messages from other agents	
Current state	1	
Next state	2	
Inputs		
Message name	Filter/Operation	From agent
MKlocation	n/a	MAPK agents
Outputs		
Message name	To agent	
ExRnewbond	MAPK agents	
Function Name	ExR_move	
Description	movement and check bond messages	
Current state	2	
Next state	3	
Inputs		
Message name	Filter/Operation	From agent
MKfinalbond	n/a	MAPK agents
Outputs		
Message name	To agent	
n/a		

Appendix A, Table 11 Summary of the transition functions used to control the exporting receptor behaviour. Function name is provided with a brief description, and the messages outputted and inputted into the transition function.

ii. Agent messages

MAPKK MESSAGES		
Message	<u>MKKlocation</u>	
Description	Details the location of MKK in the 3D coordinates and its state	
Elements		
Name	Type	Description
Id	int	id of the agent (<i>i.e.</i> MAPKK)
X	double	x coordinates
Y	double	y coordinates
Z	double	z coordinates
State	int	agent state
Range	double	the agent's message range
Message	<u>MKKnewbond</u>	
Description	Message to signifies the formation of a bond between pMAPKK and MAPK	
Elements		
Name	Type	Description
idfrom	int	The id of the agent which released the message (<i>i.e.</i> pMAPKK)
statefrom	int	The stare of the agent which released the message (<i>i.e.</i> pMAPKK)
Idto	int	The id of the agent the message is targeted to (<i>i.e.</i> MAPK)
bindunbind	int	Whether to bind or not
distance	double	Distance between agents
range	double	The agent's message range
X	double	x coordinates
Y	double	y coordinates
Z	double	z coordinates

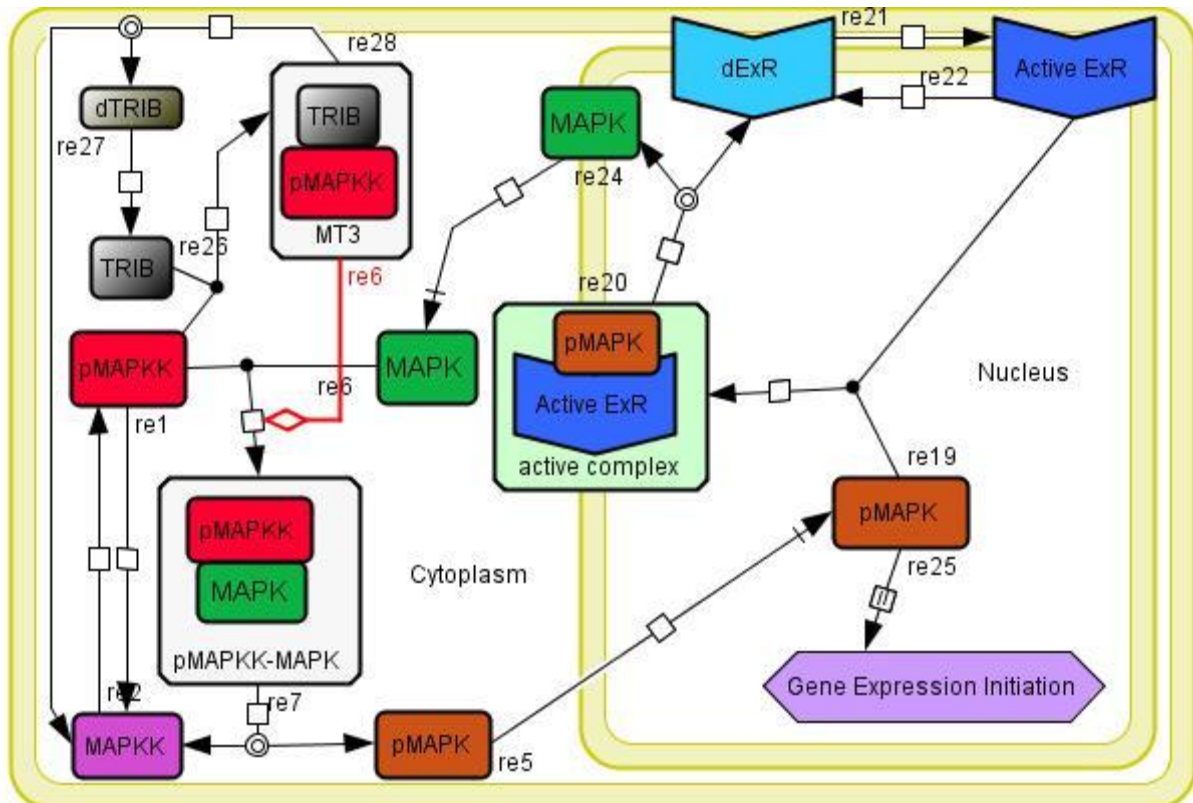
Appendix A, Table 12 Messages outputted by MAPKK into libmboard. MAPKK (MKK) outputs two messages, The first, MKKlocation, specifies the location of MAPKK within the cytoplasm with Cartesian and polar coordinates and if MAPKK is in an active or dormant state. This message is important for the interaction of MAPKK and MAPK as both agents seek to find their closest binding partners and their activation state. The second MKKnewbond specifies is important for the formation of the binding interaction between MAPK and MAPKK and the state transition. This message allows for the definition of the binding state and if it is occurring. This allows the two interacting agents to stop other agents from communicating with them while the process of bond-formation is occurring.

MAPK MESSAGES		
Message	<u>MKlocation</u>	
Description	Specifies the agent's location	
Elements		
Name	Type	Description
Id	int	identity of the agent (<i>i.e.</i> MAPK)
X	double	x coordinates
Y	double	y coordinates
Z	double	z coordinates
State	int	agent state
Range	double	the agent's message range
Message	<u>MKfinalbond</u>	
Description	Confirmation for the establishment of a bond between MAPK and either MKK or ExR	
Elements		
Name	Type	Description
idfrom	int	The id of the agent which released the message (<i>i.e.</i> MAPK)
statefrom	int	The state of the agent which released the message (<i>i.e.</i> MAPK)
Idto	int	The id of the agent the message is targeted to (<i>i.e.</i> MAPK K or ExR)
bindunbind	int	Whether to bind or not
distance	double	Distance between agents
range	double	The agent's message range
x	double	x coordinates
y	double	y coordinates
z	double	z coordinates

Appendix A, Table 13 Messages outputted by MAPK agents into the libmboard to allow for communication between the agent and its interacting partners. MKlocation is the message outputted by MAPK in order to specify its 3D coordinates both in the cytoplasm and the nucleus. This is done both in Cartesian and polar coordinates. MKfinalbond is produced when a bond is formed between MAPK and its interacting partners. This signifies no availability of MAPK for interaction with other partners. The message stores several parameters including the identity of the interacting partner, the interaction distance and the interaction state.

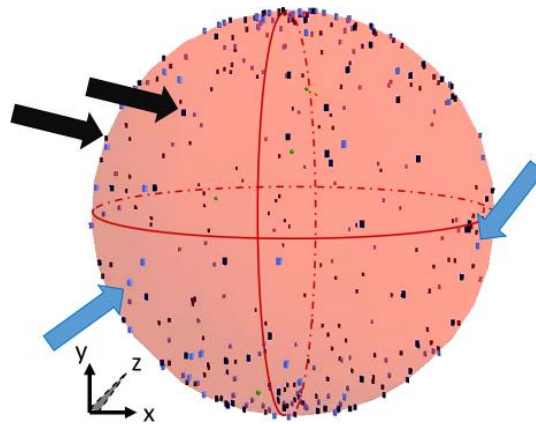
ExR MESSAGES		
Message	<u>ExRlocation</u>	
Description	Check location of agent	
Elements		
Name	Type	Description
Id	int	id of the agent (<i>i.e.</i> ExR)
X	double	x coordinates
Y	double	y coordinates
Z	double	z coordinates
State	int	agent state
Range	double	the agent's message range
Message	<u>ExRnewbond</u>	
Description	Message to signifies the formation of a bond between ExR and pMAPK	
Elements		
Name	Type	Description
idfrom	int	The id of the agent which released the message (<i>i.e.</i> ExR)
statefrom	int	The state of the agent which released the message (<i>i.e.</i> ExR)
Idto	int	The id of the agent the message is targeted to (<i>i.e.</i> MAPK)
bindunbind	int	Whether to bind or not
distance	double	Distance between agents
range	double	The agent's message range
X	double	x coordinates
Y	double	y coordinates
Z	double	z coordinates

Appendix A, Table 14 Messages outputted by exporting receptor agents (ExR). ExR outputs two messages into libmboard namely ExRlocation and ExRnewbond. The former message specifies the 3D location of the receptors within the nuclear membrane and if it is in an active or dormant state. This message is essential for the interaction between pMAPK species and the ExR and thus for the translocation of the pMAPK out of the nucleus. The ExRnewbond message is essential for the binding interaction between ExR and pMAPK, The message specifies if the bond had been formed, thus declares the availability of the ExR to bind with pMAPK species. Furthermore, the message identifies the interacting pMAPK ID and the distance between the two agents. This allows for the regulation of the binding interaction between interaction partners and stops any further interaction of ExR with other pMAPK agents which are in close proximity.



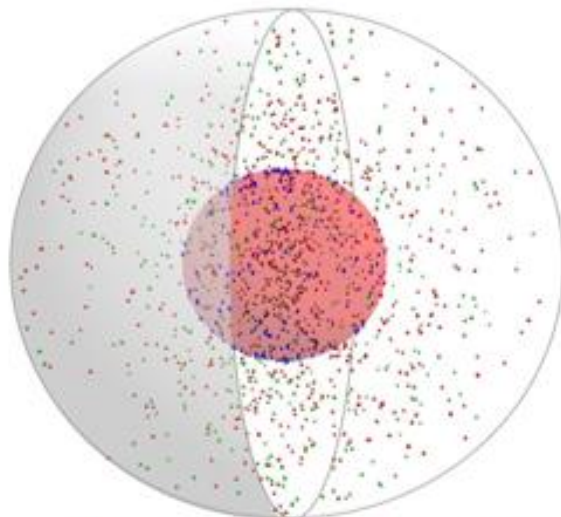
Appendix A, Figure 1 Introduction of the tribbles protein agent into the two compartment agent based model (ABM). A schematic representation using SBGN illustrating the interaction between pMAPKK and TRIB to form a complex MT3. This results in both agents changing state, whereby both become dormant (MAPKK and dTRIB). Both agents remain in this dormant state for milliseconds followed by their automatic re-activation. dTRIB is also referred to as MT3

Appendix B.



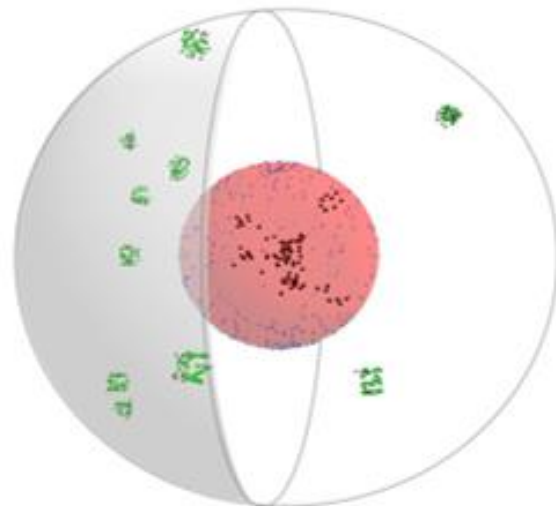
Appendix B, Figure 1 An agent based-model (ABM) simulation to validate agent interaction, behaviour and state change. A three dimensional (3D) representation illustrating the distribution of nuclear exporting receptors (ExR; blue cuboids and large red sphere) agents within the nuclear membrane (red sphere). Both ExR agent states are shown; whereby black arrows point to active ExR agents (dark blue cuboids) and blue arrows indicate dormant ExR agents (dExR, light blue cuboids). The receptors move randomly within the nuclear membrane in accordance with the fluid mosaic theory of receptor movement. The cytoplasm is the white background surrounding the nucleus.

(A)



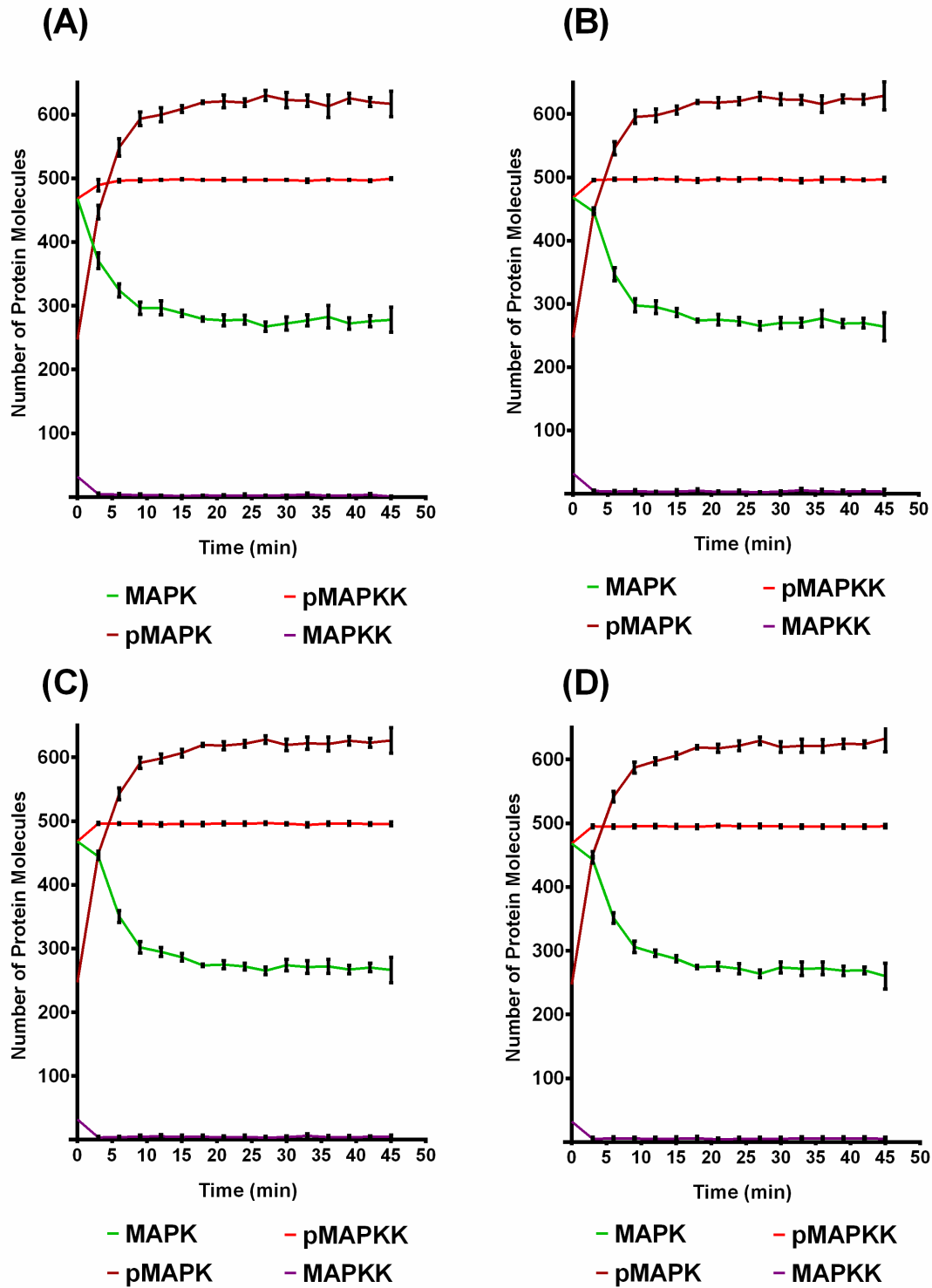
Two compartment model

(B)

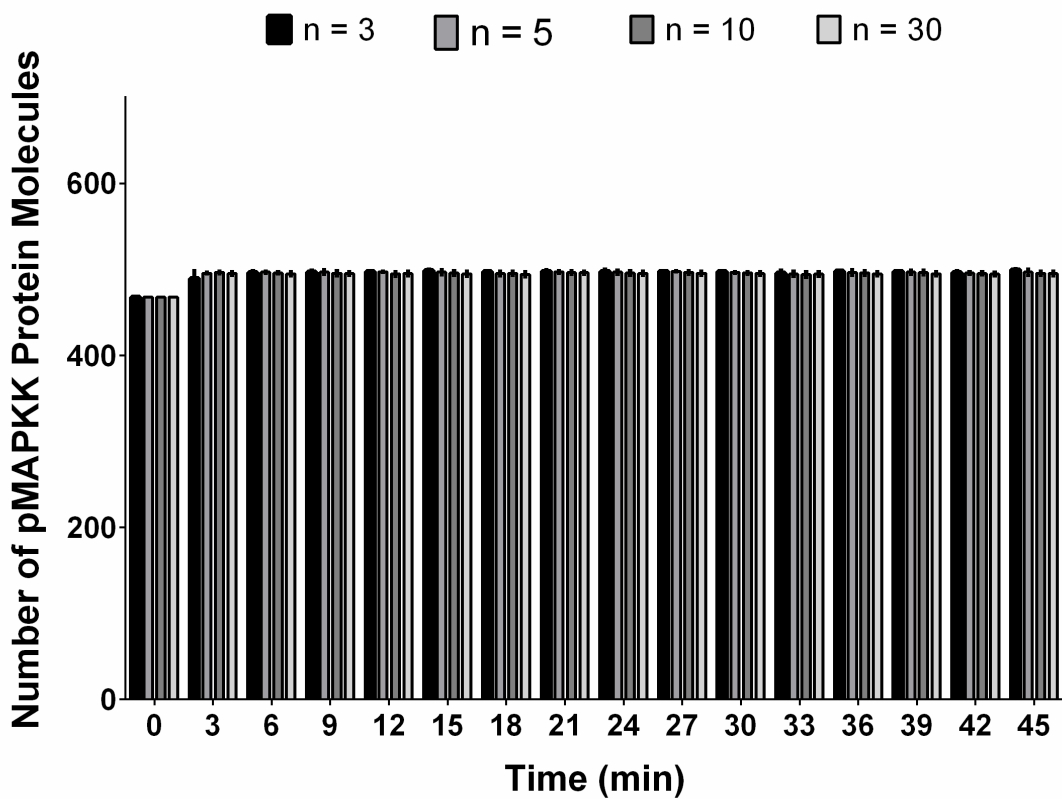
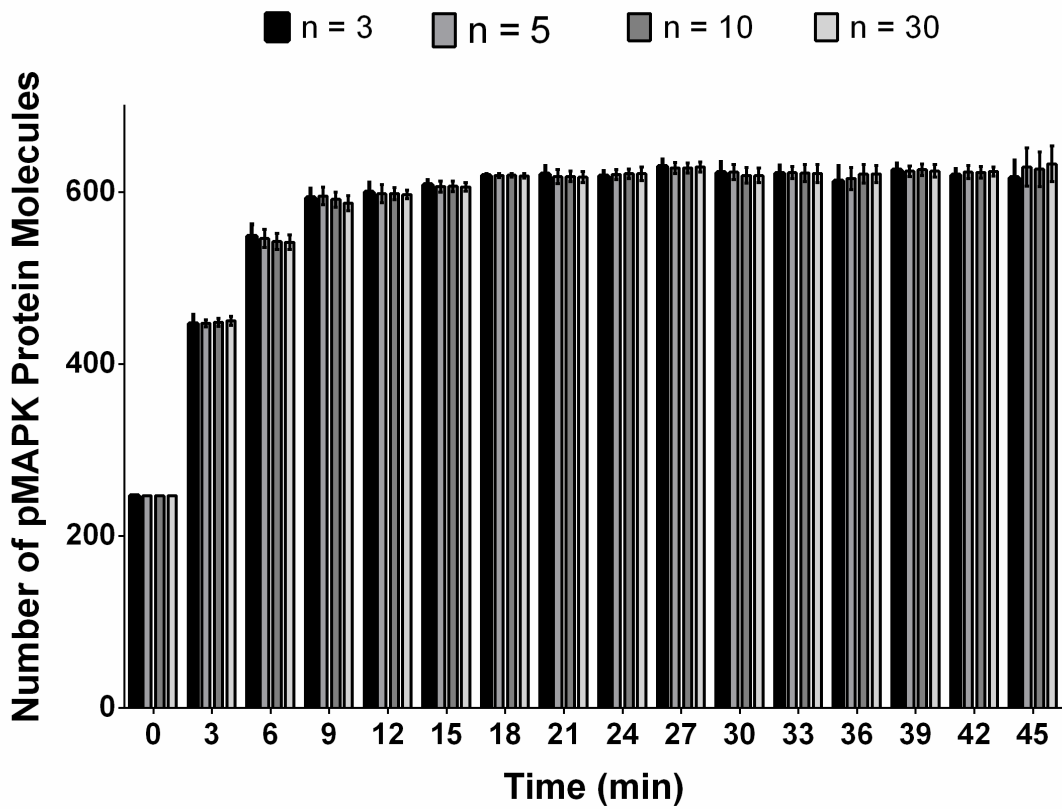


Multi compartment model

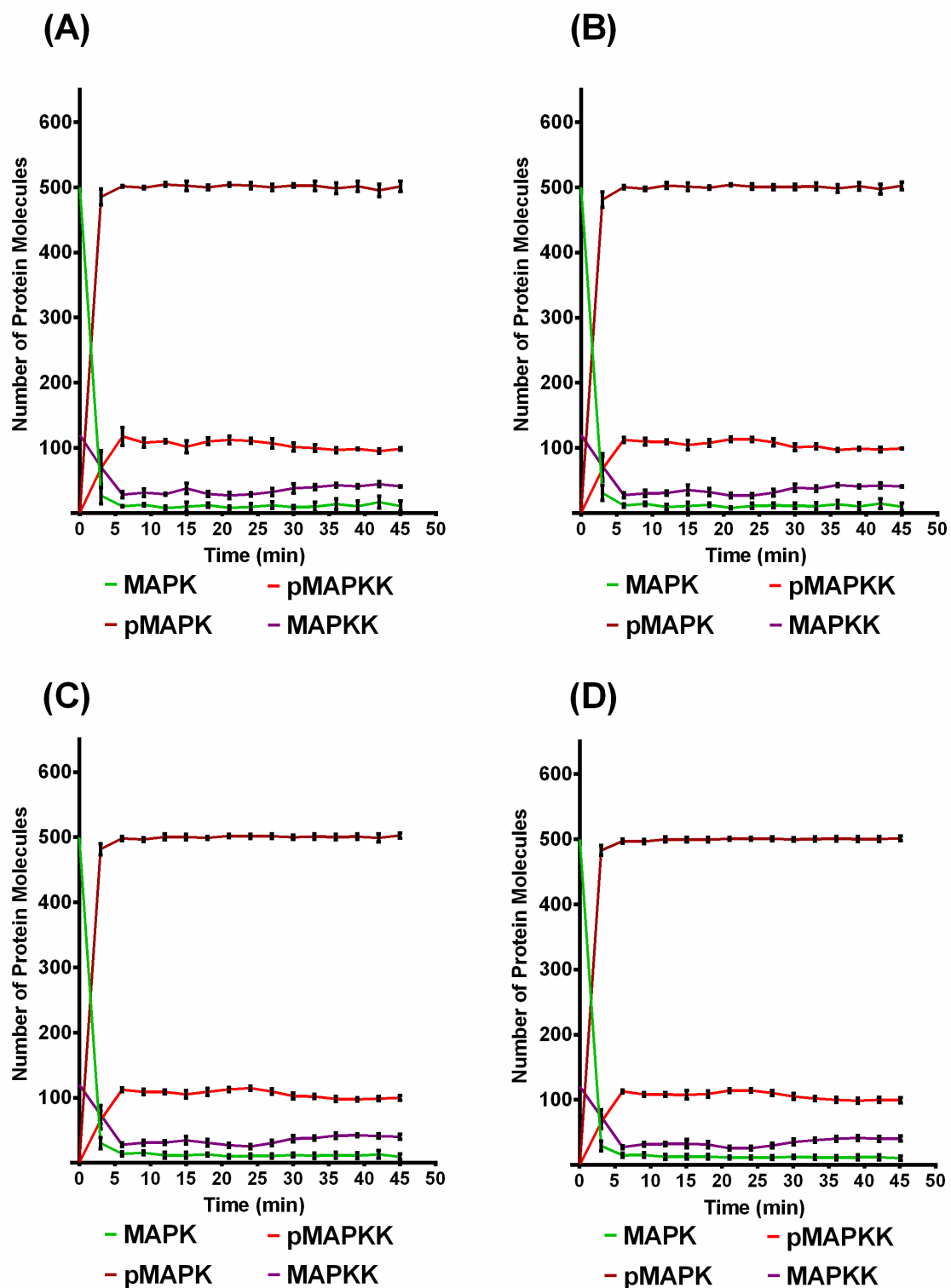
Appendix B, Figure 2 A 3D visualisation of the ABMs. The red sphere in the middle represents the nucleus and marks the nuclear membrane. In the multi compartment model, the clusters represent the cytosolic compartments. Small red spheres are MAPKK agents, green spheres are MAPK agents, purple spheres are inactive MAPKK agents and dark brown spheres (in the nucleus) are pMAPK agents. At the nuclear membrane, dark and light blue bodies are active and inactive ExR agents respectively.



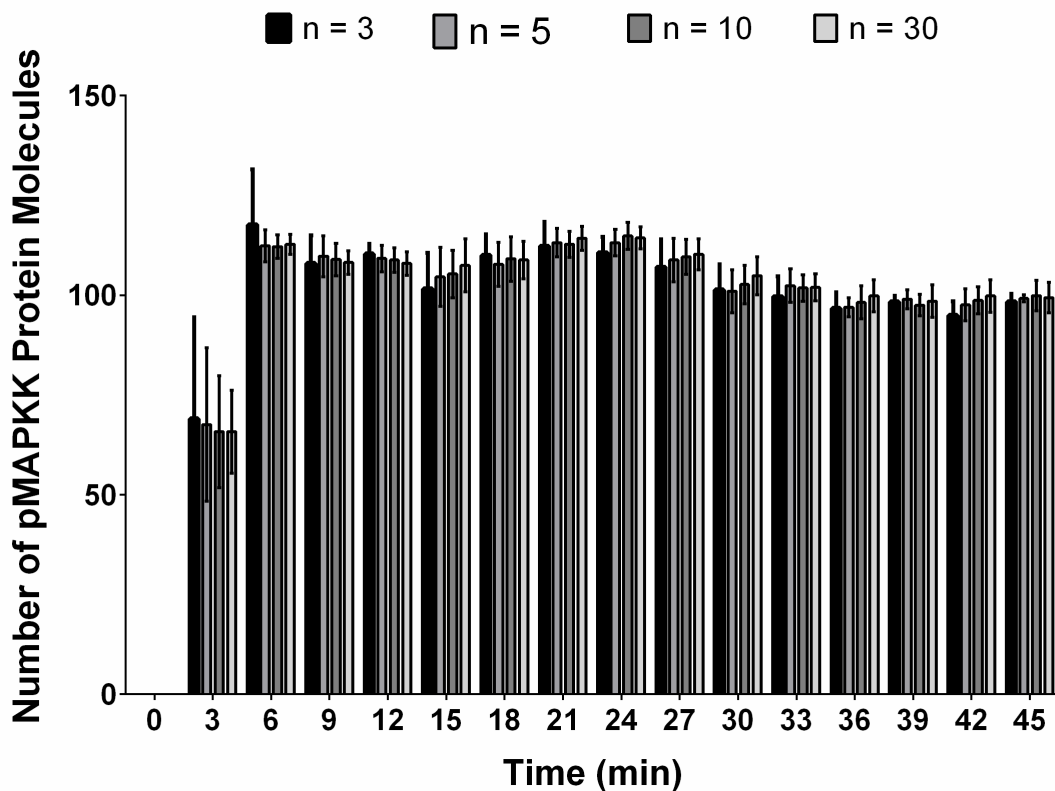
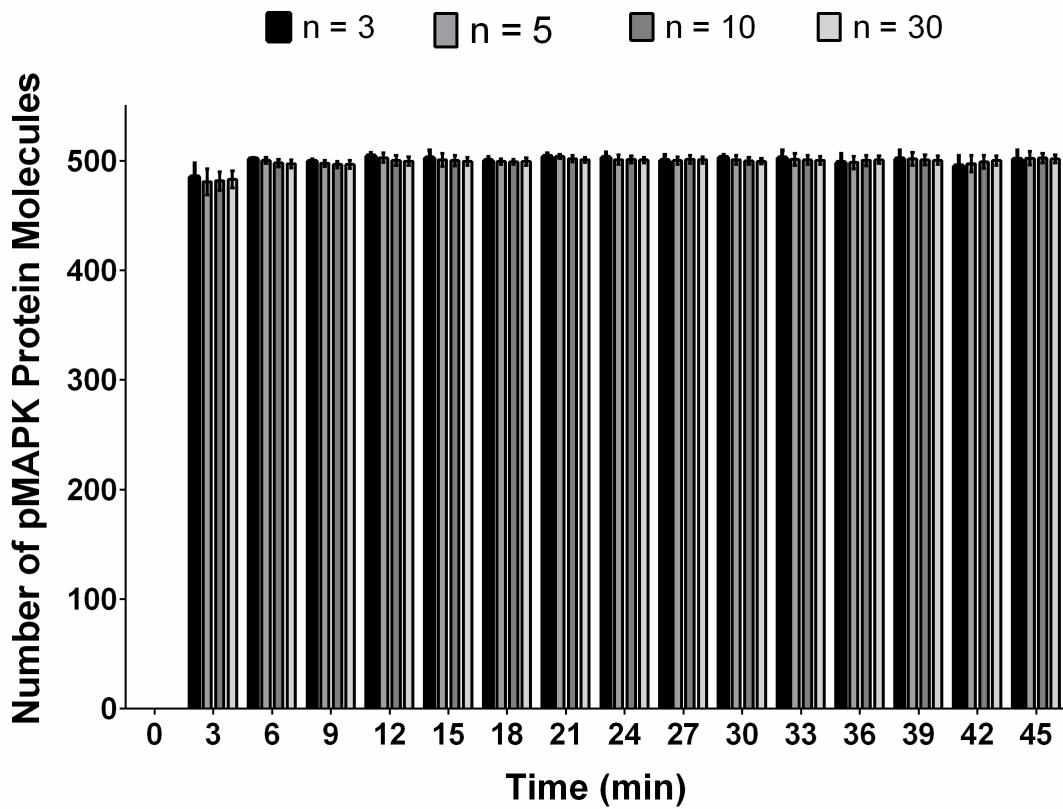
Appendix B, Figure 3 Multiple runs of the two compartment agent based mode (ABM) illustrating low variance for each time point. (A) the model was run for three times ($n = 3$), (B) the model was run for 5 times ($n = 5$). (C) The model was run for 10 times ($n = 10$). (D) The model was run for 30 times ($n = 30$). Each time point represents mean \pm standard variation (SEM).



Appendix B, Figure 4 Low variability between multiple and different two compartment ABM runs demonstrating no statistical significant difference between ABM models run for 3, 5, 10 or 30 times. (A) Demonstrates the low variation in pMAPK levels at each time point when the two-compartment ABM was simulated for 3, 5, 10 and 30 times ($n = 3$, $n = 5$, $n = 10$ and $n = 20$ respectively) . (B) Showing the low variation between the levels of pMAPKK in the same model runs. Each data point represents mean \pm SED.



Appendix B, Figure 5 Multiple runs of the multi-compartment ABM showing low variance for each time point and the visual similarities between the different simulations. (A) The model was run for three times ($n = 3$), (B) the model was run for 5 times ($n = 5$). (C) The model was run for 10 times ($n = 10$). (D) The model was run for 30 times ($n = 30$). Each time point represents mean \pm SEM.



Appendix B, Figure 6 low variability between multiple and different multi-compartment ABM rsuns demonstrating no statistical difference between ABM models run for 3, 5, 10 or 30 times. (A) Demonstrate the low variation in pMAPK levels at each time point when the two-compartment ABM was simulated for 3, 5, 10 and 30 times (n=3, n=5, n=10 and n=20 respectively). (B) Showing the low variation between the levels of pMAPKK in the same model runs. Each data point represents mean \pm SEM. model was mean. At time = 0 min the levels of both agents was close to 0.

Time (min)	n = 3	n = 5	n = 10	n = 30
0	0 ± 0.0	0 ± 0.0	0 ± 0.0	0 ± 0.0
3	485.3333 ± 12.34	481.00 ± 11.81	481.60 ± 8.53	482.90 ± 7.78
6	501.6667 ± 1.15	500.40 ± 2.61	498.10 ± 3.38	497.23 ± 3.50
9	499.3333 ± 2.08	497.60 ± 2.79	496.50 ± 3.06	496.70 ± 3.44
12	504.33 ± 3.06	502.80 ± 4.38	500.40 ± 4.72	499.77 ± 4.01
15	502.33 ± 7.23	501.00 ± 5.83	500.20 ± 4.66	499.53 ± 3.44
18	500.00 ± 3.46	499.40 ± 2.61	498.90 ± 2.23	499.37 ± 3.60
21	504.00 ± 2.65	504.00 ± 1.87	502.00 ± 2.94	500.80 ± 2.33
24	502.67 ± 5.13	501.00 ± 4.30	501.30 ± 3.30	500.67 ± 2.48
27	500.00 ± 5.20	500.20 ± 3.70	501.40 ± 3.53	500.83 ± 3.02
30	503.00 ± 2.65	500.80 ± 4.32	499.90 ± 3.21	499.63 ± 2.58
33	502.33 ± 7.23	501.40 ± 5.32	500.90 ± 4.25	500.43 ± 3.52
36	498.33 ± 8.14	498.40 ± 5.77	500.30 ± 4.69	500.83 ± 3.40
39	501.67 ± 8.08	501.80 ± 5.89	500.80 ± 4.42	500.40 ± 3.89
42	495.33 ± 9.29	497.40 ± 7.57	498.90 ± 5.99	500.17 ± 4.07
45	501.33 ± 8.08	502.40 ± 6.07	502.60 ± 4.25	501.70 ± 3.57

Appendix B, Table 1 pMAPK levels in multi-compartment ABMs showing the values demonstrated in figure B6 and B7 in tabular form. Values show mean ± SEM.

Time (min)	n = 3	n = 5	n = 10	n = 30
0	0 ± 0.00	0 ± 0.00	0 ± 0.00	0 ± 0.00
3	69.00 ± 25.53	67.6 ± 22.64	65.8 ± 20.01	65.8 ± 18.80
6	117.67 ± 13.87	112.4 ± 13.04	112.2 ± 10.07	112.8 ± 9.07
9	108.00 ± 7.00	109.8 ± 7.51	109 ± 6.77	108.2 ± 6.503
12	110.33 ± 2.52	109.2 ± 2.44	108.8 ± 5.40	107.93 ± 3.04
15	101.67 ± 9.02	104.6 ± 8.79	105.3 ± 7.57	107.5 ± 6.44
18	110.00 ± 5.29	107.8 ± 5.13	109.1 ± 4.04	108.83 ± 3.65
21	112.33 ± 6.03	113.2 ± 5.20	112.8 ± 4.42	114.27 ± 4.01
24	110.67 ± 4.04	113.2 ± 3.70	114.9 ± 2.65	114.37 ± 1.53
27	107.00 ± 7.00	108.8 ± 6.68	109.6 ± 5.20	110.27 ± 3.38
30	101.33 ± 6.43	101 ± 5.99	102.7 ± 4.07	104.9 ± 3.03
33	99.67 ± 5.03	102.4 ± 4.38	101.8 ± 3.03	102 ± 2.40
36	96.67 ± 4.04	97 ± 3.60	98.2 ± 2.77	99.83 ± 1.55
39	98.33 ± 1.53	99 ± 1.53	97.5 ± 1.48	98.5 ± 1.14
42	95.00 ± 3.46	97.6 ± 2.25	98.7 ± 1.53	99.83 ± 0.84
45	98.33 ± 2.08	99.2 ± 1.70	99.9 ± 1.48	99.37 ± 1.00

Appendix B, Table 2 pMAPKK levels in multi-compartment ABM showing the values demonstrated in figure B6 and B7 in tabular form. Values show mean ± SEM.

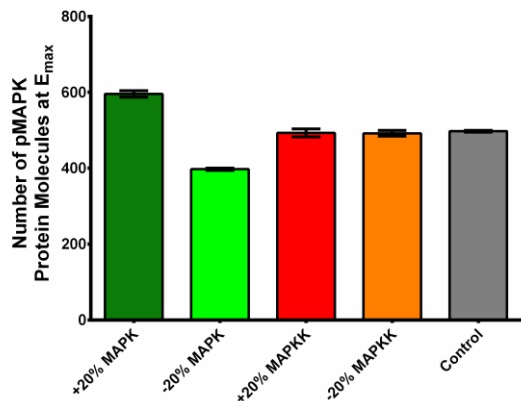
Time (min)	n = 3	n = 5	n = 10	n = 30
0	247.00 ± 0.00	247.00 ± 0.00	247.00 ± 0.00	247.00 ± 0.00
3	447.00 ± 10.39	447.40 ± 4.04	448.60 ± 4.50	450.23 ± 5.20
6	548.67 ± 13.80	546.02 ± 10.50	542.75 ± 9.38	541.66 ± 8.51
9	593.33 ± 10.69	595.40 ± 10.32	591.37 ± 8.79	587.28 ± 8.86
12	599.67 ± 11.15	598.02 ± 10.36	598.15 ± 7.23	597.13 ± 5.16
15	608.67 ± 5.13	606.60 ± 6.50	606.69 ± 5.86	605.93 ± 5.07
18	619.00 ± 2.00	619.16 ± 2.44	619.42 ± 2.13	618.95 ± 2.72
21	620.67 ± 9.87	618.16 ± 8.08	618.27 ± 6.32	617.48 ± 6.43
24	618.67 ± 6.03	620.48 ± 5.95	621.27 ± 5.54	621.43 ± 7.93
27	630.00 ± 7.81	627.90 ± 6.44	627.89 ± 6.08	629.27 ± 5.85
30	622.67 ± 12.06	623.28 ± 8.61	619.25 ± 9.04	619.25 ± 8.46
33	621.67 ± 9.07	622.56 ± 7.06	621.99 ± 9.77	621.41 ± 10.69
36	613.00 ± 17.58	615.72 ± 13.04	620.92 ± 10.77	620.86 ± 10.07
39	625.67 ± 7.51	624.38 ± 6.25	626.09 ± 6.77	624.53 ± 7.19
42	619.67 ± 7.23	623.12 ± 7.63	622.87 ± 6.68	623.82 ± 5.40
45	616.67 ± 20.01	629.00 ± 22.06	626.50 ± 20.18	632.81 ± 20.64

Appendix B, Table 3 pMAPK levels in two compartment ABM with multiple model runs. Values illustrated are mean ± SEM.

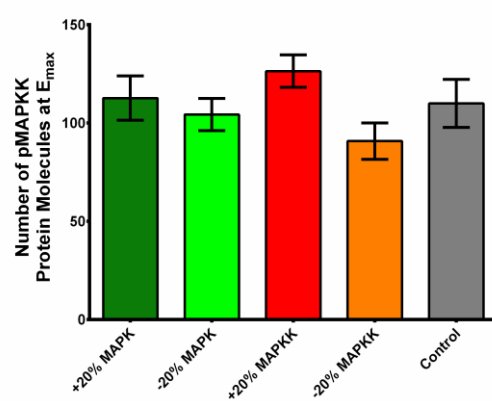
Time (min)	n = 3	n = 5	n = 10	n = 30
0	468.00 ± 0.00	468.00 ± 0.00	468.00 ± 0.00	468.00 ± 0.00
3	489.33 ± 8.96	495.60 ± 1.14	496.30 ± 1.70	495.13 ± 2.37
6	496.33 ± 2.08	496.80 ± 1.64	496.00 ± 1.49	494.73 ± 2.65
9	497.00 ± 2.00	496.80 ± 2.86	495.60 ± 3.20	495.07 ± 2.42
12	497.33 ± 0.58	497.20 ± 0.84	494.80 ± 2.86	495.20 ± 2.67
15	498.67 ± 1.15	496.80 ± 3.03	495.70 ± 2.87	495.00 ± 3.04
18	497.33 ± 0.58	495.20 ± 3.03	495.40 ± 2.63	494.40 ± 3.08
21	497.67 ± 1.53	497.20 ± 1.64	496.20 ± 2.25	496.07 ± 1.93
24	497.67 ± 2.31	496.80 ± 2.68	495.90 ± 2.81	495.50 ± 2.78
27	497.67 ± 0.58	497.80 ± 0.84	496.60 ± 2.27	495.60 ± 2.84
30	497.33 ± 0.58	496.60 ± 1.14	496.00 ± 1.76	495.13 ± 2.40
33	496.00 ± 2.65	494.80 ± 3.27	493.90 ± 3.48	494.67 ± 2.78
36	498.00 ± 1.00	496.40 ± 3.65	495.90 ± 2.85	494.73 ± 2.68
39	497.67 ± 0.58	496.80 ± 2.77	496.20 ± 2.86	494.87 ± 2.86
42	496.33 ± 1.53	495.80 ± 1.48	495.40 ± 1.84	494.57 ± 2.57
45	499.33 ± 1.15	496.80 ± 3.63	495.50 ± 2.84	495.20 ± 2.68

Appendix B, Table 4 pMAPKK levels in two compartment ABM with multiple model runs. Values illustrated are mean ± SD

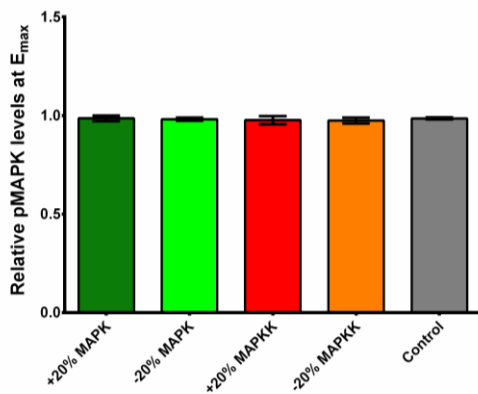
(A)



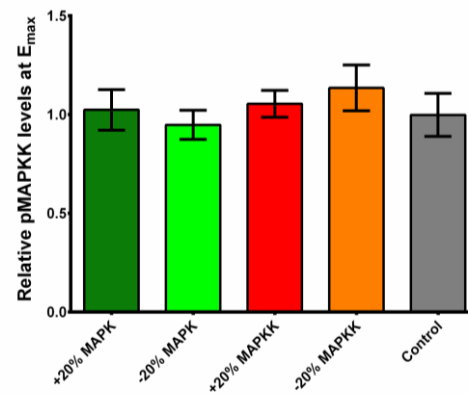
(B)



(C)

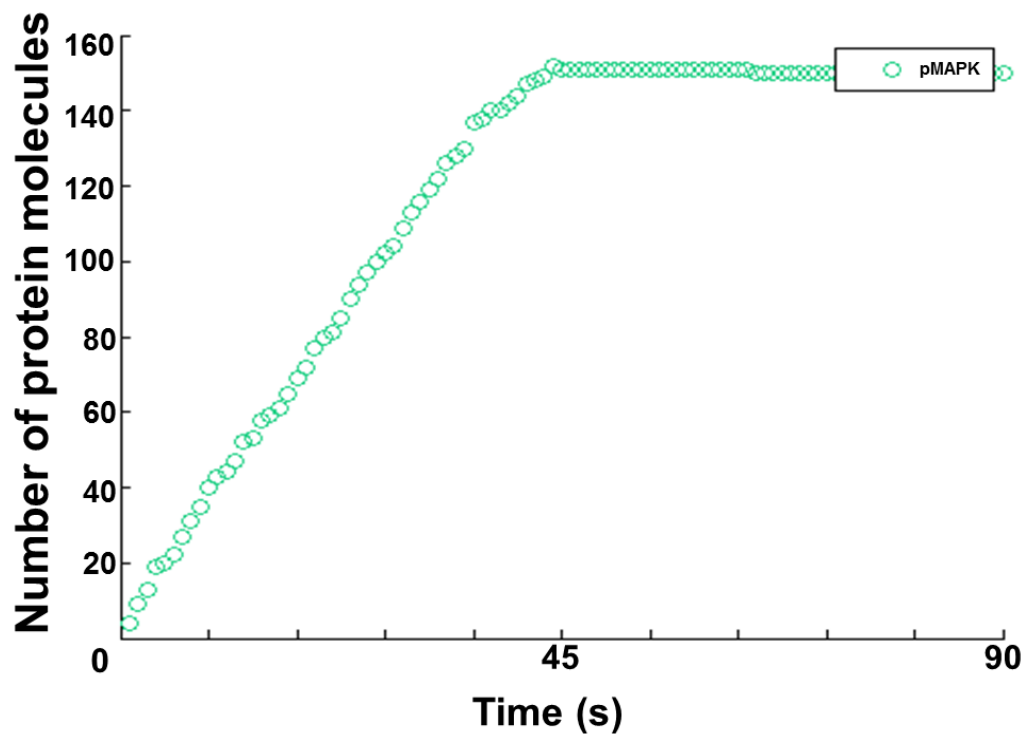


(D)

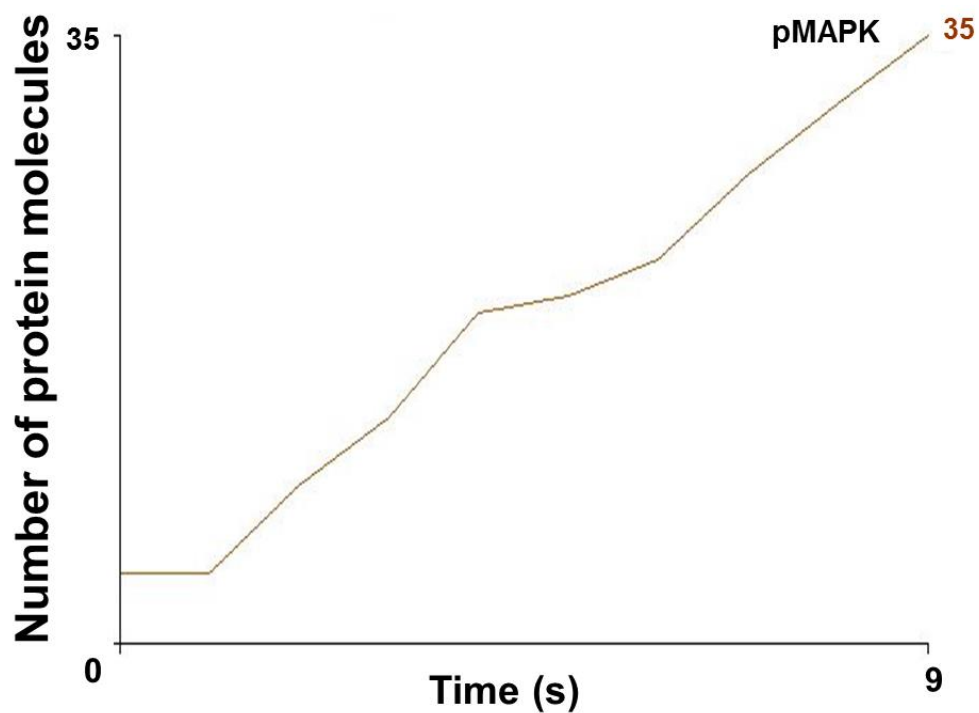


Appendix B, Figure 7 Sensitivity analysis to examine the effect MAPKK and MAPK level variation on the activation behaviour in multi-compartment models. (A) Levels of pMAPK were monitored in different ABMs where the total number of MAPKK and MAPK were varied by 20% at t_0 . (B) Levels of pMAPKK were monitored in different ABMs which contained varied MAPKK and MAPK levels at t_0 . (C) Levels of pMAPK were normalised to total MAPK present in the ABM, demonstrating that variation in the initial levels of MAPKK and MAPK agents had no statistically significant effect on pMAPK levels formed. (D) Levels of MAPKK were normalised to total MAPK present in the ABM, demonstrating that variation in the initial levels of MAPKK and MAPK agents had no statistically significant effect on pMAPKK levels formed. The model was simulated ten times ($n = 10$) The bars represent mean \pm SED. Control refers to the initial multi-compartment ABM used simulation and the agent numbers were specified in Table 3. 1(see section 3.4.1.3).

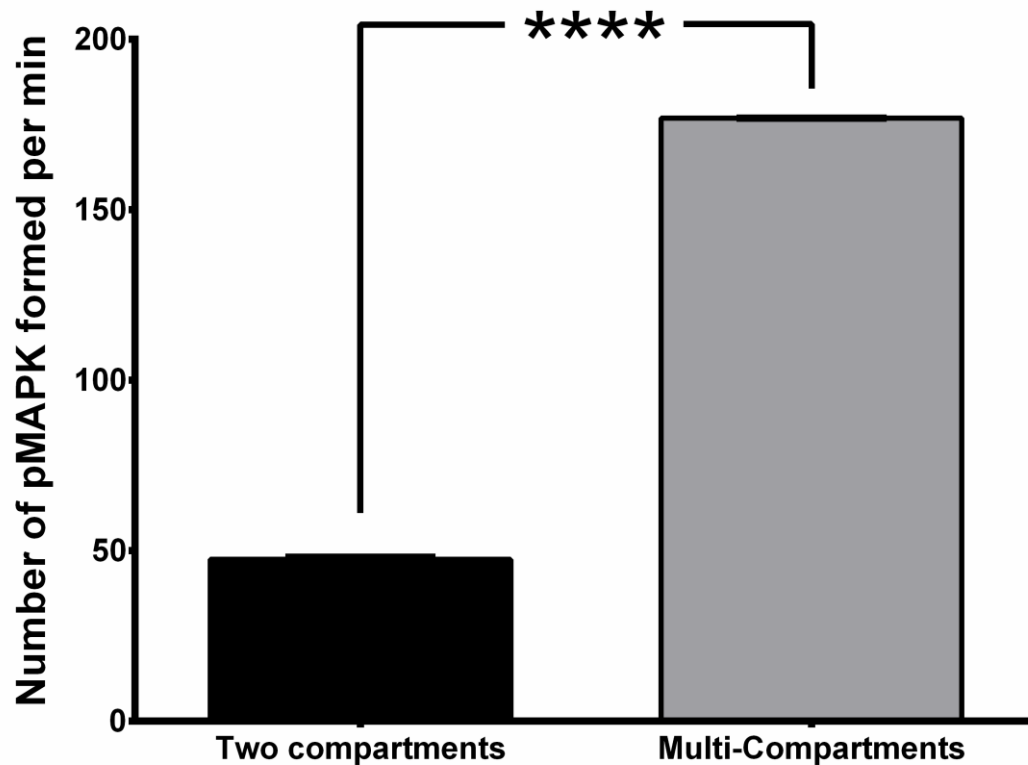
(A)



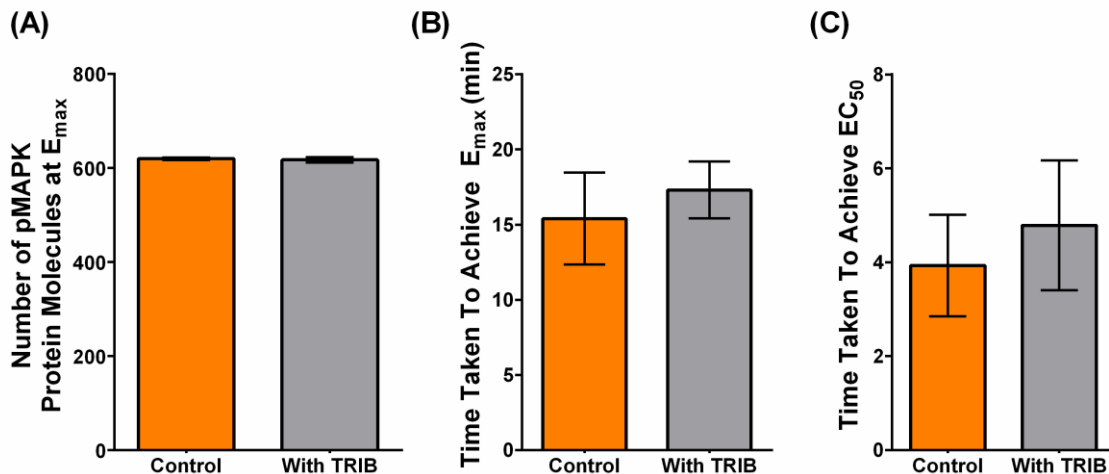
(B)



Appendix B, Figure 8 The initial plateau phase which characterises the ultrasensitive activation behaviour of MAPK was observed in both the two compartment ABM (A) and the multi-compartment model (B) . The two graphs were drawn on different scales to allow for the visualisation of the plateau phase in (B) which appears initially with a duration of 1.5 s compared to (A) where it appears after 45 s with a duration of 45 s.

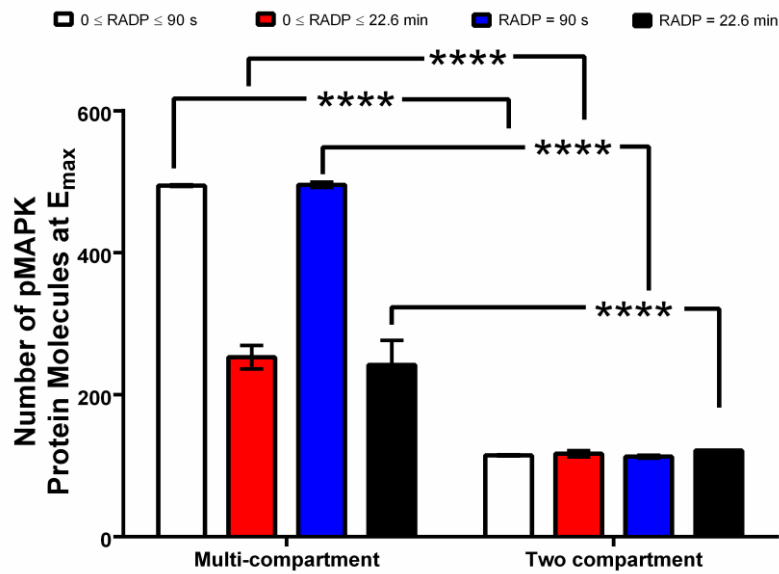


Appendix B, Figure 9 Significant difference in the rate of pMAPK formation between the two and multi-compartment ABMs. This was measured at the linear phase of pMAPK activation/formation. The model was simulated ten times (n = 10). The bars represent mean \pm SD.

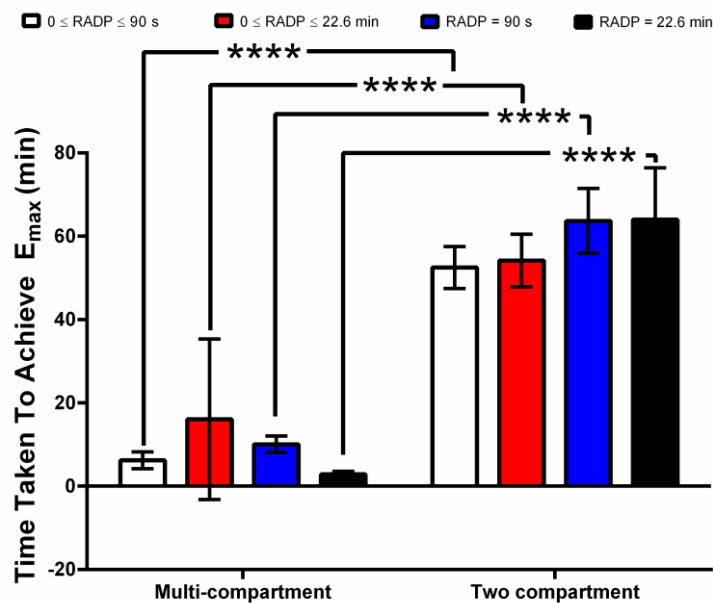


Appendix B, Figure 10 Introduction of the tribbles (TRIB) protein agent has no marked effect on the MAPK activation behaviour in the two compartment agent based model (ABM). (A) the magnitude of pMAPK generated in a two compartment ABM with and without TRIB. There was no significant statistical difference between the magnitudes generated from both models (B) This was also observed with the times taken to generate both E_{max} (B) and the EC_{50} (C). The values represented are mean \pm standard deviation (SD), and the models were run 10 times (n = 10) student t-test was used to analyse the statistical significance.

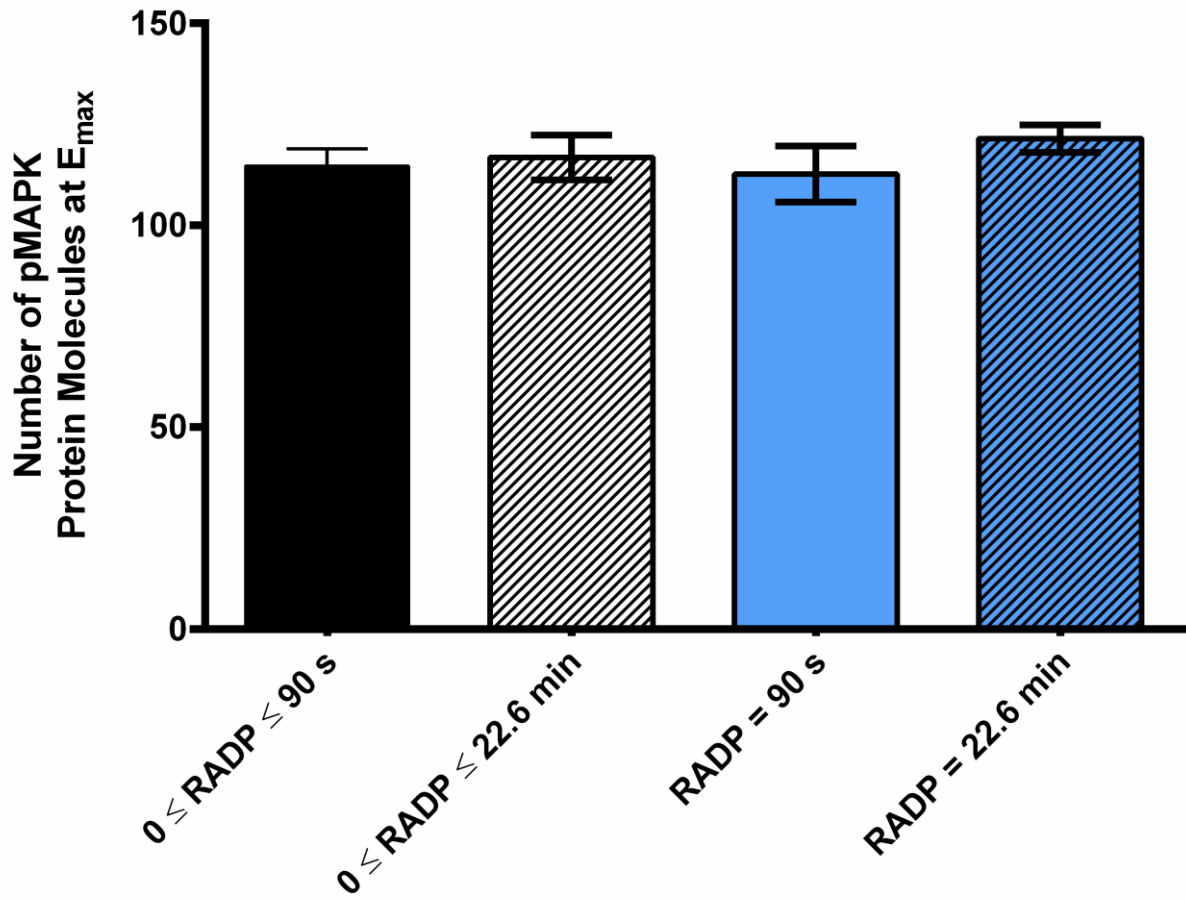
(A)



(B)

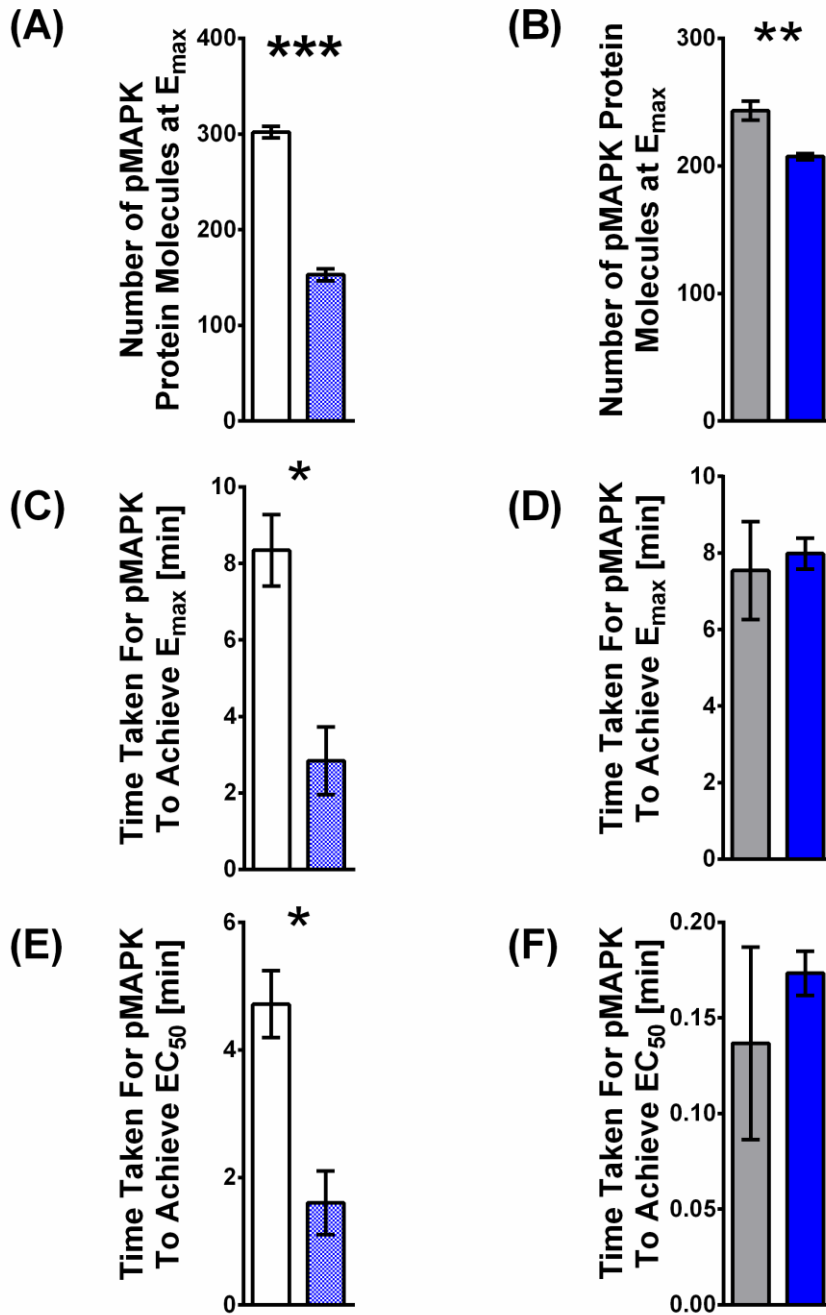


Appendix B, Figure 11 Comparison of temporal modulation effect between a multi-compartment and a two-compartment ABMs. (A) Comparison between the levels of pMAPK generated in the two ABMs where the re-activation delay period (RADP) was modelled stochastically ($0 \leq \text{RADP} \leq 90 \text{ s}$ and $0 \leq \text{RADP} \leq 22.6$) and deterministically ($\text{RADP} = 90 \text{ s}$ and $\text{RADP} = 22.6 \text{ min}$). The diagram illustrates that the multi-compartment ABM generates substantially more pMAPK compared to a two compartment model in both stochastic and deterministic RADP configurations. (B) Demonstrates that a multi-compartment ABM reaches E_{\max} in a notably shorter time compared to a two-compartment ABM using both stochastic and deterministic configurations of RADP. For each RADP configuration, a student t-test was performed to show statistical significance where **** corresponds to $(p) < 0.001$. The graphs show. The model was simulated ten times ($n = 10$) The bars represent mean \pm SD.



Appendix B, Figure 12 no extensive variation in pMAPK magnitude generated in a two compartment model where stochastic and deterministic configurations of re-activation delay period (RADP) were investigated. The bars illustrate mean \pm SD and $n = 10$ simulation runs.

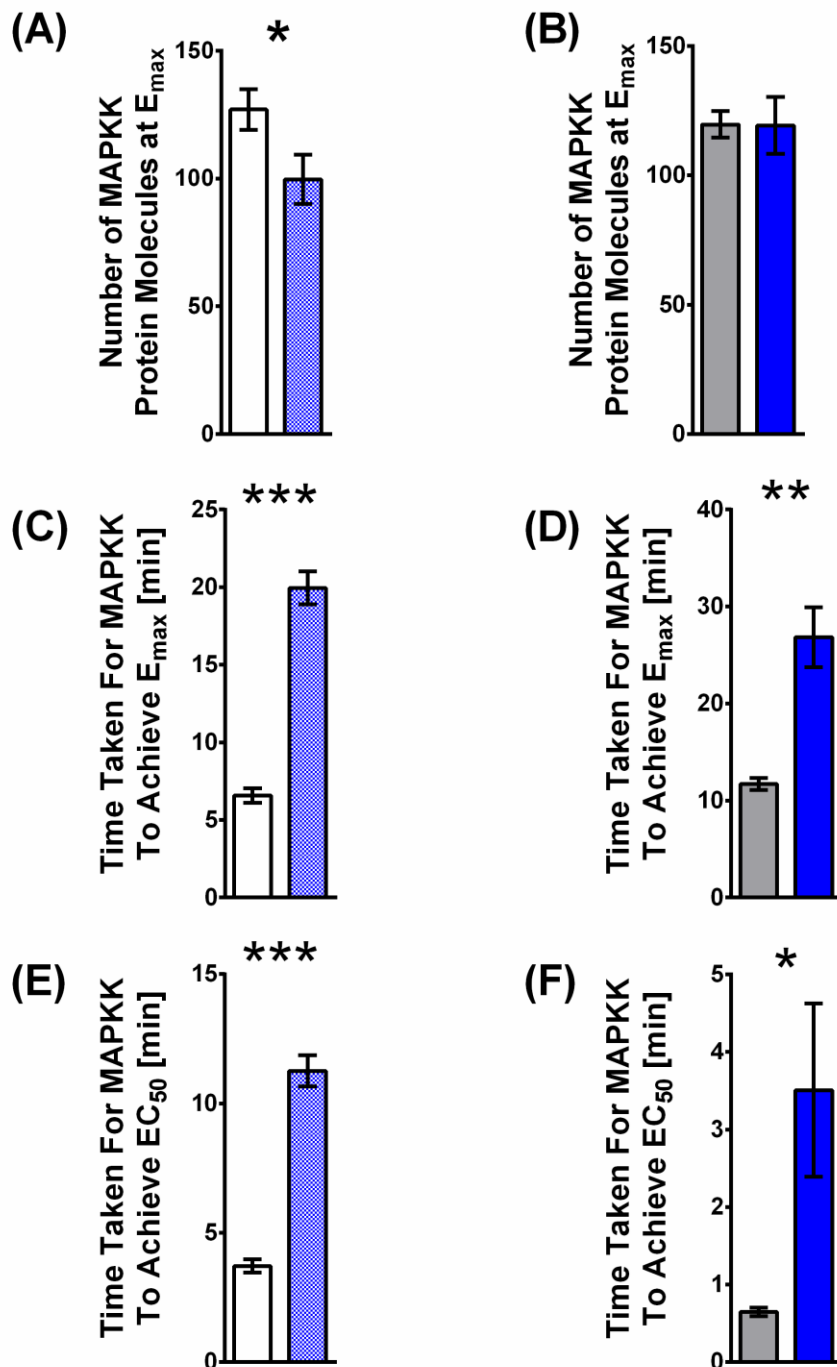
Control ($0 < \text{RADP} \leq 90 \text{ s}$) Control ($\text{RADP} = 90 \text{ s}$)
 $0 < \text{RADP} \leq 22.64 \text{ min}$ $\text{RADP} = 22.64 \text{ min}$



Appendix B, Figure 13 Short and long ($0 < \text{RADP} < 90 \text{ s}$ and $0 < \text{RADP} < 22.64 \text{ min}$, respectively) MAPKK re-activation delay periods (RADP) configurations modulate MAPK activation behaviour. Simultaneous modulation of the spatiotemporal regulatory elements in the MAPK pathway impact MAPK activation behaviour. In stochastic RADP configurations (A), (C) and (E), increasing the RADP causes a significant reduction in the levels of pMAPK generated at E_{\max} and the time to achieve both E_{\max} and EC_{50} . Conversely, using a deterministic RADP configuration, increasing RADP resulted in a significant reduction in the magnitude of pMAPK generated at E_{\max} , yet there was no significant difference in the time to achieve E_{\max} and EC_{50} . For each RADP configuration, a student t-test was performed to show statistical significance. *, ** and *** equate to $(p) > 0.05$, $(p) > 0.01$ and $(p) > 0.001$ respectively. The model was simulated ten times ($n = 10$). The bars represent mean \pm SD.

Control ($0 < \text{RADP} \leq 90 \text{ s}$)
 Control ($\text{RADP} = 90 \text{ s}$)

$0 < \text{RADP} \leq 22.64 \text{ min}$
 $\text{RADP} = 22.64 \text{ min}$



Appendix B, Figure 14 Simultaneous modulation of the spatiotemporal regulatory elements in the MAPK pathway impact MAPKK activation behaviour. Simultaneous modulation of the spatiotemporal regulatory elements in the MAPK pathway impact MAPKK activation behaviour. In stochastic RADP configurations (A), (C) and (E), increasing the RADP caused a significant reduction in the levels of pMAPK generated at E_{\max} and the time to achieve both E_{\max} and EC_{50} . Conversely, using a deterministic RADP configuration, increasing RADP resulted in a significant reduction in the magnitude of pMAPK generated at E_{\max} , yet there was no significant difference in the time to achieve E_{\max} and EC_{50} . For each RADP configuration, a student t-test was performed to show statistical significance. *, ** and *** equate to $(p) > 0.05$, $(p) > 0.01$ and $(p) > 0.001$ respectively. The model was simulated ten times ($n = 10$). The bars represent mean \pm SD.

Appendix C. References used to calibrate pMAPK activation time in the ABM.

1. Ahmed S, Grant KG, Edwards LE, Rahman A, Cirit M, Goshe MB, et al. Data-driven modeling reconciles kinetics of ERK phosphorylation, localization, and activity states. *Mol Syst Biol*. 2014;10:718. Epub 2014/02/04. doi: 10.1002/msb.134708. PubMed PMID: 24489118; PubMed Central PMCID: PMC4023404.
2. Bashor CJ, Helman NC, Yan S, Lim WA. Using engineered scaffold interactions to reshape MAP kinase pathway signaling dynamics. *Science (New York, NY)*. 2008;319(5869):1539-43. Epub 2008/03/15. doi: 10.1126/science.1151153. PubMed PMID: 18339942.
3. Bhalla US, Ram PT, Iyengar R. MAP Kinase Phosphatase As a Locus of Flexibility in a Mitogen-Activated Protein Kinase Signaling Network. *Science (New York, NY)*. 2002;297(5583):1018-23. doi: 10.1126/science.1068873.
4. Borisov N, Aksamitiene E, Kiyatkin A, Legewie S, Berkhout J, Maiwald T, et al. Systems-level interactions between insulin–EGF networks amplify mitogenic signaling. *Molecular Systems Biology*. 2009;5(1). doi: 10.1038/msb.2009.19.
5. Brightman FA, Fell DA. Differential feedback regulation of the MAPK cascade underlies the quantitative differences in EGF and NGF signalling in PC12 cells. *FEBS Letters*. 2000;482(3):169-74. doi: [http://dx.doi.org/10.1016/S0014-5793\(00\)02037-8](http://dx.doi.org/10.1016/S0014-5793(00)02037-8).
6. Chang C-w, Poteet E, Schetz JA, Gümüş ZH, Weinstein H. Towards a quantitative representation of the cell signaling mechanisms of hallucinogens: Measurement and mathematical modeling of 5-HT1A and 5-HT2A receptor-mediated ERK1/2 activation. *Neuropharmacology*. 2009;56, Supplement 1:213-25. doi: <http://dx.doi.org/10.1016/j.neuropharm.2008.07.049>.
7. Cirit M, Haugh Jason M. Data-driven modelling of receptor tyrosine kinase signalling networks quantifies receptor-specific potencies of PI3K- and Ras-dependent ERK activation. *Biochemical Journal*. 2012;441(1):77-85. doi: 10.1042/bj20110833.
8. Cirit M, Wang CC, Haugh JM. Systematic quantification of negative feedback mechanisms in the extracellular signal-regulated kinase (ERK) signaling network. *The Journal of biological chemistry*. 2010;285(47):36736-44. Epub 2010/09/18. doi: 10.1074/jbc.M110.148759. PubMed PMID: 20847054; PubMed Central PMCID: PMC2978602.
9. Derkinderen P, Valjent E, Toutant M, Corvol JC, Enslen H, Ledent C, et al. Regulation of extracellular signal-regulated kinase by cannabinoids in hippocampus. *The Journal of neuroscience : the official journal of the Society for Neuroscience*. 2003;23(6):2371-82. Epub 2003/03/27. PubMed PMID: 12657697.
10. Finch AR, Caunt CJ, Perrett RM, Tsaneva-Atanasova K, McArdle CA. Dual specificity phosphatases 10 and 16 are positive regulators of EGF-stimulated ERK activity: Indirect regulation of

ERK signals by JNK/p38 selective MAPK phosphatases. *Cellular Signalling*. 2012;24(5):1002-11. doi: <http://dx.doi.org/10.1016/j.cellsig.2011.12.021>.

11. Hatakeyama M, Kimura S, Naka T, Kawasaki T, Yumoto N, Ichikawa M, et al. A computational model on the modulation of mitogen-activated protein kinase (MAPK) and Akt pathways in heregulin-induced ErbB signalling. *The Biochemical journal*. 2003;373(Pt 2):451-63. Epub 2003/04/15. doi: 10.1042/bj20021824. PubMed PMID: 12691603; PubMed Central PMCID: PMC1223496.
12. Heitzler D, Durand G, Gallay N, Rizk A, Ahn S, Kim J, et al. Competing G protein-coupled receptor kinases balance G protein and β -arrestin signaling. *Molecular Systems Biology*. 2012;8(1). doi: 10.1038/msb.2012.22.
13. Hornberg JJ, Binder B, Bruggeman FJ, Schoeberl B, Heinrich R, Westerhoff HV. Control of MAPK signalling: from complexity to what really matters. *Oncogene*. 2005;24(36):5533-42. doi: <http://www.nature.com/onc/journal/v24/n36/supinfo/1208817s1.html>.
14. Kamioka Y, Yasuda S, Fujita Y, Aoki K, Matsuda M. Multiple decisive phosphorylation sites for the negative feedback regulation of SOS1 via ERK. *The Journal of biological chemistry*. 2010;285(43):33540-8. Epub 2010/08/21. doi: 10.1074/jbc.M110.135517. PubMed PMID: 20724475; PubMed Central PMCID: PMC1223496.
15. Kholodenko BN. Negative feedback and ultrasensitivity can bring about oscillations in the mitogen-activated protein kinase cascades. *European journal of biochemistry / FEBS*. 2000;267(6):1583-8. Epub 2000/03/11. PubMed PMID: 10712587.
16. Kiyatkin A, Aksamitiene E, Markevich NI, Borisov NM, Hoek JB, Kholodenko BN. Scaffolding Protein Grb2-associated Binder 1 Sustains Epidermal Growth Factor-induced Mitogenic and Survival Signaling by Multiple Positive Feedback Loops. *Journal of Biological Chemistry*. 2006;281(29):19925-38. doi: 10.1074/jbc.M600482200.
17. Kuhn C, Prasad KV, Klipp E, Gennemark P. Formal representation of the high osmolarity glycerol pathway in yeast. *Genome informatics International Conference on Genome Informatics*. 2010;22:69-83. Epub 2010/03/20. PubMed PMID: 20238420.
18. Li H, Ung CY, Ma XH, Li BW, Low BC, Cao ZW, et al. Simulation of crosstalk between small GTPase RhoA and EGFR-ERK signaling pathway via MEK1. *Bioinformatics*. 2009;25(3):358-64. doi: 10.1093/bioinformatics/btn635.
19. Nakakuki T, Birtwistle MR, Saeki Y, Yumoto N, Ide K, Nagashima T, et al. Ligand-Specific c-Fos Expression Emerges from the Spatiotemporal Control of ErbB Network Dynamics. *Cell*. 2010;141(5):884-96. doi: <http://dx.doi.org/10.1016/j.cell.2010.03.054>.
20. Nakayama K, Satoh T, Igari A, Kageyama R, Nishida E. FGF induces oscillations of Hes1 expression and Ras/ERK activation. *Current biology : CB*. 2008;18(8):R332-4. Epub 2008/04/24. doi: 10.1016/j.cub.2008.03.013. PubMed PMID: 18430630.

21. Purvis J, Ilango V, Radhakrishnan R. Role of Network Branching in Eliciting Differential Short-Term Signaling Responses in the Hypersensitive Epidermal Growth Factor Receptor Mutants Implicated in Lung Cancer. *Biotechnology Progress*. 2008;24(3):540-53. doi: 10.1021/bp070405o.
22. Qi Z, Ming Y, Yan L. Spatial distribution and dose–response relationship for different operation modes in a reaction–diffusion model of the MAPK cascade. *Physical Biology*. 2011;8(5):055004.
23. Santos SDM, Verveer PJ, Bastiaens PIH. Growth factor-induced MAPK network topology shapes Erk response determining PC-12 cell fate. *Nat Cell Biol*. 2007;9(3):324-30. doi: http://www.nature.com/ncb/journal/v9/n3/supinfo/ncb1543_S1.html.
24. Sarma U, Ghosh I. Different designs of kinase-phosphatase interactions and phosphatase sequestration shapes the robustness and signal flow in the MAPK cascade. *BMC Systems Biology*. 2012;6:82-. doi: 10.1186/1752-0509-6-82. PubMed PMID: PMC3508828.
25. Sarma U, Ghosh I. Oscillations in MAPK cascade triggered by two distinct designs of coupled positive and negative feedback loops. *BMC research notes*. 2012;5:287. Epub 2012/06/15. doi: 10.1186/1756-0500-5-287. PubMed PMID: 22694947; PubMed Central PMCID: PMC3532088.
26. Sasagawa S, Ozaki Y-i, Fujita K, Kuroda S. Prediction and validation of the distinct dynamics of transient and sustained ERK activation. *Nat Cell Biol*. 2005;7(4):365-73. doi: http://www.nature.com/ncb/journal/v7/n4/supinfo/ncb1233_S1.html.
27. Schoeberl B, Eichler-Jonsson C, Gilles ED, Muller G. Computational modeling of the dynamics of the MAP kinase cascade activated by surface and internalized EGF receptors. *Nat Biotech*. 2002;20(4):370-5. doi: http://www.nature.com/nbt/journal/v20/n4/supinfo/nbt0402-370_S1.html.
28. Shankaran H, Ippolito DL, Chrisler WB, Resat H, Bollinger N, Opresko LK, et al. Rapid and sustained nuclear–cytoplasmic ERK oscillations induced by epidermal growth factor. *Molecular Systems Biology*. 2009;5:332-. doi: 10.1038/msb.2009.90. PubMed PMID: PMC2824491.
29. Sulpice E, Bryckaert M, Lacour J, Contreres J-O, Tobelem G. Platelet factor 4 inhibits FGF2-induced endothelial cell proliferation via the extracellular signal–regulated kinase pathway but not by the phosphatidylinositol 3–kinase pathway. *Blood*. 2002;100(9):3087-94. doi: 10.1182/blood.V100.9.3087.
30. Vasudevan HN, Mazot P, He F, Soriano P. Receptor tyrosine kinases modulate distinct transcriptional programs by differential usage of intracellular pathways. *eLife*. 2015;4:e07186. doi: 10.7554/eLife.07186. PubMed PMID: PMC4450512.
31. Vetterkind S, Saphirstein RJ, Morgan KG. Stimulus-specific activation and actin dependency of distinct, spatially separated ERK1/2 fractions in A7r5 smooth muscle cells. *PloS one*. 2012;7(2):e30409. Epub 2012/03/01. doi: 10.1371/journal.pone.0030409. PubMed PMID: 22363435; PubMed Central PMCID: PMC3283592.
32. Wang CC, Cirit M, Haugh JM. PI3K-dependent cross-talk interactions converge with Ras as quantifiable inputs integrated by Erk. *Mol Syst Biol*. 2009;5:246. Epub 2009/02/20. doi: 10.1038/msb.2009.4. PubMed PMID: 19225459; PubMed Central PMCID: PMC32657535.

33. Wei P, Wong WW, Park JS, Corcoran EE, Peisajovich SG, Onuffer JJ, et al. Bacterial virulence proteins as tools to rewire kinase pathways in yeast and immune cells. *Nature*. 2012;488(7411):384-8. doi: <http://www.nature.com/nature/journal/v488/n7411/abs/nature11259.html#supplementary-information>.
34. Yu RC, Pesce CG, Colman-Lerner A, Lok L, Pincus D, Serra E, et al. Negative feedback that improves information transmission in yeast signalling. *Nature*. 2008;456(7223):755-61. Epub 2008/12/17. doi: 10.1038/nature07513. PubMed PMID: 19079053; PubMed Central PMCID: PMC2716709.

Appendix D. Tribbles mediate a differential response to THC-dependent cell death through alteration in protein-protein interaction with different binding partners

This appendix chapter presents preliminary biological data which were performed to further develop and optimise the agent based model of the MAPK pathway in the future. The aspect of interest is the temporal regulation of the pathway at the level of the MAPKK proteins via the Tribbles protein family (TRIBs). The biological background was outlined, the methodology undertaken during the investigation was described and the results from these *in vitro* experiments were presented and discussed. Some of the data presented here were published recently (Guan et al., 2016), see appendix E, page 277

a. Introduction

The hallmarks of cancer development include cells' uncontrolled proliferation, growth and resistance to apoptosis. These processes are regulated by multiple signalling cascades, and perturbation of signal transduction mechanisms lead to loss of control over the aforementioned processes, and ultimately to tumorigenesis (Hill and Hemmings, 2002, Kucab et al., 2005, Lim et al., 2015, Mitsiades et al., 2004). Of said processes, resistance to pro-apoptotic signals is a major hallmark, and a challenge for drug development. Recently, it was demonstrated that experimentation

with cannabinoid compounds triggers anti-tumoral effects via inhibition of cell proliferation, angiogenesis and cell growth (Blazquez et al., 2003, Blazquez et al., 2004) (Guzman, 2003). Furthermore, there is growing evidence, both in vivo and in vitro, illustrating cannabinoids' induction of cell death in a variety of cancerous cell-lines via overriding the developed pro-apoptotic-resistant mechanisms exhibited by cancer cells (Vara et al., 2011) (Galve-Roperh et al., 2000, Sanchez et al., 1998). (Carracedo et al., 2006a, Carracedo et al., 2006b, Herrera et al., 2005, Lorente et al., 2009, McAllister et al., 2005, Salazar et al., 2009). Investigation of the mechanisms with which cannabinoids (in particular Δ^9 -Tetrahydrocannabinol (THC)) trigger cell cycle inhibition and cell death in cancer cells showed the involvement of both phosphatidylinositide 3-kinases (PI3K) and the mitogen activated protein kinase (MAPK) pathway (Gaoni and Mechoulam, 1964, Pertwee, 2008) (Carracedo et al., 2006a, Carracedo et al., 2006b, Greenhough et al., 2007, Herrera et al., 2005, Sanchez et al., 2003). Both pathways play a role in the regulation of cell growth, apoptosis, and proliferation. However, though both pathways are implicated in the anti-tumoral effects of THC, the precise mechanisms are still under investigation.

The PI3K pathway is regarded as a pro-survival pathway by the inhibition of the mitochondria-dependent apoptotic pathway, and through phosphorylation of the transcription factor Forkhead box protein O (FOXO). In the former, AKT phosphorylates BAX protein, and inhibits its binding to the mitochondria, and the release of "death factors", which activate caspase enzymes and trigger apoptosis. FOXO transcription factors mediate the expression of pro-apoptotic genes (such as BIM and Fas ligand). They also inhibit the expression of pro-survival genes such as BclxL. FOXO phosphorylation by AKT mediates their nuclear export. Export into the

cytoplasm allows for the regulation of FOXO proteins levels via ubiquitination (Huang and Tindall, 2011). Furthermore, AKT was shown to mediate pro-survival effect by phosphorylation of other protein targets such as Glycogen synthase kinase 3 β (GSK-3 β) and NF-kappaB (NF- κ B). In cannabinoid mediated signalling, Sanches et al. (1998) illustrated the involvement of PI3K/AKT in transducing the cannabinoid action intracellularly. Pulgar et al. demonstrated that THC induces an activation of the PI3K pathway at the level of AKT (a downstream protein of PI3K). Further investigation had shown that cannabinoid receptor B (CB1) induced apoptosis through the activation of AKT, which in turn modulates the mTOR system, and consequently cell survival. Recently, treating cells with the cannabinoid ligand KM-233 has demonstrated a change in AKT phosphorylation status. The apoptotic effect through the PI3K/AKT pathway was shown to involve recruitment of eukaryotic translation initiation factors 4E (eIF4E) - binding proteins (4E-BP) and p8 proteins. P8 was shown to play a role in inducing endoplasmic reticulum-stress associated proteins such as CHOP, ATF4 and TRB3. This is of interest, as these proteins are involved in the MAPK signalling pathway. Furthermore, it was shown that THC treatment causes the upregulation of MAPK phosphatase MKP3 and extensively down-regulates the expression of MEK2. It is also worth noting that it was illustrated that TRB3 acts as inhibitor for MAPKs, and initially the *Drosophila* homologue of TRIB was demonstrated to associate with phosphatase enzymes during *Drosophila* development. The induction of MAPK-dependent genes such as c-Fos and BDNF were demonstrated with THC treatment in the hippocampus of murine models. This expression was blocked with the use of the MEK inhibitor SL327. Furthermore, use of the PI3K inhibitor wortmannin resulted in inhibition of cannabinoid-dependent extracellular signal-regulated kinase (ERK) activation. This is in line with the observations which show that cannabinoids such as

THC and WIN-55,212-2 trigger simultaneous effects on both MAPK pathways (ERK, c-Jun N-terminal kinases (JNK) and p38) and PI3K/AKT pathway. They also share several protein targets; and in the context of cell death, they were both shown to regulate FOXO family members, p90RSK, p70S6K and the BAD. These protein targets were also shown to be modulated during cannabinoid treatment in cancer cells. BAD protein activation, and mediating of apoptosis, were illustrated to be activated via THC-dependent ceramide formation. This intracellular accumulation of ceramide is also thought to play a part in inducing cell death through two mechanisms. These involve the inhibition of AKT and prolonged activation of Raf (therefore prolonged ERK activation). Additionally, caspase proteins recruitment by p38, and ERK activation, and AKT inhibition via ceramide accumulation, was blocked via treatment with ceramide synthesis antagonists. P38 recruitment as part of THC-induced apoptosis is reported to occur as a result of stimulation of the CB2 receptors. This stems from the observation that blocking p38 with its inhibitors resulted in the attenuation of caspase activation and CB2-mediated apoptotic response. However, this CB2-mediated activation was only reported in leukaemia cell lines, whereas in glioma cell lines the use of CB1 also recruited p38 and mediated apoptosis. JNK activation was also reported as part of the cannabinoid-dependent cell death. PC12 cell treatment with anandamide caused the phosphorylation of JNK, p38 and ERK1/2. This response was shown to be blocked with the use of the JNK inhibitor dn-JNK.

It is widely reported that PI3K and the MAPK pathway crosstalk at multiple levels of both cascades. The PI3K/AKT pathway imposes both direct and indirect regulation of the MAPK pathways. The indirect activation-loop involves PI3K activation of protein

kinase C (PKC), protein kinase D1 (PKD1) and PLD which were shown to activate the ERK pathway at the three tiers of the pathway. The direct route involves recruitment of Grb2-RasGEF complexes, the ability of AKT to inhibit Raf and p38 activation. However, the inactivation of p38 results in the activation of ERK proteins due to reduced gene expression of the phosphatase MKP2. ERK was shown to inhibit GSK-3 β activation, a substrate of AKT which is part of the positive-feedback loop for PI3K/AKT pathway, and hence causes PI3K/AKT deactivation. It was also observed that ERK1/2 is capable of inducing this inhibitory effect on GSK-3 β indirectly through activation of p90RSK. The induction of Sprouty expression by ERK results in the inhibition of the PI3K/AKT pathway, and induction of apoptosis. PI3K was demonstrated to impose a positive activation of ERK at low concentrations of growth factors, while it was demonstrated that within high concentrations of growth factor ERK induces an inhibitory effect on PI3K/AKT activation. Considering that PI3K/AKT action is mediated close to membranes, this suggests that PI3K regulates the activation of a localised pool of MAPK proteins. This pool can be responsible for eliciting the observed PI3K/AKT-dependent MAPK activation. However, with high growth factor concentrations, all MAPK populations are activated. This global activation imposes a negative feedback loop on PI3K/AKT. This hints at a spatial as well as temporal regulatory element at play. Feedback mechanisms (and thus crosstalk) are an integral part of the temporal regulatory element of signal transduction. Our multi-compartment agent based models (ABMs) of the MAPK pathway demonstrated that altering the temporal-spatial elements of MAPKK and MAPK resulted in the emergence of differential MAPK activation behaviour. Given the previous points, and considering that a population of the CB1 receptors were

	Transfection condition 1	Transfection condition 2	Transfection condition 3	Transfection condition 4	Transfection condition 5	Transfection condition 6
pTK-RLuc + Renilla construct	+	+	+	+	+	+
pFA-CHOP	-	+	+	+	+	+
pFC-MEK3	-	-	+	+	+	+
Trb1	-	-	-	++	-	+
Trb2	-	-	-	-	++	+

Appendix D, Table 1 TRIB transfection conditions using the PathDetect System_ HeLa cells were co-transfected with the DNA plasmids shown on the first column on the right. Each column shows a transfection condition a triplicate of wells was exposed to. The plus sign (+) signifies the presence of the plasmid in the transfection mix, the minus sign (-) signifies the absence of that plasmid from the transfection mix; while ++ signifies double transfection of the plasmid.

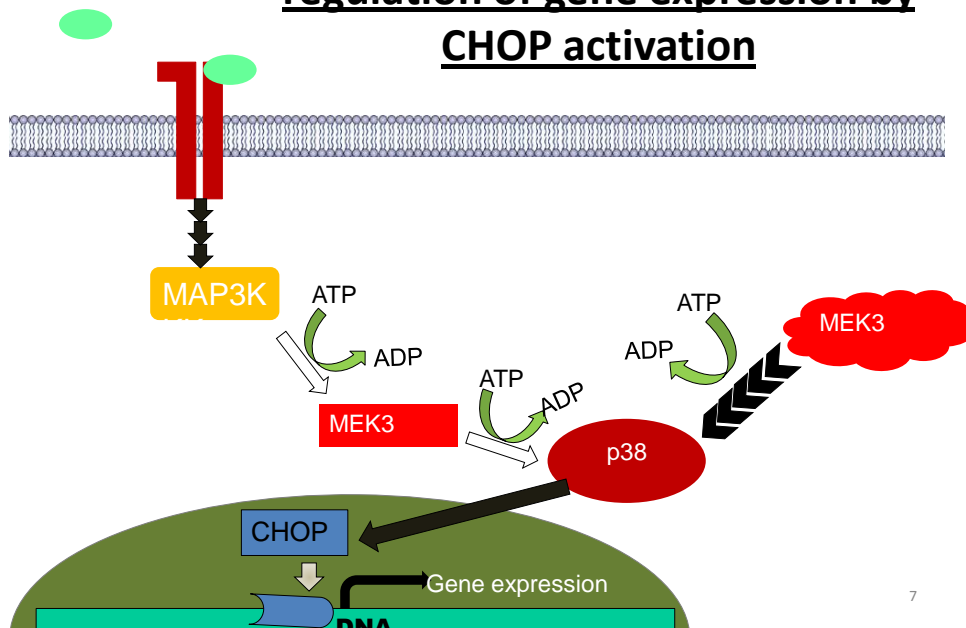
illustrated to reside in the endosomal compartment, cannabinoid-dependent signalling with the PI3K/AKT-MAPK crosstalk presented an ideal system to investigate the temporal and possible spatial modulation of the MAPK pathway in vitro to expand, optimise and improve the current ABM. Thusly, we attempted to examine the important protein-protein interactions, and protein-complexes, involved in PI3K/AKT-MAPK crosstalk, which mediate THC-dependent cell death.

b. Materials and methods.

i. Cell culture and transfection

HeLa cells were used for the transfection and Luciferase assay. HeLa cells were maintained in growth media (Dulbecco's modified Eagle's medium (DMEM) supplemented with 10% Fetal Bovine Serum (FBS), penicillin streptomycin and non-essential amino acids). Cells were seeded into 96 well plates at a density of 5×10^3 cells per well, and were incubated overnight at 37°C, and 5% O₂, to reach 40-80%

P38 MAPK pathway activation & regulation of gene expression by CHOP activation



Appendix D, Figure 1 A schematic representation of the PathDetect system in the presence of constitutively active MEK3 mutant Activation of membrane receptors such as TLR results into the activation and recruitment of the p38 pathway. p38 is phosphorylated by the MAPKK MEK3 (represented here as the red rectangle) and once it is activated it translocates to the nucleus and activates a number of transcription factors including Pfa-CHOP. Activation of CHOP allows it to bind to its DNA binding site at a promoter region, and thus initiate gene expression. In the PathDetect system, these characteristics are used, with plasmid DNA coding for luciferase enzyme driven by the yeast CHOP promoter, CHOP construct codes for a fusion protein with a yeast DNA binding domain and a mammalian activation site. The cells are also transfected with a pFC-MEK3 construct coding for a constitutively active MEK3 mutant (represented here as the red cloud). Thus luciferase will only be expressed if the chimerical CHOP binds to its promoter site and once constitutively active MEK3 is transfected p38-mediated luciferase expression will be at maximum level.

confluency prior to transfection. Transfection was carried out using PolyFect following the manufacturer's instruction. Wells were transfected with Renilla plasmids (pTK-RLuc or EF1), pFR-Luc plasmid, pFA-CHOP plasmid, pFC-MEK3 plasmid and Trb1 and/or Trb2 plasmids. When it was necessary, a sufficient amount of pcDNA3.1 empty vector was also used to allow a constant amount of DNA (100ng) to be transfected per well. The transfection was carried out as shown in Table 1. After 3 hours of transfection, the transfection media was discarded and replaced with growth media. The cells were then incubated overnight at 37°C and 5% O₂, then assayed using the Luciferase assay. For a quantitative measurement of transfection efficiency, wells were also transfected with a green fluorescent protein (pEGFP-N1)

construct. Appendix D, Figure 1 shows the design and the mechanism of action of the system.

ii. *Tribbles siRNA Knock Down (K.D)*

HeLa and U87 cells were plated on 150 mm and/or 100 mm dishes. HeLa cells were seeded at 6×10^6 cells per 150 mm, and 3×10^6 cells per 100 mm dish, and U87 cells were seeded at 1×10^6 cell per 100 mm dish. Cells were left overnight at 37°C and 5% O₂. siRNA for Trib1, Trib2, TRIB 3, and scrambled siRNA, were prepared at stock concentration of 20µM. For each HeLa 150 mm dish a 0.267 µM solution of the appropriate siRNA primer solution was prepared in DMEM, while 90ul of DARMAFECT was added to DMEM. Both DMEM mixes were left to incubate for 5 minutes at room temperature (RT). DARMAFECT-DMEM solution and siRNA-DMEM solutions were mixed thoroughly and left to incubate for 20 minutes at RT. Culture media was aspirated from the cultured 150 mm dishes and replaced with 4ml antibiotic-free complete media. This was “topped up” with 6ml of siRNA transfection solution. The cells were left to incubate overnight at 37°C in 5 % CO₂. The siRNA transfection-media was replaced with complete media after an overnight incubation. Cells were left in the complete media for 4-6 hours (h) and then were prepared for the following step.

1. *RNA isolation and Real-time quantitative PCR (RT-qPCR)*

2. RNA isolation:

siRNA K.D. was measured with qPCR. HeLa cells were seeded into 100mm dishes at a density of 8×10^5 cell/dish. For siRNA transfection 0.267 µM of the appropriate

siRNA primers were dissolved in DMEM and left to incubate at RT for 5 minutes. 45ul of DARMAFECT was mixed thoroughly with 1.44 ml of DMEM, and was left to incubate for 5 minutes at RT. siRNA-DMEM solution was mixed with the DARMAFECT-DEMEM solution thoroughly, and was left at RT for 20 minutes to incubate. Culture media was replaced with fresh antibiotic-free complete media (7ml per 100 mm dish). The siRNA transfection solution was added to the cells. The cells were left to incubate for 24 hours at 37⁰C in 5 % CO₂. The media was replaced with complete media after 24 hours, and cells were left for 4-6 hours then lysed for RNA isolation. RNA isolation was carried out at RT according to standard protocol. Briefly; Cells were washed with ice cold PBS twice, and then lysed by the addition of 500ul of TRIZOL reagent/ 100 mm dish. The cells were scraped from the dishes using cell scrappers. The cell lysates were then transferred to the appropriate eppendorfs. 100ul chloroform was added per eppendorf and was mixed thoroughly with the cell lysates. The eppendorfs were centrifuged at 12000 rpm for ten minutes at 4⁰C. This was to allow for phase separation between RNA, DNA and proteins. Following centrifugation the top RNA phase was delicately collected into new eppendorfs. 100ul of isopropanol per sample was added to precipitate the RNA. The samples were then incubated at -20⁰C for 20 minutes, and afterwards centrifuged at 12000 rpm for ten minutes. The supernatant was carefully collected and the RNA pellet was washed by the addition of 70% ethanol (500µl/eppendorf). The samples were mixed thoroughly, and then centrifuged for ten minutes at 12000 rpm and 4⁰C. Afterwards, the supernatant was removed, and the residual ethanol was air-dried (inside a vacuum hood) for 5 minutes. The RNA samples were suspended in 40µl MiliQ water per sample. 3µl of each RNA sample was aliquated to be used for qPCR analysis, while the remaining volume was stored at -80⁰C for future analysis.

Real-time quantitative PCR (RT-qPCR):

cDNA was obtained using Transcriptor (Roche Applied Science). Real-time quantitative PCR assays were performed using the FastStart Universal Probe Mastermix with Rox (Roche Applied Science), and probes were obtained from the Universal ProbeLibrary Set (Roche Applied Science). Amplifications were run in a 7900 HT-Fast Real-Time PCR System (Applied Biosystems). Each value was adjusted by using 18S RNA levels as a reference.

iii. Tetrahydrocannabinol (THC) survival assay

HeLa cells and U87 cell lines were transfected with control and Trib1, 2 and 3 siRNAs after seeding them on 100 mm dishes, as described above. After changing the media to complete media, the cells were left for 6-24 h, then were re-plated into 12 well plates at a density of 2×10^5 cell per well for U87 cells, and 1×10^5 for HeLa cells. The plates were left overnight, and then the media was changed to 0.1% FBS. This was left on for 3-4 hours, then the cells were treated with THC at the following concentrations: 0, 1 μ M, 3, μ M, 4 μ M, 5 μ M and 6 μ M . THC treatment was left for 72 h. The cell's survivability was then assayed using the MTT survival assay.

3-(4,5-dimethylthiazol-2-yl)-2,5-diphenyltetrazolium bromide (MTT) Tetrazolium survival assay

MTT solution was heated to 37°C prior to aspiration of THC containing media from cells. Once THC media was aspirated from the cells, 1ml of MTT solution was added

per well. The plates were incubated at RT for 3-4 hours. The MTT solution was aspirated and 1ml of Isopropanol was added per well. The cells were put on a plate shaker for 1-2 minutes. 200µl from the wells were aliquoted into 96 well-plate. Cell viability was measured by microplate at 570 nm.

iv. Co-Immunoprecipitation (CO-IP)

1. Covalent coupling Trib3 antibody to protein G-sepharose

The protein G-sepharose was equilibrated by washing the beads five times with PBS. Trib3 antibody (Trib3-ab) was mixed with G-seph at a ratio of 1ug antibody: 2µl Gseph up to 4 ml. This was left to mix overnight at 4°C on a rotating wheel. Trib3-ab-Gsaph conjugate was washed three times with 0.1 M Na-Borate pH 9.3. Trb3-ab-Gsaph conjugate was left to sediment, and then the supernatant was aspirated. The conjugated beads were then re-suspended in 10 volumes of 0.1 Na-Borate pH 9.3, and freshly added dimethyl pimelimidate dihydrochloride (DMP), to a concentration of 20 mM. The Trib3-ab conjugated beads were then put in a rotating wheel to mix for 30-60 minutes at RT. The beads were then spun down, the supernatant was removed carefully, and then re-suspended in another 10 volumes of 0.1 M NaBorate pH 9.3 containing 20 mM DMP. The Trib3-antibody-bead conjugate was put on the rotating wheel for mixing for 30 minutes at RT. The beads were spun gently and then washed four times with 50 mM Glycine at pH 2.5. The conjugated-beads were neutralised by washing them twice with 0.2 M Tris-HCl at pH 8.0. The Trib3-antibody-bead conjugates were re-suspended in 10 volumes of 0.2 M Tris-HCl at pH

8.0, and then mixed gently using the rotating wheel for 2 hours at RT. The antibody-bead conjugates were then re-suspended in PBS and were stored at 4°C. This results in a solution with a 1:1 ratio between Trib3-ab conjugated beads and PBS

2. Covalent coupling Trib3 antibody to protein G-sepharose

< HeLa cells were seeded on 150 mm dishes, and transfected with siRNA as described above. However, for CO-IP to ensure a high level of protein, two dishes were used per treatment. After transfection the media was aspirated from the cultures and washed twice with 20 ml of ice-cold 1 X PBS. PBS was aspirated thoroughly and 100µl of ice-cold lysis buffer per culture dish. Lysis buffer was prepared as described above. The cells were then methodically scraped using cell scrapers, and the cell lysates were collected into eppendorfs. The lysates were sonicated, then the samples were centrifuged at 14000 rpm at 4°C for 25 minutes, and then the supernatant was collected and the samples were placed on ice. 10µl per sample was used to measure the levels of protein collected using a Bradford assay. After the calculation of protein levels 1mg of the cell lysates were incubated with 10µl of the antibody-free bead slurry at 4°C for 30-60 minutes on a rotating wheel. The samples were then centrifuged for 1 minute at 4000 rpm and the supernatant was collected. 30µl of the supernatant was incubated with 80ug: 80µl of the Trib3-ab conjugated beads (160µl of the Trib3-ab conjugated beads in PBS). The rest of the supernatant was stored at -80°C. The incubated samples were incubated overnight at 4°C on a rotating wheel. The samples were centrifuged for 1 minute at 4000 rpm at 4°C. The supernatants were delicately aspirated and discarded. The

bead palette was washed four times with 500 μ l of lysis buffer. This was followed by two washes with the kinase buffer (25 mM HEPES with pH 7.5 and 50 mM KCl). 20 μ l of 1 x β -mecapthaethanol-free loading buffer was added per sample. The samples were then collected by spinning through SpinX columns for 3 minutes at 14000 rpm at 4°C. To each sample 5 μ l of 5 X loading buffer (containing β -mecapthaethanol) was added. The samples were heated to 95°C for three minutes. The samples were either loaded onto SDS-PAGE gels or stored at -80 °C. The volume of samples loaded into the wells was 25 μ l. Protein ladder was also loaded on to the gel. Gels were run at 90 volts (V) for 1 h, or until the dye front reached the bottom of the gel. The electrophoresis buffer was discarded and gels were obtained by opening the glass casts. The proteins were then transformed from gels to Polyvinylidene Difluoride (PVDF) membranes using the wet transfer method. The PDVF membranes were activated by immersion in methanol for approximately a minute. A transfer cassette was used to create a transfer stack. The transformation stack was composed of the SDS-PAGE gel and the PDVF membrane sandwiched between layers of filter papers and fibre-pads, all soaked in transfer buffer (25 mM Tris, 192 mM glycine, pH 8.3, 20% (v/v) methanol and 0.1% (w/v) SDS). The structure of the sandwich is as shown in Figure 2. 3. The sandwich was compressed with rollers to ensure there were no bubbles present. The cassette was closed tightly and placed in the transfer tank, which contained an ice cooling unite, and was filled with fresh transfer buffer. The transfer was done by running the current through at 90-100 V for 60-90 minutes. After transfer, the membrane was washed with TBST buffer and stained with ponceau red, 1 minute with agitation. The membrane was washed with undistilled water extensively to view the protein bands on the membrane. Once the bands were visible, the membrane was washed extensively with undistilled water

until ponceau S red dye disappeared (to ensure the complete transfer of proteins to the membrane). The membrane was then blocked for 1 h at RT with blocking solution (5% of fat-free milk) with gentle rocking on an orbital shaker. For protein detection, the blocking solution was discarded and the membrane was washed five times with TBST (3 minutes per wash). The membrane was left to incubate with the primary antibody solution at 4°C for 24-72 hours, while rocking gently on an orbital shaker. The primary antibody solution was discarded and the membrane was washed three times with TBST (3-5 minutes per wash). After the washes, the membrane was incubated with the secondary antibody solution for 60-90 minutes on the shaker at RT. After the secondary antibody incubation, the membrane was washed with TBST twice for 5 minutes and then was prepared for development. For the development of the membrane, the Bio-Rad ECL kit was used according to the manufacturer's instructions at RT. Briefly; horseradish peroxidase (HRP) substrate solution was prepared by the addition of kit components 1:1 to make a 7 ml solution. This was vortexed. The membrane was transferred to the developing cassette fac-up, and the HRP solution was immediately poured to completely cover the membrane. The membrane was covered with a plastic film, and bubbles were removed by passing a roller on top, and the cassette was closed. 3-5 minutes of incubation was allowed and then the development was carried out inside a dark room at RT. An X-ray film was briefly placed on top of the membrane for exposure, and then the film was imaged using digital imager.

Western blotting

Western blotting was performed on HeLa cells after they were seeded on 10 mm dishes, and were transfected with TRIB family siRNA, as described above. The media was aspirated from the cultures and washed twice with 3ml of ice-cold 1 X PBS. PBS was aspirated thoroughly and 150µl of ice-cold lysis buffer per culture dish. Lysis buffer was prepared as mentioned in the methods section. The cells were then methodically scraped using cell scrapers, and the cell lysates were collected into eppendorfs and were then sonicated. The samples were centrifuged at 14500 rpm at 4°C for 25 minutes, and then the supernatant was collected and the samples were placed on ice. 10µl per sample was used to measure the levels of protein collected, and the rest of the samples were stored at -80°C. An equal volume of Laemmli sample buffer was added per sample (140µl/sample). The samples in the Laemmli sample buffer were then boiled to 100°C for 5 minutes and aliquoted, and were then stored at -20°C. After the calculation of protein levels using the Bradford assay, equal amounts of protein-samples were loaded into the wells of the SDS-PAGE gel. The gel running procedure, gel to membrane transfer, membrane blocking and incubation with primary and secondary antibodies were similar to the description above at the co-IP section. Dilution from all primary antibodies was normally 1:1000, except for B-actin (1:100000). Secondary antibodies rabbit or mouse (GE Healthcare) dilution (1:5000)

v. Luciferase assay preparation

1. Plasmids (Bacterial transformation and plasmid isolation):

Subcloning efficiency™ DH5α™ competent bacteria cells were transformed with the following plasmids: pTK-RLuc, pFA-CHOP, pFC-MEK3 (part of the PathDetect System (Stratagene)), Trb1 and Trb2 constructs following the supplier's instruction, but briefly: the bacteria were thawed on ice, 3 µl of bacteria were mixed with 2 µl of either of the plasmid constructs, the mixture was left on ice for 30 minutes followed by a heat-shock at 42°C for 40 seconds. The mixture was left to cool for 5 minutes on ice, then was added to 1ml of antibiotic-free LB-broth in a 50 ml Falcon tube, and was left to grow 30-40 minutes at 37°C. 100 µl of the (bacterial mixture in LB-broth) was used to cover the surface of an LB plate containing 100 µg/ml ampicillin. The dish was incubated overnight at 37°C. For plasmid purification, transformed bacterial colonies were selected to be grown in 50 ml LB-broth containing 100 µg/ml ampicillin for 18 hours, the bacteria were then pelleted using the centrifuge. The plasmid isolation was performed using Invitrogen midi-kits using the vacuum method, according to the manufacturer's instruction. The concentration of the isolated plasmid was measured using the NanoDrop spectrophotometers (Thermo Scientific).

2. Restriction enzyme digests and gel electrophoresis

< After plasmid isolation, to confirm that the transformation and isolation procedures were successful, restriction enzyme digests were carried out. For pTK-RLuc Hind III and Xba I with enzyme buffer 2 were used, pFA-CHOP was digested using BamH I

and Acc65 I restriction enzymes with buffer 3, pFC-MEK3 digestion was using Acc65 I restriction enzymes with buffer 3, while Hind III enzyme with enzyme buffer 2 was used to digest the Trb1 construct. Briefly, a 30 μ l mix containing 2 μ l of DNA, 2 μ l of restriction enzyme buffer, 1 μ l of restriction enzyme and an appropriate volume of dH₂O was used. The mixes were left in the incubator at 37°C for 1 hour for complete digestion. 2 μ l of loading buffer was added to the digested mix and then loaded onto a 1% agarose gel and run for 40 minutes at 100V.

3. Fluorescence microscopy

Transfection efficiency was determined via transfection of HeLa cells with 100ng/well of pEGFP-N1 construct, using the same transfection protocol mentioned above. Transfected cells were viewed overnight at room temperature using a laser-scanning microscope (Molecular Dynamics, CLSM 2010). Laser power was set to 10 mW. pEGFP-N1 was excited at 488 nm with an argon laser, and fluorescence was collected using a band pass filter set at 530nm. The cells were viewed using a x40 objective lens.

4. Luciferase assay: Fluorescence microscopy:

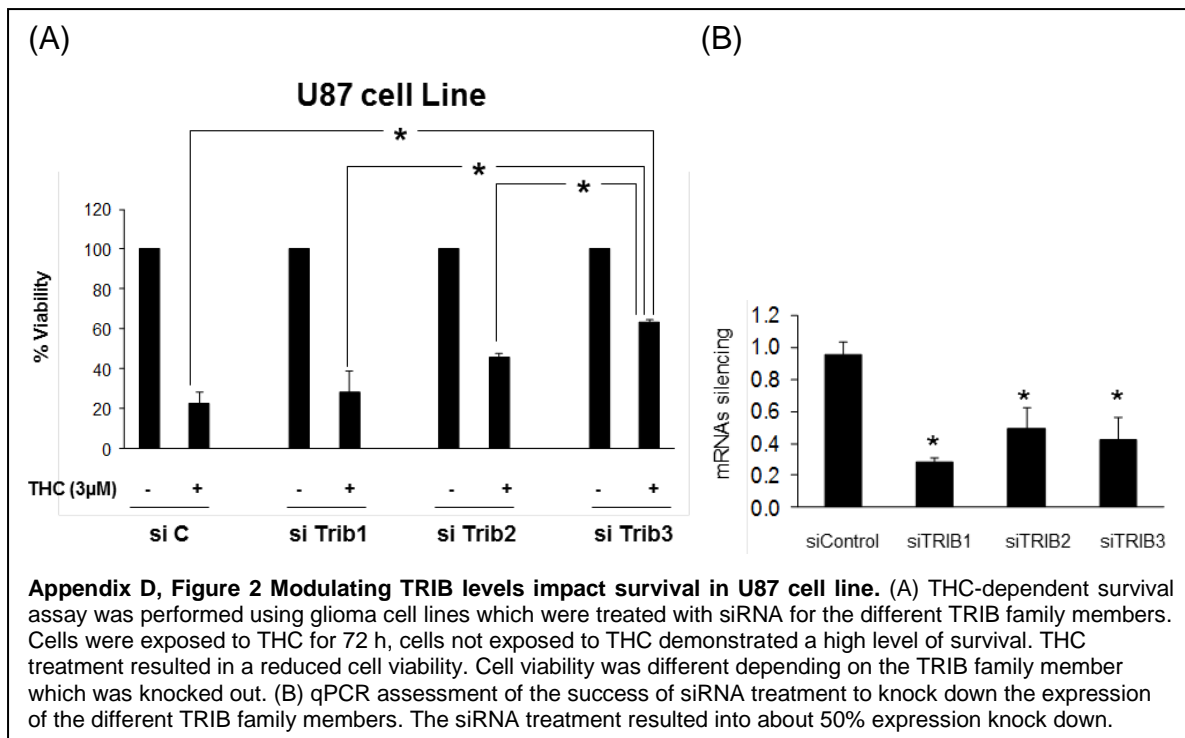
Transfected HeLa cells were prepared as follows: the growth media was discarded from the wells and then washed once with 150 μ l/well of Phosphate Buffered Saline (PBS), PBS was aspirated out, and 25 μ l of passive lysis buffer (PLB) was added per well. The PLB was left on the cells for 10-15 minutes. 5 μ l of cell lysate was transferred to a 384 well reading plate, and 10 μ l/well of luciferase assays reagent II

solution was added, and the Firefly luciferase activity was measured. This was followed by the addition of 10 µl/well of Stop & Glo® reagent solution and Renilla luciferase activity was measured. The plate was read using a Thermo Fisher Scientific Varioskan® Flash plate reader.

c. Results

i. Altering TRIB proteins levels cause a differential response to apoptosis

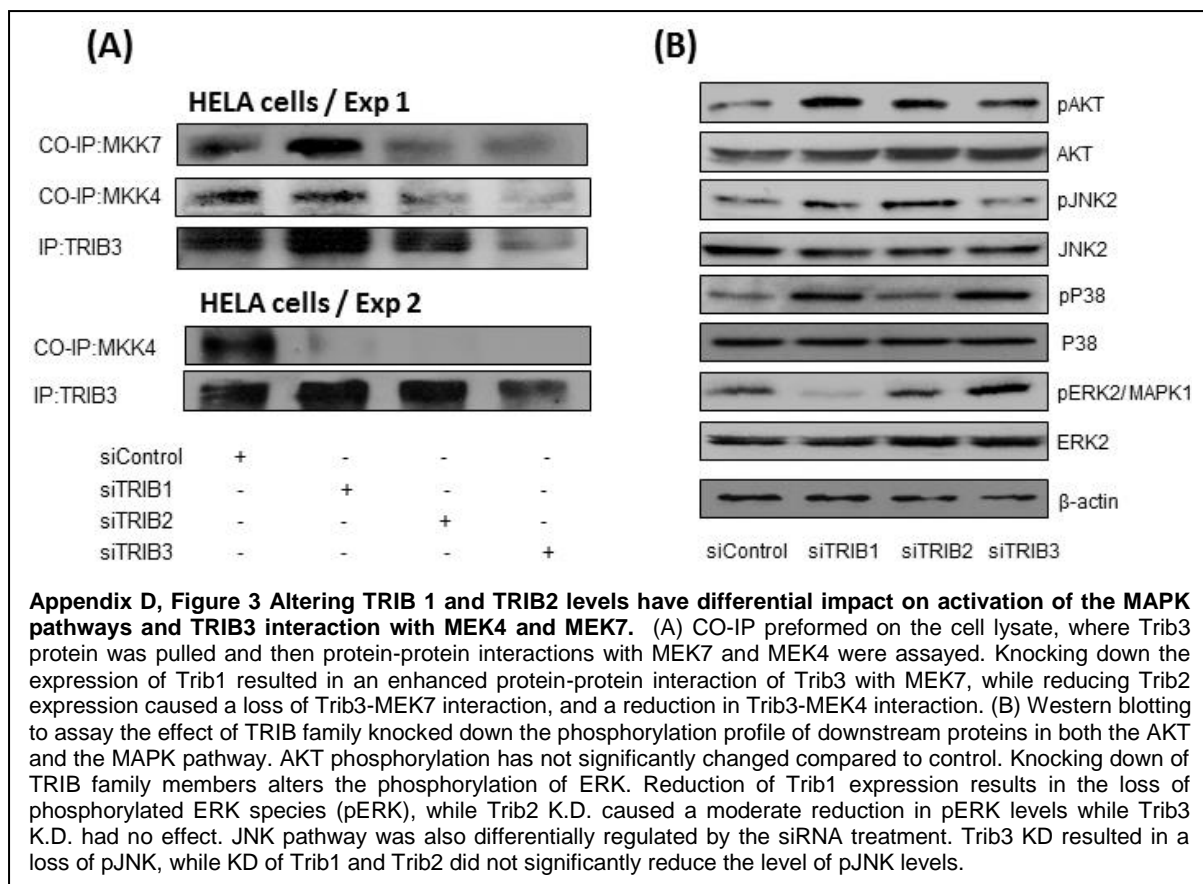
. < The differential effects of the TRB protein family was investigated in the context of cellular response to stress. This was done by assessing cellular responses while different TRB members were knocked down (KD). The ability of cells to undergo cell death due to exposure to THC was used as the measured output. It was shown previously that glioma cell treatment with THC caused an enhancement of cell death. This was reduced with the KD of TRB3 from these cells. In Figure 3. 6. 1 (A), Trib3 KD cells replicated the previous pattern of increased survival after treatment with THC in comparison to the negative control. On the other hand, the survival of Trib1 KD cells exposed to THC was level, and largely lower compared to THC untreated cells. Yet, the low survival of TRB1 KD cells was not markedly different from the levels with the control siRNA treatment exposed to THC. Also Trib2 KDed cells show a moderate apoptotic response to THC in comparison to the scrambled control. However, they demonstrate a better survival rate when they are not treated with THC. However, there is no statistical difference between the survival of cells with TRB2 and TRB1 KD exposed to THC. This differential apoptotic response observed



with the KD of different TRIB family members was also observed in the same experiments done on HeLa cells.

ii. Altering TRIB proteins levels cause a differential response to apoptosis

< The differential effects of the TRIB protein family was investigated in the context of cellular response to stress. This was done by assessing cellular responses while different TRIB members were knocked down (KD). The ability of cells to undergo cell death due to exposure to THC was used as the measured output. It was shown previously that glioma cell treatment with THC caused and enhanced cell death (Aguado et al., 2007, Blazquez et al., 2008a, Blazquez et al., 2008b) which is rescued



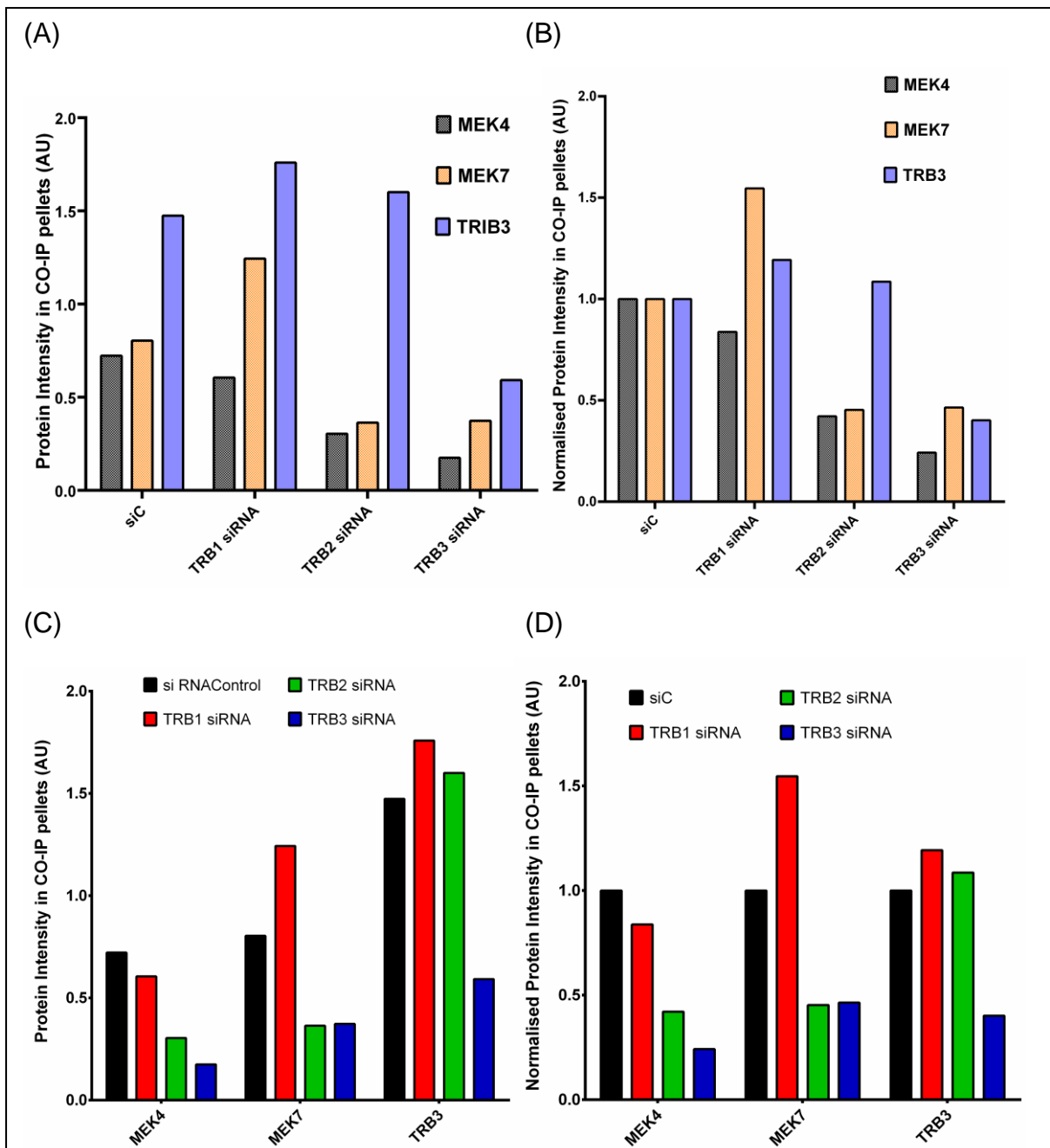
with TRIB3 KD from these cells. These observations were replicated in Appendix D, Figure 1 (A). On the other hand, the survival of TRIB1 KD cells exposed to THC was notably lower compared to THC untreated cells, yet it was not greatly different from the positive control (scrambled siRNA with THC exposure). Also TRIB2 KDed cells show a moderate survivability when treated with THC, in comparison to the scrambled siRNA treatment. Nonetheless, they demonstrate a better survival when not treated with THC. There is no statistical difference between the survival of cells with TRIB2 and TRIB1 KD exposed to THC. This differential apoptotic response observed with the KD of different TRIB family members was also observed in the same experiments done on HeLa cells.

Kinases activated	Trib1 K.D	Trib2 K.D	Trib3 K.D
AKT	+	+	+
ERK2	-	=	+
JNK2	+	+	=
P38	+	=	+

Appendix D, Table 2 Effects of knocking down (KD) tribbles family members on the activation of AKT and MAPKs. These were postulated from the western blots shown in Appendix D, Figure 2 (B). The activation was compared to control siRNA treatment. + indicates and enhancement in activation, = imply no change in activity in comparison to the control and – show a reduction in activity.

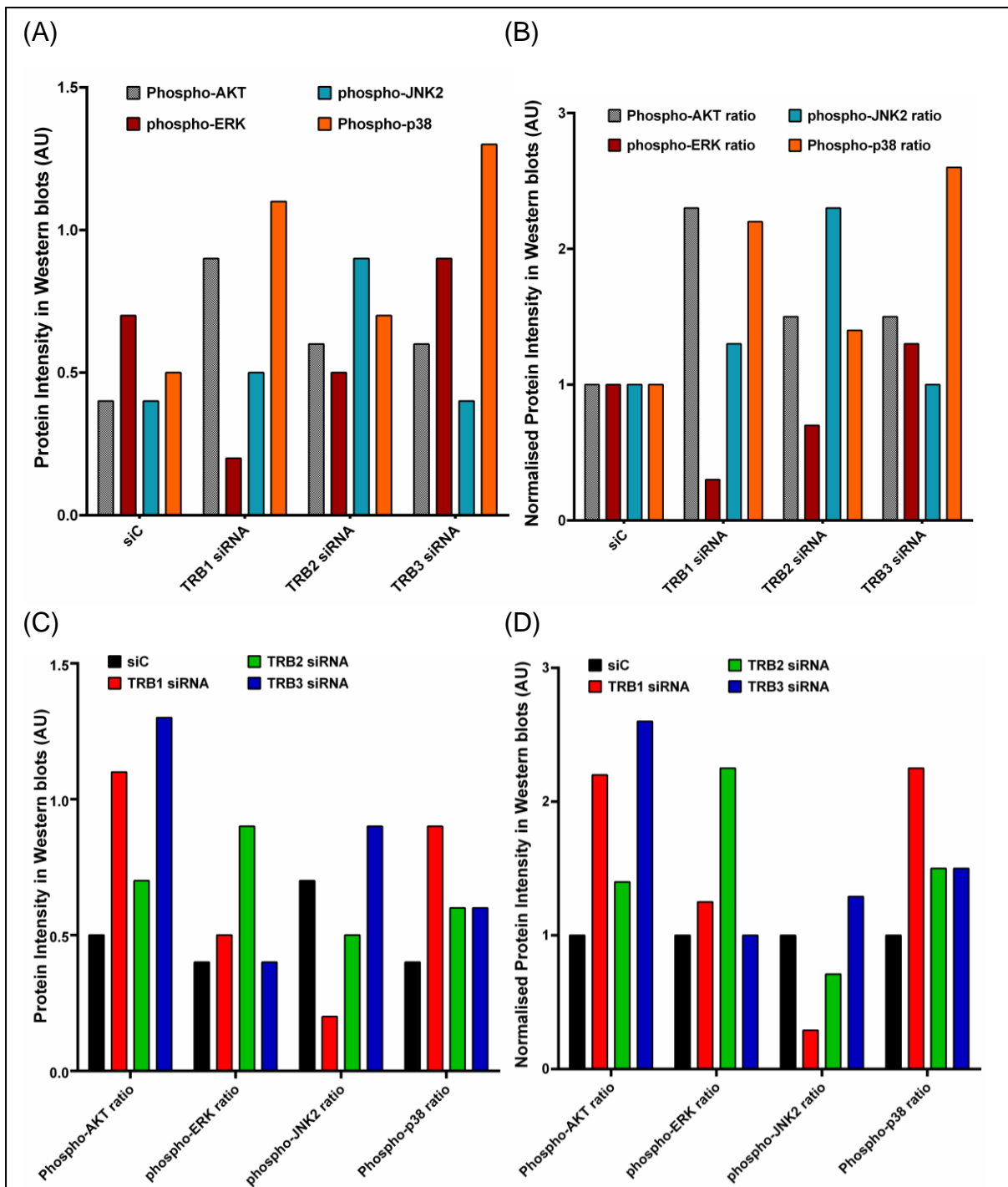
iii. Knock down (KD) of tribbles family members' expression levels influence protein-protein interaction between TRIB3 and its interaction partners.

< To elucidate how knocking down the expression of the different TRIB members resulted in a differential cellular response to THC treatment, their ability to form partnerships with other proteins was investigated. This was done using western blotting and CO-IP. As TRIB3 was shown to play a role in mediating THC-dependent cell death (Salazar et al., 2013), the focus was on protein complexes containing TRIB3. Consequently, TRIB3 antibody conjugated beads were used to pull the protein complexes, and interactions of TRIB3 with ERK, AKT, JNK, MEK4 or MEK7 were assessed while other TRIB family members were knocked down (KDed). Appendix D, Figure 2 (A) and Appendix D, Table 1 show a differential binding pattern of TRIB3 with binding partners as a result of knocking out the other TRIB members. Cells treated with scrambled siRNA demonstrate low levels of AKT, JNK2 and p38 activation, while ERK activation was moderate. Additionally, TRIB3 formed complexes with MEK7 and MEK4, with a stronger MEK7 signal observed.



Appendix D, Figure 4 Analysis of CO-IP shown in Appendix D, Figure 2.(A). (A) The intensity of protein bands were measured and analysed. The intensity of each protein band is displayed and grouped with respect to the siRNA treatment. The graph demonstrate that knocking down TRIB family members alter TRIB3 interaction with other proteins. (B) The band intensities were normalised to the siRNA control treatment. It illustrates a modulating TRIB1 and TRIB 2 induce different effects on TRIB3 interactions with MEK7 and MEK4. (C) Graph (A) was altered to show the effect of siRNA treatment with respect to TRIB3 interaction partner, whereas (D) .is a modification of normalised data displayed in (B). The data displayed are from one experiment.

(Appendix D, Figure 3) Knocking down TRIBs resulted in the activation of AKT, nonetheless, variation was observed between all KD treatments (Appendix D, Figure 4 (B) and (C)). With TRIB2 and TRIB3 causing a notable increase in AKT activation, while TRIB2 induced a moderate activation. Simultaneously, TRIB1 KD caused a



Appendix D, Figure 5 Analysis of protein levels observed in Western blots in Appendix D, Figure 2 (B).. (A) The intensity of protein bands were determined and inferred. The intensity of each protein band is displayed and grouped with respect to the siRNA treatment. The phosphorylated proteins were normalised to their corresponding total protein (e.g. AKT, ERK1/2 etc). The graph demonstrates disruption in AKT, ERK, JNK2 and p38 proteins when tribbles were knocked down. The graph also demonstrate a differential effect of altering the expression of each TRIB family member. (B) The normalisation of the data in (A) to the siRNA control. (C) The data in (A) was modified to display the effect of siRNA treatment with respect to each of the assayed proteins. (D) The data in (C) was normalised to the siRNA control.

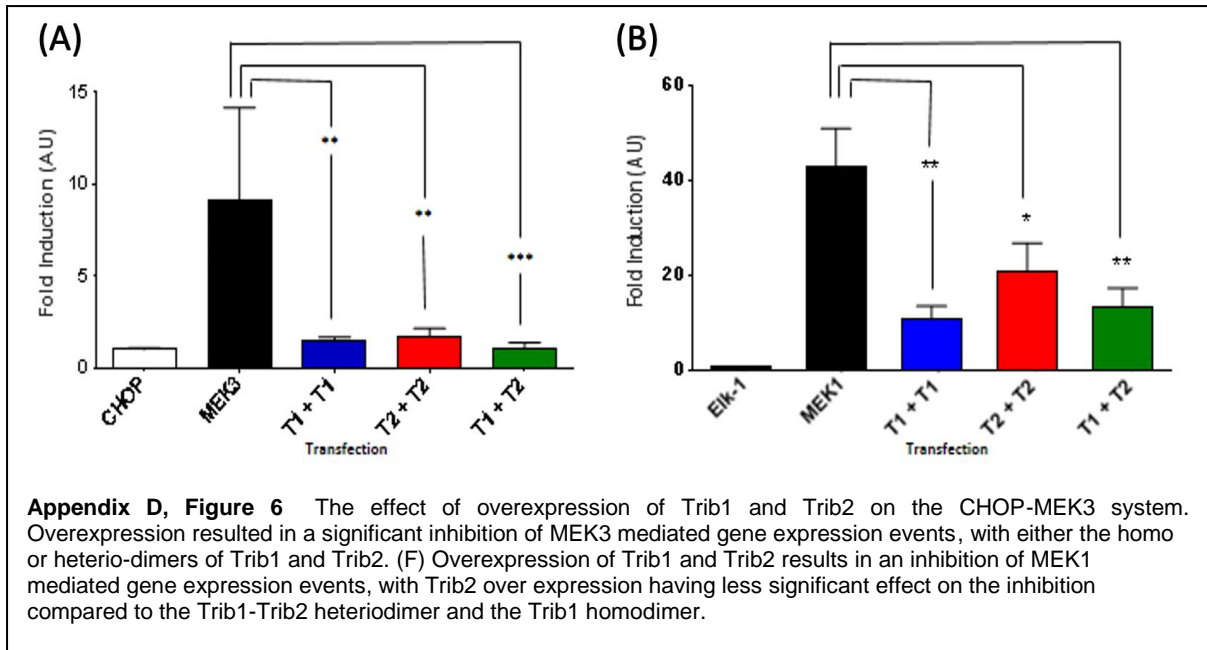
reduction in phosphorylation and activation of ERK compared to siRNA control. In contrast, TRIB1 KD caused an increase in p38 and JNK2 activation (Appendix D, Figure 4) Knocking down TRIB2 did not alter levels of phosphorylated ERK

compared to controls, while in comparison to TRIB1 KD there was an increase in ERK phosphorylation and activation. Furthermore, similar to TRIB1 KD, JNK2 activation were increased compared to control, while phosphorylated p38 levels were not affected. TRIB3 interaction with MEK7 and MEK4 were reduced in comparison to control. Furthermore, when MEK7 interaction was assessed, only TRIB1 KD enhanced MEK7 protein-protein interaction compared to control, while other KDs showed a reduction in relation to siRNA control (Appendix D, Figure 3)

iv. Over expression of TRIB1 and TRIB2 are capable of considerable reduction of p38 and ERK mediated gene expression events but with no notable difference between homo and heterodimer species.

TRIB 1 and TRIB 2 plasmids were overexpressed in HeLa cells to investigate if shifting the balance in favour of one family member results in a shift towards mediating an ERK or p38 mediated signalling response. The results in Appendix D, Figure 5 (A) show that the MEK3-CHOP system was sensitive to the presence of both TRIB1 and TRIB2 in both the hetero- and homo-dimer combination. Statistically, the heterodimer induced a more significant inhibitory effect on CHOP-dependent gene expression events compared to the two homodimers. The observations suggest an element of redundancy between TRIB1 and TRIB2.

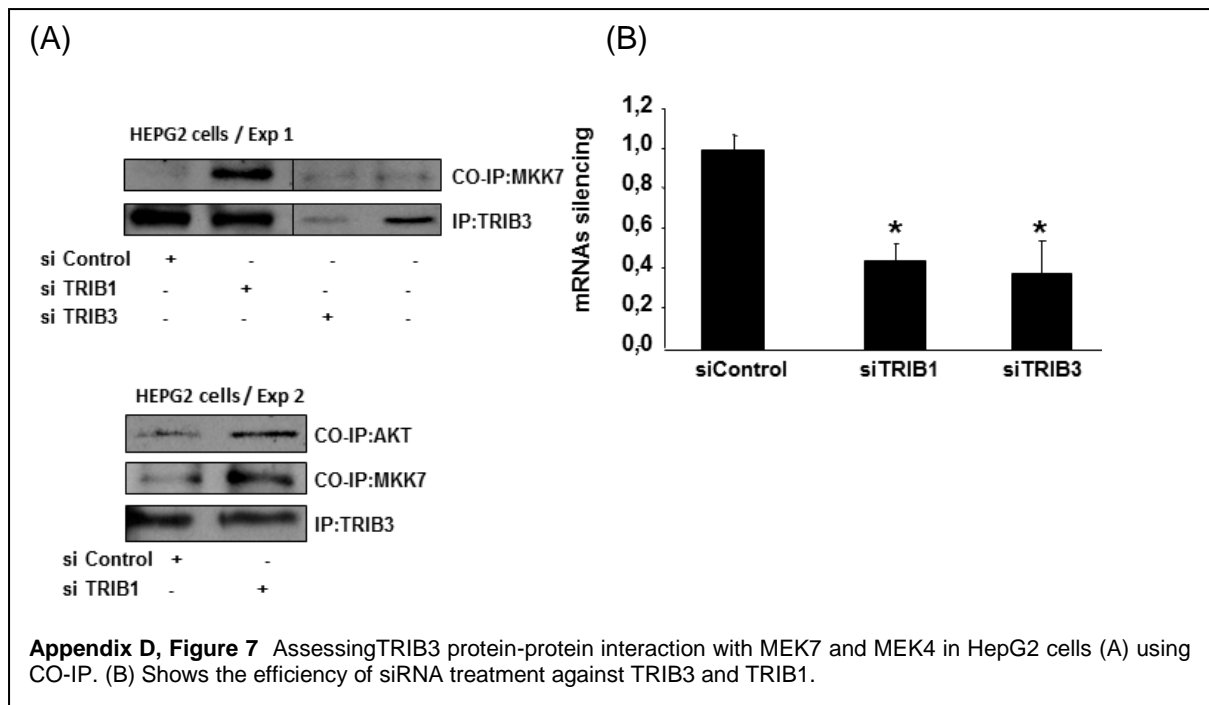
When TRIB1 and TRIB were overexpressed in the MEK1-Elk system, MEK1-dependent gene expression events by 76.6% for the TRIB1 homodimer, 53.5% for



the TRIB2 homodimer and 67.4% for the heterodimer. However, the inhibition of MEK1 mediated gene expression was stronger with the over expression of TRIB1 homodimers to that of TRIB2 homodimer overexpression (Appendix D, Figure 5). In MEK1-Elk system, the heterodimer also showed a stronger inhibition compared to that of TRIB2.

d. Discussion

< The experimental data presented shows that altering the expression of the different tribbles family members in both U87 and HeLa cells led to a different survivability in response to THC treatment. Cannabinoid mediated apoptosis and cell death in cancer cells is well documented. Some cannabinoids are capable of inducing apoptosis exclusively in cancer cells while inducing no effect, or achieving low potency in normal cells [R]. Cannabinoids (THC in particular) were shown to mediate antitumor effects both in vitro and in vivo. The mechanisms cannabinoids are thought to use are thought to be through interference with proliferation and apoptosis



signalling. It is widely established that the Akt-mTOR axis and the MAPK pathways are the main signalling networks which mediate the cannabinoid antitumor effects. Activation of the p38 and ERK pathways, and inhibition of the AKT-mTOR axis, are believed to be the main players which promote cell death. TRIB3 was recently shown to play a part in mediating THC induced apoptosis in glioma cell carcinomas and hepatocellular carcinoma (HCC) HepG2 cells (Örd and Örd, 2005, Vara et al., 2011).

There is a reported overlap between AKT and the MAPK network in mediating the cannabinoid induced proapoptotic effects. In addition TRIBs inhibits ERK. p38 and JNK pathways differentially (EKT). The results presented in this section show that TRIB1 and TRIB2 knock down in cells treated with THC for 72 hours demonstrated similar low survivability compared to scrambled siRNA cells (Appendix D, Figure 1). In glioma carcinomas and HepG2 cells THC reduced cell survivability by inhibition of the AKT-mTOR axis (Greenhough et al., 2007, Preet et al., 2008, Salazar et al., 2009, Salazar et al., 2013), and this process involved the participation of TRIB3.

TRIB3 inhibition of AKT activation was demonstrated in liver cells exposed to insulin. The data presented here with the U87 glioma cells are in line with previous findings. Knocking down TRIB3 expression rescued U87 cells from THC induced cell death. This rescue was substantially higher to those observed with TRIB1 and TRIB2 KDed cells. In glioma cells, treatment with THC was coupled with reduced AKT phosphorylation compared to control. However THC treatment in the presence of constitutive active AKT did not affect cell viability and the level of AKT phosphorylation.

Conversely, Ramer et al. showed that HeLa cell viability was not altered after exposure to different THC concentrations (Ramer and Hinz, 2008). Thus, it was concluded that THC had no toxic effects on HeLa cells. They also demonstrated that treatment with THC levels increased activated p38 and ERK levels. Our experiments with THC treated HeLa cells showed the same effect. However, when TRIB members were differentially expressed, cell survivability was reduced. TRIB3 KD caused increases in survivability compared to TRIB1 and TRIB2 KD treatment. To determine how the tribbles family mediate these effects assessment of TRIB3 protein-protein interactions with its binding partners was conducted *via* CO-IP and Western blotting. These alterations also examined the impact on activation of AKT and the MAPK network.

For both the CO-IP and Western blots, TRIB1, 2 and 3 were KDed in HeLa cells, and were not treated with THC (Appendix D, Figure 2, Appendix D, Figure 3 and Appendix D, Figure 4). This was to determine the influence of KD tribbles on protein-

protein interaction partnerships in the absence of THC, therefore reducing a layer of complexity, and therefore assessing the native interaction partnership. Since AKT and MAPK pathways are the main pathways regulating proliferation, apoptosis and survival, we looked at the level of activated proteins of these pathways. The data shows that without THC treatment, knocking down tribbles expression increased the activation of AKT. However, knocking down different TRIB proteins did not have a differential effect on AKT activation. This is consistent with previous observations in HeLa and cancerous cells. The most interesting activation variation observed was of MAPK proteins. The findings strongly support that the main targets of the TRIB protein family are within the MAPK network (Appendix D, Figure 4). With TRIB1 KD, there was a considerable increase in the activation of the AKT and p38 activation, while JNK2 activation was moderate compared to that of the control. Alternatively, ERK1/2 activation was substantially reduced. Compared to the control, knocking down the expression of TRIB2 moderately increased p38 and AKT activation, yet ERK1/2 activation was moderately reduced. Contrariwise, JNK2 activation was enhanced substantially compared to control. This substantial increase in JNK2 activation and the moderate increase in p38 activation were unexpected, as TRIB2 was reported to influence p38 activation (Wei et al., 2012), thus the expectation was that p38 activation will be increased extensively while negligible changes in ERK1/2 JNK2 activation is observed. TRIB3 KD results in a moderate increase in ERK1/2 and AKT activation compared to control, whereas there is an extensive increase in p38 activation. Conversely, JNK2 activation did not change. This was also unanticipated, considering that TRIB3 has been shown to be an important component for the activation of the JNK2. Thus, the envisaged outcome of the KD was an enhanced activation of JNK2 while p38 and ERK1/2 activation is minimal.

The data suggests that each member of the TRIB family modulate two MAPKs negatively, while mediating the activation of another.

TRIB1 KD resulted in considerable inhibition of ERK, and strong activation of p38, while no marked effect was observed with JNK2 activation. The CO-IP conducted on the lysed control cells showed TRIB3 interacts with MEK4 and MEK7 MAPKs (Appendix D, Figure 2 (A) and Appendix D, Figure 3). However, with TRIB1 KD the interaction with MEK7 increased, while interaction with MEK4 was reduced. Previous work had shown that MEK4 interacts mainly with TRIB1 while MEK7 interacts specifically with TRIB3 (Eder et al., 2008, Kiss-Toth et al., 2004, Kiss-Toth et al., 2006, Sung et al., 2006). This was in over-expression experiments of both proteins in HeLa cells. Considering that in over-expression experiments uneasiness usually stems from unspecific binding interactions and false positives. However, EKT et al. show high level of specificity in TRIB interactions with their MAPKK targets. The CO-IP data show that there is alteration in binding specificity with TRIB1 KD. Additionally, EKT et al. had shown that tribbles are capable of forming homo- and hetero-dimers. Considering the EKT results and the CO-IP results, it can be speculated that TRIB1 and TRIB3 form a dimer, and so are part of the MEK4 signalling complex/cluster. TRIB1 can also be part of the MEK7 signalling complex/cluster, as knocking it down increased MEK7-TRIB3 interaction. This increase in MEK7-TRIB3 interaction due to reduced levels of TRIB1 was confirmed in HEPG2 cells (Appendix D, Figure 6). This establishes a direct cause-effect link, as HepG2 cells lack TRIB2 proteins and do not express MEK4. In addition, in HepG2 cells TRIB1 knockdown increased the level of AKT-TRIB3 interaction. Correspondingly, knocking down TRIB2 caused a substantial reduction in MEK4 and

MEK7 interaction with TRIB3. Yet, in TRIB1 KD there was a considerable reduction in the level of activated ERK1/2 and an evident increase in JNK2 activation. These might be attributed to increased numbers of free uninhibited MEK4, due to the absence of TRIB1 in TRIB1 KD, and reduced binding to TRIB3 proteins. In regard to TRIB2 KD, the extensive reduction in TRIB3 interaction with MEK7 and MEK4 result in increased numbers of free and uninhibited MEK4 and MEK7, and consequently increased activation of JNK2 and p38. Also TRIB2 KD causes an increase in active MEK3/6, and ultimately, p38 activation.

In order to collectively explain the outcome of these knockdown experiments, and the effects on cellular response, the MAPK-AKT signalling network as a whole must be considered. Fey et al. had modelled the interaction of the three MAPK pathways and in the presence and absence of activated AKT pathways (Fey et al., 2012). They reported the effects alterations in the dynamic network behaviour had on apoptosis and proliferation. In their model they addressed activating and deactivating inputs involving feedback loops. Since the tribbles family play a role in regulating activity of both pathways, Fey's model is of relevance. Their model suggests that when the AKT pathway is not activated, JNK activation acts as a necessary switch to trigger apoptosis. This switch is modulated by the activity of both ERK and p38 pathways. AKT activation blocked JNK activation via positive feedback, and thus enhanced survival. They showed that under stressful conditions both JNK and p38 activation is enhanced considerably, while ERK activation is substantially reduced. This is in line with what the western blotting data here shows in the event of TRIB1 knock down. Furthermore, their model show that under weak AKT signalling ERK activation

dominates; JNK shows a moderate activation while p38 show minimal activation. This is similar to what the siRNA control data show.

This AKT-MAPK pathway network model by Fey et al. and our HeLa results provide a platform to explain the observation in the THC-induced cell death seen in the U87 glioma cells. In the negative control treatment, p38 and JNK pathways are not activated, while the ERK pathway is active, thus cells survival is high. THC is documented to induce cell death in cancer cells through the inhibition of the AKT pathway via the induction of TRIB3. THC in these cases is regarded as a stress inducing signal. In both the control and TRIB1 knockdowns, cell death is observed the most. This might be due to an increase in the activation of the JNK and p38 pathways (both of which are linked to stress responses), and the inhibition of ERK activation which is responsible for mediating survival. Though there is an increase in AKT activation, TRIB3 is still mediating its inhibitory actions on AKT pathway. Fey's model shows that the output from the crosstalk between p38 and ERK pathways is important for the regulation of JNK and its influence on pro-cell death response. Their model showed that increasing p38 activity reduced ERK activation and that in turn allowed for JNK to mediate cell death. This is what has been observed with TRIB1 KD experiments. With TRIB2 KD, here was a moderate increase in p38 activation coupled with a substantial reduction of ERK activation compared to siRNA control. This was also shown in the Fey et al. model where disruption of p38-ERK cross talk resulted in prevention of JNK mediated apoptosis. The cell survival assay shows that TRIB2 KD cells underwent cell death and their response to THC treatment was markedly different from those with TRIB1 KD with THC exposure. Due to the presence of TRIB3 in the system, and its inhibition of the AKT pro-survival

signal, cell death still prevailed. When the TRIB3 expression was KDed, as reported previously, THC did not induce cell death in both the U87 glioma and HeLa cells, as the TRIB3-dependent inhibition of the AKT pathway was rescinded. However contrary to Fey's model, though p38 was active, ERK activation was not hindered. This suggests that in order for the crosstalk between the p38 and ERK pathways to be efficient TRIB3 is required. Therefore, with no TRIB3 the crosstalk between p38 and ERK pathways is disrupted, and as a result the output into the JNK pathway is affected. Although JNK2 activity was as high in the TRIB3 KD experiment as the control, cell survival overcame cell death induction. In addition to blocking THC-induced cell death via blocking AKT pathway inhibition with TRIB3 KD, it was shown with Fey's model that AKT activation has an inhibitory influence on JNK activation, and thus mediation of apoptotic cell death. That might be what is being observed in the system as a whole when TRIB3 is KDed. What is being observed in glioma cell lines is that THC induces cell death by the regulation of the AKT-mTOR axis via TRIB3. What we show here experimentally is that the AKT-MAPK pathway network/crosstalk should also be considered. This point is valid when it is taken into account that gliomas which are resistant to cannabinoid-induced cell death rely on ampiregulin signalling through the activation of the ERK pathway. In addition they showed that TRIB3 and p8 (another effector in the cannabinoid-induced cell death) expression depend on ERK activation. The important role of the MAPK pathway induction of glioma cell death was further asserted by the development of the small molecule drug Vacquinol-1 as a treatment for glioblastoma multiform, where the authors believe that MAPKK 4 is a critical signalling node in this (Kitambi et al., 2014).

The data presented here suggest that protein-protein interactions within a signalling complex/cluster, in addition to the identity of the proteins in the complex, influence the activation behaviour of the MAPK signalling network. This data provides bases for constructing an ABM model which addresses these issues and their effect on MAPK activation behaviour in time and space.

e. References

AGUADO, T., CARRACEDO, A., JULIEN, B., VELASCO, G., MILMAN, G., MECHOULAM, R., ALVAREZ, L., GUZMAN, M. & GALVE-ROPERH, I. 2007. *Cannabinoids induce glioma stem-like cell differentiation and inhibit gliomagenesis. J Biol Chem*, 282, 6854-62.

BLAZQUEZ, C., CARRACEDO, A., SALAZAR, M., LORENTE, M., EGIA, A., GONZALEZ-FERIA, L., HARO, A., VELASCO, G. & GUZMAN, M. 2008a. *Down-regulation of tissue inhibitor of metalloproteinases-1 in gliomas: a new marker of cannabinoid antitumoral activity? Neuropharmacology*, 54, 235-43.

BLAZQUEZ, C., CASANOVA, M. L., PLANAS, A., GOMEZ DEL PULGAR, T., VILLANUEVA, C., FERNANDEZ-ACENERO, M. J., ARAGONES, J., HUFFMAN, J. W., JORCANO, J. L. & GUZMAN, M. 2003. *Inhibition of tumor angiogenesis by cannabinoids. FASEB J*, 17, 529-31.

BLAZQUEZ, C., GONZALEZ-FERIA, L., ALVAREZ, L., HARO, A., CASANOVA, M. L. & GUZMAN, M. 2004. *Cannabinoids inhibit the vascular endothelial growth factor pathway in gliomas. Cancer Res*, 64, 5617-23.

BLAZQUEZ, C., SALAZAR, M., CARRACEDO, A., LORENTE, M., EGIA, A., GONZALEZ-FERIA, L., HARO, A., VELASCO, G. & GUZMAN, M. 2008b.

Cannabinoids inhibit glioma cell invasion by down-regulating matrix metalloproteinase-2 expression. Cancer Res, 68, 1945-52.

CARRACEDO, A., GIRONELLA, M., LORENTE, M., GARCIA, S., GUZMAN, M., VELASCO, G. & IOVANNA, J. L. 2006a. *Cannabinoids induce apoptosis of pancreatic tumor cells via endoplasmic reticulum stress-related genes. Cancer Res, 66, 6748-55.*

CARRACEDO, A., LORENTE, M., EGIA, A., BLAZQUEZ, C., GARCIA, S., GIROUX, V., MALICET, C., VILLUENDAS, R., GIRONELLA, M., GONZALEZ-FERIA, L., PIRIS, M. A., IOVANNA, J. L., GUZMAN, M. & VELASCO, G. 2006b. *The stress-regulated protein p8 mediates cannabinoid-induced apoptosis of tumor cells. Cancer Cell, 9, 301-12.*

EDER, K., GUAN, H., SUNG, H. Y., WARD, J., ANGYAL, A., JANAS, M., SARMA, G., DUDA, E., TURNER, M., DOWER, S. K., FRANCIS, S. E., CROSSMAN, D. C. & KISS-TOTH, E. 2008. *Tribbles-2 is a novel regulator of inflammatory activation of monocytes. International Immunology, 20, 1543-1550.*

FEY, D., CROUCHER, D. R., KOLCH, W. & KHOLODENKO, B. N. 2012. *Crosstalk and Signaling Switches in Mitogen-Activated Protein Kinase Cascades. Frontiers in Physiology, 3, 355.*

GALVE-ROPERH, I., SANCHEZ, C., CORTES, M. L., GOMEZ DEL PULGAR, T., IZQUIERDO, M. & GUZMAN, M. 2000. *Anti-tumoral action of cannabinoids:*

involvement of sustained ceramide accumulation and extracellular signal-regulated kinase activation. Nat Med, 6, 313-9.

GAONI, Y. & MECHOULAM, R. 1964. *Isolation, Structure, and Partial Synthesis of an Active Constituent of Hashish. Journal of the American Chemical Society, 86, 1646-1647.*

GREENHOUGH, A., PATSOS, H. A., WILLIAMS, A. C. & PARASKEVA, C. 2007. *The cannabinoid delta(9)-tetrahydrocannabinol inhibits RAS-MAPK and PI3K-AKT survival signalling and induces BAD-mediated apoptosis in colorectal cancer cells. Int J Cancer, 121, 2172-80.*

GUZMAN, M. 2003. *Cannabinoids: potential anticancer agents. Nat Rev Cancer, 3, 745-55.*

HERRERA, B., CARRACEDO, A., DIEZ-ZAERA, M., GUZMAN, M. & VELASCO, G. 2005. *p38 MAPK is involved in CB2 receptor-induced apoptosis of human leukaemia cells. FEBS Lett, 579, 5084-8.*

HILL, M. M. & HEMMING, B. A. 2002. *Inhibition of protein kinase B/Akt. implications for cancer therapy. Pharmacol Ther, 93, 243-51.*

HUANG, H. & TINDALL, D. J. 2011. *Regulation of FOXO protein stability via ubiquitination and proteasome degradation. Biochim Biophys Acta, 1813, 1961-4.*

KISS-TOTH, E., BAGSTAFF, S. M., SUNG, H. Y., JOZSA, V., DEMPSEY, C., CAUNT, J. C., OXLEY, K. M., WYLLIE, D. H., POLGAR, T., HARTE, M., O'NEILL, L. A. J., QWARNSTROM, E. E. & DOWER, S. K. 2004. *Human Tribbles, a Protein Family Controlling Mitogen-activated Protein Kinase Cascades. Journal of Biological Chemistry, 279, 42703-42708.*

KISS-TOTH, E., WYLLIE, D. H., HOLLAND, K., MARSDEN, L., JOZSA, V., OXLEY, K. M., POLGAR, T., QWARNSTROM, E. E. & DOWER, S. K. 2006. Functional mapping and identification of novel regulators for the Toll/Interleukin-1 signalling network by transcription expression cloning. *Cellular Signalling*, 18, 202-214.

KITAMBI, SATISH S., TOLEDO, ENRIQUE M., USOSKIN, D., WEE, S., HARISANKAR, A., SVENSSON, R., SIGMUNDSSON, K., KALDERÉN, C., NIKLASSON, M., KUNDU, S., ARANDA, S., WESTERMARK, B., UHRBOM, L., ANDÄNG, M., DAMBERG, P., NELANDER, S., ARENAS, E., ARTURSSON, P., WALFRIDSSON, J., FORSBERG NILSSON, K., HAMMARSTRÖM, LARS G. J. & ERNFORS, P. 2014. Vulnerability of Glioblastoma Cells to Catastrophic Vacuolization and Death Induced by a Small Molecule. *Cell*, 157, 313-328.

KUCAB, J. E., LEE, C., CHEN, C. S., ZHU, J., GILKS, C. B., CHEANG, M., HUNTSMAN, D., YORIDA, E., EMERMAN, J., POLLAK, M. & DUNN, S. E. 2005. Celecoxib analogues disrupt Akt signaling, which is commonly activated in primary breast tumours. *Breast Cancer Res*, 7, R796-807.

LIM, H. J., CROWE, P. & YANG, J. L. 2015. Current clinical regulation of PI3K/PTEN/Akt/mTOR signalling in treatment of human cancer. *J Cancer Res Clin Oncol*, 141, 671-89.

LORENTE, M., CARRACEDO, A., TORRES, S., NATALI, F., EGIA, A., HERNANDEZ-TIEDRA, S., SALAZAR, M., BLAZQUEZ, C., GUZMAN, M. & VELASCO, G. 2009. Amphiregulin is a factor for resistance of glioma cells to cannabinoid-induced apoptosis. *Glia*, 57, 1374-85.

MCALLISTER, S. D., CHAN, C., TAFT, R. J., LUU, T., ABOOD, M. E., MOORE, D. H., ALDAPE, K. & YOUNT, G. 2005. Cannabinoids selectively inhibit proliferation and induce death of cultured human glioblastoma multiforme cells. *J Neurooncol*, 74, 31-40.

MITSIADES, C. S., MITSIADES, N. & KOUTSILIERIS, M. 2004. The Akt pathway: molecular targets for anti-cancer drug development. *Curr Cancer Drug Targets*, 4, 235-56.

ÖRD, D. & ÖRD, T. 2005. Characterization of human NIPK (TRB3, SKIP3) gene activation in stressful conditions. *Biochemical and Biophysical Research Communications*, 330, 210-218.

PERTWEE, R. G. 2008. The diverse CB1 and CB2 receptor pharmacology of three plant cannabinoids: delta9-tetrahydrocannabinol, cannabidiol and delta9-tetrahydrocannabivarin. *Br J Pharmacol*, 153, 199-215.

PREET, A., GANJU, R. K. & GROOPMAN, J. E. 2008. Delta9-Tetrahydrocannabinol inhibits epithelial growth factor-induced lung cancer cell migration in vitro as well as its growth and metastasis in vivo. *Oncogene*, 27, 339-46.

RAMER, R. & HINZ, B. 2008. Inhibition of Cancer Cell Invasion by Cannabinoids via Increased Expression of Tissue Inhibitor of Matrix Metalloproteinases-1. *Journal of the National Cancer Institute*, 100, 59-69.

SALAZAR, M., CARRACEDO, A., SALANUEVA, I. J., HERNANDEZ-TIEDRA, S., LORENTE, M., EGIA, A., VAZQUEZ, P., BLAZQUEZ, C., TORRES, S., GARCIA, S., NOWAK, J., FIMIA, G. M., PIACENTINI, M., CECCONI, F., PANDOLFI, P. P., GONZALEZ-FERIA, L., IOVANNA, J. L., GUZMAN, M., BOYA, P. & VELASCO, G.

2009. Cannabinoid action induces autophagy-mediated cell death through stimulation of ER stress in human glioma cells. *J Clin Invest*, 119, 1359-72.

SALAZAR, M., LORENTE, M., GARCIA-TABOADA, E., HERNANDEZ-TIEDRA, S., DAVILA, D., FRANCIS, S. E., GUZMAN, M., KISS-TOTH, E. & VELASCO, G. 2013. The pseudokinase tribbles homologue-3 plays a crucial role in cannabinoid anticancer action. *Biochim Biophys Acta*, 1831, 1573-8.

SANCHEZ, C., GALVE-ROPERH, I., CANOVA, C., BRACHET, P. & GUZMAN, M. 1998. Delta9-tetrahydrocannabinol induces apoptosis in C6 glioma cells. *FEBS Lett*, 436, 6-10.

SANCHEZ, M. G., RUIZ-LLORENTE, L., SANCHEZ, A. M. & DIAZ-LAVIADA, I. 2003. Activation of phosphoinositide 3-kinase/PKB pathway by CB(1) and CB(2) cannabinoid receptors expressed in prostate PC-3 cells. Involvement in Raf-1 stimulation and NGF induction. *Cell Signal*, 15, 851-9.

SUNG, H. Y., FRANCIS, S. E., CROSSMAN, D. C. & KISS-TOTH, E. 2006. Regulation of expression and signalling modulator function of mammalian tribbles is cell-type specific. *Immunology Letters*, 104, 171-177.

VARA, D., SALAZAR, M., OLEA-HERRERO, N., GUZMAN, M., VELASCO, G. & DIAZ-LAVIADA, I. 2011. Anti-tumoral action of cannabinoids on hepatocellular carcinoma: role of AMPK-dependent activation of autophagy. *Cell Death Differ*, 18, 1099-111.

WEI, S. C., ROSENBERG, I. M., CAO, Z., HUETT, A. S., XAVIER, R. J. & PODOLSKY, D. K. 2012. Tribbles 2 (Trib2) is a novel regulator of toll-like receptor 5 signaling. *Inflamm Bowel Dis*, 18, 877-88.

Appendix E. **Publications**

RESEARCH ARTICLE

Multi-Compartmentalisation in the MAPK Signalling Pathway Contributes to the Emergence of Oscillatory Behaviour and to Ultrasensitivity

Aban Shuaib^{1,2,3}, Adam Hartwell⁴, Endre Kiss-Toth^{1‡}, Mike Holcombe^{2,5‡*}

1 Department of Infection, Immunity and Cardiovascular Disease, University of Sheffield, Sheffield, United Kingdom, **2** Department of Computer Science, University of Sheffield, Sheffield, United Kingdom, **3** INSIGNEO Institute for in silico Medicine, University of Sheffield, Sheffield, United Kingdom, **4** Department of Automatic Control and Systems Engineering, University of Sheffield, Sheffield, United Kingdom, **5** Advanced Computing Research Centre, The Sheffield Bioincubator, University of Sheffield, Sheffield, United Kingdom

‡ These authors share senior responsibility for this study.

* m.holcombe@sheffield.ac.uk



CrossMark
click for updates

OPEN ACCESS

Citation: Shuaib A, Hartwell A, Kiss-Toth E, Holcombe M (2016) Multi-Compartmentalisation in the MAPK Signalling Pathway Contributes to the Emergence of Oscillatory Behaviour and to Ultrasensitivity. PLoS ONE 11(5): e0156139. doi:10.1371/journal.pone.0156139

Editor: Lisa Carlson Lyons, Florida State University, UNITED STATES

Received: April 19, 2016

Accepted: May 10, 2016

Published: May 31, 2016

Copyright: © 2016 Shuaib et al. This is an open access article distributed under the terms of the [Creative Commons Attribution License](https://creativecommons.org/licenses/by/4.0/), which permits unrestricted use, distribution, and reproduction in any medium, provided the original author and source are credited.

Data Availability Statement: Data are available from <https://github.com/MadinaJNR/Multi-Compartment-ABM-source-code-in-C-programming-language->.

Funding: Funded by Biotechnology and Biological Sciences Research Council BBSRC Doctoral Training Grant BB/F016840/1 (www.bbsrc.ac.uk).

Competing Interests: The authors have declared that no competing interests exist.

Abstract

Signal transduction through the Mitogen Activated Protein Kinase (MAPK) pathways is evolutionarily highly conserved. Many cells use these pathways to interpret changes to their environment and respond accordingly. The pathways are central to triggering diverse cellular responses such as survival, apoptosis, differentiation and proliferation. Though the interactions between the different MAPK pathways are complex, nevertheless, they maintain a high level of fidelity and specificity to the original signal. There are numerous theories explaining how fidelity and specificity arise within this complex context; spatio-temporal regulation of the pathways and feedback loops are thought to be very important. This paper presents an agent based computational model addressing multi-compartmentalisation and how this influences the dynamics of MAPK cascade activation. The model suggests that multi-compartmentalisation coupled with periodic MAPK kinase (MAPKK) activation may be critical factors for the emergence of oscillation and ultrasensitivity in the system. Finally, the model also establishes a link between the spatial arrangements of the cascade components and temporal activation mechanisms, and how both contribute to fidelity and specificity of MAPK mediated signalling.

Introduction

Cells constantly receive external signals reflecting changes in their environment, which they should respond to accordingly. An array of signal transduction pathways and signalling mechanisms have evolved that translate these external cues into specific cellular responses. One of

these central intracellular signalling pathways is known as the mitogen activated protein kinase (MAPK) pathway [1].

The pathway is a three-tiered cascade involving three enzymes, the MAPK kinase kinase (MAP3K), the MAPK kinase (MAP2K) and the MAPK. Mechanistically, pathway activation relies on the propagation of phosphorylation events downstream of the cascade [2, 3] as shown in Fig 1. The MAPK pathway plays a critical role in cells as it regulates numerous and diverse cellular responses [4–6], including regulation of the cell cycle, influencing differentiation, survival and apoptosis. Historically, these responses were attributed to distinct MAPK pathways, mediating a specific response [7–10]. Three groups of MAPKs have been characterised and were initially thought to respond to distinct signals. These include the ERK, JNK and p38 kinases; each of these is a “common name” for groups of highly similar proteins, encoded by small gene families. However, as the interest and knowledge in the molecular mechanisms that control these pathways grew, two issues have emerged: (i) a single pathway is capable of mediating opposing effects as seen with extracellular signal-regulated kinase (ERK) mediating either the differentiation or the division of PC12 cells [11, 12] (ii) Some of the responses the pathways triggered can overlap, with different MAPKs converging to mediate the same cellular responses in the same cell [13–15]. Furthermore, accumulating evidence showed that the MAPK pathways function as a network connected at different levels of the kinase cascade. Nonetheless, given this complexity, cells maintain high fidelity to the initial signal and respond efficiently. It is believed that properties arise from the activation behaviour of the pathway such as the signal magnitude, ultrasensitivity and oscillation. These thought to be influenced by the spatial and temporal aspects of MAPK pathway activation.

Temporal regulation of the MAPK pathway affects the cascade’s dynamics. It is also thought that the signal dynamics such as the magnitude of the response, duration and oscillation play a role in specifying the cellular outcome. For instance, it was long reported that sustained and transient activation of ERK caused quiescence and proliferation, respectively in Swiss 3T3 cells [16], PC12 and yeast cells [17]. In addition, high response magnitude enabled cell arrest while moderate magnitude had facilitated proliferation as seen in mouse embryonic fibroblasts

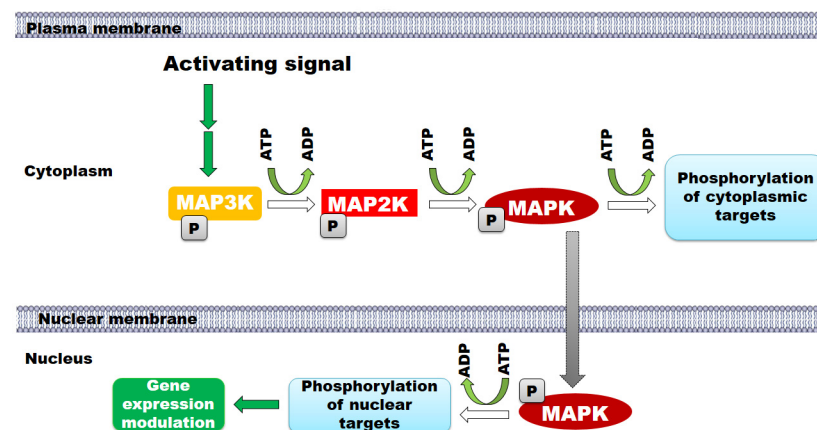


Fig 1. A schematic representation of the MAPK cascade and its activation mechanisms. The MAPK pathway is composed of three levels. The signal is transduced through phosphorylation events where mitogen activated protein kinase kinase kinase (MAP3K, also known as MAP3KK) phosphorylates mitogen activated protein kinase kinase (MAP2K, also known as MAP2KK) leading to its activation and thus the phosphorylation and activation of the mitogen activated protein kinase (MAPK). Active MAPK phosphorylates protein targets in the cytoplasm and the nucleus. For mediating nuclear events MAPK translocates to the nucleus where it phosphorylates many proteins, which control gene expression.

doi:10.1371/journal.pone.0156139.g001

(MEFs) [18, 19]. Oscillation in particular is thought to play a significant role in facilitating the specificity of the signal as the frequency and amplitude of the waves could encode for specific aspects of both gene transcription and translational changes. Oscillation is thought to emerge from regulatory mechanisms, which modulate the cascade input and output. Oscillations were observed previously in calcium signalling and in the NF- κ B pathway; however, this was only recently reported in the MAPK pathway [20, 21]. Nevertheless, oscillation in the MAPK pathway was predicted and demonstrated before using *in silico* models [22]. These models had proposed that regulatory machineries may involve feedback loops. The majority of the models had shown that negative feedback loops are chiefly responsible for the emergence of the oscillatory behaviour. Some models also propose that the interplay between positive and negative feedback is fundamental to generate signals that code for specific responses [23–26]. These oscillatory behaviours are suggested to be responsible for allowing the cell to choose to proliferate, go into senescence or differentiate. Some suggest that they may play a role in synchronising the responses of multiple cells to a signal mirroring the circadian rhythm [27].

The spatial distribution of the MAPK pathway is critical to generating specific responses. The first indications for this were coming from contrasting responses observed between nuclear and cytoplasmic ERKs triggered by the same stimulus. In fibroblasts and embryonic carcinoma cells, ERK activation and nuclear translocation caused proliferation. However, by preventing ERK translocation these cells became senescent and differentiated, respectively [28, 29]. An impact of spatial distribution was also seen during the activation of the beta-adrenergic receptors, which transiently activated ERK upon stimulation, which then translocated to the nucleus to regulate gene-expression. However, with the internalisation of receptors to the endosomal compartment, ERK activation becomes sustained and its action is confined to the cytosol. Also, Teis *et al.* have shown that there are separate pools of ERK in the plasma membrane and the endoplasmic reticulum and both of them mediate distinct actions. Depleting the endoplasmic reticulum (ER)-ERK pool led to an altered activation/inactivation dynamics of the pathway. Once the endoplasmic reticulum (ER)-ERK pool was demolished/decreased the effect disappeared and only returned with the re-introduction of the ER-ERK pool [30, 31]. Furthermore, in neuronal cells, the discrimination between the epidermal growth factor (EGF) and nerve growth factor (NGF) signalling is also thought to be due to the different compartments ERK resides in. Distinctive cellular responses were also observed when MAPKs were localised in different cellular compartments [32]. All of the above examples point to the critical role of compartments and spatial separation in mediating specific responses of the MAPK pathway.

In the work reported here, we were interested in characterising the interaction between spatial and temporal parameters in the MAPK cascade and how these influence pathway activity. We approached this by using an agent-based computer modelling approach, whereby every key molecule and compartment were explicitly modelled. This high level of detailed modelling provided an innovative basis for examining the role that compartmentalisation plays in MAPK activation. The main purpose of the model was to explain why compartmentalisation is necessary in order to achieve the various behaviours seen in biology. Less detailed modelling approaches are unlikely to be as informative.

We characterised the effect of compartmentalisation on MAPK activation and how it influences the formation of phosphorylated MAPK, thereby providing a novel insight as the issue of multi-compartmentalisation has not previously been highly addressed by *in silico* models of the cascade. We compared two types of models; a two-compartment model (which commonly used to study the cascade) and a novel, multi-compartment model. Our model shows that multi-compartments play an important role in the emergence of oscillatory behaviour in the MAPK cascade. In addition, we infer from the data that the balance between inhibitory and

activating inputs at the level of the MAPKK is critical for the appearance of oscillation in the system. Our ABM model suggests a fruitful strategy of integrating spatial and temporal regulation of the MAPK pathway and their influence on oscillation, and thus on signal specificity and efficiency.

Results

Agent Based Models of MAPK Activation

We have constructed two models of the MAPK pathway in order to address the effect of compartmentalisation of the MAPK components on pathway activation ([Fig 1](#)). The first model mimicked a two-compartment system, including the cytoplasm and the nucleus. The second model incorporated a multi-compartment system including the nucleus (with identical properties as compared to the two compartment model), cytoplasm, and ten randomly located cytoplasmic compartments. The two models share a number of common features. They both rely on binding events as the key factor to drive them. Agents move spontaneously and follow Brownian motions with few restrictions (read the agents descriptions in [Methods](#)). Both models are set and constructed in a three dimensional spherical cell as shown in [Fig 2C](#). All agents cycle between activated and deactivated states, all the MAPKK are subjected to deactivating inputs (mainly RADP) and there is no loss of agents or re-creation of agents in the system. The working mechanisms of both models are equivalent. Briefly, pMAPKK activates MAPK leading to the formation of pMAPK, which translocates to the nucleus. Once translocated to the nucleus, MAPK could interact with active exporting receptors (ExR) and removed from the nucleus ([Fig 2A and 2B](#)). Alternatively, pMAPK can interact with an active transcription factor, which triggers MAPK-dependent gene expression.

Simple rules were assigned to the agents in both models ([S1 File](#)). These rules specified the agents' movement and the manner in which they interacted amongst themselves and with their environment. The execution of the rules depends on the functions assigned to the agents and the agents' memory. Agents' memories are stored and regularly updated with every state transition of the agents and with every model iteration. A list of the memory components, messages and functions of each agent are listed in [S1 File](#).

Communication between the agents was achieved by the use of messages. The messages were inputted and outputted using the agents' functions. The messages were stored in the message board (Libmboard) and each agent accessed and read messages needed for the interaction with its interacting partner. Agents went through state transitions and the memory parameters were updated once the messages were read and the functions were performed. The physical interaction between the agents and the different agent states (DAS) were determined by assigning an interaction value. Once the interacting agents and the DAS were within the specified proximity, interaction between the agents and/or DAS occurred.

We also examined the effect of pMAPKK availability for the interaction with MAPK and how these also influence the dynamics of pathway activation. Two scenarios were modelled by introducing the parameter re-activation delay period (RADP, [Fig 2D](#)): an activation by strong stimulus *vs* weak inhibition of the signal at the level of MAPKK (when RADP < 15 min) and activation by a weak stimulus *vs* a strong signal inhibition at the level of MAPKK (when RADP > 15 min). Further details on RADP will be discussed below.

Calibration of the ABM

A critical parameter of pathway activation dynamics is the time to elicit E_{\max} of MAPK activation. In order to calibrate our ABM model, 63 experimental data points from 34 publications reported on MAPK activation time (E_{\max}) were extracted from the published literature ([S1 File](#))

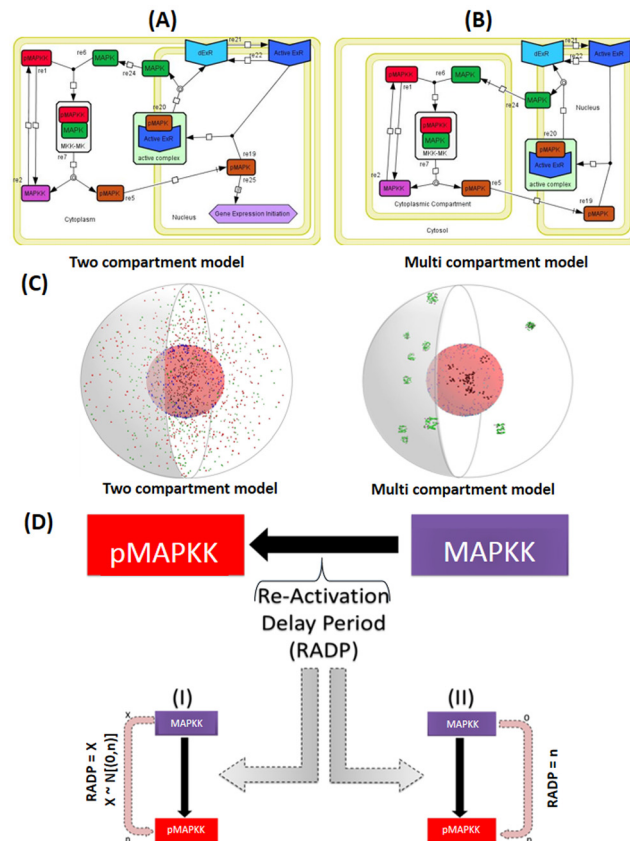


Fig 2. Graphical representation of cytoplasmic and nuclear events in the two-compartment and multi-compartment agent-based models (ABMs). The basic two dimensional design of the two and multi-compartment models of the two tier MAPK pathway represented using Systems Biology Graphical Notation (SBGN) standard annotations. (A) Illustrates the design of the two-compartment ABM whilst (B) describes the design of the multi-compartment ABM. Details of the two model design, structure and functionality are provided in the Materials and Methods section. (C) A three-dimensional (3D) visualisation of both the two-compartment vs. the multi-compartment model. The right hand side of both 3D representations is a 3D cross section of the “cell”. The cytoplasm is represented by the grey space around the nucleus. Inside the cytoplasm green spheres are MAPK, red spheres are pMAPKK, violet spheres are MAPKK, within the nuclear space, black spheres are pMAPK agents, dark blue are ExRs and light blue are dExRs. (D) Modelling the Re-Activation Delay Period (RADP) in the ABM: once pMAPKK agents change state into MAPKKs, they become dormant for period of time, and once this dormancy period is passed MAPKKs are re-activated. RADP was modelled either stochastically (I) or deterministically/periodically (II). In the stochastic model (I), RADP (X) was generated randomly for every individual pMAPKK agent, where X was a value between 0 and the chosen maximum value n ($X \sim N([0, n])$). Periodic RADP was always identical for every MAPKK formed (RADP = n).

doi:10.1371/journal.pone.0156139.g002

and analysed as shown in Fig 3A. The statistical analysis of this data revealed that the values were not normally distributed Fig 3A. In contrast, 21 E_{max} values from *in silico* models within these studies were normally distributed (Fig 3B). Therefore, the median time for maximal activation (7.63 min) was calculated from the experimental dataset and used to calibrate our model and to convert the time-step in the ABM into time values.

Sensitivity Analysis of the ABM

We tested the robustness of our models similar to approaches reported in previous studies of modelling MAPK signalling [33]. First, the two-compartment and multi-compartment models

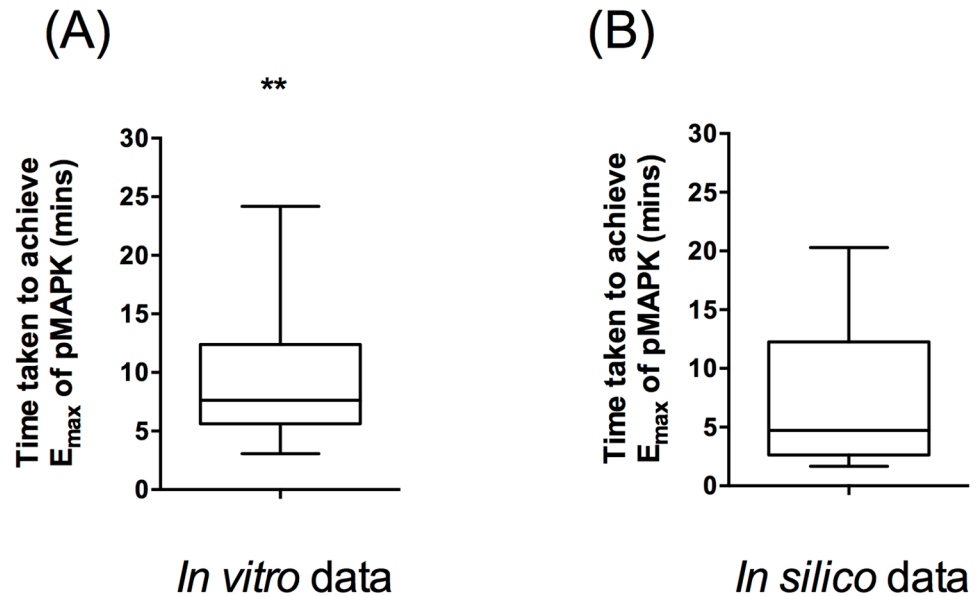


Fig 3. Analysis of MAPK activation dynamics observed *in vitro* in the published literature. 84 MAPK activation dynamics values were collected from published literature and the time to achieve E_{max} were plotted. A whisker plot with the median values are presented. (A) 63 *in vitro* data points from the analysed data were selected, plotted and analysis for normality was conducted. D'Agostino & Pearson omnibus normality test showed that the *in vitro* data for MAPK activation dynamics were not normally distributed (**: $p < 0.01$). (B) 21 *In silico* data-points were extracted from the above literature and normality analysis was performed as for (A), demonstrating that the *in silico* data was normally distributed.

doi:10.1371/journal.pone.0156139.g003

were run multiple times ($n = 3$) and the number of each species of agents were plotted at set time points for the individual runs (Fig 4A and 4B). Analysis of the standard deviation of the active MAPK species (pMAPK and pMAPKK) demonstrated that the models were robust. Whilst SD in the two-compartment model was low for both pMAPKK and pMAPK (SD pMAPK $< 3.3\%$, SD MAPKK $< 2\%$), SD for pMAPKK in the multi-compartment model were greater (1.5–37%). However, SD for pMAPK was $< 2.5\%$ at every time point, suggesting that such variation in pMAPKK levels is “tolerated” by the system, leading to a highly robust pathway activation. Next, the number of initial MAPKK and MAPK agents have been altered by 20% in the multi-compartment model, and MAPK and pMAPK agent numbers were plotted at set time points in three consecutive runs (Fig 4C and 4D). Variation between runs at each time point was $< 5\%$, further suggesting that our models were robust. Finally, the impact of altered MAPK or MAPKK levels on the dynamics of MAPK activation was analysed. Time to achieve pMAPK E_{max} and EC_{50} were determined in each of the models and conditions in Fig 4A–4D and one-way ANOVA was used to establish the impact of altered initial MAPK and MAPKK levels on the generation of pMAPK and pMAPKK (Fig 4E–4H). In short, alteration of MAPKK and MAPK levels did not affect MAPK and MAPKK activation dynamics, further supporting that our model was robust and insensitive to up-to 40% in initial agent numbers.

Compartmentalisation Is Responsible for the Rapid Responsiveness of the MAPK System

We implemented two models to investigate the effect of compartmentalisation on MAPK pathway activation. In the initial, two-compartment model (as described in the Methods), the MAPK and MAPKK agents were moving freely in the cytoplasm. We investigated the

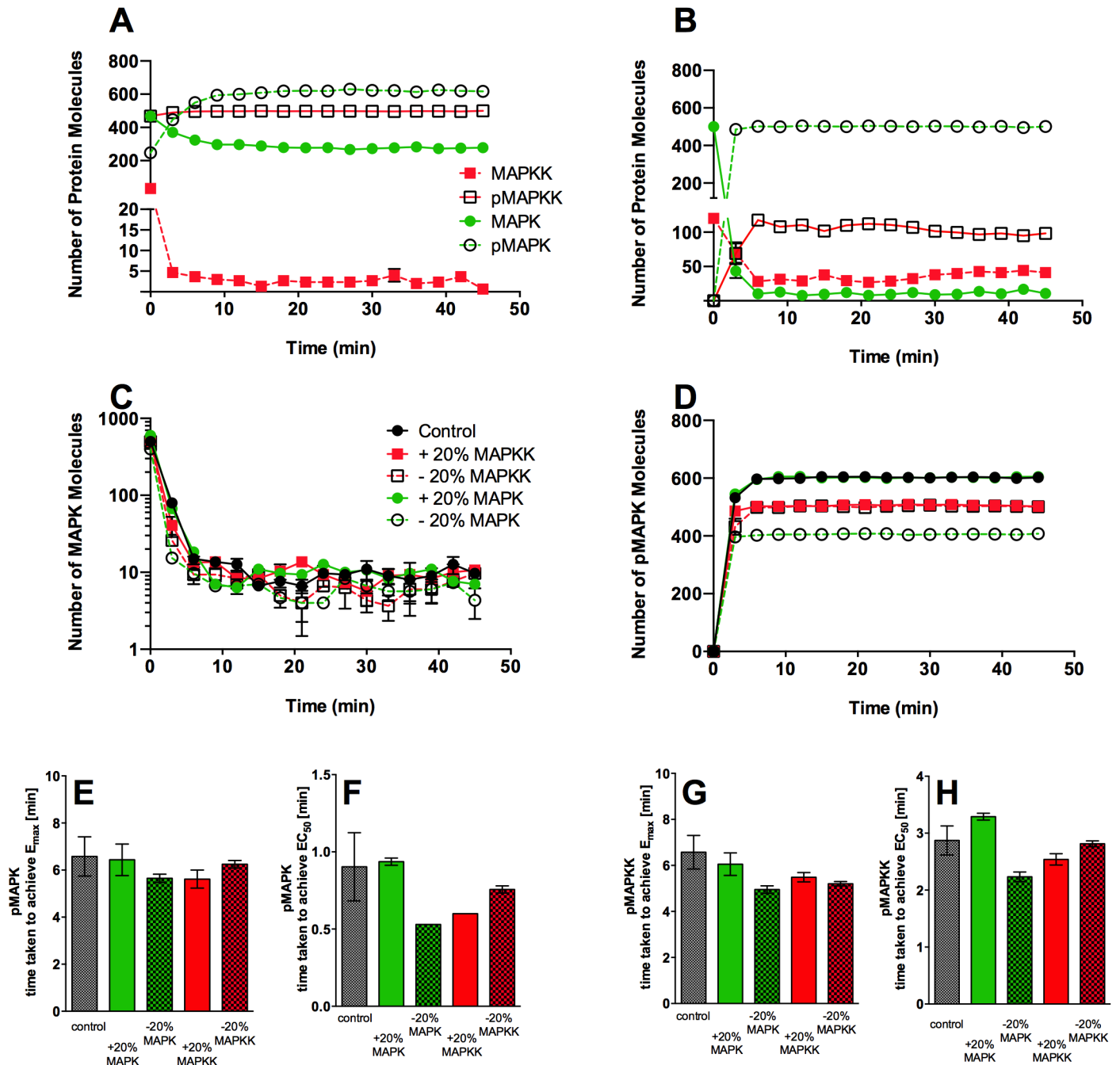


Fig 4. Robustness and sensitivity analysis of the ABM models. The basic two compartment (A) and multi-compartment models (B) were run multiple times ($n = 3$). (A) The graph shows a run of the complete two compartment model in the presence of constitutively active MAPKK agents and the emergent kinetic behaviour of pMAPK and MAPK agents. The graph shows the interaction between pMAPKKs and MAPKs until the level of pMAPKs and MAPKs plateau as the interaction reaches equilibrium. The pattern emerging is a graded ultrasensitive response (whereby $E_{max} \geq 10$ min). The model shows rapid activation of MAPK and formation of pMAPK but does not show ultrasensitive behaviour. (B) A graph generated from the multi-compartment model without a constitutively active MAPKK, this model shows that the multi-compartment system is capable of generating high level of pMAPK within a short period of time and with a gradual activation of MAPKK agents in addition to demonstrating an ultrasensitive behaviour. Individual data points for each run and the mean of the values are plotted. (C-H) Sensitivity analysis of the multi-compartment ABM to examine model sensitivity to manipulation of initial agent numbers. The number of each agent was altered by $\pm 20\%$, compared to the control model. The number of pMAPK (E, F) and pMAPKK (G, H) agents were plotted. Time to achieve both E_{max} and EC_{50} were determined under each condition and the analysis of variance (ANOVA) was used to test for statistically significant changes. The analyses showed no significant difference between the different ABM conditions.

doi:10.1371/journal.pone.0156139.g004

dynamics of the formation of the pMAPK in this model with the ratio between MAPKK and MAPK set at 1:1 and MAPKK being in a constitutively active state; this was to reflect a strong and sustained activation signal, similar to the oocyte system Ferrel investigated as a model of irreversible pathway activation [34]. As shown in Fig 4A, the levels of activated MAPKK in the system hardly changed over time in this configuration, resulting in a sharp formation of pMAPK and a rapid achievement of equilibrium. However, an initial lag-period of pMAPK accumulation (≈ 94 seconds (s)) was observed. Interestingly, an equilibrium of 1:2 MAPK to pMAPK ratio was established in the two-compartment model, different from ordinary differential equation (ODE) models that are based on Ferrel's original MAPK pathway model.

Next, a multi-compartment model was constructed to elucidate the impact of spatially restricted MAPKK/MAPK complexes on the dynamics of pMAPK formation. To simulate physiological conditions of resting cells in this model, the majority (95%) of the MAPKK agents were not active and the majority of the MAPK agents were not phosphorylated/activated initially. A model included an activation signal at 0 time point with MAPKK remaining active; this resulted in a system which was highly sensitive to activation with a rapid rate of pMAPK formation ($\approx 11.5 \pm 0.4\%$ of MAPK was converted to pMAPK per min), and thus a rapidly reaching equilibrium. In addition, in the multi-compartment model $98 \pm 0.2\%$ of MAPK was converted into pMAPK and translocated to the nucleus (Fig 4B). In contrast, the two-compartment model had generated a less sensitive system, where only $\approx 82.4\% \pm 0.2\%$ of MAPK molecules were converted to pMAPK per min. Furthermore, levels of pMAPK generated were lower in the two compartment model and only a $70.3 \pm 2.2\%$ reduction in cytoplasmic MAPK levels once the system had fully triggered (Fig 4A).

However, due to the constitutive activity of MAPKK, particularly in the multi-compartment model, the levels of MAPK did not return to the initial values. Thus we modified our model to address this and describe its results below.

MAPKK Re-Activation Delay Influence Dynamics of pMAPK Formation in a Multi-Compartment Model

In cells, activated MAPKK is deactivated by phosphatases [35, 36]. Thus the balance between activation and inactivation relies on the number of active pMAPKK molecules *versus* inactive MAPKKs, which is influenced by the rate of phosphatase activity. To address this issue in the ABM model, a re-activation delay for MAPKK was introduced. Once pMAPKK interacts with MAPK it enters a dormant state where it is not capable of activating MAPK and this period of inactivity is defined as the re-activation delay period (RADP). The effect of re-activation delay was modelled deterministically and stochastically. Initially, different RADPs were investigated and systems behaviour in stochastic vs. deterministic models were compared. Stochasticity of RADP values were analysed, employing one-sample runs test. First, RADP values were collected for five independent MAPKK agents during a model run. Secondly, RADP values were collected for the same MAPKK agent during four independent runs of the model (individual RADP values are presented in S3 File). In both scenarios, the one-sample runs test yielded $p > 0.05$ for every agent/run, demonstrating that RADP values were stochastic.

At lower RADPs ($0 \leq \text{RADP} < 90$ (s)) the MAPK system retained its rapid activation rate and high level of pMAPK formed in both deterministic and stochastic models (Fig 5A vs. 5B). In contrast, at slightly longer RADPs, the deterministic model showed graded responses during the initial activation phase (Fig 5B vs. 5D). These graded responses were also observed in the stochastic models with minimum stochasticity (for instance, $4.38 \leq \text{RADP} < 4.53$ min, S1 Fig); hence the models closely resembled the deterministic models.

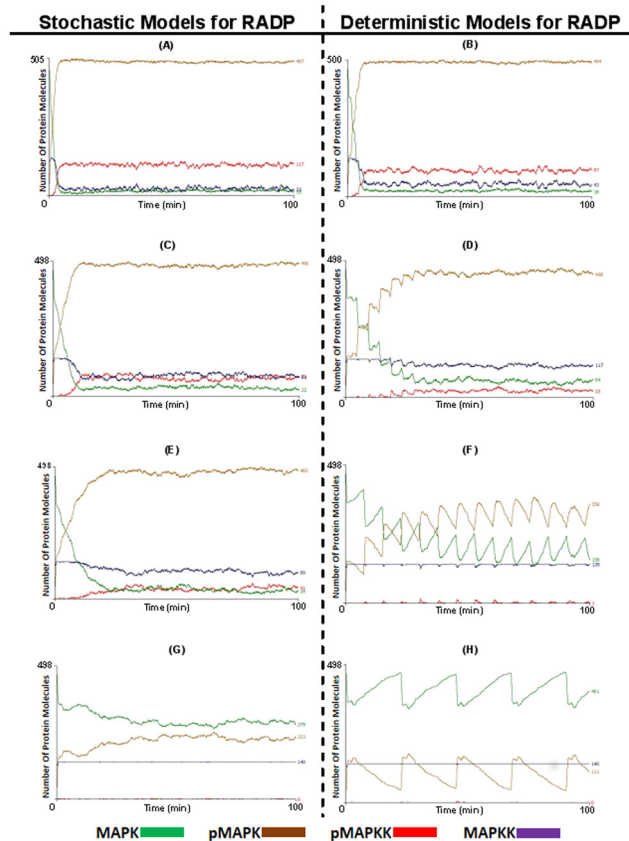


Fig 5. The effect of delaying MAPKK re-activation on the dynamics of MAPK activation and MAPKK levels. Once pMAPKK agents bind and activate MAPKs to pMAPKs, pMAPKKs convert to a dormant state (MAPKK). The length of this dormancy period was set and its effects on the levels of pMAPK, MAPK, pMAPKK and MAPKK were monitored. In (A) and (B) the re-activation delay period (RADP) was set at a short period ($0 \leq \text{RADP} \leq 90$ s), while in (C) and (D) RADP was set to an intermediate period ($0 \leq \text{RADP} \leq 4.53$ min); in (E) and (F) RADP was set to a the highest range of the intermediate period ($0 \leq \text{RADP} \leq 7.55$ min); while in (G) and (H) RADP was set to long periods ($0 \leq \text{RADP} \leq 22.6$ min). The figures on the left hand side were stochastic (where the RADP was set stochastically within the specified delay period every time pMAPKK switched state to MAPKK); while models on the right hand side were deterministic (where MAPKK returns to the active pMAPKK state after a fixed period).

doi:10.1371/journal.pone.0156139.g005

Models with longer RADPs and at maximum stochasticity ($0 \leq \text{RADP} < 7.55$ min) generally retained their ability to generate high levels of pMAPK ($93.9 \pm 1.7\%$ reduction of MAPK levels at E_{max} compared to t_0 , [S2A Fig](#)), though the rate of activation decreased and the time to achieve E_{max} increased from 6.24 ± 1.3 min to 26.7 ± 6.9 min ([Fig 5E](#) and [S2B Fig](#)). However, if the RADP was fixed to create a deterministic model ($\text{RADP} = 7.55$ min) or one with minimal stochasticity ($7.53 \leq \text{RADP} < 7.55$ min), the graded responses observed earlier evolved into an oscillatory behaviour ([Fig 5F](#)).

In a stochastic model of RADP, when the RADP was > 15 min and when E_{max} was reached, the levels of inactivated MAPK had fallen by $47.4 \pm 3.9\%$ (from 100% at t_0 and compared to $\sim 95\%$ reduction in MAPK levels observed in the other models we presented here, [S2A Fig](#)). Although this is a significant reduction, the levels of MAPK were still higher than the EC_{50} , and did not reach 5% of MAPK levels at t_0 ([Fig 5G](#)). Nonetheless, this model still demonstrated a level of responsiveness, which had arisen from the ability of extremely low levels of MAPKK agents to maintain a high level of pMAPK in the model. In contrast, the deterministic models

with RADPs higher than 15 min, the graded dynamics of pMAPK formation evolve into sustained oscillatory behaviour (Fig 5H).

In these multi-compartment models of re-activation delay, although increasing the RADP led to lower steady state pMAPK levels (Fig 5F–5H) and reduced MAPK: pMAPK ratio, neither of them were capable of re-establishing the levels of MAPK and pMAPK at t_0 . Nonetheless, in deterministic models, t_0 MAPKK levels were re-established once RADP was set at > 7.55 min. On the other hand, this behaviour was only seen at long RADP in the highly stochastic models (data not shown).

Alterations in RADP Fail to Display an Oscillatory Behaviour and to Regulate pMAPK Formation Dynamics in a Two-Compartment Model of the MAPK Cascade

Next, the re-activation delay characteristics of MAPKK were tested in the two-compartmental model. In these, neither stochastic nor deterministic models of MAPKK RADP (Fig 6A, 6C and 6B, 6D respectively) produced an oscillatory behaviour for pMAPK formation dynamics and there was no significant difference between the two models with regards to pMAPK formation, MAPKK activation and re-established MAPK levels. This was seen both at RADPs ≤ 5 min (Fig 6A and 6B) and RADPs ≥ 15 min (Fig 6C and 6D). Furthermore, whilst introducing the RADP into the two compartment model did not induce oscillation, the model still maintained the characteristic graded MAPK activation dynamics for both MAPK and pMAPKK (≈ 60 min to reach E_{max}).

Signalosome clusters have been reported previously, including lipid rafts and Ras nanoclusters [37]. In these signalling apparatus at the plasma membrane (such as rapidly accelerated fibrosarcoma1 [RAF1] and rat sarcoma [Ras]) are brought together into a very close proximity

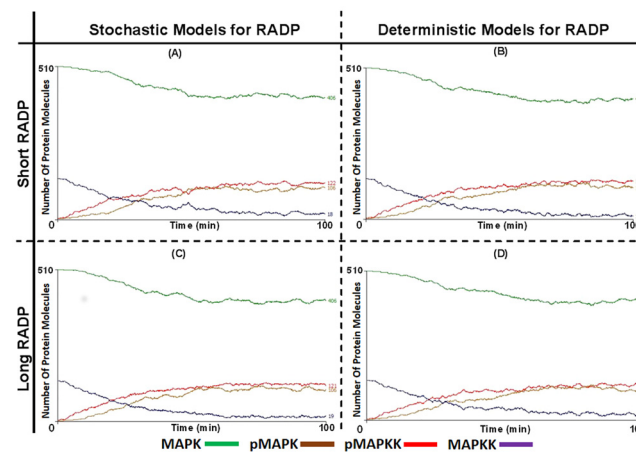


Fig 6. The effect of MAPKK re-activation delays on the dynamics of pMAPK formation and pMAPKK levels in two-compartment system. The re-activation delay characteristics of pMAPKK (red) were applied to the two-compartment ABM and the effects were monitored. Initially the effect of a deterministic versus a stochastic model were looked at. In (A) and (B) short RADPs ($0 \leq \text{RADP} \leq 90$ s) were tested, (A) was the model with stochastic RADP while (B) was the model with deterministic/periodic RADP. There was no significant difference between the graphs generated by either ABMs when the analysis of variance (ANOVA) was used. However, both of the models had generated lower activation rate and formation of pMAPK (brown) and pMAPKK (violet) in comparison to the multi-compartment system. The graphs in (C) and (D) were generated with long RADPs ($0 \leq \text{RADP} \leq 22.6$ min), pMAPK formation, pMAPKK and MAPK (green) activations patterns were similar to those with short RADP seen in (A) and (B). Unlike multi-compartment models, deterministic models with intermediate or long RADPs did not generate any oscillatory pattern.

doi:10.1371/journal.pone.0156139.g006

and randomly assemble and disassemble [38, 39]. This concept was applied by changing the multi-compartment model to a model with assembled signalosome clusters at the arrival of the activating signal; these clusters then disassembled and the signalosome components diffused into the cytoplasm by Brownian motion. The impact of signalosome cluster model was tested with both the deterministic and stochastic models and with long and short RADPs. This led to a two-phase response, an activation “turn on” phase and a tailing-off “shut-down” phase.

Looking at pMAPK formation dynamics as a surrogate of pathway activation, there was little difference between the stochastic (Fig 7A and 7C) and deterministic models (Fig 7B and 7D) as well as between the models using short or long RADPs (Fig 7A and 7B vs. Fig 7C and 7D, respectively). MAPKK-MAPK cluster formation led to a rapid accumulation of pMAPK, however, this was short lasting as MAPK levels were gradually reduced with cluster disassembly. The four models demonstrated a strong ultrasensitive response in the initial phase of activation of MAPK. However, ultrasensitive response for MAPKK was only seen in the short RADP models, while appearing to be graded in the long RADP models.

The primary differences observed between the different MAPKK-MAPK cluster models included the magnitude of pMAPK generated within the initial phase of MAPK activation. At E_{max} of the stochastic RADP model (RADP < 90 s) 60% of MAPK were activated in the initial phase. Long RADPs did not show high responsiveness and thus resulted into lower pMAPK

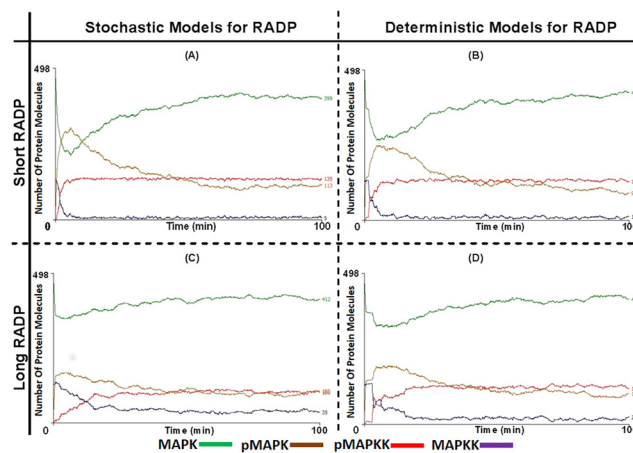


Fig 7. pMAPKK and pMAPK levels and rate of activation are significantly enhanced in the two compartmental model in the presence of signalosome clusters though with no significant difference between deterministic and stochastic re-activation delay (RADP) models. Deterministic and stochastic models of MAPKK RADPs were tested again in the two-compartment ABM, in the context of assembly and disassembly of pMAPKK-MAPK signalosome clusters. In both models the presence of the clusters caused a rapid rate for pMAPKK (red) activation and pMAPK formation (green). This observation shares similarity with the multi-compartment system; however, only at the initial MAPK activation stage. Yet, these cluster models differ with the multi-compartment model in three aspects; (1) the cluster model exhibits a two phase response (activation [turn on] and deactivation [turn off/recovery] phases); (2) the recovery of MAPK (seen in the post-activation phase of the signalosome cluster model) and (3) that high levels of active pMAPKK are incapable of re-establishing high levels of pMAPK. In (A) and (B) short RADPs ($0 \leq \text{RADP} \leq 90 \text{ s}$) were tested, (A) was the model with stochastic RADP while (B) was the model with deterministic RADP (RADP = 90 s). The graphs in (C) and (D) were generated with long RADPs ($0 \leq \text{RADP} \leq 22.6 \text{ min}$), where (C) stochastic RADP was employed while (D) deterministic RADP was utilised (RADP = 22.6 min). The dynamics of pMAPK formation, MAPKK and MAPK activations in the long RADP models were similar to those noted in the short RADP models. Student t-test no significant difference in the responses generated by stochastic and deterministic models of RADPs at long periods, except for the slightly higher pMAPKK levels in the deterministic model once the steady state was reached. This also applies to the models with short RADPs, though the stochastic models generate higher levels of pMAPK in the initial phase.

doi:10.1371/journal.pone.0156139.g007

levels and low rate for MAPK activation/pMAPK formation (33% reduction for the stochastic model and 40% for the deterministic model), though the stochastic model had shown a faster rate of pMAPK accumulation.

When assessing MAPKK activation, all models applied to this compartmental setup established maximum or near maximum pMAPKK levels at steady state, with short RADP models generating slightly higher MAPKK levels. Deterministic models of RADP, however, showed some graded responses in the initial phase of MAPKK activation (Fig 7(B) and 7(D)). Nonetheless, unlike the multi-compartment model, high levels of active MAPKK were not able to sustain high levels of pMAPK.

The pMAPK Dynamics Obtained from the ABM Are Comparable to MAPK Dynamics Observed *In Vitro*

We looked at formation of pMAPK in the ABM model and compared it to recently published results by Shankaran *et al.* where they demonstrated the oscillation of pMAPK levels experimentally [21]. Our ABM models show a good level of correlation with their *in vitro* data, as demonstrated by statistical analysis of the dynamics of MAPK activation in the experimental vs. ABM data. Their stimulation of cells with EGF showed a temporal dynamics of pMAPK formation similar to that of the periodic RADP ABM model (RADP = 22.6 min). Furthermore, when comparing the oscillatory behaviour shown by Shankaran and colleagues, the ABM model matches several features in the pMAPK response. Both Shankaran's data and the ABM model show similar "turn off" dynamics for all the oscillatory waves and the maintenance of the oscillatory behaviour past the first response trigger. The ABM (with $4.5 \leq \text{RADP} \leq 7.5$ min) and some of the oscillatory behaviour in Shankaran's paper demonstrated graded responses while continuing to oscillate until the levels of pMAPK were close to E_{max} . We also noted similarities at the phase between the turn-on and turn-off phase in the oscillatory waves. Both the ABM (when $6 \leq \text{RADP} \leq 23$ min) and some of the *in vitro* data at the initial response show some fluctuations in pMAPK levels before the "turn off" phase. In our model, we observed that this was due to a second wave of MAPKK activation which were either dormant or not in close proximity to bind to MAPK during the initial wave of activation (Fig 5F and 5H). However, the small number of available pMAPKK agents and their lengthy RADP hindered further activation of the recently available MAPKs.

The pMAPK dynamics seen in models including cluster assembly and disassembly were also similar to the results obtained with compartmentalised MAPK signalling at the endosome (S3 Fig). Lefkowitz had shown that a typical response of MAPK involving the endosome and G protein-coupled receptors (GPCRs) are divided into two phases; a GPCR- and β -arrestin-dependent phases. The GPCR-dependent phase was characterised by a rapid initial MAPK activation followed by a rapid "turn-off" phase. In contrast, the second phase is endosomal and β -arrestin-dependent and is characterised by slow activation and deactivation phases [40]. Activation dynamics of ERK (a target of the GPCR induced signalling) incorporated both the GPCR- and β -arrestin-dependent responses. In Fig 7 and S3 Fig, the ABM produced two phase MAPK activation response (a rapid activation at the initial phase followed by a slow deactivation phase). The deactivation phase was capable of lowering the levels of activated MAPK. These characteristics produced by the ABM are similar to the endosomal MAPK activation dynamics demonstrated *in vitro* by Lefkowitz. This might suggest that the formation of signalosome clusters at subcellular compartments could generate signals comparable to those triggered at membrane clusters.

A Multi-Compartment Model Combined with Multiple MAPKK Re-Activation Delay Periods (RADPs) Reveals that the Rate and Level of pMAPK Formation is Influenced by MAPKK RADPs

Cells reside in a dynamically changing environment. A highly studied example of such dynamic environments is development and/or differentiation. During somatogenesis, cells are exposed to strong signals and potent feedback control mechanisms; both of which are periodic and oscillatory in nature [41, 42].

The MAPK pathway is thought to be triggered during somatogenesis by fibroblast growth factor (FGF) with ERK and dual specificity phosphatase gene *Dusp4* both playing a role in this process [43]. ABM was used to test system recovery and the reversibility of pMAPK levels once E_{\max} had been reached by replicating the dynamic changes in external signals that have previously been reported experimentally. This was implemented by employing a combined multi-compartment model. In this model, a strong initial signal was applied which was then succeeded with a strong inhibitory response, followed by a model with a periodic activation of MAPKK. This was achieved by combining three RADP configurations and merging them into the multi-compartment ABM. Activation of the multi-compartment model was initiated with a highly stochastic-short RADP model ($0 \leq \text{RADP} < 90$ s); this led to an accelerated rate of pMAPK formation and a rapid reduction in MAPK levels (Fig 8, solid green line). Once the steady state levels of pMAPK were reached, deterministic-intermediate RADP (RADP = 7.55 min) was switched on (Fig 8, solid blue line). This was to mimic a strong inhibitory signal capable of dephosphorylating and thus deactivating MAPKK. Once the lowest steady state levels of both MAPKK and pMAPK were established, the model was switched to a stochastic-intermediate RADP model ($0 \leq \text{RADP} < 7.55$ min; Fig 8 with the solid dark lines). Switching to a deterministic model with an intermediate RADP (strong and sustained inhibitory feedback) led to reduced levels of pMAPK (ca. 50% of the maximum), while showing a very rapid inhibition of MAPKK (ca. 95.9%). Behaviour of the stochastic model with an intermediate RADP demonstrates that low levels of pMAPKK and a slow rate of conversion of MAPKK to pMAPKK were capable of rapidly establishing high pMAPK levels and producing an ultrasensitive activation behaviour.

Discussion

The dynamics of the MAPK pathway has been investigated widely using *in silico* models [33]. Since the publication of Ferrell's first model of the pathway, many more models have been reported. The majority of these papers predicted patterns and mechanisms in the pathway which explained experimental observation(s) [44]. Some of the most influential studies include the works of Levchenko who explained the contradictory experimental observations scaffold proteins have on the activation of signalling systems and the work of Ferrell *et al* and Kholodenko which explored the effect of negative and positive feedback loops on system behaviour [22, 45]. Levchenko's model showed that scaffold concentrations in the cell are responsible for these contradictions and that scaffolds have to be within a critical concentration in order to enhance MAPK signalling [46]. Other models revealed that negative and positive feedback loops are needed for the emergence of bistability and ultrasensitivity [24, 25, 47]. Furthermore, the works of Sarma *et al* had predicted that based on the architecture and feedback mechanisms of the MAPK pathway, the formation of phosphorylated species of ERK should exhibit oscillatory behaviour [23]. This was prediction was confirmed experimentally only recently [21, 48].

The most commonly used approach to model the MAPK pathway is to use ODEs to describe the pathway and the reactions, which lead to the formation of the phosphorylated

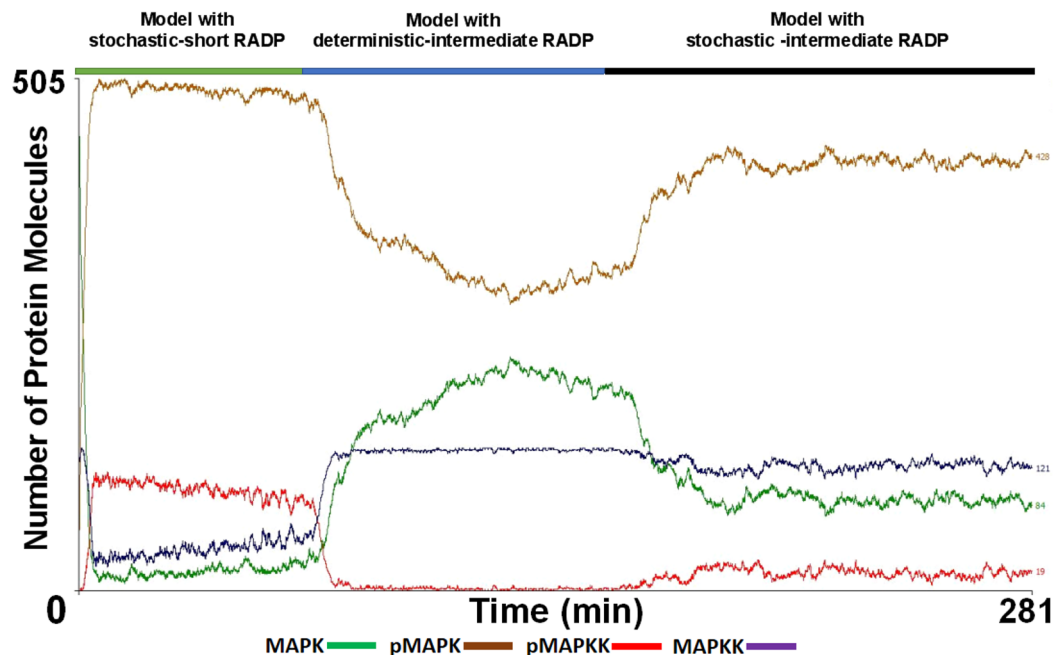


Fig 8. The effect of changeable input-output dynamics at the level of MAPKK on phosphorylated MAPK (pMAPK) formation characteristics in a multi-compartment system. Using the multi-compartment model, the MAPK pathway was run with different re-activation delay period (RADP) configurations to assess how switching between different MAPKK dormancy periods affect the formation of pMAPK. This was done to resemble a cellular system where a cell is initially faced with a strong, yet short activating signal, followed by the take-over of the inhibitory mechanisms, which is subsequently succeeded by a moderate and persistent activating signal. This simulation is similar to what cells are exposed to during somatogenesis. In the initial phase, a highly stochastic model of MAPKK RADP ($0 \leq \text{RADP} \leq 90 \text{ s}$) was used (green solid line), once pMAPK level reached its maximum and was at equilibrium, the simulation was switched to deterministic-intermediate RADP model ($\text{RADP} = 7.55 \text{ min}$, solid blue line). Once the level of pMAPK reached its lowest and was at equilibrium, the re-activation delay was switched to a model with stochastic-intermediate RADP ($0 \leq \text{RADP} \leq 7.55 \text{ min}$; solid black line). This combination of the different modes of the MAPKK re-activation shows that once strong activation inputs of MAPKK are substantially reduced, inhibitory inputs which cause the deactivation of pMAPKK for long periods are capable of rapidly reducing the levels of pMAPK. However, they are still not capable of re-establishing the initial levels of MAPK seen at t_0 as only 58.7% of t_0 MAPK level was re-established. The final stage of the simulation (solid blue lines), reflects that in a multi-compartment system, even with a high stochasticity for MAPKK activation, a low number of active pMAPKK is sufficient to fundamentally increase and maintain high pMAPK levels.

doi:10.1371/journal.pone.0156139.g008

species at the three tiers. In our study, we used an agent based model (ABM) approach as it enabled us to investigate system behaviour whilst also gaining an insight into the faith of individual proteins, the physical interaction between them and their environment in addition to the spatial parameters of the model. The latter is something unfortunately ODEs cannot address [49–51]. In this ABM approach, a generalised model of the MAPK pathway had been used. This was done for a few reasons. First, a generalised model would be able to investigate effects, which could then be applied to specific MAPK pathways and thus more transferable and testable in a number of experimental settings. Secondly, there is limited experimental information regarding to MAPK compartment numbers, the physical interactions occurring in them or the number of individual MAPKs in each compartment and their impact on signalling. Furthermore, a generalised MAPK pathway model integrates, to some extent, the influence of other pathways into the MAPK signalling network (such as feedback loops).

Our ABM, as shown in Fig 2A is composed of the second and third tiers of the MAPK pathways. It allows MAPKK to become activated by an upstream stimulus, which in biological systems is transmitted via the first tier (MAPKKK) of the cascade. The model primarily relied on

the physical interactions and binding properties between MAPKK and MAPK and was used to study the impact of compartmentalisation and the inputs into the cascade (both inhibitory and activating inputs) at the MAPKK level. The model implemented competitive inhibition and sequestration interactions between MAPKK and MAPK, as described previously in several experimental studies [52–54]. This was achieved by the change of state of pMAPKK to a dormant state once it activated MAPK. It has previously been suggested that competitive inhibition and sequestration-based-feedback between pMAPKK and MAPK play a role in the dynamics of MAPK pathway and they are capable of producing ultrasensitivity and bistability in the system and thus influence the cellular outcome [55].

The initial design of the model employed a system that contained very low competitive cooperative inhibition and sequestration of the MAPKK. Similar to the majority of previously published MAPK models, it involved two-compartments with the interacting species moving around the “cytoplasm” in Brownian motion. However, this implementation of the ABM only produced a graded activation response for the pathway. Increasing diffusion parameters in ODE models has previously been shown to be responsible for decreasing reaction orders and thus MAPK activation following Michaelis–Menten kinetics [56, 57]. Once diffusion parameters are reduced, such as when seen in the presence of scaffold proteins, the reaction order had increased, increasing the rate of phosphorylation and led to ultrasensitive MAPK response [46, 58]. In cells, if phosphorylated species were to rely only on diffusion to propagate the signal downstream, an increased probability of phosphatase action would lead to the reduction of the reaction rate [50, 59, 60]. However, *in silico* models show that this could be overcome by spatially restricting phosphatases and kinases in the cell and consequently, the formation of local pools leading to the localisation of the signal [61]. In the ABM, relying solely on Brownian motion lowers the probability of direct interactions between MAPKK and MAPK species, and even in the absence of phosphatases or inhibitory enzymes, pathway activation does not lead to strong ultrasensitivity. This behaviour matches well with findings reported in the ODE-based and experimental studies discussed above.

The introduction of multi-compartmentalisation in previous studies led to ultrasensitive response as well as oscillatory behaviour in the system. Legewie et al, Ortega et al and Qiao et al demonstrate that variations of parameters have an effect on the final response of the system and their variation might be responsible for distinct outputs [53, 56, 62]. They also show that only few of these parameters are capable of generating bistability and/or oscillation. However, they highlight that all of this hinges on phosphorylation cycles, and that the main contributors to these effects are the small numbers of regulatory molecules in the pathway. Our ABM shows that varying the input parameters at the level of MAPKK is capable of producing two distinct responses to a signal; nonetheless, it also demonstrates that compartmentalisation as well as mode of the output at the level of the MAPKK could play an important role for the generation of ultrasensitivity and oscillation.

In the ABM that included multi-compartments, a prominent ultrasensitive response emerged. This occurred in the presence of competitive inhibition and even when sequestration interaction between the pMAPKK and MAPK species was high (when RADPs > 15 min, Fig 5G). In a model where the RADP was stochastic, the rate of the phosphorylated MAPK species formation and thus the magnitude of the MAPK response had only significantly decreased when $\text{RADP} \geq 8$ min (S2A Fig). This is interesting as it was shown experimentally that pMAPK magnitude play a role in the specificity and fidelity of the MAPK pathway [38, 55]. This also implies that compartmentalisation could play a role in allowing for fidelity to a response regardless of the strength of input at the level of the MAPKK.

Oscillation in the MAPK pathway is strongly linked to negative feedback loops; though there is also a realisation that balance between positive and negative feedback is fundamental

as these are being shown both *in vitro* and *in silico* [21, 24, 63]. Several modelling approaches showed that the outcome of feedback loops differ depending on the mode of the feedback applied. Moreover, the position of these feedback loops within the cascade's three tier architecture influence the output and hence the behaviour of the cascade [23–25]. In the model presented here, balance between negative and positive feedback loops were taken into account by relying on the final output of inhibitory *versus* activating inputs from feedback loops at the level of MAPKK. This was implemented by the introduction of the re-activation delay periods (RADP). The model shows that when RADPs were deterministic (*i.e.* periodic), oscillatory behaviour emerged; in-line with previous observations which illustrate that once strong negative feedback loops were applied, oscillation was generated. In the ABM, the frequency of the oscillation and the amplitude were both influenced by RADPs. This is interesting as it was shown experimentally that frequency and amplitude of phosphorylated ERK influence the expression of specific genes such as c-Fos [20, 64]. It has also been proposed that oscillation might be a mechanism by which MAPK signalling is restricted to the cytoplasm as the frequency and amplitude would affect the MAPK targets in the cytoplasm [16]. The appearance of oscillation within the multi-compartment model strengthens this argument. Compartmentalisation and the periodicity of input at the MAPKK level could act as a filter and/or modulator for localised responses. Compartmentalised MAPK targets would be directly available to interact with phosphorylated species of MAPK, however, if there are multiple targets, their ability to react differentially to the same input signal (*i.e.* de-coding capabilities) would specify a hierarchy of interactions within the compartment and therefore control the development of the specific response.

Our results presented above demonstrated that with long periodic RADPs, oscillation becomes sustained; this is consistent with previous observations that sustained oscillation appear in models which also exhibit ultrasensitivity and strong negative feedback inhibition. However, the ABM also shows that periodic MAPKK activation and multi-compartmentalisation are essential for sustained oscillation to appear. Previously, oscillation was described as a random process, which could emerge in the absence of regulatory mechanisms, yet the ABM demonstrated that altering the periodicity of RADP at the level of MAPKK in a multi-compartment model is integral for oscillation to appear. This was confirmed when the ABM was converted to a two-compartment model and the effects of RADPs were re-tested (Fig 6). In addition, oscillation emerged in a relatively simple model suggesting that for oscillation to appear specific parameters need to be met [56, 57]. This might be plausible considering that oscillation does not appear experimentally when a population of cells is monitored, yet, it can be observed at the level of individual cells. This could suggest that the conditions required for oscillation are more easily met at the single-cell level, compared to cell populations [21, 48].

Signalosome clustering at the plasma membrane has been reported previously [37, 65] and was shown to contribute to MAPK cascade's specificity and efficacy [66]. Chiu *et al* demonstrated that Ras-nanoclusters could also be formed in cytoplasmic membranes [67]. However, Tian *et al* and others proposed that plasma membrane Ras nanoclusters are essential for MAPK activation and are major contributors to the rapid activation observed at the initial phase of global MAPK activation response [39, 68, 69]. In addition, Inder *et al* suggested that endoplasmic reticulum and Golgi Ras nanoclusters play a role in the differentiation of the incoming signal and thus determining the response output [70]. On the other hand, the off phase of MAPK activation is attributed to the disassembly of signalosome clusters, followed by diffusion into the cytoplasm [60, 68, 71]. The ABM described here (Fig 7) demonstrates, indeed, clustering of MAPKK and MAPK is responsible for the initial, robust activation of MAPK and that the disassembly of these components is responsible for the characteristics of the off phase.

Considering that compartmentalisation is a fundamental property of the cell and components of the signalosome are found inside of the compartments, the ABM reported here strengthens the argument that plasma membrane clustering might not be the sole contributor to signal efficiency and specificity and that compartments within the cytoplasm may be capable of mediating similar effects. Additionally, if both plasma membrane and cytoplasmic membrane clusters contribute to MAPK activation, their combined effects should be synergistic. This might be a valid postulation considering that Ras clusters at the ER and Golgi were experimentally shown to be triggered by Raf1, which could be triggered at the plasma membrane [70]. Such combination of plasma membrane-originated and cytoplasm-originated activation of MAPK might also be a source for generating oscillation as cytoplasmic clusters would re-trigger MAPK activation. Alternatively, if both plasma and cytosolic clusters were simultaneously activated as reported in some MAPK systems [72, 73], in order to generate the usually observed global MAPK response, strong negative feedback loops, insulation and isolation mechanisms should be present at amplification points within the MAPK system.

The ABM also showed similarities with other *in silico* models. As mentioned previously, *in silico* models in general and ODEs in particular have been very insightful in explaining and improving our understanding of signal transduction and signal processing. However, ODEs are limited in modelling spatial constraints, and with them it is challenging to model individual protein-protein interactions in multi-protein complexes. For partial differential equations (PDEs) the limitation lies in the complexity of writing several mathematical expressions and equations for every compartment and the corresponding equations, which allow those to change over time. We choose to use the ABM as it overcomes these limitations and we have validated our approach with previously published data obtained from ODEs and PDEs. Furthermore, the ABM with periodic and long RADP shared similarities with the oscillatory pattern of pMAPK vs. MAPK in a model published by Kholodenko et al, employing negative feedback and competitive inhibition [22]; the latter is also an important characteristic of the ABM. The periodicity of oscillations was also very similar between the two models. The graded response, combined with oscillation seen at the initial activation phase generated by the ABM with RADP = 4.5 min (Fig 5D); is similar to the dynamics of MAPK activation as demonstrated by a Zhao *et al* in a model of the MAPK pathway using PDEs [74]. However, there were also differences between the ABM and PDE models in the time frame of achieving E_{max} . Additionally, Zhao's model had achieved a higher frequency and continuous oscillation at E_{max} , while we did not see maintenance of high frequency in our ABM implementations.

The presented model contributes to a mechanistic analysis of the dual effects of spatio-temporal regulation of MAPK pathways and suggests that ultrasensitivity and oscillation emerge in the pathway as a product of coupled spatiotemporal modulation and that multi-compartmentalisation might be an important and integral factor for these behaviours to occur.

Concluding Remarks

In this study, we investigated the dynamics of MAPK pathway activation in both a two compartment- and a multi compartment-model. We showed that compartmentalisation has an important effect on three aspects of pathway activation. The first is the magnitude of response once the pathway is turned on, the rate by which the system reaches equilibrium and recovers from the initial activation and finally how oscillation at the level of MAPK/pMAPK could arise by periodic activation of MAPKK coupled with compartmentalisation of pathway components. Our models also demonstrated that in order to achieve levels of MAPK close to those at t_0 , the MAPKK should be under moderate to high inhibitory feedback regulation. Additionally, the

dynamics of MAPK activation obtained from the ABM model share many parallels with observed MAPK dynamics both *in vitro* and *in silico*.

Methods

For the construction of the model, the agents were modelled as stream X-machines. There are four components fundamental to X-machines, these are inputs, outputs, state memory and functions. Inputs and state memory get processed by the X-machine using finite-functions. Subsequently, the X-machine transition occurs. Transition functions map to a new X-machine state and to an output. As a result, a new X-machine state is achieved with new sets of functions. These new functions dictate the input accepted by the X-machine, the states the X-machine could transform to, the functions and outputs associated with the X-machine.

To implement this, descriptions of the agents were written in Extensible Markup Language (XML) while for the execution of the model the source code was written with C language. To create the agents and run the model, Flexible Large-scale Agent Modelling Environment (FLAME) framework was used with iterated time-steps [75–77].

Iterated time-steps were converted to minutes by first analysing MAPK activation patterns reported in the literature from *in vitro* data. The times taken to generate E_{max} response of activated MAPK species were calculated and the mean and mode values were determined from all the graphs (Fig 2). The average time was $8.98 \text{ (min)} \pm 5.08 \text{ (mean} \pm \text{SD)}$ and the median was 7.73 (min) . We opted for the median as statistical analysis shown that the data was not normally distributed. This time value was used to convert time-steps taken to generate the maximum response in the ABM model into minutes.

Initial Conditions and Basic Model Structure

Agent numbers. The number of the different components of the MAPK cascade (MAPKK and MAPK) in the model at $t = 0$ was determined from protein concentrations described by Huang et al and Chickarmane V et al [45, 78]. These concentrations were converted to moles by adapting the average number of mean corpuscular volume of red blood cells (≈ 90 femtoliter) as the volume these proteins were present in (as they are mainly cytoplasmic). Moles were then converted into number of protein molecules using Avogadro's number. See Table 1 below.

This is where MAPKK activates MAPK leading to the formation of pMAPK, which translocates to the nucleus. Once translocated to the nucleus MAPK could interact with active exporting receptors (ExR) in order to translocate out of the nucleus. This scheme is represented in Fig 2A.

Table 1.

Agent name	Number of protein agent molecules in the two compartment model	Number of protein agent molecules in the multi-compartment model
MAPKK (MAPKK)	0	100
phosph-MAPKK (pMAPKK)	500	20
MAPK (MAPK)	500	0
phosph-MAPK (pMAPK)	250	500
ExR (active)	180	180
ExR (dormant)	180	180

doi:10.1371/journal.pone.0156139.t001

Rules Governing Agents' Behaviour

Simple rules were assigned to the agents in both models. These rules specified the agents' movement and the manner with which they interacted with their interaction partners.

Agents' Description

Both models contained the same agents were. The agents were separated into cytoplasmic and nuclear species:

Cytoplasmic agents

MAPKK (MKK). MAPKK agent is found in two states, pMAPKK and MAPKK. pMAPKK only interacts with MAPK agent. It reads locations messages of the different MAPK agents, this allows it to determine the closest MAPK available for binding. pMAPKK sends location messages and binding status messages to close by MAPK agents. Once confirmation of binding availability is established between MAPK and MAPKK, binding occurs. This leads to the change in pMAPKK state to the dormant MAPKK (MAPKK). MAPKK reverts back into pMAPKK after a lag phase (the re-activation delay period, RADP). A RADP value assigned to individual MAPKKs and it becomes updated once MAPKK returns back to pMAPKK. RADP value was updated either deterministically or stochastically (Fig 2E). For the deterministic update, the value (for every MAPKK agent) was identical and it was the upper limit chosen for any particular simulation. For the stochastic updating, RADP was set (for individual MAPKK agent) randomly at a value between 0 and the chosen RADP upper limit. MAPKK moves by Brownian motion. In the two compartments model, this movement is restricted to the cytoplasm, where MAPKK deflects off the plasma membrane and the nuclear membrane. While in the multi-compartment model this movement is restricted to the individual compartment boundaries.

MAPK (MAPK). MAPK interacts with a number of agents in the model. It sends messages of its location and binding availability which are read by these agents. Once the binding availability become confirmed MAPK interact with the given agent. MAPK interacts with MAPKK in the cytoplasm, and with ExR at the internal surface of the nuclear membrane. MAPK interacts with pMAPKK leads to MAPK activation, change of status to pMAPK and the translocation to the nucleus. Once in the nucleus, pMAPK also interacts with ExR, this interaction leads to the translocation of pMAPK back to the cytoplasm and/or its specific compartment in them multi-compartment system; and the reformation of MAPK.

MAPK move by Brownian motion. However, the movements of the different states are dissimilar. MAPK is restricted to move in the cytoplasm or within the boundary of its specific compartment only. On the other hand, pMAPK are restricted to move within the cytoplasm.

Nuclear agents

Exporting Receptor (ExR). There are two states for ExR, an active (ExR) and inactive (dExR). These two states are interchangeable. Exporting receptors are shifting between active and inactive states and *vice versa*. Both receptors move around by Brownian motion, however within the nuclear membrane. dExRs shift back to ExR after a lag phase (dormancy period). ExR interacts with pMAPK. The ExR receives location messages from pMAPK, close ExR respond by sending messages to closest pMAPK confirming the availability to bind. Once ExR binds to pMAPK it changes state to dExR and triggers pMAPK translocation out of the nucleus and status change to MAPK.

ABM codes. The complete code of the ABMs presented in this study has been uploaded on GitHub: <https://github.com/MadinaJNR/Multi-Compartment-ABM-source-code-in-C-programming-language->

Supporting Information

S1 Fig. RADP stochasticity modulation and its effects on MAPK activation dynamics. Stochastic RADP configurations were tested by varying the RADP ranges in the multi-compartment ABM. (A) RADP value was set to be generated within the following range $3.77 \leq \text{RADP} < 4.55$ min. At the initial activation phase minor oscillatory responses emerge. (B) Illustrates the RADP configuration when the range was set at $4.15 \leq \text{RADP} < 4.55$ min, whereby at the initial MAPK activation phase sharper miniature oscillatory activity appears. (C) Demonstrates a RADP configuration when the range was set at $4.38 \leq \text{RADP} < 4.55$ min, there the miniature oscillatory activity become more visible. This last RADP configuration is the least stochastic due to its limited range for RADP re-setting value, thus the MAPK activation behaviour is analogous to the deterministic configuration where $\text{RADP} = 4.55$ min.

(TIF)

S2 Fig. Effects of stochastic RADP on pMAPK and MAPKK activation dynamics. (A) The pMAPK levels with each RADP configuration were examined, when RADP was less than 7.55 min, there was no significant difference between pMAPK levels compared to the control run. However, when RADP value was ≤ 7.55 min, the level of pMAPK started to become significantly lower compared to the control run, with $0 \leq \text{RADP} \leq 22.65$ min, demonstrating a substantial significance. (B) Conversely, the time to achieve E_{max} appeared to be significantly different when RADP was less than 22.63 min. (C) When the time to achieve EC_{50} was considered, only $0 \leq \text{RADP} \leq 22.63$ min configuration illustrated a significant difference compared to control run. (D) When the effect of the RADP configuration was examined in relation to MAPKK, increasing RADP caused a significant reduction in the level of active MAPKK. (E) The increasing RADP value prompted an increase in the time to achieve E_{max} when RADP configuration was $\text{RADP} \leq 22.65$ min. (F) This was also reflected with significant increase in the time to achieve EC_{50} , yet, when RADP range was within 22.63 min the time to achieve EC_{50} was significantly. This is due to the significantly small magnitude of MAPKK generated in comparison to the contro. $N = 3$, one way ANOVA test was conducted to demonstrate significance with *, ** and *** corresponding to $p < 0.05$, $p < 0.001$ and $p < 0.0001$ respectively.

(TIF)

S3 Fig. MAPK activation dynamics; AMB vs. experimental data. Relative pMAPK levels were compared between experimental data, reported by Lefkowitz RJ *et al.* [40] vs. our ABM. Multiple t-tests were performed with Holm-Sidak corrections for multiple comparisons. No significant differences were observed.

(TIFF)

S1 File. Detailed description of agent memory, messages and functions.

(DOCX)

S2 File. List of references used for calibration of MAPK activation in the ABM.

(DOCX)

S3 File. Examples of RADP values generated in the stochastic ABMs.

(XLSX)

Acknowledgments

This work was funded by the BBSRC Doctoral Training Grant BB/F016840/1. We would like to thank Dr Simon Coakley, Dr Mark Pogson and David Rhodes for their assistance and advice with FLAME and the construction of the ABM. We also would like to thank Dr Susheel Varma and Dr Andrew Narracott for their recommendations for data analysis tools and data visualisation.

Author Contributions

Conceived and designed the experiments: AAS. Performed the experiments: AAS. Analyzed the data: AAS EK-T. Contributed reagents/materials/analysis tools: AAS MH AH. Wrote the paper: AAS EK-T MH.

References

1. Seger R, Krebs EG. The MAPK signaling cascade. *FASEB journal: official publication of the Federation of American Societies for Experimental Biology*. 1995; 9(9):726–35. Epub 1995/06/01. PMID: [7601337](#).
2. Brunet A, Roux D, Lenormand P, Dowd S, Keyse S, Pouyssegur J. Nuclear translocation of p42/p44 mitogen-activated protein kinase is required for growth factor-induced gene expression and cell cycle entry. *EMBO J*. 1999; 18(3):664–74. PMID: [9927426](#)
3. Khokhlatchev AV, Canagarajah B, Wilsbacher J, Robinson M, Atkinson M, Goldsmith E, et al. Phosphorylation of the MAP Kinase ERK2 Promotes Its Homodimerization and Nuclear Translocation. *Cell*. 1998; 93(4):605–15. PMID: [9604935](#)
4. Chambard J-C, Lefloch R, Pouyssegur J, Lenormand P. ERK implication in cell cycle regulation. *Biochimica et Biophysica Acta (BBA)—Molecular Cell Research*. 2007; 1773(8):1299–310.
5. Choi TG, Lee J, Ha J, Kim SS. Apoptosis signal-regulating kinase 1 is an intracellular inducer of p38 MAPK-mediated myogenic signalling in cardiac myoblasts. *Biochimica et Biophysica Acta (BBA)—Molecular Cell Research*. 2011; 1813(8):1412–21.
6. McCubrey JA, Steelman LS, Chappell WH, Abrams SL, Wong EWT, Chang F, et al. Roles of the Raf/MEK/ERK pathway in cell growth, malignant transformation and drug resistance. *Biochimica et Biophysica Acta (BBA)—Molecular Cell Research*. 2007; 1773(8):1263–84.
7. Baldassare JJ, Bi Y, Bellone CJ. The Role of p38 Mitogen-Activated Protein Kinase in IL-1 β Transcription. *The Journal of Immunology*. 1999; 162(9):5367–73. PMID: [10228013](#)
8. Boulton TG, Nye SH, Robbins DJ, Ip NY, Radziejewska E, Morgenbesser SD, et al. ERKs: A family of protein-serine/threonine kinases that are activated and tyrosine phosphorylated in response to insulin and NGF. *Cell*. 1991; 65(4):663–75. PMID: [2032290](#)
9. Dérjard B, Hibi M, Wu IH, Barrett T, Su B, Deng T, et al. JNK1: A protein kinase stimulated by UV light and Ha-Ras that binds and phosphorylates the c-Jun activation domain. *Cell*. 1994; 76(6):1025–37. PMID: [8137421](#)
10. Johnson GL, Lapadat R. Mitogen-activated protein kinase pathways mediated by ERK, JNK, and p38 protein kinases. *Science*. 2002; 298(5600):1911–2. Epub 2002/12/10. doi: [10.1126/science.1072682](#) PMID: [12471242](#).
11. Marshall CJ. Specificity of receptor tyrosine kinase signaling: Transient versus sustained extracellular signal-regulated kinase activation. *Cell*. 1995; 80(2):179–85. PMID: [7834738](#)
12. Nguyen TT, Scimeca JC, Filloux C, Peraldi P, Carpentier JL, Van Obberghen E. Co-regulation of the mitogen-activated protein kinase, extracellular signal-regulated kinase 1, and the 90-kDa ribosomal S6 kinase in PC12 cells. Distinct effects of the neurotrophic factor, nerve growth factor, and the mitogenic factor, epidermal growth factor. *Journal of Biological Chemistry*. 1993; 268(13):9803–10. PMID: [8387505](#)
13. Colpoys WE, Cochran BH, Carducci TM, Thorpe CM. Shiga toxins activate translational regulation pathways in intestinal epithelial cells. *Cellular signalling*. 2005; 17(7):891–9. Epub 2005/03/15. doi: [10.1016/j.cellsig.2004.11.014](#) PMID: [15763431](#).
14. Harris VK, Coticchia CM, Kagan BL, Ahmad S, Wellstein A, Riegel AT. Induction of the angiogenic modulator fibroblast growth factor-binding protein by epidermal growth factor is mediated through both MEK/ERK and p38 signal transduction pathways. *The Journal of biological chemistry*. 2000; 275(15):10802–11. Epub 2001/02/07. PMID: [10753873](#).

15. Morley SJ. Signalling through either the p38 or ERK mitogen-activated protein (MAP) kinase pathway is obligatory for phorbol ester and T cell receptor complex (TCR-CD3)-stimulated phosphorylation of initiation factor (eIF) 4E in Jurkat T cells. *FEBS letters*. 1997; 418(3):327–32. Epub 1998/01/15. PMID: [9428738](#).
16. Murphy LO, MacKeigan JP, Blenis J. A network of immediate early gene products propagates subtle differences in mitogen-activated protein kinase signal amplitude and duration. *Molecular and cellular biology*. 2004; 24(1):144–53. Epub 2003/12/16. PMID: [14673150](#); PubMed Central PMCID: PMCPMC303364.
17. Sabbagh W Jr., Flatauer LJ, Bardwell AJ, Bardwell L. Specificity of MAP kinase signaling in yeast differentiation involves transient versus sustained MAPK activation. *Molecular cell*. 2001; 8(3):683–91. Epub 2001/10/05. PMID: [11583629](#); PubMed Central PMCID: PMCPMC3017497.
18. Sewing A, Wiseman B, Lloyd AC, Land H. High-intensity Raf signal causes cell cycle arrest mediated by p21Cip1. *Molecular and cellular biology*. 1997; 17(9):5588–97. Epub 1997/09/01. PMID: [9271434](#); PubMed Central PMCID: PMCPMC232407.
19. Woods D, Parry D, Cherwinski H, Bosch E, Lees E, McMahon M. Raf-induced proliferation or cell cycle arrest is determined by the level of Raf activity with arrest mediated by p21Cip1. *Molecular and cellular biology*. 1997; 17(9):5598–611. Epub 1997/09/01. PMID: [9271435](#); PubMed Central PMCID: PMCPMC232408.
20. Hillioti Z, Sabbagh W Jr., Paliwal S, Bergmann A, Goncalves MD, Bardwell L, et al. Oscillatory phosphorylation of yeast Fus3 MAP kinase controls periodic gene expression and morphogenesis. *Current biology*: CB. 2008; 18(21):1700–6. Epub 2008/11/04. doi: [10.1016/j.cub.2008.09.027](#) PMID: [18976914](#); PubMed Central PMCID: PMCPMC2602854.
21. Shankaran H, Ippolito DL, Chrisler WB, Resat H, Bollinger N, Opresko LK, et al. Rapid and sustained nuclear-cytoplasmic ERK oscillations induced by epidermal growth factor. *Molecular systems biology*. 2009; 5:332. Epub 2009/12/03. doi: [10.1038/msb.2009.90](#) PMID: [19953086](#); PubMed Central PMCID: PMCPMC2824491.
22. Kholodenko BN. Negative feedback and ultrasensitivity can bring about oscillations in the mitogen-activated protein kinase cascades. *European journal of biochemistry / FEBS*. 2000; 267(6):1583–8. Epub 2000/03/11. PMID: [10712587](#).
23. Sarma U, Ghosh I. Oscillations in MAPK cascade triggered by two distinct designs of coupled positive and negative feedback loops. *BMC research notes*. 2012; 5:287. Epub 2012/06/15. doi: [10.1186/1756-0500-5-287](#) PMID: [22694947](#); PubMed Central PMCID: PMCPMC3532088.
24. Shin SY, Rath O, Choo SM, Fee F, McFerran B, Kolch W, et al. Positive- and negative-feedback regulations coordinate the dynamic behavior of the Ras-Raf-MEK-ERK signal transduction pathway. *Journal of cell science*. 2009; 122(Pt 3):425–35. Epub 2009/01/23. doi: [10.1242/jcs.036319](#) PMID: [19158341](#).
25. Tsai TY, Choi YS, Ma W, Pomerening JR, Tang C, Ferrell JE Jr. Robust, tunable biological oscillations from interlinked positive and negative feedback loops. *Science*. 2008; 321(5885):126–9. Epub 2008/07/05. doi: [10.1126/science.1156951](#) PMID: [18599789](#); PubMed Central PMCID: PMCPMC2728800.
26. Wang X, Hao N, Dohlman HG, Elston TC. Bistability, stochasticity, and oscillations in the mitogen-activated protein kinase cascade. *Biophysical journal*. 2006; 90(6):1961–78. Epub 2005/12/20. doi: [10.1529/biophysj.105.073874](#) PMID: [16361346](#); PubMed Central PMCID: PMCPMC1386776.
27. Nakayama K, Satoh T, Igari A, Kageyama R, Nishida E. FGF induces oscillations of Hes1 expression and Ras/ERK activation. *Current Biology*. 2008; 18(8):R332–R4. doi: [10.1016/j.cub.2008.03.013](#) PMID: [18430630](#)
28. Gaumont-Leclerc MF, Mukhopadhyay UK, Goumard S, Ferbeyre G. PEA-15 is inhibited by adenovirus E1A and plays a role in ERK nuclear export and Ras-induced senescence. *The Journal of biological chemistry*. 2004; 279(45):46802–9. Epub 2004/08/28. doi: [10.1074/jbc.M403893200](#) PMID: [15331596](#).
29. Smith ER, Smedberg JL, Rula ME, Xu XX. Regulation of Ras-MAPK pathway mitogenic activity by restricting nuclear entry of activated MAPK in endoderm differentiation of embryonic carcinoma and stem cells. *The Journal of cell biology*. 2004; 164(5):689–99. Epub 2004/02/26. doi: [10.1083/jcb.200312028](#) PMID: [14981092](#); PubMed Central PMCID: PMCPMC2172165.
30. Teis D, Taub N, Kurzbauer R, Hilber D, de Araujo ME, Erlacher M, et al. p14–MP1–MEK1 signaling regulates endosomal traffic and cellular proliferation during tissue homeostasis. *The Journal of Cell Biology*. 2006; 175(6):861–8. doi: [10.1083/jcb.200607025](#) PMID: [17178906](#)
31. Teis D, Wunderlich W, Huber LA. Localization of the MP1-MAPK Scaffold Complex to Endosomes Is Mediated by p14 and Required for Signal Transduction. *Developmental cell*. 2002; 3(6):803–14. PMID: [12479806](#)
32. Vetterkind S, Saphirstein RJ, Morgan KG. Stimulus-specific activation and actin dependency of distinct, spatially separated ERK1/2 fractions in A7r5 smooth muscle cells. *PloS one*. 2012; 7(2):e30409. Epub

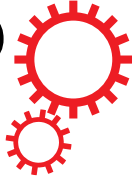
- 2012/03/01. doi: [10.1371/journal.pone.0030409](https://doi.org/10.1371/journal.pone.0030409) PMID: [22363435](https://pubmed.ncbi.nlm.nih.gov/22363435/); PubMed Central PMCID: PMC3283592.
33. Kolch W, Calder M, Gilbert D. When kinases meet mathematics: the systems biology of MAPK signalling. *FEBS Letters*. 2005; 579(8):1891–5. doi: [10.1016/j.febslet.2005.02.002](https://doi.org/10.1016/j.febslet.2005.02.002) PMID: [15763569](https://pubmed.ncbi.nlm.nih.gov/15763569/)
 34. Ferrell JE, Machleder EM. The Biochemical Basis of an All-or-None Cell Fate Switch in *Xenopus* Oocytes. *Science (New York, NY)*. 1998; 280(5365):895–8. doi: [10.1126/science.280.5365.895](https://doi.org/10.1126/science.280.5365.895)
 35. Hanada M, Kobayashi T, Ohnishi M, Ikeda S, Wang H, Katsura K, et al. Selective suppression of stress-activated protein kinase pathway by protein phosphatase 2C in mammalian cells. *FEBS letters*. 1998; 437(3):172–6. Epub 1998/11/21. PMID: [9824284](https://pubmed.ncbi.nlm.nih.gov/9824284/).
 36. Takekawa M, Maeda T, Saito H. Protein phosphatase 2C α inhibits the human stress-responsive p38 and JNK MAPK pathways. *EMBO J*. 1998; 17(16):4744–52. Epub 1998/08/26. doi: [10.1093/emboj/17.16.4744](https://doi.org/10.1093/emboj/17.16.4744) PMID: [9707433](https://pubmed.ncbi.nlm.nih.gov/9707433/); PubMed Central PMCID: PMC31170803.
 37. Lingwood D, Simons K. Lipid Rafts As a Membrane-Organizing Principle. *Science*. 2010; 327(5961):46–50. doi: [10.1126/science.1174621](https://doi.org/10.1126/science.1174621) PMID: [20044567](https://pubmed.ncbi.nlm.nih.gov/20044567/)
 38. Harding A, Tian T, Westbury E, Frische E, Hancock JF. Subcellular localization determines MAP kinase signal output. *Current biology: CB*. 2005; 15(9):869–73. Epub 2005/05/12. doi: [10.1016/j.cub.2005.04.020](https://doi.org/10.1016/j.cub.2005.04.020) PMID: [15886107](https://pubmed.ncbi.nlm.nih.gov/15886107/).
 39. Shalom-Feuerstein R, Plowman SJ, Rotblat B, Ariotti N, Tian T, Hancock JF, et al. K-ras nanoclustering is subverted by overexpression of the scaffold protein galectin-3. *Cancer research*. 2008; 68(16):6608–16. Epub 2008/08/15. doi: [10.1158/0008-5472.can-08-1117](https://doi.org/10.1158/0008-5472.can-08-1117) PMID: [18701484](https://pubmed.ncbi.nlm.nih.gov/18701484/); PubMed Central PMCID: PMC312587079.
 40. Lefkowitz RJ, Shenoy SK. Transduction of Receptor Signals by β -Arrestins. *Science*. 2005; 308(5721):512–7. doi: [10.1126/science.1109237](https://doi.org/10.1126/science.1109237) PMID: [15845844](https://pubmed.ncbi.nlm.nih.gov/15845844/)
 41. Kageyama R, Niwa Y, Isomura A, Gonzalez A, Harima Y. Oscillatory gene expression and somitogenesis. *Wiley interdisciplinary reviews Developmental biology*. 2012; 1(5):629–41. Epub 2013/06/27. doi: [10.1002/wdev.46](https://doi.org/10.1002/wdev.46) PMID: [23799565](https://pubmed.ncbi.nlm.nih.gov/23799565/).
 42. Le Dreau G, Marti E. Dorsal-ventral patterning of the neural tube: a tale of three signals. *Developmental neurobiology*. 2012; 72(12):1471–81. Epub 2012/07/24. doi: [10.1002/dneu.22015](https://doi.org/10.1002/dneu.22015) PMID: [22821665](https://pubmed.ncbi.nlm.nih.gov/22821665/).
 43. Niwa Y, Shimojo H, Isomura A, Gonzalez A, Miyachi H, Kageyama R. Different types of oscillations in Notch and Fgf signaling regulate the spatiotemporal periodicity of somitogenesis. *Genes & development*. 2011; 25(11):1115–20. Epub 2011/06/03. doi: [10.1101/gad.2035311](https://doi.org/10.1101/gad.2035311) PMID: [21632822](https://pubmed.ncbi.nlm.nih.gov/21632822/); PubMed Central PMCID: PMC3110950.
 44. Ferrell JE Jr., Pomerening JR, Kim SY, Trunnell NB, Xiong W, Huang CY, et al. Simple, realistic models of complex biological processes: positive feedback and bistability in a cell fate switch and a cell cycle oscillator. *FEBS Lett*. 2009; 583(24):3999–4005. Epub 2009/11/03. doi: [10.1016/j.febslet.2009.10.068](https://doi.org/10.1016/j.febslet.2009.10.068) PMID: [19878681](https://pubmed.ncbi.nlm.nih.gov/19878681/).
 45. Huang CY, Ferrell JE. Ultrasensitivity in the mitogen-activated protein kinase cascade. *Proceedings of the National Academy of Sciences*. 1996; 93(19):10078–83.
 46. Levchenko A, Bruck J, Sternberg PW. Scaffold proteins may biphasically affect the levels of mitogen-activated protein kinase signaling and reduce its threshold properties. *Proceedings of the National Academy of Sciences*. 2000; 97(11):5818–23. doi: [10.1073/pnas.97.11.5818](https://doi.org/10.1073/pnas.97.11.5818)
 47. Tian XJ, Zhang XP, Liu F, Wang W. Interlinking positive and negative feedback loops creates a tunable motif in gene regulatory networks. *Physical review E, Statistical, nonlinear, and soft matter physics*. 2009; 80(1 Pt 1):011926. Epub 2009/08/08. PMID: [19658748](https://pubmed.ncbi.nlm.nih.gov/19658748/).
 48. Shankaran H, Chrisler WB, Sontag RL, Weber TJ. Inhibition of ERK oscillations by ionizing radiation and reactive oxygen species. *Molecular carcinogenesis*. 2011; 50(6):424–32. Epub 2011/05/11. doi: [10.1002/mc.20724](https://doi.org/10.1002/mc.20724) PMID: [21557328](https://pubmed.ncbi.nlm.nih.gov/21557328/).
 49. Angermann BR, Klauschen F, Garcia AD, Prustel T, Zhang F, Germain RN, et al. Computational modeling of cellular signaling processes embedded into dynamic spatial contexts. *Nature methods*. 2012; 9(3):283–9. Epub 2012/01/31. doi: [10.1038/nmeth.1861](https://doi.org/10.1038/nmeth.1861) PMID: [22286385](https://pubmed.ncbi.nlm.nih.gov/22286385/); PubMed Central PMCID: PMC3448286.
 50. Klann MT, Lapin A, Reuss M. Agent-based simulation of reactions in the crowded and structured intracellular environment: Influence of mobility and location of the reactants. *BMC systems biology*. 2011; 5:71. Epub 2011/05/17. doi: [10.1186/1752-0509-5-71](https://doi.org/10.1186/1752-0509-5-71) PMID: [21569565](https://pubmed.ncbi.nlm.nih.gov/21569565/); PubMed Central PMCID: PMC3123599.
 51. Mallavarapu A, Thomson M, Ullian B, Gunawardena J. Programming with models: modularity and abstraction provide powerful capabilities for systems biology. *Journal of the Royal Society, Interface / the Royal Society*. 2009; 6(32):257–70. Epub 2008/07/24. doi: [10.1098/rsif.2008.0205](https://doi.org/10.1098/rsif.2008.0205) PMID: [18647734](https://pubmed.ncbi.nlm.nih.gov/18647734/); PubMed Central PMCID: PMC312659579.

52. Eblen ST, Slack-Davis JK, Tarcsafalvi A, Parsons JT, Weber MJ, Catling AD. Mitogen-activated protein kinase feedback phosphorylation regulates MEK1 complex formation and activation during cellular adhesion. *Molecular and cellular biology*. 2004; 24(6):2308–17. Epub 2004/03/03. PMID: [14993270](#); PubMed Central PMCID: [PMC355870](#).
53. Legewie S, Schoeberl B, Bluthgen N, Herzog H. Competing docking interactions can bring about bistability in the MAPK cascade. *Biophysical journal*. 2007; 93(7):2279–88. Epub 2007/05/29. doi: [10.1529/biophysj.107.109132](#) PMID: [17526574](#); PubMed Central PMCID: [PMC1965452](#).
54. Liu P, Kevrekidis IG, Shvartsman SY. Substrate-dependent control of ERK phosphorylation can lead to oscillations. *Biophysical journal*. 2011; 101(11):2572–81. Epub 2012/01/21. doi: [10.1016/j.bpj.2011.10.025](#) PMID: [22261044](#); PubMed Central PMCID: [PMC3297790](#).
55. Kim SY, Ferrell JE Jr. Substrate competition as a source of ultrasensitivity in the inactivation of Wee1. *Cell*. 2007; 128(6):1133–45. Epub 2007/03/27. doi: [10.1016/j.cell.2007.01.039](#) PMID: [17382882](#).
56. Qiao L, Nachbar RB, Kevrekidis IG, Shvartsman SY. Bistability and oscillations in the Huang-Ferrell model of MAPK signaling. *PLoS computational biology*. 2007; 3(9):1819–26. Epub 2007/10/03. doi: [10.1371/journal.pcbi.0030184](#) PMID: [17907797](#); PubMed Central PMCID: [PMC1994985](#).
57. Sabouri-Ghomi M, Ciliberto A, Kar S, Novak B, Tyson JJ. Antagonism and bistability in protein interaction networks. *Journal of theoretical biology*. 2008; 250(1):209–18. Epub 2007/10/24. doi: [10.1016/j.jtbi.2007.09.001](#) PMID: [17950756](#).
58. Bray D, Lay S. Computer-based analysis of the binding steps in protein complex formation. *Proceedings of the National Academy of Sciences of the United States of America*. 1997; 94(25):13493–8. Epub 1998/02/12. PMID: [9391053](#); PubMed Central PMCID: [PMC28333](#).
59. Bhalla US. Signaling in small subcellular volumes. I. Stochastic and diffusion effects on individual pathways. *Biophysical journal*. 2004; 87(2):733–44. Epub 2004/08/10. doi: [10.1529/biophysj.104.040469](#) PMID: [15298882](#); PubMed Central PMCID: [PMC1304483](#).
60. Kholodenko BN, Brown GC, Hoek JB. Diffusion control of protein phosphorylation in signal transduction pathways. *The Biochemical journal*. 2000; 350 Pt 3:901–7. Epub 2000/09/06. PMID: [10970807](#); PubMed Central PMCID: [PMC1221325](#).
61. Munoz-Garcia J, Neufeld Z, Kholodenko BN. Positional information generated by spatially distributed signaling cascades. *PLoS computational biology*. 2009; 5(3):e1000330. Epub 2009/03/21. doi: [10.1371/journal.pcbi.1000330](#) PMID: [19300504](#); PubMed Central PMCID: [PMC2654021](#).
62. Ortega F, Garcés JL, Mas F, Kholodenko BN, Cascante M. Bistability from double phosphorylation in signal transduction. Kinetic and structural requirements. *The FEBS journal*. 2006; 273(17):3915–26. Epub 2006/08/29. doi: [10.1111/j.1742-4658.2006.05394.x](#) PMID: [16934033](#).
63. Bhalla US, Ram PT, Iyengar R. MAP kinase phosphatase as a locus of flexibility in a mitogen-activated protein kinase signaling network. *Science*. 2002; 297(5583):1018–23. Epub 2002/08/10. doi: [10.1126/science.1068873](#) PMID: [12169734](#).
64. Lim S, Pnueli L, Tan JH, Naor Z, Rajagopal G, Melamed P. Negative feedback governs gonadotrope frequency-decoding of gonadotropin releasing hormone pulse-frequency. *PloS one*. 2009; 4(9):e7244. Epub 2009/09/30. doi: [10.1371/journal.pone.0007244](#) PMID: [19787048](#); PubMed Central PMCID: [PMC2746289](#).
65. Hancock JF, Parton RG. Ras plasma membrane signalling platforms. *The Biochemical journal*. 2005; 389(Pt 1):1–11. Epub 2005/06/16. doi: [10.1042/bj20050231](#) PMID: [15954863](#); PubMed Central PMCID: [PMC1184533](#).
66. Tian T, Harding A, Inder K, Plowman S, Parton RG, Hancock JF. Plasma membrane nanoswitches generate high-fidelity Ras signal transduction. *Nature cell biology*. 2007; 9(8):905–14. Epub 2007/07/10. doi: [10.1038/ncb1615](#) PMID: [17618274](#).
67. Chiu VK, Bivona T, Hach A, Sajous JB, Silletti J, Wiener H, et al. Ras signalling on the endoplasmic reticulum and the Golgi. *Nature cell biology*. 2002; 4(5):343–50. Epub 2002/05/04. doi: [10.1038/ncb783](#) PMID: [11988737](#).
68. Murakoshi H, Iino R, Kobayashi T, Fujiwara T, Ohshima C, Yoshimura A, et al. Single-molecule imaging analysis of Ras activation in living cells. *Proceedings of the National Academy of Sciences of the United States of America*. 2004; 101(19):7317–22. Epub 2004/05/05. doi: [10.1073/pnas.0401354101](#) PMID: [15123831](#); PubMed Central PMCID: [PMC409916](#).
69. Plowman SJ, Ariotti N, Goodall A, Parton RG, Hancock JF. Electrostatic interactions positively regulate K-Ras nanocluster formation and function. *Molecular and cellular biology*. 2008; 28(13):4377–85. Epub 2008/05/07. doi: [10.1128/mcb.00050-08](#) PMID: [18458061](#); PubMed Central PMCID: [PMC2447143](#).
70. Inder K, Harding A, Plowman SJ, Philips MR, Parton RG, Hancock JF. Activation of the MAPK module from different spatial locations generates distinct system outputs. *Molecular biology of the cell*. 2008;

19(11):4776–84. Epub 2008/09/12. doi: [10.1091/mbc.E08-04-0407](https://doi.org/10.1091/mbc.E08-04-0407) PMID: [18784252](https://pubmed.ncbi.nlm.nih.gov/18784252/); PubMed Central PMCID: [PMC2575182](https://pubmed.ncbi.nlm.nih.gov/PMC/PMC2575182/).

71. Mugler A, Bailey AG, Takahashi K, ten Wolde PR. Membrane clustering and the role of rebinding in biochemical signaling. *Biophysical journal*. 2012; 102(5):1069–78. Epub 2012/03/13. doi: [10.1016/j.bpj.2012.02.005](https://doi.org/10.1016/j.bpj.2012.02.005) PMID: [22404929](https://pubmed.ncbi.nlm.nih.gov/22404929/); PubMed Central PMCID: [PMC3296021](https://pubmed.ncbi.nlm.nih.gov/PMC/PMC3296021/).
72. Ahn S, Shenoy SK, Wei H, Lefkowitz RJ. Differential Kinetic and Spatial Patterns of β -Arrestin and G Protein-mediated ERK Activation by the Angiotensin II Receptor. *Journal of Biological Chemistry*. 2004; 279(34):35518–25. doi: [10.1074/jbc.M405878200](https://doi.org/10.1074/jbc.M405878200) PMID: [15205453](https://pubmed.ncbi.nlm.nih.gov/15205453/)
73. Zhou Q, Li G, Deng XY, He XB, Chen LJ, Wu C, et al. Activated human hydroxy-carboxylic acid receptor-3 signals to MAP kinase cascades via the PLC-dependent PKC and MMP-mediated EGFR pathways. *British journal of pharmacology*. 2012; 166(6):1756–73. Epub 2012/02/01. doi: [10.1111/j.1476-5381.2012.01875.x](https://doi.org/10.1111/j.1476-5381.2012.01875.x) PMID: [22289163](https://pubmed.ncbi.nlm.nih.gov/22289163/); PubMed Central PMCID: [PMC3402802](https://pubmed.ncbi.nlm.nih.gov/PMC/PMC3402802/).
74. Zhao Q, Yi M, Liu Y. Spatial distribution and dose-response relationship for different operation modes in a reaction-diffusion model of the MAPK cascade. *Physical biology*. 2011; 8(5):055004. Epub 2011/08/13. doi: [10.1088/1478-3975/8/5/055004](https://doi.org/10.1088/1478-3975/8/5/055004) PMID: [21832801](https://pubmed.ncbi.nlm.nih.gov/21832801/).
75. Adra SF, Coakley S, Kiran M, McMinn P. An Agent-Based software platform for modelling systems biology. University of Sheffield Epitheliome Project: Technical Report: University of Sheffield. 2008.
76. Coakley S, Smallwood R, Holcombe M. Using x-machines as a formal basis for describing agents in agent-based modelling. *SIMULATION SERIES*. 2006; 38(2):33.
77. Bai Hao, Rolfe Matthew D., Jia Wenjing, Coakley Simon, Poole Robert K., Green J, et al. Agent-Based Modeling of Oxygen-responsive Transcription Factors in Escherichia coli. *PLOS Comput Biol*. 2014:In press.
78. Chickarmane V, Kholodenko BN, Sauro HM. Oscillatory dynamics arising from competitive inhibition and multisite phosphorylation. *Journal of theoretical biology*. 2007; 244(1):68–76. Epub 2006/09/05. doi: [10.1016/j.jtbi.2006.05.013](https://doi.org/10.1016/j.jtbi.2006.05.013) PMID: [16949102](https://pubmed.ncbi.nlm.nih.gov/16949102/).

SCIENTIFIC REPORTS



OPEN

Competition between members of the tribbles pseudokinase protein family shapes their interactions with mitogen activated protein kinase pathways

Hongtao Guan¹, Aban Shuaib^{1,†}, David Davila De Leon², Adrienn Angyal¹, Maria Salazar², Guillermo Velasco^{2,3}, Mike Holcombe⁴, Steven K. Dower^{1,5,6} & Endre Kiss-Toth¹

Spatio-temporal regulation of intracellular signalling networks is key to normal cellular physiology; dysregulation of which leads to disease. The family of three mammalian tribbles proteins has emerged as an important controller of signalling via regulating the activity of mitogen activated protein kinases (MAPK), the PI3-kinase induced signalling network and E3 ubiquitin ligases. However, the importance of potential redundancy in the action of tribbles and how the differences in affinities for the various binding partners may influence signalling control is currently unclear. We report that tribbles proteins can bind to an overlapping set of MAPK-kinases (MAPKK) in live cells and dictate the localisation of the complexes. Binding studies in transfected cells reveal common regulatory mechanisms and suggest that tribbles and MAPKs may interact with MAPKKs in a competitive manner. Computational modelling of the impact of tribbles on MAPK activation suggests a high sensitivity of this system to changes in tribbles levels, highlighting that these proteins are ideally placed to control the dynamics and balance of activation of concurrent signalling pathways.

Spatio-temporal control of intracellular signal transduction pathways is achieved by a range of mechanisms, including regulation of receptor expression, post-translational modifications of pathway components, expression of scaffolds that bring together critical components of the signalling pathway at specific locations, as well as the action of regulatory proteins, which can augment or inhibit pathway activation. However, most intracellular signalling proteins form families with high sequence homology and often share binding partners and targets. It is generally accepted that differences in binding affinities between homologous proteins and their partners are fundamentally important in shaping signalling responses. Yet, characterising these aspects of signalling control remain technically challenging. We have investigated the interaction between MAP kinase kinases (MAPKK) and the family of tribbles (TRIB) pseudokinases, using *in vitro* systems, to exemplify such signalling control mechanisms. These data provide a semi-quantitative insight into how altered relative expression of specific TRIB proteins may lead to the enrichment (or reduction) of distinct signalling complexes.

Tribbles (TRIB) form an evolutionally ancient family of pseudokinases^{1,2} and have been shown to interact with MAP kinase kinases (MAPKK)^{3,4}, signalling molecules in the PI3K pathway⁵⁻⁷ and E3 ubiquitin ligases⁸⁻¹⁰, thereby regulating the activity of these pathways. It has been proposed that these interactions may be mechanistically important in the development of cancer¹¹⁻¹³ as well as in the control of inflammation¹⁴⁻¹⁶.

¹Department of Infection, Immunity & Cardiovascular Disease, University of Sheffield, Beech Hill road, Sheffield, S10 2RX, United Kingdom. ²Department of Biochemistry and Molecular Biology I, School of Biology, Complutense University, Madrid, Spain. ³Instituto de Investigación Sanitaria del Hospital Clínico San Carlos (IdISSC), Madrid, Spain. ⁴Department of Computer Science, University of Sheffield, Beech Hill road, Sheffield, S10 2RX, United Kingdom. ⁵Bio21 Biotechnology Institute, University of Melbourne, 30 Flemington Road, Parkville, Victoria, 3010, Australia. ⁶CSL Limited, 45 Poplar Rd, Parkville, Victoria 3052, Australia. [†]Present address: Insigneo Institute for in silico Medicine, Department of Mechanical Engineering, University of Sheffield, Sheffield, S10 2TN, United Kingdom. Correspondence and requests for materials should be addressed to E.K.-T. (email: e.kiss-toth@sheffield.ac.uk)

Also, it has been shown that both TRIB1 and TRIB2 may be oncogenes in the development of acute myeloid leukaemia via similar mechanisms¹⁷, raising questions about potential functional redundancy between these proteins. Similarly, there is no consensus in the current literature about the oncogenic vs. tumour suppressor role of tribbles proteins^{12,18–20}, suggesting that an important aspect of their activity may be context or cell type dependent. We believe that many of the currently conflicting published studies might be explained and reconciled if we understood the molecular basis of specificity and redundancy between tribbles proteins. Thus, we carried out a systematic analysis of TRIB/MAPKK interactions in mammalian cells and performed computational modelling to quantitatively assess the impact of tribbles on MAPK activation.

We report that tribbles and MAPKK proteins form inducible intermolecular complexes in live cells, mediated via the kinase-like domain of TRIBs and the N-terminus of MAPKKs. Estimation of the relative strength of TRIB-MKK4 binding revealed an up-to twenty fold differences between distinct tribbles, thereby suggesting that intracellular concentration (and trafficking) may be an important controller of TRIB action. In line with these experimental data, computational modelling of TRIB-mediated control of MAPK activation demonstrated that a ten-fold increase or decrease of TRIB concentration (or a similar change in TRIB/MAPKK affinity) is sufficient to switch the MAPK pathway between ON and OFF states.

Uncovering mechanistic details of signal transduction circuits is essential to understand how ubiquitously expressed proteins process a range of incoming signals to achieve cell-type and stimulus-specific cellular responses. Our current analysis provides experimental and computational evidence that the functional outcome from regulatory interactions between signalling kinases and TRIB proteins may be heavily influenced by the relative local abundance of both TRIBs and MAPKKs.

Results

Tribbles subcellular localisation determines the intracellular distribution of trib/mapkk complexes. We and others have demonstrated previously that tribbles proteins exert their regulatory roles, at least in part, by shaping MAPK activation at the level of MAPKKs^{13,21–23} (Fig. 1A). However, we have also shown that tribbles action in inhibiting AP-1 activation is cell-type specific²², suggesting that the expression of additional, yet unknown binding partners or tissue specific modification of tribbles may also be key to their functioning. In order to gain a further mechanistic insight into tribbles action, here we undertook a systematic study, investigating the intracellular localisation of TRIB/MAPKK complexes. Interactions between the three tribbles and MEK1, MKK6, MKK4 and MKK7 (activators of ERK, p38 and JNK MAPKs, respectively) were tested in HeLa cells, where all three tribbles are endogenously expressed and both TRIB-1 and -3 were shown to inhibit MAPK activation²³. In order to visualise the subcellular localisation of TRIB/MAPKK complexes, we used protein fragment complementation (PCA) assay, as described previously^{15,24}. The technique is based on the ability of YFP to re-fold and form a functional fluorophore when two truncated versions of the protein (encoding the N- and C-terminal regions, respectively) come to close proximity to each other. YFP was split into two fragments and each was fused to a protein of interest (TRIB or MAPKK).

First, the distribution of the overexpressed MKKs or TRIBs as EYFP fusion proteins (MAPKK/TRIB-EYFP) was studied. In order to minimise overexpression artefacts, we have selected and analysed cells with low fluorescence levels, which have previously been shown to be close to physiological levels for inflammatory signalling molecules²⁵. In agreement with previous findings, fluorescent microscopy results of TRIBs (1–3)-EYFP single transfected cells demonstrated that full-length TRIB1 and TRIB3 proteins are located in the nucleus, whereas TRIB2 protein is also expressed in the cytoplasm (Fig. 1B). Localisation of overexpressed MKKs (MEK-1, MKK6, MKK7 and -4) was examined in the same way. Full length MEK1 shows exclusive cytoplasmic expression, whereas the full length MKK6, MKK4 and MKK7 are all expressed over the whole cell (Fig. 1B). Broadly, these findings are in agreement with previous reports in the literature^{26,27}.

Building on these data, the interaction between TRIBs and MKKs and the localisation of the TRIBs-MKKs complexes were examined. A systematic survey was carried out to detect MAPKK/TRIB complexes for MEK-1, MKK6, MKK7 and -4. Representative, high magnification images are shown in Fig. 1C, low power images and nuclear counter staining of selected complexes are also shown as additional controls (Suppl. Fig. 1A,B). All tested combinations of the TRIBs-MKKs pairs formed a detectable fluorescent complex; consistent with the hypothesis that tribbles are generic regulators of MAPKK activity. As additional controls, the interaction between endogenously expressed TRIB3 and MKKs was examined by co-immunoprecipitation (Suppl. Fig. 2). Complexes between all four MKKs and either TRIB1 or TRIB3 showed nuclear localisation, whereas complexes composed of the MKKs and TRIB2 showed both cytoplasmic and nuclear localisation, with the exception of the MEK1/TRIB2 complex, which is excluded from the nucleus (Fig. 1C).

The tribbles kinase-like domain and the n-terminal region of mapkks are necessary for trib/mapkk interaction. Based on sequence homology, it is predicted that the structure of the MAPKKs and TRIBs are similar, in that both contain a kinase domain at the centre of the protein and an N- and a C-terminal domain with less understood function. The recently reported crystal structure for TRIB1 confirms these predictions²⁸. However, the kinase domain in tribbles is thought to be catalytically inactive²⁹, with the exception of TRIB2, which has recently been shown to carry a small auto-phosphorylating activity, *in vitro*³⁰. In order to characterise the protein domains necessary for the formation and localisation of TRIB/MAPKK complexes, a series of deletion mutants were generated, expressing truncated versions of MKKs and Tribbles (Suppl. Table 1). We combined wild type TRIB with the deletion mutants of MKKs, or *vice versa* to perform the PCA experiments, similar to the above.

The results demonstrate that all truncated mutants of tribbles form complexes with wild type MKKs (Fig. 2A). However, altered cellular localisation was seen for TRIB1 and TRIB3/MAPKK complexes when N-terminal, or both N- and C-terminal tribbles domains were deleted. In particular, MEK1 - TRIB1/3ΔN complexes showed

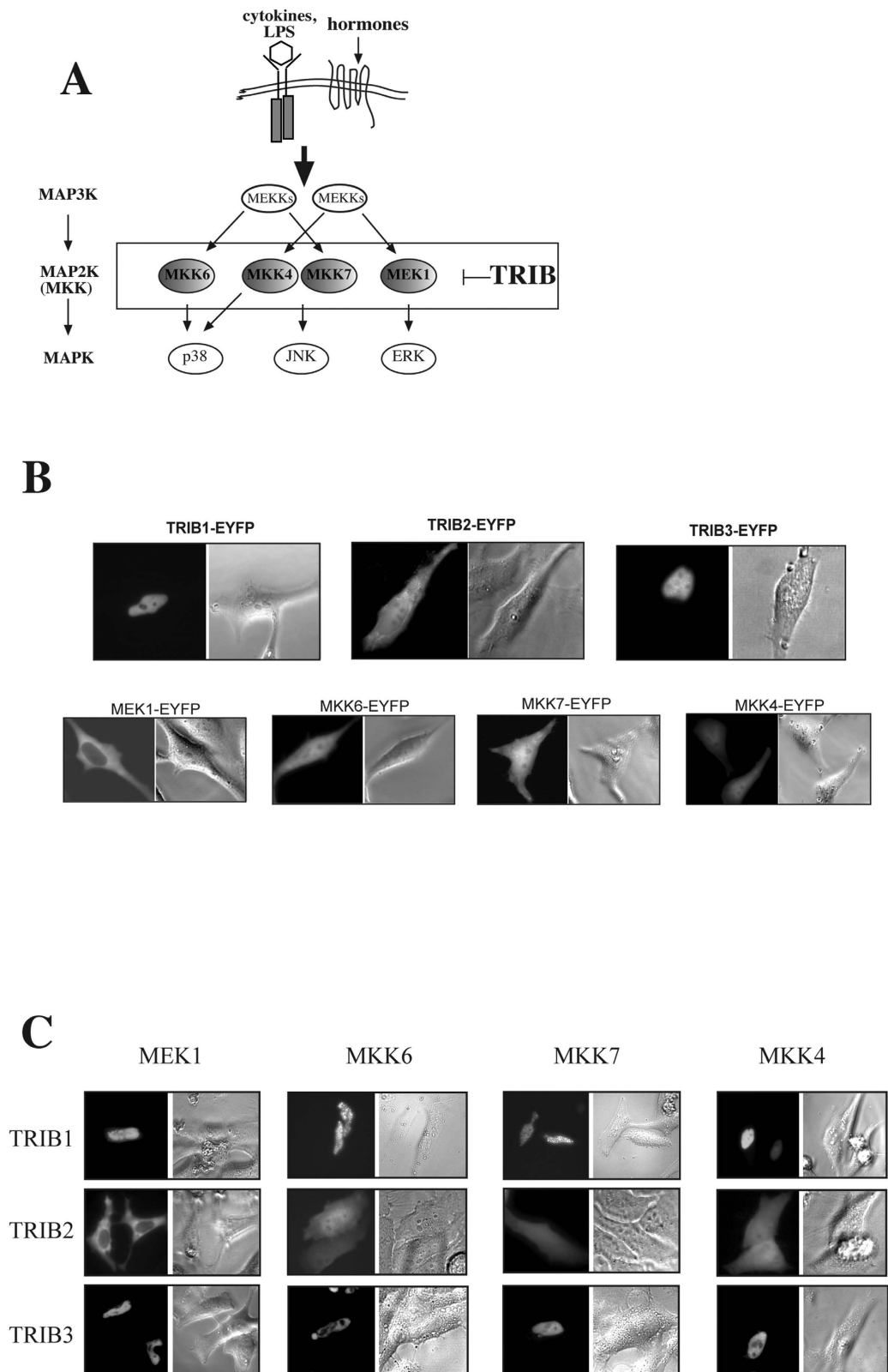


Figure 1. Members of the tribbles family interact with activators of all three groups of MAPKs. (A) A schematic diagram of TRIB mediated control of MAPK activation. **(B)** Plasmids expressing YFP tagged full length TRIBs or MKKs were transfected into HeLa cells. 24 hrs after transfection, intracellular TRIB expression profile was examined by fluorescent microscopy. Representative images are shown. **(C)** MKKs (MEK1, MKK4, 6, 7) and TRIB1-3 were fused to the V1 or V2 fragments of YFP, respectively, and co-transfected to HeLa cells. Localisation of fluorescent complexes was investigated by fluorescent microscopy. YFP fluorescent images and the corresponding phase contrast image are shown in panels B,C.

A

	TRIB1			TRIB2		TRIB3	
	Δ NC	Δ N	Δ C	Δ N	Δ C	Δ N	Δ C
MEK1	cytoplasm only	cytoplasm only	nuclear	cytoplasm only	cytoplasm only	cytoplasm only	nuclear
MKK6	whole cell	whole cell	nuclear	whole cell	cytoplasm only	whole cell	nuclear
MKK7	whole cell	whole cell	nuclear	whole cell	cytoplasm only	whole cell	nuclear
MKK4	whole cell	whole cell	nuclear	whole cell	cytoplasm only	whole cell	nuclear

	MEK1			MKK6		MKK 7	
	Δ NC	Δ N	Δ C	Δ NC	Δ C	Δ NC	Δ C
TRIB1		nuclear			nuclear		
TRIB2	No fluorescence	cytoplasm only		No fluorescence	whole cell		
TRIB3		nuclear			nuclear		

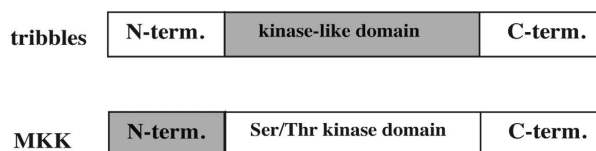
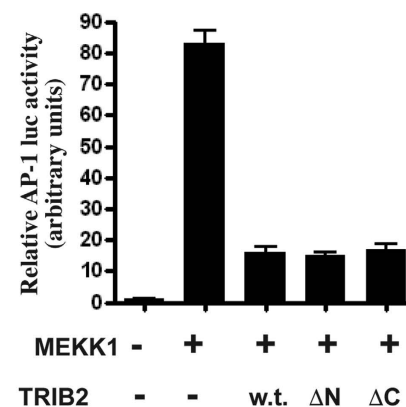
B**C**

Figure 2. The central kinase-like domain of tribbles and the N-terminal region of MKKs are required for the formation of the TRIB/MAPKK complex. (A) PCA constructs, using full length or truncated versions of TRIBs or MKKs (as indicated in the Figure) were transfected to HeLa cells to map the regions of both binding partners required for the formation of TRIB/MAPKK complex. The intracellular localisation of complexes were examined by fluorescent microscopy and listed in the Figure. (B) Schematic representation of the regions (highlighted in grey) of both TRIB and MKKs, required for complex formation. (C) Full length (w.t.) or truncated versions of TRIB2 were expressed in HeLa cells and the ability of these TRIB proteins to inhibit MEKK1 driven activation of JNK- > AP-1, as measured by an AP-1 responsive luciferase reporter, was assessed. Bar graph shows Mean \pm S.D. N = 4.

only cytoplasmic localisation, whilst MKK6/7 - TRIB1/3 Δ N complexes were seen both in the cytoplasm and in the nucleus. These data are in line with the expression patterns of the various MKKs as shown on Fig. 1C (MEK1 cytoplasm only and MKK4, 6, 7 in the whole cell) and indicate that the N-termini of the TRIB1 and TRIB3 are important for localising the TRIB/MAPKK complexes in the nucleus. In contrast to TRIB1 and TRIB3, deleting the N-terminus of TRIB2 did not alter the localisation of MKKs-TRIB2 complexes (both cytoplasmic and nuclear). However, deleting the C-terminus of TRIB2 altered the localisation of the complex with MKK4/6/7, which were observed in the cytoplasm.

To complement the above experiments, the impact of deletion of N- or C-terminal domains of MKKs on TRIB/MAPKK complex formation was tested. For MKK7, both N- and C- termini were essential for interacting with tribbles as deletions of either domains eliminated the interaction with TRIB1-3. In contrast, only the N-terminal but not the C-terminal domains of MEK1 and MKK6 were essential for complex formation with TRIB1-3 (Fig. 2A). As a control, western blotting was undertaken to confirm the expression of the N-terminal truncated MAPKK proteins (Suppl. Fig. 3). As expected, these were expressed at levels similar to that of the full-length constructs. Therefore, we conclude that the loss of PCA signal is not due to lack of expression of the MAPKK Δ N mutants.

In summary, we conclude that MKKs of all three MAPK pathways can interact with TRIBs and that TRIBs determine the localisation of the MAPKK/TRIB complex. Further, the N-termini of the MKKs and the central kinase-like domain of tribbles are indispensable for this interaction, with the exception of MKK7, where the

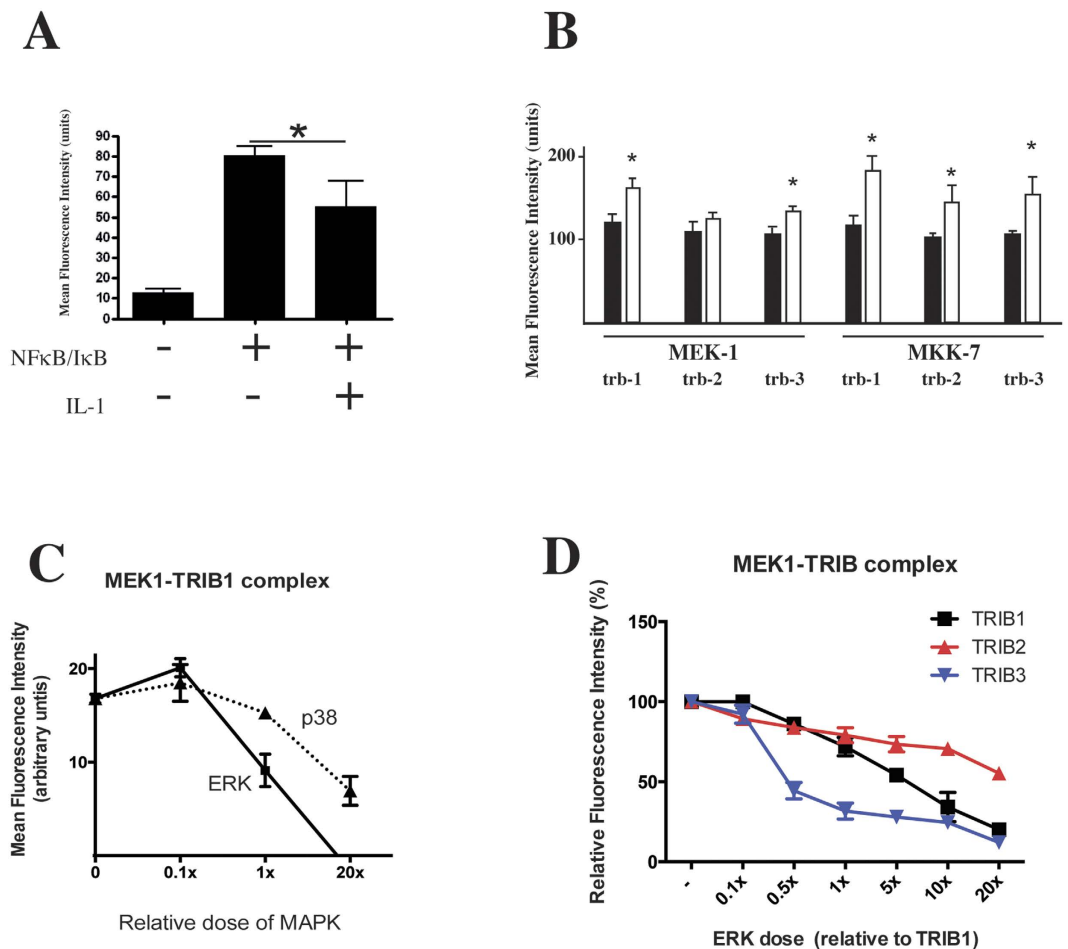


Figure 3. TRIB/MAPKK complex formation is induced by inflammatory activation and MAPKs compete with tribbles for MAPKK binding. (A) The ability of PCA to detect changes in protein complexes was verified by RelA-V1 and I κ B α -V2 cotransfected HeLa cells, which were stimulated by IL-1 α (0.1 nM, 60 min), 24 hrs after transfection. (* $p < 0.05$). (B) The impact of IL-1 α (0.1 nM, 60 min) stimulation on MEK1-TRIB and MKK7-TRIB complexes was examined using flow cytometry, 24 hrs. post-transfection (* $p < 0.05$). (C) The relative intensity of the MEK1-TRIB1 PCA complex was analysed in the presence of an increasing dose of unlabelled ERK vs. p38 expression. $N \geq 3$ (■: increasing ERK dose, ▲: increasing p38 dose). (D) The relative intensity of MEK1-TRIB PCA complexes were analysed in the presence of an increasing dose of unlabelled ERK (■: TRIB1, ▲: TRIB2, ▼: TRIB3).

C-terminus is also necessary (Fig. 2B). In line with our previous findings, N-termini of TRIB1 and TRIB3 but not of TRIB2 appear to be responsible for the nuclear localisation. However, we showed here that the C-terminal domain of TRIB2 may have a unique function as, unlike in other tribbles, its deletion leads to the exclusion of TRIB2/MAPKK complexes from the nucleus. Next, we confirmed that the kinase-like domain of TRIB2 not only is necessary for the interaction with MKKs, but it is sufficient for inhibiting MEK1 driven AP-1 activation in HeLa cells (Fig. 2C). However, we note that some of these interactions may only take place in a cell type specific manner, as we observed TRIB2/MKK7 but not TRIB2/MKK4 complexes in monocytes previously, using PCA¹⁵.

Formation of the tribbles/mapkk complex is inducible; trib and mapk proteins compete for mapkk binding.

Tribbles have previously been shown to regulate inflammatory signalling, one of the molecular mechanisms being via their interaction with MAPKKs^{14,15,23,24,31,32}. However, the dynamics of TRIB/MAPKK complex formation and the relationship between TRIBs and MAPKs is currently unclear. Thus, we tested the impact of IL-1 β stimulation on TRIB/MEK1 and TRIB/MK7 complexes, using the PCA assay, as above. As a validation of the PCA method's suitability for intervention studies, we tested this system using a well characterised protein-protein interaction pair, NF- κ B/RelA and I κ B; the complex is disrupted by IL-1 mediated cellular activation. FACS analysis showed that RelA-v1 and I κ B α -v2 formed a fluorescent complex, the intensity of which decreased significantly after 60 min of IL-1 stimulation, due to the degradation of I κ B α (Fig. 3A). These results are in line with previous reports, where the dynamics of RelA/I κ B complex was investigated using GFP-FRET³³ and validate the use of PCA in investigations of the dynamics of formation/disruption of multi-protein complexes. Serum starved HeLa cells, transfected with MEK-1/TRIB or MKK7/TRIB PCA construct pairs were stimulated by

a non-saturating dose of IL-1 (0.1 nM) for 60 min. The intensity of the PCA signal was quantified by flow cytometry. Data shown in Fig. 3B demonstrate that the formation of these complexes is induced by IL-1 treatment.

Next we wanted to characterise the relationship between TRIB and MAPK proteins, in the context of complex formation with MAPKKs. First, we used the MEK1/TRIB1 PCA complex and added increasing doses of untagged ERK (MEK1 binding MAPK) vs. p38 (non-MEK1 interacting MAPK) and shown that co-expression of equal dose of ERK vs. TRIB1 leads to a ~50% reduction in the intensity of the MEK1/TRIB1 PCA signal (Fig. 3C). In contrast, co-expression of p38 had no detectable impact at this dose, suggesting that there was a competitive relationship between TRIB and MAPK proteins for interacting with their MAPKK partner. Finally, we tested whether ERK disrupts MEK1/TRIB1-3 complexes with equal efficiency. Our data demonstrates that the MEK1/TRIB3 complex is most sensitive to co-expressed ERK (~50% of the MEK1/TRIB3 complex disrupted, in the presence of 0.5x the dose of TRIB3), followed by TRIB1 and TRIB2 (Fig. 3D). Interestingly, about 50% of the MEK1/TRIB2 PCA signal was preserved, even when 20 fold excess of ERK was co-expressed.

Tribbles family members compete for binding with mapkks. Since members of the tribbles family interact with an overlapping set of MAPKKs, the interactome between TRIBs-MAPKKs may be a continuously balanced, dynamic system, with tribbles turnover and expression levels being tightly regulated^{34–36}. Given the data presented in Fig. 3C,D, we hypothesised that TRIB proteins may not only compete with MAPKKs but they themselves bind to MAPKKs cross-competitively. However, in addition to differing expression levels, the binding affinities between distinct TRIBs and MAPKKs may also vary, resulting in an additional layer of complexity for pathway control. To address these questions in live cells, we have used the PCA assay as above and tested the binding of tribbles to MKK4. MKK4-V1 was co-transfected with a tribbles-V2 expression plasmid (Fig. 4A). We have then co-transfected an increasing dose of untagged tribbles expression plasmid, encoding TRIB-1, -2 or -3, respectively. Each MKK4/TRIB complex behaved similarly in that the level of fluorescent signal reduced as an increasing dose of untagged tribbles was co-expressed. In addition, TRIB-3 was substantially more potent in inhibiting fluorescent complex formation. Next, we confirmed that the three recombinant tribbles proteins are expressed at similar levels, when an identical dose of the expression plasmids is transfected, thus enabling comparison of relative binding affinity in live cells (Fig. 4B, left panel). In addition, transfection of an increasing dose of tribbles expression plasmid resulted in a parallel increase of tribbles expression levels (Fig. 4B). Data presented above led us to hypothesise that distinct TRIBs may have differential effects on signalling, in part due to their different “affinities” to their binding partners. This was addressed by using siRNA knockdown of individual tribbles in monocytes and showed that whilst knockdown of any of the three tribbles led to an increase in basal p-p38 levels, the impact on IL-1 induced p38 activation was distinct; siTrib-2 substantially augmented p-p38 levels, whilst siTrib-3 rendered monocyte p-p38 non-inducible by IL-1 (Fig. 4C).

The above competitive PCA assay demonstrated that TRIB-3 could titrate out the MKK4-TRIB binding most efficiently (Fig. 4A), indicating that the affinity of MKK4/TRIB-3 may be the highest among the three. Next, we quantitatively analysed the data by applying a reversible competition-binding model (Fig. 5A). Unlabelled TRIB protein binds MKK4-V1 as a competitor (“B” in equations, Fig. 5A), whilst fusion protein TRIB-V2 being the binding agent (“A”, Fig. 5A). In our experiment setting, equal amount (ng) of TRIB-V2 was added into each sample mix, and 0 to 10x competitor TRIB (relative to the TRIB-V2 dose) was added. We introduced an “f” coefficient in the equation so that $[B] = f[A]$ for fitting the optimal curves. This competition binding model assumes that 1) the interactions are reversible; 2) The binding agents already reached equilibrium when the FACS analysis was undertaken, 3) The degree of AR complex formation is proportional to the mean fluorescent intensity, and 4) Dose (μg) of plasmids transfected into the cells are proportional to the expression of the protein.

Based on these results, we conclude that of the three tribbles, TRIB-3 has ca 15 fold greater affinity to MKK4, compared to TRIB2, thus being the most efficient in competing with other tribbles in the formation of TRIB/MKK4 complex; with TRIB1 having an intermediate affinity (Fig. 5B).

Putting the above data together raises the possibility that altering the expression levels of specific tribbles may have an indirect impact on cell signalling and function by “liberating binding partners” for interaction with other TRIB proteins. We have explored this by knocking down TRIB1, TRIB2 or TRIB3 in HepG2 cells and measuring the level of interactions between TRIB3 and MKK7 under these conditions by co-immunoprecipitation (Fig. 5C and Suppl. Fig. 4). Our results demonstrate that reducing TRIB1 or TRIB2 levels leads to an enhanced TRIB3/MKK7 interaction, supporting the notion that TRIBs form a protein family which controls cell signalling in an integrated fashion.

Model for inhibition of map kinase activity by tribbles proteins. In our original report on the characterisation of tribbles proteins²³, we showed that when TRIB3 expression plasmid was titrated in HeLa cells, all 3 MAPK cascades were maximally inhibited to the same extent (ca. 60–70%), but the mid points of the dose responses differed in the rank order $p38 < JNK < ERK$, and approximately at relative levels of 1:3:10, possibly reflecting differing affinities of TRIB3 for specific MKKs. This data fits well with results presented in Fig. 3D, demonstrating that ERK was most efficient in disrupting (and probably replacing) TRIB3 in its complex with MEK1. Data presented above (Fig. 4A) indicate that specific tribbles may also bind to the same MAPKK with varying affinity. Taken these results together, we wished to use a computational model and test the hypothesis that 10–20 fold change in the binding affinity of tribbles to its binding partner, or a similar change in TRIB expression levels is able to control the activation of MAPK cascades. Modelling was based on a 3 step map kinase cascade:



with each protein kinase requiring two sequential phosphorylation steps for activation. The properties of this type of model have been analysed elsewhere; for example taking Km values in the range 60–1500 nM for the individual protein kinase reactions yields ultrasensitive input/output characteristics for the system, with Hill coefficients for

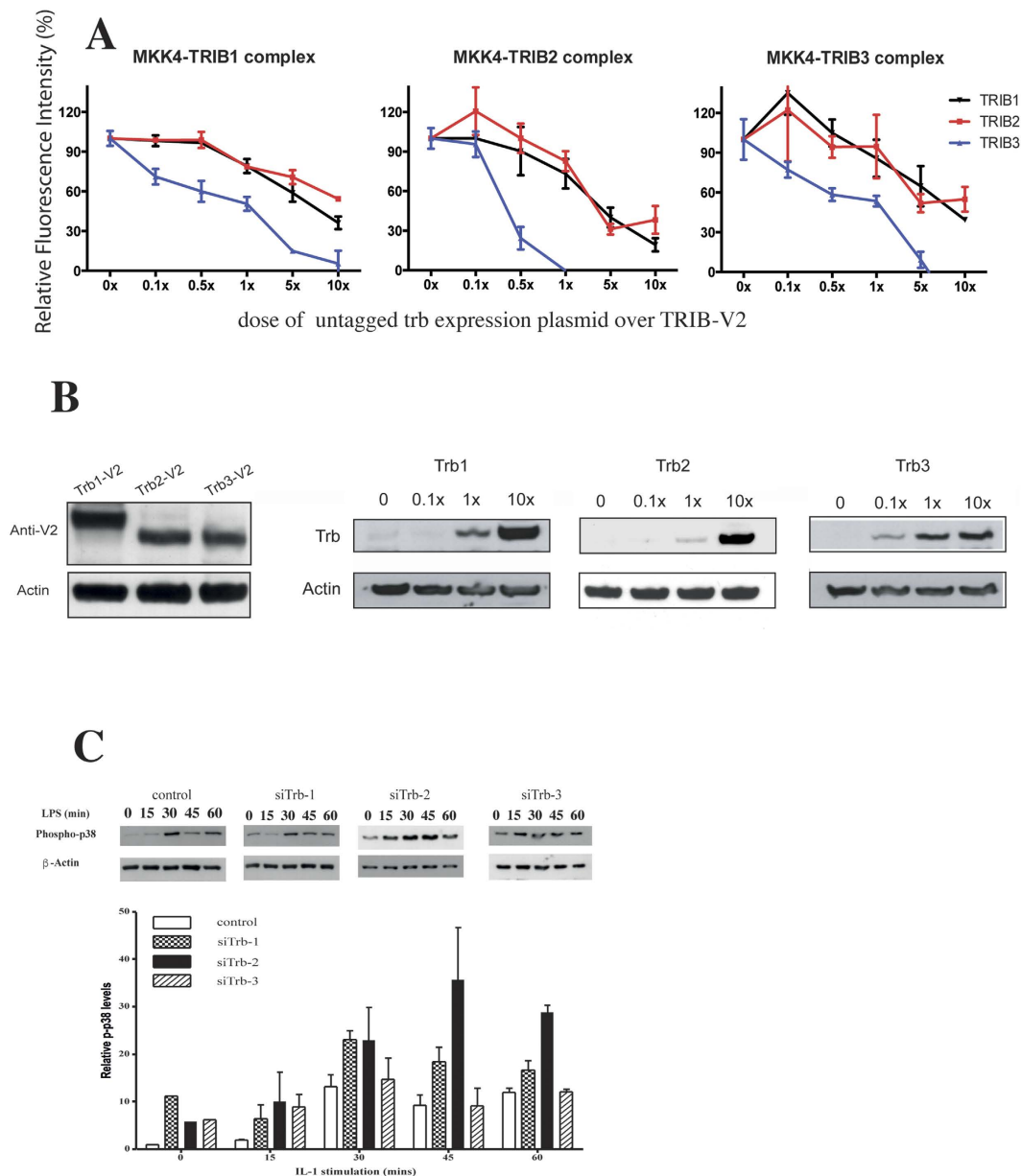


Figure 4. TRIB proteins compete with each other for MAPKK binding. (A) The relative intensity of the MKK4-TRIB PCA complexes were analysed in the presence of an increasing dose of unlabelled tribbles. $N \geq 3$ (▼: TRIB1, ■: TRIB2, ▲: TRIB3) (B). Left panel: 400 ng expression plasmids, encoding for individual tribbles-V2 fusion proteins were transfected into HeLa cells and expression levels were detected by an anti-GFP western blot. Middle and right panels: Tribbles expression levels in HeLa cells increase in a dose dependent manner. Transfected doses of untagged tribbles, relative to the TRIB-PCA dose used in panel A are indicated above the individual panels. Representative western blots are shown ($N = 3$). (C) The differential impact of knockdown of specific tribbles on p38 MAPK activation was assessed in THP-1 cells. Cells transfected with non-targeting control or si-Trib constructs were stimulated by LPS for the stated length of time and the activation of p38 was detected by a phospho-p38 specific western blot. As loading control, the membrane was re-probed for β -actin. Upper panel: a representative result, Lower panel: quantitative assessment of p-p38 from three independent experiments. Data is expressed relative to the β -actin signal.

the MKPP output in the range of 3–6 and 50% maximal output as a function of E1 concentration ca 1000–10,000 lower than the K_m values used for the individual kinase reactions³⁷.

Our previous data suggest that tribbles proteins interact specifically with MKKs, and act as inhibitors of MAPK signalling²³. We approached this problem by adopting the MAPK signalling model, originally described by Ferrell *et al.*³⁸ and incorporated tribbles action into this system. Based on this (but *vide infra*), the full model for this analysis is shown in Suppl. Fig. 5, and the ODE system is presented in Appendix 1. Parameter values for enzyme concentrations and rate constants were taken from refs 37,38.

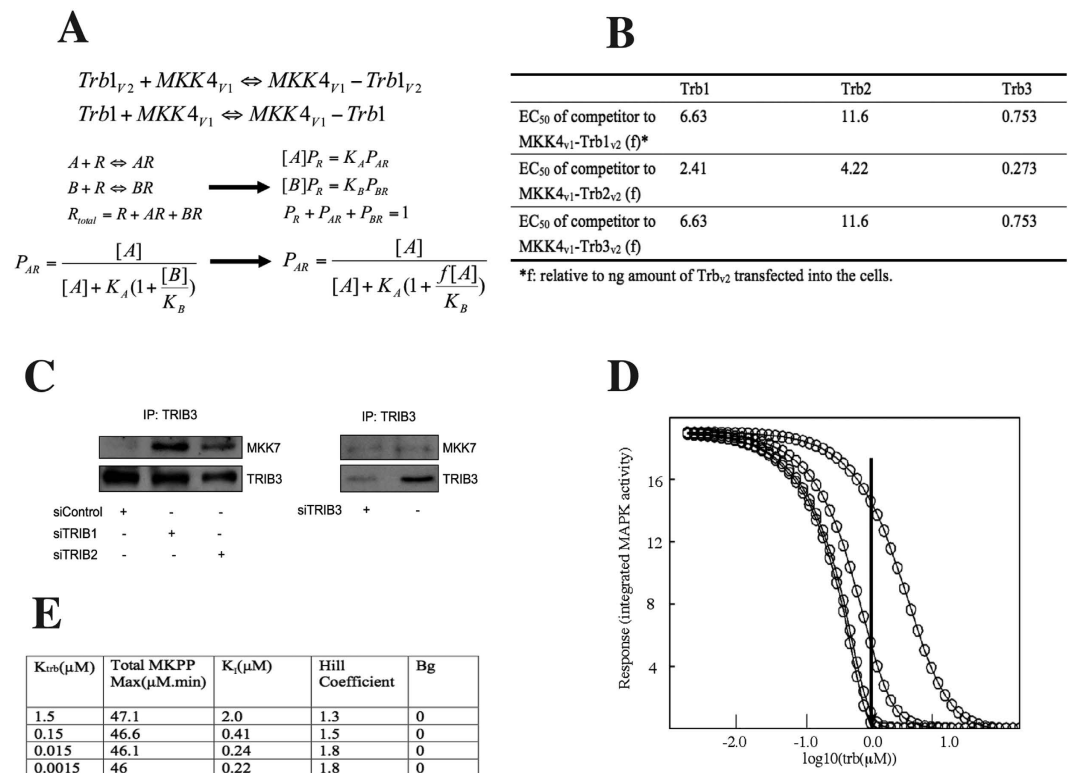


Figure 5. An ODE model to characterise the impact of tribbles mediated inhibition of MAPK activation. (A) A reversible competitive binding model was used to analyse FACS data presented on panel A by MLAB (Civilized Software Inc). (B) The EC₅₀ values (f, fold to ng amount of TRIB-v2 transfected) indicate the amount of the untagged TRIB protein required to interrupt half of the MKK4V1-TRIBV2 complexes. (C) HepG2 cells were transfected with the indicated siRNA, followed by an IP for TRIB3. The level of MKK7 interacting with TRIB3 was measured by Western blot. (D) The effect of varying K_{TRIB} on the integrated response to the E1 pulse was calculated using the ODE system. TRIB concentrations were varied over ca 10⁵ range; time courses were simulated and integrated. (E) The integrated output dose responses were fitted with a cooperative inhibition model, the results are shown here.

To model the transient responses typically observed in immune and inflammatory mediator action, in contrast to differentiation or cell cycle progression which are switch like and irreversible, we simulated a receptor generated signal rapidly attenuated for example by ligand-receptor complex internalisation and degradation, by replacing the E1 activator enzyme input concentration with the piecewise linear function:

$$E1(t) = \text{if } t < t1 \text{ then } E_0 \text{ else (if } t < t2 \text{ } E1_{max} \text{ else } E_0) \quad (2)$$

where t is time in minutes, such that $t2 > t1$, defining a square wave pulse at $t1$, width $t2-t1$ and amplitude $E1_{max}$ above a constant background of E_0 . Using this input we tested a model based on that described by Ferrell and Machleder³⁸, which incorporates an MK to MKKK positive feedback loop, and found, as expected, that this showed bistability in the response to the square wave input as either $t2-t1$ or $E1_{max}$ were varied, and hence the system once ON, it did not return to baseline as $t \rightarrow \infty$. This was not therefore useful for transient response modelling. Consequently, we did not incorporate positive feedback loops in the model.

We designated the specific locus of tribbles action, based on our and others findings. Specifically:

- Tribbles proteins act by binding to MKKs as above^{15,23,24}.
- Tribbles proteins attenuate MK phosphorylation/activity as above^{23,24}.
- Tribbles proteins do not attenuate MAPKK phosphorylation²⁴.
- Tribbles are phosphoproteins and phosphorylation is induced by similar inputs to those that activate MKs³⁹.

These observations suggest that a minimal plausible mechanism for tribbles action is competitive inhibition of MK phosphorylation by active MKKs; (MKKPP in the model used here). Thus either TRIBs do not bind to non-phospho- and mono-phospho-MAPKK, or if so then these complexes are also substrates for E1.MKPK, and the interaction has no functional impact on system behaviour. Finally, given (d) above, we examined whether requiring that tribbles be phosphorylated to be active, i.e. to bind to MKKPP, significantly modified TRIB effects when compared to a model where TRIB is intrinsically active (binding to MKKPP) without phosphorylation. We tested this experimentally by PCA and measured the effect of inhibiting MAPK activity on the capacity of all three

TRIB proteins to bind to MKKs. IL1 treatment induced complex formation between TRIBs and MKKs (Fig. 3B). These data suggest that MK or elements downstream of MK act on the MAPKK step to potentiate MAPKK/TRIB interactions. To model this, given (d) we assumed that the tribbles kinase is MKPP and that it is the phosphorylation of TRIBs that activates binding to MKKPP, thus creating a negative feedback loop. While the evidence for this is circumstantial, it is a minimal assumption, avoiding arbitrarily introducing additional tribbles kinases into the system. In the parameter range close to that previously reported by Ferrel *et al.*, sensitivity analysis over a wide range of values for TRIB interactions with both MKPP and MKKPP, suggested that introduction of the phosphorylation mediated negative feedback loop did not give rise to system behaviour qualitatively different from that produced by the simpler model in which unmodified TRIB was the active form. A credible biological explanation for this observation may be that TRIB phosphorylation impacts on its intracellular distribution, thus only the phospho form may be co-localised with MKPP. Nevertheless, given earlier reports in the literature and the data in Figs 2 and 3, we used the more complex model for further analysis.

To examine the predicted quantitative impact of varying TRIB/MAPKK affinity on the inhibition dose response curve (Fig. 5D), K_{TRIB} was set at 1.5, 0.15, 0.015 and 0.0015 μM and initial TRIB ($t = 0$) varied from 100 to 0.001 μM , with all other initials and constants fixed (Fig. 4G). Again, a square wave E1 input was used. The simulations show that once $K_{\text{TRIB}} < 0.1 K_m$, little further effect on the inhibition dose response is found. However in the 0.1 to 10 range of the K_{TRIB}/K_m ratio, and at TRIB concentrations in the range 1 to 10 μM , selective inhibition of parallel MAPK pathways would be predicted to occur. Thus, as the arrow in Fig. 3F indicates, when TRIB is 1 μM , if K_{TRIB} for 3 different MKKs were in the ratio 0.1:1:10 – the relative pathway activities would be 0:0.4:1. Further, the relative mid points in the inhibition dose response curves are 1:2:8.5, similar to those observed experimentally (ref. 23 and Fig. 4). Thus, a 100-fold range of K_{TRIB} could produce selective responses from the 3 MAPK cascades even if they all were intrinsically equally responsive to an input, provided that TRIB concentration was in slight ($< 1.5\text{--}2x$) excess over MAPKK.

Discussion

Since the original description of tribbles as regulators of morphogenesis and several signalling pathways, this family of proteins have increasingly been recognised as an important controller of cellular processes; dysregulation of tribbles expression/function has been implicated in a number of diseases, including hyperlipidaemia and myocardial infarction (reviewed in refs 14,40,41). One significant aspect of tribbles action, still ill defined, is the specificity and redundancy between the three mammalian proteins. Whilst TRIB1 and TRIB2 but not TRIB3 have been suggested to play a role in the development of acute myeloid leukemia (AML)⁴², TRIB2 and TRIB3 have both been shown to interact with PI3K and Akt^{6,12,19}. On the other hand, the action of tribbles has been proposed to be cell type specific, the molecular basis for which is still not well understood. Whilst it is tempting to speculate that differences in intracellular localisation of distinct tribbles, their affinity to their binding partners as well as their expression levels may vary in a cell type specific manner, thus ultimately leading to specificity in tribbles action, most of these parameters have not been assessed systematically.

In the current study, we attempted to carry out a comprehensive study to ask the question: how does tribbles binding to MAPKK translate into specific signalling responses? We addressed this question by investigating the localisation of TRIB/MAPKK complexes, the requirement of specific protein domains for these interactions, the control of complex formation and by studying the impact of tribbles on MAPK activation, using a combined experimental and computational approach.

In line with previous data⁴³, we show in here that TRIB1 and TRIB3 are expressed in the nucleus, whilst TRIB2 is predominantly expressed in the cytoplasm. In agreement with historical reports^{26,27}, expression of MKKs, however, (with the exception of MEK1) appears to be less specific with respect to cellular compartmentalisation. The importance of TRIB localisation is reflected in the specific intracellular localisation pattern of their complexes with MKKs (Fig. 1C), raising the possibility that distinct pools of MKKs may interact with specific tribbles, and these complexes may be coupled to responses to specific stimuli. Whilst we have no direct evidence to support this hypothesis, it is tempting to speculate that distinct intracellular pools of signalling molecules, such as MKKs, with specific signalling functions may exist. Given these considerations, the relative “affinity” between TRIBs and MKK4 measured in live cells in our PCA system may not be comparable directly to values that would be obtained in a system using purified proteins, bearing in mind that most proteins with cells are likely not in free solution. Rather, it reflects a more complex “measure” of interactions by taking the physical availability of binding partners into account. However, it is clear from our data (Fig. 3D) that intracellular localisation may not be the sole determinant of the effectiveness by which distinct tribbles “compete” for MKKs. There is a notable difference in relative binding “affinity” between TRIB1 and TRIB3, despite the fact that both of these proteins appear to be expressed in the nuclear compartment (Fig. 1B).

The technique we chose to use here to investigate the binding between tribbles and MKKs has some limitations. Once a fluorescent complex forms, it “locks” the binding partners together, thus quantification of dynamic disruption of complexes with reversible binding is not possible. However, induction of complex formation can be followed (Fig. 3B). It has also been demonstrated previously that that dynamics of protein complexes can be studied in the limited cases of formation of new complexes, prevention of formation of new complexes or changes in localization of constitutive complexes with the YFP PCA^{44,45}. Additionally, degradation mediated disruption of complexes may also be detected via the loss of fluorescent signal, as we show for the NF κ B/I κ B α complex (Fig. 3A). These limitations were taken into consideration in the design and interpretation of experiments presented here by investigating the impact of “competition” between PCA tagged and untagged TRIBs 24 hrs post-transfection, when the system reached a steady state. Thus, prevention of complex formation, rather than an impact on existing complexes were measured in the experiments, results of which were used for the modelling.

Finally, we and others have shown previously that expression level of specific tribbles varies substantially in a tissue²³ and differentiation³⁴ specific manner. This provides experimental support for the hypothesis that tribbles

levels may be important in regulating qualitative, dynamic aspects of signalling. Using our experimental data, we have simulated the impact of altered tribbles concentration/affinity on the activation of MAPKs, utilising an ODE model initially developed by Ferrell and his colleagues to analyse MAPK signalling in oocytes^{37,38}. Output from this analysis predicts that a ten-fold change in tribbles “affinity” (or in expression levels), a range observed experimentally, is sufficient to alter signalling outcome in the MAPK system.

However, ODE models have clear limitations when used for modelling of signalling events. For instance, they treat the cell as a homogeneous solution. Whilst they are undoubtedly useful to probe the impact of altered availability of certain components (in this case tribbles) on signal propagation, quantitative conclusions from these studies need to be interpreted with some caution. It is well established that MAPK activation (and other signalling events) take place in a specialised intracellular microenvironment, in scaffolded multi-protein complexes. Our data suggest that TRIBs may only interact with a small proportion of MAPKs. For instance, whilst most MEK1 is seen in the cytoplasm (Fig. 1B), the TRIB1/MEK1 complex is located in the nucleus. This may explain (at least in part), why TRIBs that are often expressed at relatively low levels are still able to regulate signalling effectively. In these scaffolded complexes, local concentrations of components may be vastly different from those that is usually measured by most traditional biochemical analyses, using whole cell lysates. Consequently, the ratios between the components of the ODE modelled pathway are best interpreted to reflect local protein concentrations required within signalling complexes, rather than cell-wide expression levels.

Lately, novel modelling approaches are being developed and utilised to study signalling, that have the ability to account for spatio-temporal aspects of signal propagation. We have recently published the first agent-based model for MAPK signalling and demonstrated that the presence of scaffolded complexes may explain the ultrasensitivity of MAPK activation, as observed experimentally⁴⁶. Current work in our group includes the incorporation of TRIB proteins into this framework to further our understanding of the molecular mechanisms of TRIB mediated signalling control.

Of note, our modelling analysis here have focussed on the inhibitory action of TRIB proteins in signalling. However, we have previously reported a concentration dependent, bi-phasic regulatory role for these proteins²³ and potentiation of TRIB mediated potentiation of MEK1/ERK signalling has also been reported^{13,47}. Whilst it is possible that complex alterations between specific MAPK complexes due to changes in specific TRIB levels could explain these results, such hypothesis is yet to be tested, both experimentally and theoretically, via computational models.

Whilst the experiments reported here have focussed on the interactions between TRIBs and MKKs, we believe that the same paradigm could also be applied for their molecular interactions with other partners, such as members of the PI3K signalling network and E3 Ub ligases. Therefore, we believe that lessons learned in this system and our main conclusions are generalizable and thus provide a holistic model that contributes a better understanding of how TRIB pseudokinases function at the molecular level.

Materials and Methods

Protein-fragment Complementation Assay (PCA). In order to examine the physical interactions between tribbles and MAP kinase kinases, MEK1, MKK6, MKK4 and MKK7 in live cells, we used the yellow fluorescent protein (YFP) based protein fragment complementation assay (PCA). This strategy was developed and previously described by Michnick and his colleagues^{48,49}. We have validated this approach to study interactions between tribbles-1 and MKKs^{15,24,50}. The Venus variant of YFP was used in this study, since it provides a greater signal than EYFP (Venus variant YFP fragments were termed as V1 and V2 throughout this study). Full length GFP or YFP fragments were fused to the C-terminus of TRIB and MAPKK proteins, respectively.

Plasmids. The plasmids encoding for full length TRIB and MAPKK in fusion with GFP or the Venus fragment have been generated as described before^{15,24}.

Cell culture and transfection. HeLa, THP1 and HepG2 cells were purchased from ATCC and maintained according to the supplier’s recommendations. siRNA SmartPools against human TRIBs -1, -2 and -3, and non-targeting siRNA (siNC) were purchased from Dharmacon and used as recommended by the manufacturer. Polyfect (Qiagen, Crawley, UK) was used for transfection into HeLa and HepG2 cells, according to the manufacturer’s instructions. THP-1 cells were transfected using Nucleofector (Amaxa).

Fluorescence microscopy. Fluorescence images were taken by a Leica DMI4000B Inverted microscope (Leica Geosystems Ltd., Milton Keynes, UK). Representative fluorescent and phase contrast images were taken at 40x objective lens.

FACS analysis. 24 h after transfection, the cells were collected and flow cytometric analysis (FACS) was performed on a FACSCalibur (Becton Dickinson, USA) following the general guidelines from the manufacturer. Data were analysed using Cell Quest Pro software (Becton Dickinson, USA). The fluorescent intensity values were normalised by subtracting the background fluorescent values for mock-transfected cells. 20,000 cells were analysed for each sample.

Western blotting. Anti MKK4 and MKK7 antibodies was purchased from Cell Signalling Technology (Beverly, USA). Rabbit polyclonal GFP (ab290, 1/2500 dilution) and anti-TRIB3 (ab50516) were purchased from Abcam (Cambridge, UK). Anti-actin (c-11) antibody was purchased from Santa Cruz Biotechnology, Inc.

Immunoprecipitation. HepG2 cells were lysed in HEPES lysis buffer (40 mM HEPES, pH 7.5; 120 mM NaCl, 1 mM EDTA, 10 mM sodium pyrophosphate, 10 mM sodium glycerophosphate, 50 mM NaF, 0.5 mM sodium orthovanadate; 0.3% CHAPS). Lysate (1–4 mg) was precleared by incubating with 5–20 µl of protein

G-Sepharose conjugated to pre-immune IgG. The lysate extracts were then incubated with 5–20 µl of protein G-Sepharose conjugated to 5–20 µg of the anti-TRIB3 antibody (ab50516) or pre-immune IgG. TRIB3 antibody was covalently conjugated to protein G-Sepharose using dimethyl pimelimidate. Immunoprecipitations were carried out for 1 h at 4 °C on a rotatory wheel. The immunoprecipitates were washed 4 times with HEPES lysis buffer, followed by 2 washes with HEPES kinase buffer. The immunoprecipitates were resuspended in 30 µl of sample buffer (not containing 2-mercaptoethanol) and filtered through a 0.22-µm Spin-X filter, and 2-mercaptoethanol was added to a concentration of 1% (vol/vol). Samples were subjected to electrophoresis and immunoblot analysis.

Luciferase assay. The dual luciferase reporter assay system (Promega, Madison, WI) was used following the manufacturer's instructions. Normalised relative luciferase activity was calculated as a ratio of firefly to Renilla luciferase activity for each sample.

IL-1 α treatment. IL-1 α was a kind gift from Immunex Inc., USA.

Statistical Analysis. All the experiments were repeated a minimum of three times, all graphs show a mean \pm S.D. One-way ANOVA (followed by Tukey's Multiple Comparison Test) or two-way ANOVA (followed by Bonferroni post-tests) were used to assess statistical significance, as appropriate.

References

- Hegedus, Z., Czibula, A. & Kiss-Toth, E. Tribbles: novel regulators of cell function; evolutionary aspects. *Cell Mol Life Sci* **63**, 1632–1641 (2006).
- Kiss-Toth, E. Tribbles: 'puzzling' regulators of cell signalling. *Biochem Soc Trans* **39**, 684–687 (2011).
- Kiss-Toth, E. *et al.* Functional mapping of Toll/interleukin-1 signalling networks by expression cloning. *Biochem Soc Trans* **33**, 1405–1406 (2005).
- Sung, H. Y., Francis, S., Crossman, D. C. & Kiss-Toth, E. Tribbles-1, a mitogen activated protein kinase (MAPK) scaffold regulates inflammation in vascular smooth muscle cells (VSMC) and atherosclerosis. *Heart* **91**, A15–A15 (2005).
- Cunard, R. Mammalian Tribbles Homologs at the Crossroads of Endoplasmic Reticulum Stress and Mammalian Target of Rapamycin Pathways. *Scientifica (Cairo)* **2013**, 750871 (2013).
- Naiki, T., Saijou, E., Miyaoka, Y., Sekine, K. & Miyajima, A. TRB2, a mouse tribbles ortholog, suppresses adipocyte differentiation by inhibiting AKT and C/EBP β . *J Biol Chem* **282**, 24075–24082 (2007).
- Du, K., Herzig, S., Kulkarni, R. N. & Montminy, M. TRB3: a tribbles homolog that inhibits Akt/PKB activation by insulin in liver. *Science* **300**, 1574–1577 (2003).
- Uljon, S. *et al.* Structural Basis for Substrate Selectivity of the E3 Ligase COP1. *Structure* **24**, 687–696 (2016).
- Xu, S. *et al.* TRIB2 inhibits Wnt/ β -Catenin/TCF4 signaling through its associated ubiquitin E3 ligases, β -TrCP, COP1 and Smurf1, in liver cancer cells. *FEBS Lett* **588**, 4334–4341 (2014).
- Qi, L. *et al.* TRB3 links the E3 ubiquitin ligase COP1 to lipid metabolism. *Science* **312**, 1763–1766 (2006).
- Stein, S. J., Mack, E. A., Rome, K. S. & Pear, W. S. Tribbles in normal and malignant haematopoiesis. *Biochem Soc Trans* **43**, 1112–1115 (2015).
- Salazar, M. *et al.* TRIB3 suppresses tumorigenesis by controlling mTORC2/AKT/FOXO signaling. *Mol Cell Oncol* **2**, e980134 (2015).
- Yokoyama, T. *et al.* Trib1 links the MEK1/ERK pathway in myeloid leukemogenesis. *Blood* **116**, 2768–2775 (2010).
- Johnston, J., Basatvat, S., Ilyas, Z., Francis, S. & Kiss-Toth, E. Tribbles in inflammation. *Biochem Soc Trans* **43**, 1069–1074 (2015).
- Eder, K. *et al.* Tribbles-2 is a novel regulator of inflammatory activation of monocytes. *Int Immunol* **20**, 1543–1550 (2008).
- Yamamoto, M. *et al.* Enhanced TLR-mediated NF-IL6 dependent gene expression by Trib1 deficiency. *J Exp Med* **204**, 2233–2239 (2007).
- Liang, K. L., Rishi, L. & Keeshan, K. Tribbles in acute leukemia. *Blood* **121**, 4265–4270 (2013).
- Link, W. Tribbles breaking bad: TRIB2 suppresses FOXO and acts as an oncogenic protein in melanoma. *Biochem Soc Trans* **43**, 1085–1088 (2015).
- Salazar, M. *et al.* Loss of Tribbles pseudokinase-3 promotes Akt-driven tumorigenesis via FOXO inactivation. *Cell Death Differ* **22**, 131–144 (2015).
- Hua, F. *et al.* TRB3 links insulin/IGF to tumour promotion by interacting with p62 and impeding autophagic/proteasomal degradations. *Nat Commun* **6**, 7951 (2015).
- Zhang, L., Zhang, J., Liu, X., Liu, S. & Tian, J. Tribbles 3 Regulates the Fibrosis Cytokine TGF- β 1 through ERK1/2-MAPK Signaling Pathway in Diabetic Nephropathy. *J Immunol Res* **2014**, 240396 (2014).
- Sung, H. Y., Francis, S. E., Crossman, D. C. & Kiss-Toth, E. Regulation of expression and signalling modulator function of mammalian tribbles is cell-type specific. *Immunol Lett* **104**, 171–177 (2006).
- Kiss-Toth, E. *et al.* Human tribbles, a protein family controlling mitogen-activated protein kinase cascades. *J Biol Chem* **279**, 42703–42708 (2004).
- Sung, H. Y. *et al.* Human tribbles-1 controls proliferation and chemotaxis of smooth muscle cells via MAPK signaling pathways. *J Biol Chem* **282**, 18379–18387 (2007).
- Carlotti, F., Chapman, R., Dower, S. K. & Qwarnstrom, E. E. Activation of nuclear factor kappaB in single living cells. Dependence of nuclear translocation and anti-apoptotic function on EGFPRELA concentration. *J Biol Chem* **274**, 37941–37949 (1999).
- Tournier, C., Whitmarsh, A. J., Cavanagh, J., Barrett, T. & Davis, R. J. The MKK7 gene encodes a group of c-Jun NH2-terminal kinase kinases. *Mol Cell Biol* **19**, 1569–1581 (1999).
- Zheng, C. F. & Guan, K. L. Cytoplasmic localization of the mitogen-activated protein kinase activator MEK. *J Biol Chem* **269**, 19947–19952 (1994).
- Murphy, J. M. *et al.* Molecular Mechanism of CCAAT-Enhancer Binding Protein Recruitment by the TRIB1 Pseudokinase. *Structure* (2015).
- Hegedus, Z., Czibula, A. & Kiss-Toth, E. Tribbles: A family of kinase-like proteins with potent signalling regulatory function. *Cell Signal* **19**, 238–250 (2007).
- Bailey, F. P. *et al.* The Tribbles 2 (TRB2) pseudokinase binds to ATP and autophosphorylates in a metal-independent manner. *Biochem J* **467**, 47–62 (2015).
- Lohan, F. & Keeshan, K. The functionally diverse roles of tribbles. *Biochem Soc Trans* **41**, 1096–1100 (2013).
- Wei, S. C. *et al.* Tribbles 2 (Trib2) is a novel regulator of toll-like receptor 5 signaling. *Inflamm Bowel Dis* **18**, 877–888 (2012).
- Yang, L., Ross, K. & Qwarnstrom, E. E. RelA control of IkappaBalpha phosphorylation: a positive feedback loop for high affinity NF-kappaB complexes. *J Biol Chem* **278**, 30881–30888 (2003).

34. Ashton-Chess, J. *et al.* Tribbles-1 as a Novel Biomarker of Chronic Antibody-Mediated Rejection. *J Am Soc Nephrol* **19**, 1116–1127 (2008).
35. Ohoka, N., Sakai, S., Onozaki, K., Nakanishi, M. & Hayashi, H. Anaphase-promoting complex/cyclosome-cdh1 mediates the ubiquitination and degradation of TRB3. *Biochem Biophys Res Commun* **392**, 289–294 (2010).
36. Zhou, Y. *et al.* E3 ubiquitin ligase SIAH1 mediates ubiquitination and degradation of TRB3. *Cell Signal* **20**, 942–948 (2008).
37. Huang, C. Y. & Ferrell, J. E. J. Ultrasensitivity in the mitogen-activated protein kinase cascade. *Proc Natl Acad Sci USA* **93**, 10078–10083 (1996).
38. Ferrell, J. E. J. & Machleder, E. M. The biochemical basis of an all-or-none cell fate switch in *Xenopus* oocytes. *Science* **280**, 895–898 (1998).
39. Wilkin, F. *et al.* Characterization of a phosphoprotein whose mRNA is regulated by the mitogenic pathways in dog thyroid cells. *Eur J Biochem* **248**, 660–668 (1997).
40. Dugast, E., Kiss-Toth, E., Soulillou, J. P., Brouard, S. & Ashton-Chess, J. The Tribbles-1 protein in Humans: roles and functions in health and disease. *Curr Mol Med* **13**, 80–85 (2013).
41. Angyal, A. & Kiss-Toth, E. The tribbles gene family and lipoprotein metabolism. *Curr Opin Lipidol* **23**, 122–126 (2012).
42. Dedhia, P. H. *et al.* Differential ability of Tribbles family members to promote degradation of C/EBPalpha and induce acute myelogenous leukemia. *Blood* **116**, 1321–1328 (2010).
43. Kiss-Toth, E. *et al.* Functional mapping and identification of novel regulators for the Toll/Interleukin-1 signalling network by transcription expression cloning. *Cell Signal* **18**, 202–214 (2006).
44. MacDonald, M. L. *et al.* Identifying off-target effects and hidden phenotypes of drugs in human cells. *Nat Chem Biol* **2**, 329–337 (2006).
45. Remy, I., Montmarquette, A. & Michnick, S. W. PKB/Akt modulates TGF-beta signalling through a direct interaction with Smad3. *Nat Cell Biol* **6**, 358–365 (2004).
46. Shuaib, A., Hartwell, A., Kiss-Toth, E. & Holcombe, M. Multi-Compartmentalisation in the MAPK Signalling Pathway Contributes to the Emergence of Oscillatory Behaviour and to Ultrasensitivity. *Plos ONE* **11**, e0156139 (2016).
47. Yokoyama, T. *et al.* Identification of TRIB1 R107L gain-of-function mutation in human acute megakaryocytic leukemia. *Blood* (2012).
48. Remy, I. & Michnick, S. W. Mapping biochemical networks with protein-fragment complementation assays. *Methods Mol Biol* **261**, 411–426 (2004).
49. Remy, I. & Michnick, S. W. Dynamic visualization of expressed gene networks. *J Cell Physiol* **196**, 419–429 (2003).
50. Gilby, D. C. *et al.* Tribbles-1 and -2 are tumour suppressors, down-regulated in human acute myeloid leukaemia. *Immunol Lett* **130**, 115–124 (2010).

Acknowledgements

This work was supported by a Transatlantic Network of Excellence grant 10CVD03 from the Fondation Leducq, BBSRC Doctoral Training Grant BB/F016840/1, the British Heart Foundation project grant PG/05/100, the State Plan for R&D + I2013–2016 [with funding provided by the Instituto de salud Carlos III (ISCIII) and the European Regional Development Fund (ERDF) (PS09/01401; P112/02248 and P115/00339 grants)] and a Santander Research Mobility Award.

Author Contributions

M.S., G.V., M.H. and E.K.-T. designed the experiments. H.G., A.S., D.D.D.L. and A.A. carried out the experiments; S.K.D. designed and implemented the ODE model of MAPK signalling. S.K.D. and E.K.-T. led the analysis of results; all authors contributed to the writing and editing of the manuscript.

Additional Information

Supplementary information accompanies this paper at <http://www.nature.com/srep>

Competing financial interests: The authors declare no competing financial interests.

How to cite this article: Guan, H. *et al.* Competition between members of the tribbles pseudokinase protein family shapes their interactions with mitogen activated protein kinase pathways. *Sci. Rep.* **6**, 32667; doi: 10.1038/srep32667 (2016).



This work is licensed under a Creative Commons Attribution 4.0 International License. The images or other third party material in this article are included in the article's Creative Commons license, unless indicated otherwise in the credit line; if the material is not included under the Creative Commons license, users will need to obtain permission from the license holder to reproduce the material. To view a copy of this license, visit <http://creativecommons.org/licenses/by/4.0/>

© The Author(s) 2016